



pennsylvania

DEPARTMENT OF TRANSPORTATION

Guidelines for Analyzing Curved and Skewed Bridges and Designing Them for Construction

FINAL REPORT

August 15, 2010

By Daniel Linzell, Abner Chen, Mohammad
Sharafbayani, Junwon Seo, Deanna Nevling,
Tanit Jaissa-Ard and Omar Ashour

The Thomas D. Larson
Pennsylvania Transportation Institute

PENNSTATE



COMMONWEALTH OF PENNSYLVANIA
DEPARTMENT OF TRANSPORTATION

CONTRACT No. 510602
PROJECT No. PSU-009



1. Report No. FHWA-PA-2010-013-PSU 009		2. Government Accession No.		3. Recipient's Catalog No.	
4. Title and Subtitle Guidelines for Analyzing Curved and Skewed Bridges and Designing Them for Construction			5. Report Date August 15, 2010		
			6. Performing Organization Code		
7. Author(s) Daniel Linzell, PhD, PE, Abner Chen, PhD, Mohammad Sharafbayani, Junwon Seo, PhD, Deanna Nevling, PhD, Tanit Jaissa-Ard, and Omar Ashour			8. Performing Organization Report No. LTI 2010-18		
9. Performing Organization Name and Address The Thomas D. Larson Pennsylvania Transportation Institute The Pennsylvania State University 201 Transportation Research Building University Park, PA 16802-4710			10. Work Unit No. (TRAIS)		
			11. Contract or Grant No. 510602, PSU 009		
12. Sponsoring Agency Name and Address The Pennsylvania Department of Transportation Bureau of Planning and Research Commonwealth Keystone Building 400 North Street, 6 th Floor Harrisburg, PA 17120-0064			13. Type of Report and Period Covered Final Report 8/16/2007 – 8/15/2010		
			14. Sponsoring Agency Code		
15. Supplementary Notes COTR: Tom Macioce, 717-787-2881, tmacioce@state.pa.us					
16. Abstract Although the use of curved and skewed bridges continues to increase steadily throughout the United States, certain aspects of their behavior during construction and while in service still are not well understood. The effects of design, fabrication, and construction on the geometry and load distribution in a curved or skewed bridge system are areas in which further study and understanding are required. This project utilized remote acquisition capabilities for instruments on two structures in the Interstate 99 corridor: a horizontally curved, steel, I-girder bridge, and a skewed, pre-stressed, concrete bridge. Data obtained from these structures were examined and the numerical model accuracy for curved and skewed, steel, I-girder bridges and select appropriate model types and software was investigated. Parametric studies were undertaken on a group of representative curved and skewed steel bridge structures to numerically examine the influence of specific variables on behavior during construction. Results enabled the identification of preferred erection sequencing approaches. Among other results, girder vertical deflections were decreased when paired-girder erection methods were used and paired inner erection was preferred for structures with severe curvature. Erection methods examined herein did not show appreciable influence on skewed bridge behavior. Drop-in erection would be an acceptable approach for either curved or skewed bridges. The findings and the numerical modeling from the parametric studies formed the basis for suggesting possible modifications to relevant PennDOT publications. Web out-of-plumbness did not cause appreciable bridge deflection and stress increases when the out-of-plumbness was within the limit (1%) specified in the Structural Welding Code. Exceeding the 1% limit of the web out-of-plumbness can result in slightly higher deformations and stresses. The use of temporary construction shoring can significantly reduce girder deflections, leading to a more constructible condition. Inconsistent cross-frame detailing increased vertical and radial deflections in curved bridges and lateral deflections in skewed bridges. Replacing solid plate diaphragms in skewed bridges slightly increased deformations but did not severely affect cross-frame stresses. The applied temperature change did not have an appreciable impact on overall bridge deflections and stresses for all of the radii, skew angles and cross-frame spacings studied.					
17. Key Words Bridge design, curved and skewed bridges, behavior, construction, numerical modeling, guidelines			18. Distribution Statement No restrictions. This document is available from the National Technical Information Service, Springfield, VA 22161		
19. Security Classif. (of this report) Unclassified		20. Security Classif. (of this page) Unclassified		21. No. of Pages 421	22. Price

This work was sponsored by the Pennsylvania Department of Transportation, the Mid-Atlantic Universities Transportation Center, and the U.S. Department of Transportation, Federal Highway Administration. The contents of this report reflect the views of the authors, who are responsible for the facts and the accuracy of the data presented herein. The contents do not necessarily reflect the official views or policies of the Federal Highway Administration, U.S. Department of Transportation, the Mid-Atlantic Universities Transportation Center, or the Commonwealth of Pennsylvania at the time of publication. This report does not constitute a standard, specification, or regulation.

Table of Contents

1	INTRODUCTION	1
2	UPDATED LITERATURE SEARCH.....	1
3	DATA ACQUISITION SYSTEM MAINTENANCE.....	1
	3.1 Instrumentation Summary	2
	3.1.1 Structure #207.....	2
	3.1.2 Structure #314.....	4
	3.2 Data Collection	4
	3.3 Data Reduction and Results	4
	3.3.1 Structure #207.....	4
	3.3.2 Structure #314.....	6
4	NUMERICAL MODELING	9
	4.1 Parametric Study Modeling Procedure.....	10
5	PARAMETRIC STUDIES	10
	5.1 Parametric Structure Selection and Design	10
	5.1.1 Initial Bridge Parameter Identification and Final Structure Down Selection.....	10
	5.1.2 Structure Design and Final Proportions	18
	5.2 Girder and Cross-Frame Erection Sequencing	21
	5.2.1 Parametric Studies - Curved.....	22
	5.2.2 Parametric Studies - Skewed.....	81
	5.2.3 Final Results and Discussion	88
	5.3 Web-Plumbness	88
	5.3.1 Parametric Studies.....	89
	5.3.2 Results and Discussion.....	90
	5.4 Temporary Shoring Placement and Settlement Effects	106
	5.4.1 Parametric Studies.....	106
	5.4.2 Results and Discussion.....	114
	5.5 Cross Frame Consistent Detailing	132
	5.5.1 Parametric Studies.....	132
	5.5.2 Results and Discussion.....	134
	5.6 Solid Plate Diaphragms.....	144
	5.6.1 Parametric Studies.....	144
	5.6.2 Results and Discussion.....	145
	5.7 Temperature Change	158
	5.7.1 Parametric Studies.....	159
	5.7.2 Results and Discussion.....	160
6	CONCLUSIONS.....	177
	6.1 Project Overview	177
	6.2 Parametric Study Findings.....	178
7	REFERENCES	186

8	APPENDIX A: LITERATURE SEARCH REPORT	188
	TABLE OF CONTENTS	190
	8.1 INTRODUCTION	191
	8.2 GENERAL DESIGN GUIDELINE AND LITERATURE SEARCH	191
	8.2.1 General Design Provisions and Guidelines	192
	8.2.2 Updated Literature Search.....	193
	8.2.3 Summary.....	196
	8.3 PROPOSED DESIGN FOR CONSTRUCTION DOCUMENT TEMPLATE	196
	8.4 REFERENCES	197
9	APPENDIX B: FINAL INTERIM REPORT: NUMERICAL MODELING	201
	Table of Contents	203
	9.1 Introduction	204
	9.2 Structure Descriptions	204
	9.2.1 Structure #207	204
	9.2.2 Structure #7A	205
	9.2.3 Missing Ramps Bridge.....	206
	9.2.4 Structure #28.....	215
	9.3 Modeling Techniques	216
	9.3.1 Model Construction.....	216
	9.3.2 Analysis Techniques	218
	9.4 Comparisons and Modifications	219
	9.4.1 Comparisons – Structure #207	219
	9.4.2 Modifications	237
	9.5 Additional Evaluations	242
	9.5.1 Evaluations – Curved Bridges.....	242
	9.5.2 Evaluations – Skewed Bridge	250
	9.6 Conclusions	253
	9.7 References	254
	Appendix A – Representative Moment and Stress Calculations	255
10	APPENDIX C: PARAMETRIC STUDY BRIDGES	258
	APPENDIX C-1: Curved Bridge Drawings	259
	APPENDIX C-2: Skewed Bridge Drawings	272
11	APPENDIX D: PENNDOT DOCUMENTS	284

List of Figures

Figure 1. Structure #207 Instrument Locations.	3
Figure 2. Structure #314 Instrument Locations.	4
Figure 3. Structure #207 Section A-A Strain Variation.....	5
Figure 4. Structure #207 Section B-B Strain Variation.	5
Figure 5. Structure #207 Section C-C Strain Variation.	6
Figure 6. Structure #314 Section B-B Strain Variation.	6
Figure 7. Structure #314 Section C-C Strain Variation.	7
Figure 8. Structure #314 Section D-D Strain Variation.....	7
Figure 9. Structure #314 Section E-E Strain Variation.....	8
Figure 10. Structure #314 Section F-F Strain Variation.	8
Figure 11. Structure #314 Section G-G Strain Variation.....	9
Figure 12. Structure #314 Section H-H Strain Variation.....	9
Figure 13. Curved Bridge Statistics, Radius of Curvature.....	11
Figure 14. Curved Bridge Statistics, Span Number.	12
Figure 15. Curved Bridge Statistics, Number of Girders.....	12
Figure 16. Curved Bridge Statistics, Span Length.....	13
Figure 17. Curved Bridge Statistics, Girder Spacing.....	13
Figure 18. Curved Bridge Statistics, Cross-Frame Spacing.	14
Figure 19. Skewed Bridge Statistics, Skew Angle.	15
Figure 20. Skewed Bridges Statistics, Span Number.	15
Figure 21. Skewed Bridges Statistics, Number of Girders.	16
Figure 22. Skewed Bridges Statistics, Span Length.	16
Figure 23. Skewed Bridges Statistics, Girder Spacing.	17
Figure 24. Skewed Bridges Statistics, Cross-Frame Spacing.....	17
Figure 25. 3-D Modeling in SAP2000 of a Representative Curved Bridge.	19
Figure 26. 3-D Modeling in SAP2000 of a Representative Skewed Bridge.	19
Figure 27. Girder Boundary Conditions.	20
Figure 28. Models for Initial Curved Bridge Study.....	22
Figure 29. Simplified Framing Plan, Single-Span, 4-Girder, 305-m (1000-ft) Radius Bridge.....	24
Figure 30. Simplified Framing Plan, Single-Span, 4-Girder, 91-m (300-ft) Radius Bridge, R/L = 13.33.	24
Figure 31. Simplified Framing Plan, Balanced Two-Span, 4-Girder, 305-m (1000-ft) Radius Bridge.....	25
Figure 32. Simplified Framing Plan, Balanced Two-Span, 4-Girder, 91-m (300-ft) Radius Bridge, R/L = 13.33.	25
Figure 33. Simplified Framing Plan, Unbalanced Two-Span, 4-Girder, 305-m (1000-ft) Radius Bridge.....	27
Figure 34. Simplified Framing Plan, Unbalanced Two-Span, 4-Girder, 91-m (300-ft) Radius Bridge, R/L = 13.33.	28
Figure 35. Stage 1 of Construction for Paired Girder (Inner Girders Placed First) Erection of Single-Span, 4-Girder, 305-m (1000-ft) Radius Bridge.	28
Figure 36. Stage 2 of Construction for Paired Girder (Inner Girders Placed First) Erection of Single-Span, 4-Girder, 305-m (1000-ft) Radius Bridge.....	28

Figure 37. Stage 1 of Construction for Single Girder (Inner Girder Placed First) Erection of Single-Span, 4-Girder, 305-m (1000-ft) Radius Bridge.....	29
Figure 38. Stage 2 of Construction for Single Girder (Inner Girder Placed First) Erection of Single-Span, 4-Girder, 305-m (1000-ft) Radius Bridge.....	29
Figure 39. Stage 3 of Construction for Single Girder (Inner Girder Placed First) Erection of Single-Span, 4-Girder, 305-m (1000-ft) Radius Bridge.....	29
Figure 40. Stage 4 of Construction for Single Girder (Inner Girder Placed First) Erection of Single-Span, 4-Girder, 305-m (1000-ft) Radius Bridge.....	29
Figure 41. Stage 1 of Construction for Paired Girder (Inner Girders Placed First) Erection of Single-Span, 5-Girder, 305-m (1000-ft) Radius Bridge.....	30
Figure 42. Stage 2 of Construction for Paired Girder (Inner Girders Placed First) Erection of Single-Span, 5-Girder, 305-m (1000-ft) Radius Bridge.	30
Figure 43. Stage 3 of Construction for Paired Girder (Inner Girders Placed First) Erection of Single-Span, 5-Girder, 305-m (1000-ft) Radius Bridge.....	30
Figure 44. Stage 1 of Construction for Single Girder (Inner Girder Placed First) Erection of Single-Span, 5-Girder, 305-m (1000-ft) Radius Bridge.....	30
Figure 45. Stage 2 of Construction for Single Girder (Inner Girder Placed First) Erection of Single-Span, 5-Girder, 305-m (1000-ft) Radius Bridge.....	31
Figure 46. Stage 3 of Construction for Single Girder (Inner Girder Placed First) Erection of Single-Span, 5-Girder, 305-m (1000-ft) Radius Bridge.....	31
Figure 47. Stage 4 of Construction for Single Girder (Inner Girder Placed First) Erection of Single-Span, 5-Girder, 305-m (1000-ft) Radius Bridge.....	31
Figure 48. Stage 5 of Construction for Single Girder (Inner Girder Placed First) Erection of Single-Span, 5-Girder, 305-m (1000-ft) Radius Bridge.....	31
Figure 49. Stage 1 of Construction for Paired Girder (Inner Girders Placed First) Erection of Two Equal Span, 4-Girder, 305-m (1000-ft) Radius Bridge.....	32
Figure 50. Stage 2 of Construction for Paired Girder (Inner Girders Placed First) Erection of Two Equal Span, 4-Girder, 305-m (1000-ft) Radius Bridge.....	32
Figure 51. Stage 3 of Construction for Paired Girder (Inner Girders Placed First) Erection of Two Equal Span, 4-Girder, 305-m (1000-ft) Radius Bridge.....	32
Figure 52. Stage 4 of Construction for Paired Girder (Inner Girders Placed First) Erection of Two Equal Span, 4-Girder, 305-m (1000-ft) Radius Bridge.....	32
Figure 53. Slab Pour Sequence for Two Equal Span, 4- and 5-Girder, 305-m (1000-ft) Radius Bridges.....	33
Figure 54. Stage 1 of Construction for Paired Girder (Inner Girders Placed First) Erection of Two Unequal Spans, 4-Girder, 305-m (1000-ft) Radius Bridge.....	33
Figure 55. Stage 2 of Construction for Paired Girder (Inner Girders Placed First) Erection of Two Unequal Spans, 4-Girder, 305-m (1000-ft) Radius Bridge.....	33
Figure 56. Stage 3 of Construction for Paired Girder (Inner Girders Placed First) Erection of Two Unequal Spans, 4-Girder, 305-m (1000-ft) Radius Bridge.....	33
Figure 57. Stage 4 of Construction for Paired Girder (Inner Girders Placed First) Erection of Two Unequal Spans, 4-Girder, 305-m (1000-ft) Radius Bridge.....	34
Figure 58. Slab Pour Sequence for Two Unequal Spans, 4- and 5-Girder, 305-m (1000-ft) Radius Bridge.....	34
Figure 59. Structure 7A Framing Plan.....	35
Figure 60. Plan View Detailing Deflection Directions.....	36

Figure 61. Girder 1 Bottom Flange Vertical Deflections for Single-Span, 4-Girder, 305m (1000 ft.) Radius Bridge.	37
Figure 62. Girder 1 Bottom Flange Radial Deflections for Single-Span, 4-Girder, 305m (1000 ft.) Radius Bridge.	38
Figure 63. Girder 1 Bottom Flange Radial Deflections for Single-Span, 4-Girder, 305m (1000 ft.) Radius Bridge.	39
Figure 64. Girder 4 Bottom Flange Vertical Deflections for Single-Span, 4-Girder, 305m (1000 ft.) Radius Bridge.	40
Figure 65. Girder 4 Bottom Flange Radial Deflections for Single-Span, 4-Girder, 305m (1000 ft.) Radius Bridge.	41
Figure 66. Girder 4 Bottom Flange Tangential Deflections for Single-Span, 4-Girder, 305m (1000 ft.) Radius Bridge.	42
Figure 67. Construction Method Influence on Fitted Mean Vertical Deflections.	50
Figure 68. Construction Method Influence on Fitted Mean Radial Deflections.	52
Figure 69. Fitted Means Radial Deflection Comparison for the Interaction of Construction Method and R/L Ratio.	53
Figure 70. Construction Method Influence on Fitted Mean Tangential Deflections.	55
Figure 71. Fitted Mean Tangential Deflection Comparison for the Interaction of Construction Method and Span Type.	56
Figure 72. Radial Deformations, Single Girder Erection. First Erected Girder.	61
Figure 73. Vertical Deformations, Single Girder Erection. First Erected Girder.	61
Figure 74. Radial Deformations, Single Girder Erection. Last Erected Girder.	62
Figure 75. Vertical Deformations, Single Girder Erection. Last Erected Girder.	62
Figure 76. Radial Deformations, Paired Girder Erection. First Erected Girder.	63
Figure 77. Vertical Deformations, Paired Girder Erection. First Erected Girder.	64
Figure 78. Radial Deformations, Paired Girder Erection. Last Erected Girder.	64
Figure 79. Vertical Deformations, Paired Girder Erection. Last Erected Girder.	65
Figure 80: Simplified Framing Plan, Bridge C3: Two-Span, 4-Girder, 91.4 m Radius, R/L=13.3.	68
Figure 81: Simplified Framing Plan, Bridge C6: Two-Span, 4-Girder, 198.1 m Radius, R/L=28.9.	68
Figure 82: Simplified Framing Plan, Bridge C9: Two-Span, 4-Girder, 304.8 m Radius, R/L=44.4.	68
Figure 83: Simplified Framing Plan, Bridge C10: Balanced, Three-Span, 4-Girder, 91.4 Radius, R/L=13.3.	69
Figure 84: Simplified Framing Plan, Bridge C11: Unbalanced, Three-Span, 4-Girder, 91.4 Radius, R/L=13.3.	69
Figure 85: Stage 1 to Stage 6 for Paired-Girder (inner girders placed first) Erection of Two-Equal-Span, 4-Girder bridges.	70
Figure 86: Stage 1 to Stage 6 for Paired-Girder (outer girders placed first) Erection of Two-Equal-Span, 4-Girder Bridges.	71
Figure 87: Stage 1 to Stage 12 of Construction for Single-Girder (inner girder placed first) Erection of Two-Equal-Span, 4-Girder Bridges.	72
Figure 88: Stage 1 to Stage 12 of Construction for Single-Girder (outer girder placed first) Erection of Two-Equal-Span, 4-Girder Bridges.	73
Figure 89: Stage 1 to Stage 14 of Construction for “Drop-In” Erection of Bridge C-10.	75

Figure 90: Stage 1 to Stage 8 of Construction for “Drop-	75
Figure 91: Ratio of Maximum Vertical Deflections for Bridge C3.....	76
Figure 92: Ratio of Maximum Vertical Deflections for Bridge C6.....	77
Figure 93: Ratio of Maximum Vertical Deflections for Bridge C9.....	77
Figure 94: Ratio of Maximum Vertical Deflections for Bridge C10.....	78
Figure 95: Ratio of Maximum Vertical Deflections for Bridge C11.....	78
Figure 96: Ratio of Maximum Radial Deflections for Bridge C3.	79
Figure 97: Ratio of Maximum Radial Deflections for Bridge C6.	79
Figure 98: Ratio of Maximum Radial Deflections for Bridge C9.	80
Figure 99: Ratio of Maximum Radial Deflections for Bridge C10.	80
Figure 100: Ratio of Maximum Radial Deflections for Bridge C11.	81
Figure 101: Simplified Framing Plan of Bridge S2: Single-Span, 50° Skew.....	82
Figure 102: Simplified Framing Plan of Bridge S6: Two-Span, 50° Skew.....	82
Figure 103: Simplified Framing Plan of Bridge S8: Two-Span , 70° Skew.....	82
Figure 104: Simplified Framing Plan of Bridge S9: Balanced, Three-Span, 50° Skew.....	82
Figure 105: Simplified Framing Plan of Bridge S10: Unbalanced, Three-Span, 50° Skew.....	82
Figure 106: Stage 1 to Stage 6 of Construction for Paired-Girder Erection of Two Equal-Span, 4-Girder Bridges.	83
Figure 107: Stage 1 to Stage 12 of Construction for Single-Girder Erection of Two-Equal-Spans, 4-Girder Bridges.	84
Figure 108: Stage 1 to Stage 10 of Construction for “Drop-In” Erection of Bridge S-9 and Bridge S-10.	85
Figure 109: Ratio of Maximum Vertical Deflections for Bridge S2, Single-Span, 50° Skew.....	86
Figure 110: Ratio of Maximum Vertical Deflections for Bridge S6, Two-Span, 50° Skew.	86
Figure 111: Ratio of Maximum Vertical Deflections for Bridge S8, Two-Span, 70° Skew.	87
Figure 112: Ratio of Maximum Vertical Deflections For Bridge S9, Balanced Three-Span, 50° Skew.	87
Figure 113: Ratio of Maximum Vertical Deflections for Bridge S10, Unbalanced Three-Span, 50° Skew.....	87
Figure 114: Girder Web Out-Of-Plumbness Information.....	89
Figure 115: Ratio of Maximum Vertical Deflections for Bridge C1.....	91
Figure 116: Ratio of Maximum Vertical Deflections for Bridge C3.....	91
Figure 117: Ratio of Maximum Vertical Deflections for Bridge C6.....	92
Figure 118: Ratio of Maximum Vertical Deflections for Bridge C7.....	92
Figure 119: Ratio of Maximum Vertical Deflections for Bridge C9.....	93
Figure 120: Ratio of Maximum Radial Deflections for Bridge C1.	93
Figure 121: Ratio of Maximum Radial Deflections for Bridge C3.	94
Figure 122: Ratio of Maximum Radial Deflections for Bridge C6.	94
Figure 123: Ratio of Maximum Radial Deflections for Bridge C7.	95
Figure 124: Ratio of Maximum Radial Deflections for Bridge C9.	95
Figure 125: Ratio of Maximum Von Mises Stresses in Cross Frames for Bridge C1.....	96
Figure 126: Ratio of Maximum Von Mises Stresses in Cross Frames for Bridge C3.....	96
Figure 127. Ratio of Maximum Vertical Deflections for Bridge C3, 6% Out-of-Plumbness.	97
Figure 128. Ratio of Maximum Radial Deflections for Bridge C3, 6% Out-of-Plumbness.....	97

Figure 129 Ratio of Maximum Von Mises Stresses in Cross Frames for Bridge C3, 6% Out-of-Plumbness.	98
Figure 130: Ratio of Maximum Vertical Deflections for Bridge S2.	98
Figure 131: Ratio of Maximum Vertical Deflections for Bridge S5.	99
Figure 132: Ratio of Maximum Vertical Deflections for Bridge S6.	99
Figure 133: Ratio of Maximum Vertical Deflections for Bridge S7.	100
Figure 134: Ratio of Maximum Vertical Deflections for Bridge S8.	100
Figure 135: Ratio of Maximum Radial Deflections for Bridge S2.	101
Figure 136: Ratio of Maximum Radial Deflections for Bridge S5.	101
Figure 137: Ratio of Maximum Radial Deflections for Bridge S6.	102
Figure 138: Ratio of Maximum Radial Reflections for Bridge S7.	102
Figure 139: Ratio of Maximum Radial Deflections for Bridge S8.	103
Figure 140: Ratio of Maximum Von Mises Stresses in Cross Frames for Bridge S5.	103
Figure 141: Ratio of Maximum Von Mises Stresses in Cross Frames for Bridge S6.	104
Figure 142: Ratio of Maximum Vertical Deflections for Bridge S6, 6% Out-of-Plumbness.	104
Figure 143: Ratio of Maximum Lateral Deformations for Bridge S6, 6% Out-of-Plumbness.	105
Figure 144: Ratio of Maximum Von Mises Stresses in Cross Frames for Bridge S6, 6% Out-of-Plumbness.	105
Figure 145: Shoring Conditions for Two-Span Bridges.	109
Figure 146: Shoring Conditions for Bridge C10.	110
Figure 147: Shoring Conditions for Bridge C11.	111
Figure 148: Shoring Conditions for Bridge C12.	111
Figure 149: Shoring Conditions for Single-Span Skewed Bridge.	113
Figure 150: Shoring Conditions for Two-Span Skewed Bridges.	113
Figure 151: Shoring Conditions for Three-Span Skewed Bridges.	114
Figure 152: Ratio of Maximum Vertical Deflections for Bridge C1.	115
Figure 153: Ratio of Maximum Vertical Deflections for Bridge C3.	115
Figure 154: Ratio of Maximum Vertical Deflections for Bridge C6.	116
Figure 155: Ratio of Maximum Vertical Deflections for Bridge C7.	116
Figure 156: Ratio of Maximum Vertical Deflections for Bridge C9.	117
Figure 157: Ratio of Maximum Vertical Deflections for Bridge C10.	117
Figure 158: Ratio of Maximum Vertical Deflections for Bridge C11.	118
Figure 159: Ratio of Maximum Vertical Deflections for Bridge C12.	118
Figure 160: Ratio of Maximum Vertical Deflections for Bridge C3.	119
Figure 161: Ratio of Maximum Vertical Deflections for Bridge C6.	119
Figure 162: Ratio of Maximum Vertical Deflections for Bridge C9.	120
Figure 163: Ratio of Maximum Von Mises Stresses for Bridge C3.	120
Figure 164: Ratio of Maximum Von Mises Stresses for Bridge C6.	121
Figure 165: Ratio of Maximum Von Mises Stresses for Bridge C9.	121
Figure 166: Ratio of Maximum Von Mises Stress for Bridge C3 with Various Settlement Conditions.	122
Figure 167: Ratio of Maximum Vertical Deflections for Bridge S2.	123
Figure 168: Ratio of Maximum Vertical Deflections for Bridge S5.	123
Figure 169: Ratio of Maximum Vertical Deflections for Bridge S6.	124

Figure 170: Ratio of Maximum Vertical Deflections for Bridge S7.	124
Figure 171: Ratio of Maximum Vertical Deflections for Bridge S8.	125
Figure 172: Ratio of Maximum Vertical Deflections for Bridge S9.	125
Figure 173: Ratio of Maximum Vertical Deflections for Bridge S10.	126
Figure 174: Ratio of Maximum Vertical Deflections for Bridge S11.	126
Figure 175: Ratio of Maximum Vertical Deflections for Three Shoring Conditions in Bridge S5.	127
Figure 176: Ratio of Maximum Vertical Deflections for Three Shoring Conditions in Bridge S-6.	127
Figure 177: Ratio of Maximum Vertical Deflections for Three Shoring Conditions in Bridge S7.	128
Figure 178: Ratio of Maximum Vertical Deflections for Three Shoring Conditions in Bridge S8.	128
Figure 179: Ratio of Maximum Von Mises Stresses for Bridge S5.	129
Figure 180: Ratio of Maximum Von Mises Stresses for Bridge S6.	129
Figure 181: Ratio of Maximum Von Mises Stresses for Bridge S7.	130
Figure 182: Ratio of Maximum Von Mises Stresses for Bridge S8.	130
Figure 183: Ratio of Maximum Von Mises Stress for Bridge S6 with Various Settlement Conditions.	131
Figure 184: Cross Frame Geometries for Inconsistent Detailing.	132
Figure 185: Ratio of Maximum Vertical Deflections for Bridge C3.	135
Figure 186: Ratio of Maximum Vertical Deflections for Bridge C11.	135
Figure 187: Ratio of Maximum Radial Deflections for Bridge C3.	136
Figure 188: Ratio of Maximum Radial Deflections for Bridge C11.	136
Figure 189: Ratio of Maximum Von Mises Stresses for Bridge C3.	137
Figure 190: Ratio of Maximum Von Mises Stresses for Bridge C11.	137
Figure 191: Ratio of Maximum Vertical Deflections for Bridge S5.	138
Figure 192: Ratio of Maximum Vertical Deflections for Bridge S6.	138
Figure 193: Ratio of Maximum Vertical Deflections for Bridge S7.	139
Figure 194: Ratio of Maximum Vertical Deflections for Bridge S8.	139
Figure 195: Ratio of Maximum Radial Deflections for Bridge S5.	140
Figure 196: Ratio of Maximum Radial Deflections for Bridge S6.	140
Figure 197: Ratio of Maximum Radial Deflections for Bridge S7.	141
Figure 198: Ratio of Maximum Radial Deflections for Bridge S8.	141
Figure 199: Ratio of Maximum Von Mises Stresses for Bridge S5.	142
Figure 200: Ratio of Maximum Von Mises Stresses for Bridge S6.	142
Figure 201: Ratio of Maximum Von Mises Stresses for Bridge S7.	143
Figure 202: Ratio of Maximum Von Mises Stresses for Bridge S8.	143
Figure 203: Ratio of Maximum Vertical Deflections for Bridge C1.	146
Figure 204: Ratio of Maximum Vertical Deflections for Bridge C3.	146
Figure 205: Ratio of Maximum Vertical Deflections for Bridge C7.	147
Figure 206: Ratio of Maximum Vertical Deflections for Bridge C9.	147
Figure 207: Ratio of Maximum Radial Deflections for Bridge C1.	148
Figure 208: Ratio of Maximum Radial Deflections for Bridge C3.	148
Figure 209: Ratio of Maximum Radial Deflections for Bridge C7.	149
Figure 210: Ratio of Maximum Radial Deflections for Bridge C9.	149

Figure 211: Ratio of Maximum Von Mises Stresses in Cross Frames for Bridge C1.....	150
Figure 212: Ratio of Maximum Von Mises Stresses in Cross Frames for Bridge C3.....	150
Figure 213: Ratio of Maximum Von Mises Stresses in Cross Frames for Bridge C7.....	151
Figure 214: Ratio of Maximum Von Mises Stresses in Cross Frames for Bridge C9.....	151
Figure 215: Ratio of Maximum Vertical Deflections for Bridge S5.	152
Figure 216: Ratio of Maximum Vertical Deflections for Bridge S6.	153
Figure 217: Ratio of Maximum Vertical Deflections for Bridge S7.	153
Figure 218: Ratio of Maximum Vertical Deflections for Bridge S8.	154
Figure 219: Ratio of Maximum Lateral Deflections for Bridge S5.....	154
Figure 220: Ratio of Maximum Lateral Deflections for Bridge S6.....	155
Figure 221: Ratio of Maximum Lateral Deflections for Bridge S7.....	155
Figure 222: Ratio of Maximum Lateral Deflections for Bridge S8.....	156
Figure 223: Ratio of Maximum Von Mises Stresses in Cross Frames for Bridge S5	156
Figure 224: Ratio of Maximum Von Mises Stresses in Cross Frames for Bridge S6.	157
Figure 225: Ratio of Maximum Von Mises Stresses in Cross Frames for Bridge S7.	157
Figure 226: Ratio of Maximum Von Mises Stresses in Cross Frames for Bridge S8.	158
Figure 232: Ratio of Maximum Vertical Deflections for Bridge C9.....	163
Figure 234: Ratio of Maximum Vertical Deflections for Bridge C11.....	164
Figure 248: Ratio of Maximum Vertical Deflections for Bridge S7.	171
Figure 249: Ratio of Maximum Vertical Deflections for Bridge S8.	171
Figure 250: Ratio of Maximum Vertical Deflections for Bridge S9.	172
Figure 232. Plan Views, Missing Ramps Bridge.....	209
Figure 233. Typical Cross-Sections, Missing Ramps Bridge.....	209
Figure 234. Unit 1, Girder Erection Details, Missing Ramps Bridge.....	211
Figure 235. Unit 2, Girder Erection Details, Missing Ramps Bridge.....	212
Figure 236. Unit 1 Deck Placement Sequence, Missing Ramps Bridge.....	214
Figure 237. Unit 2 Deck Placement Sequence, Missing Ramps Bridge.....	215
Figure 238. Representative B31 Flange Element.	218
Figure 239. Typical Cross-Section, Shell and Beam Model Construction.	218
Figure 240. Structure #207 Construction Stage.....	220
Figure 241. Structure #207 Instrumented Sections.....	221
Figure 242. Stage 6 Vertical Bending Moment Distribution for Section B-B, Structure #207.....	222
Figure 243. Stage 8b Vertical Bending Moment Distribution for Section B-B, Structure #207.....	223
Figure 244. Stage 5 Vertical Bending Moment Distribution for Section C-C, Structure #207.....	224
Figure 245. Stage 6 Vertical Bending Moment Distribution for Section C-C, Structure #207.....	225
Figure 246. Stage 8b Vertical Bending Moment Distribution for Section C-C, Structure #207.....	226
Figure 247. Stage 8b Lateral Bending Moment Distribution for Section B-B, Structure #207.....	227
Figure 248. Stage 8b Lateral Bending Moment Distribution for Section C-C, Structure #207.....	228
Figure 249. Deck Placement Sequence, Structure #207.	229

Figure 250. Stress Comparisons for Girder 1 Bottom Flange Section A-A, Structure #207.....	230
Figure 251. Stress Comparisons for Girder 1 Bottom Flange Section B-B, Structure #207.....	231
Figure 252. Stress Comparisons for Girder 3 Top Flange Section B-B, Structure #207.....	232
Figure 253. Change in Girder 1 Vertical Displacements between Erection of Entire Steel Superstructure and Placement of the Slab, Structure #207.....	233
Figure 254. Change in Girder 2 Vertical Displacements between Erection of Entire Steel Superstructure and Placement of the Slab, Structure #207.....	234
Figure 255. Change in Girder 3 Vertical Displacements between Erection of Entire Steel Superstructure and Placement of the Slab, Structure #207.....	235
Figure 256. Change in Girder 4 Vertical Displacements between Erection of Entire Steel Superstructure and Placement of the Slab, Structure #207.....	236
Figure 257. Change in Girder 5 Vertical Displacements between Erection of Entire Steel Superstructure and Placement of the Slab, Structure #207.....	237
Figure 258. Vertical Deflection Comparison, Concentrated Load at Midspan, Heins and Spates (1968) Tests.....	238
Figure 259. Rotation Comparison, Concentrated Load at Three-Tenths Point, Heins and Spates (1968) Tests.....	239
Figure 260. Vertical Deflection Comparisons, Original and Modified Slab Placement Techniques, Structure #207.....	240
Figure 261. Radial Deflection Comparisons, Original and Modified Slab Placement Techniques, Structure #207.....	241
Figure 262. Stage 8b Vertical Bending Moment Distribution for Section C-C, Including Flange Offset, Structure #207.....	242
Figure 263. ABAQUS Model, Structure #7A.....	243
Figure 264. G1 Vertical Displacement Changes During Realignment of Spans 4 and 5, Structure #7A.....	244
Figure 265. G2 Vertical Displacement Changes During Realignment of Spans 4 and 5, Structure #7A.....	244
Figure 266. G3 Vertical Displacement Changes During Realignment of Spans 4 and 5, Structure #7A.....	245
Figure 267. G4 Vertical Displacement Changes During Realignment of Spans 4 and 5, Structure #7A.....	246
Figure 268. G5 Vertical Displacement Changes During Realignment of Spans 4 and 5, Structure #7A.....	246
Figure 269. ABAQUS Model, Missing Ramps Bridge.....	247
Figure 270. ABAQUS Model Detailing Cross-Frame Labels, Missing Ramps Bridge.....	247
Figure 271. Girder Radial Translations at Web-Flange Junction, Cross-Frame 10, Completion of Unit 1 Girder Erection, Missing Ramps Bridge.....	248
Figure 272. Girder Radial Translations at Web-Flange Junction, Cross-Frame 50, Completion of Unit 2 Girder Erection, Missing Ramps Bridge.....	249
Figure 273. Girder Radial Translations at Web-Flange Junction, Cross-Frame 55, Completion of Unit 2 Girder Erection, Missing Ramps Bridge.....	250
Figure 274. ABAQUS Model, Structure #28.....	251
Figure 275. Girder Lateral Displacements, Completion of Deck Pour, Structure #28.....	251
Figure 276. G1 Vertical Displacements, Completion of Deck Pour, Structure #28.....	252
Figure 277. G7 Vertical Displacements, Completion of Deck Pour, Structure #28.....	252

List of Tables

Table 1. Preliminary Curved Steel Bridge Global Information.....	14
Table 2. Preliminary Skewed Steel Bridge Global Information.....	18
Table 3. Final Curved Bridge Global Information.....	21
Table 4. Final Skewed Bridge Global Information.....	21
Table 5. Single-Span Bridge Proportions.	23
Table 6. Balanced, Two-Span Bridge Proportions.	24
Table 7. Unbalanced, Two-Span Bridge Proportions.....	27
Table 8. Independent ANOVA Variables.....	42
Table 9. R/L Ratios Used in ANOVA Analysis.	42
Table 10. ANOVA Results for Initial Vertical Deflection Statistical Model.....	46
Table 11. ANOVA Results for Modified Vertical Deflection Statistical Model.....	47
Table 12. ANOVA Results for Final Vertical Deflection Statistical Model.	49
Table 13. ANOVA Results for Final Radial Deflection Model.....	51
Table 14. ANOVA Results for Final Tangential Deflection Model.....	55
Table 15. Recommended Construction Methods for Single-Span Bridges, Initial Studies.....	57
Table 16. Construction Methods Not Recommended for Single-Span Bridges, Initial Studies.....	57
Table 17. Recommended Construction Methods for Balanced Two-Span Bridges, Initial Studies.....	58
Table 18. Construction Methods Not Recommended for Balanced Two-Span Bridges, Initial Studies.	58
Table 19. Recommended Construction Methods for Unbalanced Two-Span Bridges, Initial Studies.	58
Table 20. Construction Methods Not Recommended for Unbalanced Two-Span Bridges, Initial Studies.	59
Table 21: Selected Curved Bridge Erection Study Bridge Information	68
Table 22: Information From Representative Bridges.	81
Table 23 Selected Curved Bridge Web-Plumbness Study Information.....	90
Table 24 Selected Skewed Bridge Web-Plumbness Study Information.....	90
Table 25: Selected Curved Bridge Temporary Shoring Study Information.	108
Table 26: Selected Settlement Conditions.	112
Table 27: Selected Skewed Bridge Temporary Shoring Study Information.	112
Table 28: Selected Inconsistent Detailing Study Bridge Information	134
Table 29: Selected Skewed Bridge Consistent Detailing Study Bridge Information	134
Table 30: Selected Curved Bridge Diaphragm Study Bridge Information.....	144
Table 31: Selected Curved Bridge Diaphragm Study Bridge Information.....	145
Table 32: Selected Curved Bridge Temperature Change Study Information.....	159
Table 33: Selected Skewed Bridge Temperature Change Study Information.....	160
Table 34. Summary Table.....	181
Table 35. Girder Lengths, Radii, and Field Splice Locations (see Figure 1).	207
Table 36. Structure #207 Examined Construction Stages.	219

1 INTRODUCTION

This report summarizes research activities and findings in association with Work Order 009, “Guidelines for Analyzing Curved and Skewed Bridges and Designing Them for Construction.” The report is intended to serve as a compendium of activities related to the project and, as such, follows the final Work Order 009 scope document with respect to organization.

As discussed in the scope document, the objectives of the project were to: (1) continue to develop and maintain remote acquisition capabilities (via cell phone) for instruments on two structures in the I-99 corridor – #207, a horizontally curved, steel, I-girder bridge, and #314, a skewed, pre-stressed, concrete bridge; (2) develop, examine, and reduce data produced from these structures as needed; (3) continue examination of numerical model accuracy for curved and skewed, steel, I-girder bridges and select appropriate model types and software; (4) extend numerical studies to examine prevalent issues affecting curved and skewed steel, I-girder bridge behavior during construction (detailed under tasks below and within the enclosed draft guidelines document); and (5) develop relevant guidelines for curved and skewed, steel, I-girder bridges during construction.

The project was divided into seven tasks, listed below:

1. Updated Literature Search
2. Data Acquisition System Maintenance
3. Numerical Modeling
4. Parametric Studies
5. Draft Final Report
6. Final Report
7. Invoice Submission

Tasks that are relevant to this report are numbers 1 through 4. Each will be discussed in the sections that follow.

2 UPDATED LITERATURE SEARCH

As discussed in the project scope, an updated literature search was completed that summarized recent publications relevant to topics of interest on curved and skewed bridges. These topics included items related to construction response, numerical modeling, information on the development of any design for construction documents, and information on areas more specific to the parametric studies that were completed. More specific topics that were researched included: the effects of bearing type and restraint on curved and skewed, steel, I-girder behavior; the effects of temperature on curved and skewed, steel, I-girder behavior during construction; the effects of web-plumbness and twist imperfections on curved and skewed, steel, I-girder behavior; the effects of connection detailing on curved and skewed, steel, I-girder behavior; and the influence of solid plate diaphragms and cross frames on curved and skewed, steel, I-girder behavior.

An updated literature search report summarizing the information obtained was submitted to PennDOT in August 2008 (Linzell et al. 2008). The main body of that report is included as Appendix A of this document.

3 DATA ACQUISITION SYSTEM MAINTENANCE

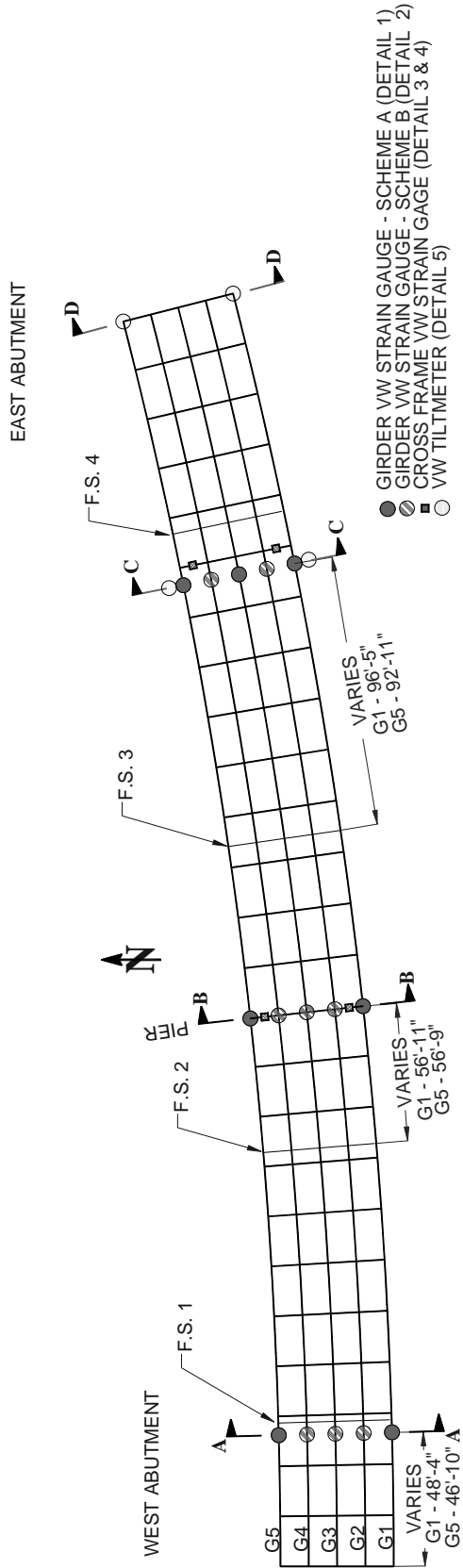
As discussed previously and in the project scope, bridge data acquisition and power supply systems were maintained and monitored throughout the project on Structures 207 and 314. Data recorded during the current project encompassed monitoring the effects of temperature cycles on the structures.

3.1 Instrumentation Summary

Summaries of the structures, instruments used, and their quantities and locations can be found in earlier submittals to PennDOT (Linzell et al. 2003; Hiltunen et al. 2004; Linzell et al. 2006). To assist with discussions of results that were obtained, short summaries of the instrumentation on each of the structures are provided in the sections that follow.

3.1.1 Structure #207

A combination of vibrating wire strain gages and vibrating wire tiltmeters were used to monitor superstructure response. Instruments were placed at various locations on the girders and cross frames as shown in Figure 1. Data were acquired at specified increments throughout the construction process and after the bridge was placed into service.



BRIDGE S-207 - INSTRUMENT LOCATION PLAN

Figure 1. Structure #207 Instrument Locations.

3.1.2 Structure #314

Similar to Structure #207, a combination of vibrating wire strain gages and tiltmeters were used to measure superstructure response for Structure #314. Strain gages were mounted to the girders and diaphragms, and tiltmeters were mounted to the girders with instruments being placed at various times during construction. Figure 2 details the instrumented sections on the bridge. Data were acquired at specified increments throughout the construction process and after the bridge was placed into service.

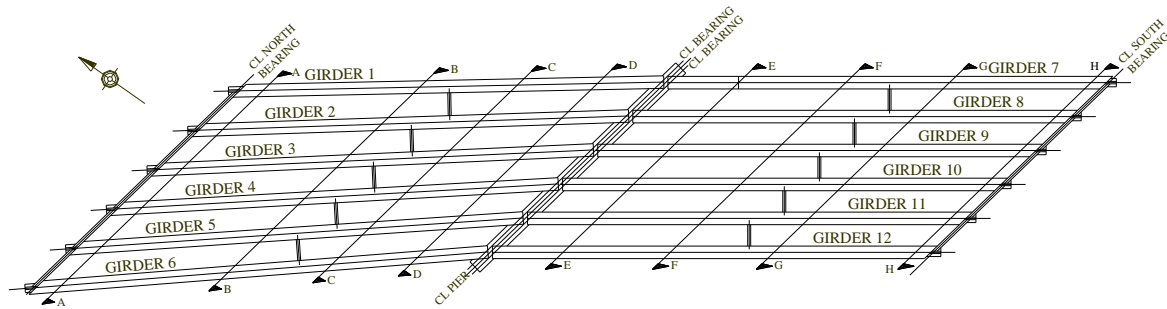


Figure 2. Structure #314 Instrument Locations.

3.2 Data Collection

As stated earlier, data collection summarized herein involved monitoring in-service bridge behavior. Given the instruments and data acquisition systems that were used, this largely consisted of tracking responses due to temperature changes. Data that deviated from what was anticipated or historically recorded for a given instrument could be identified. Data were downloaded from the acquisition systems at both structures approximately monthly throughout the duration of the project. Data readings that were downloaded were recorded by the acquisition systems at one-hour intervals. The time period over which recorded data is provided is between August 2008 and April 2010.

3.3 Data Reduction and Results

Downloaded data were merged with values for each instrument from previous downloads. Since weigh-in-motion systems were not included with the instrumentation suite for the bridges, data were plotted with respect to time for each instrument. Representative plots for each structure are provided in the sections that follow.

3.3.1 Structure #207

Representative changes in strain during the data recording period are provided at the instrumented locations discussed above. Data are plotted as response versus time in days and provide a snapshot and some insight related to gross changes in bridge behavior. Observed strains did not vary by more than approximately 200 $\mu\epsilon$ during the representative period. No obvious trends were noted from the data.

207-G3 AA

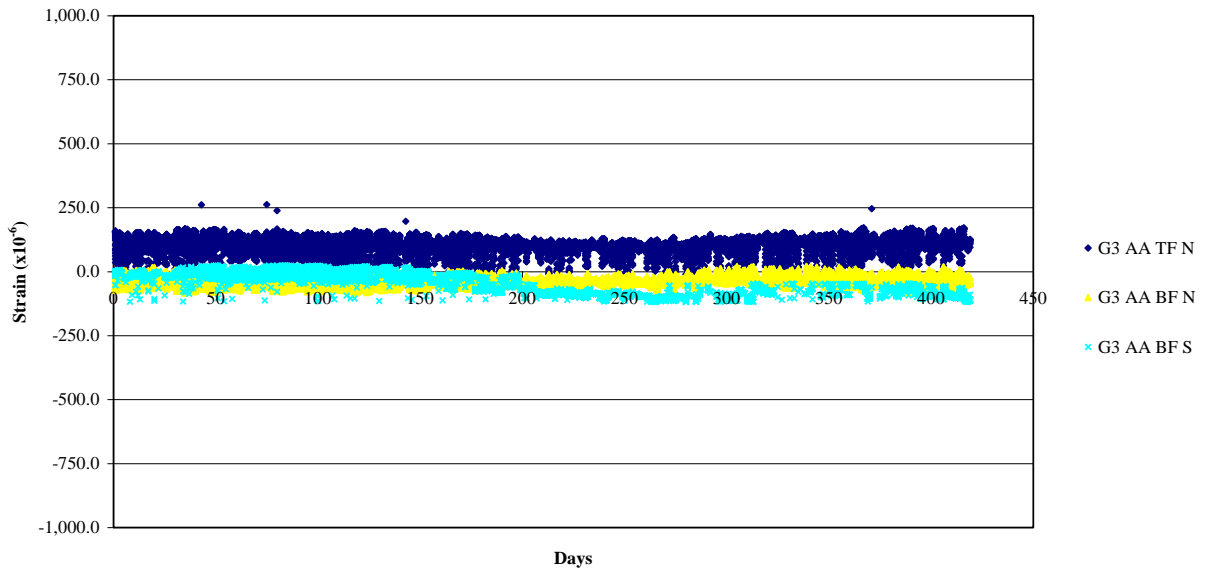


Figure 3. Structure #207 Section A-A Strain Variation.

207-G2 BB

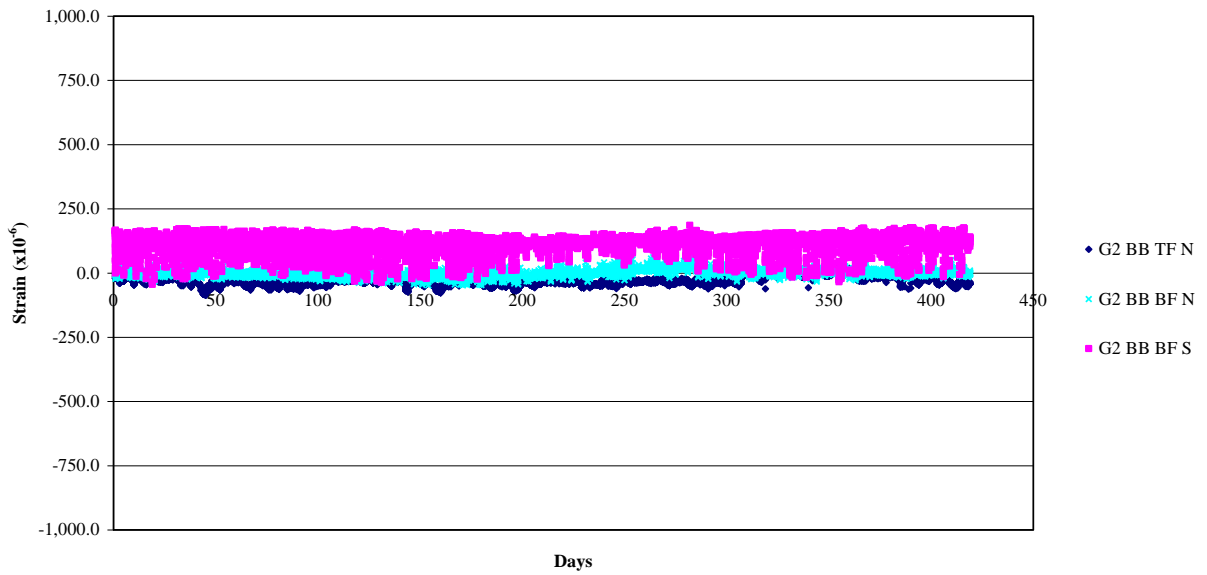


Figure 4. Structure #207 Section B-B Strain Variation.

207-G1 CC

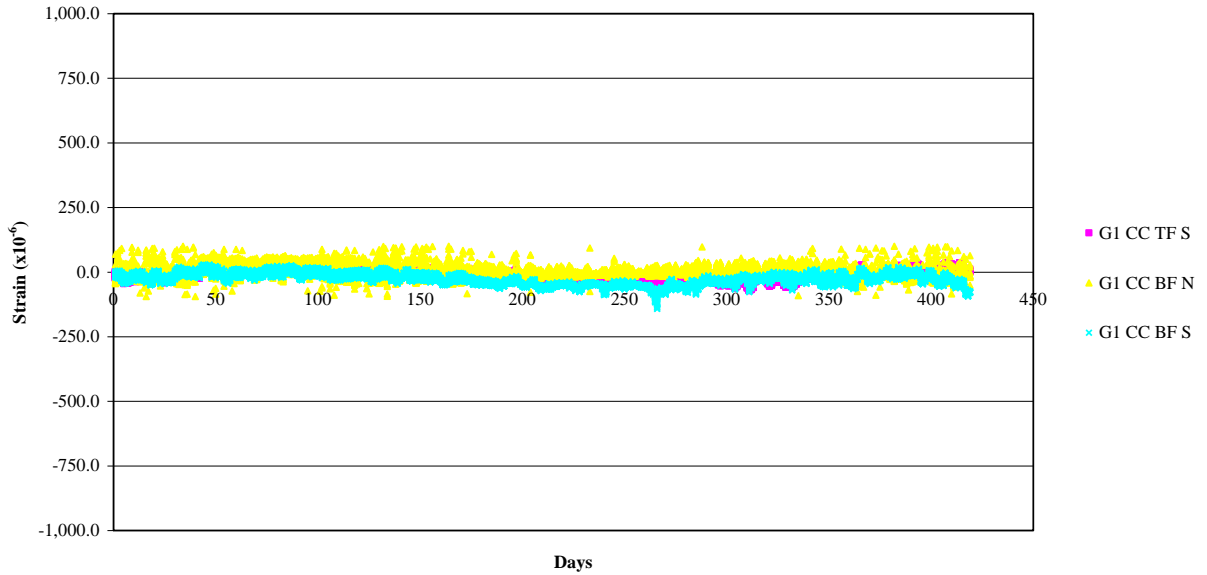


Figure 5. Structure #207 Section C-C Strain Variation.

3.3.2 Structure #314

Data are again plotted verses time in days and provide a snapshot and some insight related to gross changes in bridge behavior. Observed strains did not vary by more than approximately $30 \mu\epsilon$ during the representative period. Again, no obvious trends were noted from the data.

314-G6 BB

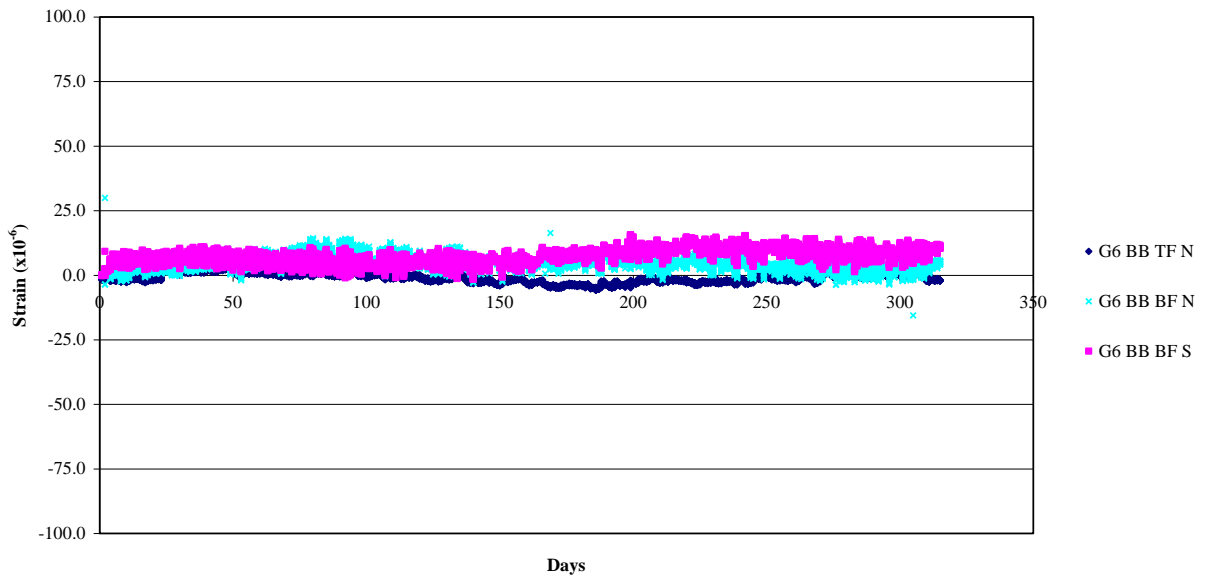


Figure 6. Structure #314 Section B-B Strain Variation.

314-G1 CC

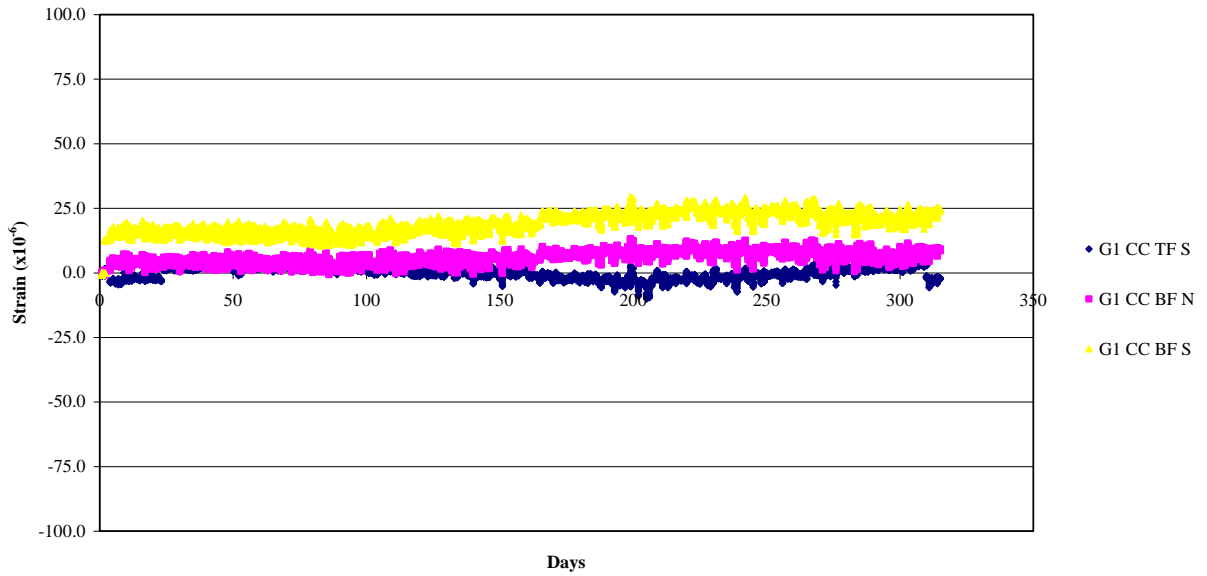


Figure 7. Structure #314 Section C-C Strain Variation.

314-G1 DD

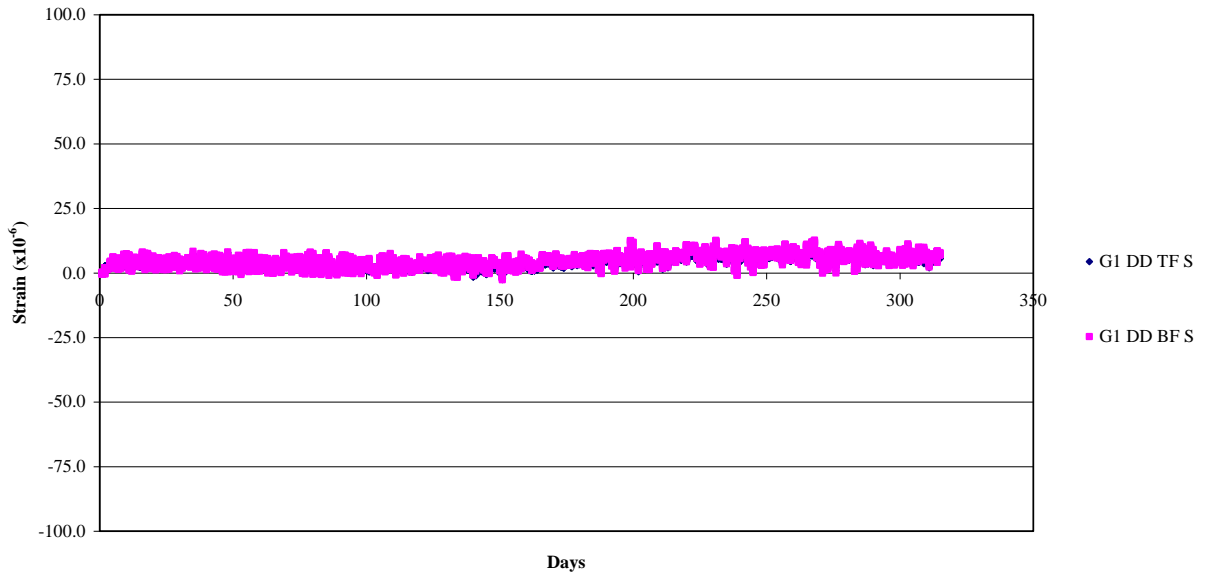


Figure 8. Structure #314 Section D-D Strain Variation.

314-G12 EE

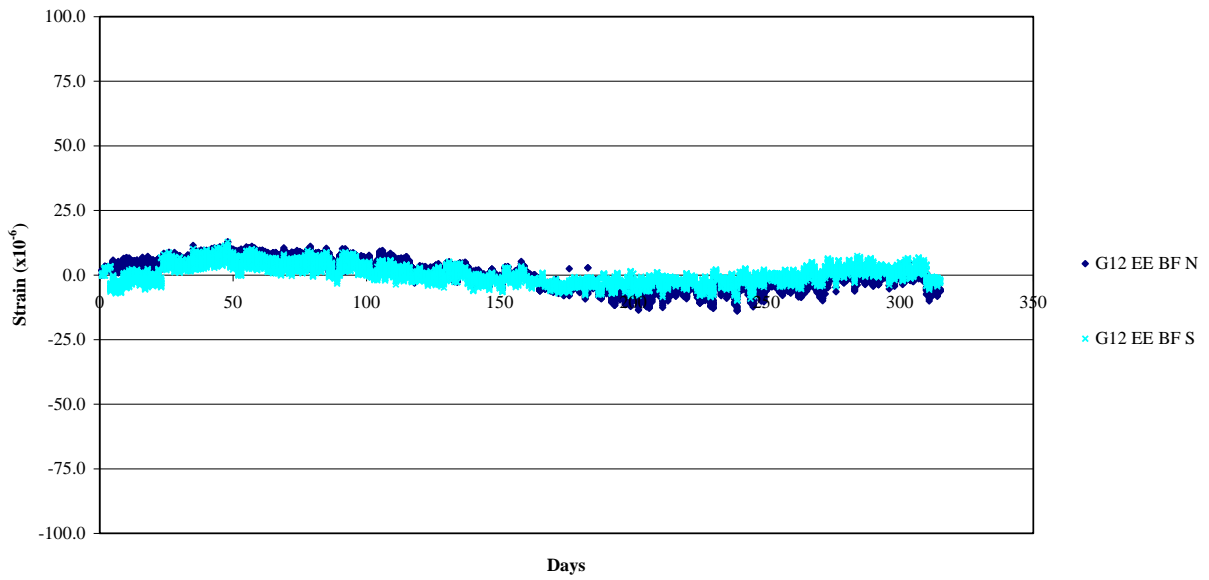


Figure 9. Structure #314 Section E-E Strain Variation.

314-G9 FF

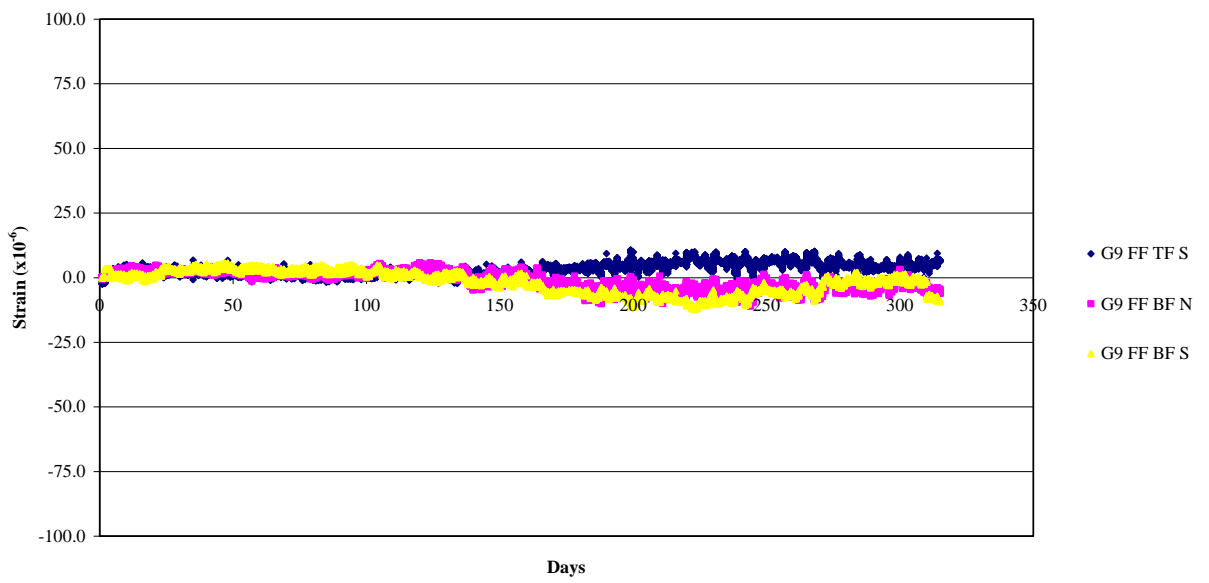


Figure 10. Structure #314 Section F-F Strain Variation.

314-G9 GG

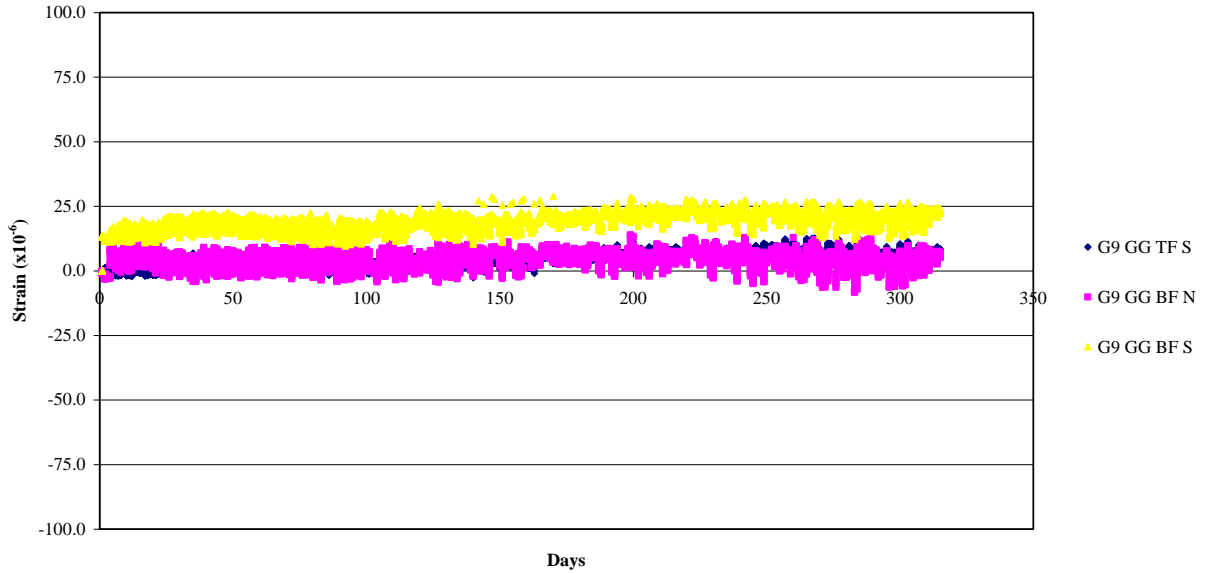


Figure 11. Structure #314 Section G-G Strain Variation.

314-G7 HH

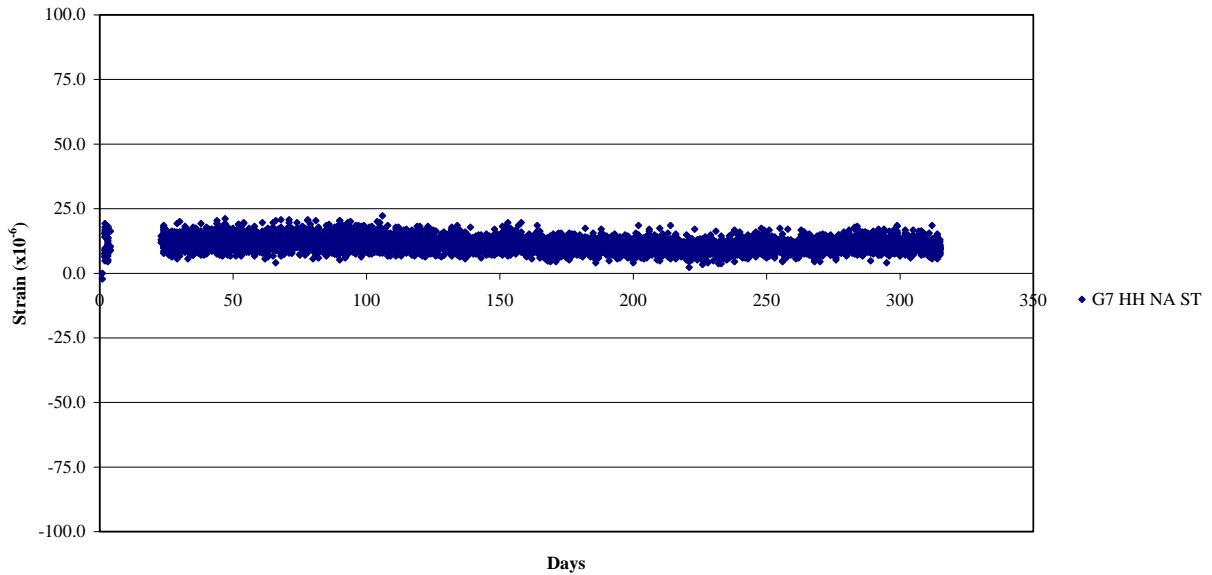


Figure 12. Structure #314 Section H-H Strain Variation.

4 NUMERICAL MODELING

As discussed in the scope, work was completed that established appropriate model types for application in the parametric studies that are outlined and discussed in sections that follow. Models of differing complexities were developed and compared to field data from the structures discussed earlier. Some additional structures and, via these comparisons, a recommended modeling scheme were developed for the parametric studies.

A numerical modeling report, summarizing work that was done and decisions that were made to establish the modeling procedure outlined below, was initially submitted to PennDOT in August 2008 (Linzell et al. 2008). The main body of that report is included as Appendix B of this document.

4.1 Parametric Study Modeling Procedure

As discussed in the previously submitted numerical modeling report (Linzell et al. 2008), models that were recommended for the parametric studies consisted of shell elements for the girder webs and bridge decks and beam elements for the girder flanges and cross frame members. The shell elements used for the girder webs and the bridge deck were ABAQUS S4R elements having 1:1 and 1:2 aspect ratios, respectively. The beam elements used for flanges were ABAQUS B31 beam elements. The report also suggested that using a first-order deformation analysis provides an effective method to predict deflections, including rotations, for a bridge with severe horizontal curvature. Therefore, analyses were performed using a first-order deformation approach.

The analysis procedure for each parametric study discussed in the sections that follow consisted of sequential analysis of curved and skewed bridges that incorporated various parameters examined in this study. The sequential analyses were performed by creating multiple steps involving analyses of each construction stage. During each step, the program analyzed the structure having the given structural components, loads, and boundary conditions based on that construction stage. The program completed the analysis when all girders were erected and the concrete deck was placed. Results from the sequential analyses were used to examine the effects of those parameters on bridge constructability. Details on how each parameter was incorporated in the finite element model are described in the following chapter.

5 PARAMETRIC STUDIES

The majority of the work discussed in the current report relates to this task, which encompasses a number of aspects as discussed in the project scope. In a general sense, the parametric studies that were performed examined the influence of construction methodology and sequencing on the resulting stresses and deformations in both curved and skewed, steel, I-girder bridges.

More specifically, the parametric studies examined the effects of a specific number of variables involved in curved, steel, I-girder bridge construction on the response of a group of representative bridge structures, which encompassed a specific range of geometries. Variables that were examined as the studied structures were numerically “constructed” included: (1) web-plumbness; (2) temporary shoring placement and settlement effects; (3) cross-frame consistent detailing (i.e., applying the work by Chavel and Earls to other bridge geometries); (4) girder and cross-frame erection sequencing along the span and with respect to girder radius and the effects of “drop-in” erection; (5) solid plate diaphragms verses cross frames; and (6) global temperature change during placement of the deck.

5.1 Parametric Structure Selection and Design

Background information related to how the representative structures were selected and designed is provided prior to discussing any information related to the parametric studies and their subsequent results. The discussion includes information related to: statistical studies completed to assist with significant curved and skewed bridge global design variable identification and selection; down-select decisions used to establish the final representative curved and skewed bridge designs used for the parametric studies; and specific information related to how final proportions were obtained for the representative bridges that were analyzed.

5.1.1 Initial Bridge Parameter Identification and Final Structure Down Selection

The identification and selection of significant parameters and parameter ranges used to initiate design of the representative curved and skewed bridges for the parametric studies began with an inventory survey of a

large set of bridge design plans from Maryland, New York, and Pennsylvania. A total of 355 bridges, consisting of horizontally curved, steel, I-girder structures with and without skew, were included in the inventory study. Of these 355 bridges, 129 had no skew (36% of the total) and 226 were a combination of skewed and curved steel I-girder bridges (64% of the total).

5.1.1.1 Curved Bridges Statistics

The statistical study completed herein focused on curved bridges with no skew and having a single center of curvature. This initial examination assisted with establishing the initial design parameters for curved bridges and provided some input for the initial design parameters for skewed bridges. Of the 129 curved bridges that had no skew, 102 were constructed using a single horizontal curve. These 102 bridges were investigated in more detail to identify statistically significant values of selected global geometric parameters. Curved bridge parameters that were investigated included the radius of curvature, span and girder numbers, span length, and girder and cross-frame spacing. Figure 13 through Figure 18 show the resulting frequency distributions for each of these parameters from the bridge sample.

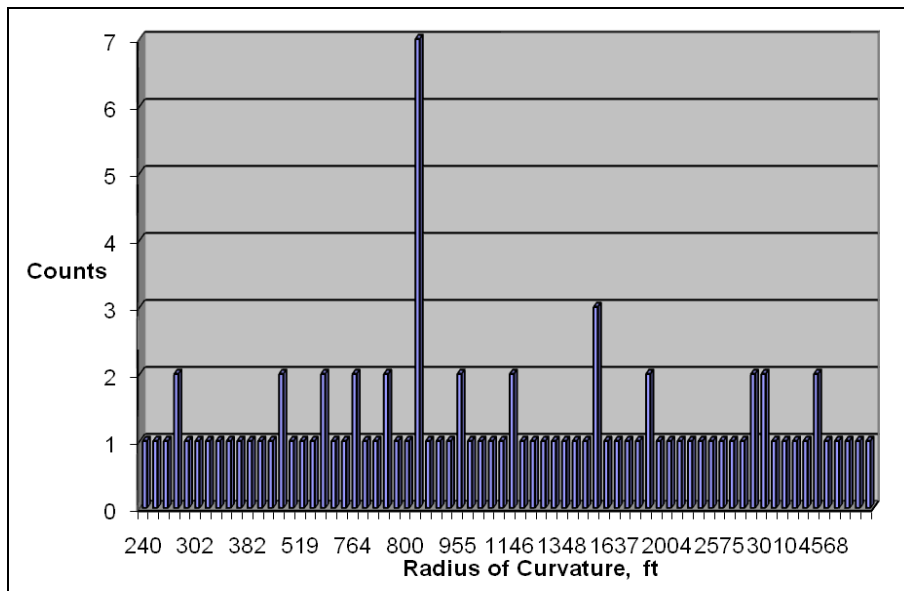


Figure 13. Curved Bridge Statistics, Radius of Curvature.

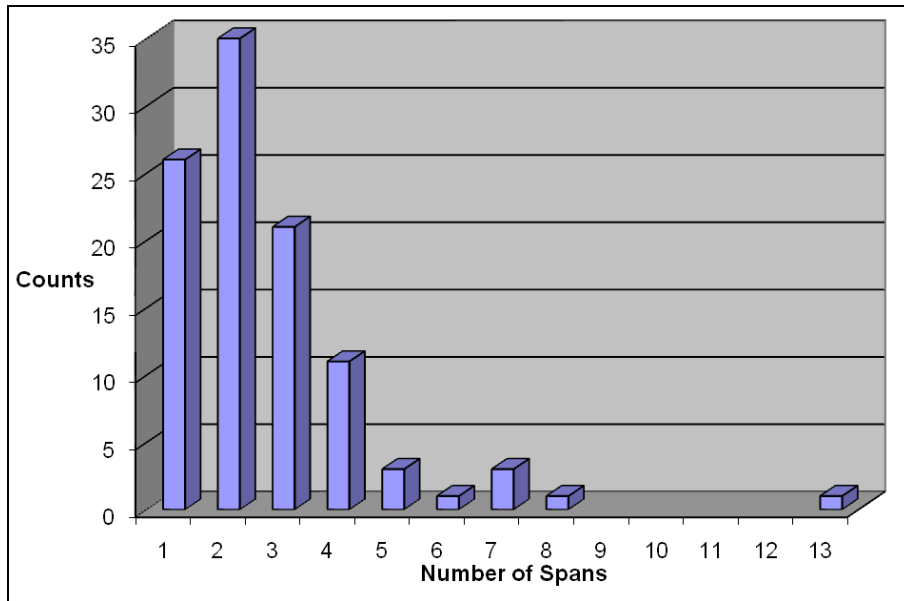


Figure 14. Curved Bridge Statistics, Span Number.

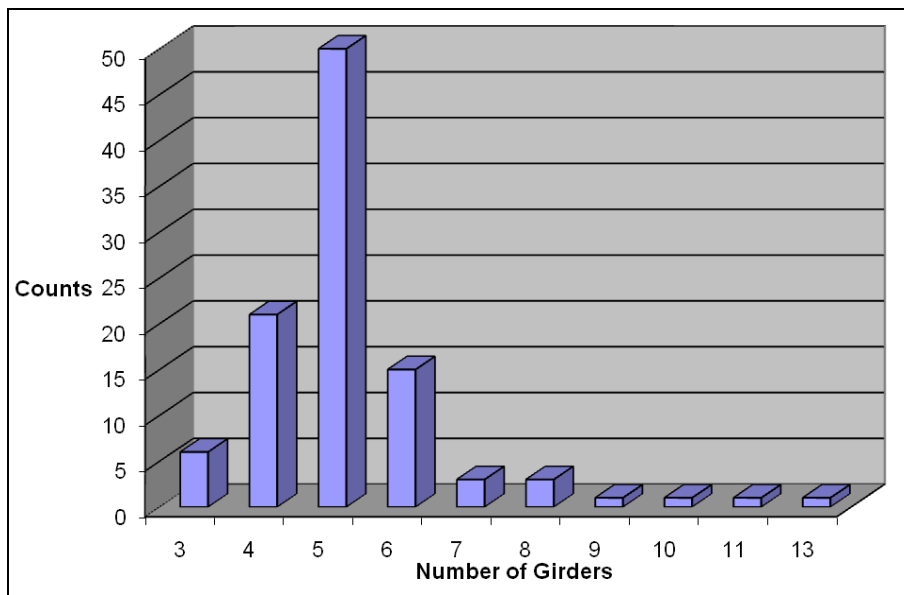


Figure 15. Curved Bridge Statistics, Number of Girders.

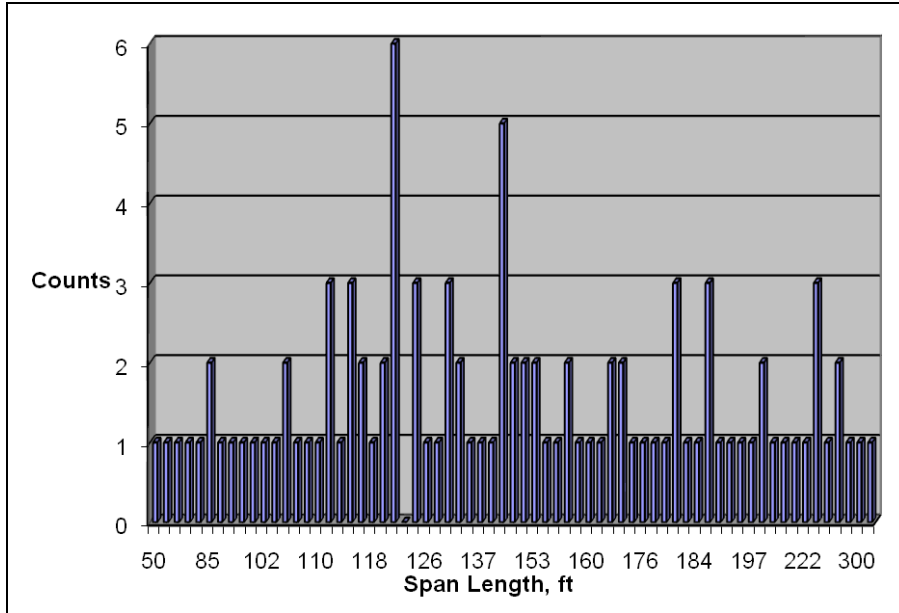


Figure 16. Curved Bridge Statistics, Span Length.

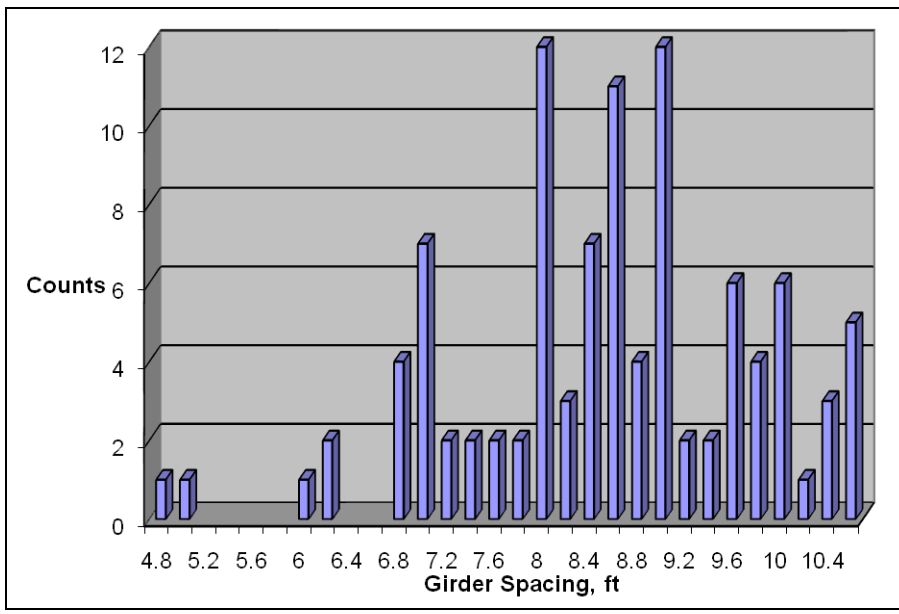


Figure 17. Curved Bridge Statistics, Girder Spacing.

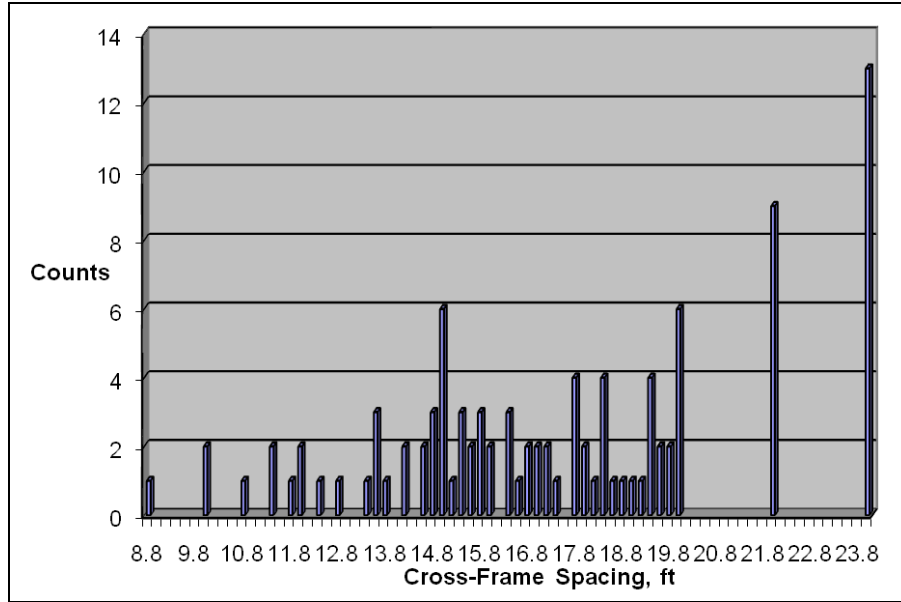


Figure 18. Curved Bridge Statistics, Cross-Frame Spacing.

The study of the bridge statistics in conjunction with examining the current design specifications was a starting point for developing an initial, proposed set of curved bridges that would be examined parametrically. Twelve horizontally curved steel bridges, shown in Table 1, were preliminarily selected for the planned parametric studies. They consisted of nine balanced, two-span structures and three balanced and unbalanced three-span continuous structures. Preliminary analyses and designs of these structures were completed with the aid of SAP2000, and the process that was followed is presented in subsequent sections.

Table 1. Preliminary Curved Steel Bridge Global Information.

Bridge No.	Radius of Curvature, ft	Cross-Frame Spacing, ft	Girder-Spacing, ft	Span-Length, ft	Number of Girder, ft
1	300	15	8	225	4
2	300	18	8	225	4
3	300	22.5	8	225	4
4	650	15	8	225	4
5	650	18	8	225	4
6	650	22.5	8	225	4
7	1000	15	8	225	4
8	1000	18	8	225	4
9	1000	22.5	8	225	4

5.1.1.2 Skewed Bridges Statistics

For the skewed bridges, similar statistical analyses were completed using the same inventory for the curved bridges to identify global geometric parameters of interest. This study focused only on bridges with skewed abutments. The parameters investigated for skewed bridges included the skew angle, span and girder numbers, span length, and girder and cross-frame spacing. Figure 19 through Figure 24 show the resulting frequency distributions for each of these parameters from the bridge sample.

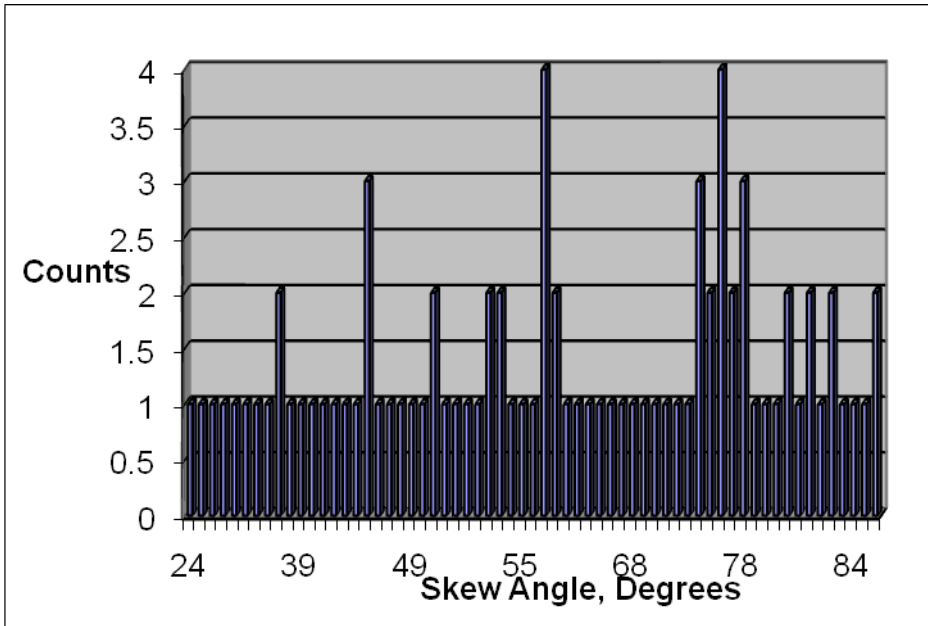


Figure 19. Skewed Bridge Statistics, Skew Angle.

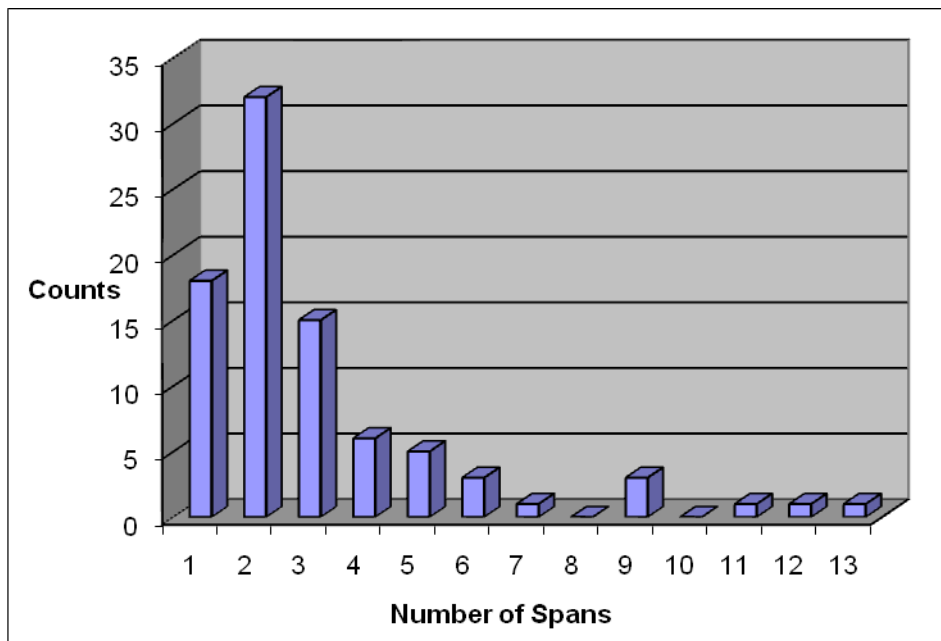


Figure 20. Skewed Bridges Statistics, Span Number.

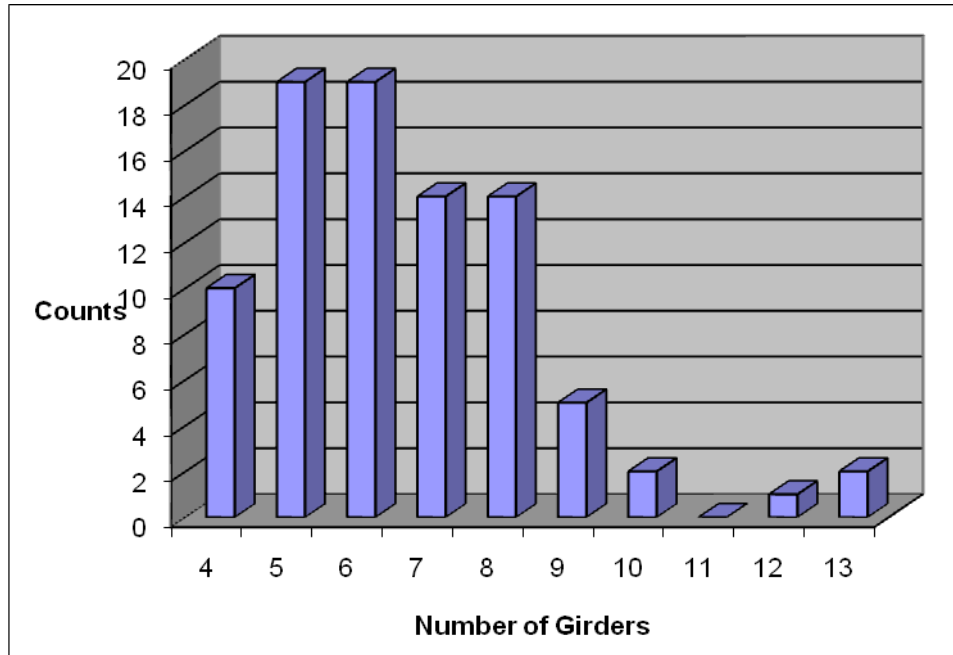


Figure 21. Skewed Bridges Statistics, Number of Girders.

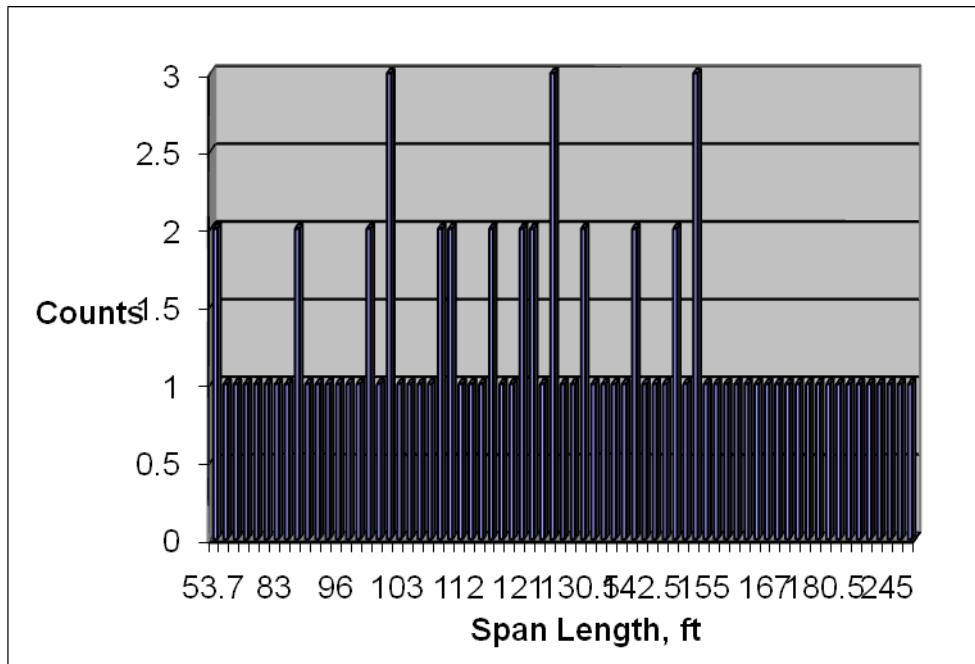


Figure 22. Skewed Bridges Statistics, Span Length.

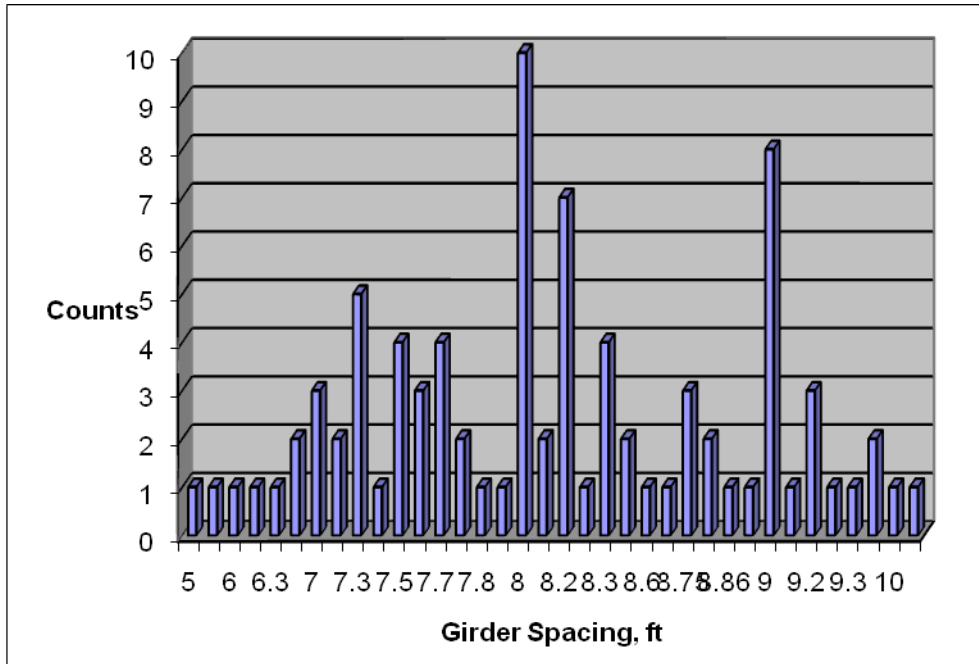


Figure 23. Skewed Bridges Statistics, Girder Spacing.

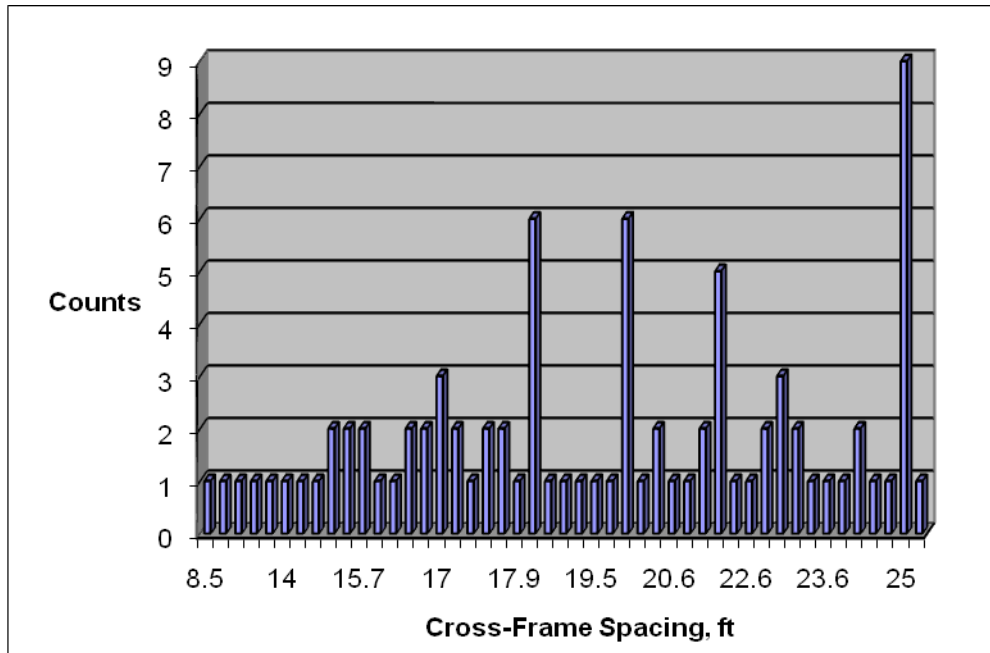


Figure 24. Skewed Bridges Statistics, Cross-Frame Spacing.

Based on the statistical analysis, an initial, proposed set of skewed bridges that would be examined parametrically was defined. Nine straight, skewed steel bridges, shown in Table 2, were preliminarily selected for the planned parametric studies. They consisted of four single-span structures, four balanced, two-span structures, and three balanced and unbalanced three-span continuous structures. Preliminary analyses and designs of these structures were completed with the aid of SAP2000, and the process that was followed to finalize the group that would be examined parametrically is presented in subsequent sections.

Table 2. Preliminary Skewed Steel Bridge Global Information

Bridge No.	Skew Angle, degree	Cross-Frame Spacing, ft	Girder-Spacing, ft	Number of Spans	Span-Length, ft	Number of Girders
1	50	15	10	1	168	4
2	60	20	10	1	168	4
3	80	24	10	1	168	4
4	50	15	10	2	168-168	4
5	60	20	10	2	168-168	4
6	80	24	10	2	168-168	4
7	50	24	10	3	168-168-168	4
8	50	24	10	3	120-168-168	4
9	50	24	10	3	120-168-120	4

5.1.2 Structure Design and Final Proportions

5.1.2.1 Preliminary Designs

Based on the statistical analyses discussed in the previous section, initial bridge global geometries were selected and preliminary designs were completed for both the curved and skewed bridges. Designs for the concrete deck design and steel superstructure were completed following relevant chapters from the *AASHTO LRFD Bridge Design Specifications* (AASHTO, 2007) and the *PennDOT Design Manual* (PennDOT, 2007). Irrespective of structure type, all bridges were initially assumed to support two lanes of traffic with shoulders and barriers; these assumptions resulted in an initial deck width of 38 ft. The deck was designed assuming one-way action and acted compositely with the supporting plate girders. Its thickness was selected to satisfy the requirements for flexure and shear strength limit states according to AASHTO and PennDOT. The initial steel superstructures all consisted of four plate girders spaced at 10 feet that were braced using X-shape cross frames with top and bottom cords. Lower lateral bracing was also included in the initial designs. Preliminary plate girder dimensions were selected for both curved and skewed bridge sets following the cross-section proportion limits from relevant AASHTO and PennDOT DM4 articles. Plate girders were assumed to be braced at the maximum allowable limits for curved plate girders from AASHTO. Although there is no unbraced length limit for straight plate girders in the specifications, to have an efficient and consistent design for the skewed structures that avoided lateral torsional buckling, applicable limits from AASHTO for curved plate girders were also used for the girders in the skewed bridges. To have an efficient cross section design, flanges were sized to be either compact or non-compact, and webs were sized to be slender following the slenderness limits from AASHTO and PennDOT DM4. Cross frames and horizontal bracings were initially sized for anticipated wind loads on girder-developed surfaces, and they were initially designed assuming they acted solely as tension or compression members. Initial sizes for all the bridge components were used to create models in SAP2000 that assisted with completion of the final designs.

5.1.2.2 Final Designs

Analyses that helped with establishing final curved and skewed bridge designs were completed using 3D SAP2000 finite element models. In these models, the plate girders were represented using shell elements for the top and bottom flanges and the webs. The concrete deck was also modeled using shell elements. Cross frames were incorporated into the models using frame elements. Representative curved and skewed bridge models are shown in Figure 25 and Figure 26, respectively. All plate girders were assumed to be homogeneous with a yield stress of 50 ksi, and the deck concrete was assumed to have a 4 ksi compressive strength. Single-span bridges were assumed to be simply supported, while multi-span structures had

pinned supports at one interior pier and roller supports everywhere else. Figure 27 details the boundary conditions applied to the bridges.

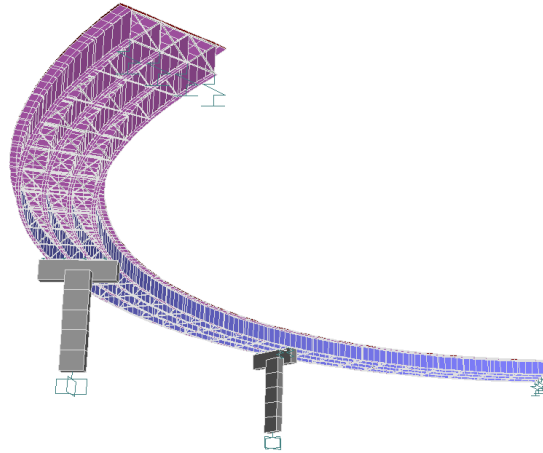


Figure 25. 3-D Modeling in SAP2000 of a Representative Curved Bridge.

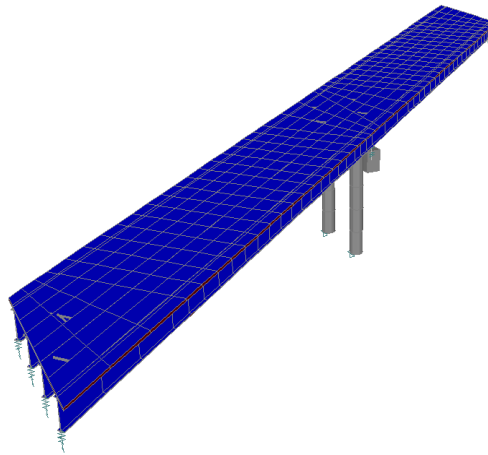


Figure 26. 3-D Modeling in SAP2000 of a Representative Skewed Bridge.

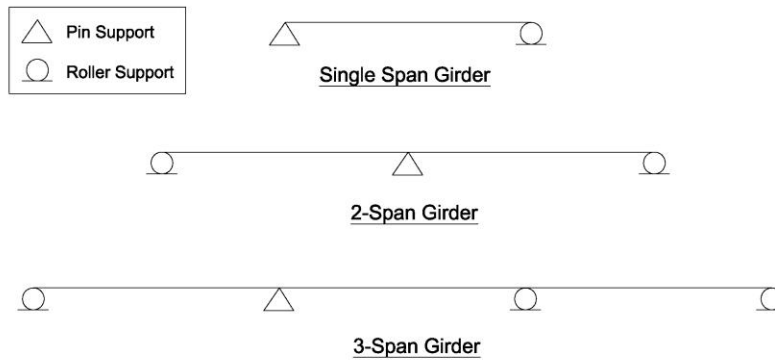


Figure 27. Girder Boundary Conditions.

Loading Criteria

Refined loads were then used to modify the initial plate girder and cross frames section geometries. Self weights for bridge structural components were obtained directly from preliminary design member sizes (D_{C1} in AASHTO). Dead loads due to wearing surface (D_w) and other non-structural components (D_{C2}) were applied to the concrete deck as distributed loads. HL-93 vehicular live loads were applied to the deck as well.

Plate Girder Flexural Design

The AASHTO and PennDOT DM4 STRI load combination was used for strength limits for flexure, with Service II being used for service limits and $1.25*DC1$ being used for constructability limits. For both curved and skewed bridges, final section designs changed as a function of positive and negative moment magnitudes. Splices were located at dead-load contraflexure points. Where section sizes could be modified due to positive and negative moment magnitudes, factors such as web depths, web thicknesses, and top and bottom flange widths were kept constant, and only top and bottom flange thicknesses changed. Following the preliminary designs, webs were slender in all cross sections, and top and bottom flanges were either compact or non-compact.

Plate Girder Shear Design

AASHTO and PennDOT DM4 STRI were used to check strength limits for shear, and $1.25*DC1$ was used to check constructability limits. To enhance the web shear capacity, transverse stiffeners were added to the plate girder web. Bearing stiffeners were also included in the final design. These stiffeners were sized in accordance with AASHTO.

Cross Frame Refined Design

According to the design specifications, cross frames are considered to be primary members in curved and severely skewed bridges, and so their initial cross section geometries were checked again here against the final design loads. AASHTO and PennDOT DM4 design provisions for compression and tension members were considered again for the final design of these members. The lateral bracing were designed as secondary members according to the specifications, and their preliminary designs were used in the final design.

Based on design refinements and section optimization as well as input from PennDOT personnel related to design decisions, two final sets of 12 horizontally curved and 11 skewed bridges were obtained for examination in the parametric studies that are summarized in the following sections. The final design

global parameters are summarized in Table 3 and Table 4. Corresponding plans for those bridges are found in Appendix C. These final bridge geometries were used to create numerical models in ABAQUS for the parametric studies.

Table 3. Final Curved Bridge Global Information.

Bridge No.	Radius of Curvature, ft	Cross-Frame Spacing, ft	Girder-Spacing, ft	Number of Spans	Span-Length, ft	Number of Girders
C1	300	15	10	2	225-225	4
C2	300	18	10	2	225-225	4
C3	300	22.5	10	2	225-225	4
C4	650	15	10	2	225-225	4
C5	650	18	10	2	225-225	4
C6	650	22.5	10	2	225-225	4
C7	1000	15	10	2	225-225	4
C8	1000	18	10	2	225-225	4
C9	1000	22.5	10	2	225-225	4
C10	300	22.5	10	3	225-225-225	4
C11	300	22.5	10	3	157.5-225-225	4
C12	300	22.5	10	3	157.5-225-157.5	4

Table 4. Final Skewed Bridge Global Information.

Bridge No.	Skew Angle, degree	Cross-Frame Spacing, ft	Girder-Spacing, ft	Number of Spans	Span-Length, ft	Number of Girders
S1	50	15	10	1	180	4
S2	50	25.7	10	1	180	4
S3	70	15	10	1	180	4
S4	70	25.7	10	1	180	4
S5	50	15	10	2	180-180	4
S6	50	25.7	10	2	180-180	4
S7	70	15	10	2	180-180	4
S8	70	25.7	10	2	180-180	4
S9	50	25.7	10	3	180-180-180	4
S10	50	25.7	10	3	180-180-128.75	4
S11	50	25.7	10	3	128.75-180-128.75	4

5.2 Girder and Cross-Frame Erection Sequencing

The effects of erection sequencing decisions on curved and skewed bridge responses are the first parametric study item discussed here, as findings from this portion of the project influenced the other parametric studies that were completed.

Studying the effects of erection sequencing began with the examination of their effects on curved, I-girder structures. Prior to the final curved structure down-select for the parametric studies outlined herein, examinations of a broader range of single- and two-span structures and of a single three-span structure were conducted to ascertain erection performance and assist with sequencing recommendations. Discussion of those studies, their findings, and how those findings were applied to the selected curved bridge set are

presented in the sections that follow. The final curved structures were selected, based on those findings, to include significant parameters that may influence the effects of erection sequencing methods on bridge response. Various erection sequencing scenarios used in the initial studies were applied to the final structures to reaffirm findings from the initial studies.

For the skewed structures, final structures were selected to include variables similar to those used for curved structures. Similar erection sequencing scenarios used for curved structures were applied to the skewed structures to study their effects.

5.2.1 Parametric Studies - Curved

5.2.1.1 Initial Studies - Background

The initial set of studies involving single- and two-span structures examined a total of thirty bridges under the influence of the following erection sequencing parameters: (1) varying radii; (2) single-span structures and two-span structures with varying span ratios; (3) four- and five-girder cross sections; (4) different erection sequencing options that including erecting single girders and girders in pairs; (5) erecting the girders from inner to outer radius of curvature and from outer to inner radius of curvature; and (6) the influence of temporary shoring.

As shown in Figure 28, the three centerline radii investigated for these initial studies were 91.4 m (300.0 ft), 198.1 m (650.0 ft), and 304.8 m (1000.0 ft) and were intended to represent a severely curved bridge (91.4 m), a moderately curved bridge (304.8 m), and a curved bridge that fell in between the extremes (198.1 m). Three different R/L values, which represent the ratio of radius of the girder to unbraced length, were investigated for the severely curved bridge: 10, 13.33, and 20. The 198.1-m (650.0-ft) and 304.8-m (1000.0-ft) bridges were studied for a single R/L ratio. Based on the parameters being considered and their combinations, a total of 240 different scenarios were investigated. Finite element models of the bridges were created and analyzed in ABAQUS/Standard using the recommended modeling procedure discussed earlier and in previous submittals to PennDOT. The structures were analyzed for all construction stages, including placement of the concrete deck. Figure 28 summarizes the scenarios that were analyzed for this preliminary study.

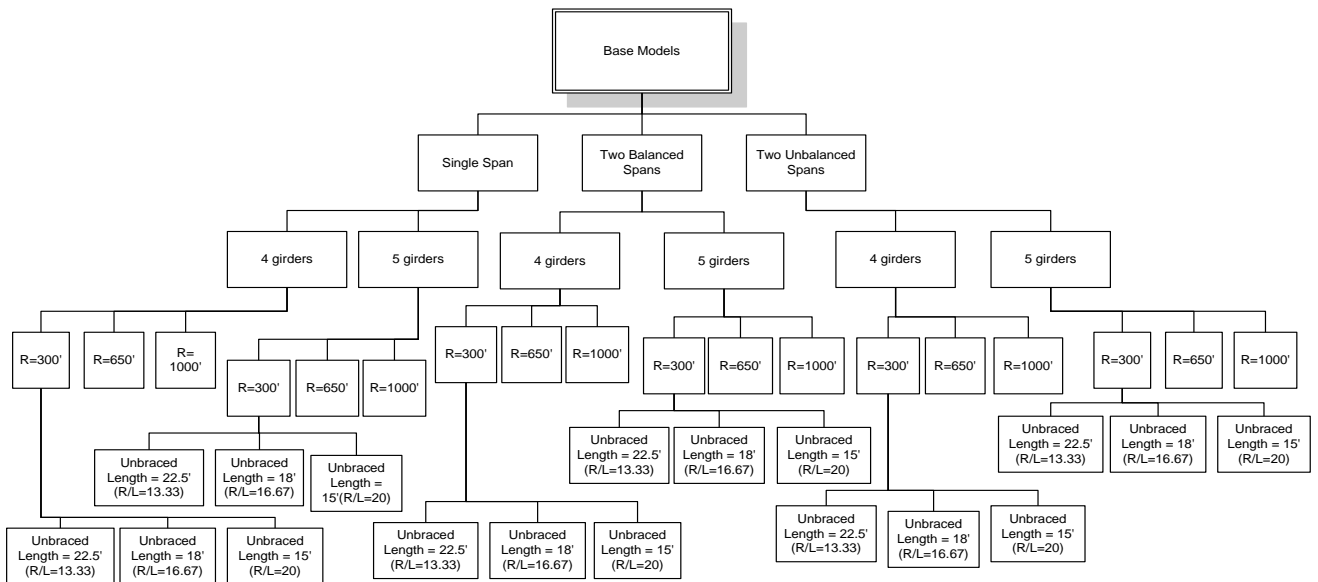


Figure 28. Models for Initial Curved Bridge Study.

The thirty bridges shown in the figure were designed following the *AASHTO Guide Specification* (AASHTO 2003) and the *AASHTO LRFD Bridge Design Specifications* (AASHTO 2008). Girders were cambered vertically, but bridge superelevation and vertical curvature were not considered. Grade 50 steel was used, and all flanges were compact and all webs transversely stiffened. A girder spacing of 2.4 m (8.0 ft) was used for all of the designs along with a 1.2-m (4.0-ft) deck overhang and a 203-mm (8-in) slab thickness. Bearing types and locations, along with cross-frame member proportions, were kept as similar as possible for all structures. SAP2000 grillage models were used to assist with the initial design and design optimization for all bridges.

Resulting single-span bridges had a span length of 68.6 m (225.0 ft), and all girders were prismatic. Table 5 details the proportions of all steel superstructure components for the single-span four- and five-girder bridge designs. Figure 29 and Figure 30 show some representative four-girder framing plans.

Table 5. Single-Span Bridge Proportions.

Bridge (No. of Girders; Radius, m (ft); R/L Ratio)	Web Dimensions, mm (in)	Flange Dimensions, mm (in)	Cross Frame Members	Transverse Stiffener Dimensions, mm (in) and Spacings, m (ft)	Bearing Stiffener Dimensions, mm (in)
4, 305 (1000), 35.59	2794 x 22.225 (110 x 0.875)	63.5 x 711 (2.5 x 28)	L3x2.5x0.25	9.525 x 152 (0.375 x 6) @ 4 (13)	25 x 254 (1.0 x 10)
4, 198 (650), 23.13	2845 x 25.400 (112 x 1.00)	76.2 x 838 (3.0 x 33)	L3.5x2.5x0.5	15.875 x 216 (0.625 x 8.5) @ 2.4 (8.0)	25 x 254 (1.0 x 10)
4, 91 (300), 13.33	2896 x 31.750 (114 x 1.250)	120.65 x 1118 (4.75 x 44)	L6x6x0.4375	15.875 x 216 (0.625 x 8.5) @ 2.9 (9.5)	25 x 356 (1.0 x 14)
4, 91 (300), 16.67	2896 x 31.750 (114 x 1.250)	120.65 x 1118 (4.75 x 44)	L6x6x1	15.875 x 216 (0.625 x 8.5) @ 2.9 (9.5)	25 x 305 (1.0 x 12)
4, 91 (300), 20.00	2896 x 31.750 (114 x 1.250)	120.65 x 1118 (4.75 x 44)	L6x6x0.375	15.875 x 216 (0.625 x 8.5) @ 2.9 (9.5)	32 x 406 (1.25 x 16)
5, 305 (1000), 35.59	2794 x 22.225 (110 x 0.875)	57.15 x 711 (2.25 x 28)	L3x2.5x0.25	12.7 x 178 (0.5 x 7) @ 4 (13)	25 x 254 (1.0 x 10)
5, 198 (650), 23.13	2845 x 25.400 (112 x 1.00)	76.2 x 838 (3.0 x 33)	L3.5x2.5x0.5	15.875 x 209.55 (0.625 x 8.25) @ 2.7 (9.0)	31.75 x 254 (1.25 x 10)
5, 91 (300), 13.33	2896 x 31.750 (114 x 1.250)	120.65 x 1118 (4.75 x 44)	L6x6x0.4375	19.05 x 305 (0.75 x 12) @ 2.9 (9.5)	35 x 356 (1.375 x 14)
5, 91 (300), 16.67	2896 x 31.750 (114 x 1.250)	120.65 x 1118 (4.75 x 44)	L6x6x1	19.05 x 305 (0.75 x 12) @ 2.0 (9.5)	35 x 356 (1.375 x 14)
5, 91 (300), 20.00	2896 x 31.750 (114 x 1.250)	120.65 x 1118 (4.75 x 44)	L6x6x0.375	19.05 x 305 (0.75 x 12) @ 2.0 (9.5)	35 x 356 (1.375 x 14)

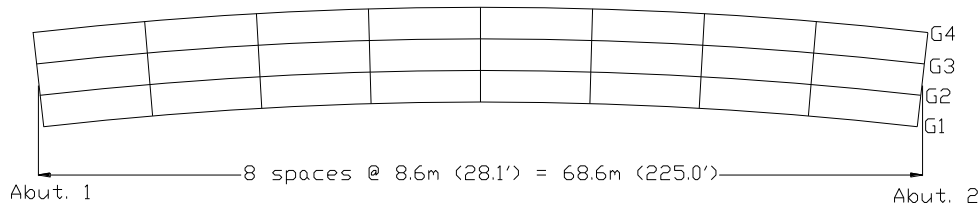


Figure 29. Simplified Framing Plan, Single-Span, 4-Girder, 305-m (1000-ft) Radius Bridge.

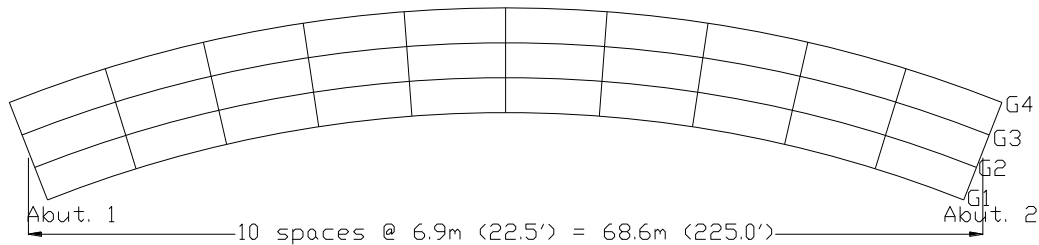


Figure 30. Simplified Framing Plan, Single-Span, 4-Girder, 91-m (300-ft) Radius Bridge, R/L = 13.33.

Similar to the single-span bridge, the balanced, two-span bridges had span lengths of 68.6 m (225.0 ft), and again, prismatic sections were used for the initial studies. Table 6 details proportions of all steel superstructure components for the balanced, two-span, four- and five-girder bridge designs. Figure 31 and Figure 32 show some representative four-girder framing plans.

Table 6. Balanced, Two-Span Bridge Proportions.

Bridge (No. of Girders; Radius, m (ft); R/L Ratio)	Web Dimensions, mm (in)	Flange Dimensions, mm (in)	Cross Frame Members	Transverse Stiffener Dimensions, mm (in) and Spacings, m (ft)	Bearing Stiffener Dimensions, mm (in)
4, 305 (1000), 35.59	2794 x 22.225 (110 x 0.875)	50.8 x 559 (2 x 22)	L3.5x2.5x0.25	9.525 x 152 (0.375 x 6) @ 4 (13)	25 x 254 (1.0 x 10)
4, 198 (650), 23.13	2845 x 25.4 (112 x 1.0)	50.8 x 610 (2 x 24)	L3.5x2.5x0.5	15.875 x 216 (0.625 x 8.5) @ 2.7 (9.0)	25 x 254 (1.0 x 10)
4, 91 (300), 13.33	2896 x 31.75 (114 x 1.25)	63.5 x 711 (2.5 x 28)	L6x6x0.4375	15.875 x 216 (0.625 x 8.5) @ 2.9 (9.5)	25 x 279 (1.0 x 11)
4, 91 (300), 16.67	2896 x 31.75 (114 x 1.25)	57.2 x 711 (2.25 x 28)	L6x6x1	15.875 x 216 (0.625 x 8.5) @ 2.9 (9.5)	25 x 305 (1.0 x 12)
4, 91 (300), 20.00	2896 x 31.75 (114 x 1.25)	57.2 x 711 (2.25 x 28)	L6x6x0.375	15.875 x 216 (0.625 x 8.5) @ 2.9 (9.5)	34.9 x 305 (1.375 x 12)
5, 305 (1000), 35.59	2794 x 22.225 (110 x 0.875)	44.5 x 508 (1.75 x 20)	L3.5x2.5x0.25	9.525 x 152 (0.375 x 6) @ 4 (13)	25 x 254 (1.0 x 10)
5, 198 (650),	2845 x 25.4	50.8 x 508	L3.5x2.5x0.5	15.875 x 216	25 x 254

23.13	(112 x 1.0)	(2.0 x 20)		(0.625 x 8.5) @ 2.7 (9.0)	(1.0 x 10)
5, 91 (300), 13.33	2896 x 31.75 (114 x 1.25)	57.2 x 660 (2.25 x 26)	L6x6x0.4375	15.875 x 216 (0.625 x 8.5) @ 2.9 (9.5)	25 x 279 (1.0 x 11)
5, 91 (300), 16.67	2896 x 31.75 (114 x 1.25)	57.2 x 610 (2.25 x 24)	L6x6x1	15.875 x 216 (0.625 x 8.5) @ 2.9 (9.5)	25 x 305 (1.0 x 12)
5, 91 (300), 20.00	2896 x 31.75 (114 x 1.25)	57.2 x 610 (2.25 x 24)	L6x6x0.375	15.875 x 216 (0.625 x 8.5) @ 2.9 (9.5)	34.9 x 305 (1.375 x 12)

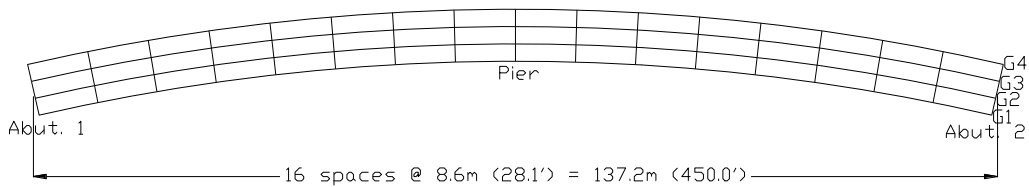


Figure 31. Simplified Framing Plan, Balanced Two-Span, 4-Girder, 305-m (1000-ft) Radius Bridge.

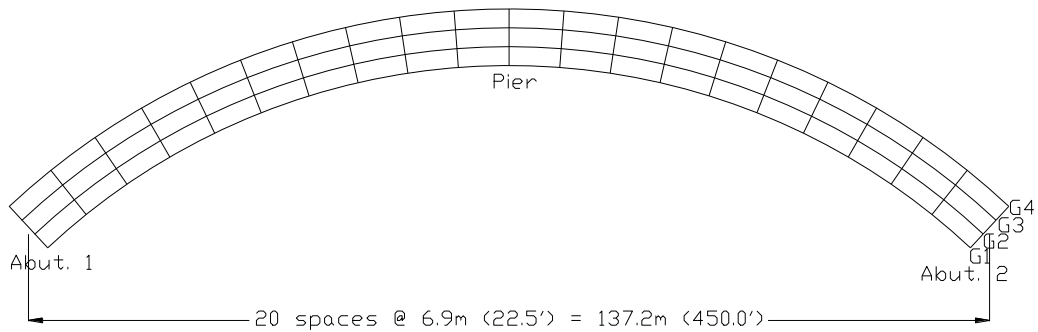


Figure 32. Simplified Framing Plan, Balanced Two-Span, 4-Girder, 91-m (300-ft) Radius Bridge, R/L = 13.33.

The unbalanced, two-span bridges had span lengths of 68.6 m (225.0 ft) and 34.3 m (112.5 ft). Prismatic sections were again used for the initial erection studies.

Table 7 details the proportions of all steel superstructure components for the balanced, two-span, four- and five-girder bridge designs. Figure 33 and Figure 34 show some representative four-girder framing plans.

Table 7. Unbalanced, Two-Span Bridge Proportions

Bridge (No. of Girders; Radius, m (ft); R/L Ratio	Web Dimensions, mm (in)	Flange Dimensions, mm (in)	Cross Frame Members	Transverse Stiffener Dimensions, mm (in) and Spacings, m (ft)	Bearing Stiffener Dimensions, mm (in)
4, 305 (1000), 35.59	2794 x 22.225 (110 x 0.875)	50.8 x 559 (2 x 22)	L3.5x2.5x0.25	9.525 x 152 (0.375 x 6) @ 4 (13)	25 x 254 (1.0 x 10)
4, 198 (650), 23.13	2845 x 25.4 (112 x 1.0)	50.8 x 660 (2 x 26)	L3.5x2.5x0.5	15.875 x 216 (0.625 x 8.5) @ 2.7 (9.0)	25 x 254 (1.0 x 10)
4, 91 (300), 13.33	2896 x 31.75 (114 x 1.25)	57.2 x 711 (2.25 x 28)	L6x6x0.4375	15.875 x 216 (0.625 x 8.5) @ 2.9 (9.5)	25 x 279 (1.0 x 11)
4, 91 (300), 16.67	2896 x 31.75 (114 x 1.25)	57.2 x 610 (2.25 x 24)	L6x6x1	15.875 x 216 (0.625 x 8.5) @ 2.9 (9.5)	25 x 305 (1.0 x 12)
4, 91 (300), 20.00	2896 x 31.75 (114 x 1.25)	57.2 x 610 (2.25 x 24)	L6x6x0.375	15.875 x 216 (0.625 x 8.5) @ 2.9 (9.5)	25 x 254 (1.0 x 10)
5, 305 (1000), 35.59	2794 x 22.225 (110 x 0.875)	44.5 x 508 (1.75 x 20)	L3.5x2.5x0.25	9.525 x 152 (0.375 x 6) @ 4 (13)	25 x 254 (1.0 x 10)
5, 198 (650), 23.13	2845 x 25.4 (112 x 1.0)	50.8 x 508 (2 x 20)	L3.5x2.5x0.5	15.875 x 216 (0.625 x 8.5) @ 2.7 (9.0)	25 x 254 (1.0 x 10)
5, 91 (300), 13.33	2896 x 31.75 (114 x 1.25)	57.2 x 660 (2.25 x 26)	L6x6x0.4375	15.875 x 216 (0.625 x 8.5) @ 2.9 (9.5)	25 x 279 (1.0 x 11)
5, 91 (300), 16.67	2896 x 31.75 (114 x 1.25)	50.8 x 610 (2 x 24)	L6x6x1	15.875 x 216 (0.625 x 8.5) @ 2.9 (9.5)	25 x 254 (1.0 x 10)
5, 91 (300), 20.00	2896 x 31.75 (114 x 1.25)	50.8 x 610 (2 x 24)	L6x6x0.375	15.875 x 216 (0.625 x 8.5) @ 2.9 (9.5)	25 x 229 (1 x 9)

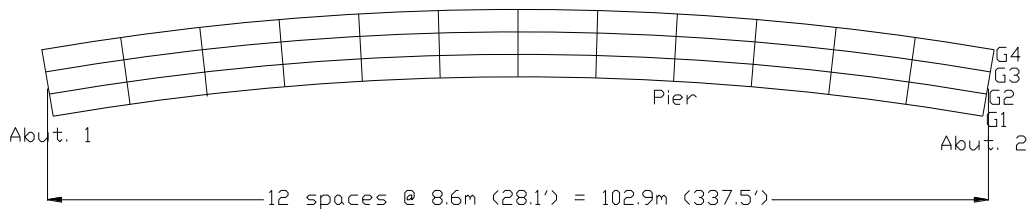


Figure 33. Simplified Framing Plan, Unbalanced Two-Span, 4-Girder, 305-m (1000-ft) Radius Bridge.

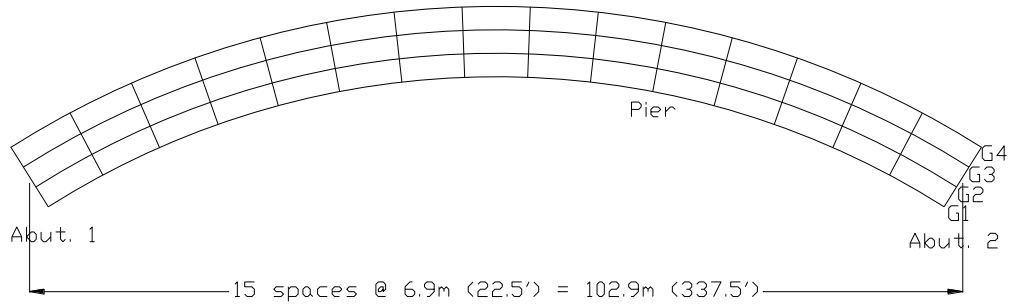


Figure 34. Simplified Framing Plan, Unbalanced Two-Span, 4-Girder, 91-m (300-ft) Radius Bridge, R/L = 13.33.

Single-span bridges were statically analyzed following the procedure outlined in previous submittals for PennDOT (Linzell et al. 2008) for the following four construction scenarios: (1) paired girder erection placing the interior girders first; (2) paired girder erection placing the exterior girders first; (3) single girder erection that placed the interior girder first; and (4) single girder erection that placed the exterior girder first. The construction techniques were selected based on common erection procedures used by contractors to erect horizontally curved, steel, I-girder bridges. Paired girder erection for the five-girder bridges involved placing the two interior girders first, then placing the middle girder, and finally placing the two exterior girders last. The reverse was done for paired girder erection by placing the exterior girders first. All analyses involved applying dead load to the components of the structure that were erected during the current phase of construction. The final stage for all construction scenarios involved placing the entire slab on the structure. Figure 35 through Figure 40 detail the analyzed construction sequences for a representative single-span, four-girder, 305-m (1000-ft) radius bridge undergoing paired and single girder erection. Figure 41 through Figure 48 detail analyzed construction sequences for a representative single-span, five-girder, 305-m (1000-ft) radius bridge undergoing paired and single girder erection.

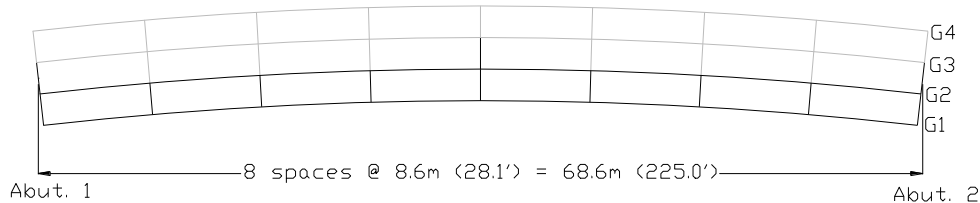


Figure 35. Stage 1 of Construction for Paired Girder (Inner Girders Placed First) Erection of Single-Span, 4-Girder, 305-m (1000-ft) Radius Bridge.

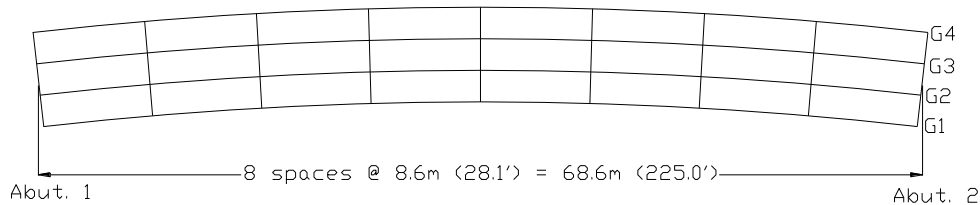


Figure 36. Stage 2 of Construction for Paired Girder (Inner Girders Placed First) Erection of Single-Span, 4-Girder, 305-m (1000-ft) Radius Bridge.

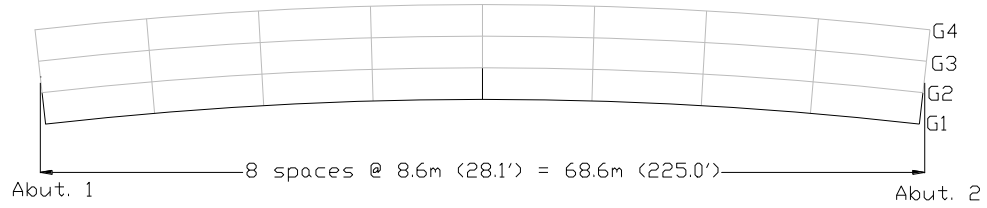


Figure 37. Stage 1 of Construction for Single Girder (Inner Girder Placed First) Erection of Single-Span, 4-Girder, 305-m (1000-ft) Radius Bridge.

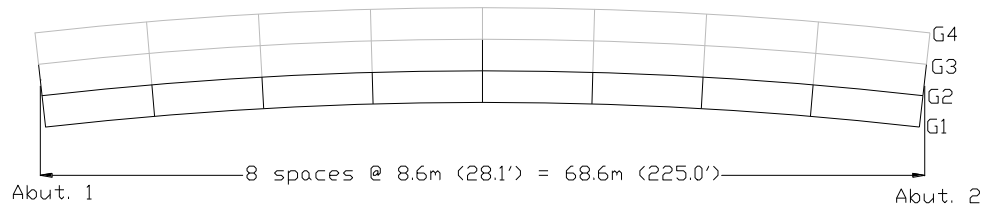


Figure 38. Stage 2 of Construction for Single Girder (Inner Girder Placed First) Erection of Single-Span, 4-Girder, 305-m (1000-ft) Radius Bridge.

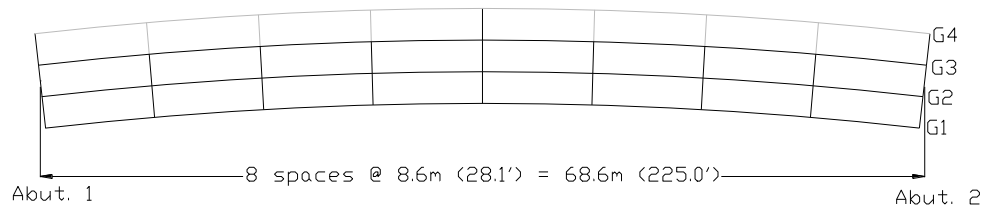


Figure 39. Stage 3 of Construction for Single Girder (Inner Girder Placed First) Erection of Single-Span, 4-Girder, 305-m (1000-ft) Radius Bridge.

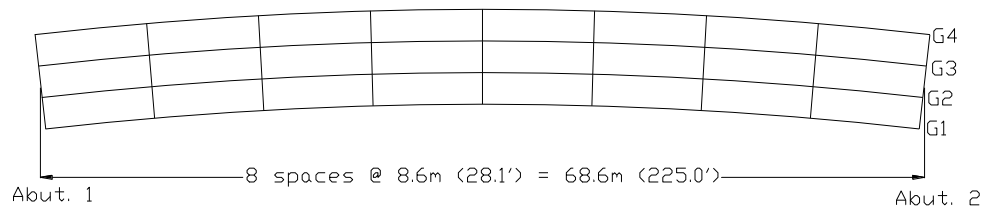


Figure 40. Stage 4 of Construction for Single Girder (Inner Girder Placed First) Erection of Single-Span, 4-Girder, 305-m (1000-ft) Radius Bridge.

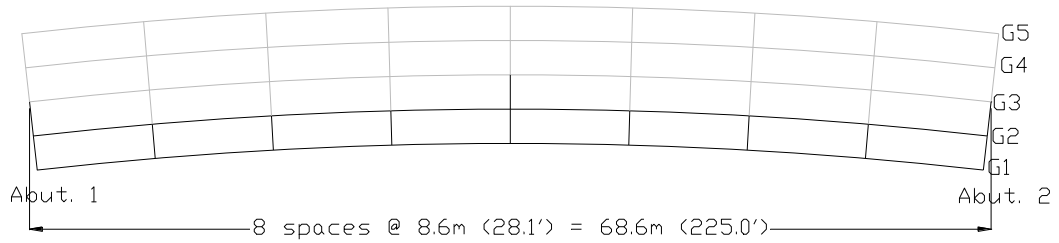


Figure 41. Stage 1 of Construction for Paired Girder (Inner Girders Placed First) Erection of Single-Span, 5-Girder, 305-m (1000-ft) Radius Bridge.

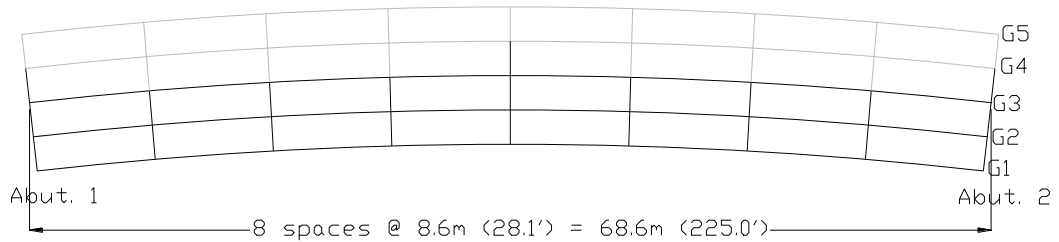


Figure 42. Stage 2 of Construction for Paired Girder (Inner Girders Placed First) Erection of Single-Span, 5-Girder, 305-m (1000-ft) Radius Bridge.

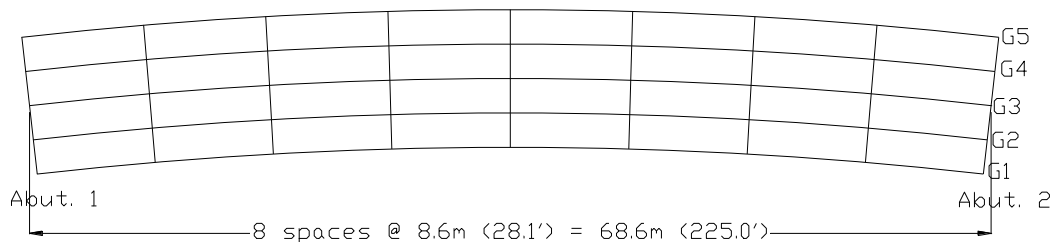


Figure 43. Stage 3 of Construction for Paired Girder (Inner Girders Placed First) Erection of Single-Span, 5-Girder, 305-m (1000-ft) Radius Bridge.

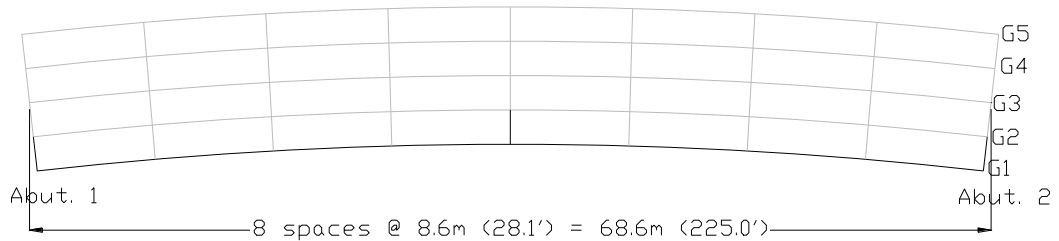


Figure 44. Stage 1 of Construction for Single Girder (Inner Girder Placed First) Erection of Single-Span, 5-Girder, 305-m (1000-ft) Radius Bridge.

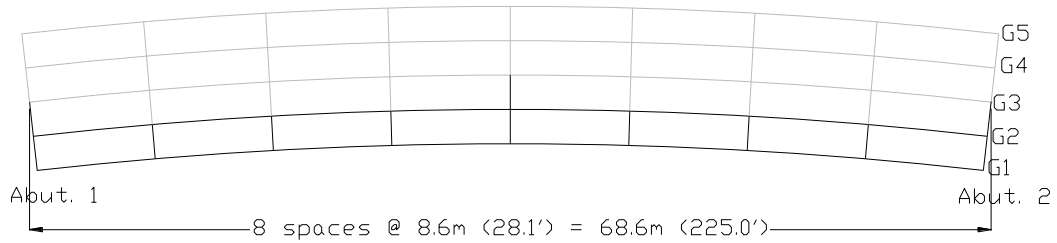


Figure 45. Stage 2 of Construction for Single Girder (Inner Girder Placed First) Erection of Single-Span, 5-Girder, 305-m (1000-ft) Radius Bridge.

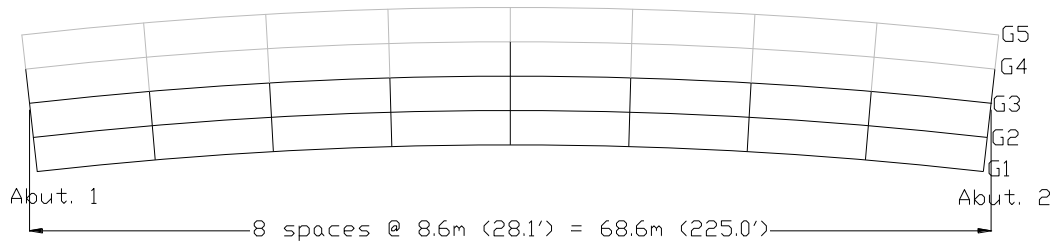


Figure 46. Stage 3 of Construction for Single Girder (Inner Girder Placed First) Erection of Single-Span, 5-Girder, 305-m (1000-ft) Radius Bridge.

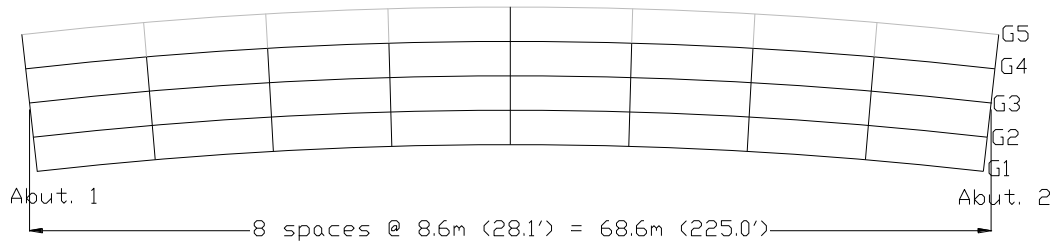


Figure 47. Stage 4 of Construction for Single Girder (Inner Girder Placed First) Erection of Single-Span, 5-Girder, 305-m (1000-ft) Radius Bridge.

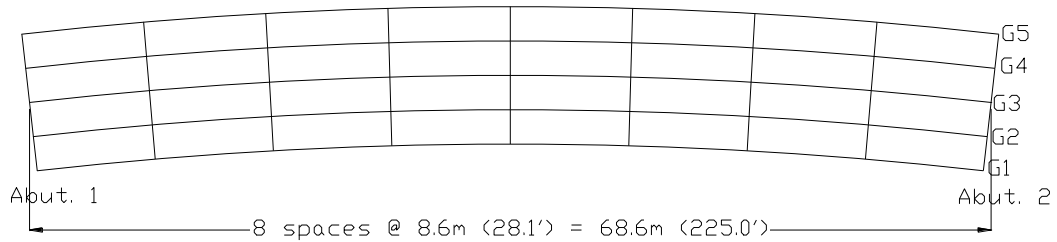


Figure 48. Stage 5 of Construction for Single Girder (Inner Girder Placed First) Erection of Single-Span, 5-Girder, 305-m (1000-ft) Radius Bridge.

The two equal span bridges were analyzed using the same four construction scenarios: (1) paired girder erection placing the interior girders first; (2) paired girder erection placing the exterior girders first; (3) single girder erection that placed the interior girder first; and (4) single girder erection that placed the

exterior girder first. The first stages of construction involved placing the girders from Abutment 1 to 18.1 m (59.3 ft) beyond the pier. The next set of stages involved placing the girder from 18.1 m (59.3 ft) beyond the pier to Abutment 2. The final stages of construction involved placing the slab on the structure in three different stages. The slab was placed in the negative moment regions first, and then the final two stages involved placing the concrete in the positive moment regions. Figure 49 through Figure 52 show the studied construction sequences for a representative two-equal-span, four-girder, 305-m (1000-ft) radius bridge. Figure 53 shows the modeled slab pour sequence for the two-equal-span, four- and five-girder, 305-m (1000-ft) radius bridges.

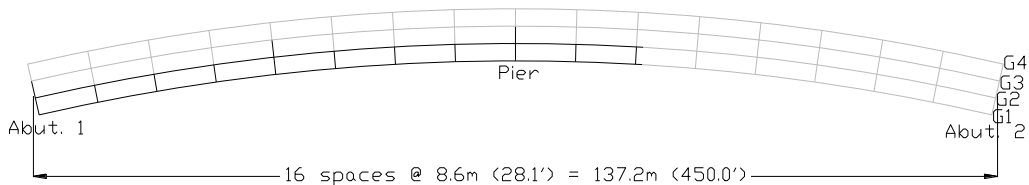


Figure 49. Stage 1 of Construction for Paired Girder (Inner Girders Placed First) Erection of Two Equal Span, 4-Girder, 305-m (1000-ft) Radius Bridge.

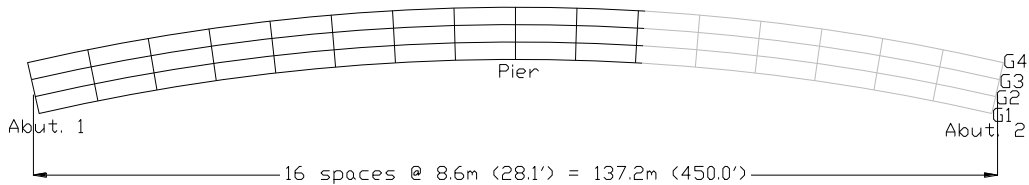


Figure 50. Stage 2 of Construction for Paired Girder (Inner Girders Placed First) Erection of Two Equal Span, 4-Girder, 305-m (1000-ft) Radius Bridge.

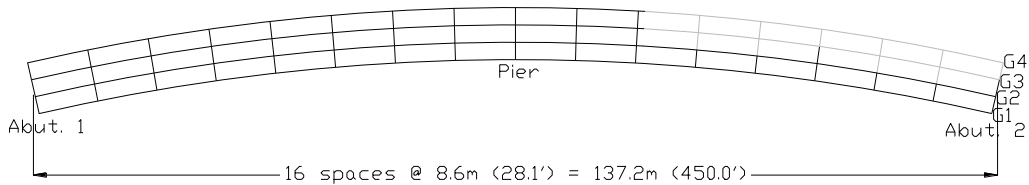


Figure 51. Stage 3 of Construction for Paired Girder (Inner Girders Placed First) Erection of Two Equal Span, 4-Girder, 305-m (1000-ft) Radius Bridge.

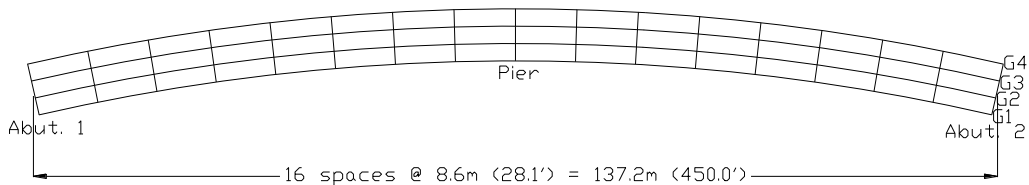
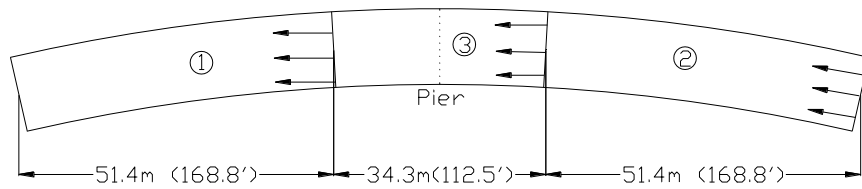


Figure 52. Stage 4 of Construction for Paired Girder (Inner Girders Placed First) Erection of Two Equal Span, 4-Girder, 305-m (1000-ft) Radius Bridge.



Note: All Distances are Measured Along the Centerline Arc

Figure 53. Slab Pour Sequence for Two Equal Span, 4- and 5-Girder, 305-m (1000-ft) Radius Bridges.

The two-unequal-span bridges were analyzed using the same four aforementioned construction scenarios. The first stages of construction involved placing the girders from Abutment 1 to 8.6 m (28.1 ft) beyond the pier. The next set of stages involved placing the girders from 8.6 m (28.1 ft) beyond the pier to Abutment 2. The final stages of construction involved placing the slab on the structure in three different stages. Figure 54 through Figure 57 show the studied construction sequences for a two-unequal-span, four-girder, 305-m (1000-ft) radius bridge. Figure 58 shows the modeled slab pour sequence for the two-unequal-span, four- and five-girder, 305-m (1000-ft) radius bridges.

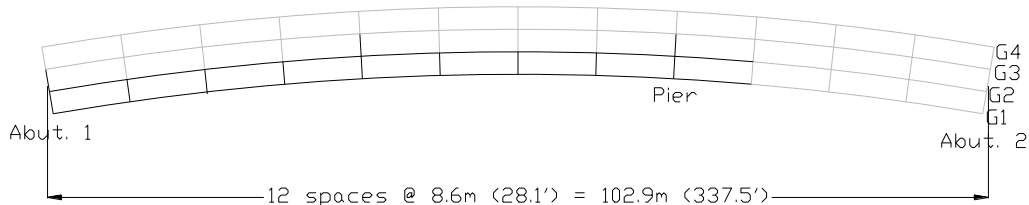


Figure 54. Stage 1 of Construction for Paired Girder (Inner Girders Placed First) Erection of Two Unequal Spans, 4-Girder, 305-m (1000-ft) Radius Bridge.

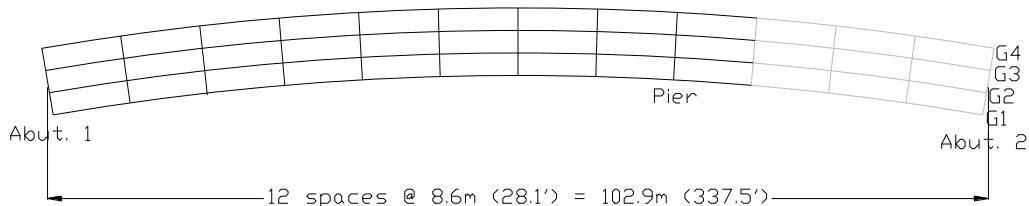


Figure 55. Stage 2 of Construction for Paired Girder (Inner Girders Placed First) Erection of Two Unequal Spans, 4-Girder, 305-m (1000-ft) Radius Bridge.

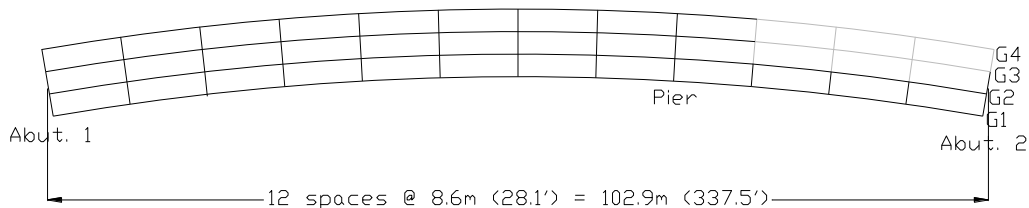


Figure 56. Stage 3 of Construction for Paired Girder (Inner Girders Placed First) Erection of Two Unequal Spans, 4-Girder, 305-m (1000-ft) Radius Bridge.

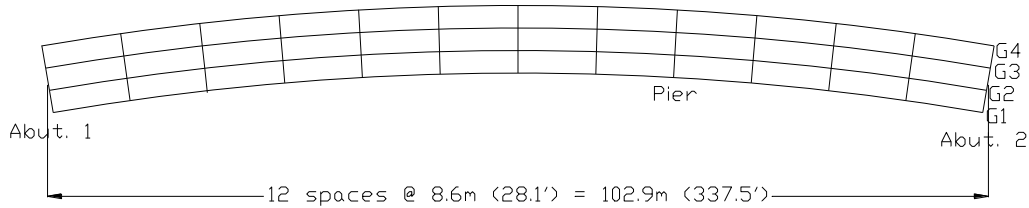
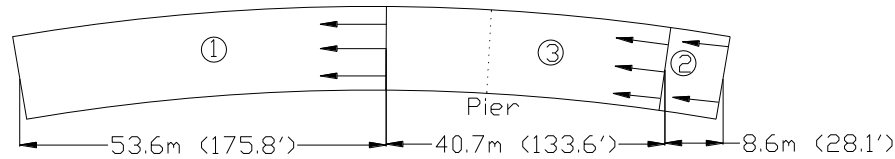


Figure 57. Stage 4 of Construction for Paired Girder (Inner Girders Placed First) Erection of Two Unequal Spans, 4-Girder, 305-m (1000-ft) Radius Bridge.



Note: All Distances are Measured Along the Centerline Arc

Figure 58. Slab Pour Sequence for Two Unequal Spans, 4- and 5-Girder, 305-m (1000-ft) Radius Bridge.

The initial study involving structures with more than two spans involved examining the effects of erecting the girders on the response of a single structure, Structure #7A, using two methods: from the inner to outer radius of curvature, and from the outer to inner radius of curvature. Its geometry and proportions are described in detail in previous submittals to PennDOT that summarized how the structure was monitored during construction and how it was used to assist with developing the modeling procedure (Linzell et al. 2003; Hiltunen et al. 2004; Linzell et al. 2006; Linzell et al. 2008). The structure is six spans, composed of five girders; it is divided into 2 three-span continuous units, and one of those units containing Spans 4 through 6 was examined. A simplified framing plan of the examined spans is shown in Figure 59.

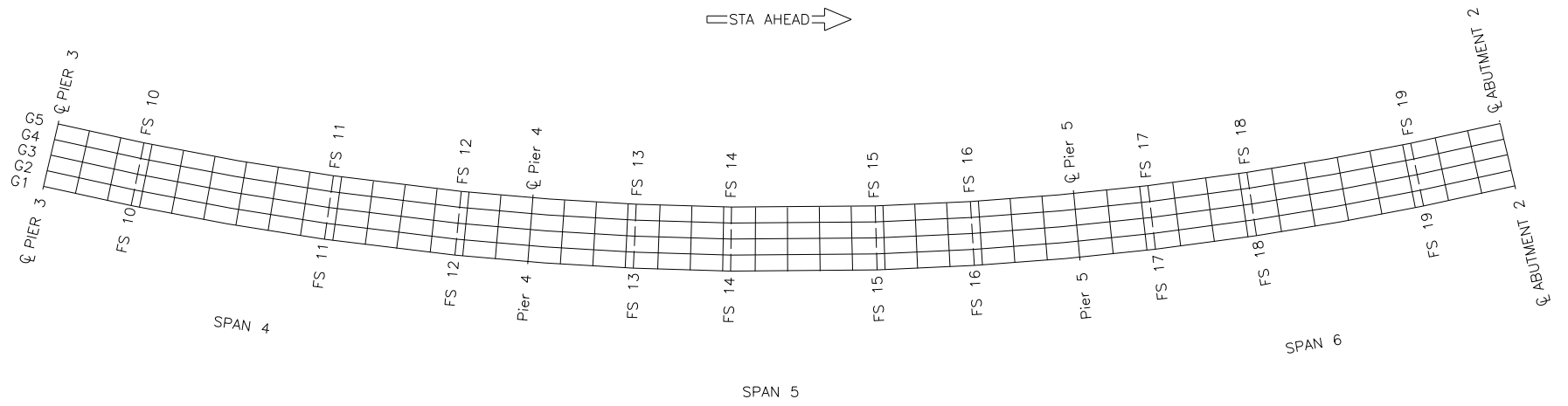


Figure 59. Structure 7A Framing Plan.

5.2.1.2 Initial Studies - Results

Results from static, sequential analyses of the initial group of single- and two-span curved bridges were examined statistically to identify preferred erection sequencing approaches from the previously discussed group of examined erection sequencing options. Preferred sequences were identified based on deflections from the analyses, since previous results for this study and other published work indicated that during construction, bridge performance is largely controlled by stiffness and not strength (Linzell et al. 2003; Hiltunen et al. 2004; Linzell et al. 2006; Linzell et al. 2008; Galambos et al. 1996). It should be noted that for the initial group of bridges that were studied, top and bottom flange stresses were never observed to reach yield.

Deflection results and discussions are presented in perceived order of importance to contractors that erect the structures. Vertical deflection is classified as the deflection direction with the highest importance, followed by radial deflections, and finally tangential deflections, which varied slightly for different erection methods. Figure 60 details the three deflection directions and boundary condition orientations. Deflections were obtained for each node along the bottom flange of each girder for each stage of construction. Depending on the span type and the number of girders, deflection results were generated for a minimum of 5 construction stages and a maximum of 13 stages. Due to the large number of generated deflection values, only the paired construction deflection results for fascia Girders 1 and 4 for the single -span, four-girder, 305-m (1000 ft.) radius bridge are presented herein.

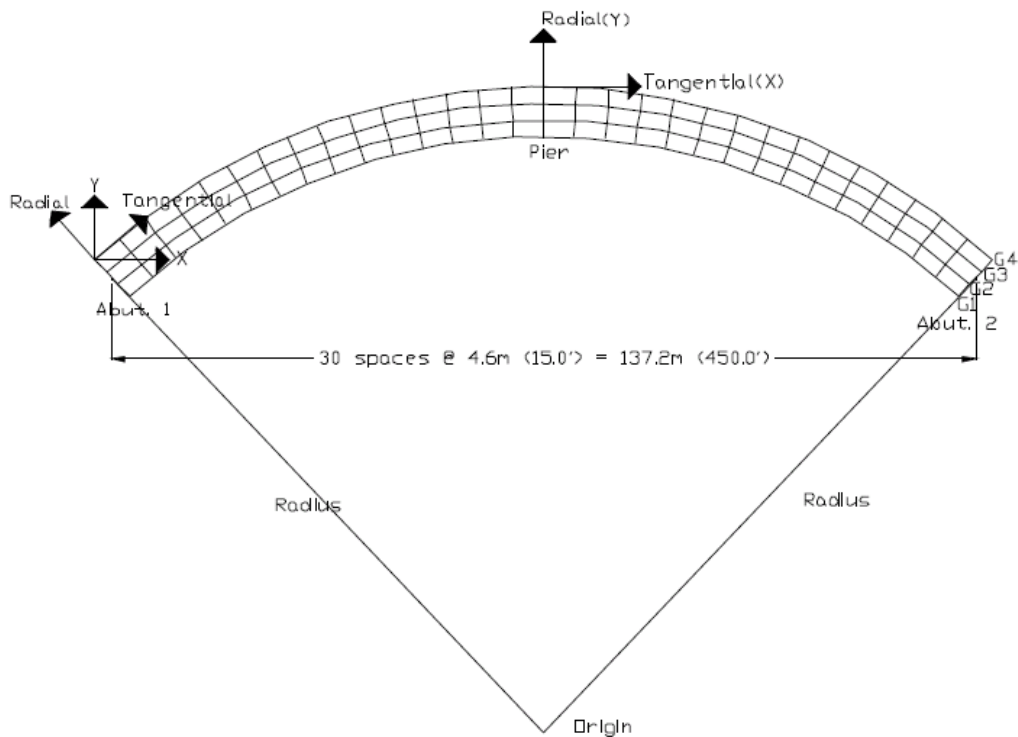


Figure 60. Plan View Detailing Deflection Directions.

Representative deflections for one of the thirty single- and two-span structures that were examined are presented. After presenting these representative results, a discussion of the statistical methods used to determine the influence of certain parameters on construction response is provided.

Figure 61 to Figure 63 show interior girder G1 vertical, radial, and tangential bottom flange deflections for the paired inner and paired outer construction options, respectively, for the single-span, four-girder, 305-m (1000 ft.) radius bridge. Stage 1 of the paired inner construction method corresponds to the erection of G1 and G2. Stage 2

corresponds to the addition of G3 and G4. For paired outer construction, Stage 1 is not shown because G1 had not been erected. Stage 2 of the paired outer construction method corresponds to the addition of G1 and G2 to the structure when G3 and G4 are in place. Stage 3 of both the paired inner and paired outer construction methods corresponds to the placement of the entire slab on the structure.

Figure 61 shows that Stage 3 of the paired inner construction method resulted in the largest vertical deflection. The figure also shows that during paired inner construction, the placement of G3 and G4 (Stage 2 paired inner) decreased the vertical deflection for G1, which demonstrates the benefits of adding additional stiffness to the superstructure.

Figure 62 indicates that all radial deflections are nearly equal to zero at Abutment 1 (see Figure 60) due to the restraint of translations normal to the plane of the superstructure and in the plane of the superstructure (“pinned” supports). Abutment 2 also restrains translations normal to the plan (“roller” supports) and, as a result, maximum radial displacements occur at Abutment 2 for all stages of paired construction. The largest radial deflections for G1 occurred for paired inner construction Stages 2 and 3, which shows that the initial placement of G1 and G2 increases the magnitude of the G1 radial deflection in subsequent stages. The radial deflection of G1 decreases significantly at the cross frame locations for Stages 2 and 3 of the paired outer construction method.

Figure 63 shows that tangential deflections for G1 are consistently smaller in magnitude than the radial and vertical deflections. The cumulative effect of the three stages of the paired inner construction method results in larger tangential deflections for G1 when compared to the tangential deflections from the two stages of the paired outer construction method.

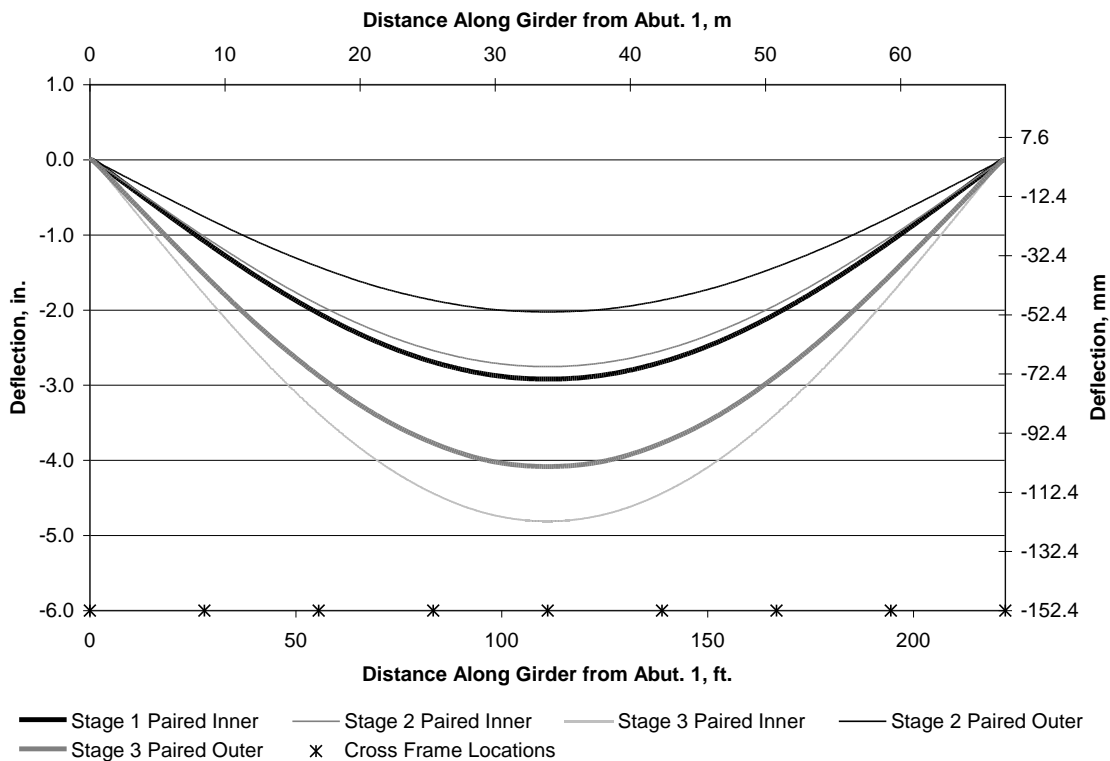


Figure 61. Girder 1 Bottom Flange Vertical Deflections for Single-Span, 4-Girder, 305m (1000 ft.) Radius Bridge.

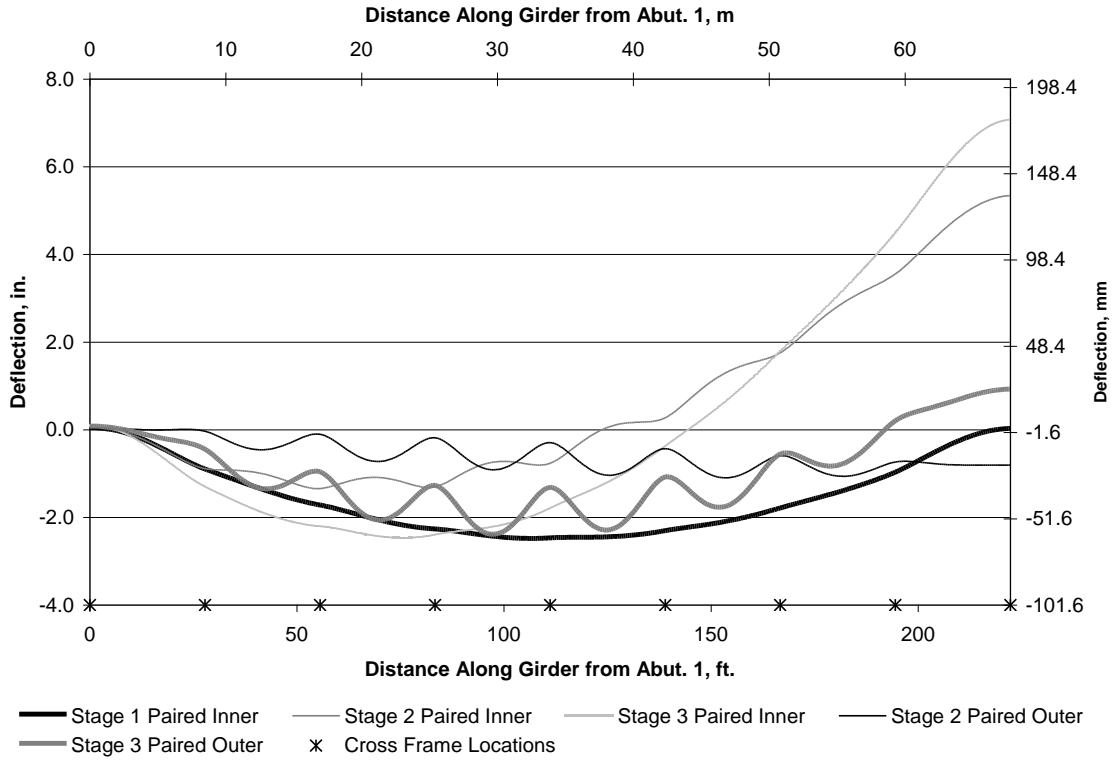


Figure 62. Girder 1 Bottom Flange Radial Deflections for Single-Span, 4-Girder, 305m (1000 ft.) Radius Bridge.

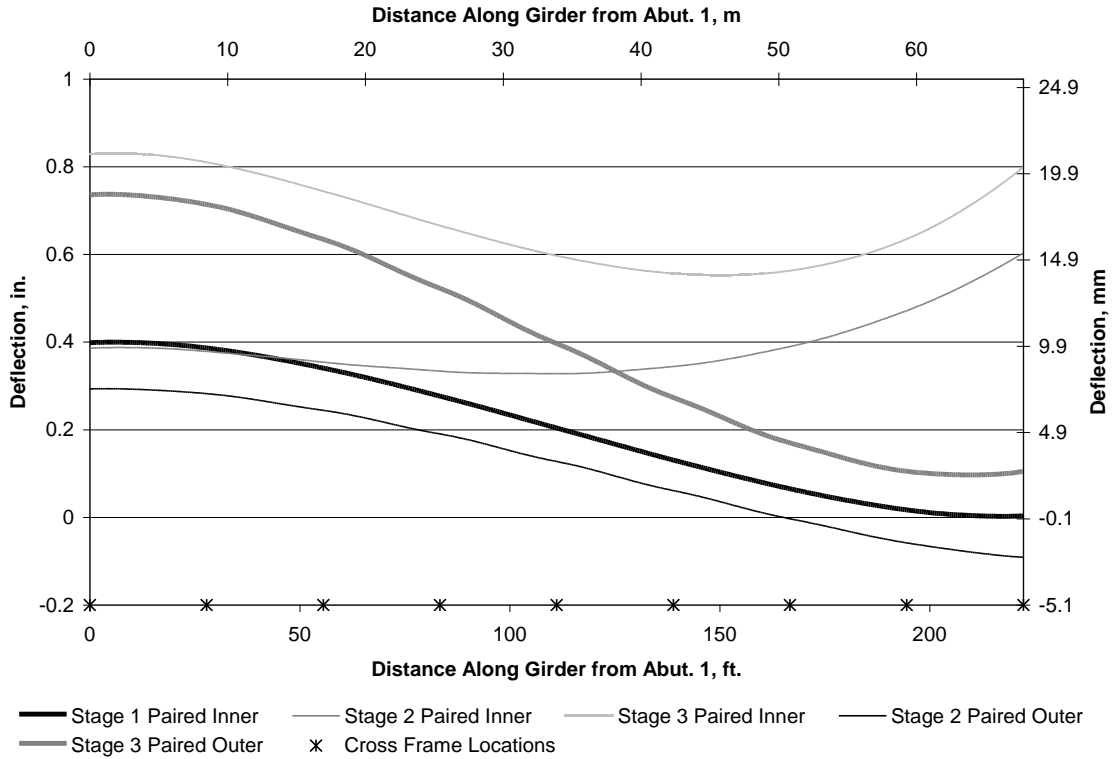


Figure 63. Girder 1 Bottom Flange Radial Deflections for Single-Span, 4-Girder, 305m (1000 ft.) Radius Bridge.

Figure 64 to Figure 66 show vertical, radial, and tangential bottom flange deflection values for paired inner and paired outer construction approaches for exterior girder G4 of the single-span, four-girder, 305-m (1000 ft.) radius bridge. In similar fashion to what was shown for certain stages for G1, Stage 1 for the paired inner construction method is not presented because G4 had not yet been erected. To reiterate, Stage 2 of the paired inner construction method corresponds to the addition of G3 and G4 to the structure when G1 and G2 are in place. Stage 1 of the paired outer construction method corresponds to the erection of G3 and G4. Stage 2 of the paired outer construction method corresponds to the addition of G1 and G2 to the structure. Stage 3 of both the paired inner and paired outer construction methods corresponds to the placement of the entire slab on the structure.

Figure 64 shows that when maximum vertical deflections for G4 for both paired construction methods are compared, Stage 3 of the paired outer construction method results in the largest vertical deflections. The cumulative effect of placing G4 during Stage 1 of the paired outer construction method results in larger vertical deflections than waiting to erect G4 during Stage 2 of the paired inner construction method.

Boundary conditions existed at the abutments for G4 that were similar to those discussed for G1. Therefore, Figure 65 shows that the maximum radial deflections for G4 occurred at Abutment 2 for all stages of paired construction. The figure also shows that Stage 3 of the paired outer construction method results in the largest radial deflection for G4.

Figure 66 shows smaller tangential deflections than vertical or radial deflections for G4, which is similar to the results for G1. The figure also shows the maximum tangential deflections for Stage 3 of the paired outer construction method.

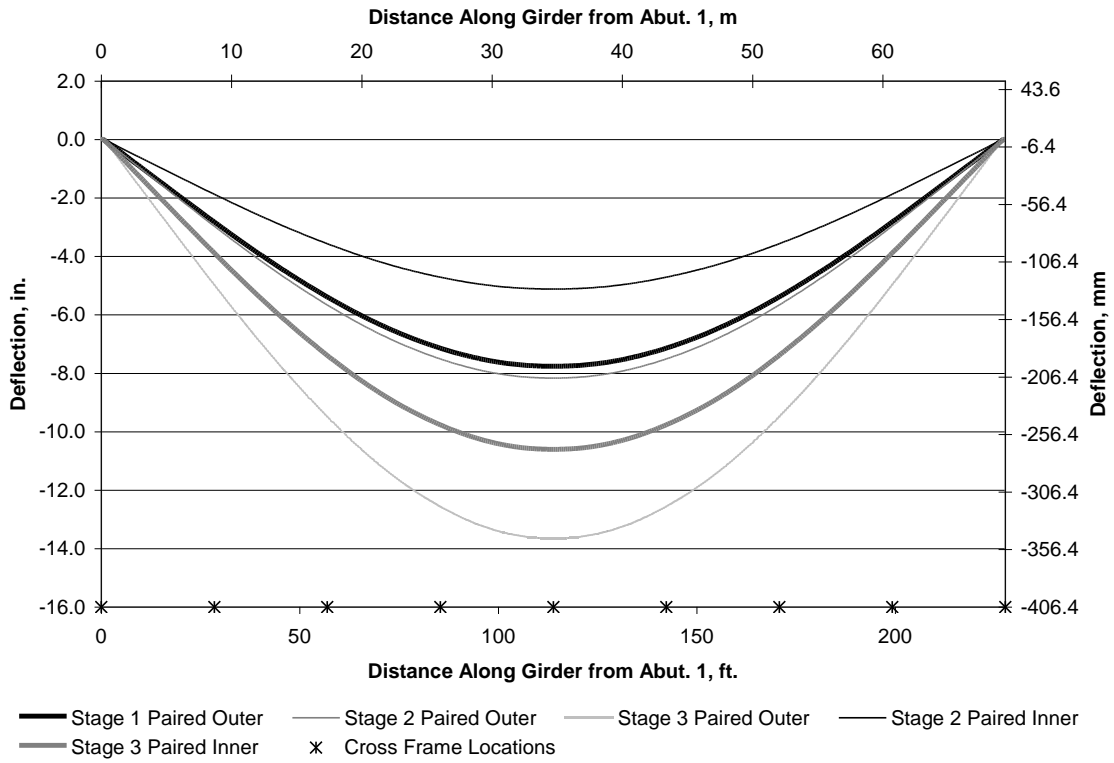


Figure 64. Girder 4 Bottom Flange Vertical Deflections for Single-Span, 4-Girder, 305m (1000 ft.) Radius Bridge.

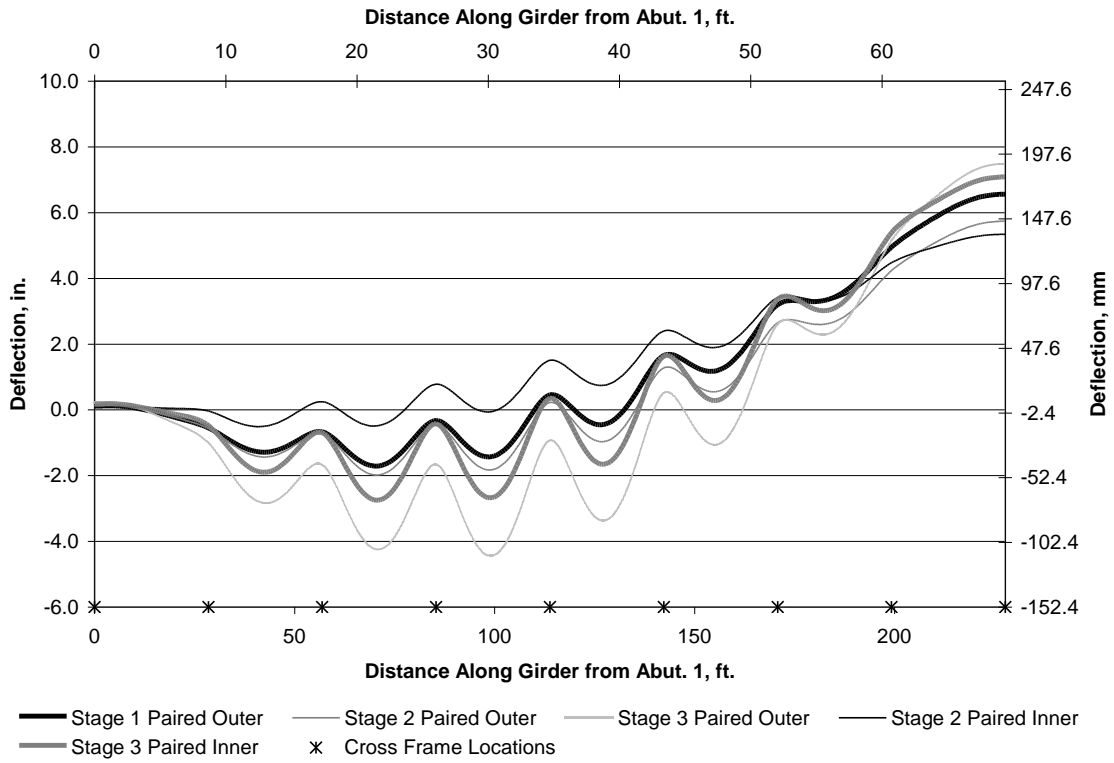


Figure 65. Girder 4 Bottom Flange Radial Deflections for Single-Span, 4-Girder, 305m (1000 ft.) Radius Bridge.

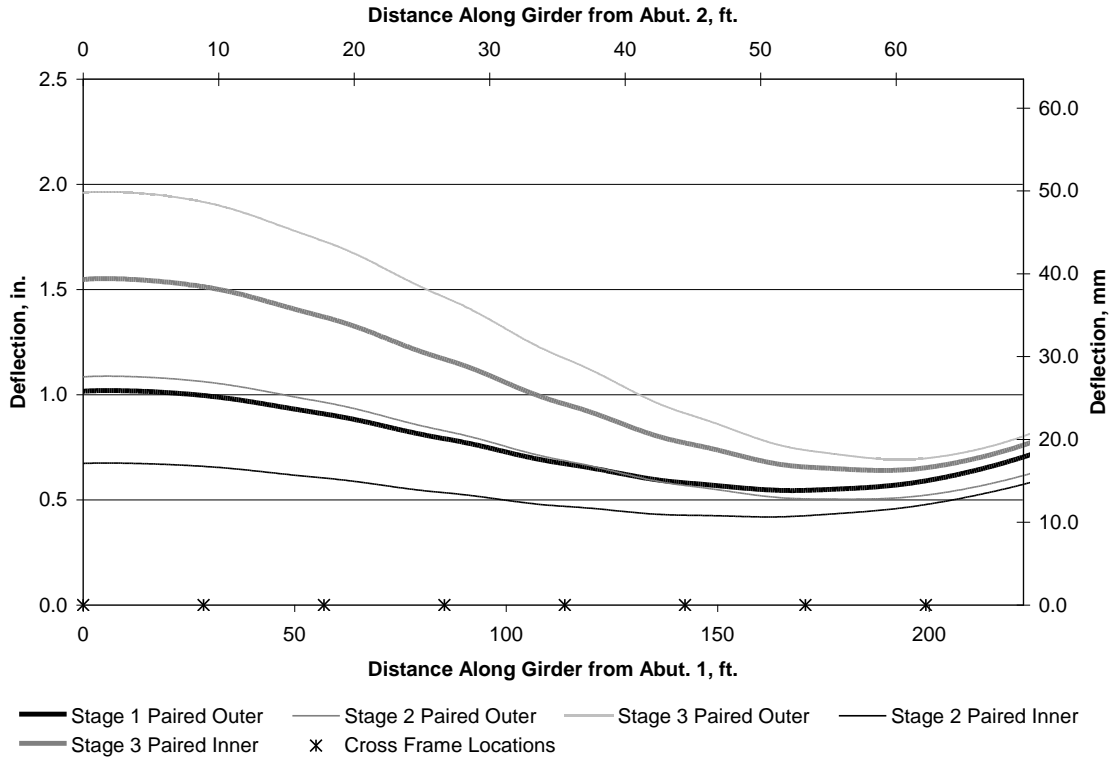


Figure 66. Girder 4 Bottom Flange Tangential Deflections for Single-Span, 4-Girder, 305m (1000 ft.) Radius Bridge.

An analysis of variance (ANOVA) procedure was selected to examine the influence of not only the construction method, but also the number of girders, radius, unbraced length, and span type on maximum radial, tangential, and vertical deflection values for the 120 one-and two-span bridge finite element models that were constructed (30 parametric bridges analyzed using 4 different construction methods). A general linear ANOVA model was selected in Minitab (Minitab 2007) because it can test the influence of a number of different parameters on one response variable (deflection). The three dependant variables were the vertical, radial, and tangential deflections. The aforementioned five independent variables and their different levels as included in the ANOVA are shown in Table 8.

Table 8. Independent ANOVA Variables.

Variable	Levels
Construction Method	Single-Inner, Single-Outer, Paired-Inner, Paired Outer
Number of Girders	4, 5
Radius	91m (300'), 198m (650'), 305m (1000')
Unbraced Length	4.6m (15.0'), 5.3m (17.3'), 6.9m (22.5'), 9.6m (28.1')
Span Type	Single, Two Balanced, Two Unbalanced

To facilitate the ANOVA analysis, the radius and unbraced length independent variables were combined into a single independent variable set, as shown in Table 9.

Table 9. R/L Ratios Used in ANOVA Analysis.

Radius, m (ft.)	Unbraced Length, m (ft.)	R/L Ratio
91 (300)	4.6 (15.0)	20.00
91 (300)	5.3 (17.3)	17.34
91 (300)	6.9 (22.5)	13.33
198 (650)	9.6 (28.1)	23.13
305 (1000)	9.6 (28.1)	35.59

Similar full statistical models were used for the ANOVA analyses to examine the influence of previously discussed independent variable combinations on deflections. A full ANOVA statistical model includes the largest list of variables that could be influencing the deflection response variable, and this full ANOVA statistical model was first tested to determine which variables and which variable combinations had the largest influence on the resulting deflections. As an example, Equation 1 shows the results from the full ANOVA examination of independent variable influence on vertical deflections generated during construction. The equation indicates that there are 4 main-effects terms, 6 two-way interaction terms, 3 three-way interaction terms, and 1 four-way interaction term for the full, vertical deflection ANOVA model. Main-effect terms are multiplied together to create interaction terms, which are included in the statistical model to determine if the combination of any of the main-effect terms is influencing the deflection response. All four-way interaction terms are typically dropped from ANOVA analyses and were done so here for all deflections.

$$\text{Deflection} = (\text{Span} + \text{No. of Girders} + \text{Construction Method} + \text{R/L Ratio}) + (\text{Span} * \text{No. of Girders} + \text{Span} * \text{Construction Method} + \text{Span} * \text{R/L Ratio} + \text{No. of Girders} * \text{Construction Method} + \text{No. of Girders} * \text{R/L Ratio} + \text{Construction Method} * \text{R/L Ratio}) + (\text{Span} * \text{No. of Girders} * \text{Construction Method} + \text{Span} * \text{No. of Girders} * \text{R/L Ratio} + \text{No. of Girders} * \text{Construction Method} * \text{R/L Ratio}) + (\text{Span} * \text{No. of Girders} * \text{Construction Method} * \text{R/L Ratio})$$

Equation 1

In an attempt to further simplify the statistical models that were examined, a full ANOVA was performed using Equation 1, with the last term removed, to ascertain which of the independent variables and which of their combinations had the most significant effects on vertical deflections. Results from the ANOVA can be summarized as shown in

Table 10. ANOVA Results for Initial Vertical Deflection Statistical Model.

Source	DF	Seq SS, m2 (ft. ²)	Adj SS, m2 (ft. ²)	Adj MS, m2 (ft. ²)	F	P
Span	2	0.12023 (1.29418)	0.12023 (1.29418)	0.06012 (0.64709)	22.52	0.000
No. of Girders	1	0.02526 (0.27187)	0.02526 (0.27187)	0.02526 (0.27187)	9.46	0.003
Construction Method	3	0.43598 (4.69282)	0.43598 (4.69282)	0.14533 (1.56427)	54.44	0.000
R/L Ratio	4	0.39616 (4.26423)	0.39616 (4.26423)	0.09904 (1.06606)	37.10	0.000
Span*No. of Girders	2	0.00359 (0.03863)	0.00359 (0.03863)	0.00180 (0.01932)	0.67	0.515
Span*Construction Method	6	0.03399 (0.36583)	0.03399 (0.36583)	0.00566 (0.06097)	2.12	0.068
Span*R/L Ratio	8	0.08496 (0.91447)	0.08496 (0.91447)	0.01062 (0.11431)	3.98	0.001
No. of Girders*Construction Method	3	0.01648 (0.17740)	0.01648 (0.17740)	0.00549 (0.05913)	2.06	0.118
No. of Girders*R/L Ratio	4	0.02774 (0.29861)	0.02774 (0.29861)	0.00694 (0.07465)	2.60	0.048
Construction Method*R/L Ratio	12	0.02680 (0.28849)	0.02680 (0.28849)	0.00223 (0.02404)	0.84	0.613
Span*No. of Girders*Construction Method	6	0.02926 (0.31492)	0.02926 (0.31492)	0.00488 (0.05249)	1.83	0.114
Span*No. of Girders*R/L Ratio	8	0.02368 (0.25380)	0.02368 (0.25380)	0.00295 (0.03172)	1.10	0.377
No. of Girders*Construction Method*R/L Ratio	12	0.01404 (0.15110)	0.01404 (0.15110)	0.00117 (0.01250)	0.44	0.939
Error	48	0.12814 (1.37928)	0.12814 (1.37928)	0.00267 (0.02874)		
Total	119	1.36620 (14.70563)				
S = 0.05167 (0.16951) R2 = 90.62% R2 (adj) = 76.75%						

The DF column in the table represents the degrees of freedom for each factor, which indicates the amount of information the ANOVA statistical model factors provides for determining values for vertical deflection. The sequential sum of squares (Seq SS) measures the amount of variation in the deflection response explained by adding terms sequentially to the statistical model in the order listed in the table. The adjusted sum of squares (Adj SS) measures the amount of additional variation in deflection explained by a specific factor, given that all other terms are already in the statistical model. It can be noted that the sequential sum of squares values equaled the adjusted sum of squares values for the vertical deflection, which shows that the order of the terms in the statistical model did not affect the results. The adjusted mean of squares (Adj MS) is calculated by dividing the adjusted sum of squares by the degrees of freedom. The S value, which comes from estimating the variance in the data and is calculated by taking the square root of the adjusted mean squares of the error, represented the standard distance the data values fell from any fitted values, with S being measured in deflection units, m (ft.). The better the model predicted vertical deflection, the lower the S value. The R² term, termed the coefficient of determination, represents the amount of

variation in the observed vertical deflections as a function of the independent variables (span, number of girders, construction method, and R/L ratio). The adjusted R^2 term was a modified R^2 value adjusted for the number of terms in the statistical model. The final columns in the table listed the F- and P-factors, respectively. Both represent standard statistical tests, with the F-values found by dividing the adjusted mean squares by the adjusted mean squares of the error term, and then being used as inputs to determine the P-values. The P-values determined whether or not an independent variable or variable combination was a significant influence on determining vertical deflections. P-values less than or equal to 0.05 correspond to variables or variable combinations that significantly affected vertical deflections.

Table 10. ANOVA Results for Initial Vertical Deflection Statistical Model.

Source	DF	Seq SS, m ² (ft. ²)	Adj SS, m ² (ft. ²)	Adj MS, m ² (ft. ²)	F	P
Span	2	0.12023 (1.29418)	0.12023 (1.29418)	0.06012 (0.64709)	22.52	0.000
No. of Girders	1	0.02526 (0.27187)	0.02526 (0.27187)	0.02526 (0.27187)	9.46	0.003
Construction Method	3	0.43598 (4.69282)	0.43598 (4.69282)	0.14533 (1.56427)	54.44	0.000
R/L Ratio	4	0.39616 (4.26423)	0.39616 (4.26423)	0.09904 (1.06606)	37.10	0.000
Span*No. of Girders	2	0.00359 (0.03863)	0.00359 (0.03863)	0.00180 (0.01932)	0.67	0.515
Span*Construction Method	6	0.03399 (0.36583)	0.03399 (0.36583)	0.00566 (0.06097)	2.12	0.068
Span*R/L Ratio	8	0.08496 (0.91447)	0.08496 (0.91447)	0.01062 (0.11431)	3.98	0.001
No. of Girders*Construction Method	3	0.01648 (0.17740)	0.01648 (0.17740)	0.00549 (0.05913)	2.06	0.118
No. of Girders*R/L Ratio	4	0.02774 (0.29861)	0.02774 (0.29861)	0.00694 (0.07465)	2.60	0.048
Construction Method*R/L Ratio	12	0.02680 (0.28849)	0.02680 (0.28849)	0.00223 (0.02404)	0.84	0.613
Span*No. of Girders*Construction Method	6	0.02926 (0.31492)	0.02926 (0.31492)	0.00488 (0.05249)	1.83	0.114
Span*No. of Girders*R/L Ratio	8	0.02368 (0.25380)	0.02368 (0.25380)	0.00295 (0.03172)	1.10	0.377
No. of Girders*Construction Method*R/L Ratio	12	0.01404 (0.15110)	0.01404 (0.15110)	0.00117 (0.01250)	0.44	0.939
Error	48	0.12814 (1.37928)	0.12814 (1.37928)	0.00267 (0.02874)		
Total	119	1.36620 (14.70563)				
S = 0.05167 (0.16951) R ² = 90.62% R ² (adj) = 76.75%						

Examination of the results from the table indicate that the following independent variables or variable combinations had significant effect on vertical deflections: (1) Span; (2) Number of Girders; (3) Construction Method; (4) R/L Ratio; (5) Span * R/L Ratio; and (6) Number of Girders * R/L Ratio. As a result of these findings, a revised vertical deflection ANOVA statistical model was developed that included these significant factors only. This model appears as follows:

$$\text{Vertical Deflection} = \text{Span} + \text{No. of Girders} + \text{Construction Method} + \text{R/L Ratio} + \text{No. of Girders} * \text{R/L Ratio} + \text{Span} * \text{R/L Ratio}$$

Equation 2

A second ANOVA was performed to ascertain if additional revisions to the vertical deflection statistical model were necessary. Results from analyses of this model are shown in Table 11. They indicate that the P-value for the combination of number of girders and R/L ratio was 0.052, and this term was removed from the final vertical deflection statistical model, which is shown in Equation 3.

Table 11. ANOVA Results for Modified Vertical Deflection Statistical Model.

Source	DF	Seq SS, m ² (ft. ²)	Adj SS, m ² (ft. ²)	Adj MS, m ² (ft. ²)	F	P
Span	2	0.12023 (1.29418)	0.12023 (1.29418)	0.06012 (0.64709)	21.14	0.000
No. of Girders	1	0.02526 (0.27187)	0.02526 (0.27187)	0.02526 (0.27187)	8.88	0.004
Construction Method	3	0.43598 (4.69282)	0.43598 (4.69282)	0.14533 (1.56427)	51.10	0.000
R/L Ratio	4	0.39616 (4.26423)	0.39616 (4.26423)	0.09904 (1.06606)	34.82	0.000
No. of Girders*R/L Ratio	4	0.02774 (0.29861)	0.02774 (0.29861)	0.00694 (0.07465)	2.44	0.052
Span*R/L Ratio	8	0.08496 (0.91447)	0.08496 (0.91447)	0.01062 (0.11431)	3.73	0.001
Error	97	0.27587 (2.96945)	0.27587 (2.96945)	0.00284 (0.03061)		
Total	119	1.36620 (14.70563)				
S = 0.05333 (0.17497) R ² = 79.18% R ² (adj) = 75.23%						

$$\text{Vertical Deflection} = \text{Span} + \text{No. of Girders} + \text{Construction Method} + \text{R/L Ratio} + \text{Span} * \text{R/L Ratio}$$

Equation 3

The final ANOVA statistical model included four significant single variables and one significant two-way interaction term that contained the and R/L ratio. To ascertain if this final statistical model was acceptable for all future studies, a final ANOVA was performed, with results shown in

Table 12. All P-values are less than 0.05, which shows that the factors in the final statistical model are significant. The adjusted R^2 value is 73.82%, which shows that 73.82% of the variation in the vertical deflections is explained by the final statistical model.

Table 12. ANOVA Results for Final Vertical Deflection Statistical Model.

Source	DF	Seq SS, m ² (ft. ²)	Adj SS, m ² (ft. ²)	Adj MS, m ² (ft. ²)	F	P
Span	2	0.12023 (1.29418)	0.12023 (1.29418)	0.06012 (0.64709)	20.00	0.000
No. of Girders	1	0.02526 (0.27187)	0.02526 (0.27187)	0.02526 (0.27187)	8.40	0.005
Construction Method	3	0.43598 (4.69282)	0.43598 (4.69282)	0.14533 (1.56427)	48.34	0.000
R/L Ratio	4	0.39616 (4.26423)	0.39616 (4.26423)	0.09904 (1.06606)	32.95	0.000
Span * R/L Ratio	8	0.08957 (0.91447)	0.08957 (0.91447)	0.01062 (0.11431)	3.53	0.001
Error	101	0.30361 (3.26805)	0.30361 (3.26805)	0.00301 (0.03236)		
Total	119	1.36620 (14.70563)				
S = 0.05483 (0.17988) R ² = 77.78% R ² (adj) = 73.82%						

Using the final ANOVA from Equation 3, the influence of the four studied construction sequencing methods on fitted mean vertical deflections for the 120 initially studied one- and two-span bridges was examined. Results are shown in Figure 67, which indicates that construction methods did influence vertical deflection. However, an additional statistical test was conducted to determine which differences in the fitted mean vertical deflections shown in the figure were statistically significant. The Tukey method (Minitab 2007) was selected to perform this investigation. The Tukey method produced adjusted P-values for each pair of fitted means, which represents the probability that important differences exist between a pair of fitted means when, at first glance, that difference does not appear statistically significant. For example, Figure 67 indicates that the single inner and paired inner construction methods result in similar fitted mean vertical deflection values. The Tukey adjusted P-value for the difference between the single inner and paired inner construction methods is 0.9937, which indicates that this difference was not statistically significant, and thus supports what the figure shows. In other words, no significant difference in the fitted mean vertical deflection exists when Girder 1 is first placed individually, assuming it is adequately braced, versus placing both Girders 1 and 2 first. Erecting the interior girder (girder with the smallest radius) first and then sequentially erecting the remaining girders in the structure minimizes the vertical deflection of the structure irrespective of whether a single girder is placed first or a pair of girder is placed first. Placing the interior girders first limits the final vertical deflections by reducing the structure's tendency to rotate towards the exterior girder. The figure clearly shows that the single outer construction method results in larger vertical deflections when compared to the other three methods via examination of the fitted means. The Tukey adjusted P-values for the differences between the paired inner, paired outer, and single inner construction methods and the single outer construction method are 0.0000, 0.0000, 0.0000, respectively, which further substantiate what the figure shows with respect to first erecting the outer girder. Again, girders in the bridge tend to rotate towards the exterior girder, and placing the exterior girder first magnifies this effect. When the fitted mean magnitudes were compared, the smallest mean was for the single inner construction method, which would tend to indicate that this would be a preferred erection approach for the group of bridges that was initially studied.

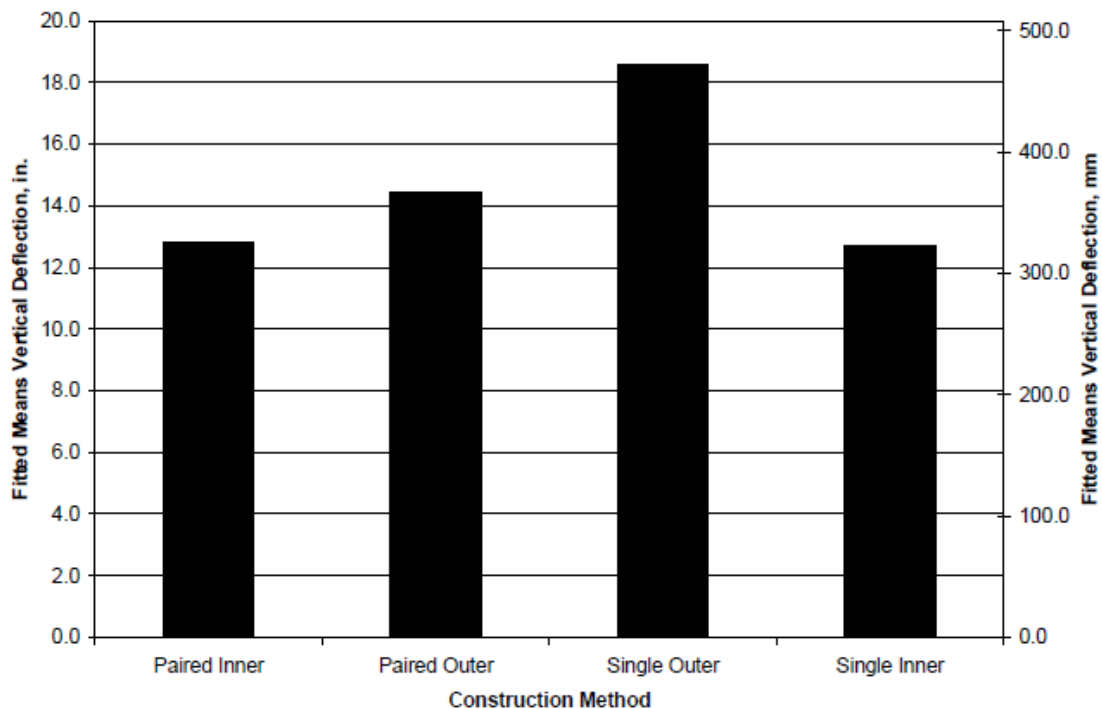


Figure 67. Construction Method Influence on Fitted Mean Vertical Deflections.

A similar ANOVA procedure was used to examine the influence of construction sequencing on radial deflections obtained from the 120 one- and two-span bridges that were initially studied. After developing the full ANOVA

statistical model and reducing it, the final statistical model selected to examine sequencing effects on radial deflections appears as shown below:

$$\text{Radial Deflection} = \text{Span} + \text{No. of Girders} + \text{Construction Method} + \text{R/L Ratio} + \text{Span} * \text{No. of Girders} + \text{Span} * \text{R/L Ratio} + \text{Construction Method} * \text{R/L Ratio}$$

Equation 4

Table 13 shows the ANOVA results for the final radial deflection statistical model. The table indicates that all factors included in the model were significant (P-values less than 0.05). The adjusted R² value for the final radial deflection statistical model is 69.36%.

Table 13. ANOVA Results for Final Radial Deflection Model.

Source	DF	Seq SS, m ² (ft. ²)	Adj SS, m ² (ft. ²)	Adj MS, m ² (ft. ²)	F	P
Span	2	0.00766 (0.08240)	0.00766 (0.08240)	0.00383 (0.04120)	1.49	0.231
No. of Girders	1	0.00176 (0.01894)	0.00176 (0.01894)	0.00176 (0.01894)	0.68	0.410
Construction Method	3	0.20241 (2.17876)	0.20241 (2.17876)	0.06747 (0.72625)	26.24	0.000
R/L Ratio	4	0.30886 (3.32450)	0.30886 (3.32450)	0.07721 (0.83113)	30.03	0.000
Span * No. of Girders	2	0.02900 (0.31216)	0.02900 (0.31216)	0.01450 (0.15608)	5.64	0.005
Span * R/L Ratio	8	0.05882 (0.63311)	0.05882 (0.63311)	0.00735 (0.07914)	2.86	0.007
Construction Method * R/L Ratio	12	0.16662 (1.79353)	0.16662 (1.79353)	0.01389 (0.14946)	5.40	0.000
Error	87	0.22371 (2.40804)	0.22371 (2.40804)	0.00257 (0.02768)		
Total	119	0.99884 (10.75144)				
S = 0.05071 (0.16637) R ² = 77.60% R ² (adj) = 69.36%						

Figure 68 shows the effect of construction method on the radial deflection, again via examination and comparison of fitted means. The figure clearly shows that the single outer construction method results in larger radial deflection fitted mean values when compared to the other three methods. The Tukey adjusted P-values for the differences between the paired inner, paired outer, and single inner construction methods and the single outer construction method are 0.0000, 0.0000, 0.0000, respectively. Erecting the exterior girder (girder with the largest radius) first and then sequentially erecting the remaining girders in the structure individually leads to excessive radial deflections when compared to the other three construction methods.

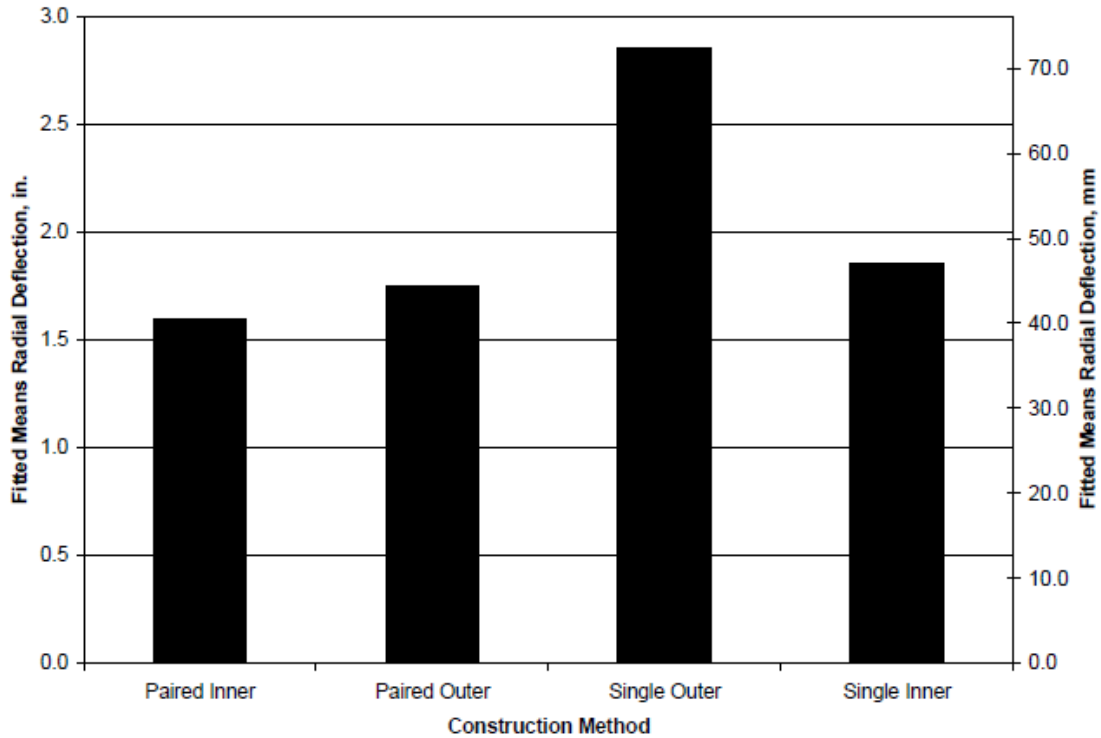


Figure 68. Construction Method Influence on Fitted Mean Radial Deflections.

ince the final ANOVA statistical model for radial deflections included an interaction term that involved the construction method, the effects of this interaction term on fitted mean radial deflections also needed to be examined. Figure 69 details the effects of a combination of construction method and R/L ratio on radial deflection fitted mean values. For R/L ratios of 23.13 and 35.59, the single outer construction method results in fitted mean radial deflections that are significantly different when compared to the other three construction methods at those R/L ratios. The results indicate that placing the exterior girder first results in larger radial deflections that cannot be counteracted by the larger cross-frame spacings for the R/L values of 23.13 and 35.59.

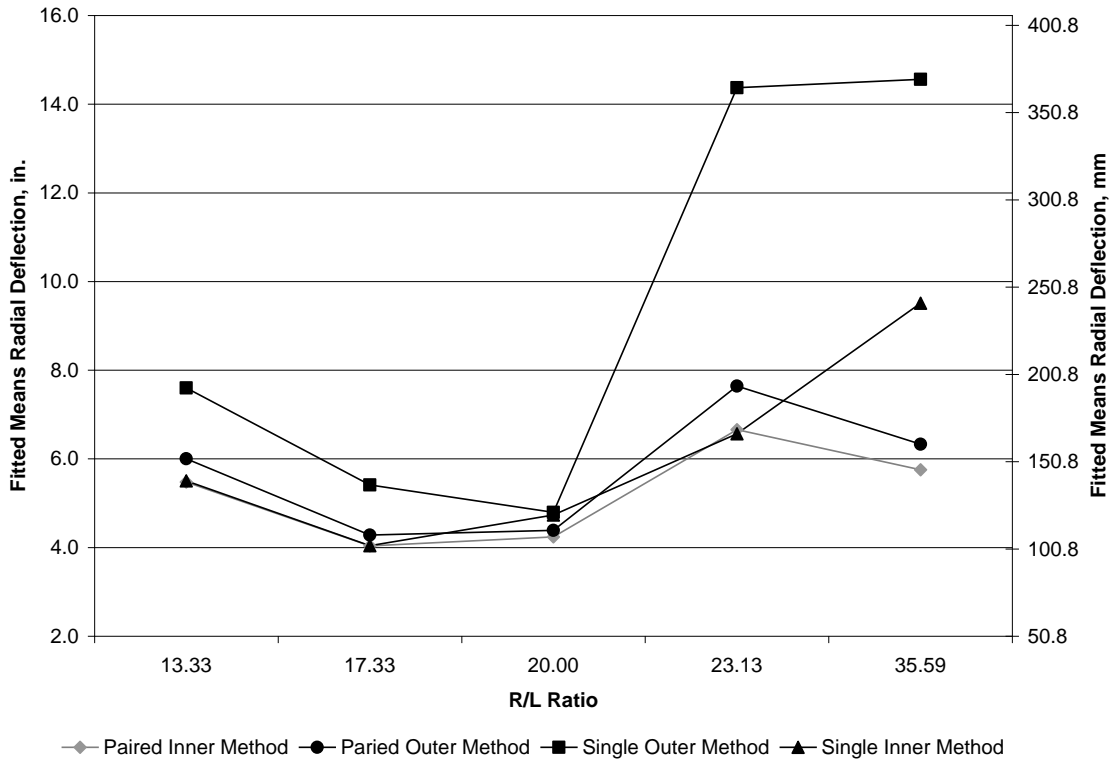


Figure 69. Fitted Means Radial Deflection Comparison for the Interaction of Construction Method and R/L Ratio.

The final statistical model for tangential deflections appears as shown in Equation 5. ANOVA results for the final model are shown in

Table 14. The table indicates that all factors included in the model were significant (P-values less than 0.05). The adjusted R² value for the final statistical model is 84.51%.

$$\text{Tangential Deflection} = \text{Span} + \text{Construction Method} + \text{R/L Ratio} + \text{Span} * \text{Construction Method} + \text{Span} * \text{R/L Ratio}$$

Equation 5

Table 14. ANOVA Results for Final Tangential Deflection Model.

Source	DF	Seq SS, m ² (ft. ²)	Adj SS, m ² (ft. ²)	Adj MS, m ² (ft. ²)	F	P
Span	2	0.01913 (0.20596)	0.01913 (0.20596)	0.00957 (0.10298)	216.37	0.000
Construction Method	3	0.00184 (0.01976)	0.00184 (0.01976)	0.00061 (0.00659)	13.84	0.000
R/L Ratio	4	0.00641 (0.06904)	0.00641 (0.06904)	0.00160 (0.01726)	36.26	0.000
Span*Construction Method	6	0.00151 (0.01625)	0.00151 (0.01625)	0.00025 (0.00271)	5.69	0.000
Span*R/L	8	0.00083 (0.00890)	0.00083 (0.00890)	0.00010 (0.00111)	2.34	0.024
Error	96	0.00424 (0.04569)	0.00424 (0.04569)	0.00004 (0.00048)		
Total	119	0.03397 (0.36560)				
S = 0.00665 (0.02182) R ² = 87.50% R ² (adj) = 84.51%						

Figure 70 shows the effect of construction method on tangential deflection via an examination of fitted means. The figure shows that the single outer construction method results in larger tangential deflection fitted means when compared to the other three methods. The Tukey adjusted P-values for the differences between the paired inner, paired outer, and single inner construction methods fitted means and the single outer construction method are 0.0000, 0.0014, 0.0000, respectively.

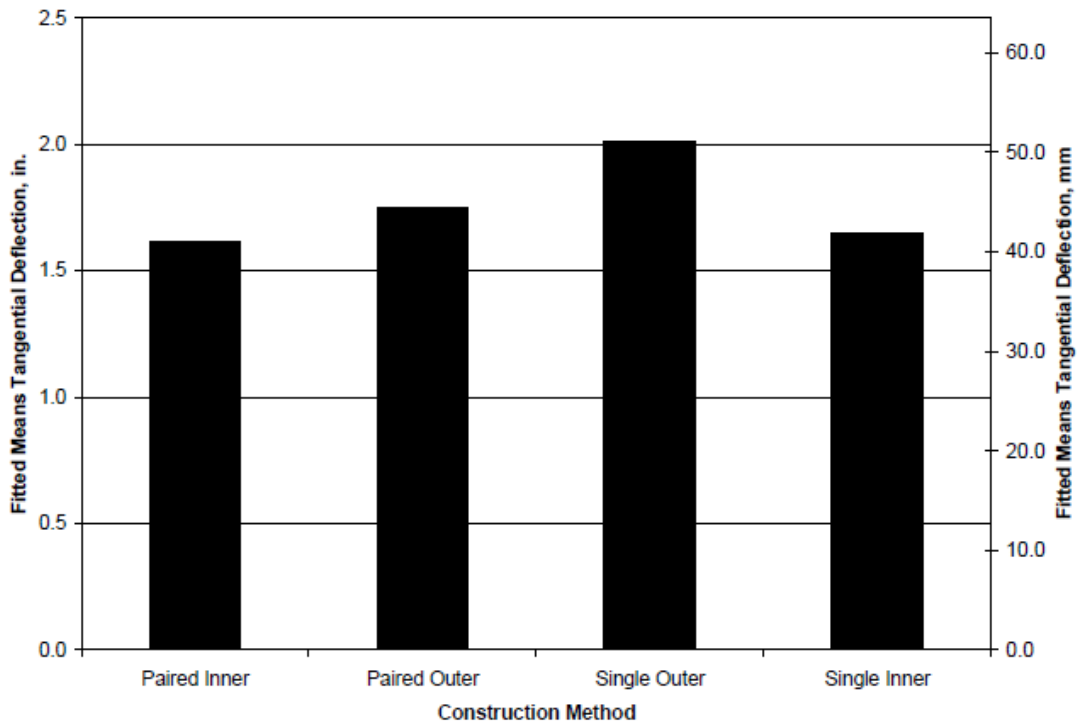


Figure 70. Construction Method Influence on Fitted Mean Tangential Deflections.

The final ANOVA statistical model for tangential deflections also included an interaction term that involved the construction method, similar to the final radial deformation statistical model. So, again, the effects of this interaction term on fitted mean radial deflections were examined. Figure 71 details the effects of a combination of construction method and span type (i.e. single span, two span) on tangential deflection fitted means. The figure shows that for all 4 construction methods, the single-span bridges experience mean tangential deflection values larger than those observed for the two-span bridges, and that the two-span bridges do not differ significantly with respect to construction sequencing effects.

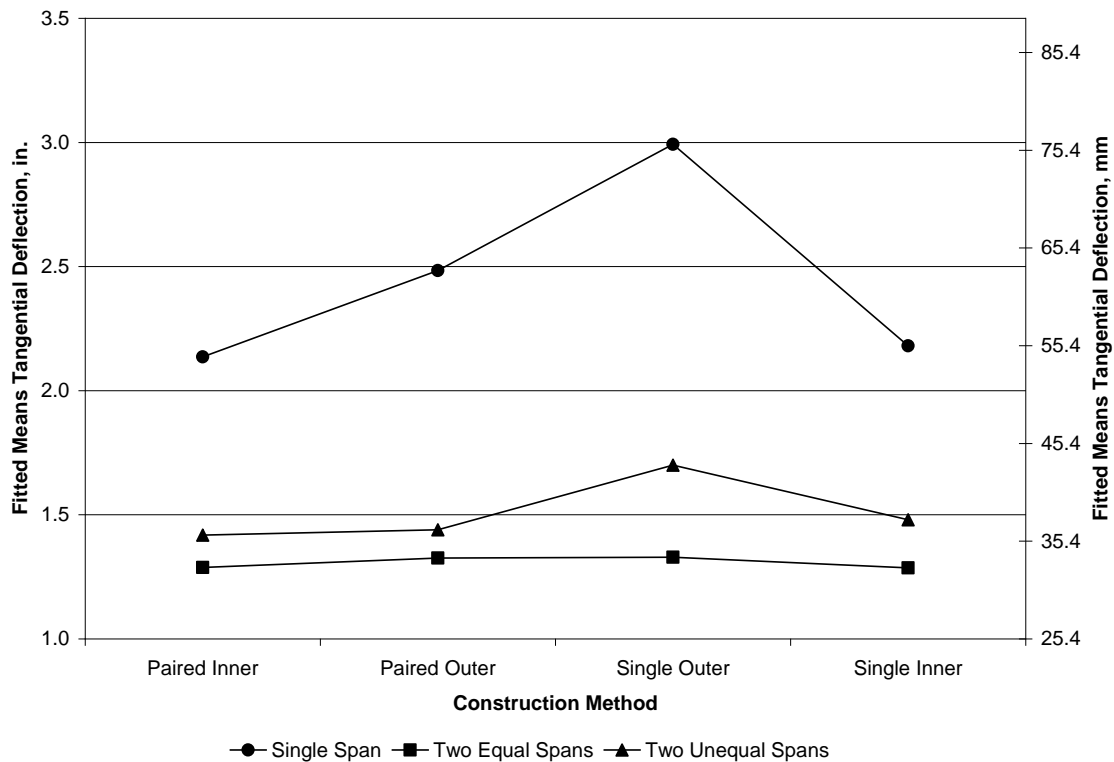


Figure 71. Fitted Mean Tangential Deflection Comparison for the Interaction of Construction Method and Span Type.

In summary, based on the ANOVA vertical, radial and tangential deflection statistical models of the 120 one- and two-span bridges that were initially studied, it can be concluded that the single outer construction method generally resulted in the largest deflections, irrespective of bridge geometry. However, of the other methods, it was not clear which would be preferred for a given bridge framing plan. Therefore, it was of interest to expand upon the ANOVA statistical work to assist with future parametric studies. Results from each of the one- and two-span bridge analyses were examined in greater detail to assist with providing a more comprehensive list of recommendations related to preferred construction methods.

Each bridge was examined to determine if one of the investigated construction methods could be clearly identified as that which minimized all three possible deformation components (i.e. radial, tangential, and vertical). Conversely, the models were also examined to identify a construction method that maximized those deformations. For the single-span bridges, the focus was at the end of all stages of construction, while for the two-span bridges, the focus was the field splice locations when only the first portion of a girder section was in place. Comparisons between deflections for different stages of construction greater than 6.35 mm (0.25 in.) were deemed significant. Results from these examinations are summarized in Table 15 through

Table 20. Construction Methods Not Recommended for Unbalanced Two-Span Bridges, Initial Studies.

No. of Girders	Radius, m (ft.)	R/L Ratio	Method
4	91 (300)	20.00	Single Outer
4	91 (300)	17.33	Single Inner
4	91 (300)	13.33	Single Outer
4	198 (650)	23.13	Single Inner
4	305 (1000)	35.59	Single Outer
5	91 (300)	20.00	Single Outer
5	91 (300)	17.33	Single Outer
5	91 (300)	13.33	Single Outer
5	198 (650)	23.13	Single Outer
5	305 (1000)	35.59	Paired Outer Single Outer

and are differentiated based on span number.

Table 15. Recommended Construction Methods for Single-Span Bridges, Initial Studies.

No. of Girders	Radius, m (ft.)	R/L Ratio	Method
4	91 (300)	20.00	Single Inner
4	91 (300)	17.33	Paired Outer, Paired Inner, Paired Outer
4	91 (300)	13.33	Paired Inner (Min. Radial) Single Inner (Min. Vertical)
4	198 (650)	23.13	Paired Inner (Min. Radial) Single Inner (Min. Vertical)
4	305 (1000)	35.59	Paired Inner
5	91 (300)	20.00	Single Inner
5	91 (300)	17.33	Paired Inner (Min. Radial) Single Inner (Min. Vertical)
5	91 (300)	13.33	Paired Inner
5	198 (650)	23.13	Paired Inner (Min. Radial) Single Inner (Min. Vertical)
5	305 (1000)	35.59	Paired Inner (Min. Radial) Single Inner (Min. Vertical)

Table 16. Construction Methods Not Recommended for Single-Span Bridges, Initial Studies.

No. of Girders	Radius, m (ft.)	R/L Ratio	Method
4	91 (300)	20.00	Single Outer
4	91 (300)	17.33	Single Outer
4	91 (300)	13.33	Single Outer
4	198 (650)	23.13	Single Outer
4	305 (1000)	35.59	Single Outer
5	91 (300)	20.00	Single Outer
5	91 (300)	17.33	Single Outer
5	91 (300)	13.33	Single Inner
5	198 (650)	23.13	Single Outer Paired Outer
5	305 (1000)	35.59	Single Outer

Table 17. Recommended Construction Methods for Balanced Two-Span Bridges, Initial Studies.

No. of Girders	Radius, m (ft.)	R/L Ratio	Method
4	91 (300)	20.00	Paired Inner
4	91 (300)	17.33	Paired Inner
4	91 (300)	13.33	Paired Inner
4	198 (650)	23.13	Paired Outer
4	305 (1000)	35.59	Paired Outer
5	91 (300)	20.00	Paired Inner (Min. Radial) Single Inner (Min. Vertical)
5	91 (300)	17.33	Paired Outer
5	91 (300)	13.33	Paired Outer (Min. Radial) Single Inner (Min. Vertical)
5	198 (650)	23.13	Paired Inner
5	305 (1000)	35.59	Paired Outer

Table 18. Construction Methods Not Recommended for Balanced Two-Span Bridges, Initial Studies.

No. of Girders	Radius, m (ft.)	R/L Ratio	Method
4	91 (300)	20.00	Single Outer
4	91 (300)	17.33	Single Outer
4	91 (300)	13.33	Single Outer Paired Outer
4	198 (650)	23.13	Single Outer
4	305 (1000)	35.59	Single Outer
5	91 (300)	20.00	Single Outer Single Inner
5	91 (300)	17.33	Single Outer
5	91 (300)	13.33	Single Outer
5	198 (650)	23.13	Single Outer Single Inner
5	305 (1000)	35.59	Single Outer

Table 19. Recommended Construction Methods for Unbalanced Two-Span Bridges, Initial Studies.

No. of Girders	Radius, m (ft.)	R/L Ratio	Method
4	91 (300)	20.00	Paired Outer (Min. Radial) Paired Inner (Min. Vertical)
4	91 (300)	17.33	Single Outer
4	91 (300)	13.33	Paired Outer
4	198 (650)	23.13	Paired Inner
4	305 (1000)	35.59	Paired Outer
5	91 (300)	20.00	Paired Inner
5	91 (300)	17.33	Paired Inner (Min. Radial) Single Inner (Min. Vertical)
5	91 (300)	13.33	Paired Inner (Min. Radial) Single Inner (Min. Vertical)
5	198 (650)	23.13	Paired Outer
5	305 (1000)	35.59	Paired Inner

Table 20. Construction Methods Not Recommended for Unbalanced Two-Span Bridges, Initial Studies.

No. of Girders	Radius, m (ft.)	R/L Ratio	Method
4	91 (300)	20.00	Single Outer
4	91 (300)	17.33	Single Inner
4	91 (300)	13.33	Single Outer
4	198 (650)	23.13	Single Inner
4	305 (1000)	35.59	Single Outer
5	91 (300)	20.00	Single Outer
5	91 (300)	17.33	Single Outer
5	91 (300)	13.33	Single Outer
5	198 (650)	23.13	Single Outer
5	305 (1000)	35.59	Paired Outer Single Outer

The results listed above indicate the following for the initial set of single- and two-span horizontally curved bridges that were examined:

- Construction methods that initiate with the inner (lowest radius) girder are preferred for single-span horizontally curved structures, but a clear preference between erecting single girders and erecting girders in pairs, from a strength and stiffness standpoint, is not apparent;
- Paired construction methods, irrespective of the initial placement scheme relative to the center of curvature, are preferred for two-span structures irrespective of span ratio; and
- Regardless of span number and geometry, construction that initiates with a single outer girder is not recommended from a strength and stiffness standpoint.

As was stated previously, the initial examination of effects of the aforementioned construction methods on the response of structures containing more than two spans occurred via the study a single curved bridge, Structure #7A. Three-dimensional models of the three-span continuous framing system comprised of Spans 4, 5, and 6 were sequentially constructed in SAP 2000, and the aforementioned single- and paired-girder erection sequences were completed computationally. Their effects on the structure were examined via the tangential, radial, and vertical deflections that were induced during construction.

Single inner erection was examined by placing the smallest radius of curvature girder first from splice to splice, followed by the next higher radius girder and so on until the entire superstructure was erected. Single outer girder placement was investigated using a similar procedure, with the only difference being the initiation of the erection from outer to inner girder. Outer and inner paired erection was also investigated in similar fashion, with the paired girders and the fifth, single girder, being erected from splice to splice.

To evaluate and compare erection sequences for this structure, the final deformed shapes for the first and last girder line erected for each were compared. Single girder approaches will be compared initially, followed by paired girder approaches, and finally the four methods will be examined collectively.

Girder G5 was the first to be placed for the single outer erection procedure, while G1 was the first to be erected for the single inner approach. The resulting final vertical and radial deformed shapes for the first and last girders erected are shown in Figure 72 through Figure 75. Discontinuities evident in some of the plots were caused by SAP's sequential analysis capabilities, which, at the time these analyses were completed, added new sections in their undeformed positions to already deformed portions of the erected portions of the bridge. These discontinuities were localized at the field splice locations and, since they affected all analyses that were completed, did not affect the comparisons that were completed.

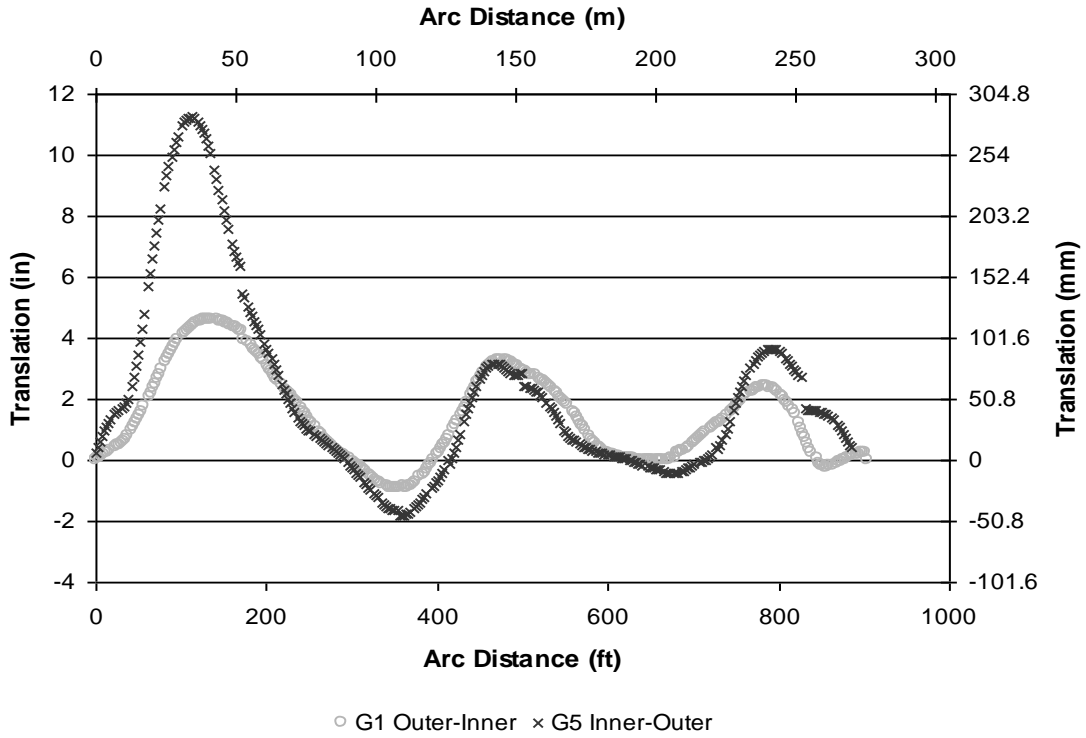


Figure 72. Radial Deformations, Single Girder Erection. First Erected Girder.

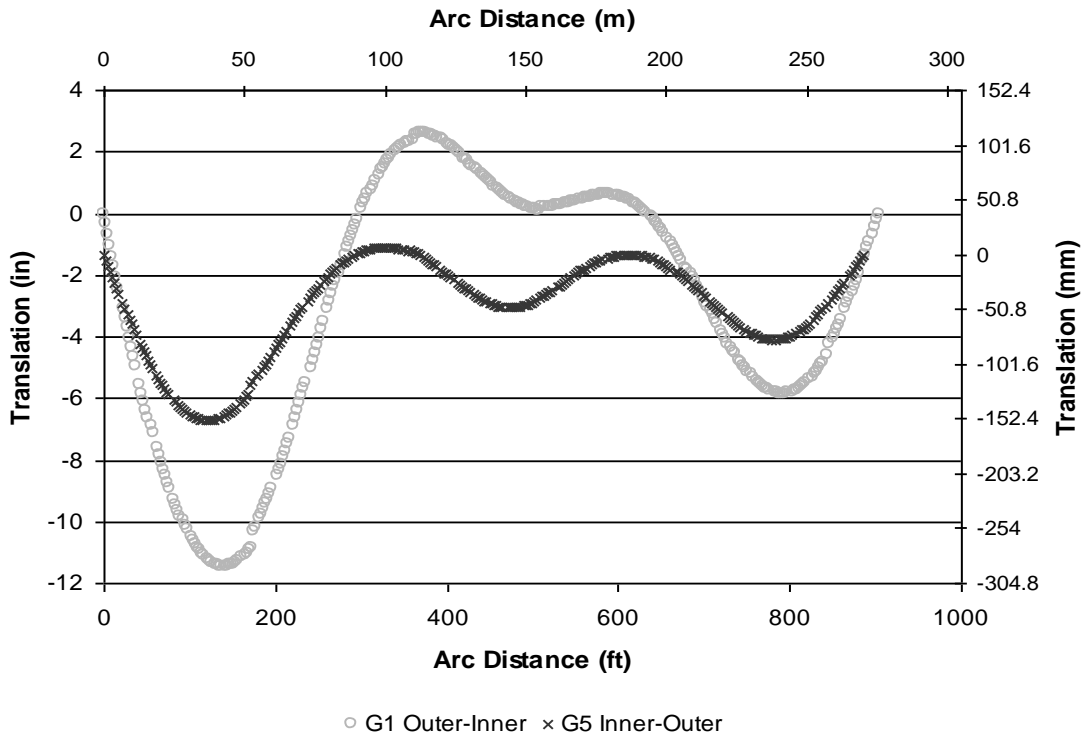


Figure 73. Vertical Deformations, Single Girder Erection. First Erected Girder.

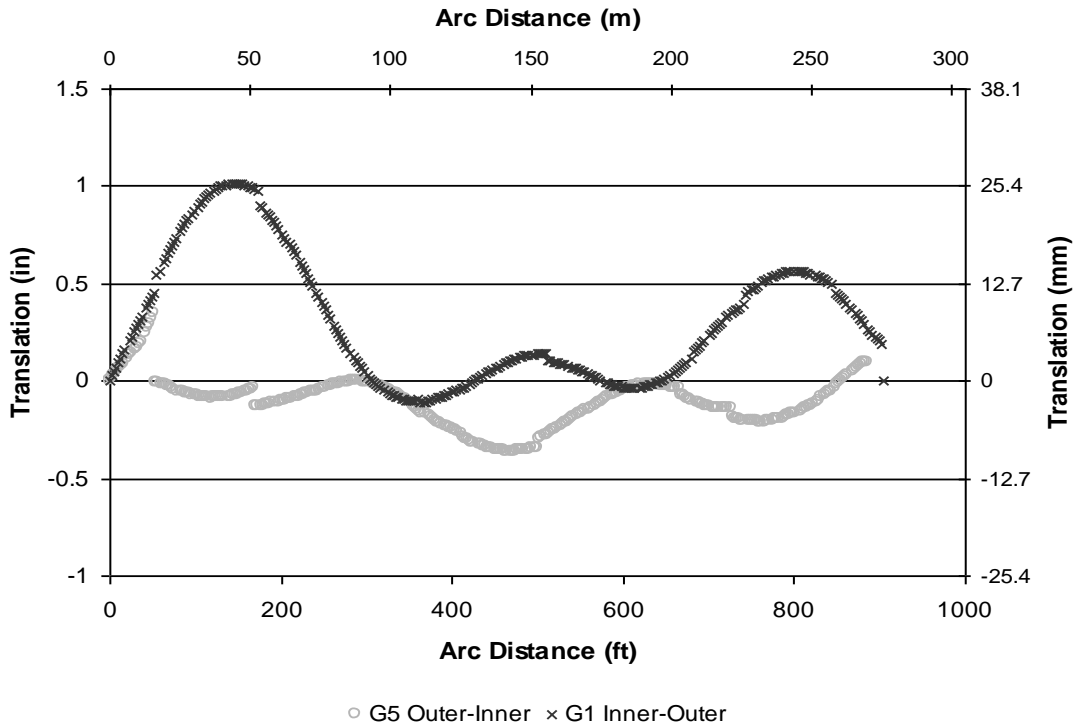


Figure 74. Radial Deformations, Single Girder Erection. Last Erected Girder.

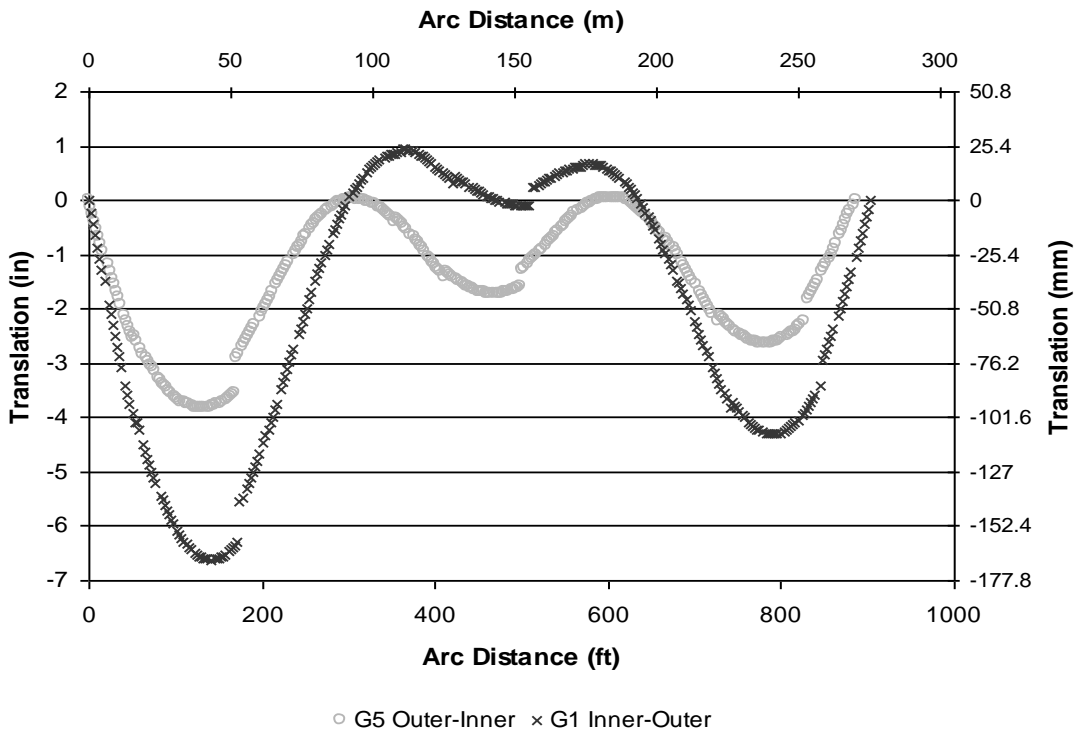


Figure 75. Vertical Deformations, Single Girder Erection. Last Erected Girder.

Examination of the results from these comparisons appeared to support conclusions drawn from the initial single- and two-span girder studies discussed earlier. These conclusions are that, if single-girder erection procedures are used, choosing a single outer approach tends to result in greater displacements than a single inner approach.

Similar comparisons for the paired inner and outer approaches are shown in Figure 76 through Figure 79.

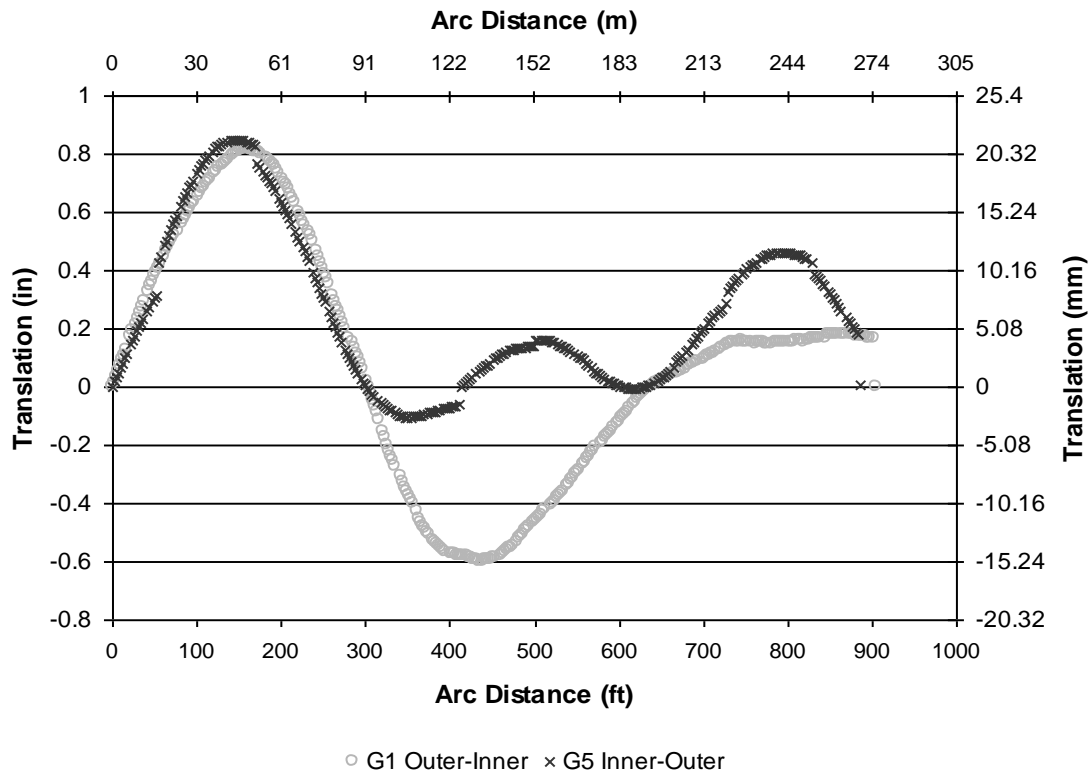


Figure 76. Radial Deformations, Paired Girder Erection. First Erected Girder.

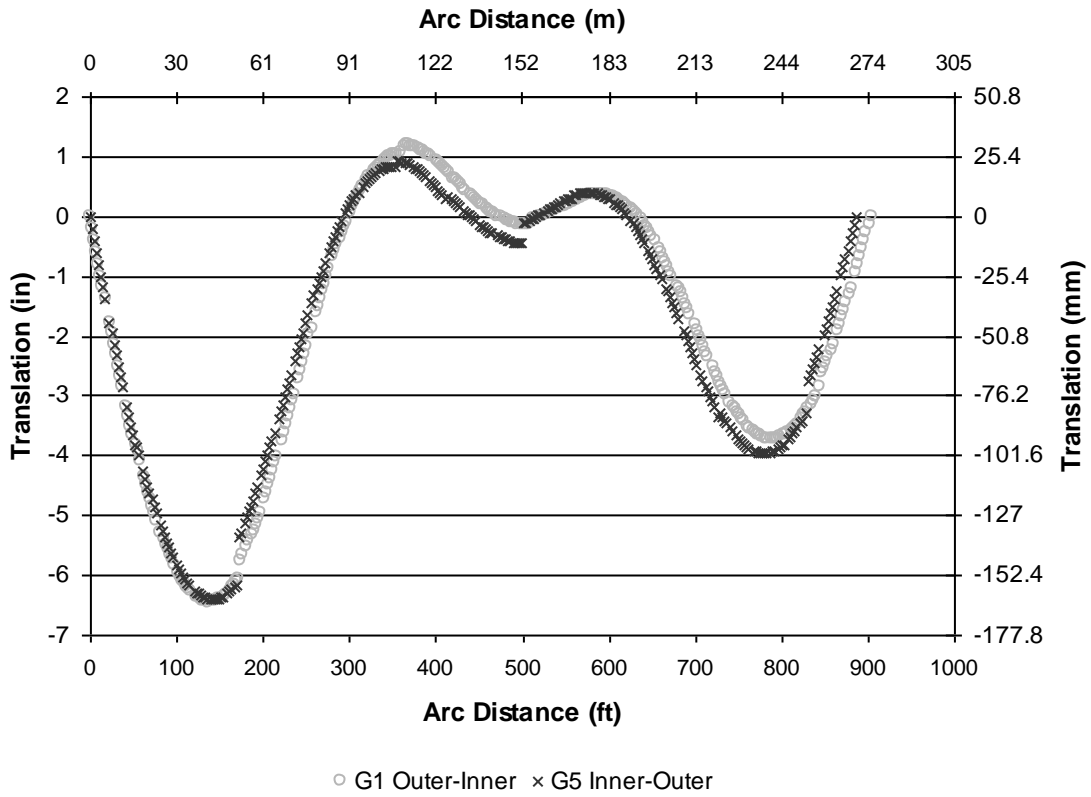


Figure 77. Vertical Deformations, Paired Girder Erection. First Erected Girder.

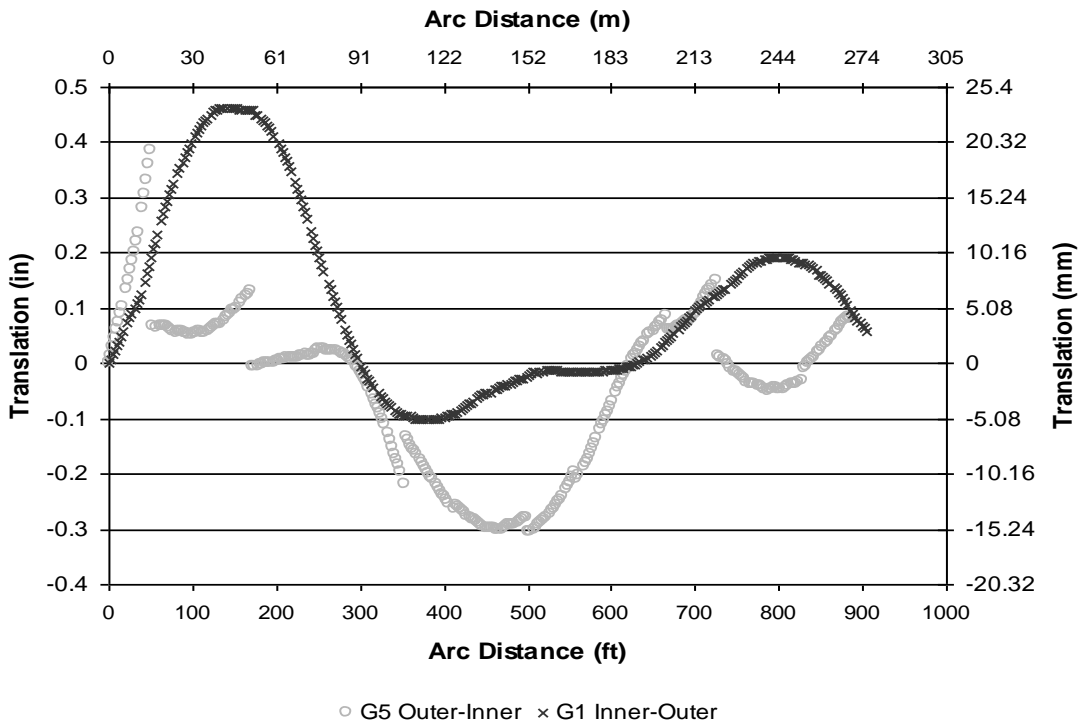


Figure 78. Radial Deformations, Paired Girder Erection. Last Erected Girder.

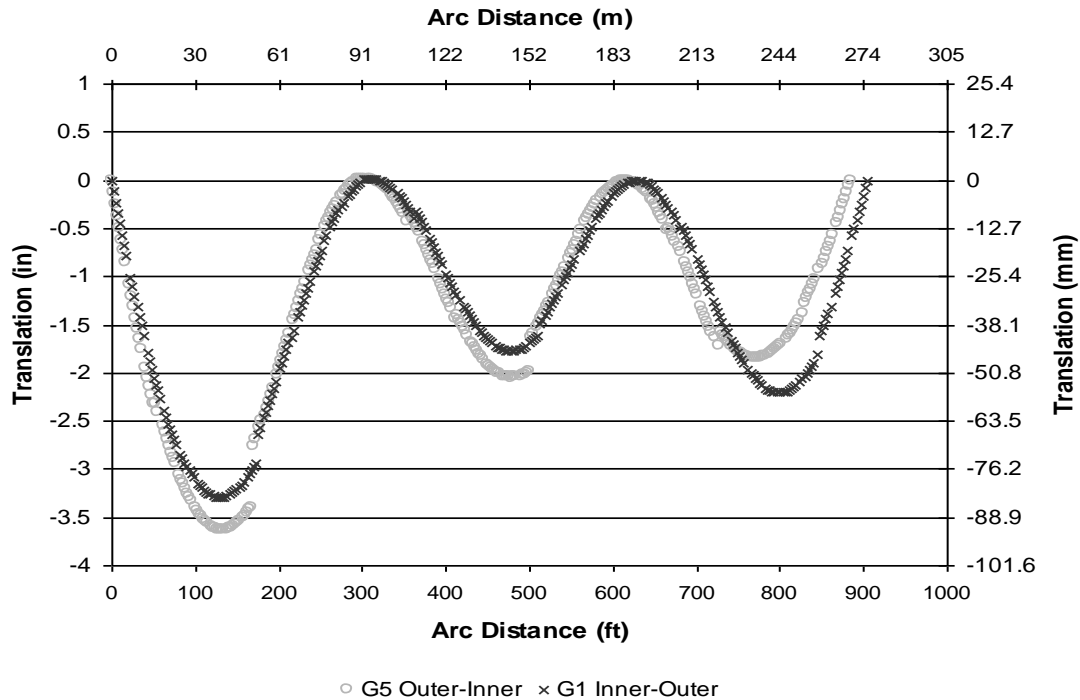


Figure 79. Vertical Deformations, Paired Girder Erection. Last Erected Girder.

The paired girder comparisons indicate that the paired inner approach produced, in general, smaller deformations than the paired outer approach. However, the differences in deformation magnitude were not nearly as dramatic as for single girder comparisons, which again appear to support conclusions drawn from the single- and two-span initial studies.

When all four studied erection procedures are compared, paired-girder erection procedures were preferred over single-girder for the single three-span structure that was initially investigated. Again, these final conclusions appear to support the conclusions obtained for the initial single- and two-span structure studies summarized in Table 15 through

Table 20. Construction Methods Not Recommended for Unbalanced Two-Span Bridges, Initial Studies.

No. of Girders	Radius, m (ft.)	R/L Ratio	Method
4	91 (300)	20.00	Single Outer
4	91 (300)	17.33	Single Inner
4	91 (300)	13.33	Single Outer
4	198 (650)	23.13	Single Inner
4	305 (1000)	35.59	Single Outer
5	91 (300)	20.00	Single Outer
5	91 (300)	17.33	Single Outer
5	91 (300)	13.33	Single Outer
5	198 (650)	23.13	Single Outer
5	305 (1000)	35.59	Paired Outer Single Outer

5.2.1.3 Representative Structure Studies - Background

Five bridges from the set described in the Final Design section were selected for additional verification with respect to erection sequencing effect results. It was of interest to ensure that the recommended preliminary study erection schemes were mimicked in the final design structure. The selected bridges were two-span structures having varying radii and three-span bridges having balanced and unbalanced spans. These bridges were selected so they included important parameters examined in the preliminary studies, such as extreme R/L ratio and incorporation of the unbalanced spans. The radii for the three two-span, four-girder bridges selected were 91.4 m (300 ft), 198.1 m (650 ft), and 304.8 m (1000 ft), and the radius of the single balanced and the single unbalanced three-span, four-girder bridges selected was 91.4 m (300ft). The unbalanced three-span bridge span ratio was 1:1.4. The designed girder spacing and cross-frame spacing for the selected representative bridges were 3 m (10 ft) and 6.9 m (22.5 ft), respectively. Consequently, three different R/L ratios (13.3, 28.9, and 44.4) were investigated. In addition, the deck was designed following the deck dimensions used in the previous initial studies. The span length for the two-span bridges and the balanced, three-span bridge was 68.6 m (225 ft), and the span lengths for the unbalanced, three-span bridge were 48.1 m (157.5 ft) and 68.6 m (225 ft).

Table 21 lists the parameters of the selected representative bridges. Simplified framing plans for the selected bridges are shown in Figure 80 to Figure 84.

Table 21: Selected Curved Bridge Erection Study Bridge Information

Bridge No.	Radius of Curvature, m (ft)	Cross-Frame Spacing, m (ft)	Girder Spacing, m (ft)	Number of Spans	Span-Length, m (ft)	Number of Girder, m (ft)
C3	91.4 (300)	6.9 (22.5)	3 (10)	2	68.6-68.6 (225-225)	4
C6	198.1 (650)	6.9 (22.5)	3 (10)	2	68.6-68.6 (225-225)	4
C9	304.8 (1000)	6.9 (22.5)	10	2	68.6-68.6 (225-225)	4
C10	91.4 (300)	6.9 (22.5)	3 (10)	3	68.6-68.6-68.6 (225-225-225)	4
C11	91.4 (300)	6.9 (22.5)	3 (10)	3	48.1-68.6-68.6 (157.5-225-225)	4

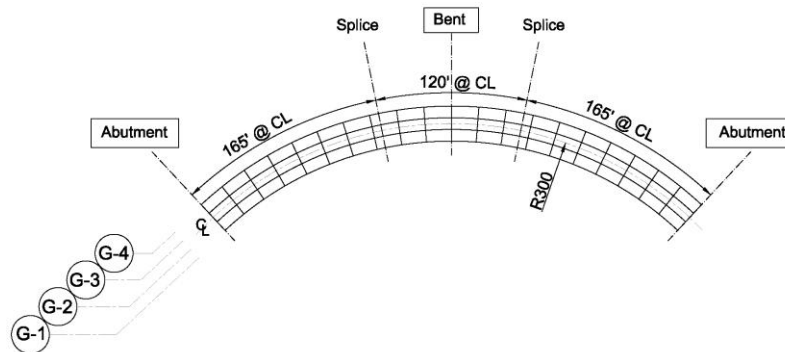


Figure 80: Simplified Framing Plan, Bridge C3: Two-Span, 4-Girder, 91.4 m Radius, R/L=13.3

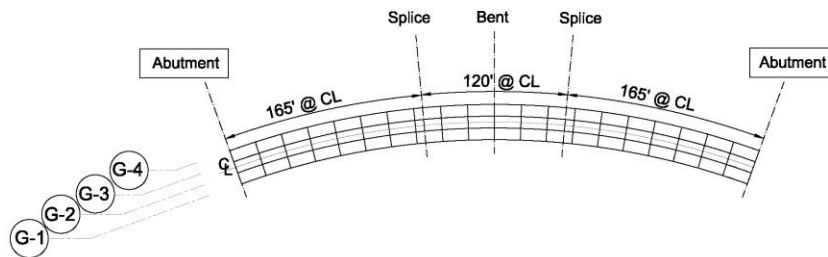


Figure 81: Simplified Framing Plan, Bridge C6: Two-Span, 4-Girder, 198.1 m Radius, R/L=28.9

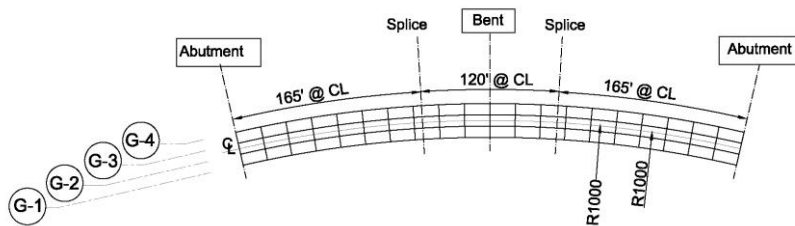


Figure 82: Simplified Framing Plan, Bridge C9: Two-Span, 4-Girder, 304.8 m Radius, R/L=44.4

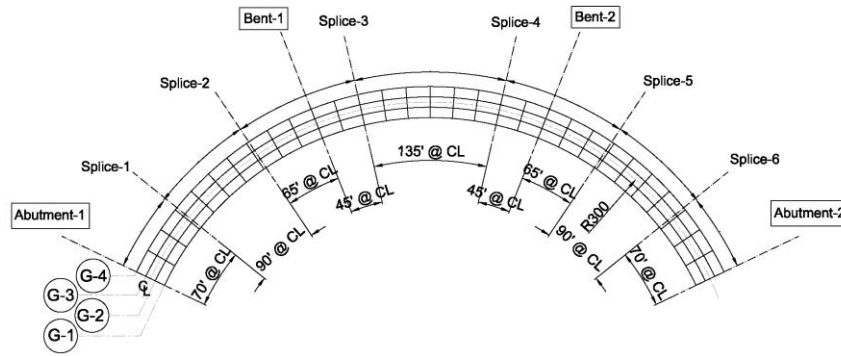


Figure 83: Simplified Framing Plan, Bridge C10: Balanced, Three-Span, 4-Girder, 91.4 Radius, R/L=13.3

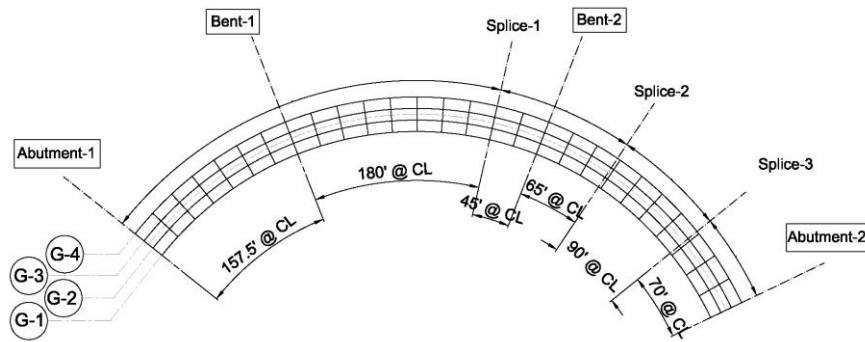


Figure 84: Simplified Framing Plan, Bridge C11: Unbalanced, Three-Span, 4-Girder, 91.4 Radius, R/L=13.3

Four erection scenarios were applied to the selected structures to reaffirm results from the preliminary studies by investigating the effects of erection sequencing decisions on construction behavior. The four erection scenarios were: 1) paired-girder erection placing the interior girders first; 2) paired-girder erection placing the exterior girders first; 3) single-girder erection placing the interior girder first; and 4) single-girder erection placing the exterior girder first. The behavior of the structures under self weight was analyzed using ABAQUS/Standard, with sequential analysis being performed to examine the behavior for construction stages that involved girder erection and concrete deck placement, with the final stage for the sequential analysis being deck placement. Figure 85 through Figure 88 detail the superstructure erection stages for the four scenarios for a representative two-span bridge. A similar erection approach was used for the three-span bridges, with the number of erection stages differing due to an increased number of splices. In addition to erection sequencing study, the effects of “drop-in” erection on the constructability of curved bridges were examined for balanced and unbalanced three-span structures having a severe curvature. The “drop-in” erection sequences for Bridges C-10 and C-11, the two bridges studied, are shown in Figure 89 and Figure 90.

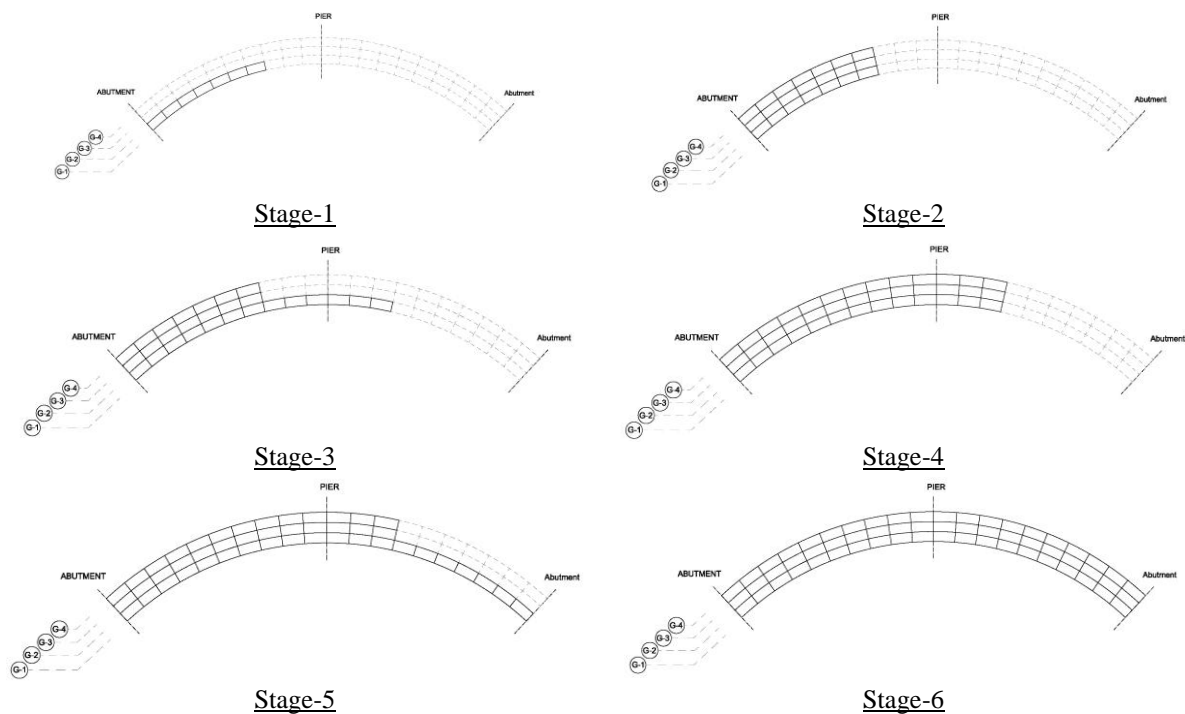


Figure 85: Stage 1 to Stage 6 for Paired-Girder (inner girders placed first) Erection of Two-Equal-Span, 4-Girder bridges.

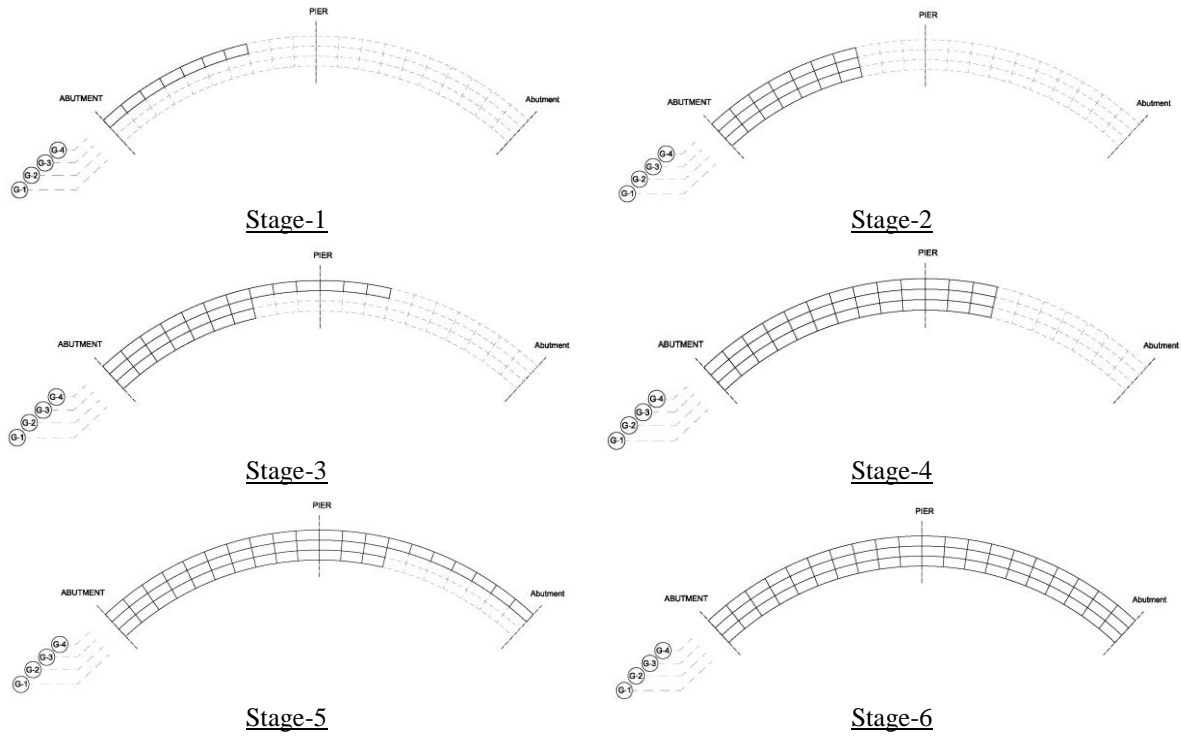


Figure 86: Stage 1 to Stage 6 for Paired-Girder (outer girders placed first) Erection of Two-Equal-Span, 4-Girder Bridges.

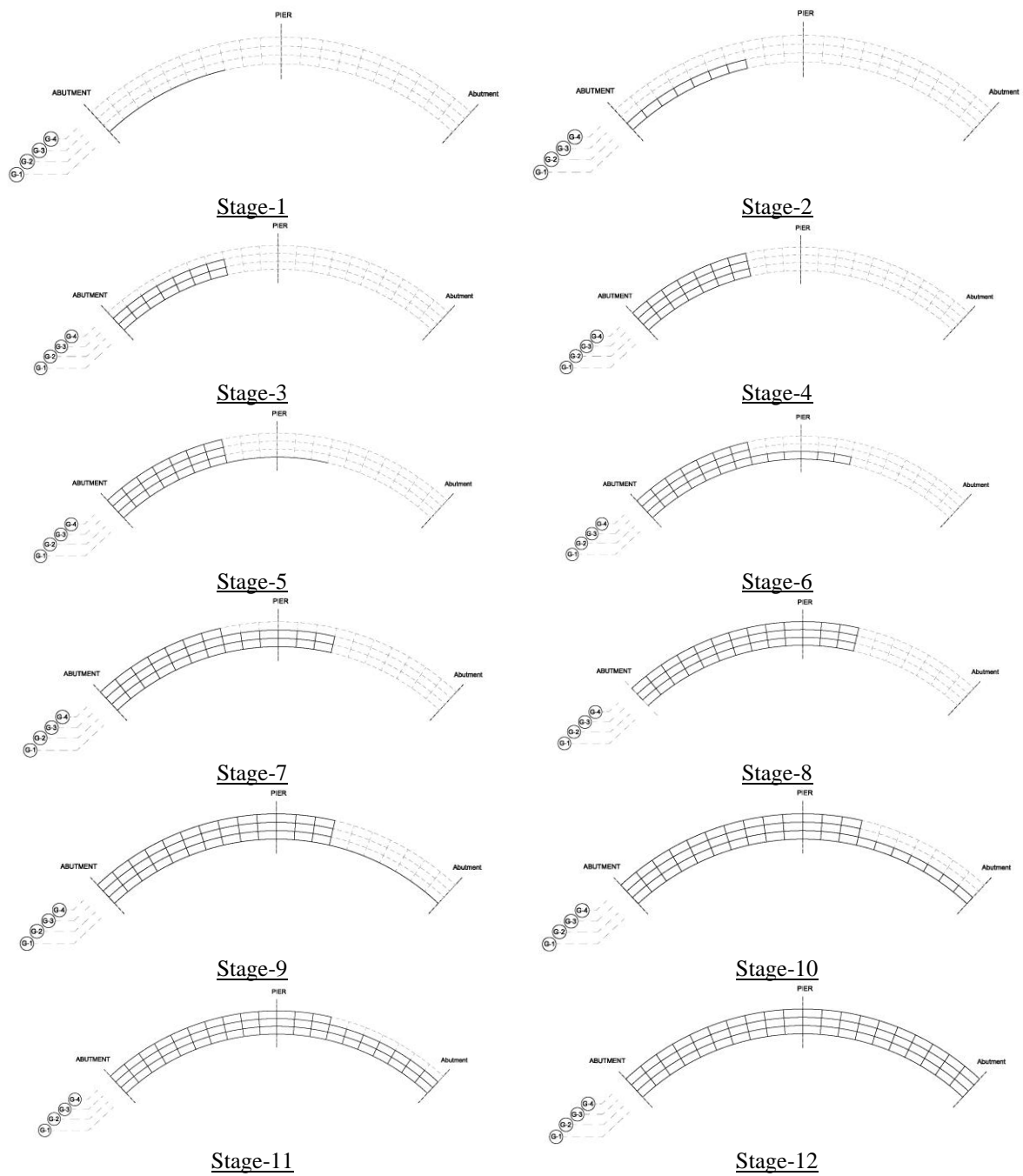


Figure 87: Stage 1 to Stage 12 of Construction for Single-Girder (inner girder placed first) Erection of Two-Equal-Span, 4-Girder Bridges.

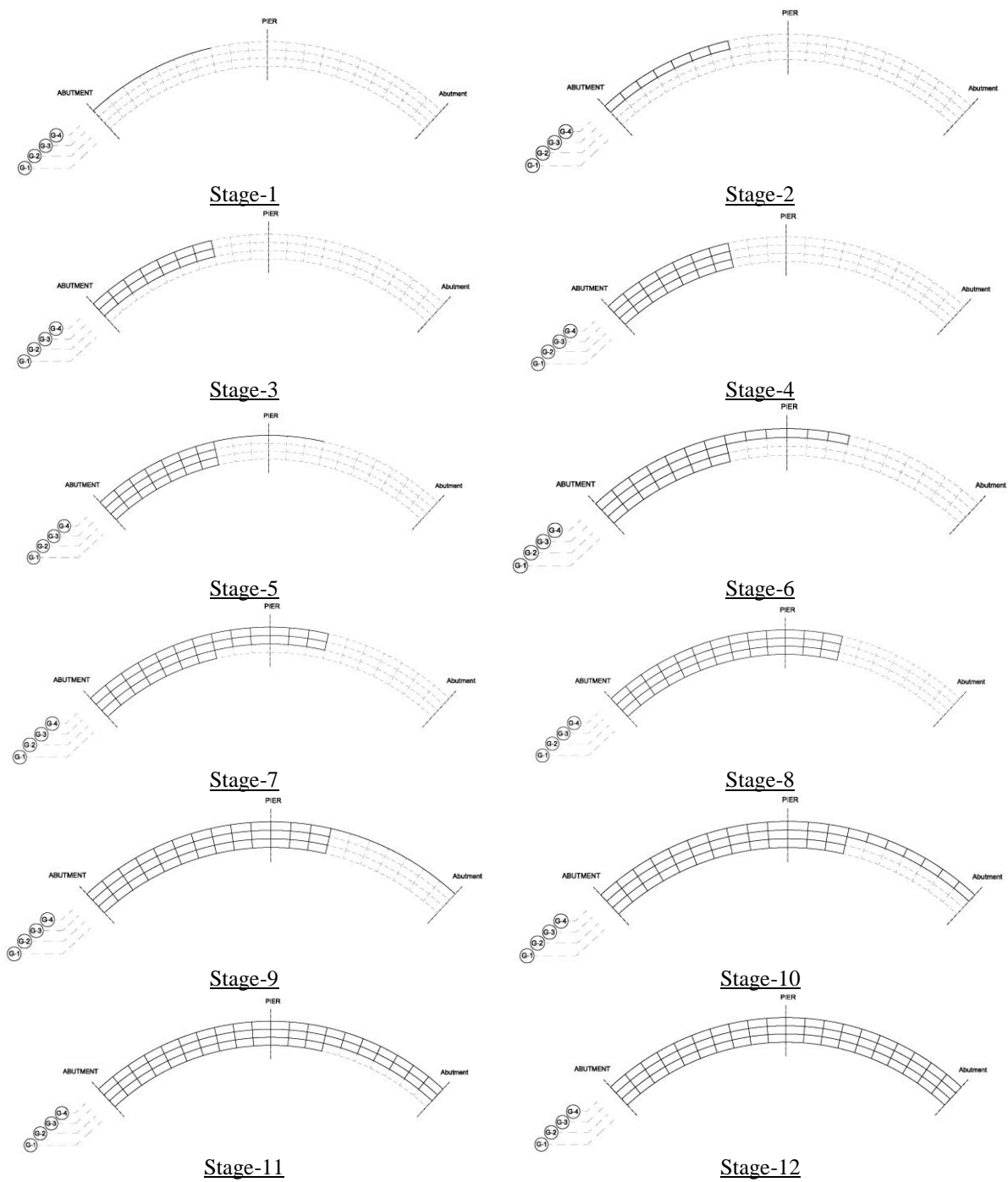
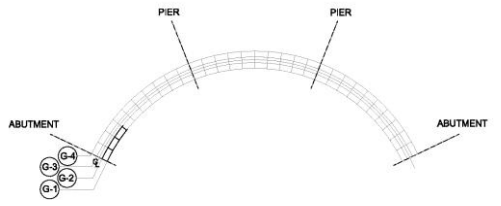
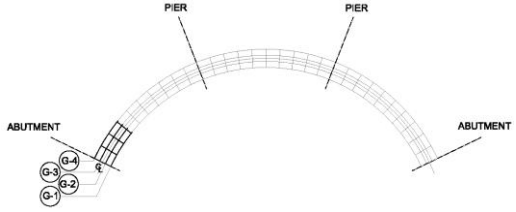


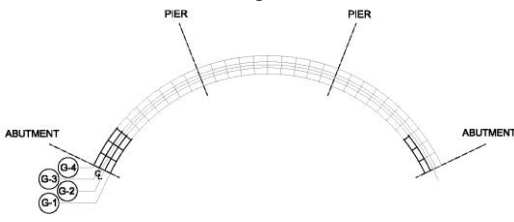
Figure 88: Stage 1 to Stage 12 of Construction for Single-Girder (outer girder placed first) Erection of Two-Equal-Span, 4-Girder Bridges.



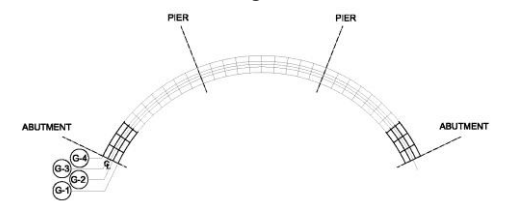
Stage-1



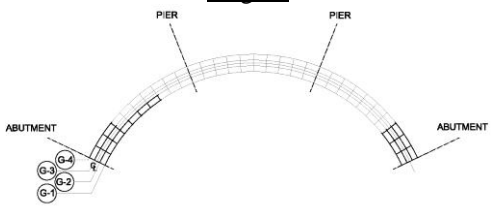
Stage-2



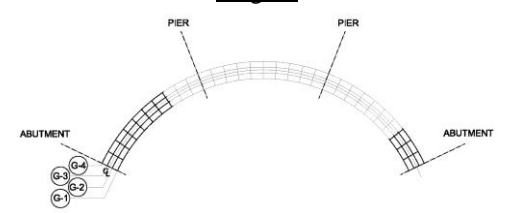
Stage-3



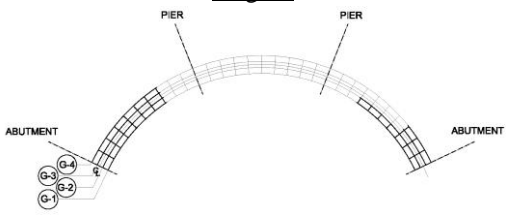
Stage-4



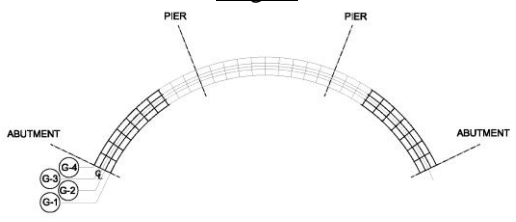
Stage-5



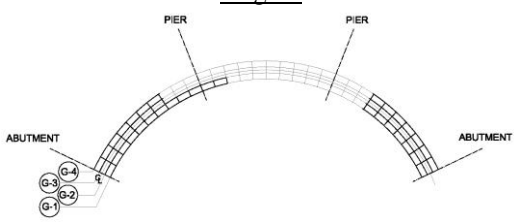
Stage-6



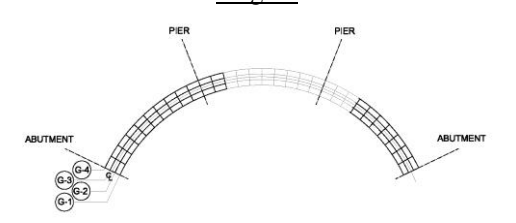
Stage-7



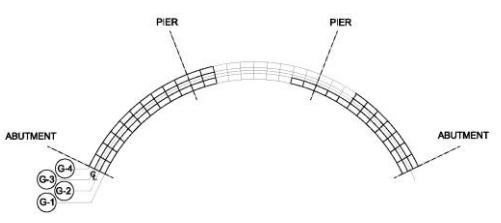
Stage-8



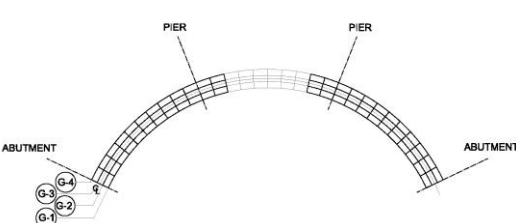
Stage-9



Stage-10



Stage-11



Stage-12

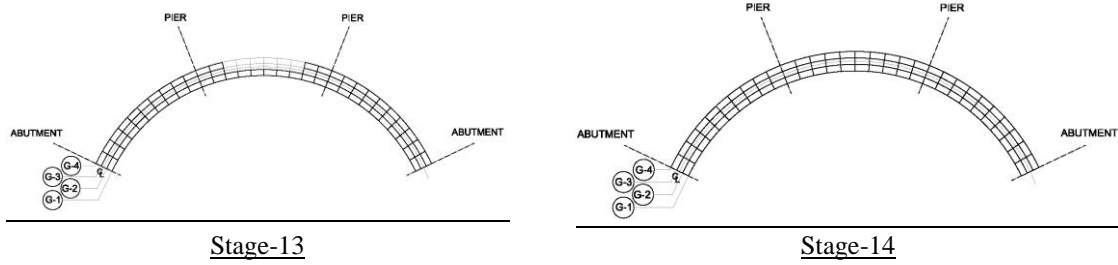


Figure 89: Stage 1 to Stage 14 of Construction for “Drop-In” Erection of Bridge C-10.

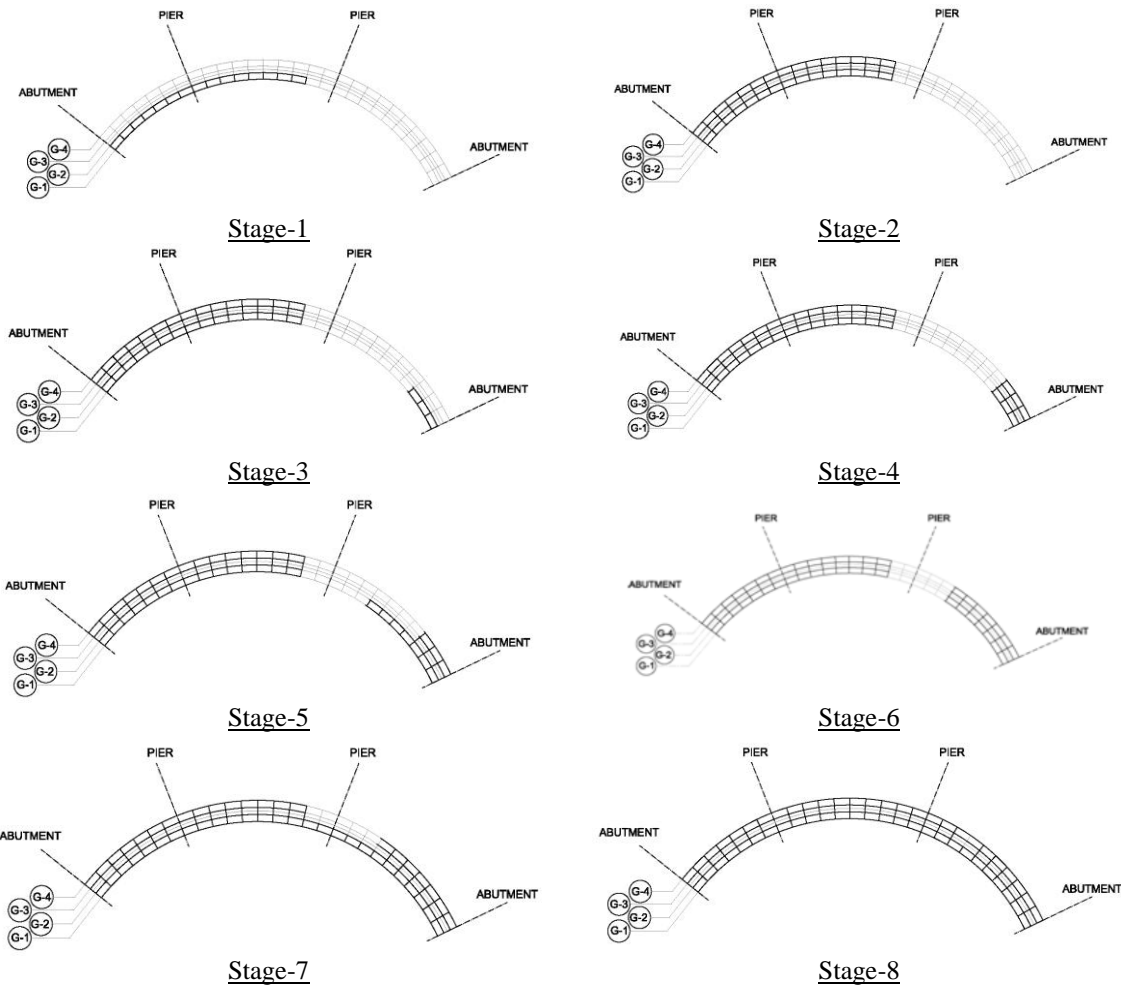


Figure 90: Stage 1 to Stage 8 of Construction for “Drop-In” Erection of Bridge C-11.

5.2.1.4 Representative Structure Studies - Results

Based on the results of the initial studies, vertical and radial deflections were classified as the two most important indexes for evaluating the adequacy of various erection approaches. Therefore, vertical and radial deflections from sequential analyses were compared herein to assist with the current evaluation. To compare the different erection sequences, vertical and radial deflections where maximum values were anticipated to occur were compared. These

locations were at splice locations and at 0.4L, where L is the span of the girder, measured from the abutment for the exterior spans and at mid-span for interior spans.

For these analyses, comparisons were made by examining non-dimensionalized deflections that consisted of maximum deflections normalized with respect to maximums from the recommended preliminary study erection scenario (paired inner). The maximum deflection was defined as the maximum deflection at the selected locations in the girders for a given stage. Results are presented in Figure 91 through Figure 100, with the construction stages corresponding to those for the paired-girder approach. As observed in the figures, vertical deflections were decreased when paired-girder erection approaches were used, while radial deflections were not significantly influenced between the different erection methods. These results confirmed the findings from the initial studies of the final bridge designs that were examined. If enough crane capacity is available, paired-girder erection approaches would be the preferred erection methods for the curved bridges examined in this study. More specifically, the paired inner erection approach was preferred for curved bridges having severe curvature. Maximum vertical and radial girder deflections at splice locations obtained from the drop-in effect study were all close to those from previous results, which permitted the drop-in erection approach to be adopted as an alternative method. Consequently, those deflections were found to be functions of R/L values, boundary conditions, and span lengths, but not the drop-in effect. Therefore, if adequate control of the already erected sections can be maintained, the use of drop-in erection sequencing should not positively or adversely affect bridge constructability for the bridges studied.

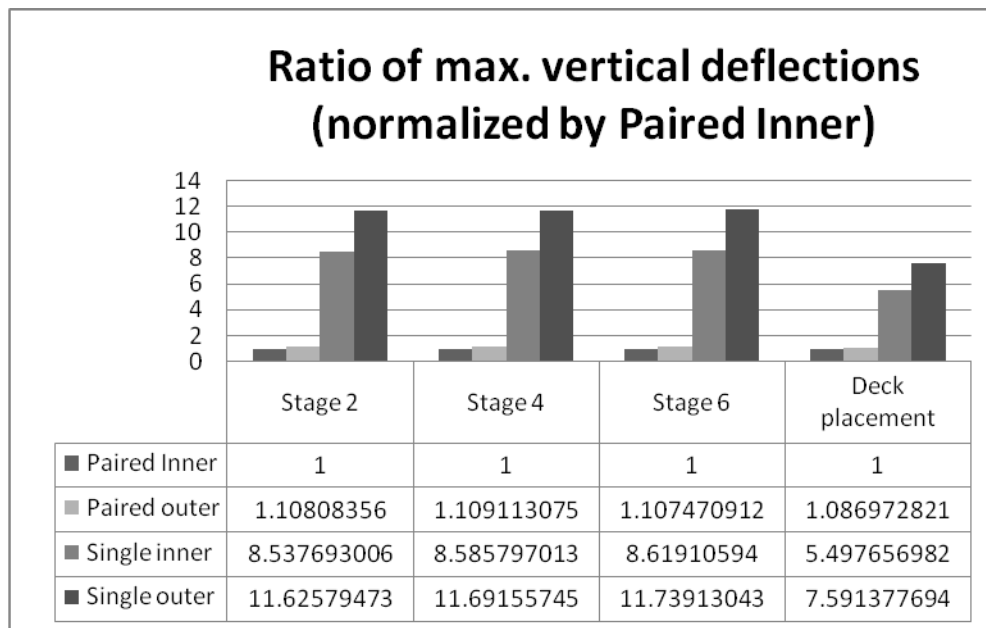


Figure 91: Ratio of Maximum Vertical Deflections for Bridge C3.

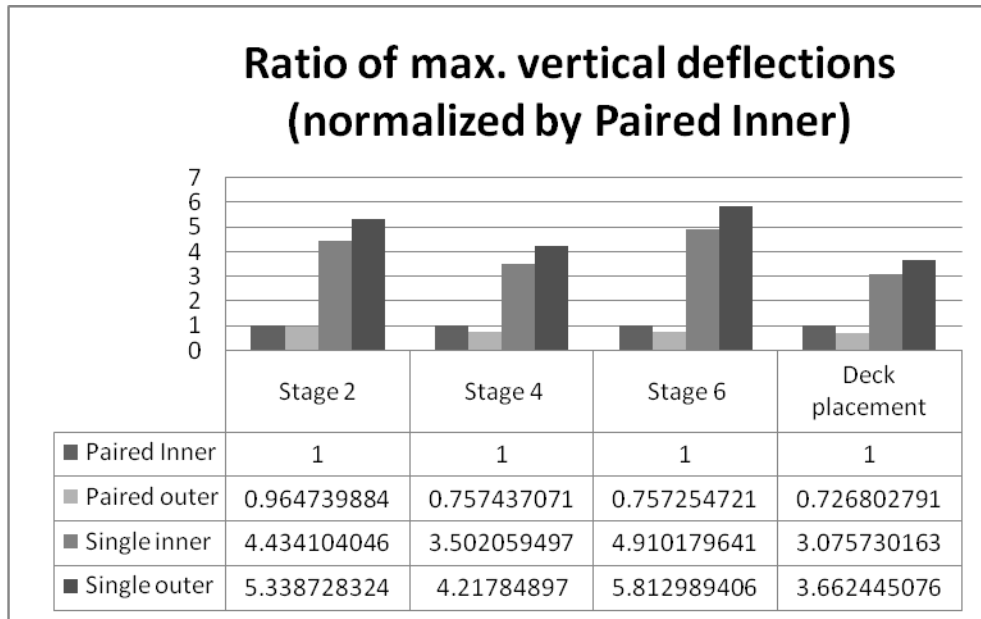


Figure 92: Ratio of Maximum Vertical Deflections for Bridge C6.

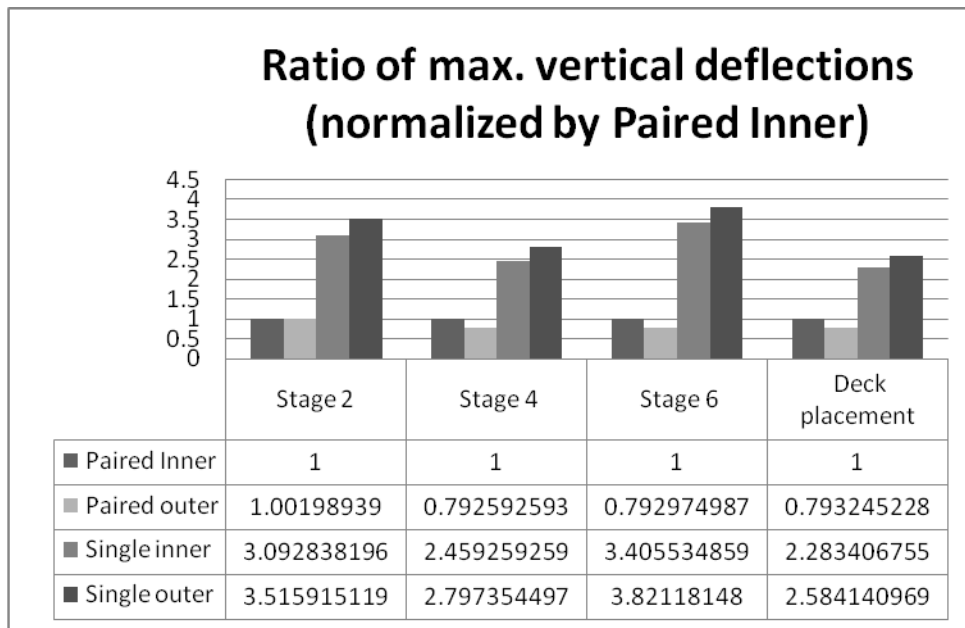


Figure 93: Ratio of Maximum Vertical Deflections for Bridge C9.

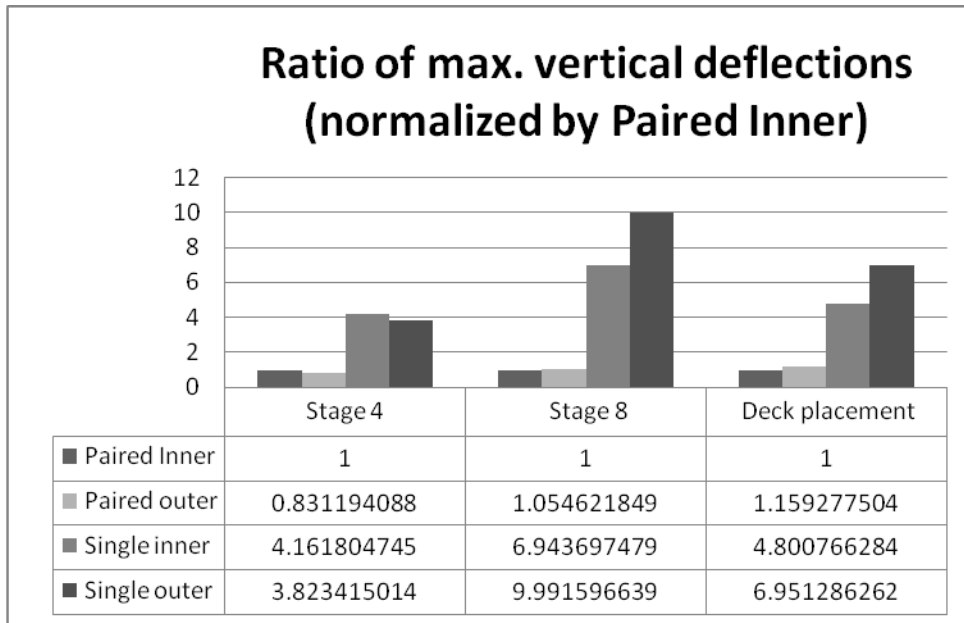


Figure 94: Ratio of Maximum Vertical Deflections for Bridge C10.

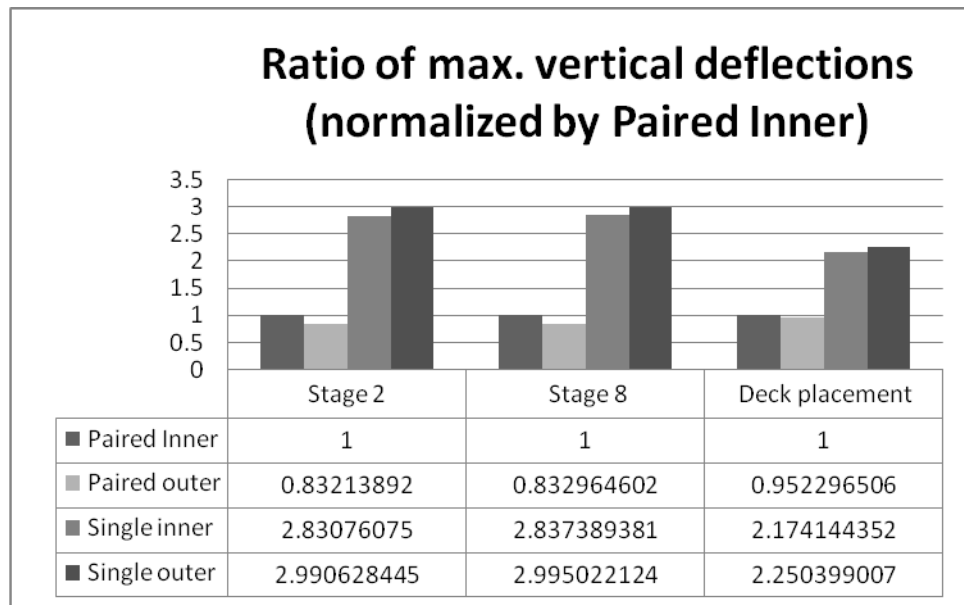


Figure 95: Ratio of Maximum Vertical Deflections for Bridge C11.

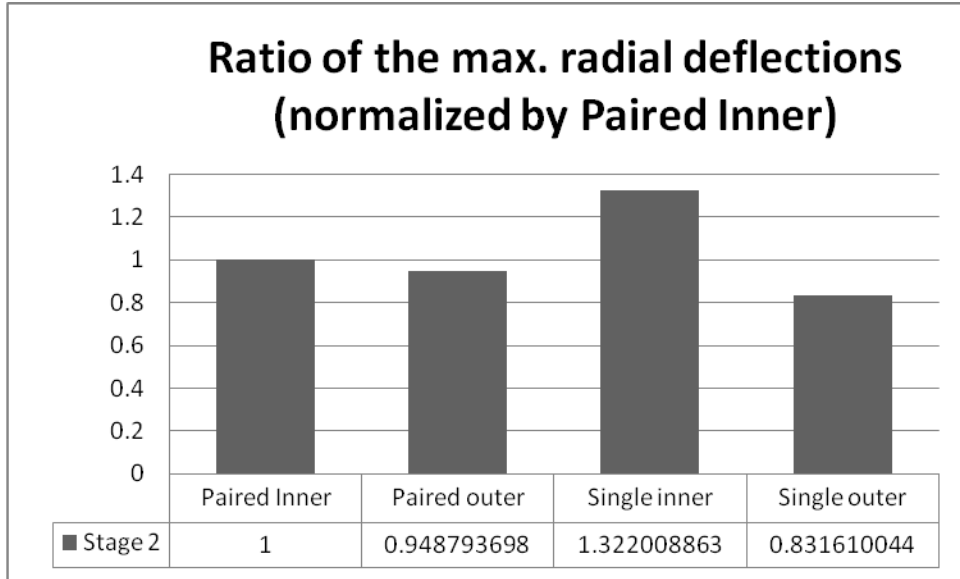


Figure 96: Ratio of Maximum Radial Deflections for Bridge C3.

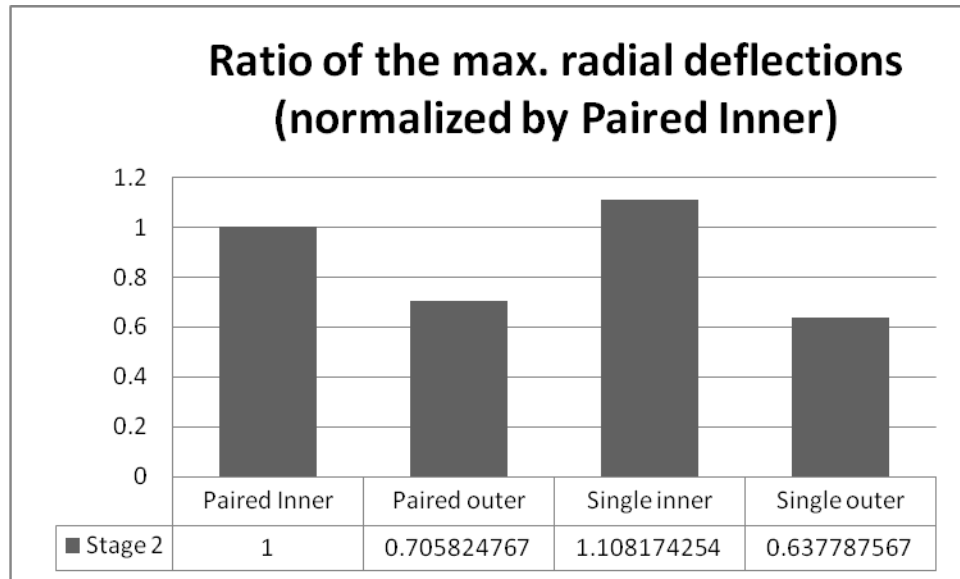


Figure 97: Ratio of Maximum Radial Deflections for Bridge C6.

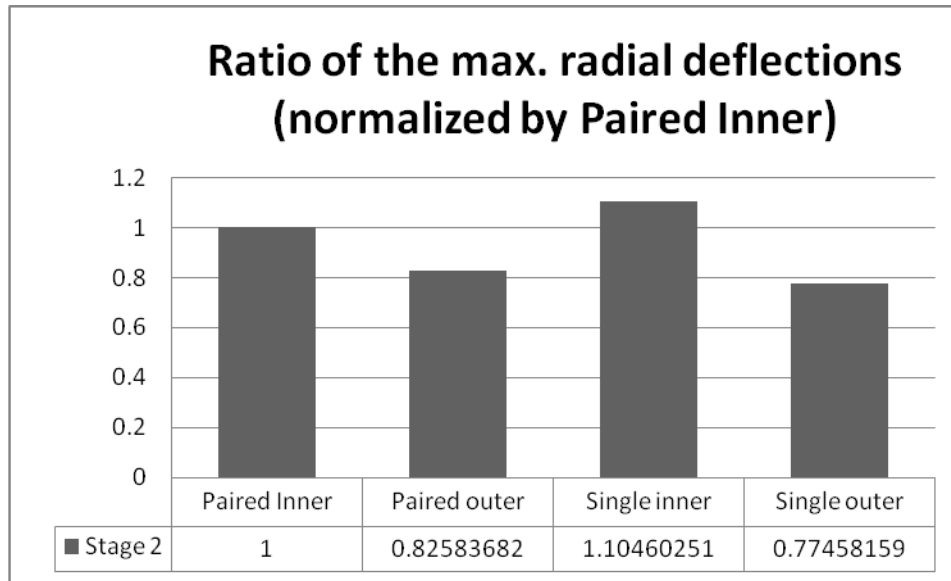


Figure 98: Ratio of Maximum Radial Deflections for Bridge C9.

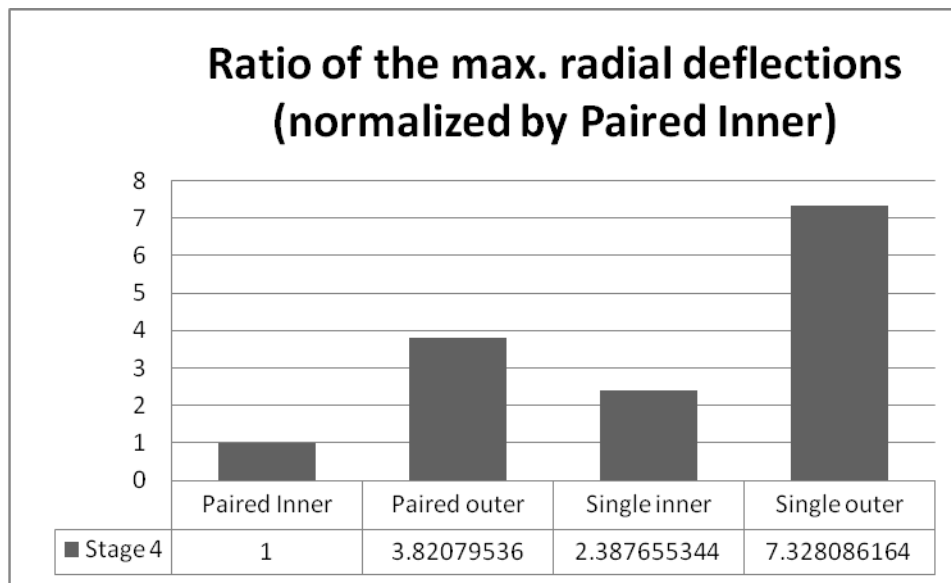


Figure 99: Ratio of Maximum Radial Deflections for Bridge C10.

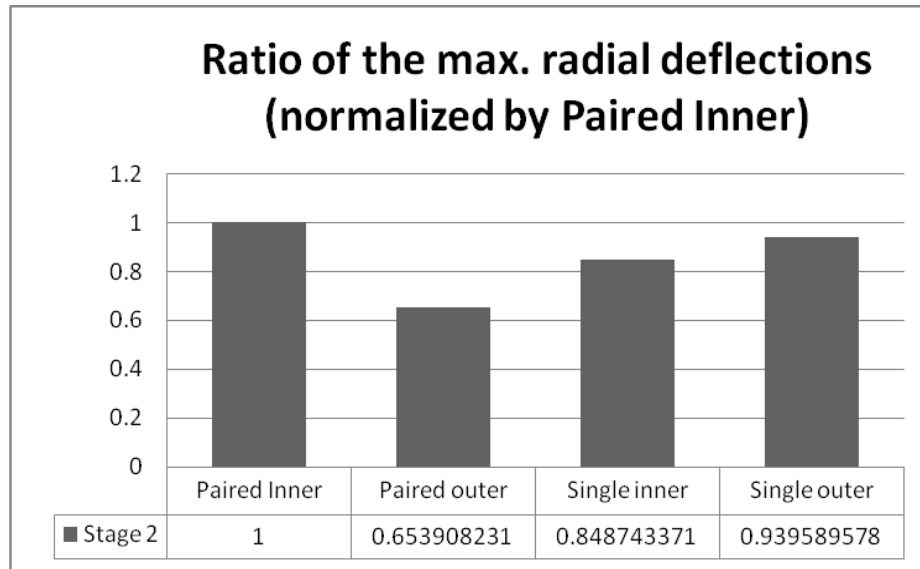


Figure 100: Ratio of Maximum Radial Deflections for Bridge C11.

5.2.2 Parametric Studies - Skewed

5.2.2.1 Representative Structure Studies – Background

Similar to the study of the representative curved bridges, a total of five representative skewed structures were examined. One single-span bridge with severely skewed supports, two two-span bridges with varying skew angles, and two triple-span bridges with balanced/unbalanced spans were selected to examine erection sequencing effects. These bridges were selected in order to address all of the important parameters assumed to have an impact on skewed bridge constructability. Single- and two-span bridges were chosen to investigate the effects of span continuity. Varying the skew angle in two-span bridges was considered to examine the behavior of varying skews during construction. Three-span bridges having balanced and unbalanced spans were selected to examine different span-ratio effects. The supports in the single- and three-span bridges had a severe skew of 50°, and the two-span bridges were skewed of 70° and 50° relative to their supports. The unbalanced three-span bridge had a span ratio of 1:1.4. The designed girder spacing and cross-frame spacing for the selected representative bridges was 3 m (10 ft) and 7.8 m (25.7 ft), respectively. The span length for the single-span, two-span bridges and the balanced, three-span bridge was 54.86 m (180 ft), and the span lengths for the unbalanced, three-span bridge were 39.24 m (128.75 ft) and 54.86 m (180 ft). Table 22 lists the parameters of the selected representative bridges. Simplified framing plans for the selected representative bridges are shown in Figure 101 through Figure 105.

Table 22: Information From Representative Bridges.

Bridge No.	Skew Angle	Cross-Frame Spacing, m (ft)	Girder-Spacing, m (ft)	Number of Spans	Span-Length, m (ft)	Number of Girder, m (ft)
S2	50°	7.8 (25.7)	3 (10)	1	54.86 (180)	4
S6	50°	7.8 (25.7)	3 (10)	2	54.86-54.86 (180-180)	4
S8	70°	7.8 (25.7)	3 (10)	2	54.86-54.86 (180-180)	4
S9	50°	7.8 (25.7)	3 (10)	3	54.86-54.86-54.86 (180-180-180)	4
S10	50°	7.8 (25.7)	3 (10)	3	54.86-54.86-39.24 (180-180-128.75)	4

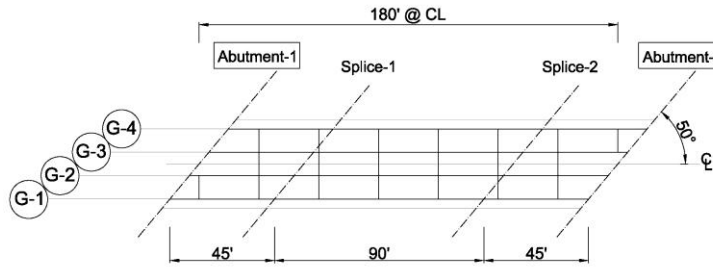


Figure 101: Simplified Framing Plan of Bridge S2: Single-Span, 50° Skew.

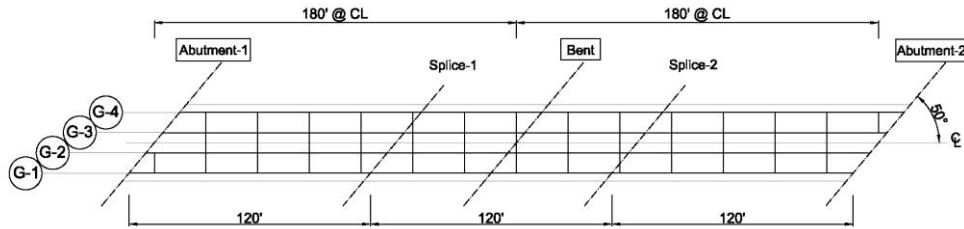


Figure 102: Simplified Framing Plan of Bridge S6: Two-Span, 50° Skew.

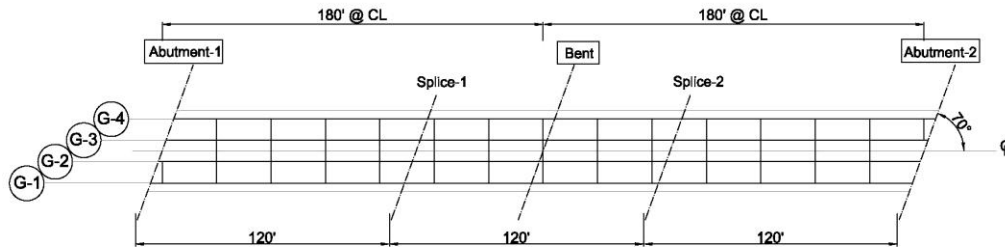


Figure 103: Simplified Framing Plan of Bridge S8: Two-Span, 70° Skew.

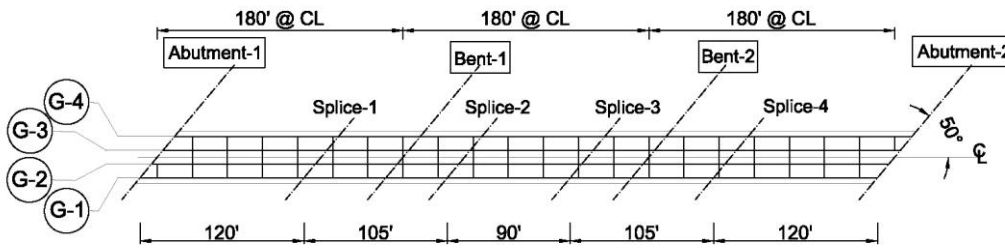


Figure 104: Simplified Framing Plan of Bridge S9: Balanced, Three-Span, 50° Skew.

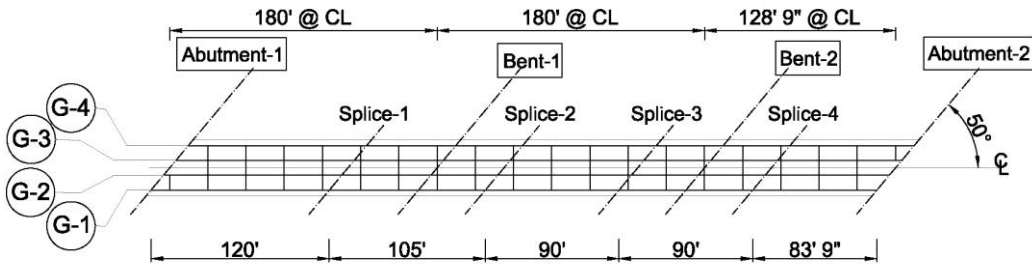


Figure 105: Simplified Framing Plan of Bridge S10: Unbalanced, Three-Span, 50° Skew.

Unlike curved bridges, there is no differentiation between “inner or outer” placement of the girders for the skewed bridges that are studied due to the lack of a center of curvature and the resulting identical span lengths of adjacent bridge girders. Therefore, two erection scenarios were applied to the representative structures to investigate the effects of erection sequencing on their behavior during construction: 1) paired girder erection; and 2) single girder erection. Similar to the curved bridges that were examined, sequential analysis was performed using ABAQUS to examine skewed structure behavior after each construction stage that included girder erection and concrete deck placement. Figure 106 and Figure 107 show the construction stages for the two types of erection sequences that were examined for representative two-span bridge. A similar approach for erection sequencing was used for the single-span and balanced and unbalanced three-span bridges.

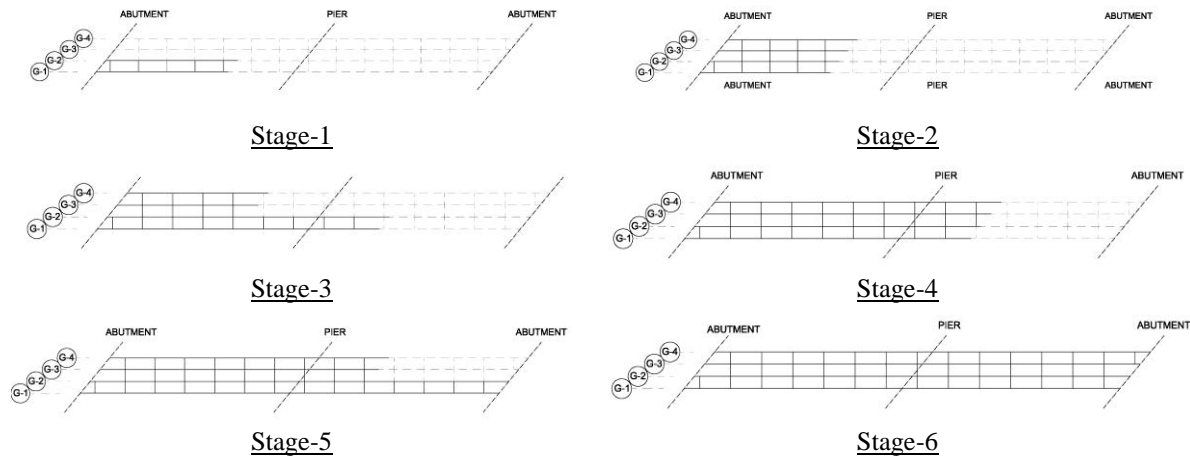


Figure 106: Stage 1 to Stage 6 of Construction for Paired-Girder Erection of Two Equal-Span, 4-Girder Bridges.

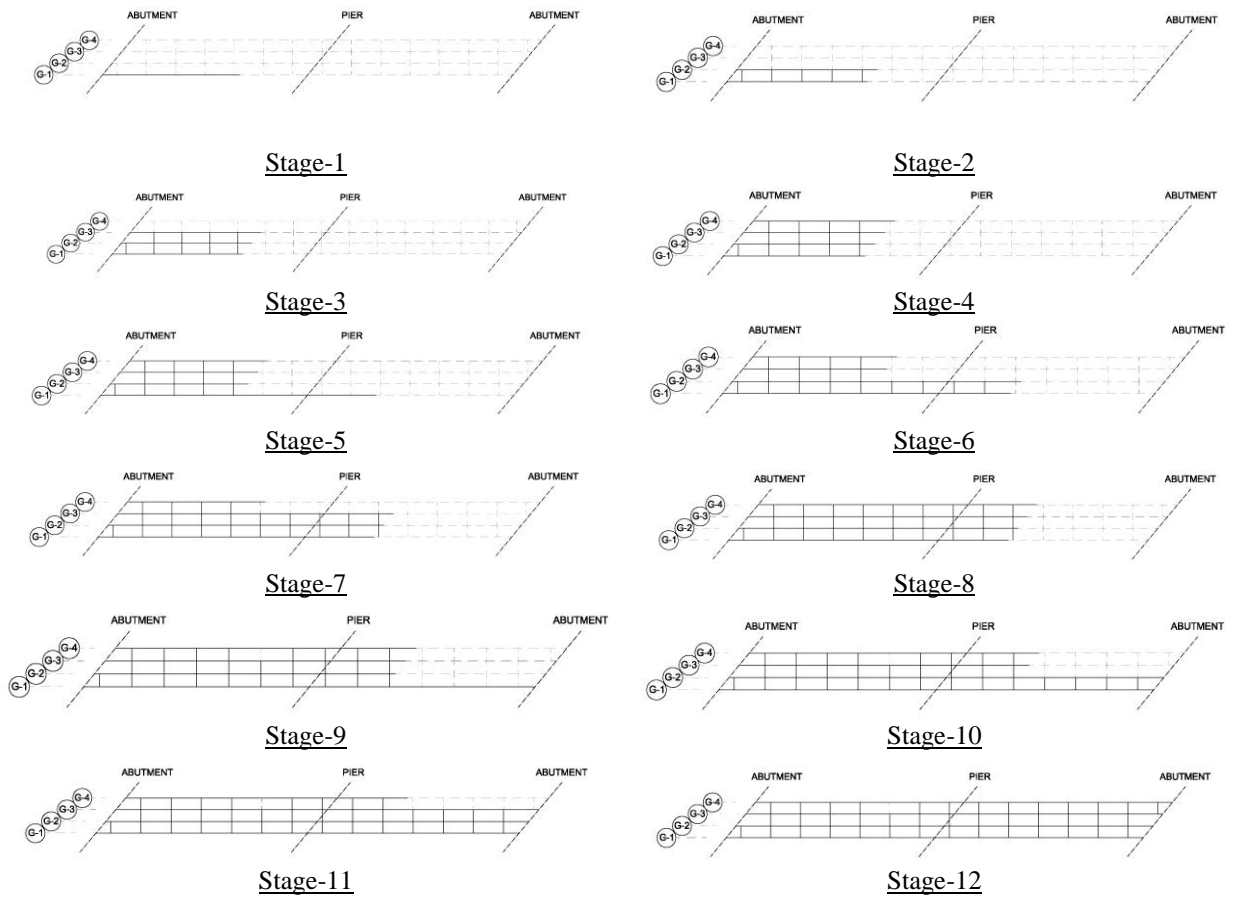


Figure 107: Stage 1 to Stage 12 of Construction for Single-Girder Erection of Two-Equal-Spans, 4-Girder Bridges.

The effects of “drop-in” erection on the constructability of skewed bridges were also examined for balanced and unbalanced three-span structures having a severe skew. The “drop-in” erection sequences for Bridge S-9 and S-10 are shown in Figure 108.

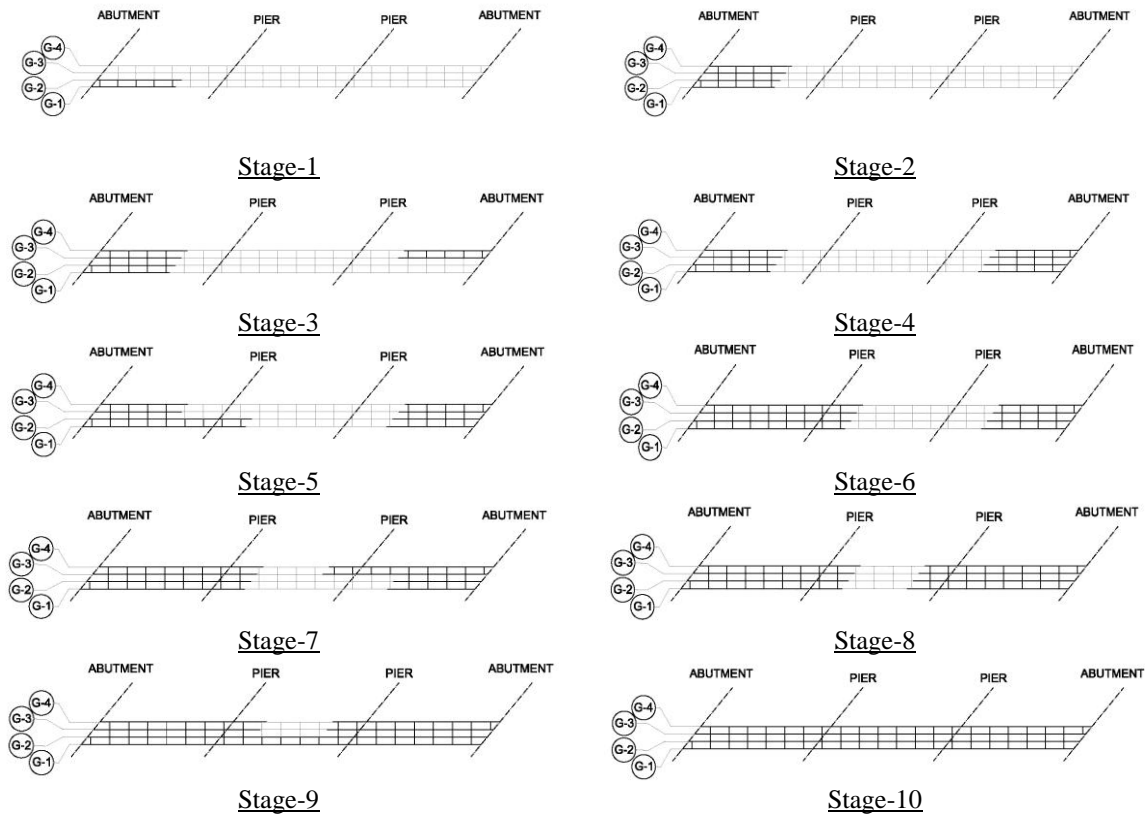


Figure 108: Stage 1 to Stage 10 of Construction for “Drop-In” Erection of Bridge S-9 and Bridge S-10.

5.2.2.2 Representative Structure Studies - Results

As opposed to the curved bridges, lateral deformation of skewed girders during their erection is not significant. Girder twist becomes important during the concrete deck pour for skewed bridges, after the whole steel superstructure has been erected. Therefore, only vertical deflections from the sequential analyses were compared herein to evaluate the influences of different erection scenarios. Vertical deflections were compared at 0.4L from the abutment for the exterior spans and at mid-span for the interior spans, since these locations are where maximum deflections were assumed to occur. In addition, similar the curved bridge study, for each stage of construction the maximum deflections, normalized with respect to the maximum deflection for the paired erection scenario, were examined. Results are shown in Figure 109 through Figure 113, with stage numbers representing the paired erection cases. As can be inferred from the figures, vertical deflections did not change much between the two erection techniques. For the skewed bridges as well as the curved bridges, maximum vertical and radial girder deflections at mid-span and splice locations obtained from the drop-in effect study were all close to those from previous results, which permitted the drop-in erection approach to be adopted as an alternative method. As a result, it is apparent that drop-in erection can not significantly affect the constructability of the skewed structures.

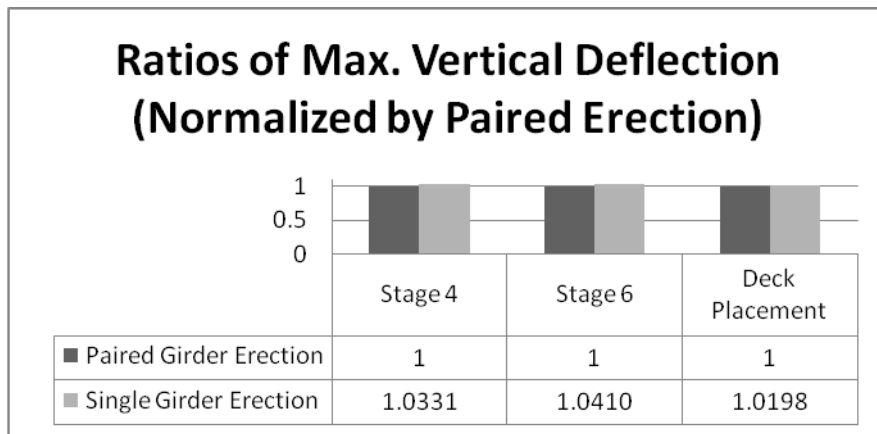


Figure 109: Ratio of Maximum Vertical Deflections for Bridge S2, Single-Span, 50° Skew.

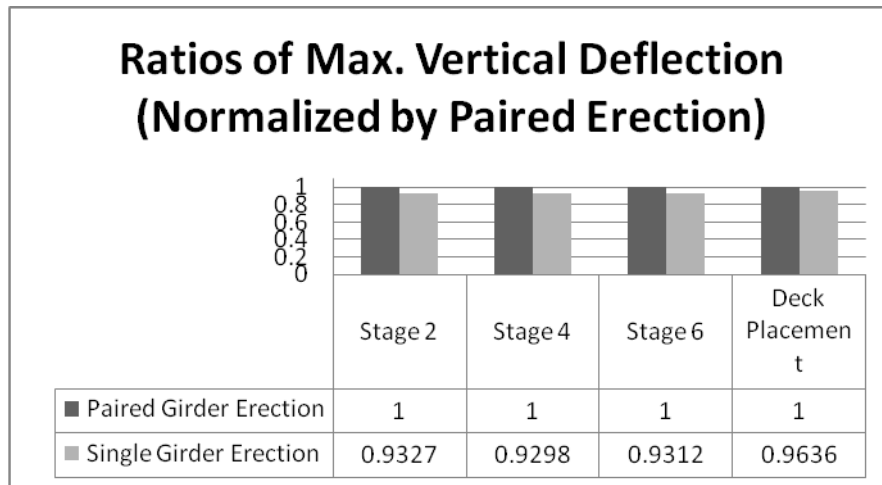


Figure 110: Ratio of Maximum Vertical Deflections for Bridge S6, Two-Span, 50° Skew.

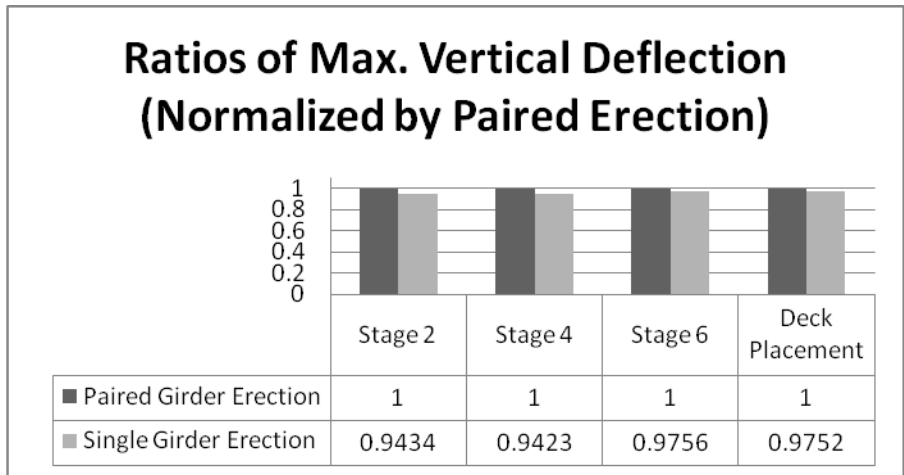


Figure 111: Ratio of Maximum Vertical Deflections for Bridge S8, Two-Span, 70° Skew.

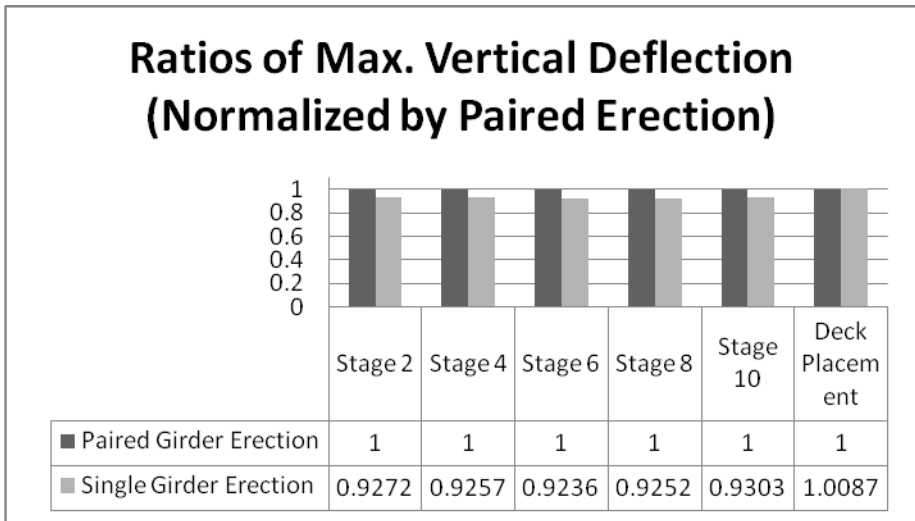


Figure 112: Ratio of Maximum Vertical Deflections For Bridge S9, Balanced Three-Span, 50° Skew.

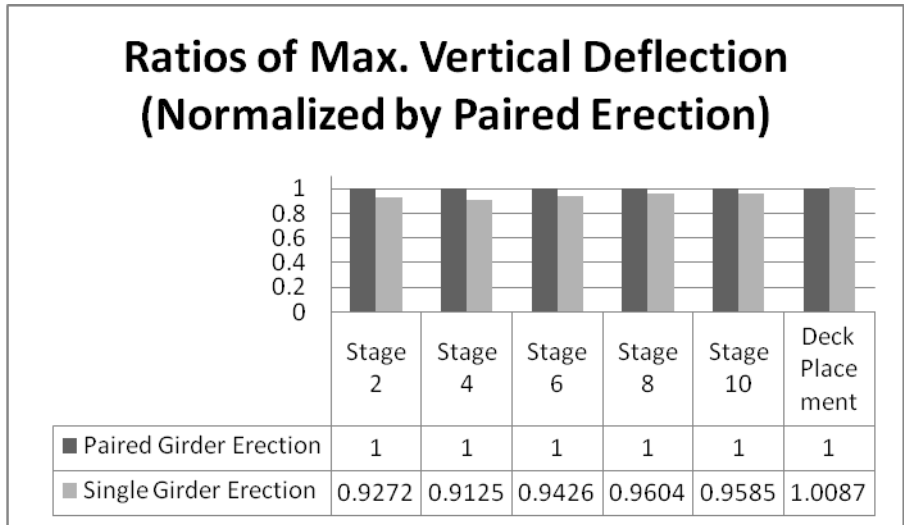


Figure 113: Ratio of Maximum Vertical Deflections for Bridge S10, Unbalanced Three-Span, 50° Skew

5.2.3 Final Results and Discussion

The results from the preliminary and final curved bridge erection sequence studies completed herein indicated that, should adequate crane capacity be available and stability concerns be mitigated, vertical deflections were decreased when paired-girder erection approaches were employed. Radial deflections did not significantly change between the different erection methods that were examined. Of the paired-girder approaches that were studied, paired inner erection was preferred for curved bridges with severe curvature. In addition, it was observed from the results that bridge deflections were mainly controlled by R/L values, boundary conditions, and span lengths, but not by the “drop-in” effect. The observed rotations for sections prior to drop-in erection were small enough to allow for this erection approach should adequate control of the previously erected sections be provided.

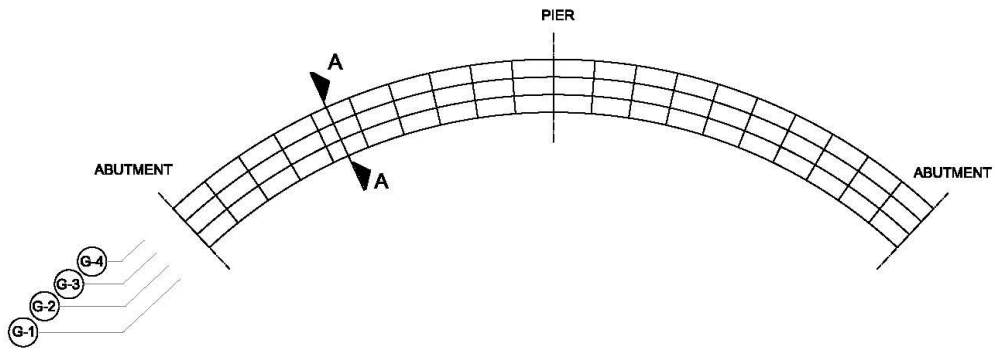
For the skewed structures that were studied, the results indicated very small differences between examined erection techniques for all bridges that were examined. Although paired erection can result in slightly lower vertical deformations compared to single-girder erection, in general there was no marked difference between the techniques. Drop-in erection methods were also permissible for skewed bridges because of the small rotations of the previously erected girders.

In summary, findings from the erection sequencing parametric studies for the curved and skewed bridges that were examined included:

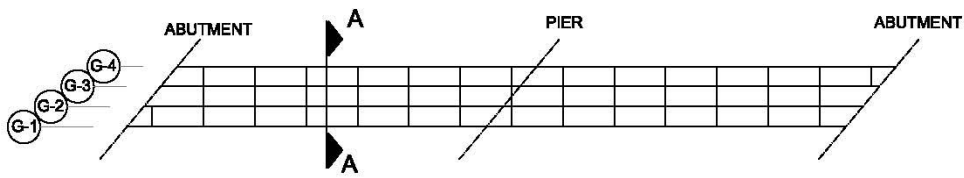
- Curved
 - Girder vertical deflections were decreased when paired girder erection methods were used.
 - Paired inner erection was preferred for structures with severe curvature.
 - Drop-in erection would be an acceptable approach.
- Skewed
 - Erection methods examined herein did not show appreciable influence on skewed bridge behavior.
 - Drop-in erection would be an acceptable approach.

5.3 Web-Plumbness

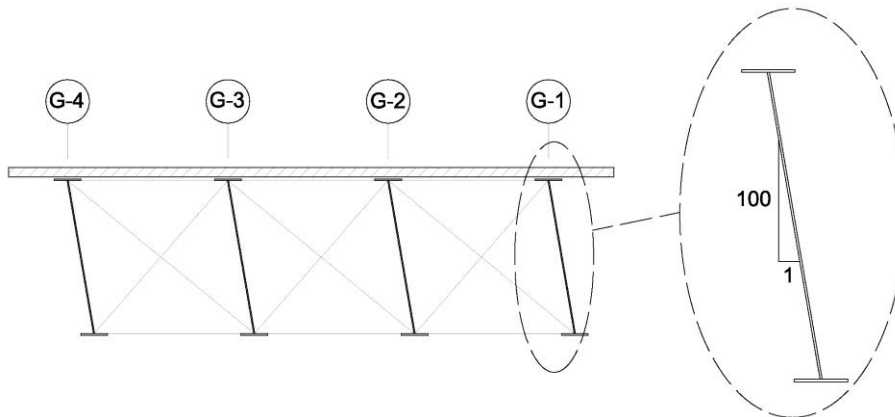
This section examines the effects of web-plumbness on bridge behavior during construction. According to section 5.23 of the Structural Welding Code (AWS, 2004), maximum out-of-straightness of 1 in 100 is allowed for the web of the plate girders. Hence, a 1% web out-of-plumbness was introduced to representative bridges to investigate its effects on the constructability of curved and skewed bridges. This out of plumbness was applied to the girders in a fashion that increased any twist in the girders caused by curvature or global twisting of the structure during deck placement. In the models, the out-of-plumbness was introduced by intentionally tilting whole girder webs by 1% of the web depth (as shown in Figure 114), and the geometries of the cross frames were modified accordingly. The same magnitude and direction for out-of-plumbness was maintained along the entire length of the girders.



a) Curved Bridge Representative Plan



b) Skewed Bridge Representative Plan



c) Section A-A Indicating Web-Out of Plumbness Orientation for Girders in Curved and Skewed Bridges

Figure 114: Girder Web Out-Of-Plumbness Information.

5.3.1 Parametric Studies

5.3.1.1 Curved

In curved bridges, web out-of-plumbness can aggravate the effects of torsional moment due to the curvature. These effects are influenced by the radius and cross-frame spacing. Consequently, the R/L value can be used as a key parameter for this parametric study to ascertain web out-of-plumbness effects. Examination of the effects of web-plumbness on curved bridges consisted of five representative bridges having varying radii and cross-frame spacings. The radii of the selected curved bridges were 91.4 m (300 ft), 198.1 m (650 ft), and 304.8 m (1000 ft), and the cross-frame spacings were 4.57 m (15 ft) and 6.86 m (22.5 ft). These parameters were selected so they included moderately to severely curved bridges with different cross-frame spacings, resulting in a broad range of R/L values (from 13.3 to 66.7). To investigate the effects of web-plumbness, a 1% web out-of-plumbness (as shown in Figure 114) was introduced to girder webs in a fashion that aggravated the curvature effects. Sequential analysis was

performed to examine the effects at each stage, with the paired inner erection method being adopted for this study, since it was considered the preferred erection approach. Table 23 lists parameters for the bridges that were examined.

Table 23 Selected Curved Bridge Web-Plumbness Study Information.

Bridge No.	Radius of Curvature, ft	Cross-Frame Spacing, ft	Girder-Spacing, ft	Number of Spans	Span-Length, ft	Number of Girder, ft
C1	300	15	10	2	225-225	4
C3	300	22.5	10	2	225-225	4
C6	650	22.5	10	2	225-225	4
C7	1000	15	10	2	225-225	4
C9	1000	22.5	10	2	225-225	4

5.3.1.2 Skewed

Five representative skewed bridges were also considered in order to investigate the effects of web-plumbness on their construction behavior. Representative bridges included 1 single-span bridge with a 50° skew and four two-span bridges with 50° and 70° skews and varying cross-frame spacing. The cross-frame spacings in the one-span bridge were 7.8m (25.7 ft), and they were 4.57 m (15 ft) and 7.8 m (25.7 ft) in the two-span bridges. Similar to the study of the curved structures, these parameters were selected so they included both moderately to severely skewed bridges with different cross-frame spacings, and one- and two-span bridges were selected to examine the influence of continuity. Sequential analysis was performed to simulate bridge behavior for each construction stage, and the paired-girder erection method was again adopted. Table 24 lists parameters of the selected representative skewed bridges.

Table 24 Selected Skewed Bridge Web-Plumbness Study Information.

Bridge No.	Skew Angle, degree	Cross-Frame Spacing, ft	Girder-Spacing, ft	Number of Spans	Span-Length, ft	Number of Girder, ft
S2	50	25.7	10	1	180	4
S5	50	15	10	2	180-180	4
S6	50	25.7	10	2	180-180	4
S7	70	15	10	2	180-180	4
S8	70	25.7	10	2	180-180	4

5.3.2 Results and Discussion

5.3.2.1 Curved

Similar to the erection sequencing study, vertical and radial deflections were primarily compared to examine the effects of web-plumbness on construction response. At each stage, maximum girder vertical deflections and maximum radial deflections at splice locations were examined for the out-of-plumb cases, with those maximum deflections being normalized by the maximum deflections for the baseline case that had plumb webs. Comparisons are shown in Figure 115 to Figure 124.

The results showed that the effects of web out-of-plumbness on both vertical and radial deflections were insignificant. Not surprisingly, the change in vertical deflections due to web out-of-plumbness was negligible (typically less than 1%). Although the change in ratios of radial deflections was larger than that for vertical deflections, those deflection changes were small compared to the radial deflections due to curvature effects. Furthermore, cumulative stresses in the cross frames were checked for two of the severely curved bridges (R=300'). To examine out-of-plumbness effects on stresses in the structures, comparisons of maximum Von Mises stresses,

which account for the effects of axial, bending and shear stresses in the cross frames, are presented in Figure 125 and Figure 126. Similar findings were observed from the stress results. The changes in stresses in cross frames were less than 1%. Hence, the effects of a 1% web out-of-plumbness on bridge constructability are considered small for the structures that were studied.

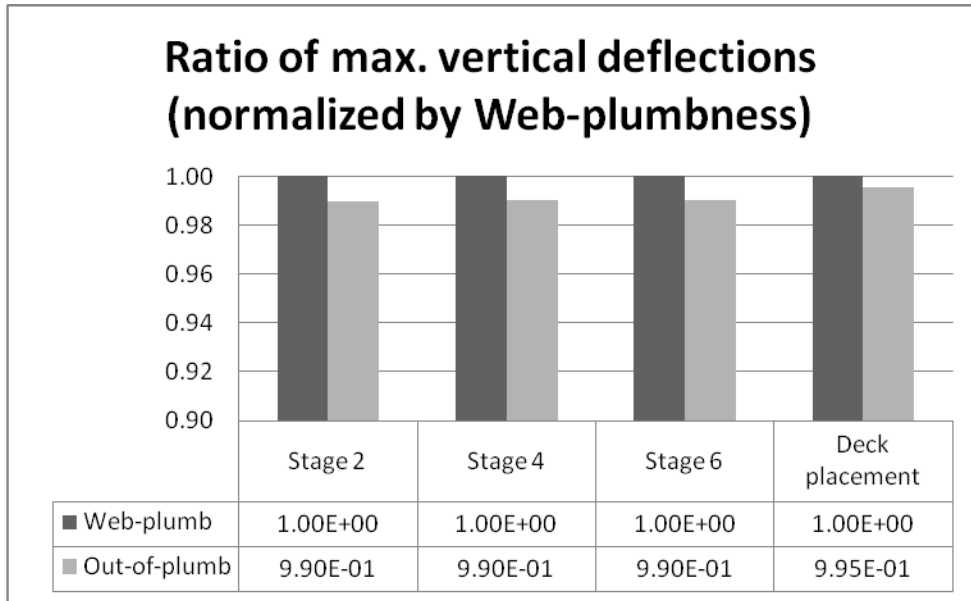


Figure 115: Ratio of Maximum Vertical Deflections for Bridge C1.

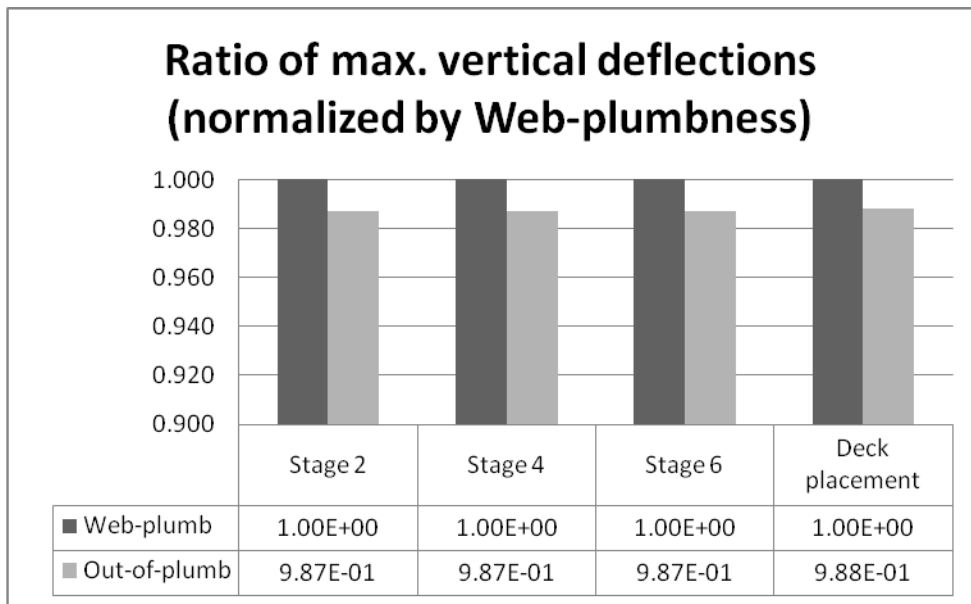


Figure 116: Ratio of Maximum Vertical Deflections for Bridge C3.

Ratio of max. vertical deflections (normalized by Web-plumbness)

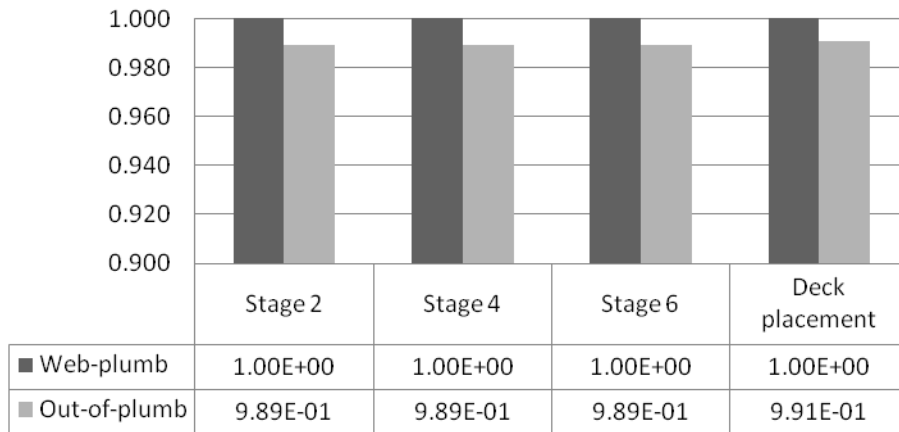


Figure 117: Ratio of Maximum Vertical Deflections for Bridge C6.

Ratio of max. vertical deflections (normalized by Web-plumbness)

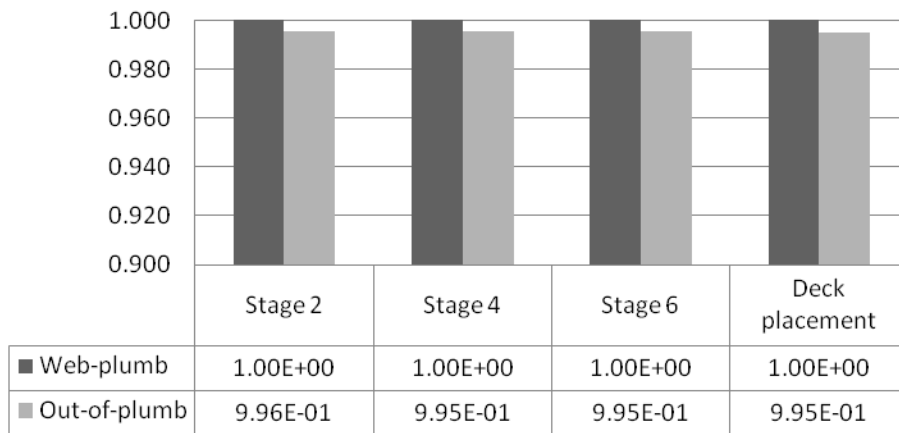


Figure 118: Ratio of Maximum Vertical Deflections for Bridge C7.

Ratio of max. vertical deflections (normalized by web-plumbness)

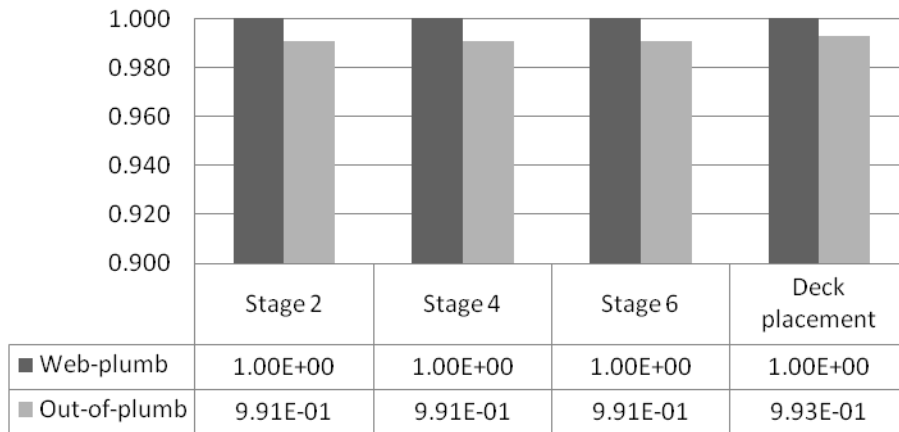


Figure 119: Ratio of Maximum Vertical Deflections for Bridge C9.

Ratio of max. radial deflections (normalized by Web-plumbness)

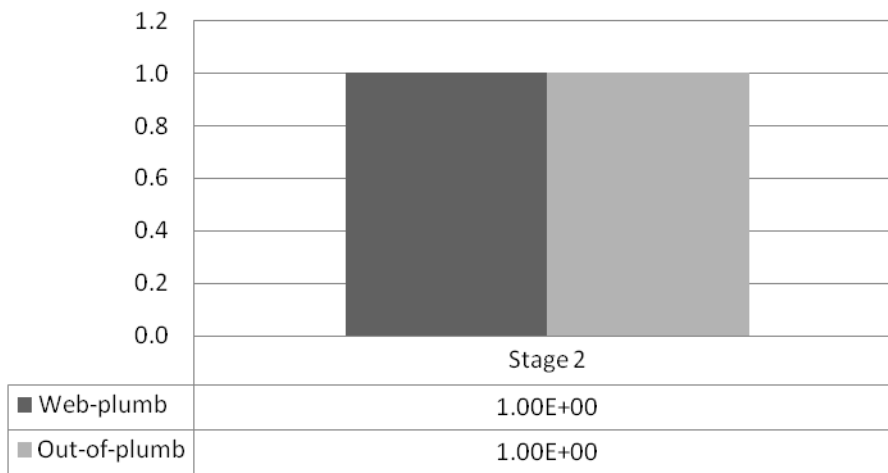


Figure 120: Ratio of Maximum Radial Deflections for Bridge C1.

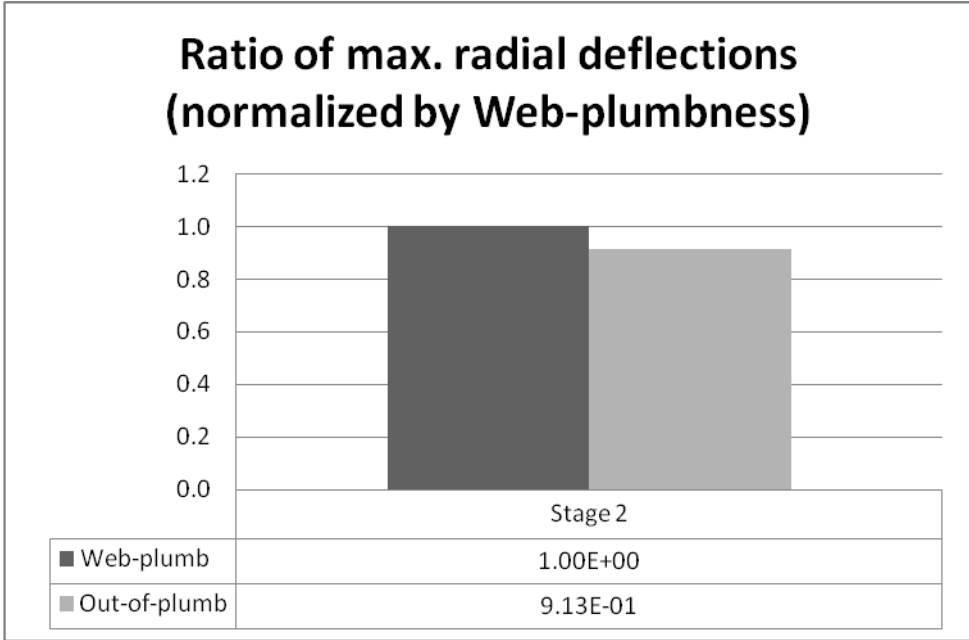


Figure 121: Ratio of Maximum Radial Deflections for Bridge C3.

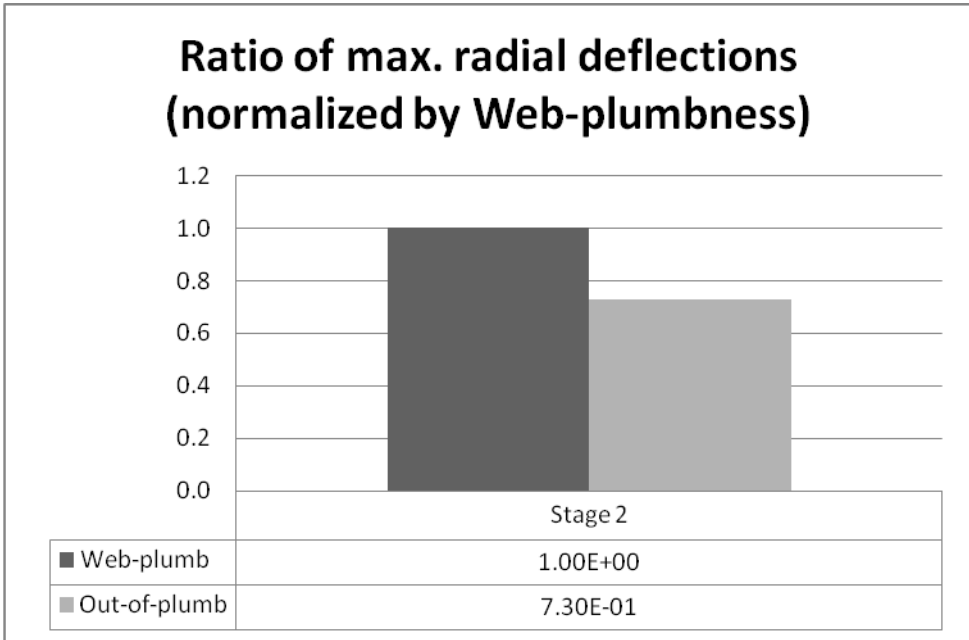


Figure 122: Ratio of Maximum Radial Deflections for Bridge C6.

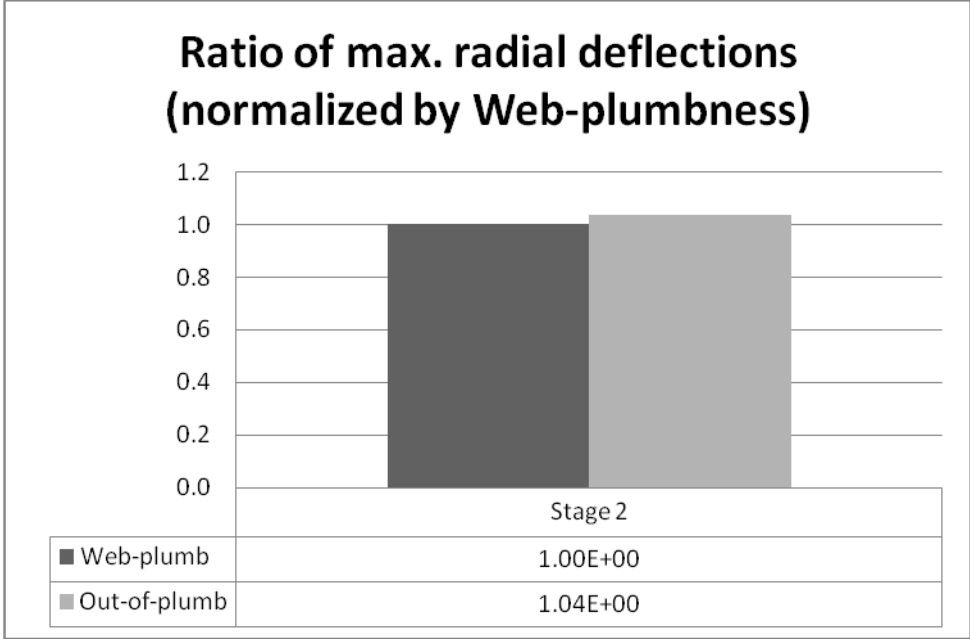


Figure 123: Ratio of Maximum Radial Deflections for Bridge C7.

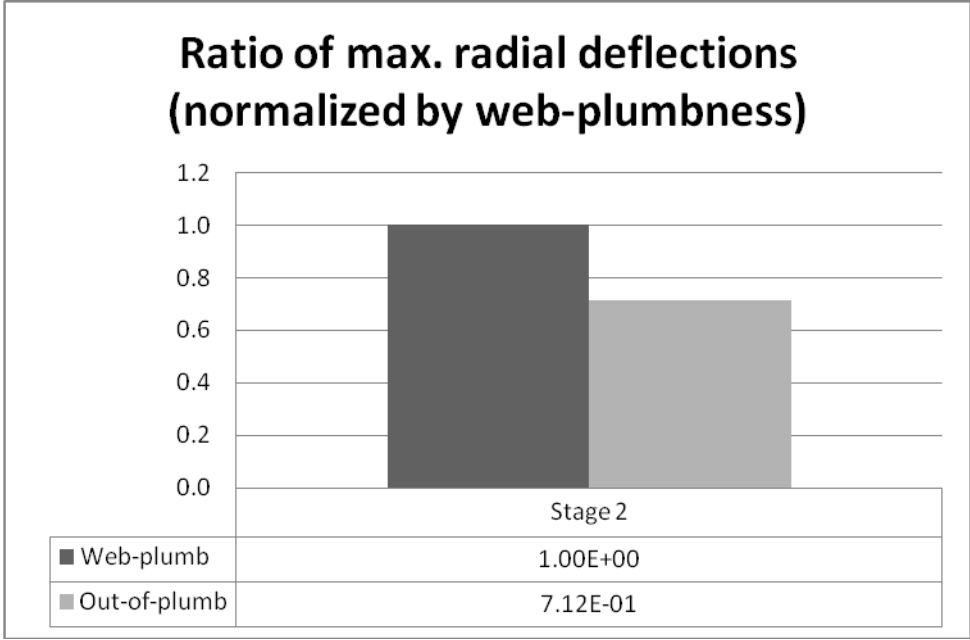


Figure 124: Ratio of Maximum Radial Deflections for Bridge C9.

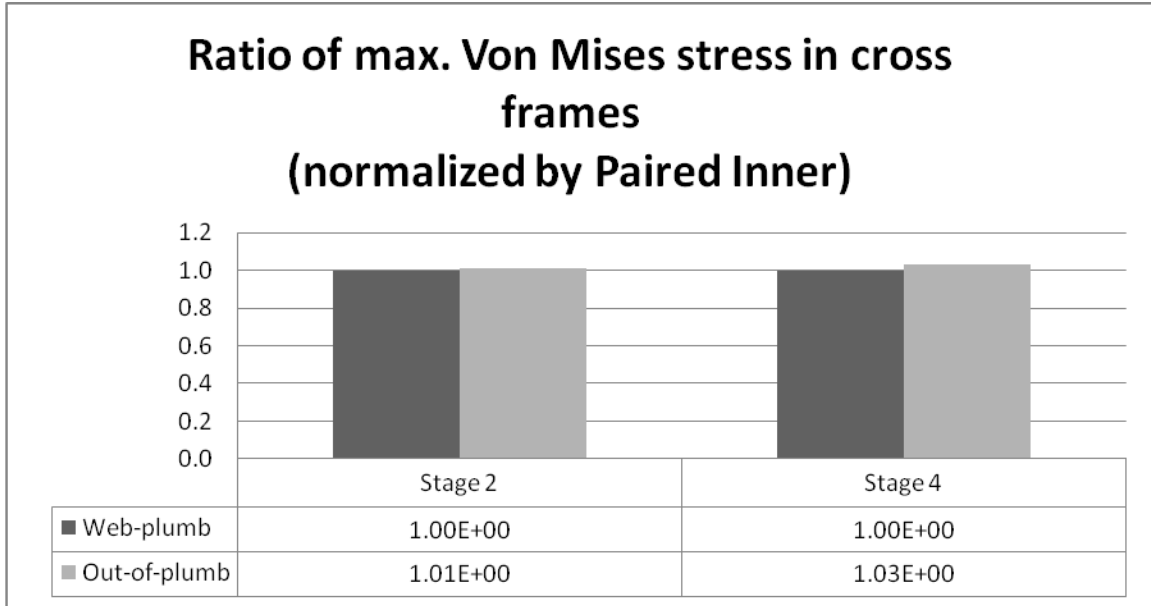


Figure 125: Ratio of Maximum Von Mises Stresses in Cross Frames for Bridge C1.

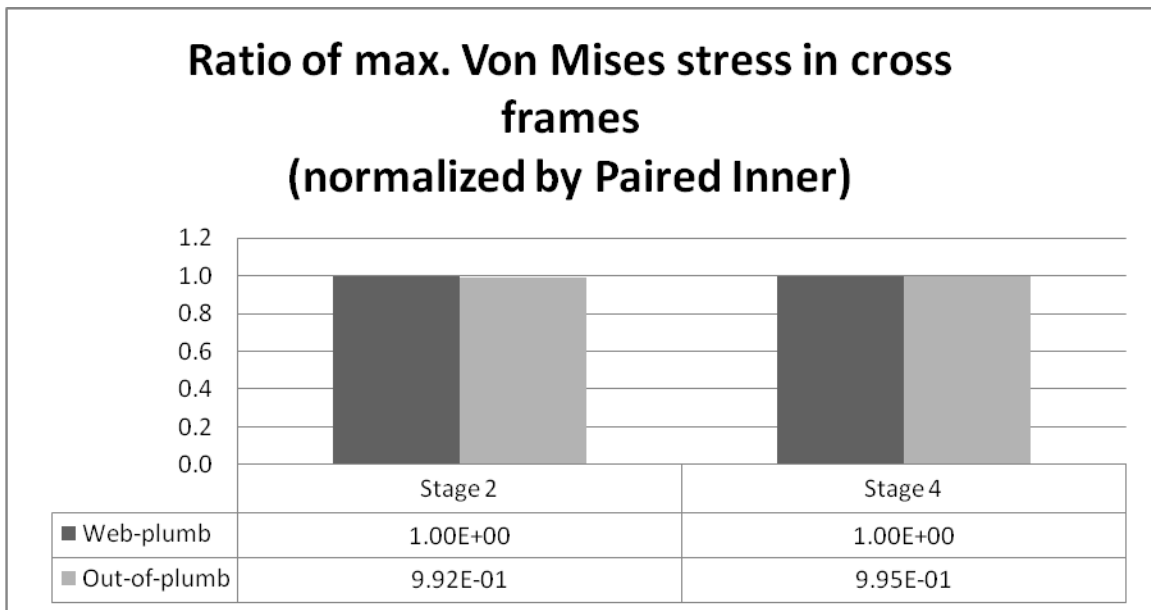


Figure 126: Ratio of Maximum Von Mises Stresses in Cross Frames for Bridge C3.

An additional investigation into the effects of unintentional web out-of-plumbness on the behavior of curved bridges occurred via the examination of six times the allowable value (6%) for Bridge C3, a structure with critical R/L values from those that were studied and one that showed slightly larger changes in deformations and stresses for 1% out-of-plumbness when compared to the other structures that were examined (see Table 4). The 6% value was applied to the girders in the same fashion as that used for 1% and vertical and radial deflections and Von Mises stresses in the cross frames were compared to the baseline, web plumb case, to examine their effects. Comparisons are shown in Figure 127 through Figure 129. As shown in these figures, with an extreme web out-of-plumbness of 6%, changes in deformations and stresses were 20% or less. This indicates that these levels of out-of-plumbness, which are certainly a concern from a constructability perspective, do not impose a drastic change to curved bridge behavior during construction and that global curvature effects dominate the construction behavior. It should also be noted that web out-of-plumbness was shown to have a slightly larger influence on radial deformations than on vertical deformations and cross frame stresses, irrespective of the out-of-plumbness magnitude.

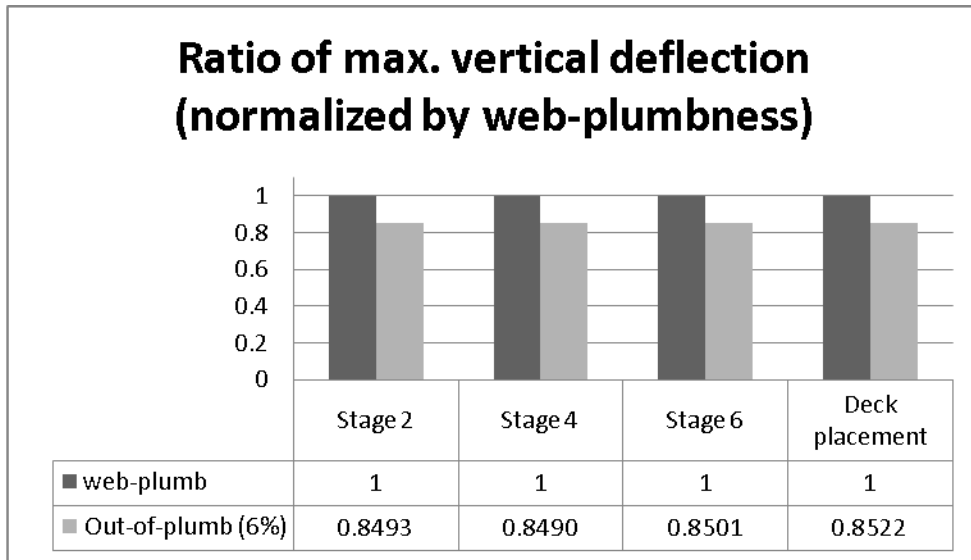


Figure 127. Ratio of Maximum Vertical Deflections for Bridge C3, 6% Out-of-Plumbness.

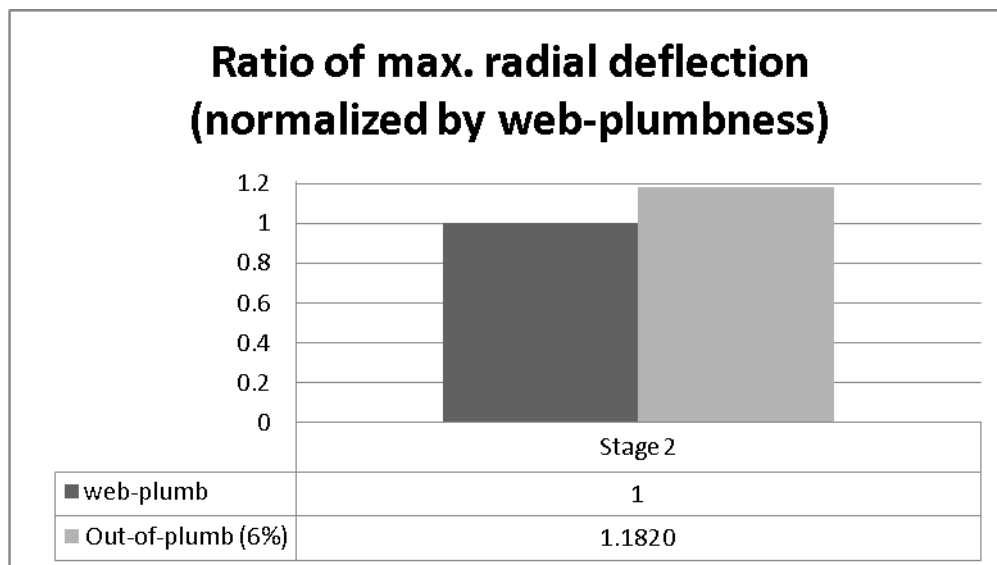


Figure 128. Ratio of Maximum Radial Deflections for Bridge C3, 6% Out-of-Plumbness.

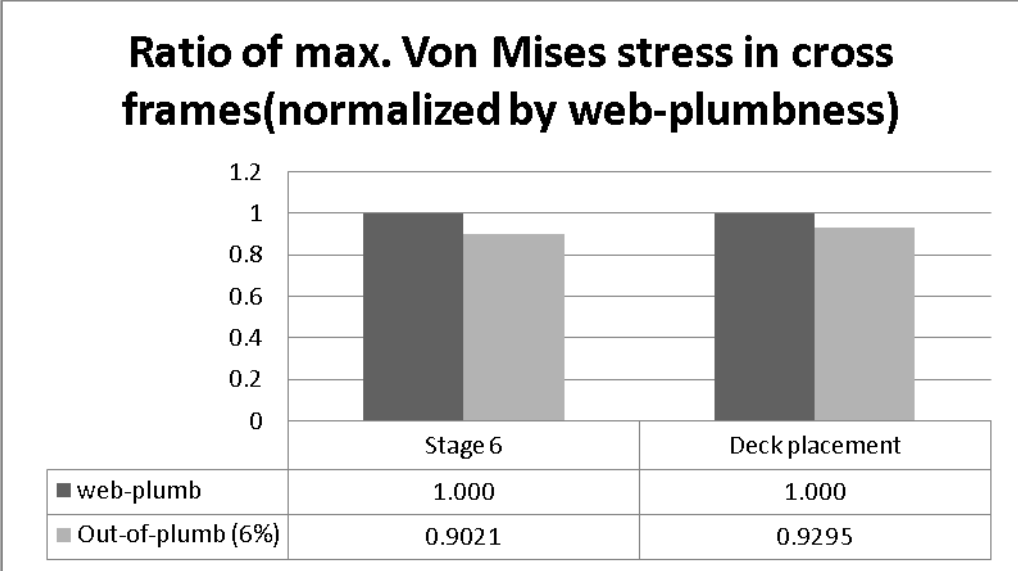


Figure 129 Ratio of Maximum Von Mises Stresses in Cross Frames for Bridge C3, 6% Out-of-Plumbness.

5.3.2.2 Skewed

Vertical and radial deflections were also assumed to be important indices for examining the effects of web-plumbness on skewed bridges. At each stage, the maximum vertical deflections in girders and the maximum radial deflections at splice locations for web-plumb and web out-of-plumb structures were compared. All the deformation values were normalized with respect to these results from the web-plumb bridges. Comparisons of deflections between web-plumb and web out-of-plumb structures are shown in Figure 130 through Figure 139.

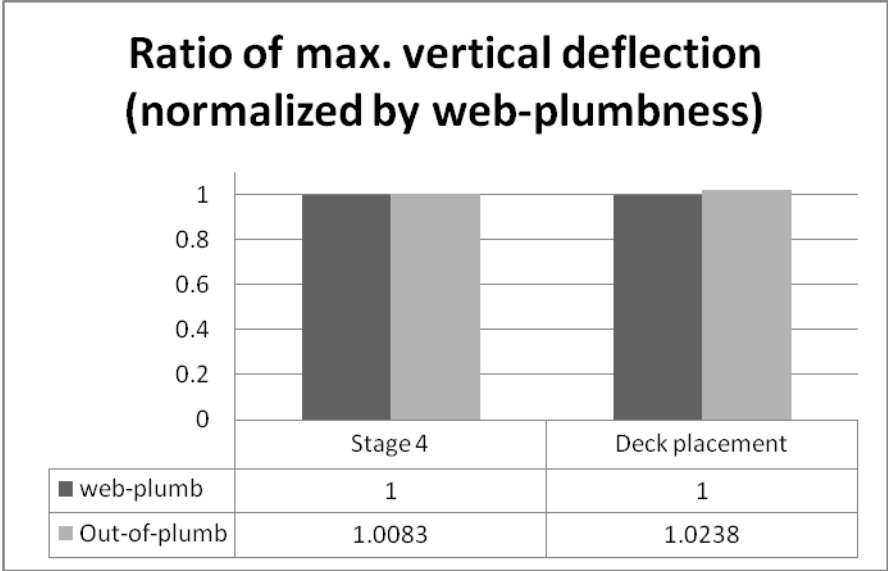


Figure 130: Ratio of Maximum Vertical Deflections for Bridge S2.

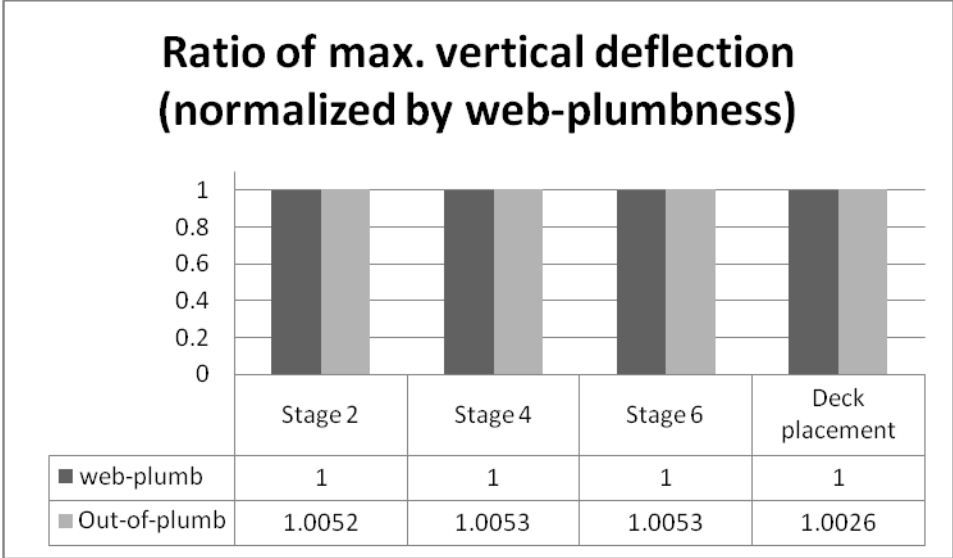


Figure 131: Ratio of Maximum Vertical Deflections for Bridge S5.

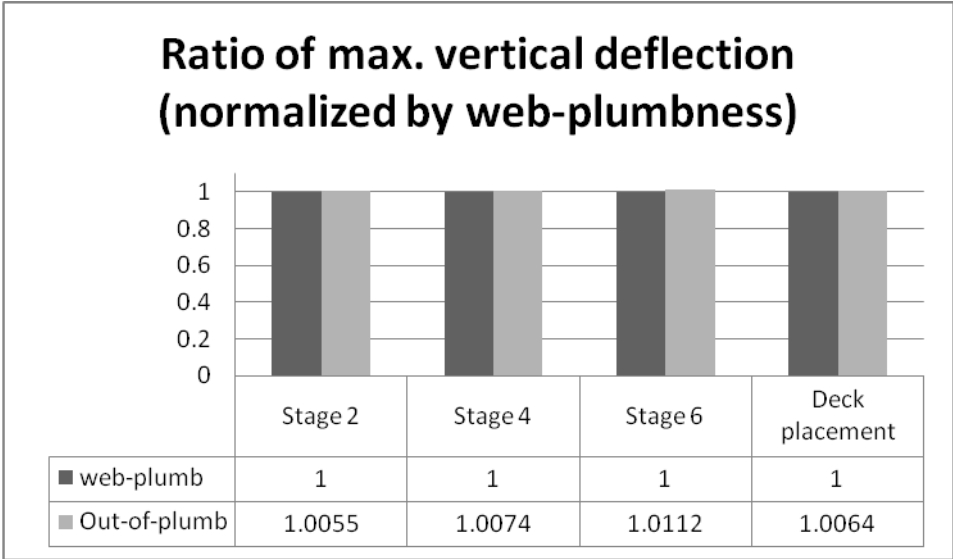


Figure 132: Ratio of Maximum Vertical Deflections for Bridge S6.

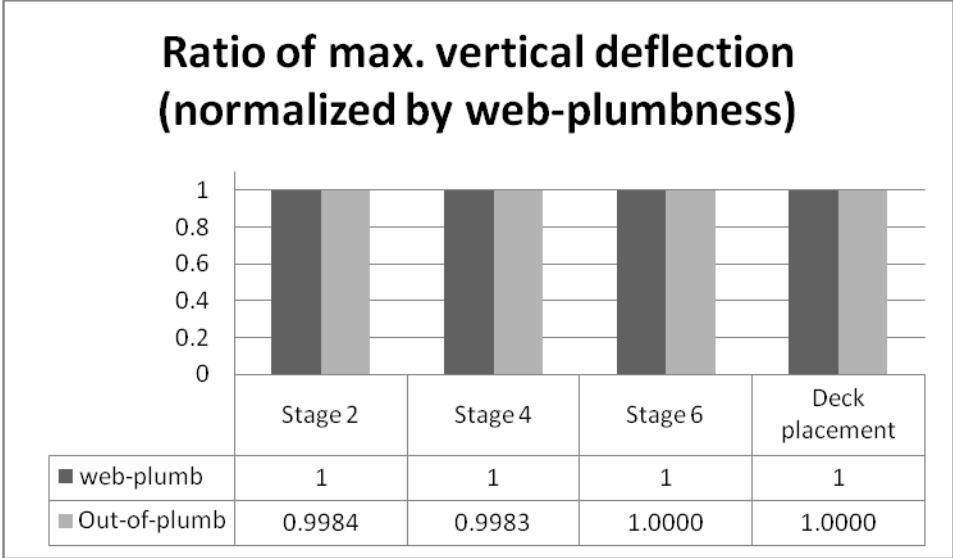


Figure 133: Ratio of Maximum Vertical Deflections for Bridge S7.

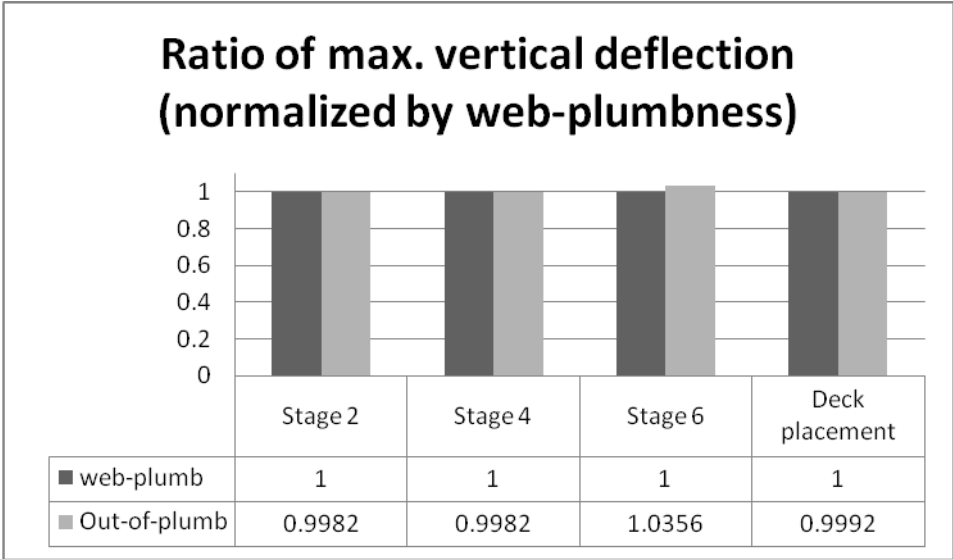


Figure 134: Ratio of Maximum Vertical Deflections for Bridge S8.

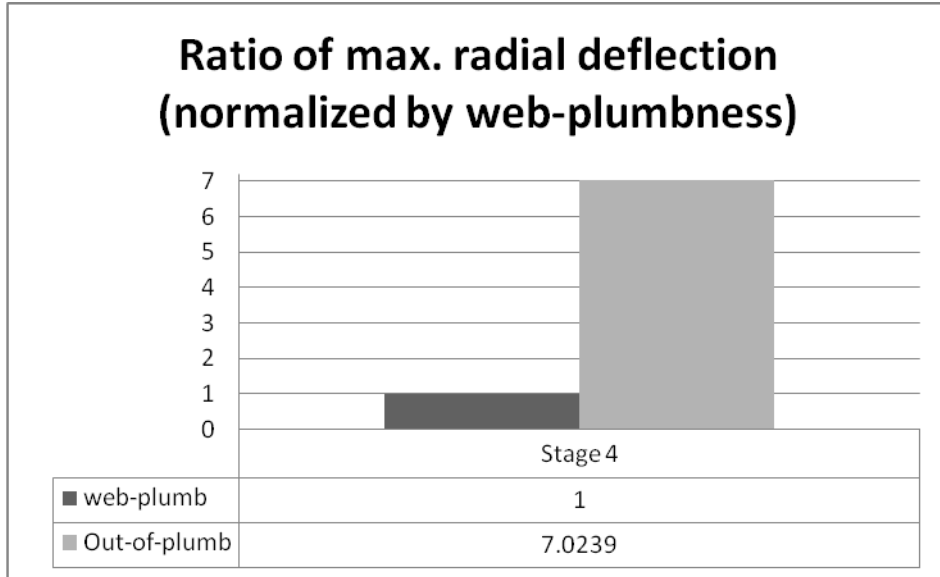


Figure 135: Ratio of Maximum Radial Deflections for Bridge S2.

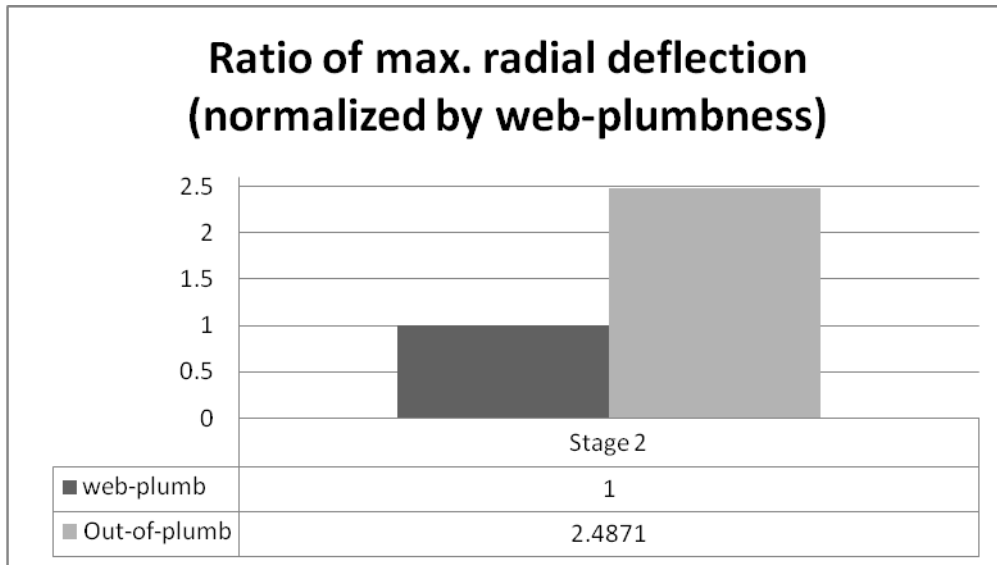


Figure 136: Ratio of Maximum Radial Deflections for Bridge S5.

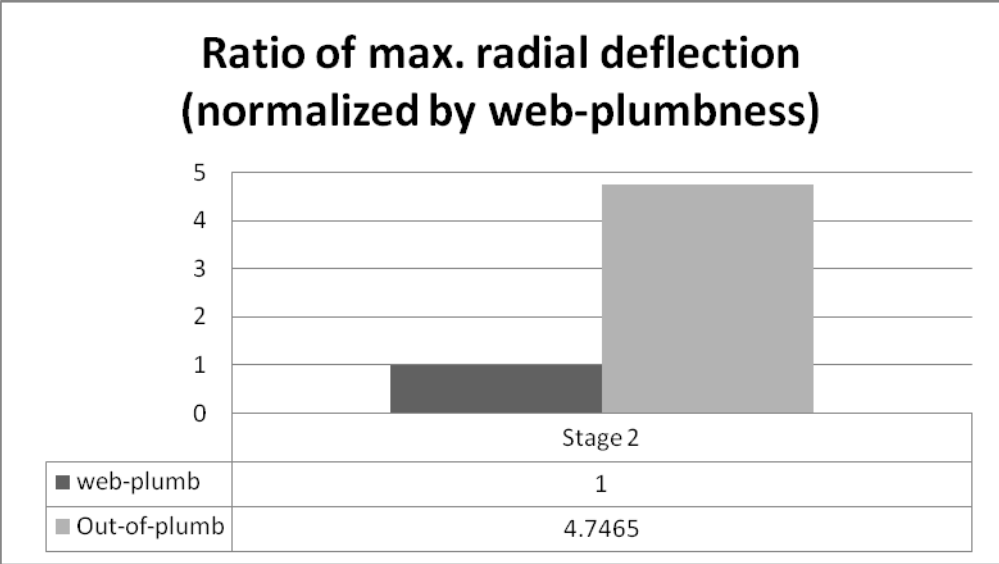


Figure 137: Ratio of Maximum Radial Deflections for Bridge S6.

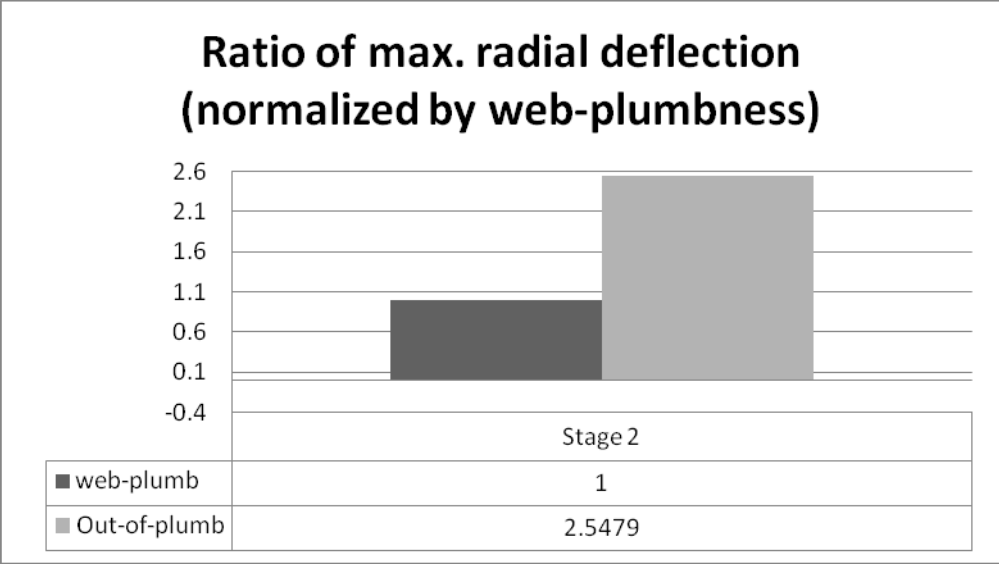


Figure 138: Ratio of Maximum Radial Reflections for Bridge S7.

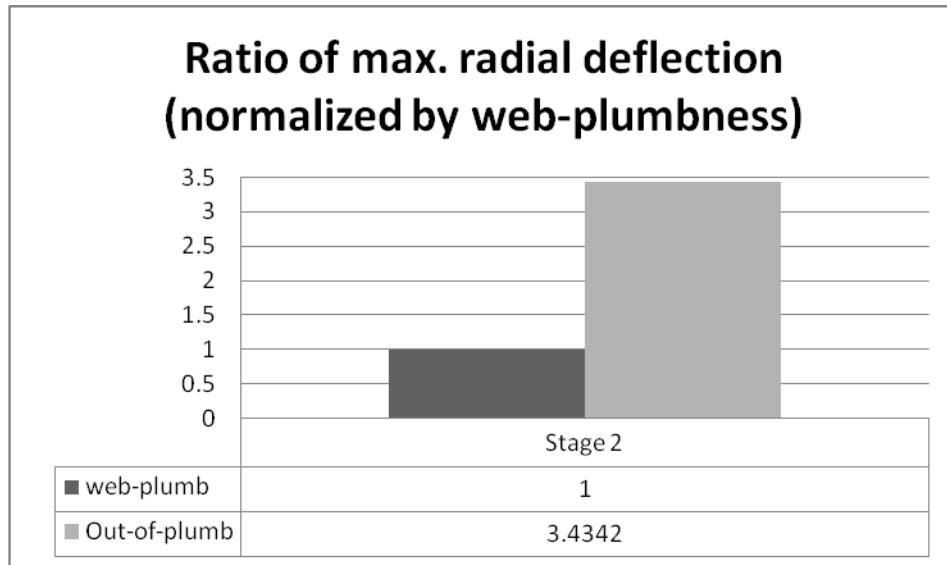


Figure 139: Ratio of Maximum Radial Deflections for Bridge S8.

Similar to the study of curved bridges, the results showed that web out-of-plumbness had a very small impact on vertical deformations, with effects being smaller than those on the curved bridges. For lateral deformations, as shown in the figures, the web out-of-plumbness caused a large increase in nondimensional ratios. As discussed in the previous section, the large difference is caused by a slight increase in lateral deformation, and it not a significant issue during the construction of these bridges. Cross-frame cumulative stresses were also checked for two of the severely skewed bridges (50° skew). Comparisons of maximum Von Mises stresses in the cross frames are presented in Figure 140 and Figure 141. Similar findings to the curved structures were observed, with changes in cross-frames stresses being less than about 1%. Based on previously discussed results from this parametric study, it was surmized that the effects of 1% web out-of-plumbness on skewed bridges during their construction were small.

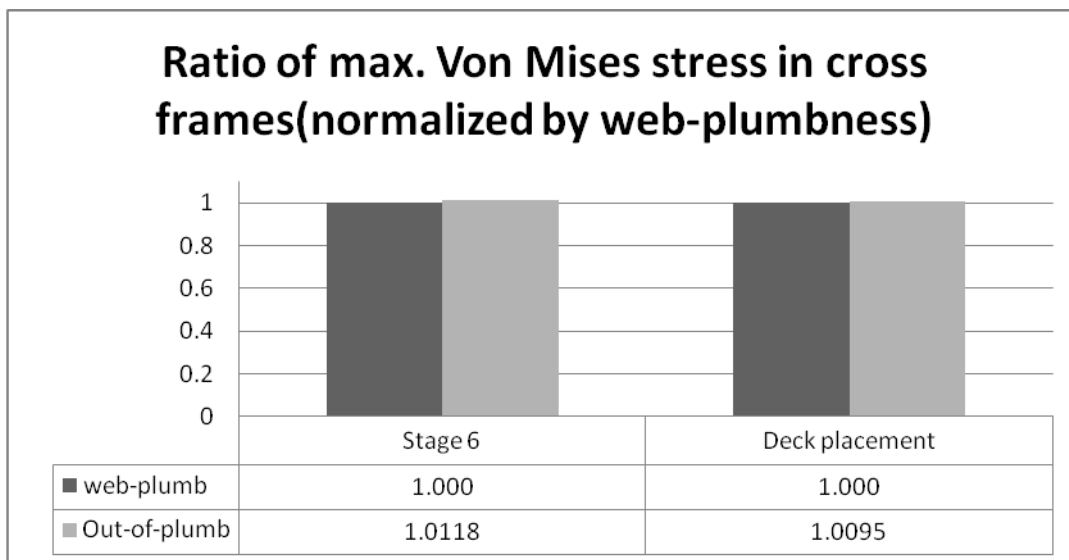


Figure 140: Ratio of Maximum Von Mises Stresses in Cross Frames for Bridge S5.

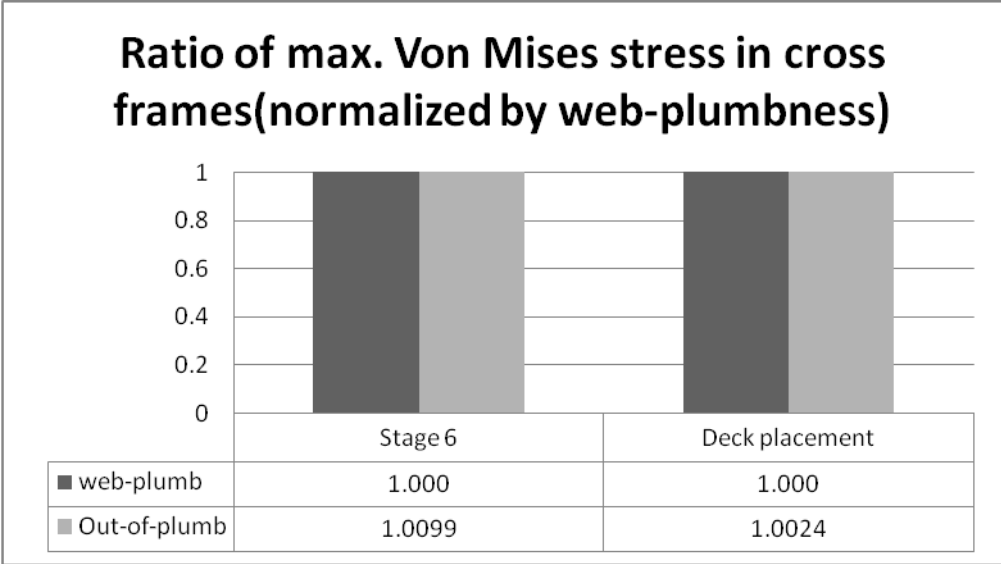


Figure 141: Ratio of Maximum Von Mises Stresses in Cross Frames for Bridge S6.

In similar fashion to the curved bridges, a 6% web out-of-plumbness was considered for Bridge S6, a structure having the largest skew angle and cross frame spacing and one that was shown to have a slightly larger influence on its behavior for 1% out-of-plumbness among those that were studied (Table 4). The 6% out-of-plumbness was applied in the same fashion that was used for 1% and vertical and lateral girder deflections and Von Mises stresses in the cross frames were compared to the baseline, web-plumb, case. Comparisons are shown in Figure 142 through Figure 144.

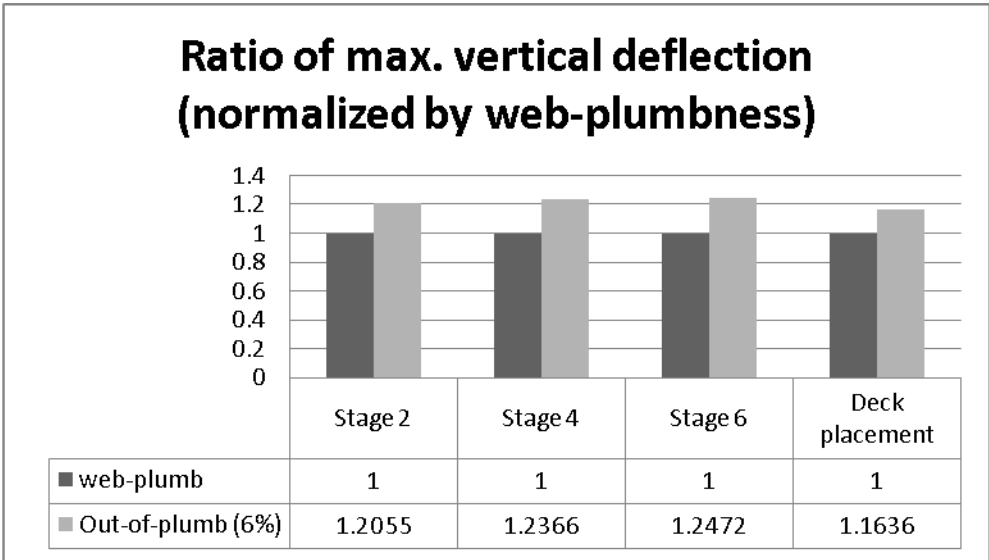


Figure 142: Ratio of Maximum Vertical Deflections for Bridge S6, 6% Out-of-Plumbness..

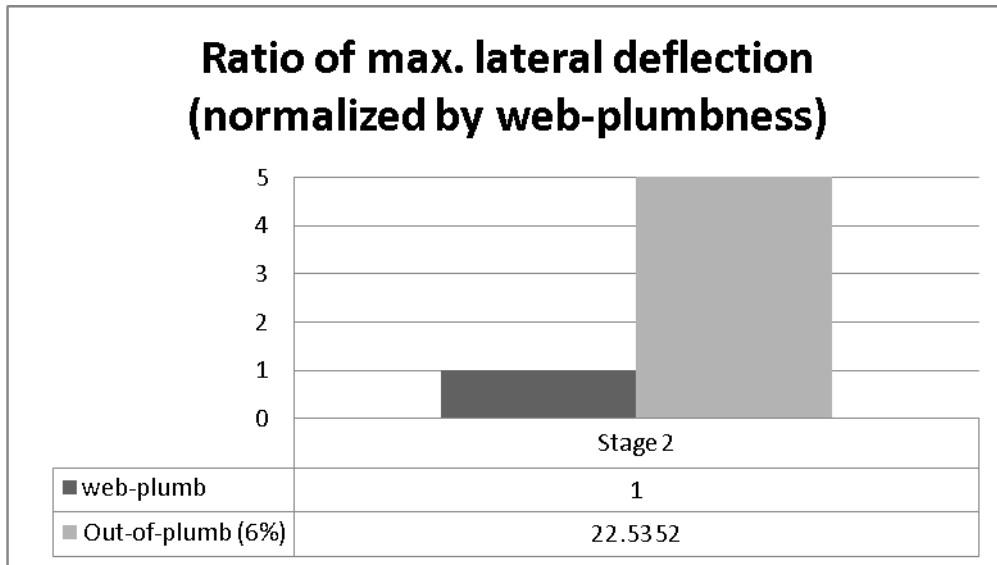


Figure 143: Ratio of Maximum Lateral Deformations for Bridge S6, 6% Out-of-Plumbness.

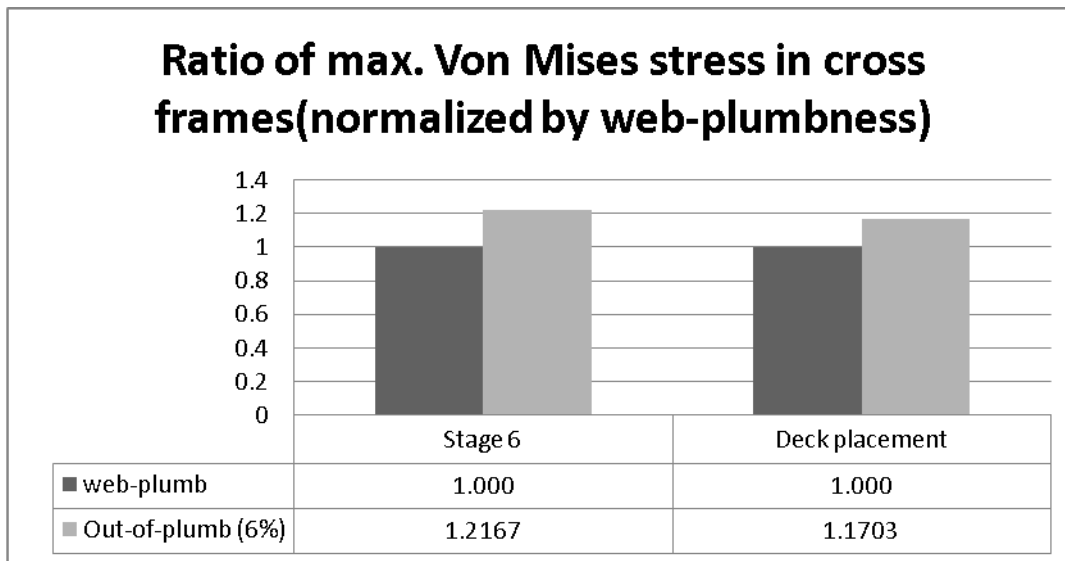


Figure 144: Ratio of Maximum Von Mises Stresses in Cross Frames for Bridge S6, 6% Out-of-Plumbness.

Based on the results, the 6% web out-of-plumbness in the skewed bridge could change vertical deflections of the girders and stresses in the cross frames by a maximum of approximately 25% when compared to the web-plumb case, values that are slightly larger than those seen for the curved bridge with similar web out-of-plumbness. For girder lateral deformations, however, a sixfold increase in web out-of-plumbness resulted in an increase in their values by approximately six times. This demonstrates that, unlike for curved bridges where global curvature dominates the behavior, for skewed structures the effects of web out-of-plumbness are more pronounced and, if accounted for during erection, can be taken advantage of to ensure a web-plumb position at the completion of construction.

5.3.2.3 Summary

This section examined the effects of web-plumbness on bridge constructability for curved and skewed structures by comparing girder deflections and cross-frame stresses. A 1% web out-of-plumbness was applied to all bridge girders in a fashion that increased any twist in the girders caused by curvature or global twisting of the structure during deck placement. Results showed that no appreciable deflection and stress changes were observed between the web-

plumbness and web out-of-plumbness cases. Therefore, the effects of web-plumbness on curved and skewed bridge constructability are considered not significant.

In summary, findings from the web-plumbness parametric studies for the curved and skewed bridges that were examined included:

- Curved
 - Web out-of-plumbness did not cause appreciable bridge deflection and stress increases when the out-of-plumbness was within the limit (1%) specified in the Structural Welding Code (AWS, 2004).
 - Exceeding the 1% limit of the web out-of-plumbness can result in slightly higher vertical and lateral deformations and also stresses. However, the effects of horizontal curvature on these parameters are much larger than those from the web out-of-plumbness.

- Skewed
 - Web out-of-plumbness did not cause appreciable bridge deflection and stress increases when the out-of-plumbness was within the limit (1%) specified in the Structural Welding Code (AWS, 2004).
 - Exceeding the 1% limit of the web out-of-plumbness can result in slightly higher vertical deformations and stresses. However, the effects on lateral deformations are more pronounced. As a result, the effects of web-out-of plumbness, which could be beneficial to ensure web-plumb at the completion of construction, should be considered during the erection of structures having a skew less than 70°.

5.4 Temporary Shoring Placement and Settlement Effects

5.4.1 Parametric Studies

5.4.1.1 Curved

Eight representative bridges were selected to investigate the effects of temporary shoring placement on curved bridge behavior during construction. The selected bridges were two-span structures with varying radii and cross-frame spacings and three-span structures with balanced and unbalanced spans. The radii of the two-span bridges were 91.4 m (300 ft), 198.1 m (650 ft), and 304.8 m (1000 ft), and the cross-frame spacings were 4.57 m (15 ft) and 6.86 m (22.5 ft). These parameters were selected so that they included moderately to severely curved bridges with different cross-frame spacings, resulting in R/L values from 13.3 to 66.7. The balanced and unbalanced three-span, four-girder bridges had the same radius (91.4 m (300ft)) and cross-frame spacing (6.86 m (22.5 ft)), with the unbalanced span ratio being 1:1.4. Sequential analysis was performed to simulate bridge behavior for each construction stage. The paired inner erection method was adopted in this study since it was considered the preferred erection approach from the erection sequencing investigations.

Table 25 lists the parameters of the selected representative bridges.

Table 25: Selected Curved Bridge Temporary Shoring Study Information.

Bridge No.	Radius of Curvature, m (ft)	Cross-Frame Spacing, m (ft)	Girder-Spacing, m (ft)	Number of Spans	Span-Length, m (ft)	Number of Girder
C1	91.4 (300)	4.57 (15)	3 (10)	2	68.6-68.6 (225-225)	4
C3	91.4 (300)	6.86 (22.5)	3 (10)	2	68.6-68.6 (225-225)	4
C6	198.1 (650)	6.86 (22.5)	3 (10)	2	68.6-68.6 (225-225)	4
C7	304.8 (1000)	4.57 (15)	3 (10)	2	68.6-68.6 (225-225)	4
C9	304.8 (1000)	6.86 (22.5)	3 (10)	2	68.6-68.6 (225-225)	4
C10	91.4 (300)	6.86 (22.5)	3 (10)	3	68.6-68.6-68.6 (225-225-225)	4
C11	91.4 (300)	6.86 (22.5)	3 (10)	3	48-68.6-68.6 (157.5-225-225)	4
C12	91.4 (300)	6.86 (22.5)	3 (10)	3	48-68.6-48 (157.5-225-157.5)	4

Three shoring conditions were investigated to determine their effects on bridge constructability. The first shoring condition was to place supports at splice locations only; the second condition was to place supports at splice locations as well as at 0.4L (for the exterior span) and 0.5L (for the interior span) of the span when the span was longer than 100 ft; and the third condition was to place supports at 0.75L of the span.

Figure 145 through Figure 148 show the three shoring conditions for the selected two-span and three-span bridges.

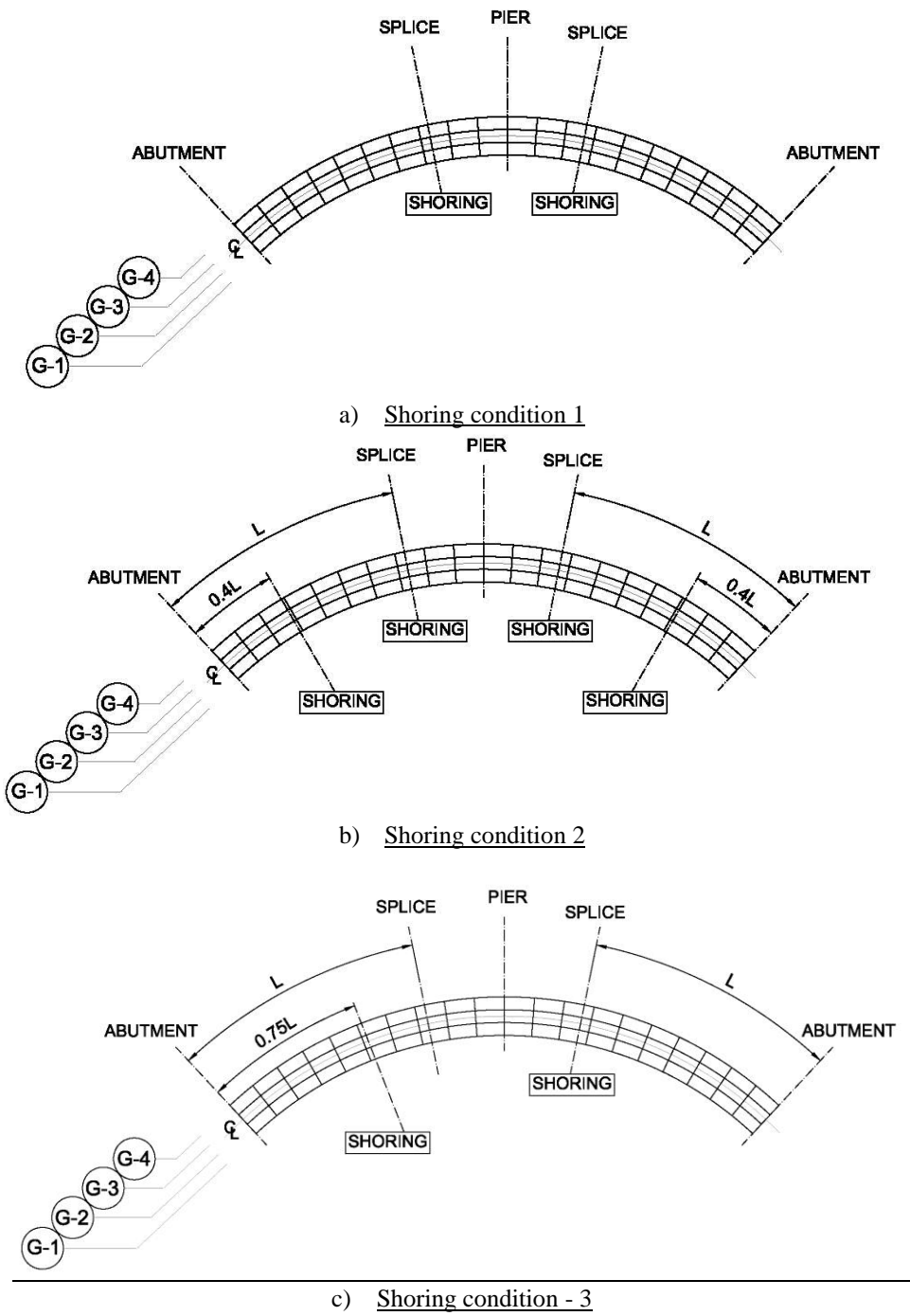
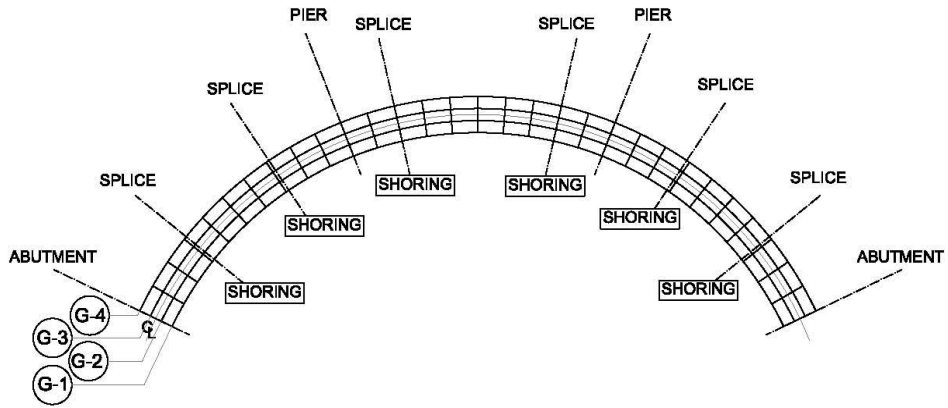
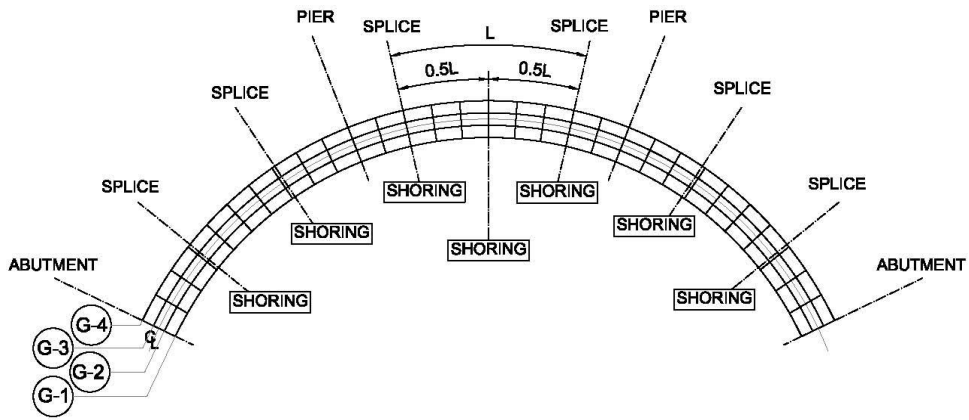


Figure 145: Shoring Conditions for Two-Span Bridges.

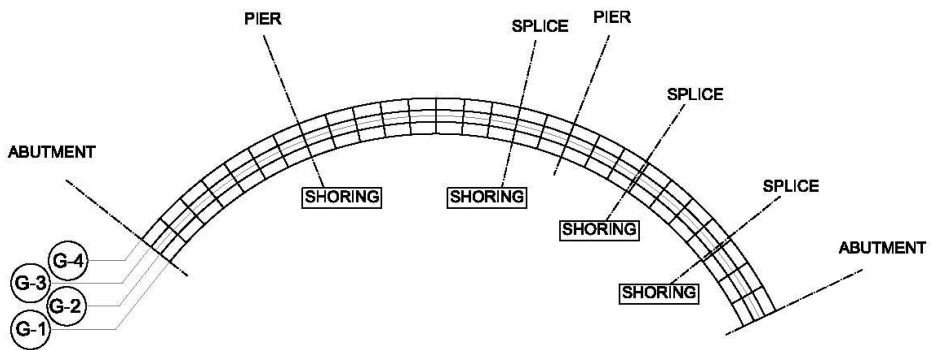


a) Shoring condition 1

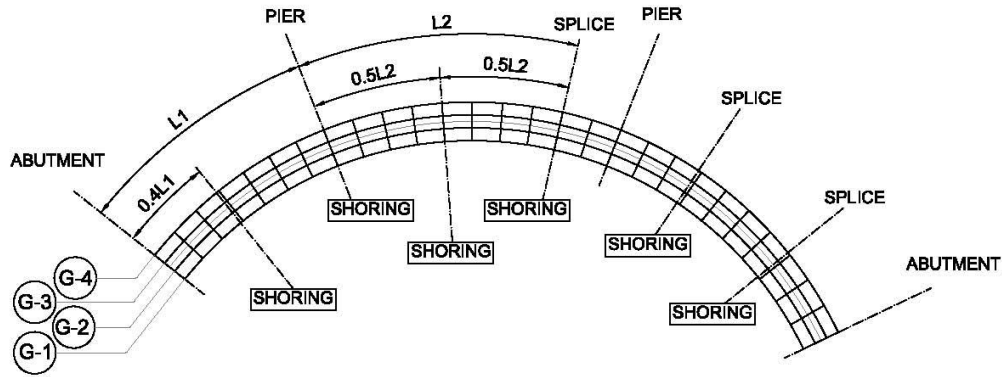


b) Shoring condition 2

Figure 146: Shoring Conditions for Bridge C10.

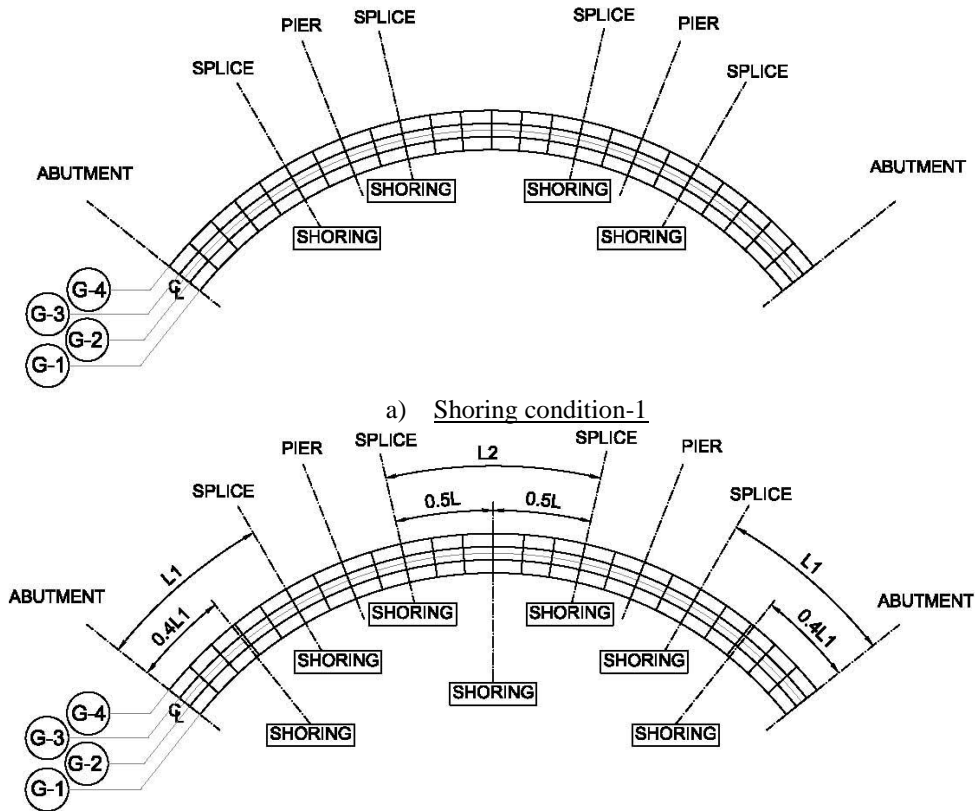


a) Shoring condition-1



b) Shoring condition 2

Figure 147: Shoring Conditions for Bridge C11.



a) Shoring condition-1

b) Shoring condition-2

Figure 148: Shoring Conditions for Bridge C12.

After the study of temporary shoring effects, the effects of settlement were studied for Bridge C3, which was the most severely curved structure with the largest cross-frame spacing. A total of six settlement conditions were examined (listed in Table 26), which included two settlement scenarios having three different settlement magnitudes. The first scenario introduced a settlement at one support at one splice location, while the second scenario introduced a settlement at supports at two splice locations. The three different settlement magnitudes that were applied were $0.001L$, $0.002L$, and $0.004L$, where L is the span length between the abutment and pier. These

values gave settlements between approximately 2 ½" and 10". Consequently, the effects of increasing settlement could be observed.

Table 26: Selected Settlement Conditions.

Settlement conditions	Scenario	Settlement
Condition-1	Settlement at one support	0.001L
Condition-2	Settlement at one support	0.002L
Condition-3	Settlement at one support	0.004L
Condition-4	Settlement at two supports	0.001L
Condition-5	Settlement at two supports	0.002L
Condition-6	Settlement at two supports	0.004L

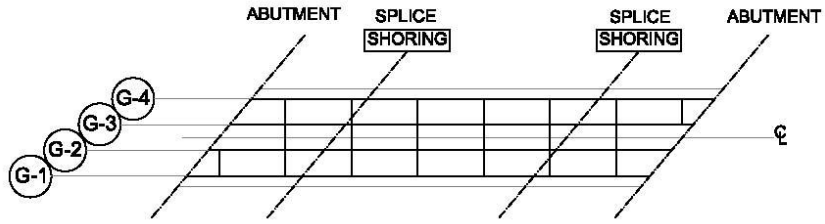
5.4.1.2 Skewed

Eight representative bridges were also selected from the skewed bridge set to investigate the effects of temporary shoring placement on bridge behavior during construction. The selected bridges included one single-span bridge with severely skewed abutments and maximum cross-frame spacing, four two-span bridges with varying skew angles and cross-frame spacings and three three-span bridges with balanced and unbalanced spans. The skew angle of the single-span bridge was 50°, and the cross-frame spacing was 7.8 m (25.7 ft). The varying skew angles of the two-span bridges were 50° and 70°, each with two different cross-frame spacings of 4.57 m (15 ft) and 7.8 m (25.7 ft). These parameters were selected so that they included a range from moderately to severely skewed bridges with different cross-frame spacings. Two symmetric three-span bridges with balanced and unbalanced spans and one non-symmetric three-span bridge with unbalanced spans were also included in this parametric study. All three-span bridges had the same skew angle (50°), the same cross frame spacing (7.8 m (25.7 ft)), and a 1:1.4 span ratio. Similar to the curved bridges, the paired-girder erection method was adopted for analysis consistency between curved and skewed models. Table 27 lists the parameters of the selected representative bridges.

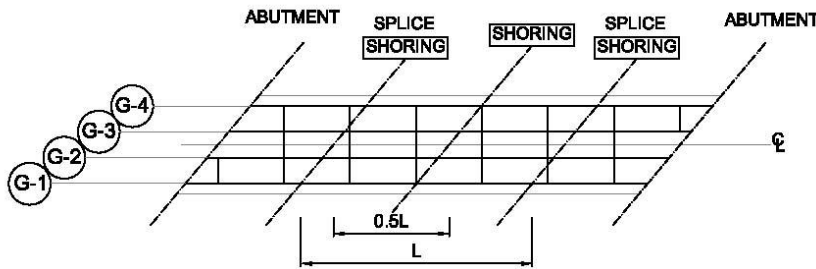
Table 27: Selected Skewed Bridge Temporary Shoring Study Information.

Bridge No.	Skew Angle, degrees	Cross-Frame Spacing, m (ft)	Girder-Spacing, m (ft)	Number of Spans	Span-Length, m (ft)	Number of Girder
S2	50	7.8 (25.7)	3 (10)	1	54.9 (180)	4
S5	50	4.57 (15)	3 (10)	2	54.9-54.9 (180-180)	4
S6	50	7.8 (25.7)	3 (10)	2	54.9-54.9 (180-180)	4
S7	70	4.57 (15)	3 (10)	2	54.9-54.9 (180-180)	4
S8	70	7.8 (25.7)	3 (10)	2	54.9-54.9 (180-180)	4
S9	50	7.8 (25.7)	3 (10)	3	54.9-54.9-54.9 (180-180-180)	4
S10	50	7.8 (25.7)	3 (10)	3	54.9-54.9-39.2 (180-180-128.75)	4
S11	50	7.8 (25.7)	3 (10)	3	39.2-54.9-39.2 (128.75-180-128.75)	4

Similar to the study of the representative curved bridges, three shoring conditions were investigated to determine their effects on bridge constructability. The first shoring condition was to place supports at splice locations only, the second condition was to place supports at splice locations as well as at 0.4L of the span for exterior spans and and/or 0.5L for interior spans, and the third condition was to place supports at 0.75L of the first span and at splice locations for the second span of the two-span bridges. Figure 149 through Figure 151 show the three shoring conditions for the selected two-span and three-span bridges.

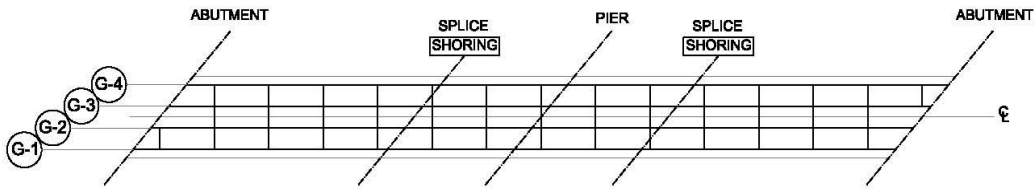


a) Shoring condition-1

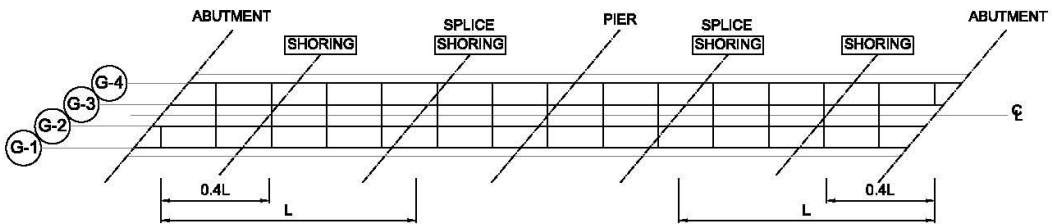


b) Shoring condition-2

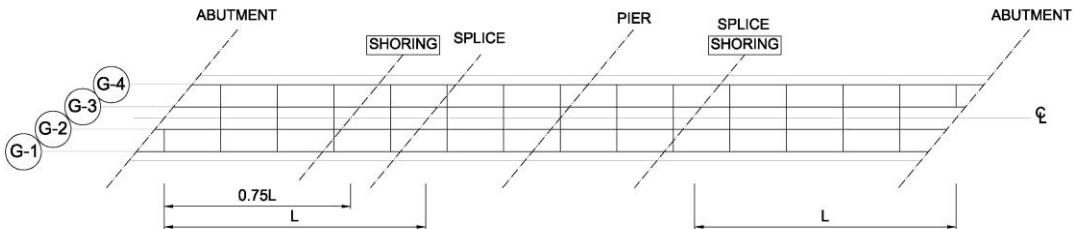
Figure 149: Shoring Conditions for Single-Span Skewed Bridge.



a) Shoring condition-1



b) Shoring condition-2



c) Shoring condition-3

Figure 150: Shoring Conditions for Two-Span Skewed Bridges.

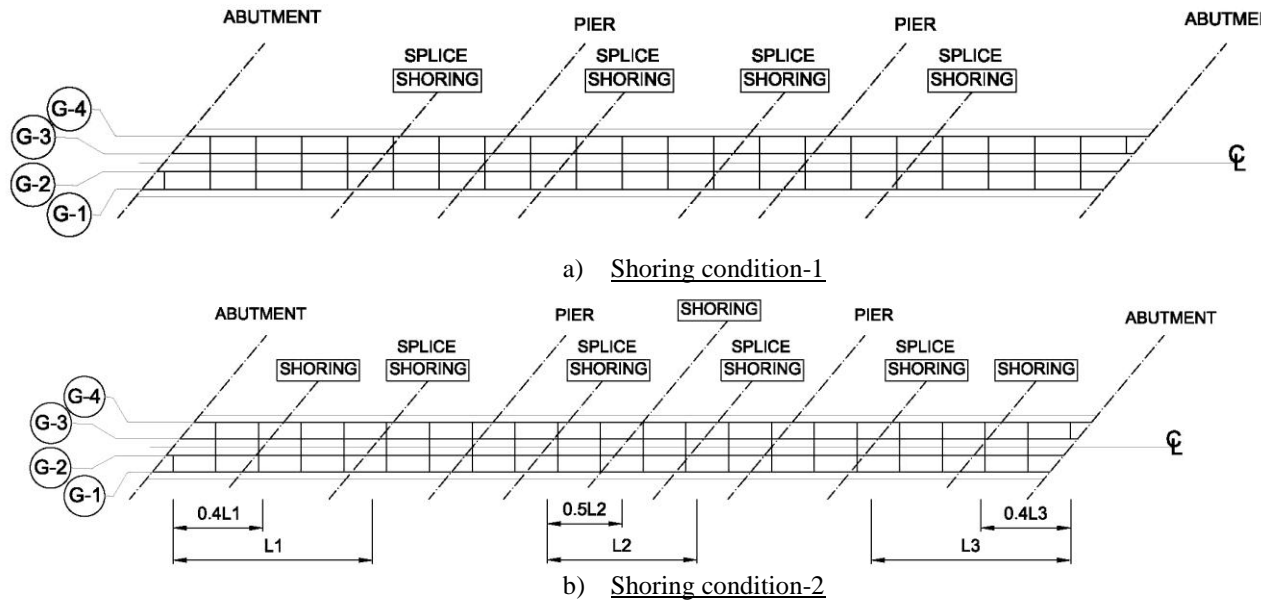


Figure 151: Shoring Conditions for Three-Span Skewed Bridges.

Similar to the study of the representative curved bridges, the settlement effects on the skewed structures were investigated by considering six settlement conditions (Table 26) for Bridge S6 (the most severely skewed structure with the largest cross-frame spacing). The first settlement scenario introduced a settlement at one support at one splice location, while the second scenario introduced settlement at supports at both splice locations. The three different settlements applied were $0.001L$, $0.002L$, and $0.004L$, where L is the span length between the abutment and pier, which gave settlement values between approximately 2" and 9". Consequently, the effects of increasing settlement could be observed.

5.4.2 Results and Discussion

5.4.2.1 Curved

Maximum girder vertical deflections and Von Mises stresses in cross frames were compared to study the effects of temporary shoring placement on bridge behavior during construction. Figure 152 through Figure 159 show the comparisons of deflections between the first two shoring conditions. Not surprisingly, adding additional supports in girders with span lengths of more than 100 ft considerably reduced girder deflections, leading to a more stable structure and therefore a more desirable construction condition. Secondly, considering that under certain circumstances contractors might not be able to provide the additional shoring between supports, the third shoring condition (shoring at $0.75L$) was studied to provide an alternative to contractors for mitigating girder deflections. Figure 160 through Figure 165 show the representative results of vertical deflections and Von Mises stresses for all three shoring conditions. Interestingly, as observed from the results, the maximum girder deflections and stresses in cross frames could be significantly reduced by placing one shoring tower at $0.75L$. The results also show that more reductions in deflections and stresses were observed for severely curved structures than for moderately curved structures when a temporary support was provided at $0.75L$ instead of at splice locations. This finding suggested that, for the erection of a long span (>100 ft), severely curved ($R=300$ ft) bridges, placing one support between the splice location and mid-span could increase the stability and constructability of the structure over one that does not have any intermediate shoring.

Ratio of max. vertical deflections (normalized by Shoring condition 1)

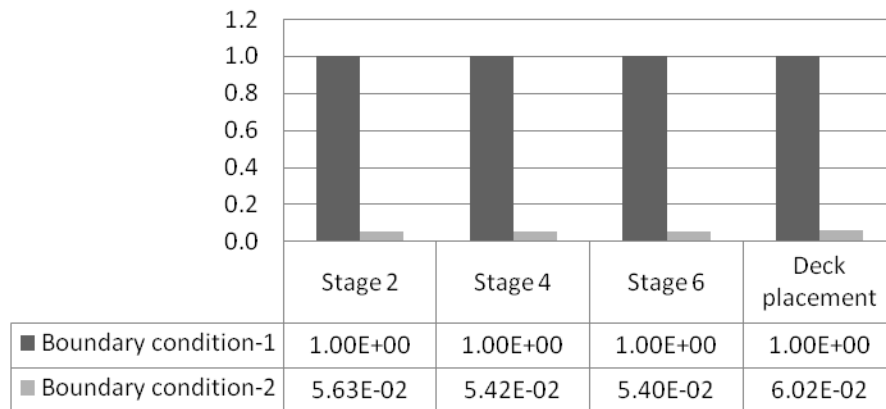


Figure 152: Ratio of Maximum Vertical Deflections for Bridge C1.

Ratio of max. vertical deflections (normalized by Shoring condition 1)

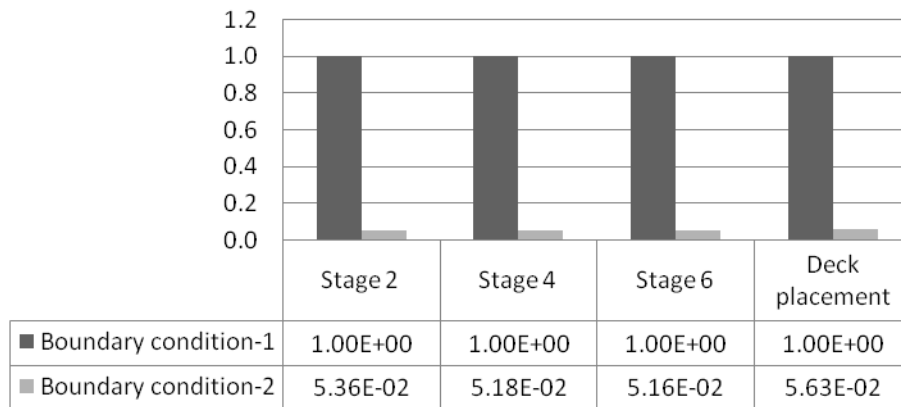


Figure 153: Ratio of Maximum Vertical Deflections for Bridge C3.

Ratio of max. vertical deflections (normalized by Shoring condition 1)

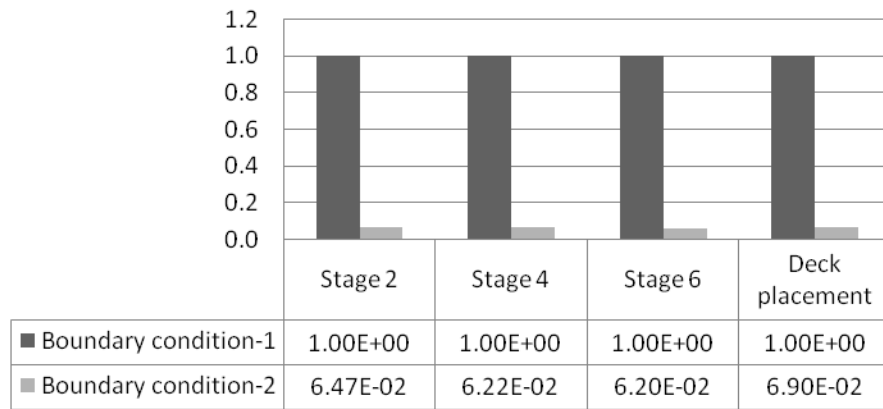


Figure 154: Ratio of Maximum Vertical Deflections for Bridge C6.

Ratio of max. vertical deflections (normalized by Shoring condition 1)

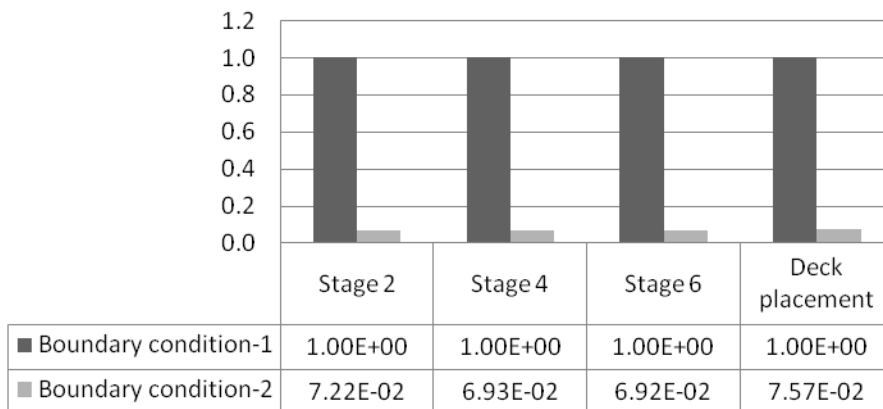


Figure 155: Ratio of Maximum Vertical Deflections for Bridge C7.

Ratio of max. vertical deflections (normalized by Shoring condition 1)

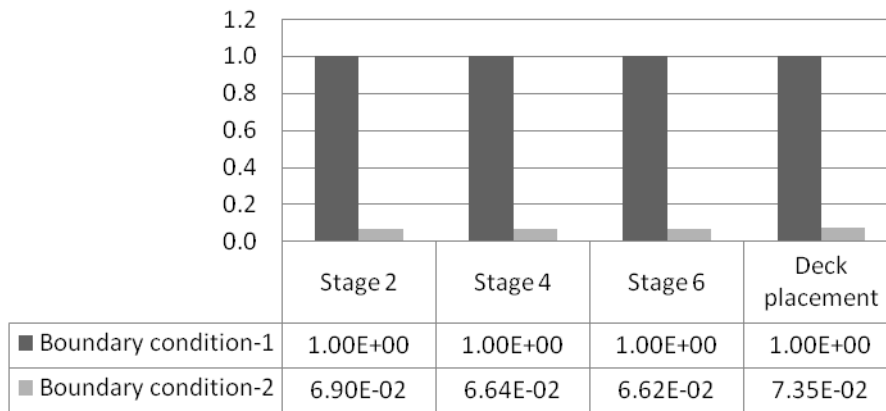


Figure 156: Ratio of Maximum Vertical Deflections for Bridge C9.

Ratio of max. vertical deflections (normalized by Shoring condition 1)

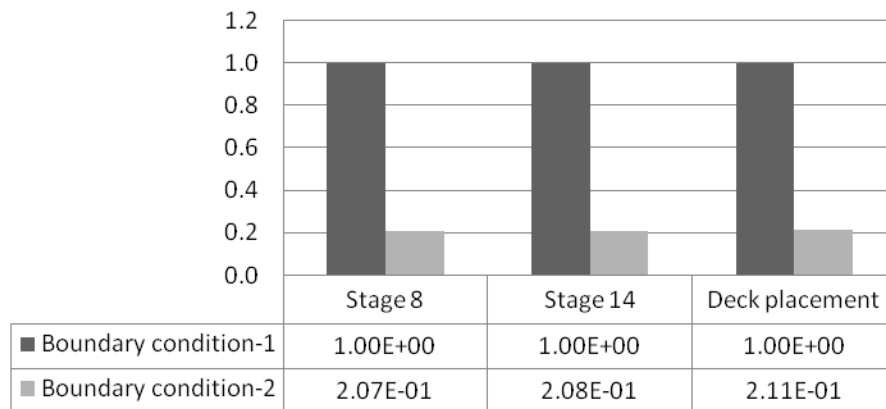


Figure 157: Ratio of Maximum Vertical Deflections for Bridge C10.

Ratio of max. vertical deflections (normalized by Shoring condition 1)

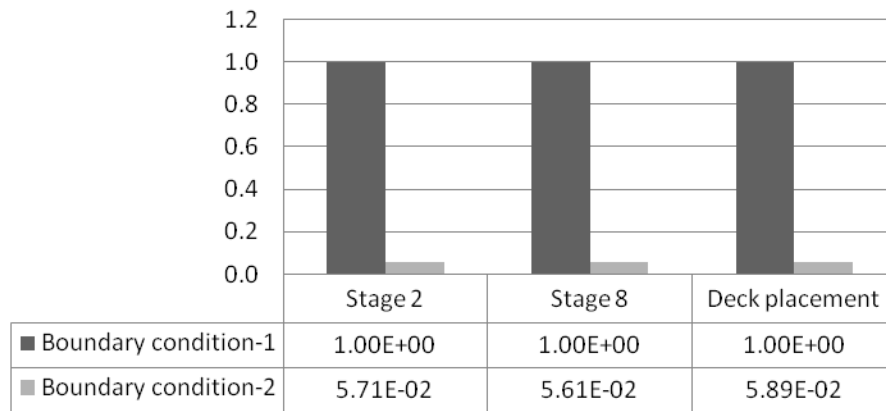


Figure 158: Ratio of Maximum Vertical Deflections for Bridge C11.

Ratio of max. vertical deflections (normalized by Shoring condition 1)

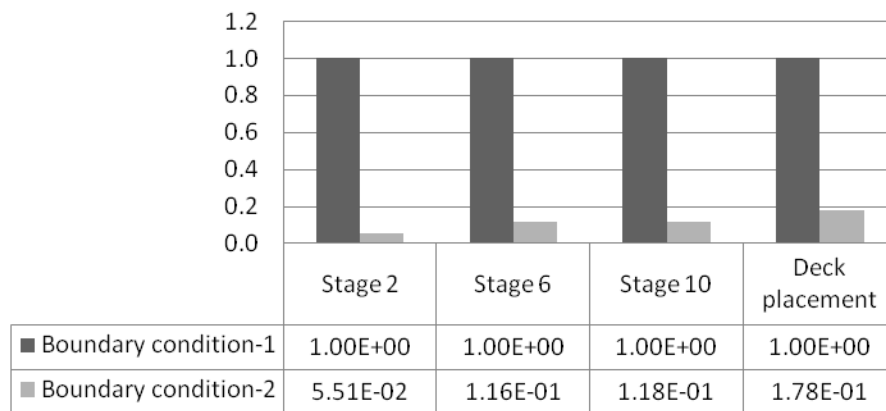


Figure 159: Ratio of Maximum Vertical Deflections for Bridge C12.

Ratio of max. vertical deflections (normalized by Shoring condition 1)

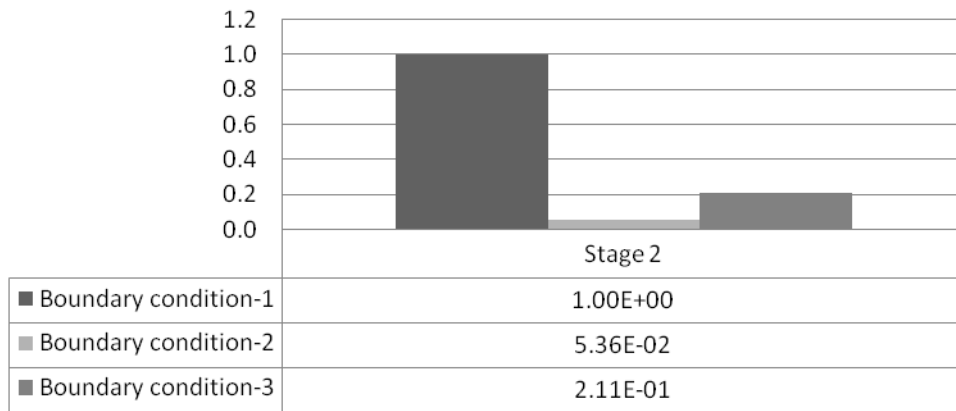


Figure 160: Ratio of Maximum Vertical Deflections for Bridge C3.

Ratio of max. vertical deflections (normalized by Shoring condition 1)

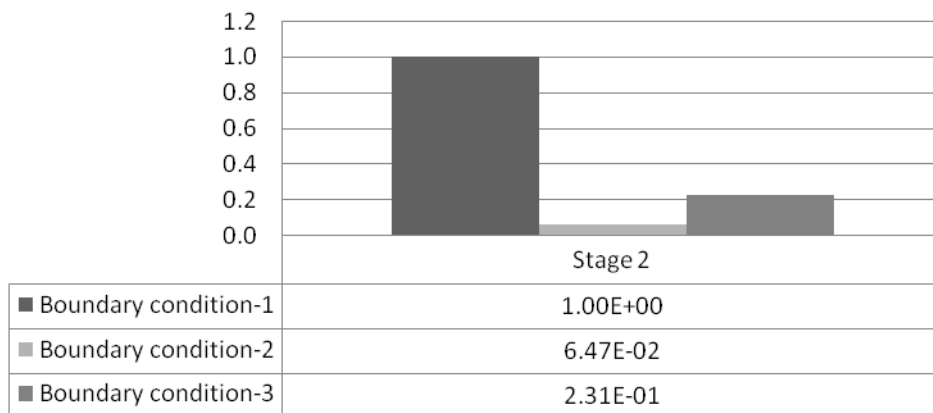


Figure 161: Ratio of Maximum Vertical Deflections for Bridge C6.

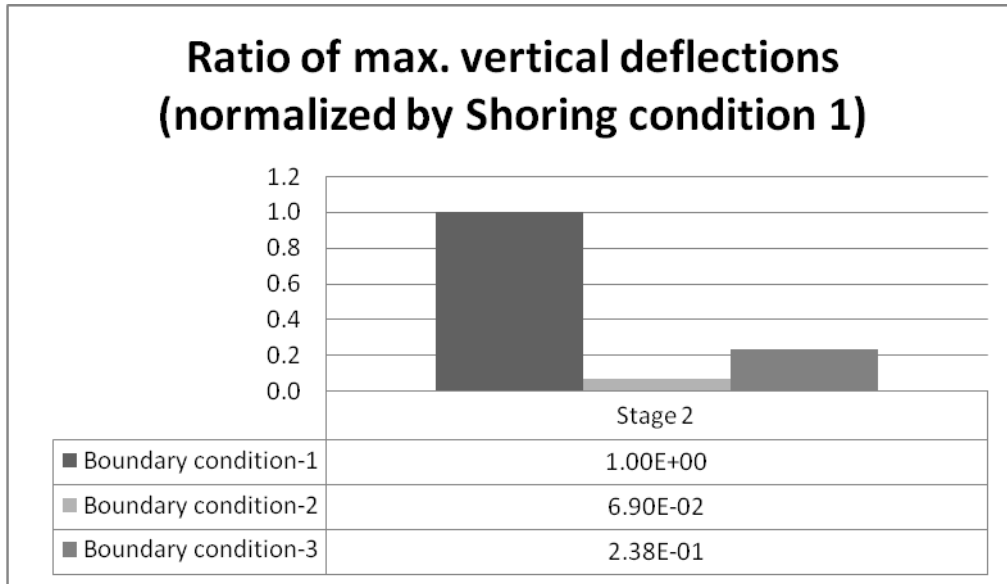


Figure 162: Ratio of Maximum Vertical Deflections for Bridge C9.

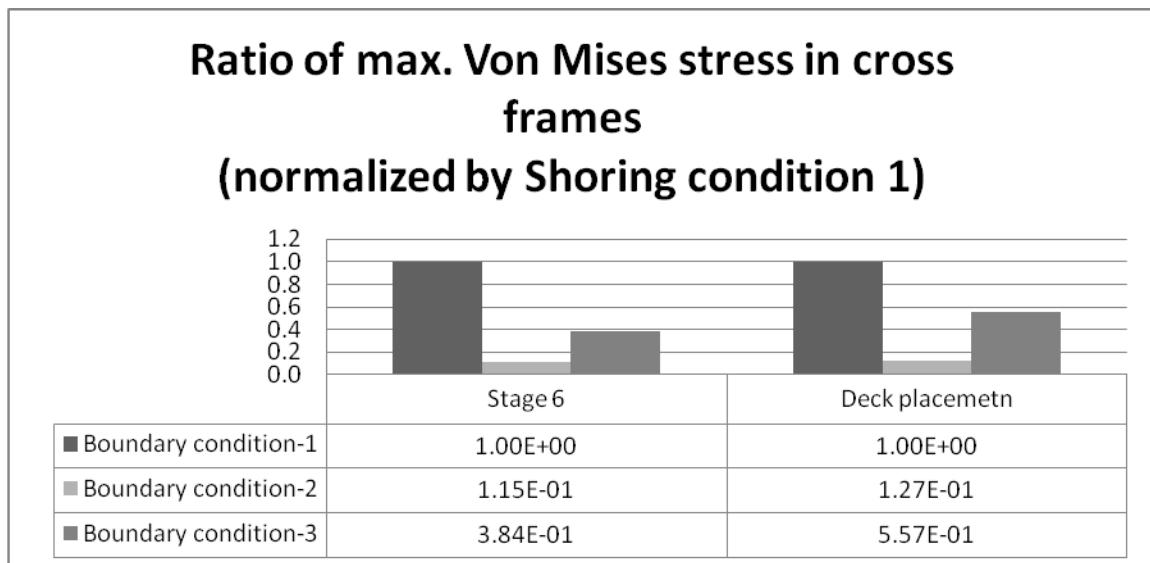


Figure 163: Ratio of Maximum Von Mises Stresses for Bridge C3.

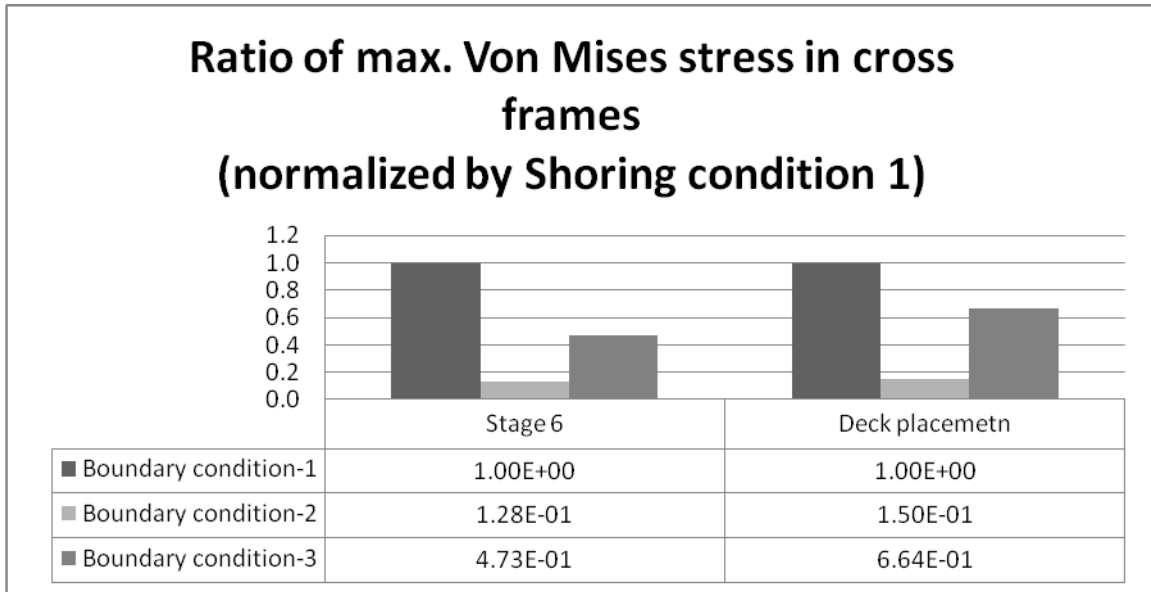


Figure 164: Ratio of Maximum Von Mises Stresses for Bridge C6.

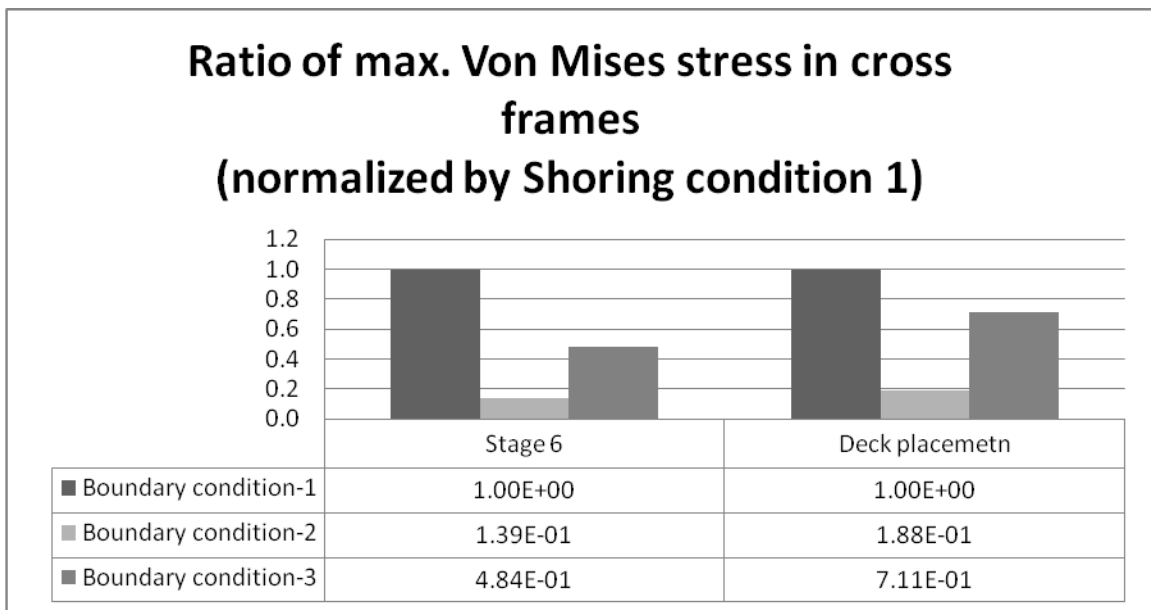


Figure 165: Ratio of Maximum Von Mises Stresses for Bridge C9.

Settlement effects on the stresses in cross frames were also examined for the six settlement conditions. The cross frame having the maximum Von Mises stress before support settlement was checked for stress increases after settlement.

Figure 166 shows the results for the ratio of maximum Von Mises stresses. First, as seen in Figure 166, stresses were increased due to the support settlements; nevertheless, no significant difference in the increase of stress was observed between the one-support settlement and two-support settlement conditions, with the two-support settlement condition having a slightly higher stress increase. Second, stresses were increased proportionally with increasing settlement. An average of 25% stress increase in cross frames was observed with every increase of 0.0001L settlement for the bridge studied.

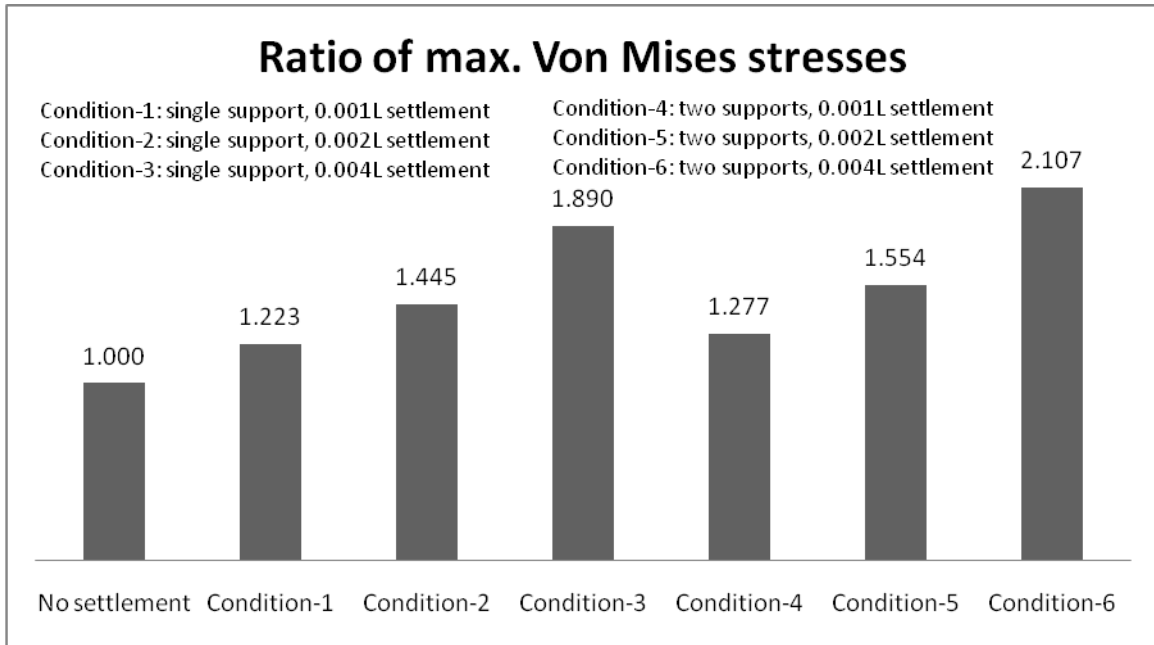


Figure 166: Ratio of Maximum Von Mises Stress for Bridge C3 with Various Settlement Conditions.

5.4.2.2 Skewed

Maximum vertical deflections in the girders and maximum Von Mises stresses in the cross frames were also examined for the skewed bridge shoring cases. Figure 167 through Figure 174 show the comparisons of deflections between the first two shoring conditions for all representative bridges and all construction stages. As was expected, additional shoring at the mid spans of the girders dramatically decreased the maximum vertical deformations which, in turn, could enhance the stability of all the bridges. The behavior of the structures under the third shoring condition (at 0.75L) was studied by looking at the results from vertical deflections for the two-span representative skewed bridges at the second stage of construction. The results for the other stages were shown to be the same as the results for Shoring condition-1 because of the similarity of the support conditions for those stages. Figure 175 through Figure 178 show the ratios of maximum girder vertical deformation at Stage-2. Finally, maximum Von Mises stresses in the cross frames were then compared in the two-span bridges for all three shoring conditions, and results are shown in Figure 179 through Figure 182. Similar to the representative curved bridges, in comparison with Shoring condition-1 (placing the shoring at a splice location), the maximum girder deflections and stresses in cross frames could be significantly reduced by moving the shoring to 0.75L of the first span. For all three conditions, the ratios of maximum deflection and maximum Von Mises stress are nearly the same for all four examined skewed bridges.

Ratio of max. vertical deformation (normalized by Shoring condition-1)

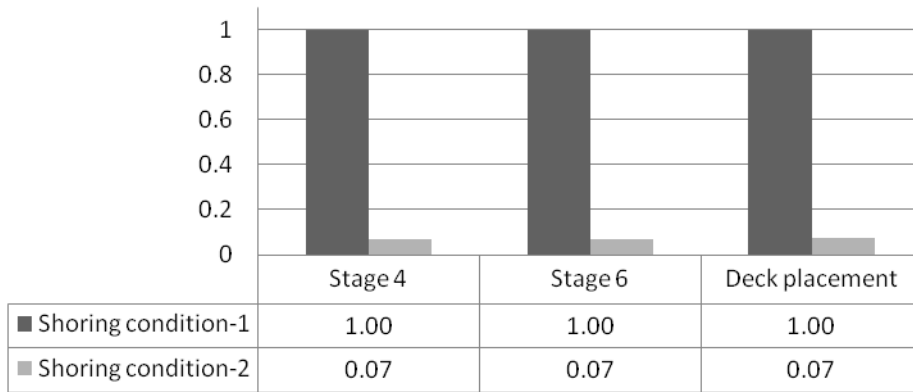


Figure 167: Ratio of Maximum Vertical Deflections for Bridge S2.

Ratio of max. vertical deformation (normalized by Shoring condition-1)

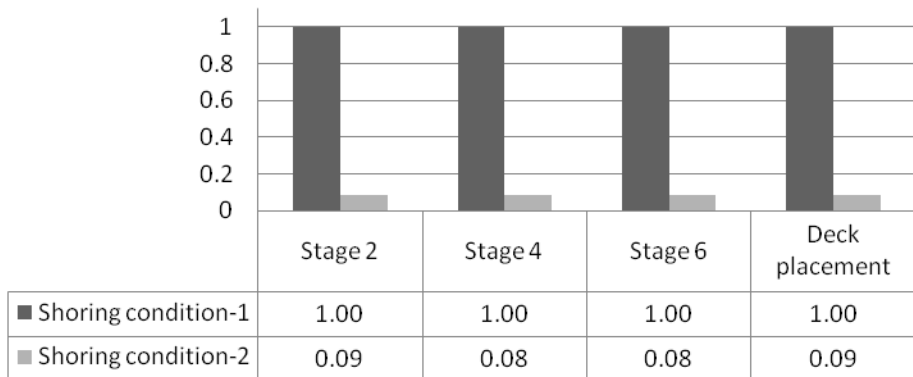


Figure 168: Ratio of Maximum Vertical Deflections for Bridge S5.

Ratio of max. vertical deformation (normalized by Shoring condition-1)

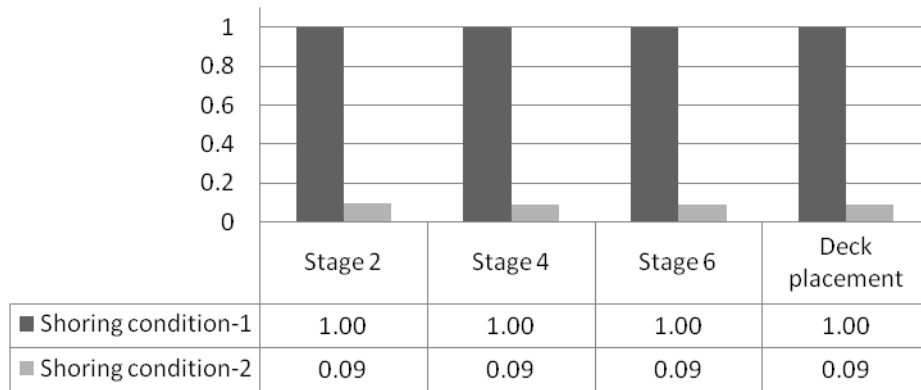


Figure 169: Ratio of Maximum Vertical Deflections for Bridge S6.

Ratio of max. vertical deformation (normalized by Shoring condition-1)

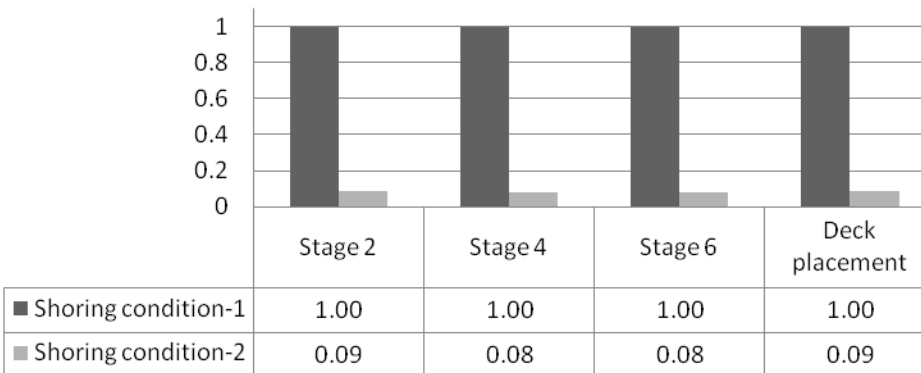


Figure 170: Ratio of Maximum Vertical Deflections for Bridge S7.

Ratio of max. vertical deformation (normalized by Shoring condition-1)

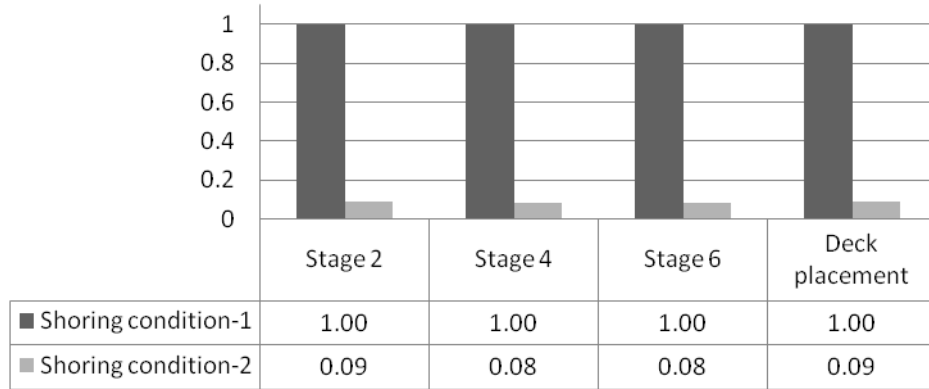


Figure 171: Ratio of Maximum Vertical Deflections for Bridge S8.

Ratio of max. vertical deformation (normalized by Shoring condition-1)

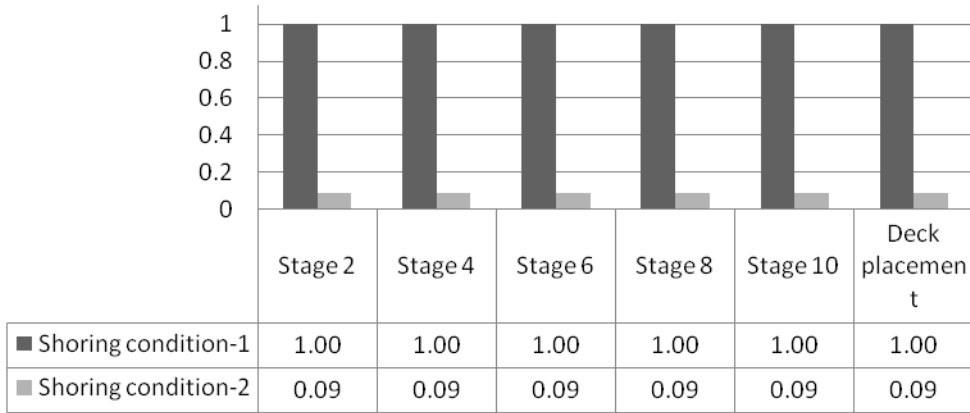


Figure 172: Ratio of Maximum Vertical Deflections for Bridge S9.

Ratio of max. vertical deformation (normalized by Shoring condition-1)

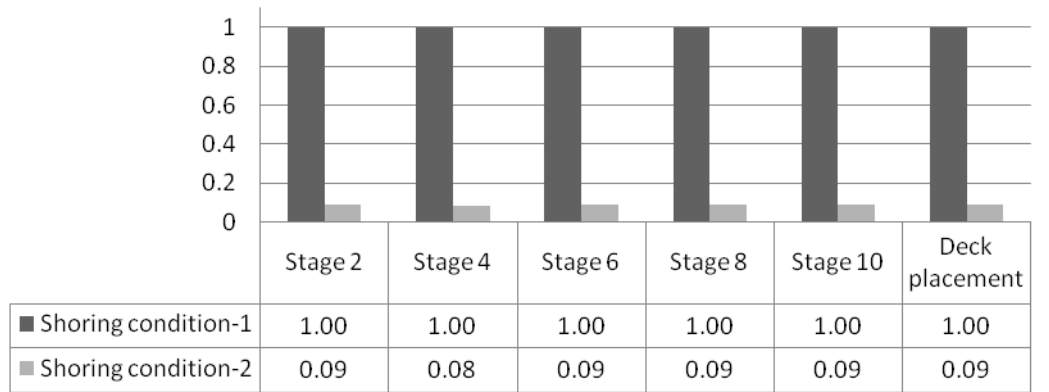


Figure 173: Ratio of Maximum Vertical Deflections for Bridge S10.

Ratio of max. vertical deformation (normalized by Shoring condition-1)

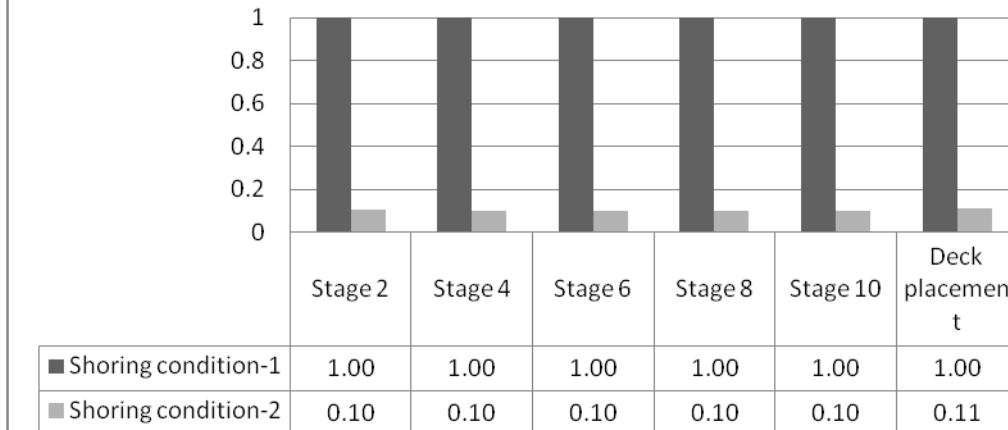


Figure 174: Ratio of Maximum Vertical Deflections for Bridge S11.

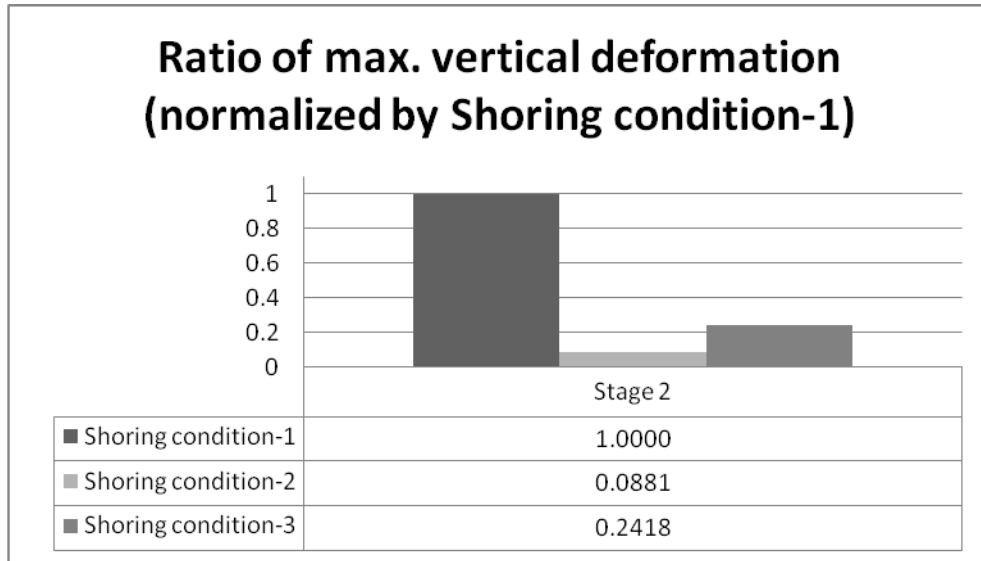


Figure 175: Ratio of Maximum Vertical Deflections for Three Shoring Conditions in Bridge S5.

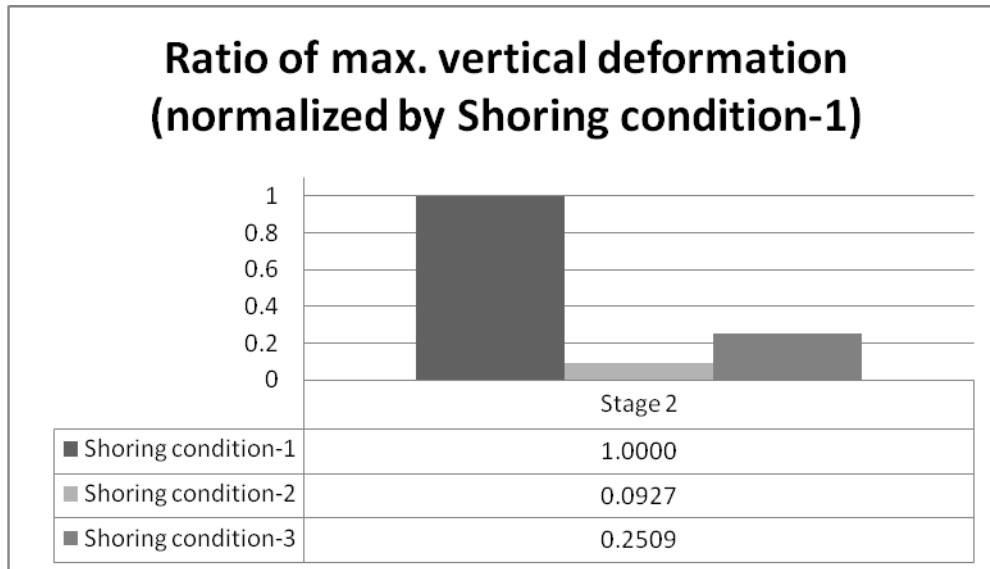


Figure 176: Ratio of Maximum Vertical Deflections for Three Shoring Conditions in Bridge S-6.

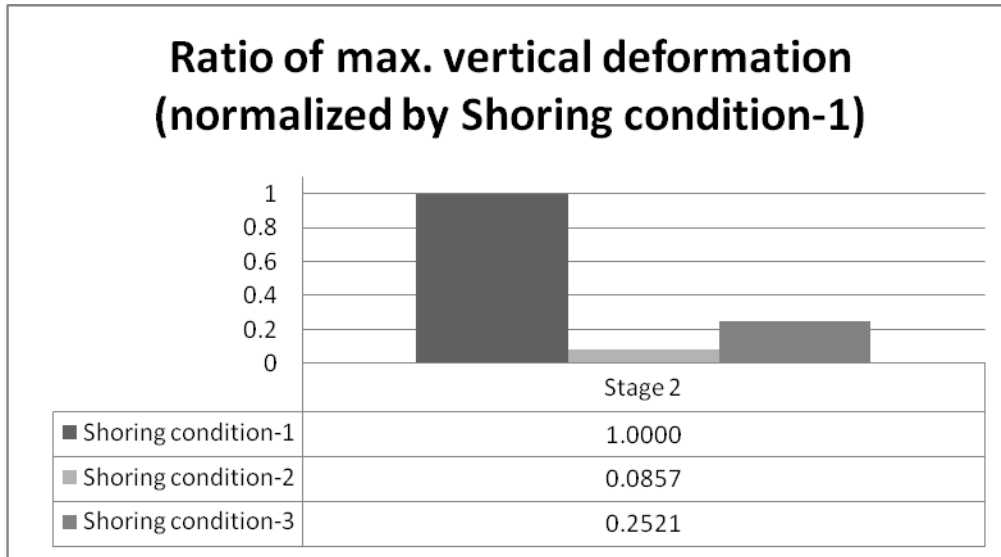


Figure 177: Ratio of Maximum Vertical Deflections for Three Shoring Conditions in Bridge S7.

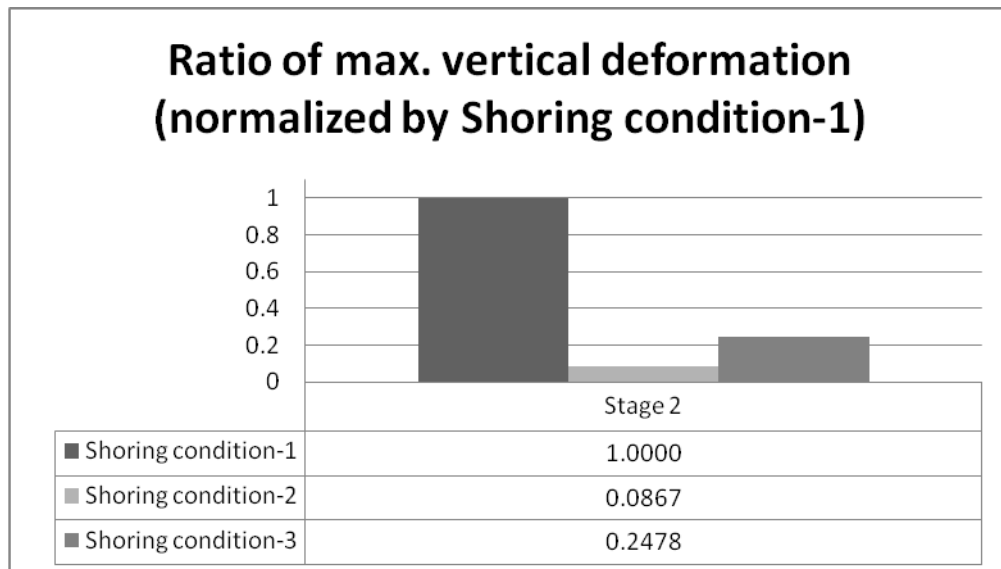


Figure 178: Ratio of Maximum Vertical Deflections for Three Shoring Conditions in Bridge S8.

Ratio of max. Von Mises stress in cross frames (normalized by Shoring condition-1)

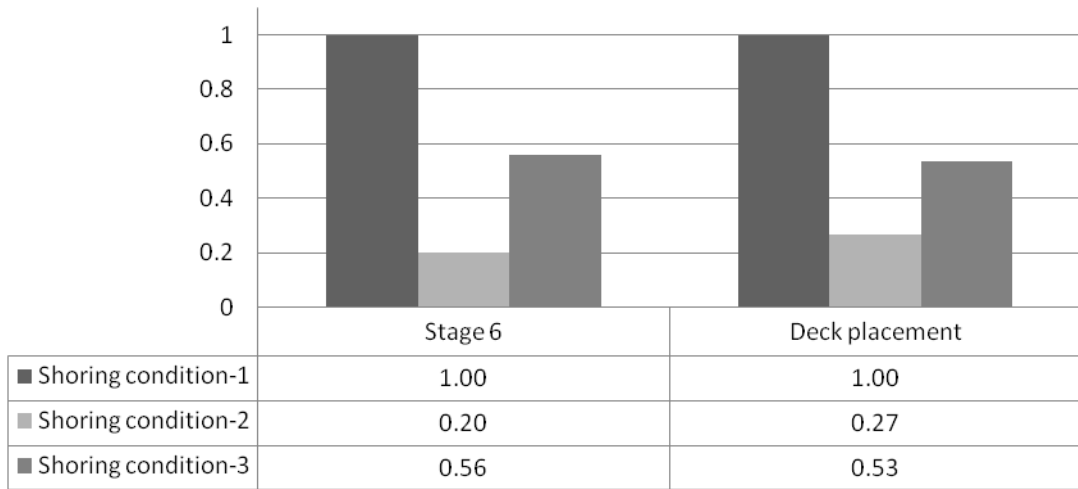


Figure 179: Ratio of Maximum Von Mises Stresses for Bridge S5.

Ratio of max. Von Mises stress in cross frames (normalized by Shoring condition-1)

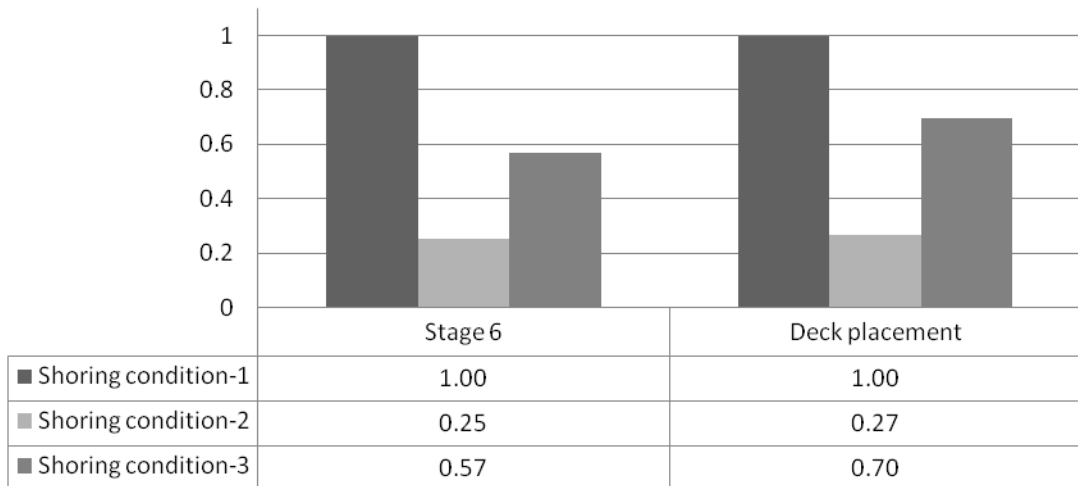


Figure 180: Ratio of Maximum Von Mises Stresses for Bridge S6.

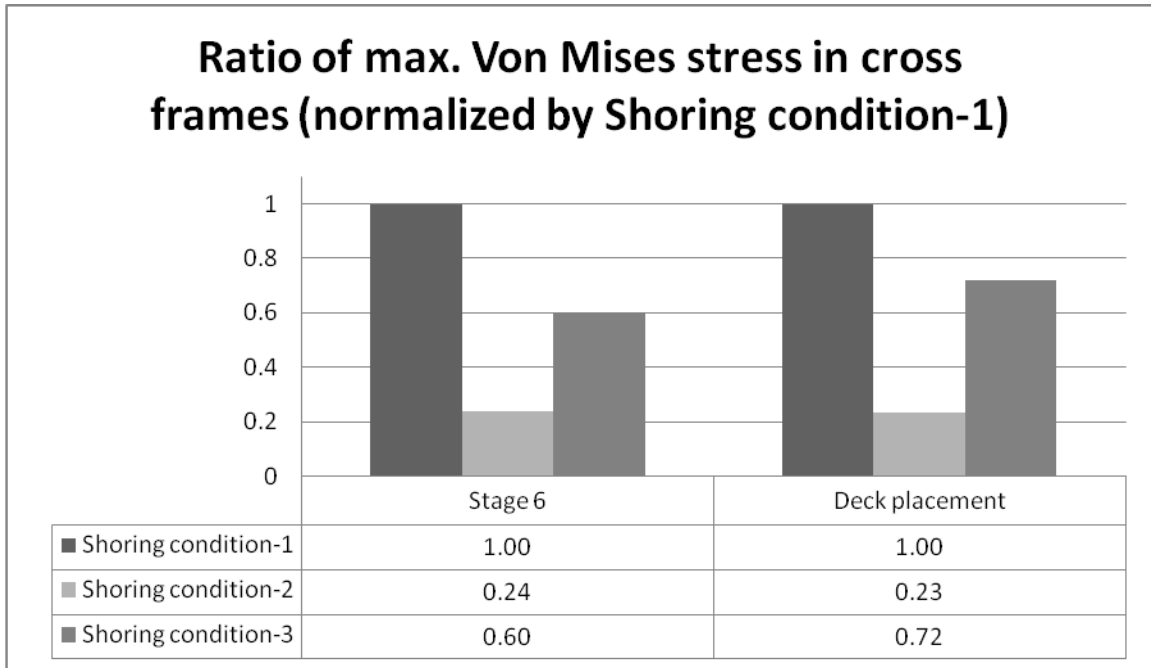


Figure 181: Ratio of Maximum Von Mises Stresses for Bridge S7.

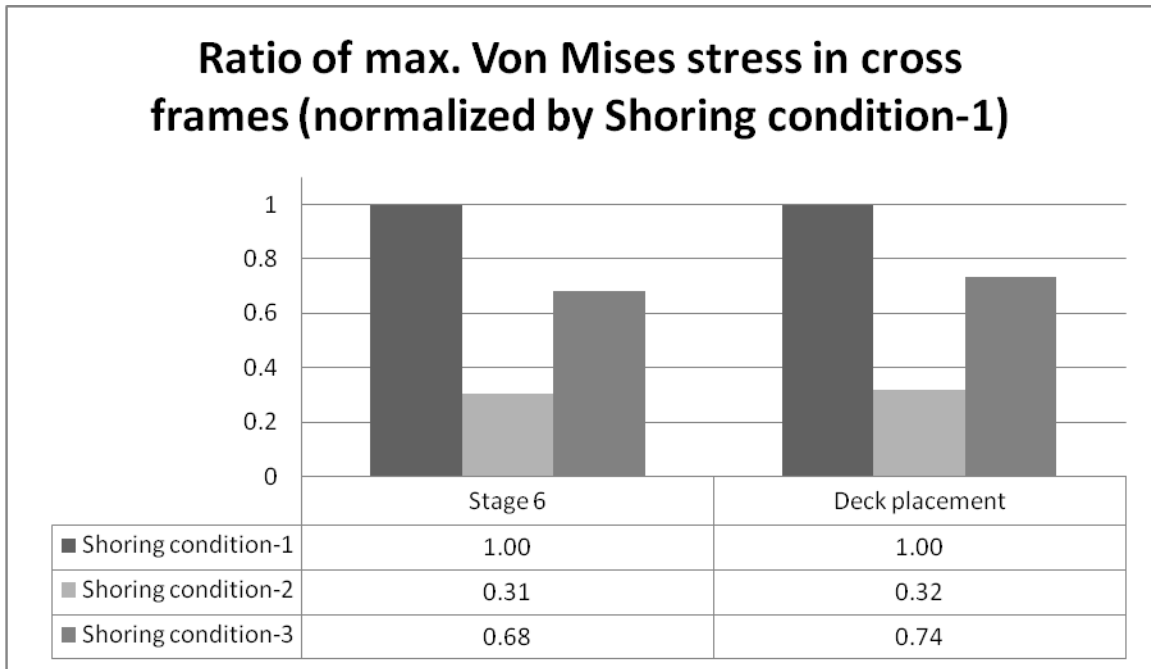


Figure 182: Ratio of Maximum Von Mises Stresses for Bridge S8.

The effect of settlement on cross-frames stresses was also examined for the six settlement conditions. The cross frame with the maximum Von Mises stress before support settlement was checked for stress increases after settlement. Figure 183 shows the results for the ratio of maximum Von Mises stresses. In comparison with the results from the curved bridges, the cross frames experienced a relatively large increase in stress for all settlement conditions. It can also be observed from Figure 183 that, unlike the curve bridges, there is an appreciable difference between the effects of settlement of a single support and settlement of two supports for skewed bridges. The reason for these effects is the relatively small stresses on the cross frames due to dead load torsional effects in the skewed bridges for the no settlement condition. By comparison, in the curved bridges, the cross frames experienced larger

stresses as a result of curvature effects. Therefore, the increase in stress for skewed bridges becomes more prominent because it largely reflects the settlement effects. However, the magnitudes of these stresses are smaller overall than those in curved bridges under settlement effects.

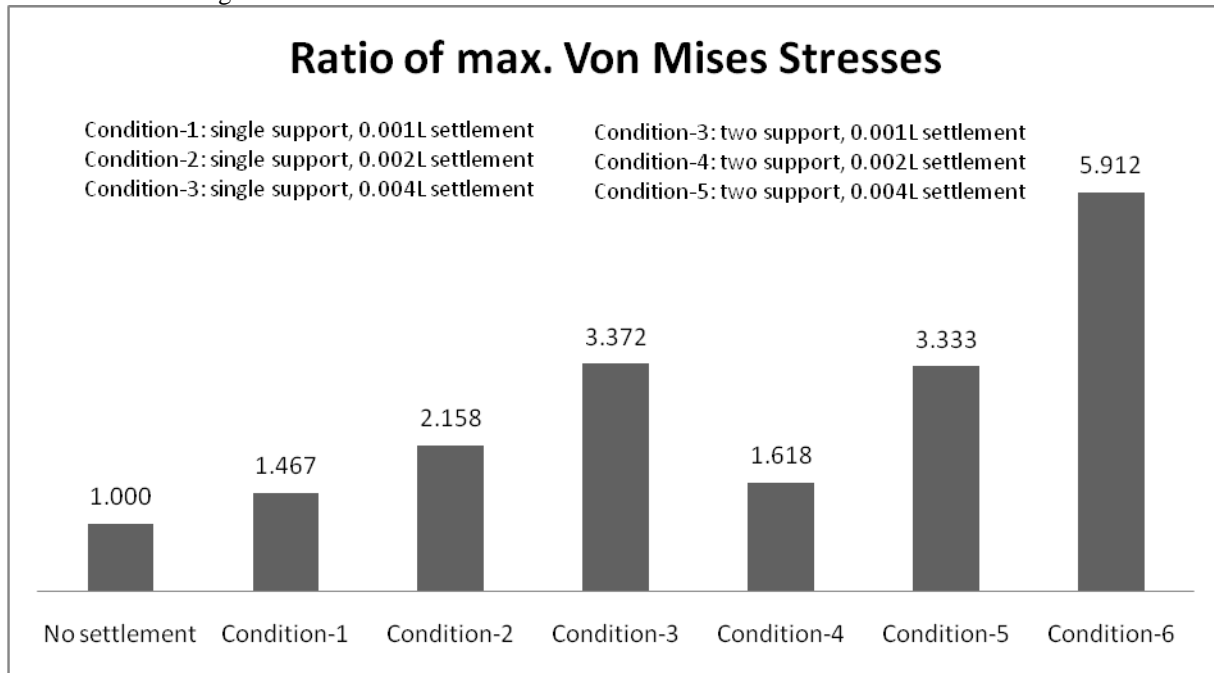


Figure 183: Ratio of Maximum Von Mises Stress for Bridge S6 with Various Settlement Conditions.

5.4.2.3 Summary

This section examined temporary shoring and settlement effects on curved and skewed bridge behavior during construction. In the first part of this study, the effectiveness of three shoring scenarios (1. splice locations; 2. splice locations and 0.4L; 3. 0.75L) was investigated. It was observed that placing one temporary shoring at 0.75L between the abutment and splice location effectively reduced girder deflections and improved bridge constructability for both curved and skewed structures. The second part of this study investigated settlement effects on curved and skewed bridge behaviors during construction. Two settlement scenarios (one-support settling and two-supports settling) with three various amounts of settlement were studied. Results showed appreciable cross-frame stress increases due to support settlement effects. Therefore, settlement effects on bridge constructability should be taken into account for construction planning.

In summary, findings from the temporary shoring parametric studies for the curved and skewed bridges that were examined included:

- Curved
 - In addition to the shoring at splice locations, placing one temporary support at 0.4L could significantly reduce girder deflections, leading to a more constructible condition.
 - When adding additional shoring at 0.4L was not feasible, placing one support at 0.75L between the abutment and splice location could reduce girder vertical deflections by more than 75% for the structures studied when compared to the deflections of placing one support at the splice location.
 - Attempts should be made to limit support settlements to less than 0.001L (L=span length) during construction to mitigate stress increases in bridge members.
 - Small differences were observed between one-support settling and two-supports settling.

- Skewed
 - In addition to the shoring at splice locations, placing one temporary support at $0.4L$ could significantly reduce girder deflections, leading to a more constructible condition.
 - When adding additional shoring at $0.4L$ was not feasible, placing one support at $0.75L$ between the abutment and splice location could reduce girder vertical deflections by more than 70% for the structures studied when compared to the deflections of placing one support at the splice location.
 - Attempts should be made to limit support settlement to less than $0.001L$ (L =span length) during construction to mitigate stress increases in bridge members.
 - Two-supports settling had a larger impact on stresses than one-support settling.

5.5 Cross Frame Consistent Detailing

Earlier work (Chavel and Earls 2006) indicated that detailing curved girders and cross frames for different load conditions during construction can lead to undesirable and costly fit-up problems. Typically, this inconsistent detailing occurs when girders are detailed to be web-plumb under one construction condition (e.g., no load) and cross frames are detailed to be web-plumb under another condition (e.g., full dead load). To model these effects in ABAQUS, the studied curved and skewed bridge models were initially run in SAP 2000 for a web-plumb under no load condition to define the geometry of cross frames and girders in the ABAQUS models. The SAP models also assisted with finding the geometry of inconsistently detailed cross frames by providing vertical deformations of the girders at their connection with each cross frame under full dead load. The new geometries of the cross frames were defined assuming the webs were plumb in this deformed shape, as shown in Figure 184. When compared against a consistent detailing case, the geometries resulted in elongation of one cross-frame diagonal and shortening of the other. To mimic the forces applied to the structures as a result of this inconsistent detailing, positive or negative temperatures that would give these length changes were calculated for each diagonal. These temperatures were then applied to the members in the ABAQUS models to investigate the effects of inconsistent detailing on curved and skewed bridge constructability.

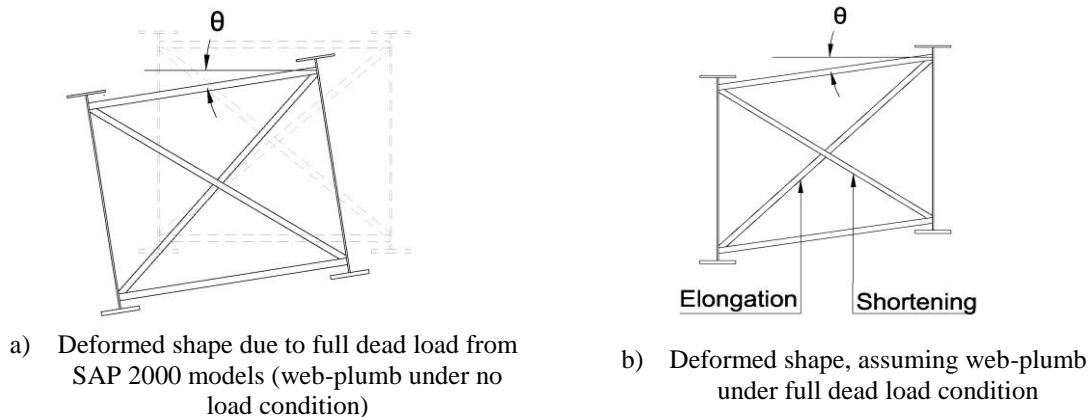


Figure 184: Cross Frame Geometries for Inconsistent Detailing.

5.5.1 Parametric Studies

5.5.1.1 Curved

To examine inconsistent detailing effects on curved bridges, one two-span curved bridge with a severe curvature and one unbalanced three-span bridge were selected.

Table 28 lists parameters for the bridges that were examined.

Table 28: Selected Inconsistent Detailing Study Bridge Information

Bridge No.	Radius of Curvature, m (ft)	Cross-Frame Spacing, m (ft)	Girder-Spacing, m (ft)	Number of Spans	Span-Length, m (ft)	Number of Girder
C3	91.4 (300)	6.86 (22.5)	3 (10)	2	68.6-68.6 (225-225)	4
C11	91.4 (300)	6.86 (22.5)	3 (10)	3	48-68.6-68.6 (157.5-225-225)	4

5.5.1.2 Skewed

Similar to the curved bridges, the effects of the inconsistent detailing of the cross frame on the constructability of the skewed bridges was investigated by considering four two-span bridges with varying skew angles and cross-frame spacings. Table 29 lists the parameters for the bridges that were examined.

Table 29: Selected Skewed Bridge Consistent Detailing Study Bridge Information

Bridge No.	Skew Angle, degree	Cross-Frame Spacing, ft	Girder-Spacing, ft	Number of Spans	Span-Length, ft	Number of Girder, ft
S5	50	15	10	2	180-180	4
S6	50	25.7	10	2	180-180	4
S7	70	15	10	2	180-180	4
S8	70	25.7	10	2	180-180	4

5.5.2 Results and Discussion

5.5.2.1 Curved

To examine the effects of inconsistent detailing on bridge constructability and the resulting locked-in stresses in the cross frames, girder splice vertical and radial deflections and cross-frame Von Mises stresses were again examined. Comparisons are shown in Figure 185 through Figure 190. As shown in the results, inconsistent cross-frame detailing resulted in higher vertical and radial deflections. More importantly, it was also observed that stresses in cross frames were increased due to locked-in stresses caused by inconsistent detailing. This change in stress occurred more or less in all cross frames along the bridge; however, cross frames near the supports experienced slightly higher increases.

Ratio of max. vertical deflections (normalized by Consistent Detailing)

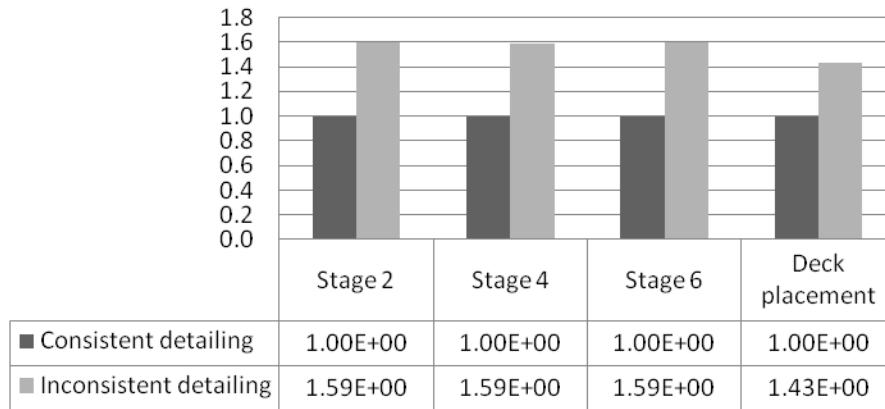


Figure 185: Ratio of Maximum Vertical Deflections for Bridge C3.

Ratio of max. vertical deflections (normalized by Consistent Detailing)

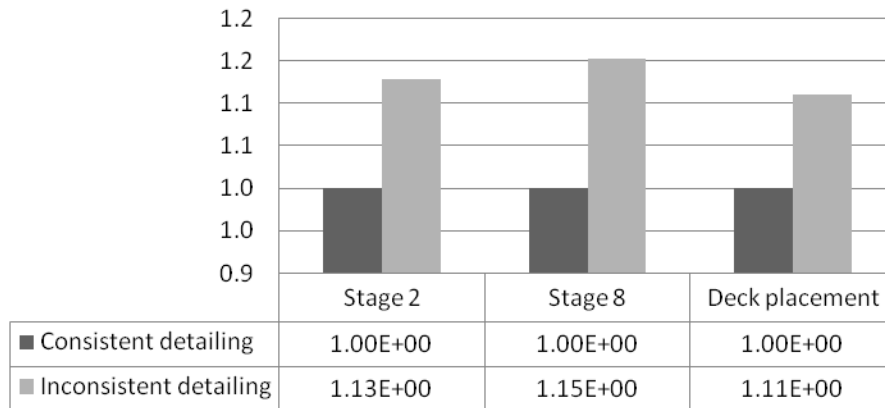


Figure 186: Ratio of Maximum Vertical Deflections for Bridge C11.

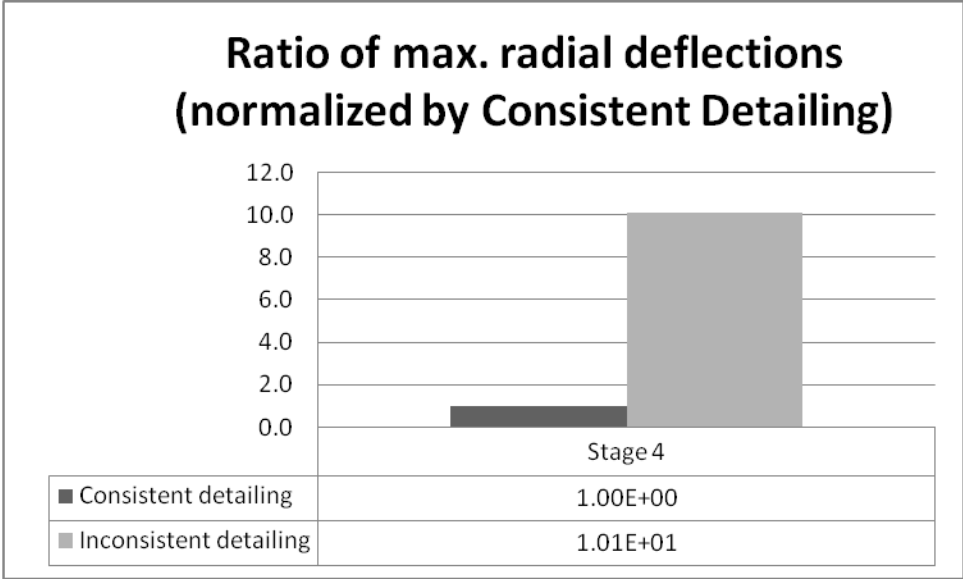


Figure 187: Ratio of Maximum Radial Deflections for Bridge C3.

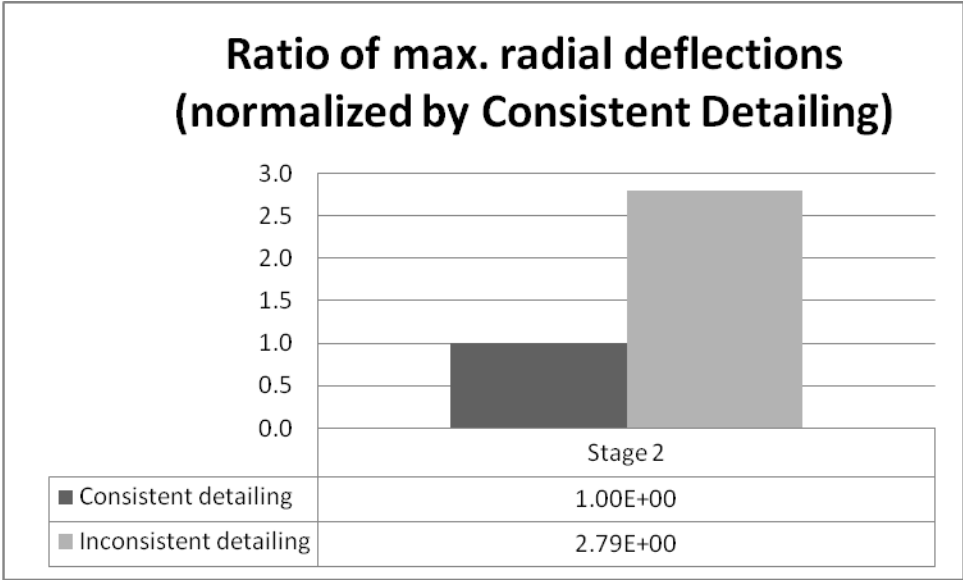


Figure 188: Ratio of Maximum Radial Deflections for Bridge C11.

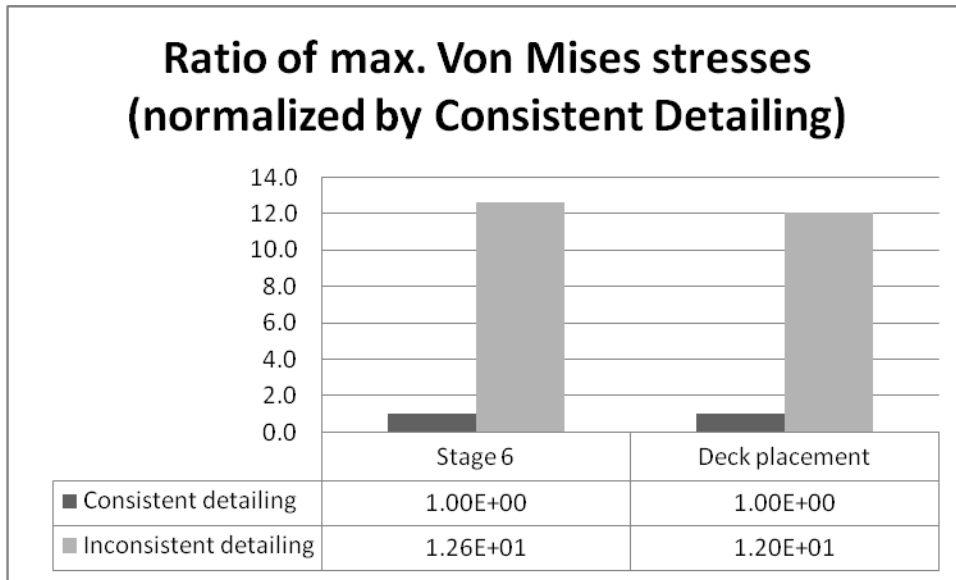


Figure 189: Ratio of Maximum Von Mises Stresses for Bridge C3.

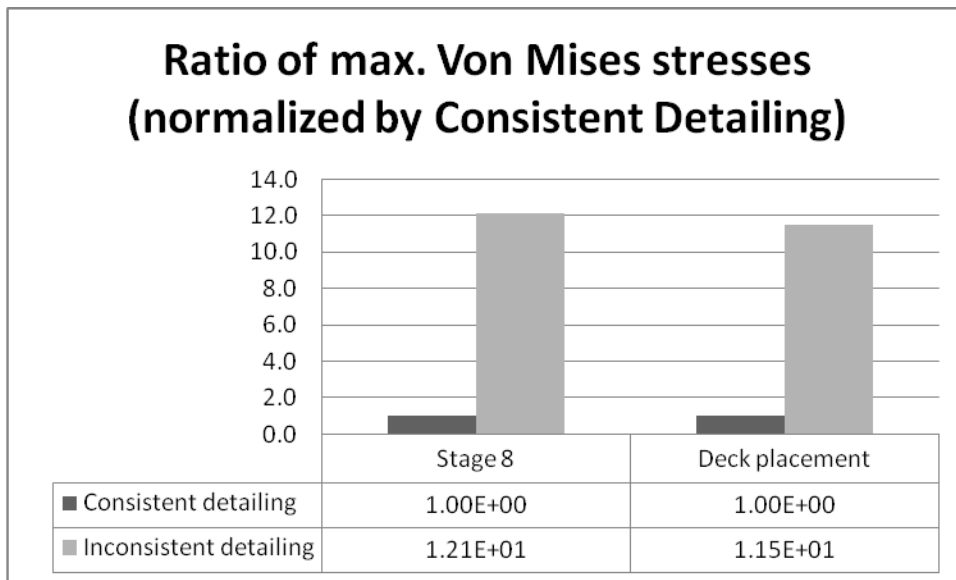


Figure 190: Ratio of Maximum Von Mises Stresses for Bridge C11.

5.5.2.2 Skewed

Similar to the representative curved bridges, to examine the effects of inconsistent detailing on bridge constructability and the resulting locked-in stresses in the skewed bridge cross frames, girder splice deflections and cross-frame Von Mises stresses were examined. Results are shown in Figure 191 through Figure 202. The results show a very small change in vertical deflection in all representative bridges for consistent and inconsistent detailing. However, inconsistent detailing appreciably increased girder lateral deflections and Von Mises stresses in the cross frames. In similar fashion to the curved bridges, cross frames near the supports experienced higher stresses as a result of inconsistent detailing. Moreover, increases for bridges with larger cross-frame spacings were slightly larger than those with smaller cross-frame spacings.

Ratio of max. vertical deflections (normalized by Consistent Detailing)

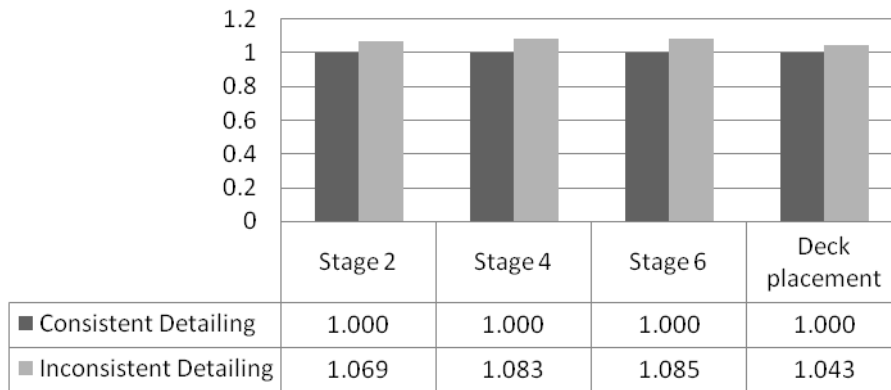


Figure 191: Ratio of Maximum Vertical Deflections for Bridge S5.

Ratio of max. vertical deflections (normalized by Consistent Detailing)

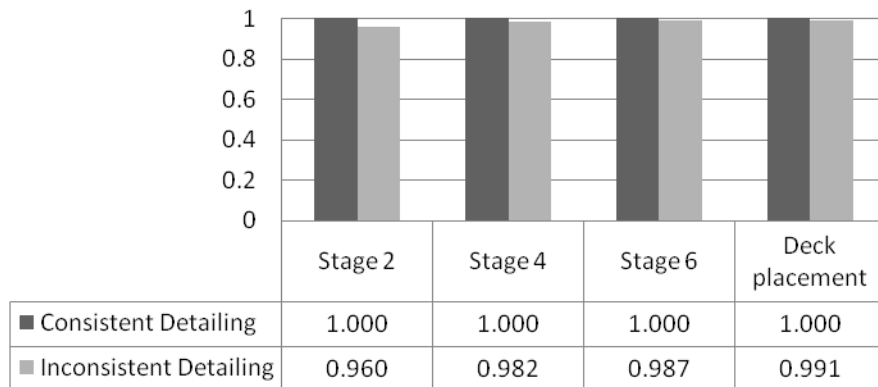


Figure 192: Ratio of Maximum Vertical Deflections for Bridge S6.

Ratio of max. vertical deflections (normalized by Consistent Detailing)

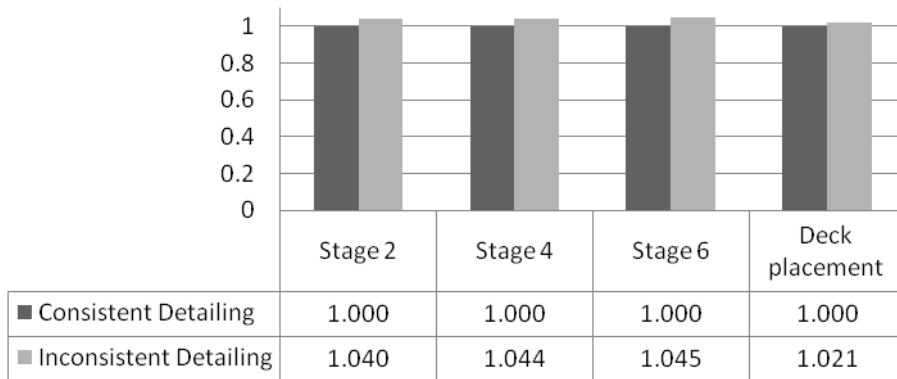


Figure 193: Ratio of Maximum Vertical Deflections for Bridge S7.

Ratio of max. vertical deflections (normalized by Consistent Detailing)

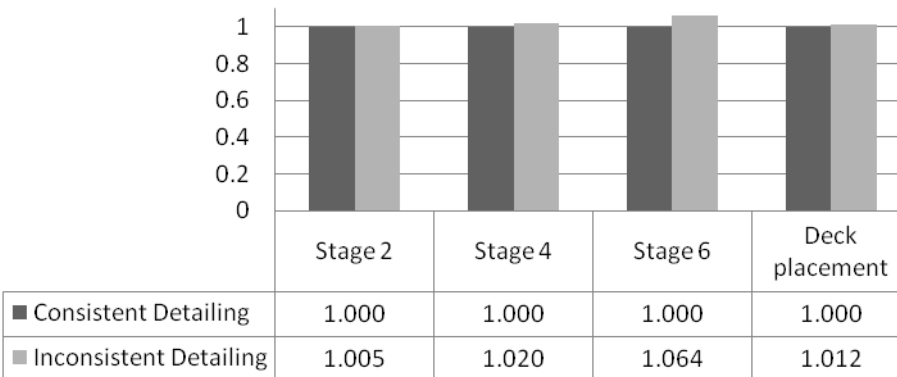


Figure 194: Ratio of Maximum Vertical Deflections for Bridge S8.

Ratio of max. lateral deformations (normalized by Consistent Detailing)

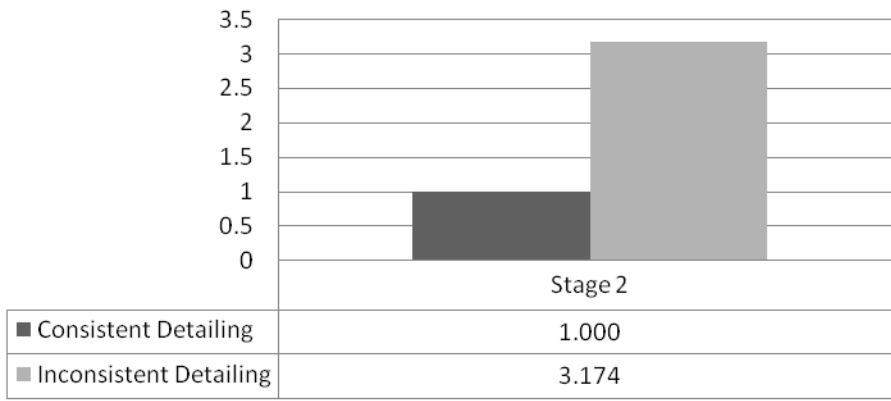


Figure 195: Ratio of Maximum Radial Deflections for Bridge S5.

Ratio of max. lateral deformations (normalized by Consistent Detailing)

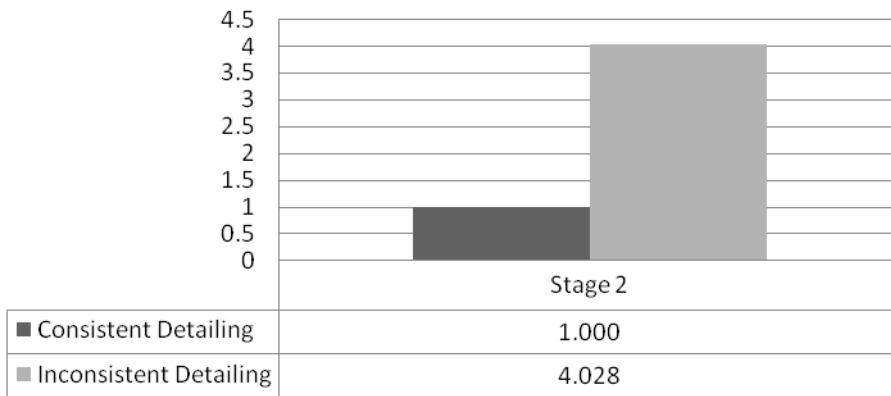


Figure 196: Ratio of Maximum Radial Deflections for Bridge S6.

Ratio of max. lateral deformations (normalized by Consistent Detailing)

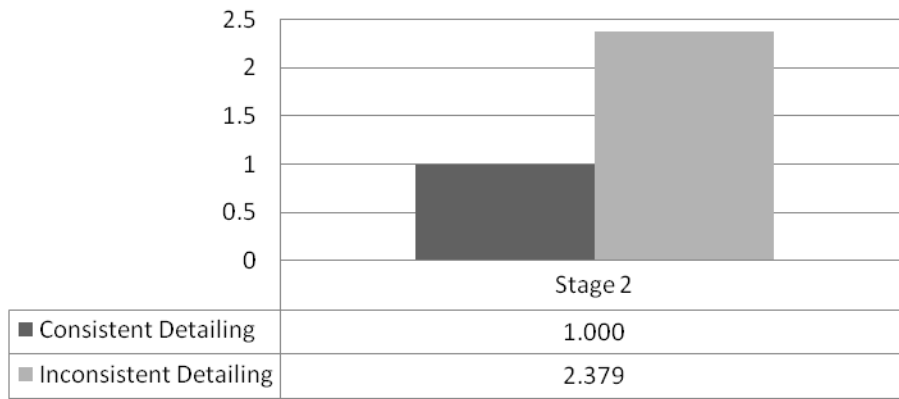


Figure 197: Ratio of Maximum Radial Deflections for Bridge S7.

Ratio of max. lateral deformations (normalized by Consistent Detailing)

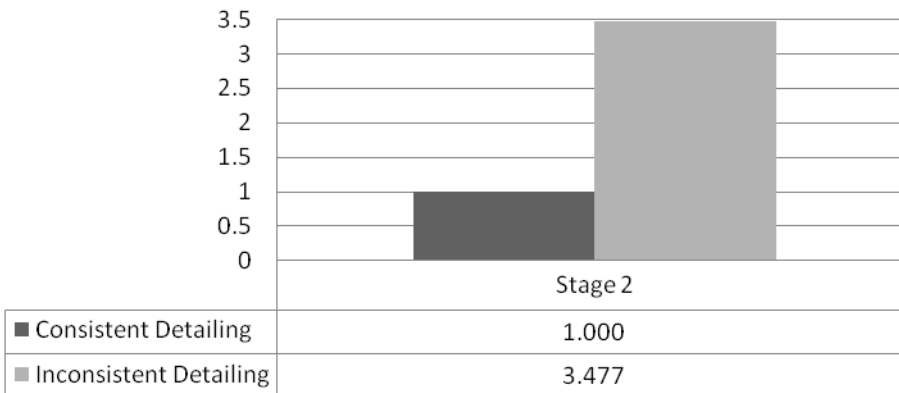


Figure 198: Ratio of Maximum Radial Deflections for Bridge S8.

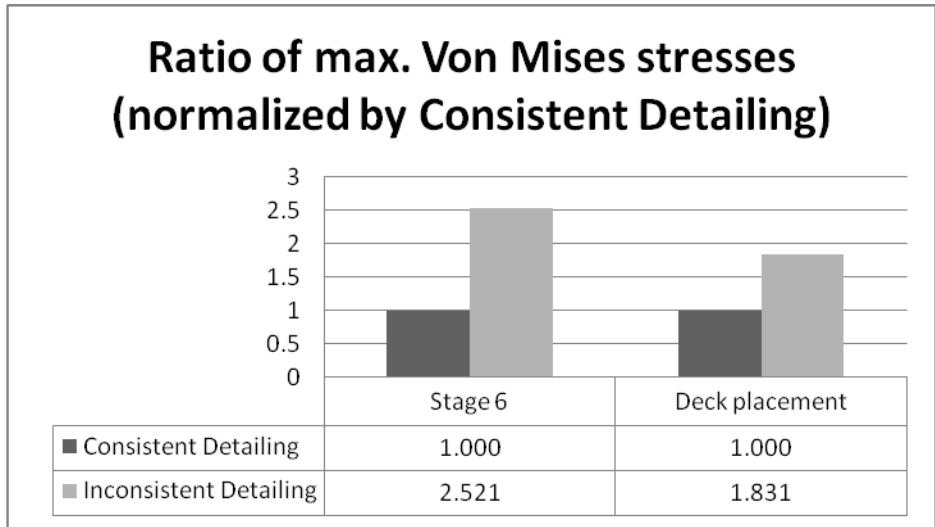


Figure 199: Ratio of Maximum Von Mises Stresses for Bridge S5.

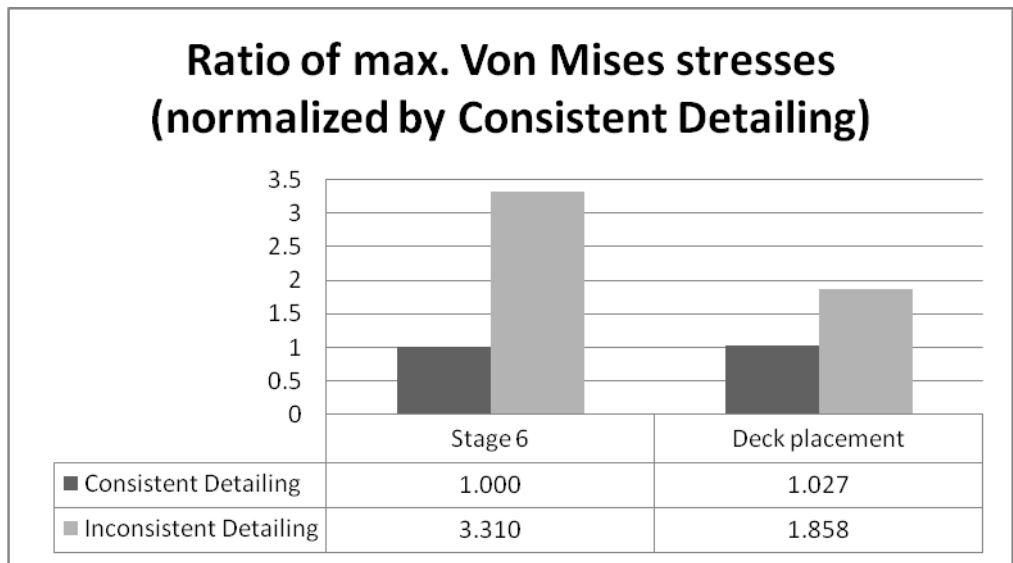


Figure 200: Ratio of Maximum Von Mises Stresses for Bridge S6.

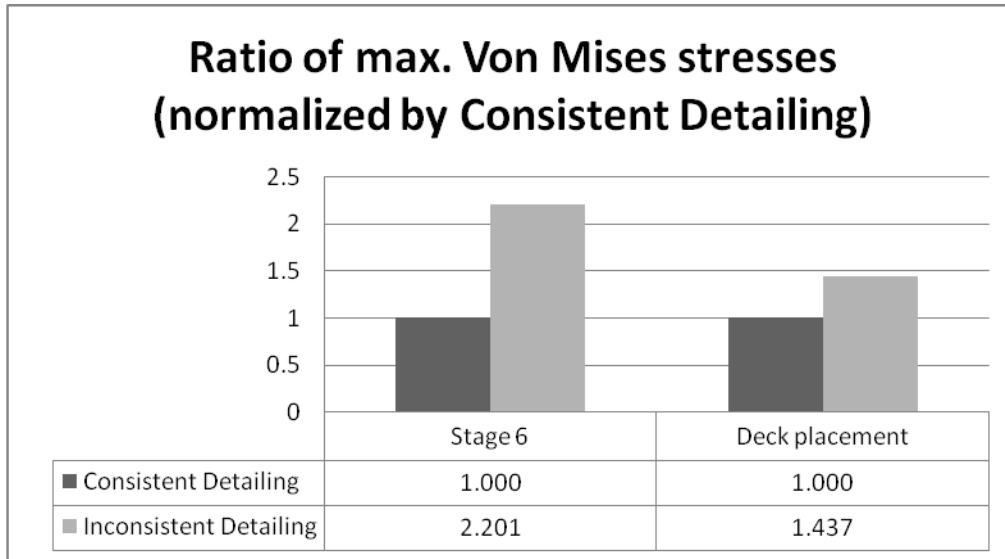


Figure 201: Ratio of Maximum Von Mises Stresses for Bridge S7.

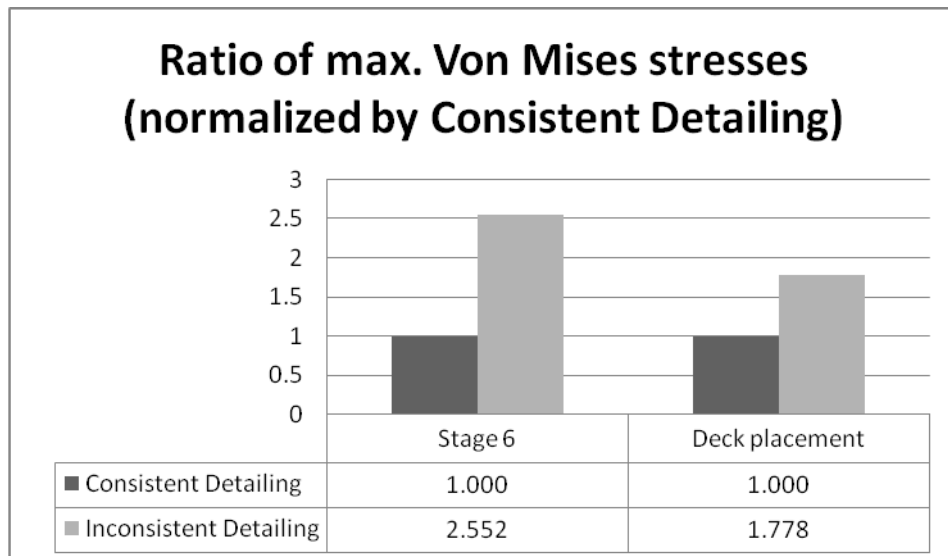


Figure 202: Ratio of Maximum Von Mises Stresses for Bridge S8.

5.5.2.3 Summary

This section examined the effects of inconsistent cross-frame detailing on bridge behavior during construction for curved and skewed structures. Temperature loads were applied to cross frames to mimic the external forces applied to them during construction. The inconsistent detailing was caused by detailing girders and cross frames for different load conditions. In this study, girders were detailed to be web-plumb under no load, and cross frames were detailed to be web-plumb under full dead load. The results suggest that, for both curved and skewed structures, inconsistent cross-frame detailing had a detrimental impact on girder rotations and cross-frame stresses, but had little influence on girder vertical deflections.

- Curved
 - Inconsistent cross-frame detailing increased vertical and radial deflections.
 - Cross-frame stresses were appreciably increased as a result of the locked-in stresses due to the inconsistent detailing. This increase was more pronounced for cross frames near the supports.
 - Irrespective of the radius and cross-frame spacing, inconsistent cross-frame detailing should be avoided for all curved structures to mitigate locked-in stresses and increased deformations. The

effects of inconsistent detailing can be more pronounced in bridges with larger cross frame spacings.

- Skewed
 - Inconsistent cross-frame detailing did not have a crucial impact on girder vertical deflections.
 - Inconsistent cross-frame detailing increased lateral deflections.
 - Cross-frame stresses were appreciably increased as a result of the locked-in stresses due to inconsistent detailing. This increase was more pronounced for cross frames near the supports.
 - Irrespective of the skew and cross-frame spacing, inconsistent cross-frame detailing should be avoided for all skewed structures to mitigate locked-in stresses and increased deformations. The effects of inconsistent detailing can be more pronounced in bridges with larger cross frame spacings.

5.6 Solid Plate Diaphragms

This section explored the effects of replacing cross-frame members with solid plate diaphragms on the construction response of horizontally curved and skewed steel bridges. Three scenarios to replace cross frames with diaphragms were investigated: (1) diaphragms at abutments only, (2) diaphragms at abutments and piers, and (3) diaphragms at abutments, piers and mid-span locations. Diaphragms were designed as short, deep plate girder sections and were initially sized according to appropriate slenderness limits from AASHTO and PennDOT DM4. Once again, SAP 2000 models were employed for final design where appropriate cross frames were replaced. Design forces were then extracted from the analysis results, and the initial cross sections were checked for bending and shear based on relevant AASHTO and Penn DOT DM4 criteria. These final diaphragm sections were used in the subsequent ABAQUS models in place of the cross frames. In these models, similar to the study performed for the girders, diaphragms were modeled utilizing beam elements for their top and bottom flanges and shell elements for their webs, and were tied to the girder webs.

5.6.1 Parametric Studies

5.6.1.1 Curved bridges

Cross frames and diaphragms in curved bridges play an important role in transferring loads, distributing live and dead loads to the girders, providing stability to the compression flanges during erection, and providing torsional stiffness for the overall structure. The examination of the effects of replacing cross frames with diaphragms at abutments, piers, and mid-span locations focused on four representative bridges. The radii of the selected curved bridges were 91.4 m (300 ft) and 304.8 m (1000 ft), and the cross-frame spacings were 4.57 m (15 ft) and 6.86 m (22.5 ft). Table 30 lists the parameters for the bridges that were examined. The paired inner erection method was used for all sequential analyses.

Table 30: Selected Curved Bridge Diaphragm Study Bridge Information.

Bridge No.	Radius of Curvature, m (ft)	Cross-Frame Spacing, m (ft)	Girder-Spacing, m (ft)	Number of Spans	Span-Length, m (ft)	Number of Girder
C1	91.4 (300)	4.57 (15)	3 (10)	2	68.6-68.6 (225-225)	4
C3	91.4 (300)	6.86 (22.5)	3 (10)	2	68.6-68.6 (225-225)	4
C7	304.8 (1000)	4.57 (15)	3 (10)	2	68.6-68.6 (225-225)	4
C9	304.8 (1000)	6.86 (22.5)	3 (10)	2	68.6-68.6 (225-225)	4

5.6.1.2 Skewed bridges

Similar to their role in curved bridges, cross frames and diaphragms in skewed bridges with skew angles smaller than 70° (Penn DOT, 2007) play an important role in load distribution and enhancing stability of the overall structure. As for the curved bridges, the effects of replacing cross frames with diaphragms at sections close to the abutments, piers, and mid-span locations on skewed bridge construction response were studied by looking at four representative two-span bridges. The selected bridges had skew angles of 50° and 70 and cross-frame spacings of 4.57 m (15 ft) and 7.8 m (25.7 ft). Table 31 lists the parameters for the skewed bridges that were examined.

Table 31: Selected Curved Bridge Diaphragm Study Bridge Information.

Bridge No.	Skew Angle, degrees	Cross-Frame Spacing, m (ft)	Girder-Spacing, m (ft)	Number of Spans	Span-Length, m (ft)	Number of Girder
S5	50	4.57 (15)	3 (10)	2	54.9-54.9 (180-180)	4
S6	50	7.8 (25.7)	3 (10)	2	54.9-54.9 (180-180)	4
S7	70	4.57 (15)	3 (10)	2	54.9-54.9 (180-180)	4
S8	70	7.8 (25.7)	3 (10)	2	54.9-54.9 (180-180)	4

5.6.2 Results and Discussion

5.6.2.1 Curved bridges

At each stage the maximum girder vertical deflection and maximum radial deflections at splice locations were examined and normalized against maximum values of the base model, which was the bridge with all cross frames (no diaphragms). Furthermore, maximum Von Mises stresses were compared in cross-frame members after completed erection of the superstructure and deck placement for each scenario. Figure 203 through Figure 214 show comparisons of the deflections and stresses.

Results indicated that the use of diaphragms instead of cross frames caused an increase in both vertical and radial deflections and Von Mises stresses. Diaphragms replacing cross frames at abutments only or at abutments and pier (scenario 1 and 2) showed an average 5% increase in maximum girder vertical deflection. However, when the cross frames were also replaced with diaphragms at mid-span locations (scenario 3), it caused a vertical deflection increase of 7% in 4.57m (15 ft) cross-frame spacing and 9% in 6.86m (22.5 ft) cross-frame spacing, compared to bridge models without diaphragms. Von Mises stresses in cross frames showed an average increase of 13% in all models when compared to the base models with no diaphragms. Diaphragms placement for all 3 scenarios caused an average increase of 10% in radial deflections at the first splice location, and no major changes in deflections at the second splice location. Consequently, it is concluded from these results that the addition of diaphragms instead of cross frames at support and mid-span locations has no appreciable effects on reducing deflections and stresses during the construction of horizontally curved steel bridges.

Ratio of max. vertical deflections (Normalized by No Diaphragm case)

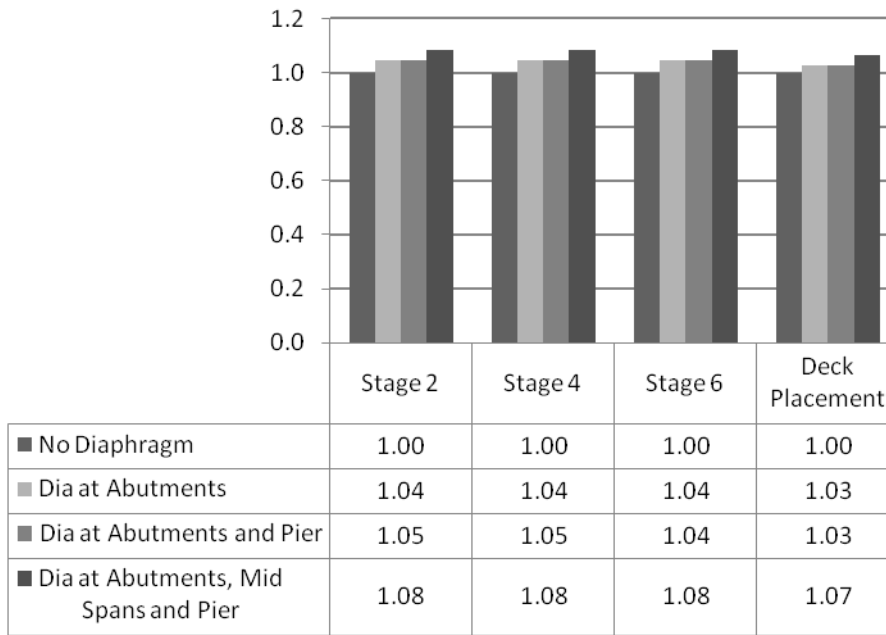


Figure 203: Ratio of Maximum Vertical Deflections for Bridge C1.

Ratio of max. vertical deflections (Normalized by No Diaphragm case)

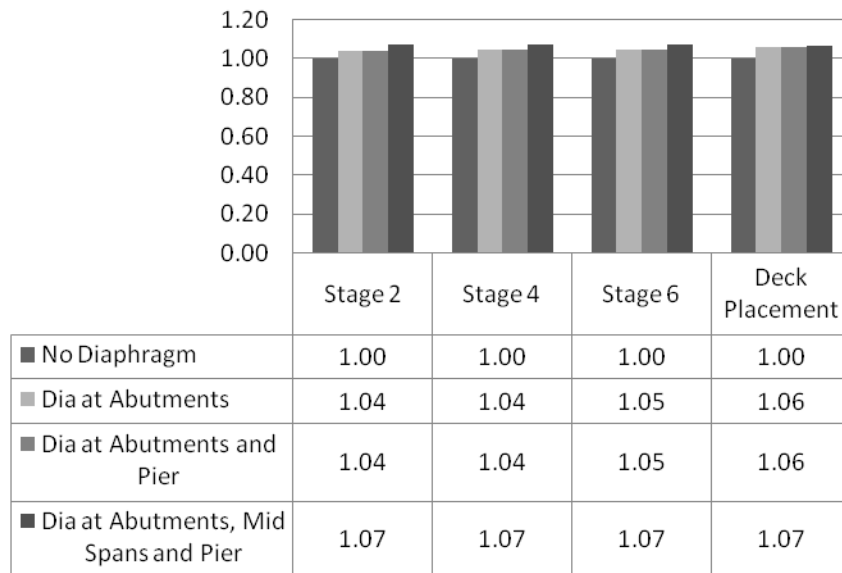


Figure 204: Ratio of Maximum Vertical Deflections for Bridge C3.

Ratio of max. vertical deflections (Normalized by No Diaphragm case)

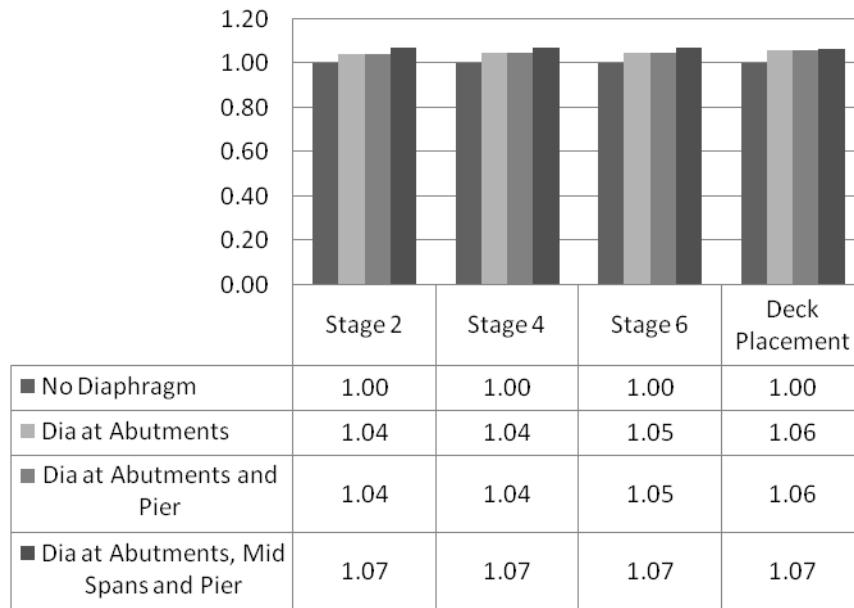


Figure 205: Ratio of Maximum Vertical Deflections for Bridge C7.

Ratio of max. vertical deflections (Normalized by No Diaphragm case)

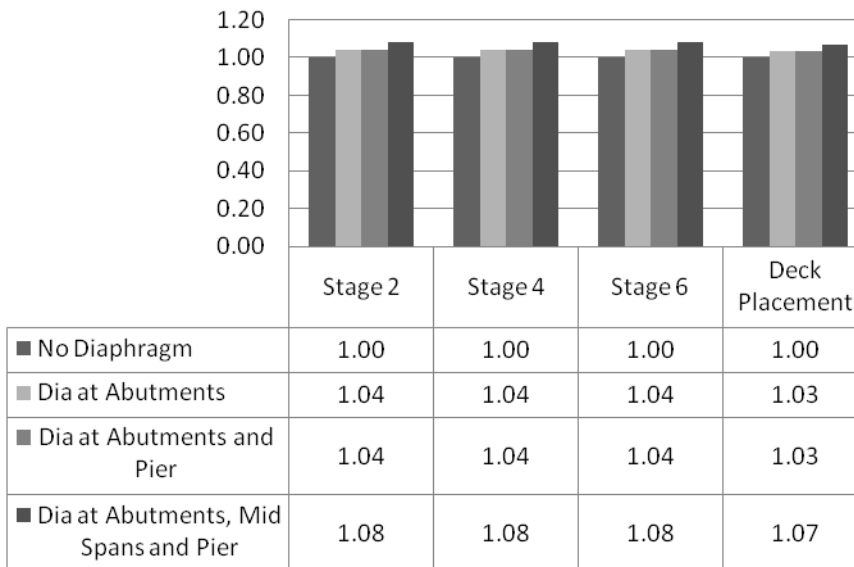


Figure 206: Ratio of Maximum Vertical Deflections for Bridge C9.

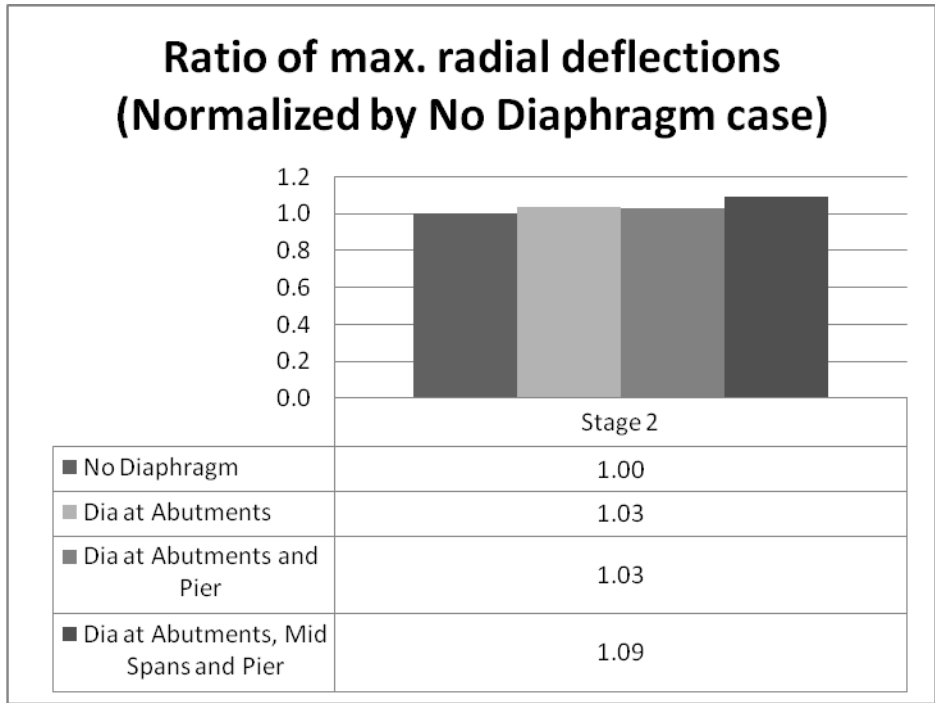


Figure 207: Ratio of Maximum Radial Deflections for Bridge C1.

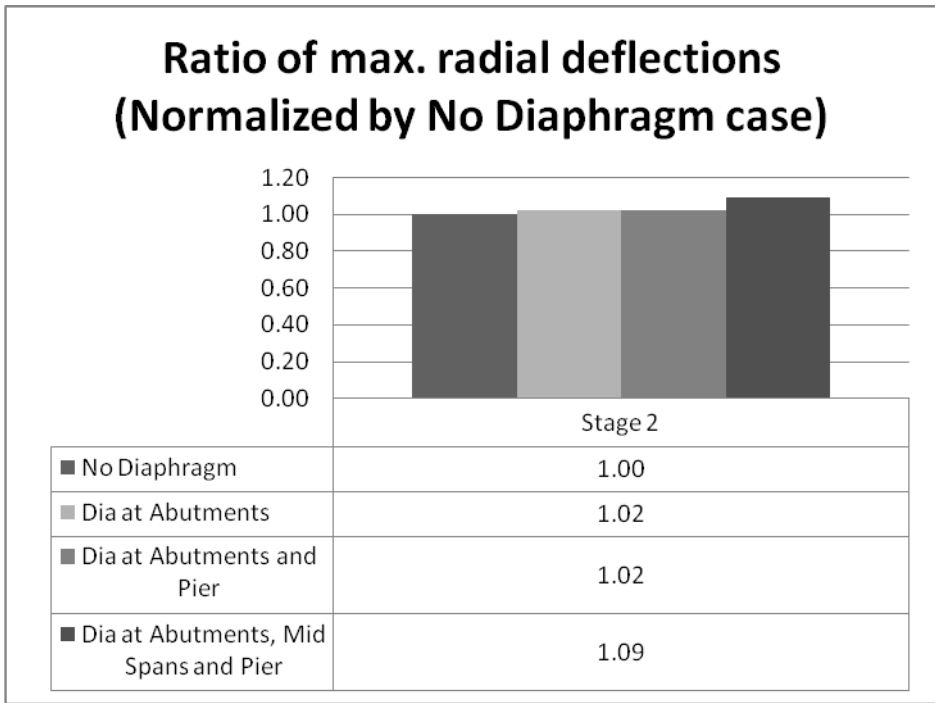


Figure 208: Ratio of Maximum Radial Deflections for Bridge C3.

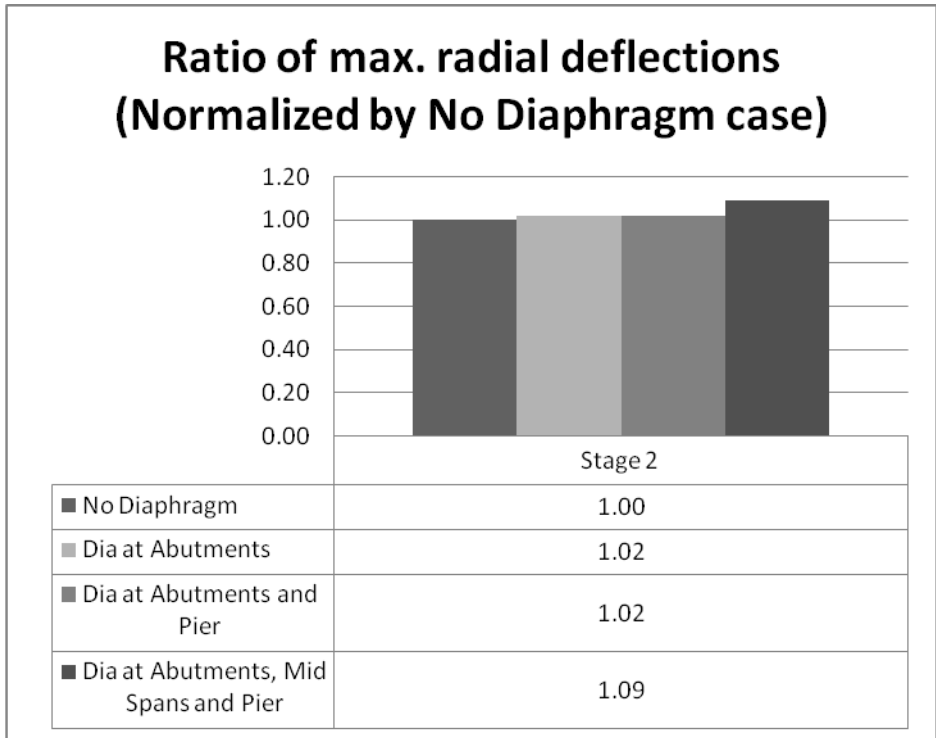


Figure 209: Ratio of Maximum Radial Deflections for Bridge C7.

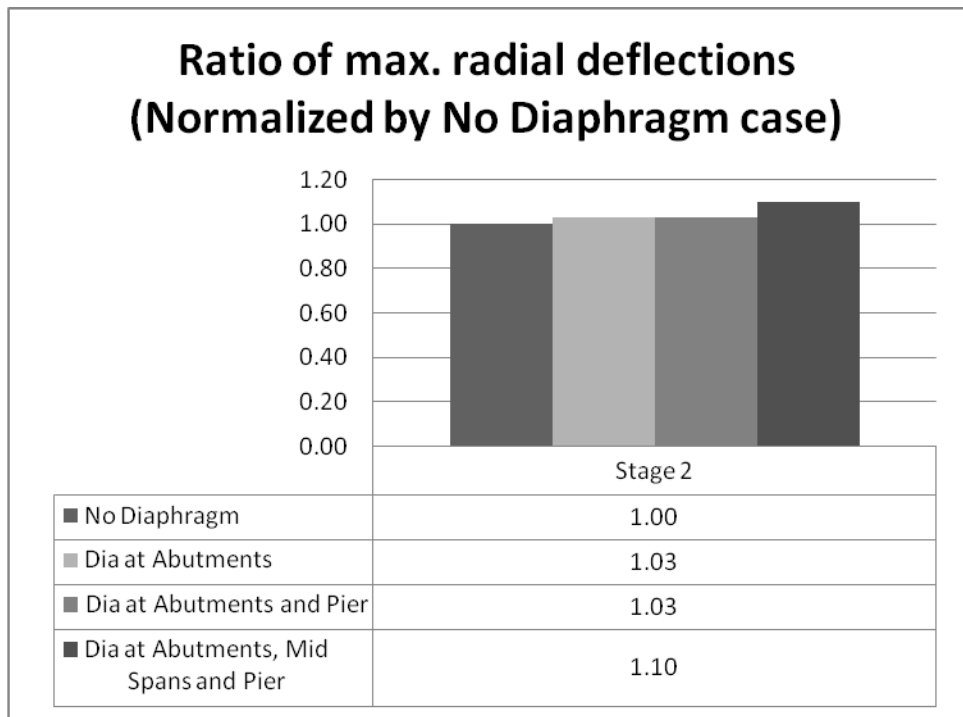


Figure 210: Ratio of Maximum Radial Deflections for Bridge C9.

Ratio of max Von Mises Stress in Cross Frames (Normalized by No Diaphragm case)

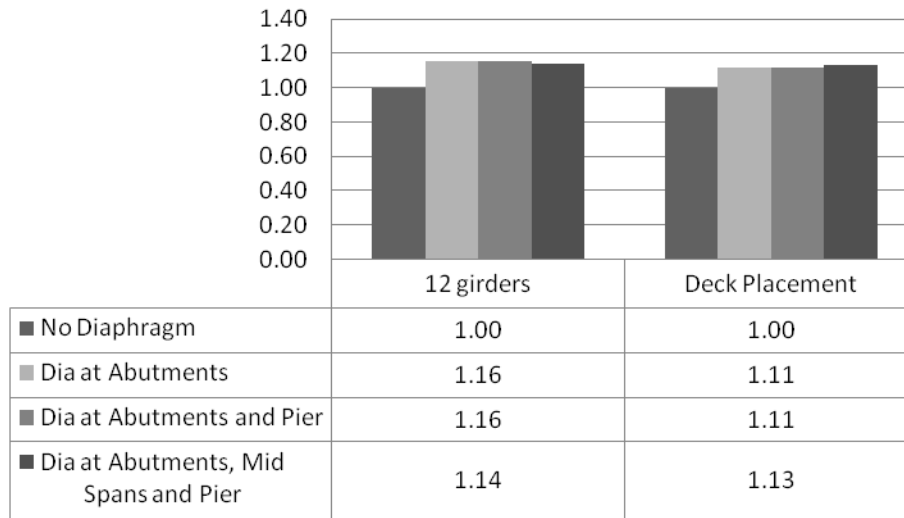


Figure 211: Ratio of Maximum Von Mises Stresses in Cross Frames for Bridge C1.

Ratio of max Von Mises Stress in Cross Frames (Normalized by No Diaphragm case)

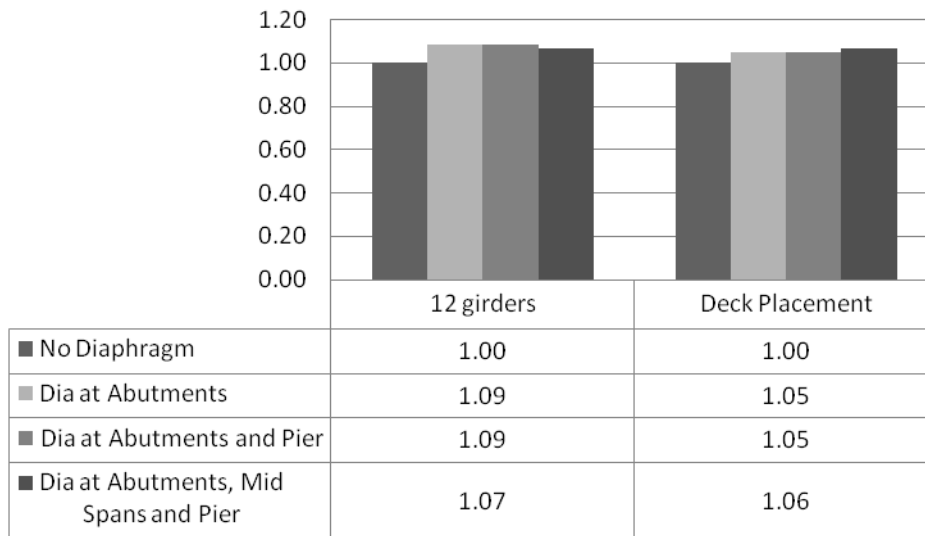


Figure 212: Ratio of Maximum Von Mises Stresses in Cross Frames for Bridge C3.

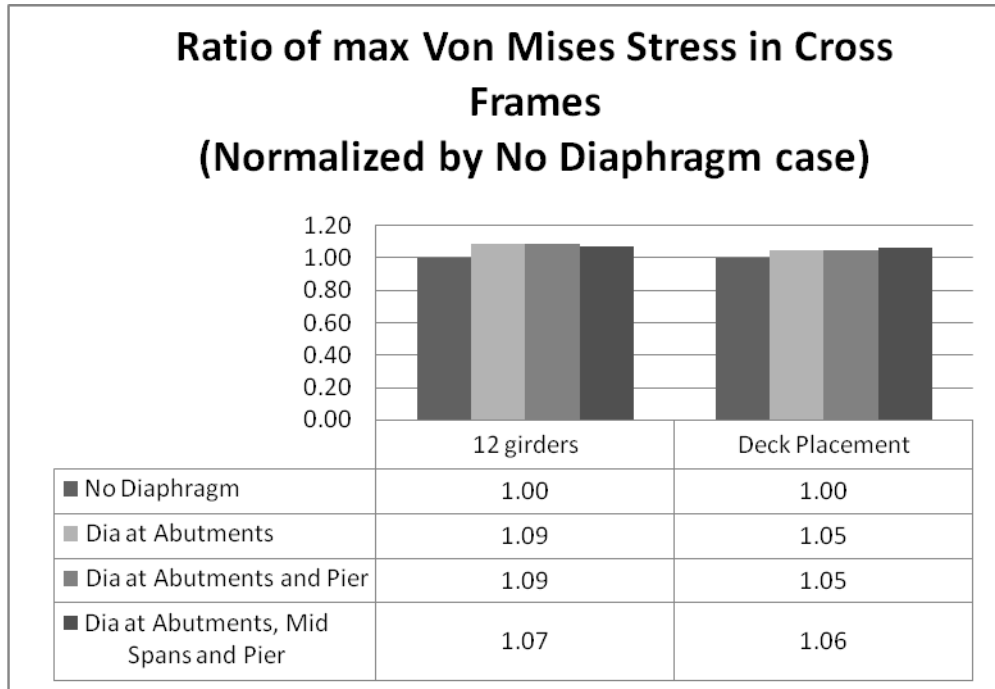


Figure 213: Ratio of Maximum Von Mises Stresses in Cross Frames for Bridge C7.

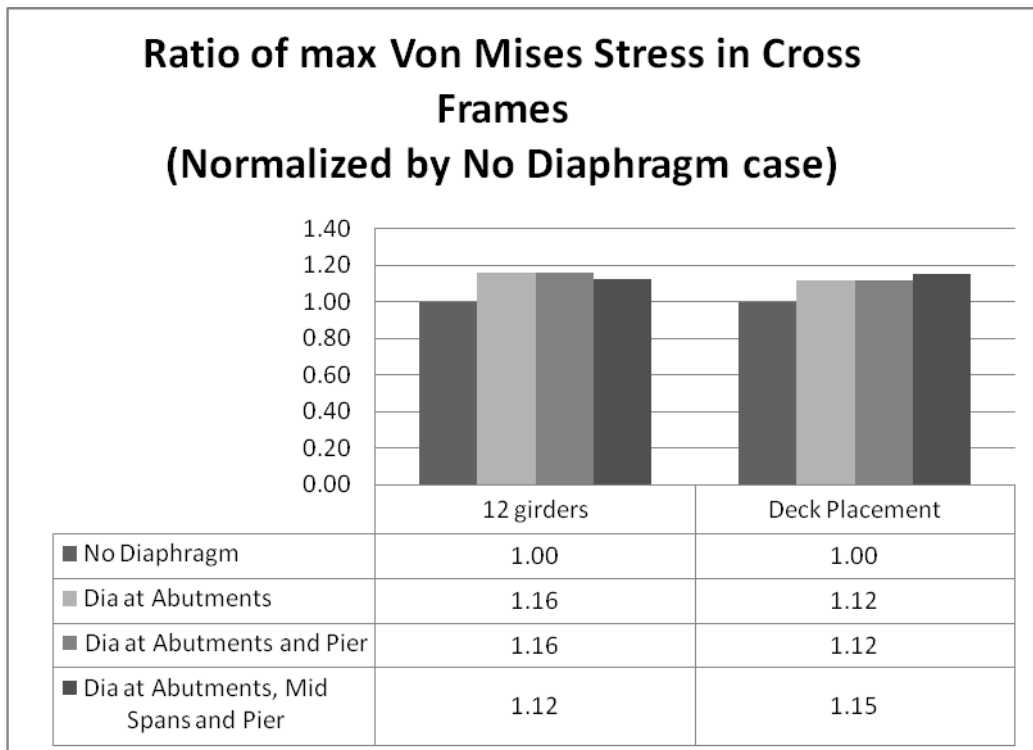


Figure 214: Ratio of Maximum Von Mises Stresses in Cross Frames for Bridge C9.

5.6.2.2 Skewed bridges

Vertical deflection of the girders, lateral deformations at splice locations, and maximum Von Mises stresses in cross frames were also compared for the representative skewed bridges. These values were normalized with their

corresponding values for the bridge models which had only cross frames and no diaphragms. Figure 215 through Figure 226 show comparisons of the deformations and stresses.

As can be observed in the results, maximum vertical deformation of the girders at mid-span and lateral deformations at splice location increased slightly for bridges with diaphragms when compared to those values for bridges with no diaphragms. The reason for this increase is the additional load imposed to the structure due to the self weight of the diaphragm elements, which are relatively heavy when compared to the cross frames they replaced. This increase in deformations is higher, to some degree, for those bridges that have larger cross-frame spacing (Bridge S-6 and Bridge S-8). For maximum stresses in cross frames, the effect of replacing cross frames with diaphragms is not significant for any of the cases. In general, it can be concluded from these results that using diaphragms instead of cross frames at supports and mid-span locations of the skewed bridges had insignificant influence on their behavior during construction.

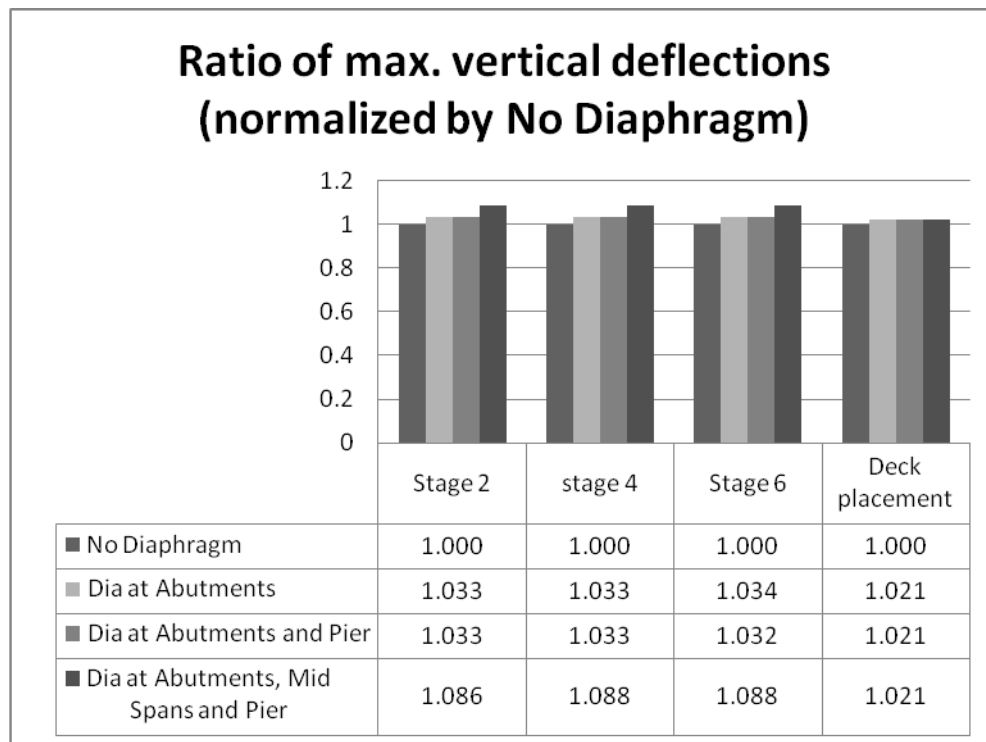


Figure 215: Ratio of Maximum Vertical Deflections for Bridge S5.

Ratio of max. vertical deflections (normalized by No Diaphragm)

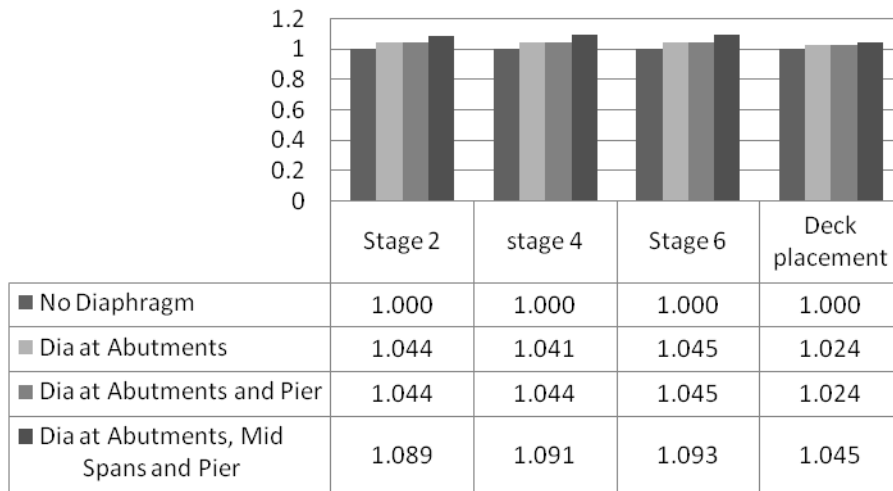


Figure 216: Ratio of Maximum Vertical Deflections for Bridge S6.

Ratio of max. vertical deflections (normalized by no diaphragm)

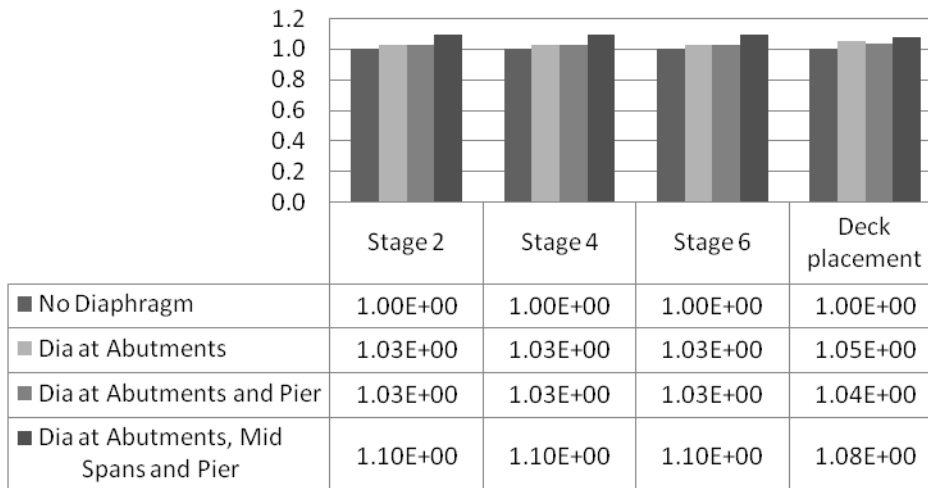


Figure 217: Ratio of Maximum Vertical Deflections for Bridge S7.

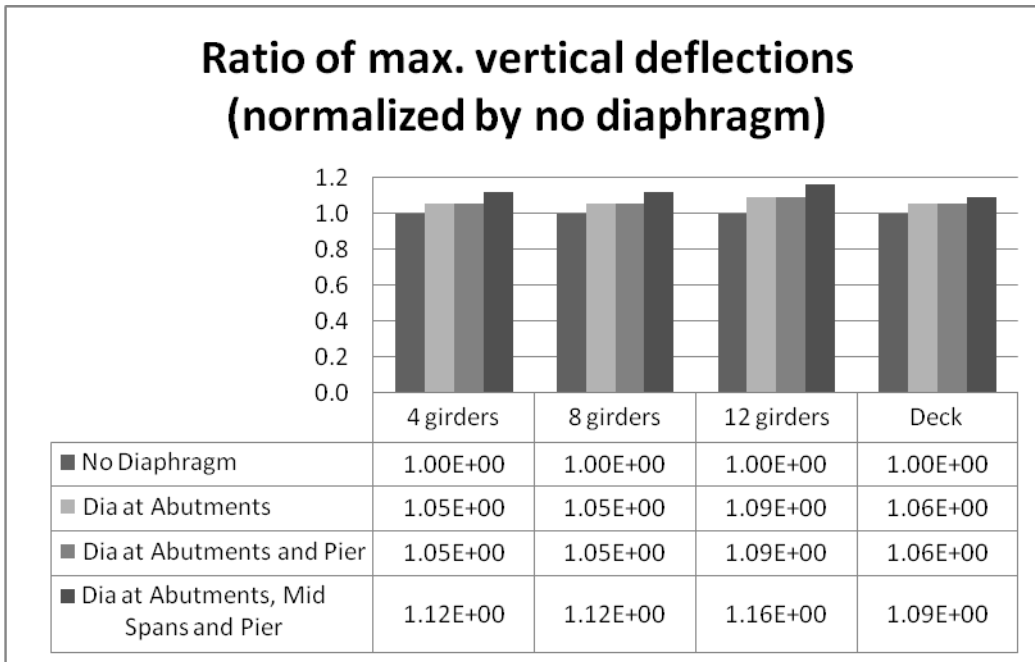


Figure 218: Ratio of Maximum Vertical Deflections for Bridge S8.

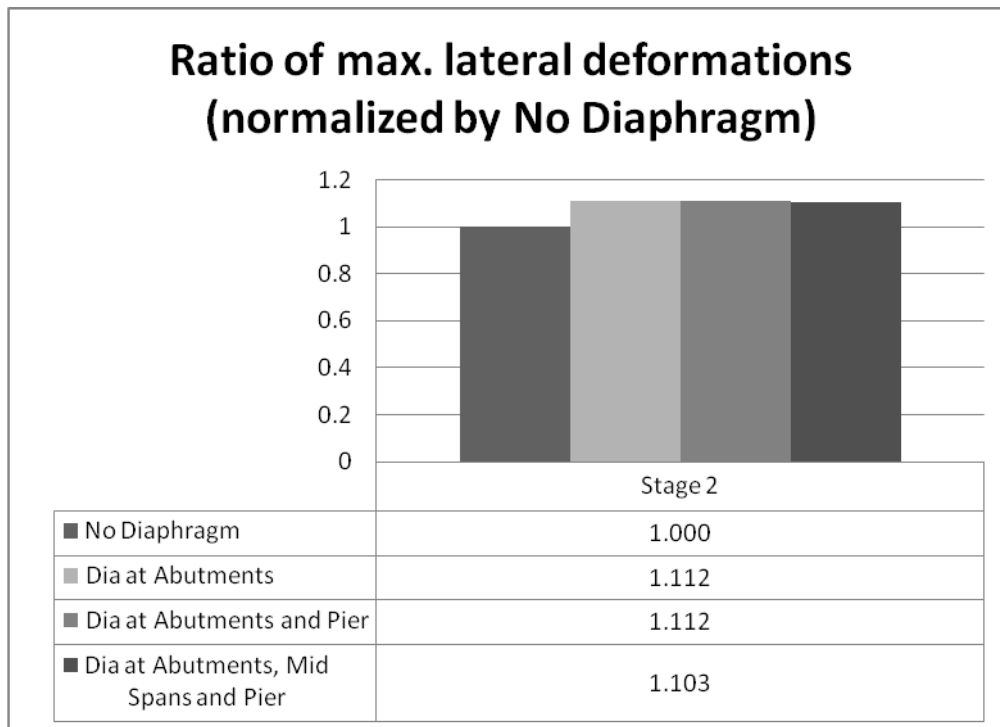


Figure 219: Ratio of Maximum Lateral Deflections for Bridge S5.

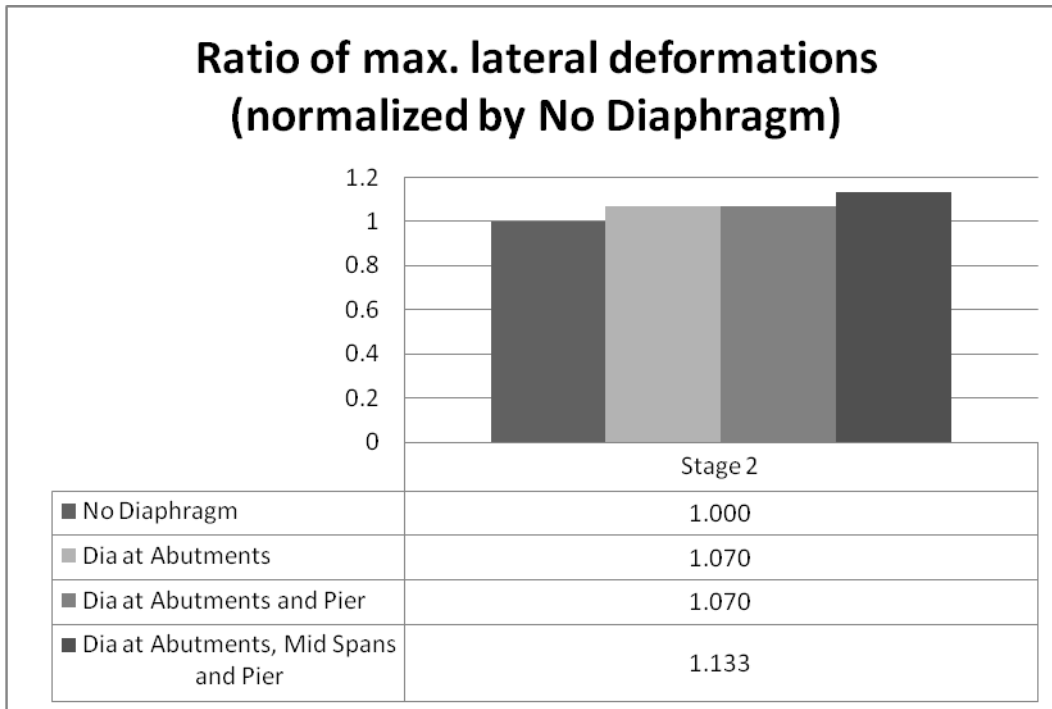


Figure 220: Ratio of Maximum Lateral Deflections for Bridge S6.

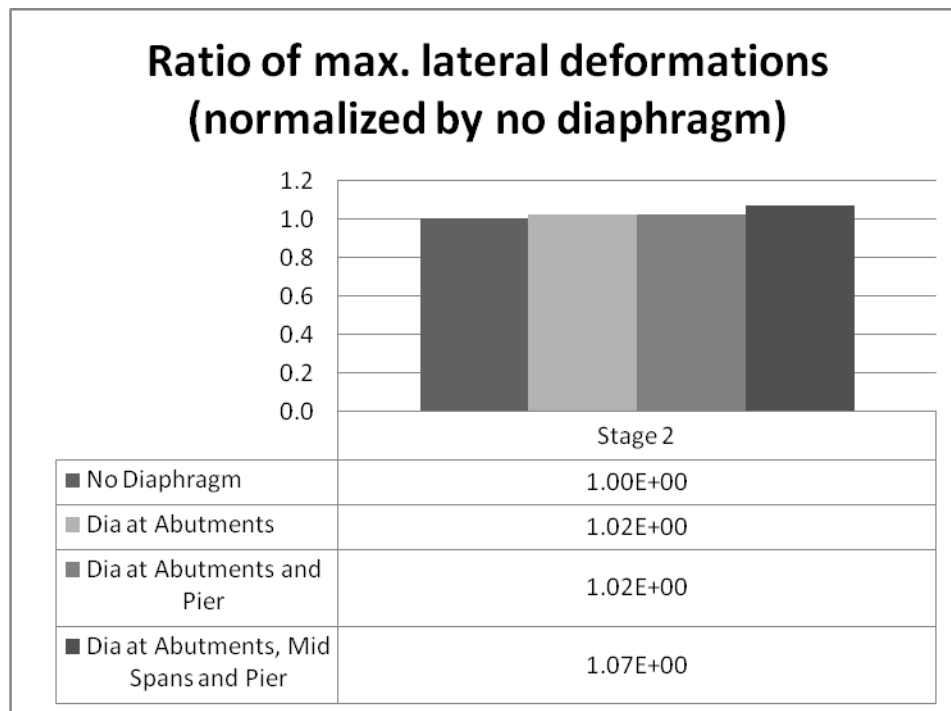


Figure 221: Ratio of Maximum Lateral Deflections for Bridge S7.

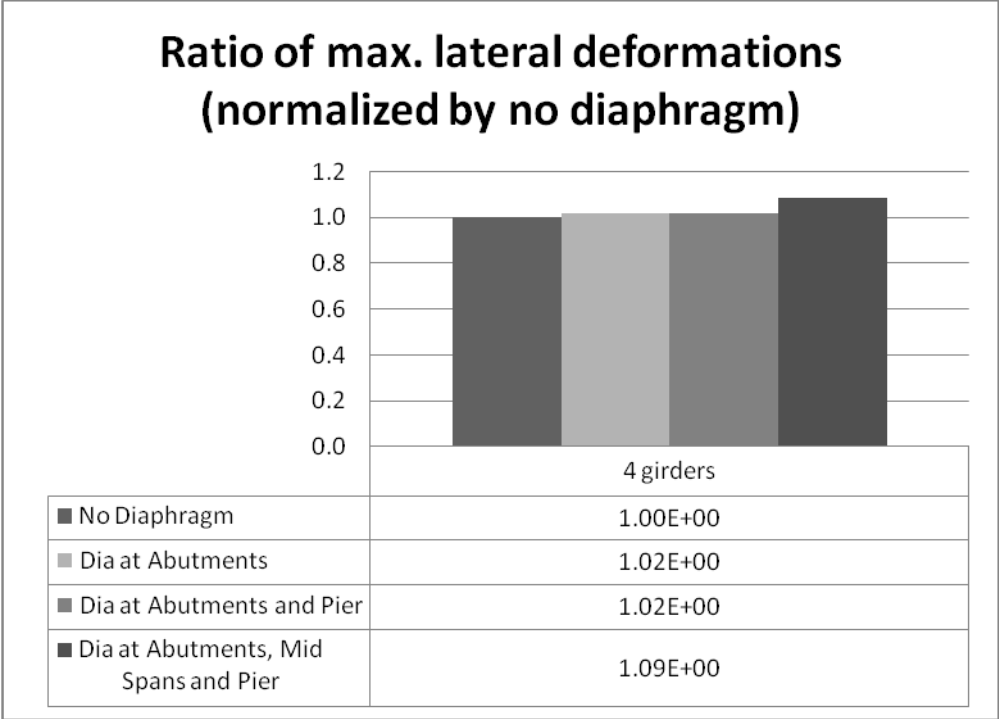


Figure 222: Ratio of Maximum Lateral Deflections for Bridge S8.

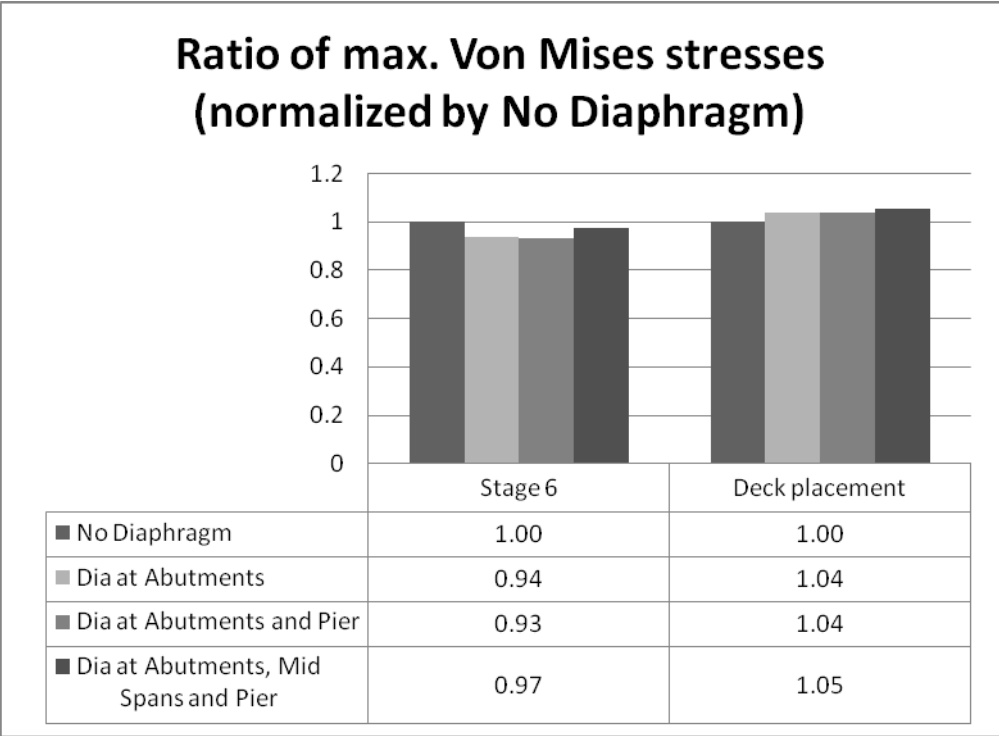


Figure 223: Ratio of Maximum Von Mises Stresses in Cross Frames for Bridge S5

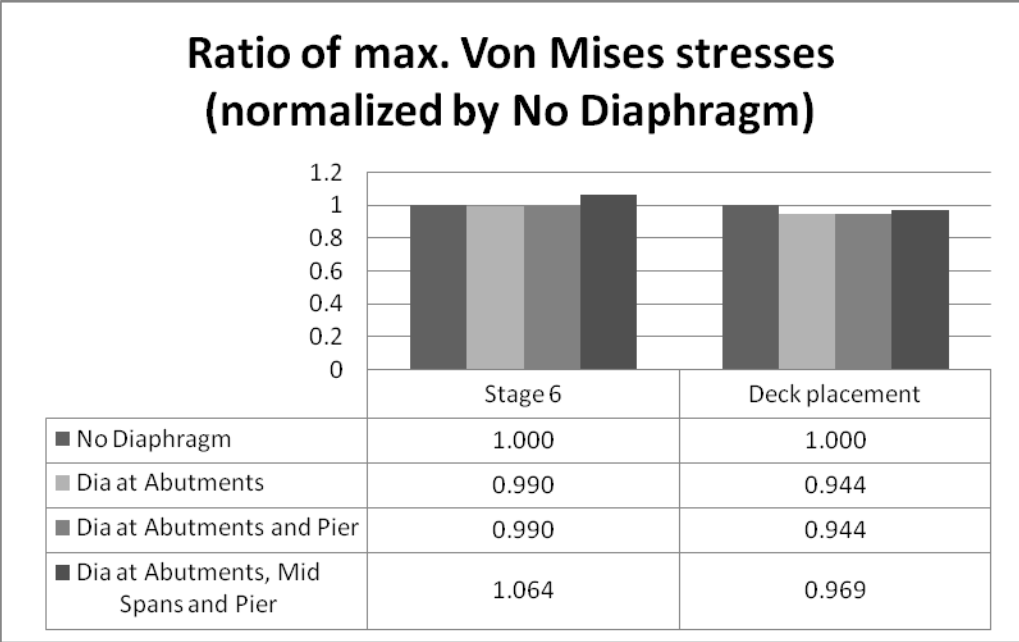


Figure 224: Ratio of Maximum Von Mises Stresses in Cross Frames for Bridge S6.

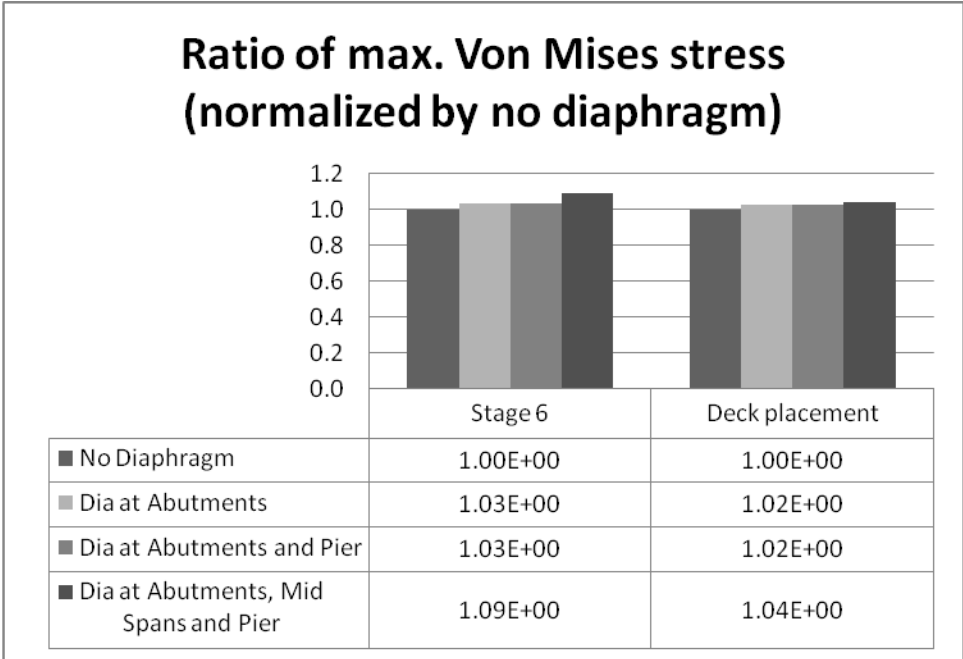


Figure 225: Ratio of Maximum Von Mises Stresses in Cross Frames for Bridge S7.

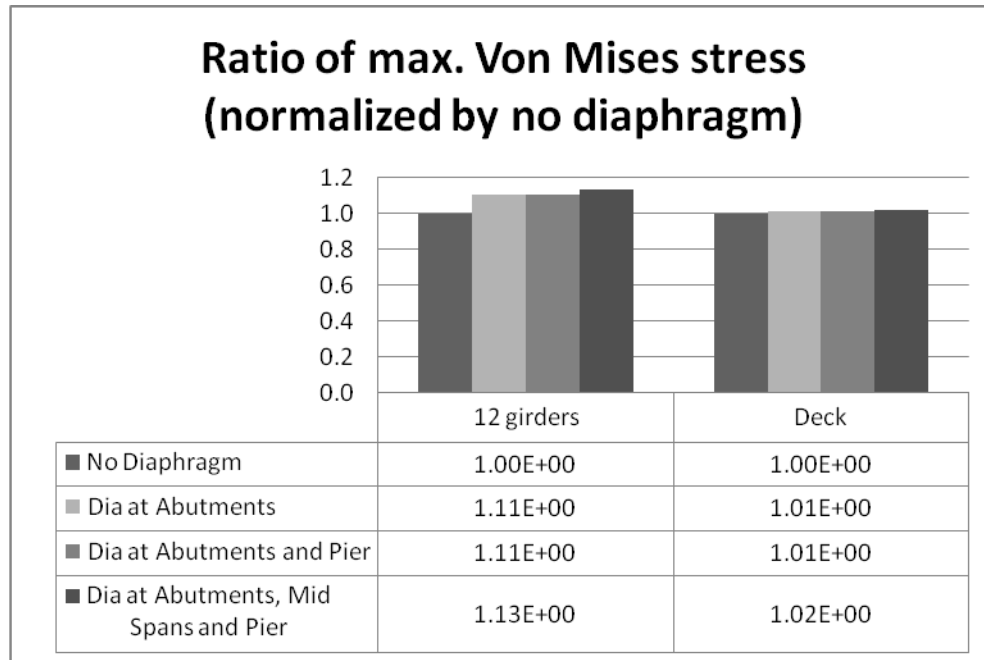


Figure 226: Ratio of Maximum Von Mises Stresses in Cross Frames for Bridge S8.

5.6.2.3 Summary

This section examined the effects of replacing cross frames with diaphragms at the abutments, piers, and mid-span locations on curved and skewed bridge behavior during construction. Results showed no significant changes in girder deflections and cross-frame stresses between bridges with diaphragms and without diaphragms. The girder deflections and cross-frame stresses were slightly increased due to the diaphragm self weight. Therefore, replacing cross frames with diaphragms had no appreciable benefit to the bridge constructability for both curved and skewed structures.

In summary, findings from the diaphragm parametric studies for the curved and skewed bridges that were examined included:

- Curved
 - o Replacing cross frames with solid plate diaphragms did not severely affect bridge vertical and radial deflections and cross-frame stresses during construction, irrespective of the radius and cross-frame spacing.
 - o Replacing cross frames with solid plate diaphragms at the abutment and pier locations for the curved bridges that were studied did not adversely affect or appreciably benefit their construction behavior. Nevertheless, using diaphragms at the mid-span locations can cause slightly higher deformations for the girders when compared to the use of cross frames at those locations.
- Skewed
 - o Placing solid plate diaphragms in skewed bridges slightly increased deformations due to the self weight of the diaphragms, but did not severely affect cross-frame stresses.
 - o Replacing cross frames with solid plate diaphragms at the abutment and pier locations for the skewed bridges did not adversely affect or appreciably benefit their construction behavior. However, using diaphragms at the mid-span locations can cause slightly higher deformations for the girders when compared to the use of cross frames at those locations.

5.7 Temperature Change

This section examined the effects of temperature change during deck placement. To study this effect, daily temperature change data from National Oceanic and Atmospheric Administration's (NOAA) National Weather Service (2010) for central Pennsylvania was used to determine the value of temperature change to be applied to

structures during a given construction event. Figure 227 presents daily high and low temperatures in central Pennsylvania from 2003 to 2007 obtained from NOAA. The maximum temperature change in a day from 2003 to 2007 was 43 °F. To be conservative, a 50 °F temperature rise was applied to the structures during deck placement, so the resulting maximum cross-frame stress was the highest. To model temperature effects in ABAQUS, temperature loads were applied to the entire steel superstructure, with the initial temperature being 20 °F and the final temperature being 70 °F. These values were arbitrarily selected to give the desired temperature change, and their actual magnitudes had no bearing on ABAQUS results. Deflections and stresses were monitored before and after the temperature change.

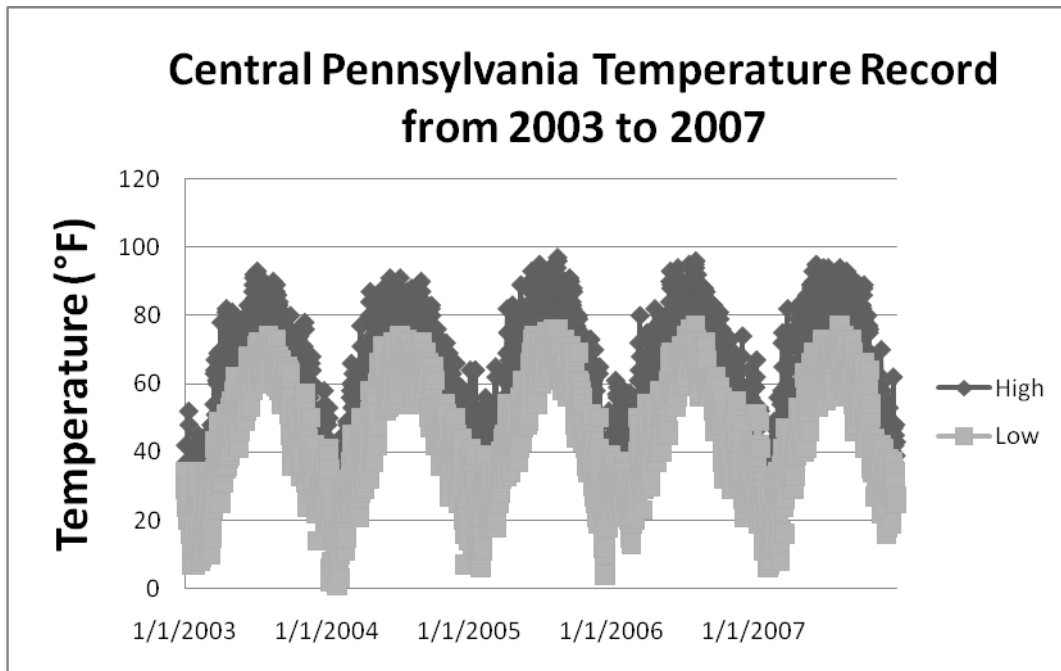


Figure 227: Central Pennsylvania High and Low Temperatures. (NOAA, 2010).

5.7.1 Parametric Studies

5.7.1.1 Curved

Examination of the effects of temperature change during deck placement on curved structures consisted of comparisons of deflection and stress changes after the temperature change occurred. To investigate the effects of radius, cross-frame spacing, and unbalanced spans in conjunction with temperature change during deck placement, eight representative bridges involving different parameters (radius, cross-frame spacing, and span ratio) were selected. The selected bridges were two-span structures with varying radii and cross-frame spacings and three-span structures with balanced and unbalanced spans. The radii of the two-span bridges were 91.4 m (300 ft), 198.1 m (650 ft), and 304.8 m (1000 ft), and the cross-frame spacings were 4.57 m (15 ft) and 6.86 m (22.5 ft). These parameters were selected so that they included moderately to severely curved bridges with different cross-frame spacings, resulting in R/L values from 13.3 to 66.7. The balanced and unbalanced three-span, four-girder bridges had the same radius (91.4 m (300ft)) and cross-frame spacing (6.86 m (22.5 ft)), with the unbalanced span ratio being 1:1.4. Table 32 lists the parameters of the selected representative bridges.

Table 32: Selected Curved Bridge Temperature Change Study Information.

Bridge No.	Radius of Curvature, m (ft)	Cross-Frame Spacing, m (ft)	Girder-Spacing, m (ft)	Number of Spans	Span-Length, m (ft)	Number of Girder
C1	91.4 (300)	4.57 (15)	3 (10)	2	68.6-68.6 (225-225)	4

C3	91.4 (300)	6.86 (22.5)	3 (10)	2	68.6-68.6 (225-225)	4
C6	198.1 (650)	6.86 (22.5)	3 (10)	2	68.6-68.6 (225-225)	4
C7	304.8 (1000)	4.57 (15)	3 (10)	2	68.6-68.6 (225-225)	4
C9	304.8 (1000)	6.86 (22.5)	3 (10)	2	68.6-68.6 (225-225)	4
C10	91.4 (300)	6.86 (22.5)	3 (10)	3	68.6-68.6-68.6 (225-225-225)	4
C11	91.4 (300)	6.86 (22.5)	3 (10)	3	48-68.6-68.6 (157.5-225-225)	4
C12	91.4 (300)	6.86 (22.5)	3 (10)	3	48-68.6-48 (157.5-225-157.5)	4

5.7.1.2 Skewed

Similar to the curved bridges, the effects of temperature change during deck placement was investigated by considering eight representative bridges. These bridges were selected to include the effects of skew angle, cross-frame spacing, and unbalanced spans in conjunction with temperature change. The selected bridges were two single-span bridges with severely skewed abutments (50°) and varying cross-frame spacing, four two-span bridges with varying skew angle (50° and 70°) and cross-frame spacing, and two three-span bridges with balanced and unbalanced spans. The cross frame-spacings in the single- and two-span bridges were 4.57 m (15 ft) and 7.8 m (25.7 ft). The balanced and unbalanced three-span, four-girder bridges had the same skew angle (50°) and cross-frame spacing (7.8 m (25.7 ft)), with the unbalanced span ratio being 1:1.4. Table 33 lists the parameters of the selected representative bridges.

Table 33: Selected Skewed Bridge Temperature Change Study Information.

Bridge No.	Skew Angle, degrees	Cross-Frame Spacing, m (ft)	Girder-Spacing, m (ft)	Number of Spans	Span-Length, m (ft)	Number of Girder
S1	50	4.57 (15)	3 (10)	1	54.9 (180)	4
S2	50	7.8 (25.7)	3 (10)	1	54.9 (180)	4
S5	50	4.57 (15)	3 (10)	2	54.9-54.9 (180-180)	4
S6	50	7.8 (25.7)	3 (10)	2	54.9-54.9 (180-180)	4
S7	70	4.57 (15)	3 (10)	2	54.9-54.9 (180-180)	4
S8	70	7.8 (25.7)	3 (10)	2	54.9-54.9 (180-180)	4
S9	50	7.8 (25.7)	3 (10)	3	54.9-54.9-54.9 (180-180-180)	4
S10	50	7.8 (25.7)	3 (10)	3	54.9-54.9-39.2 (180-180-128.75)	4

5.7.2 Results and Discussion

5.7.2.1 Curved

Comparisons of deflections and stresses are presented in Figure 228 through Figure 2. Girder deflection changes between bridges studied caused by the temperature change were not as noticeable as stress changes in the cross frames. The results showed that stress changes due to temperature increased with increasing curvature and

decreasing cross-frame spacing. These findings suggested: (1) temperature changes could aggravate curvature effects on cross-frame stresses, and (2) smaller cross-frame spacings could lead to higher stress increases caused by temperature changes.

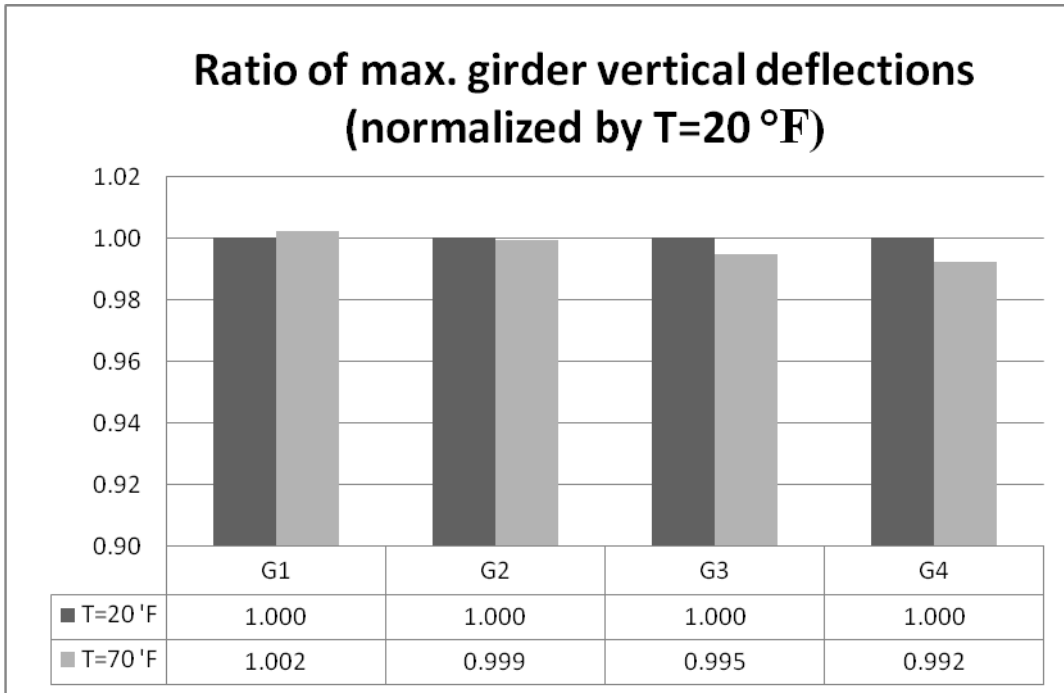


Figure 228: Ratio of Maximum Vertical Deflections for Bridge C1.

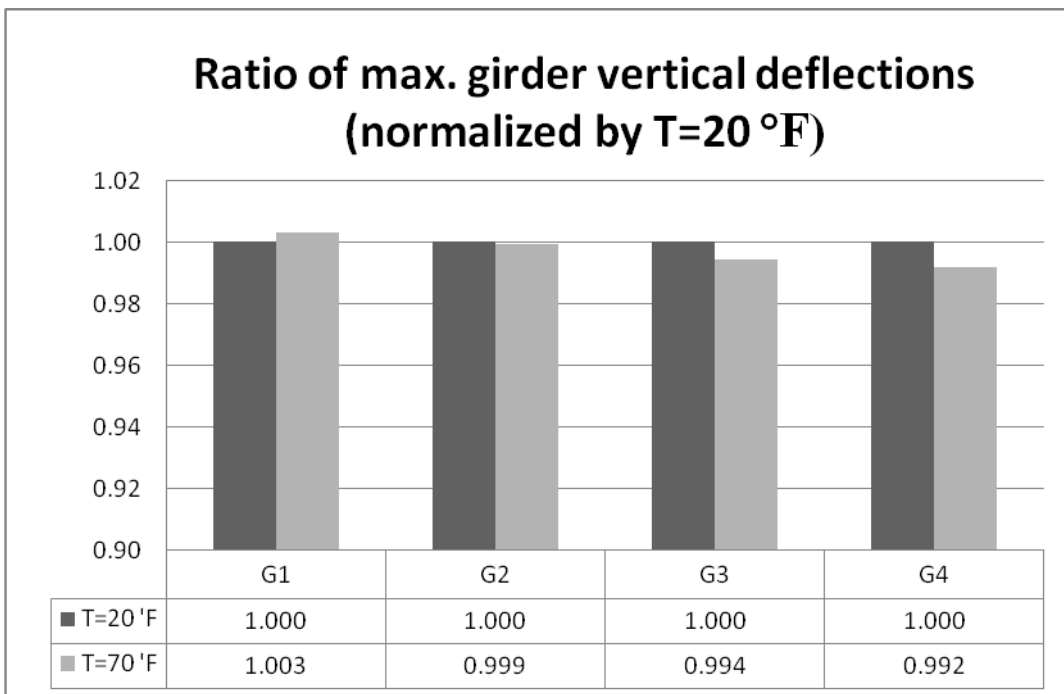


Figure 229: Ratio of Maximum Vertical Deflections for Bridge C3.

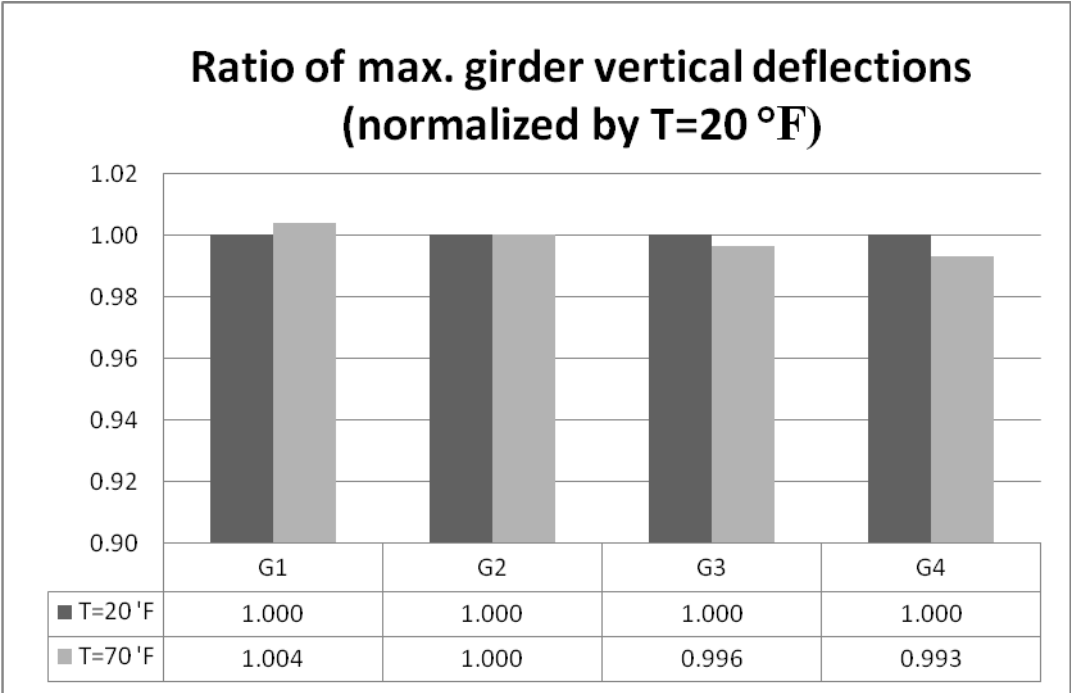


Figure 230: Ratio of Maximum Vertical Deflections for Bridge C6.

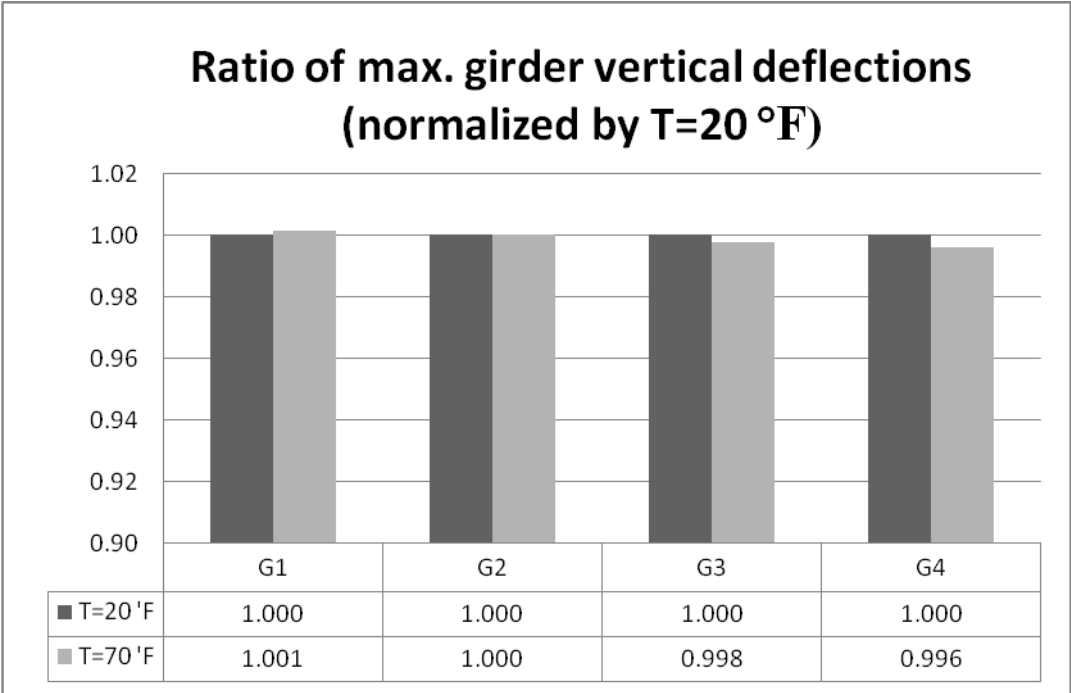


Figure 231: Ratio of Maximum Vertical Deflections for Bridge C7.

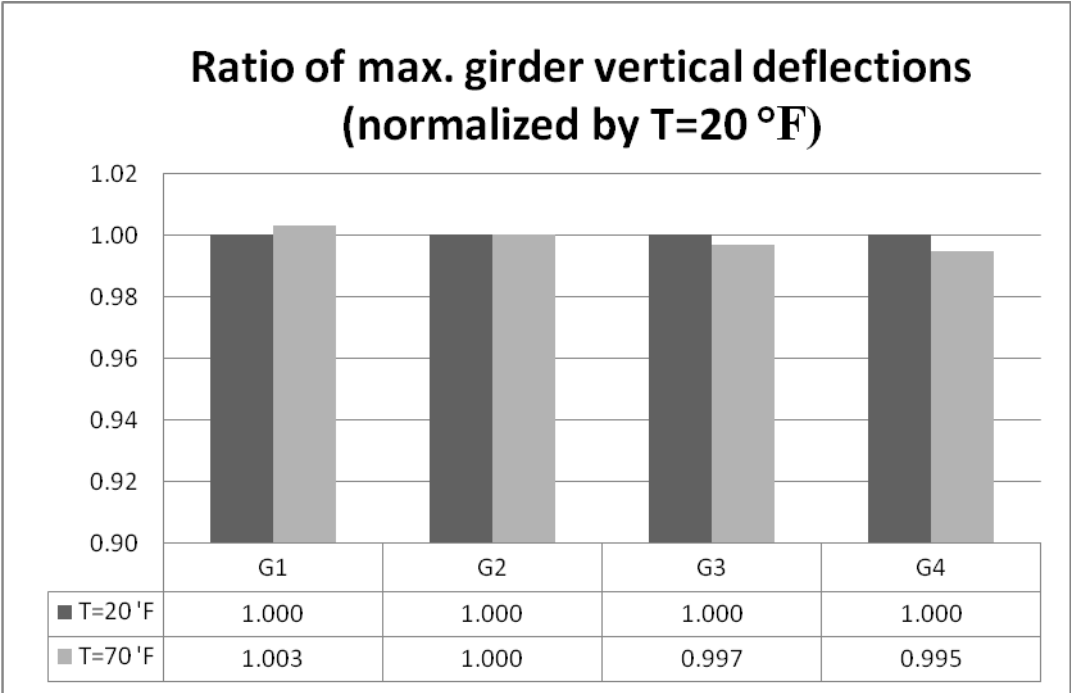


Figure 227: Ratio of Maximum Vertical Deflections for Bridge C9.

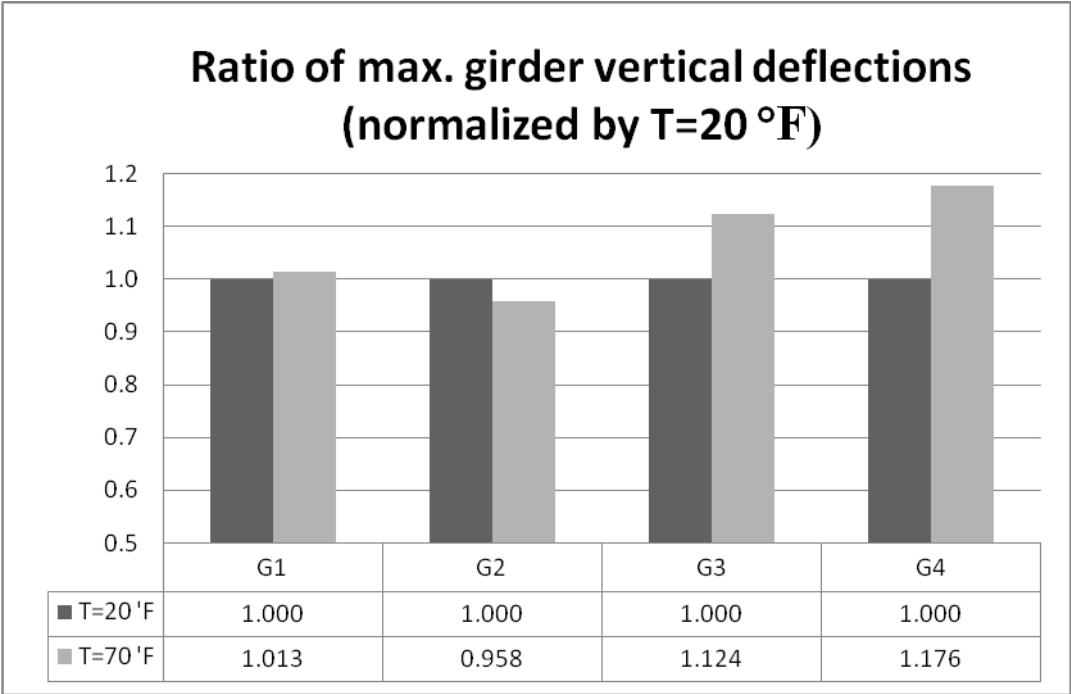


Figure 233: Ratio of Maximum Vertical Deflections for Bridge C10.

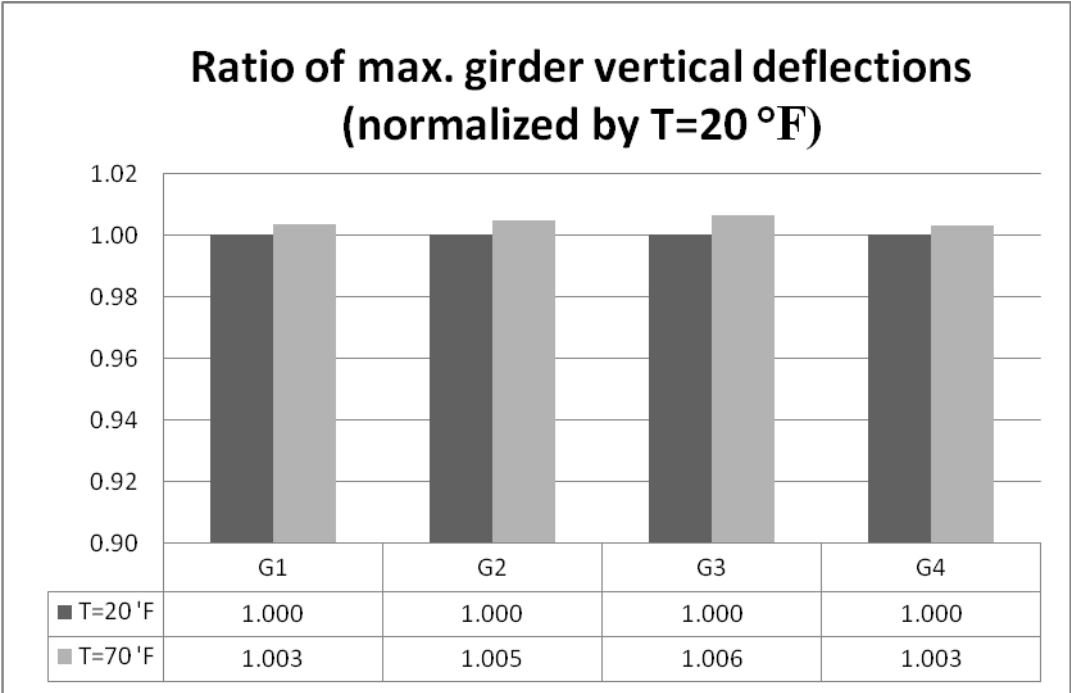


Figure 228: Ratio of Maximum Vertical Deflections for Bridge C11.

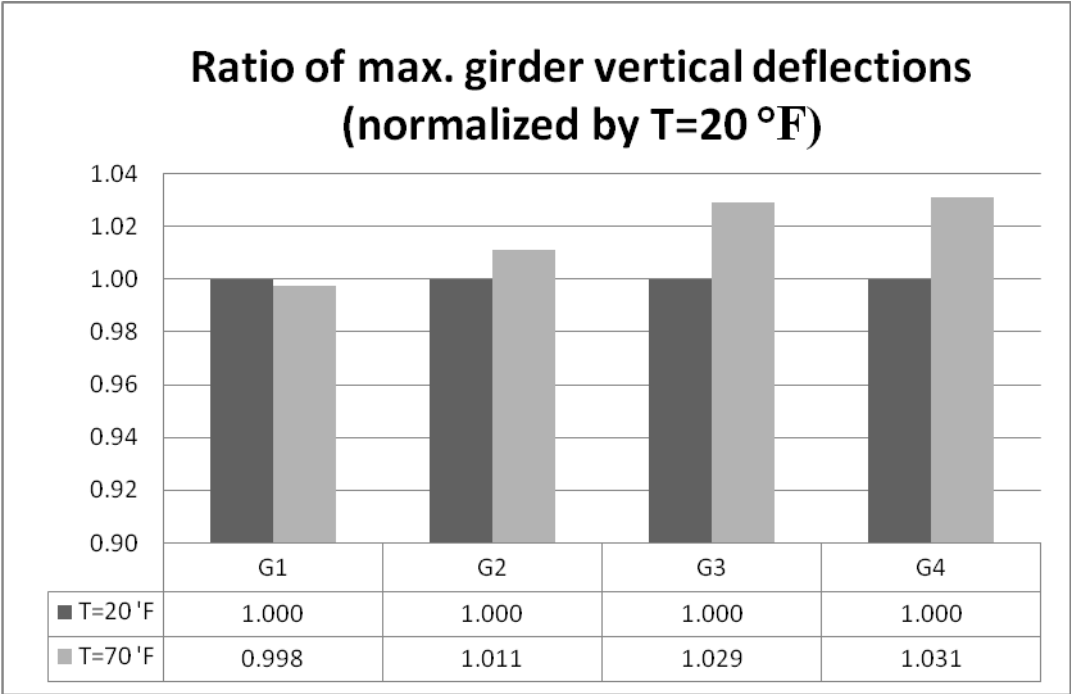


Figure 235: Ratio of Maximum Vertical Deflections for Bridge C12.

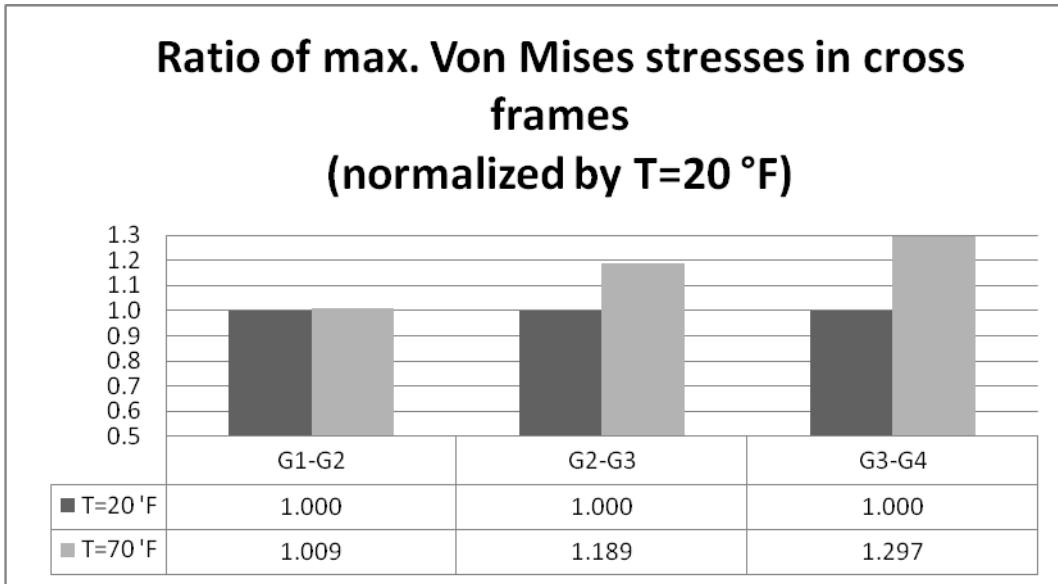


Figure 236: Ratio of Maximum Von Mises Stresses for Bridge C1.

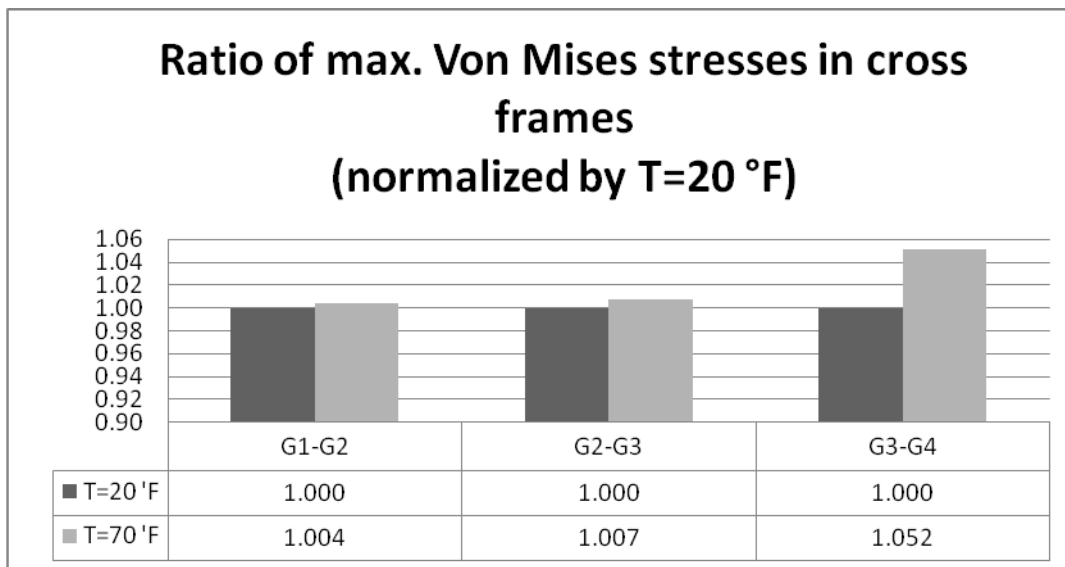


Figure 237: Ratio of Maximum Von Mises Stresses for Bridge C3.

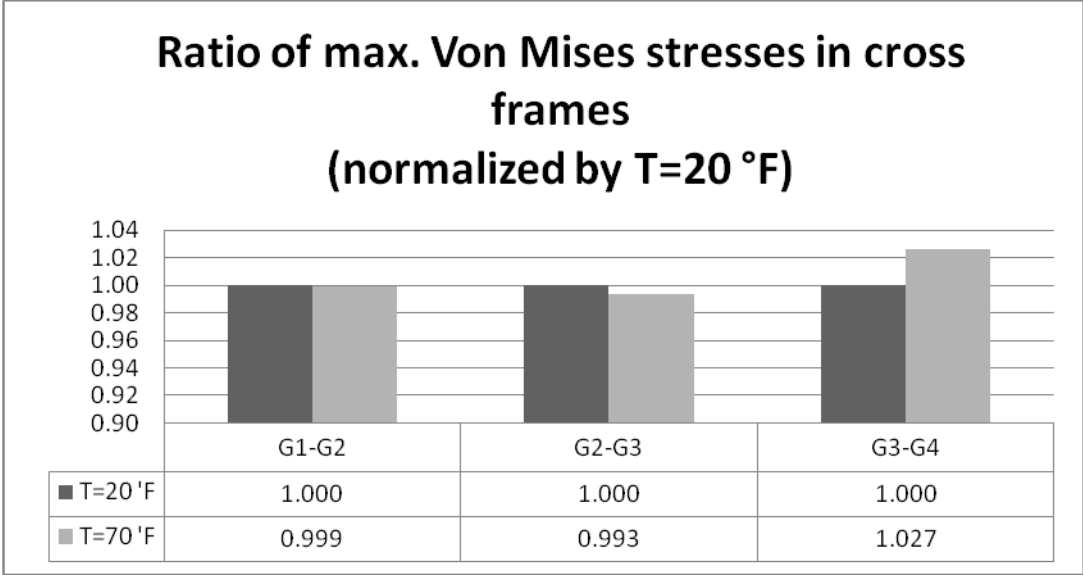


Figure 238: Ratio of Maximum Von Mises Stresses for Bridge C6.

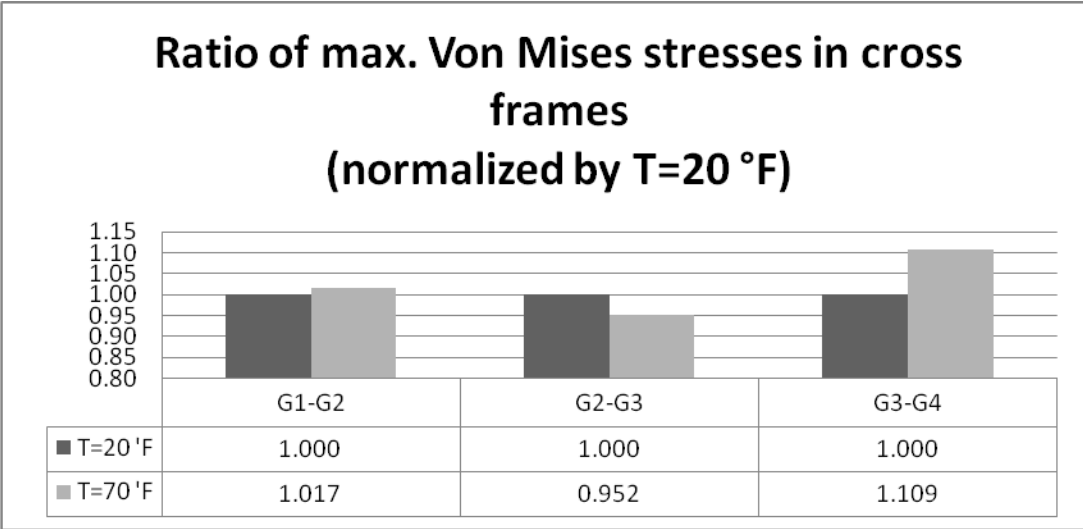


Figure 239: Ratio of Maximum Von Mises Stresses for Bridge C7.

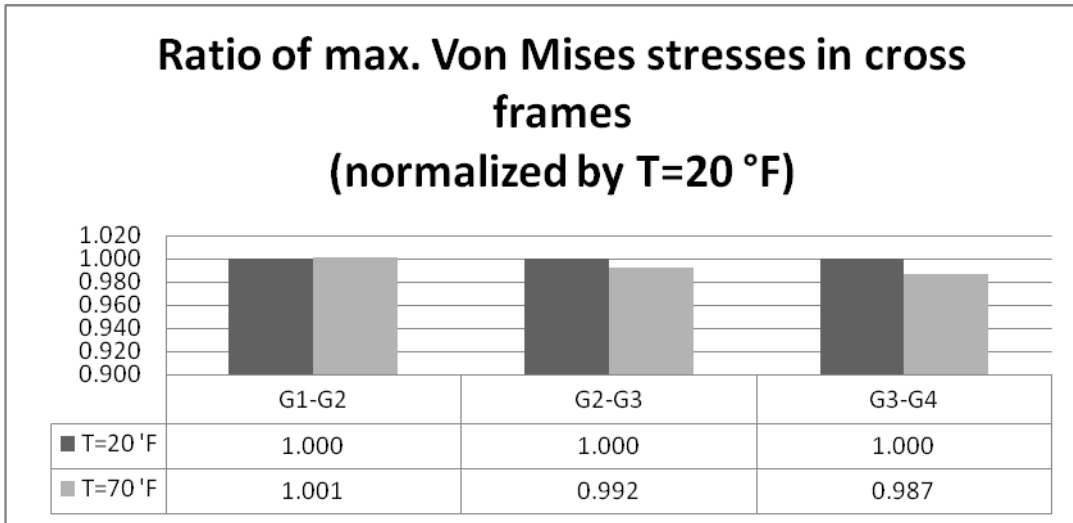


Figure 240: Ratio of Maximum Von Mises Stresses for Bridge C9.

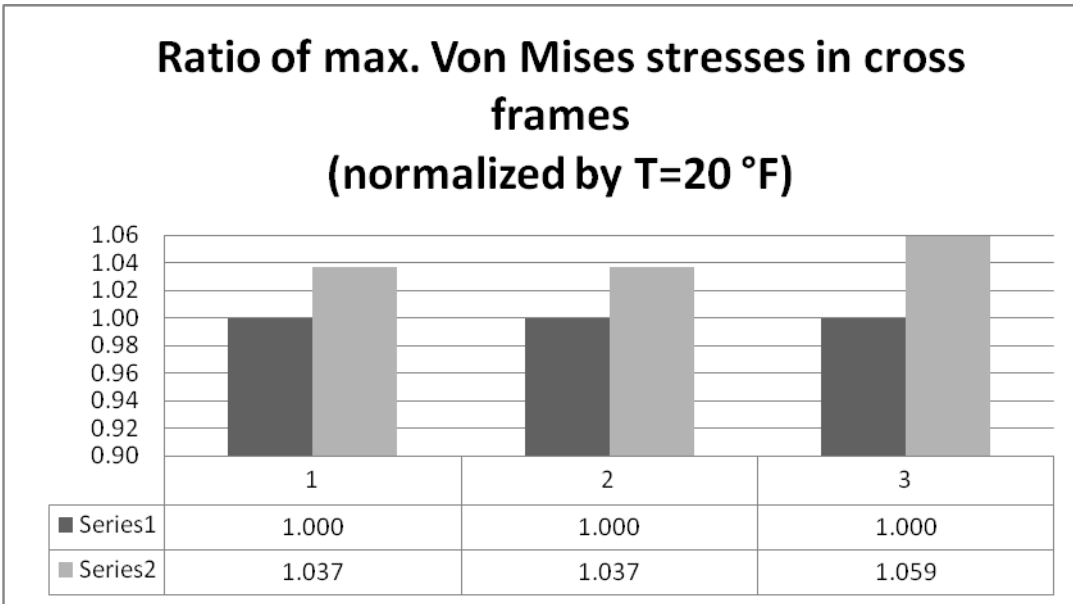


Figure 241: Ratio of Maximum Von Mises Stresses for Bridge C10.

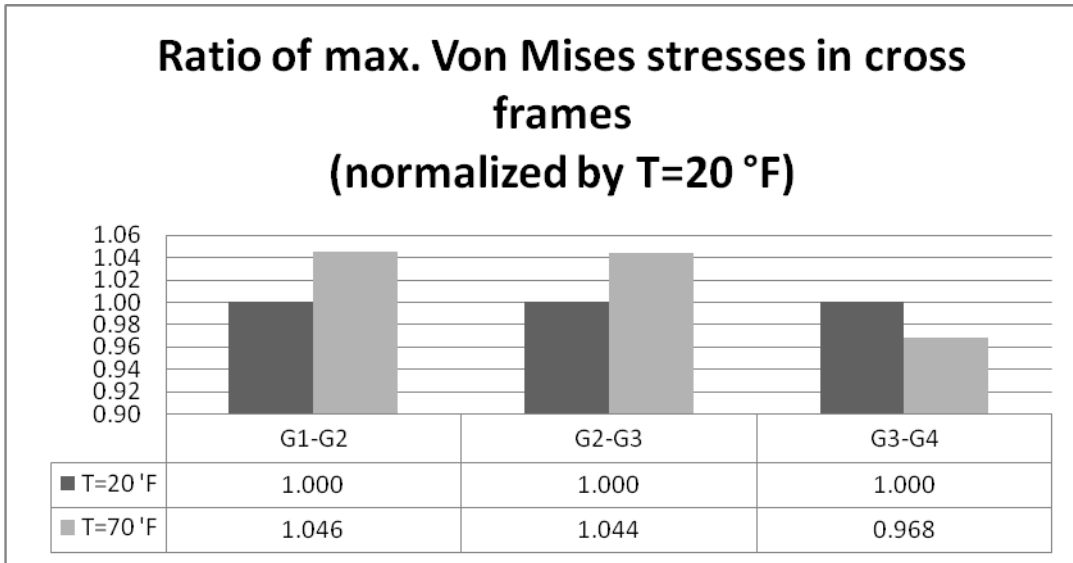


Figure 242: Ratio of Maximum Von Mises Stresses for Bridge C11.

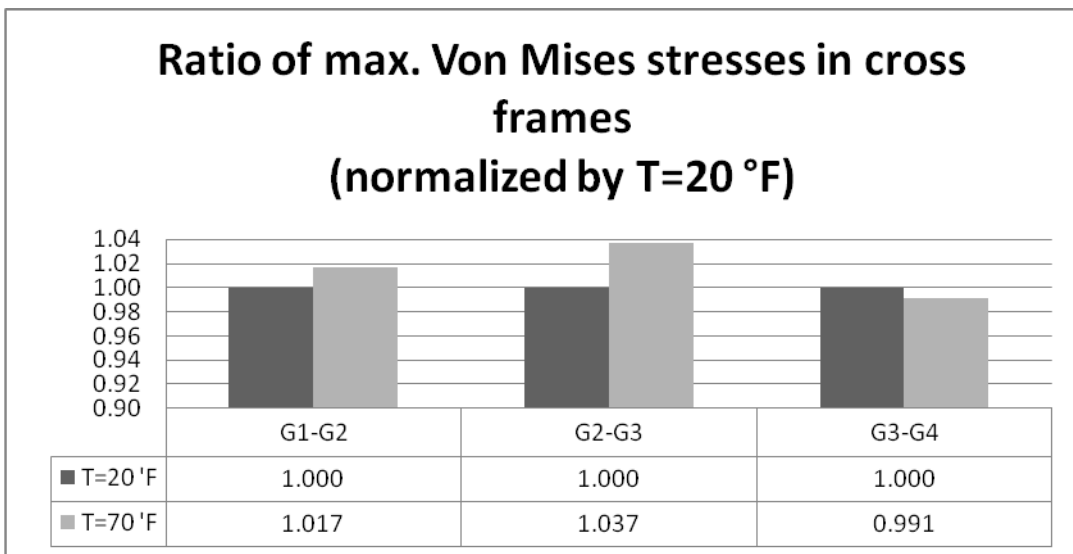


Figure 243: Ratio of Maximum Von Mises Stresses for Bridge C12.

5.7.2.2 Skewed

Ratios of maximum girder vertical deflections and cross-frame stresses are compared in Figure 244 through Figure . There is no marked change in vertical deformation or stresses due to temprature change in skewed bridges.

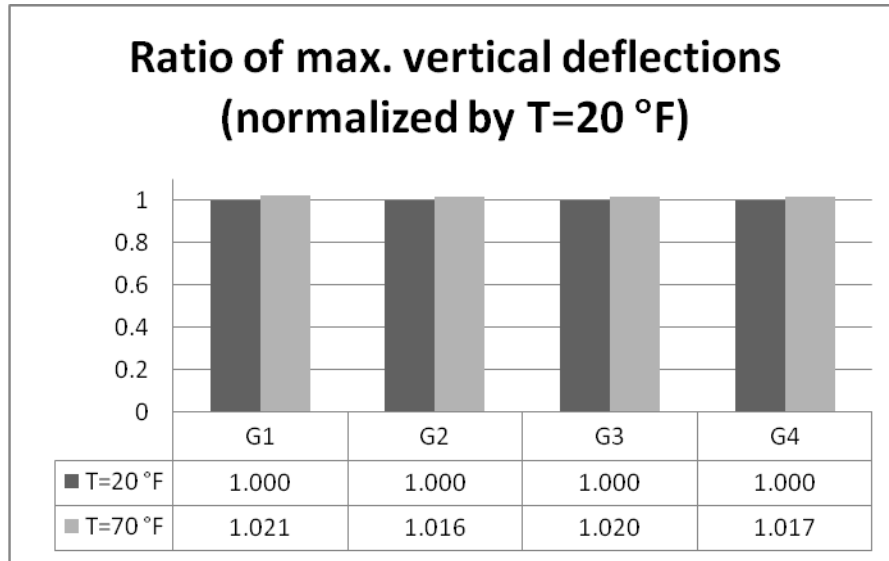


Figure 244: Ratio of Maximum Vertical Deflections for Bridge S1.

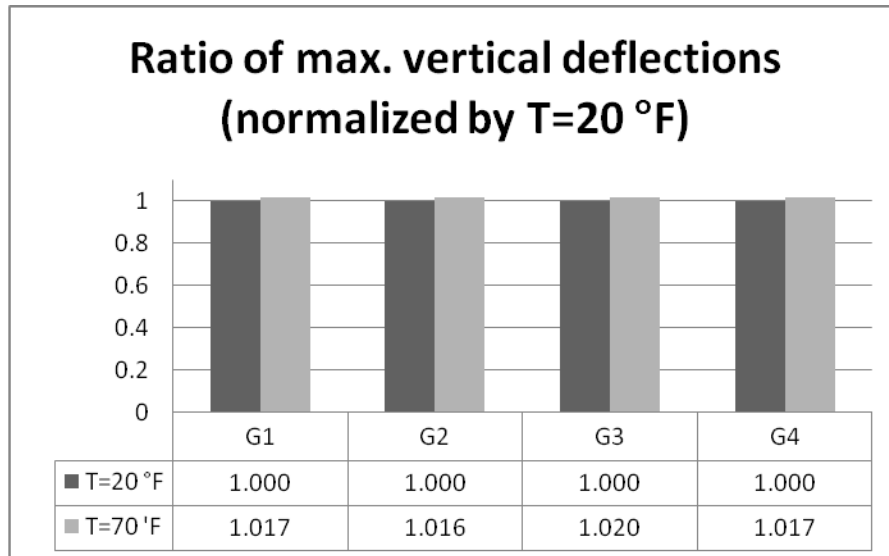


Figure 245: Ratio of Maximum Vertical Deflections for Bridge S3.

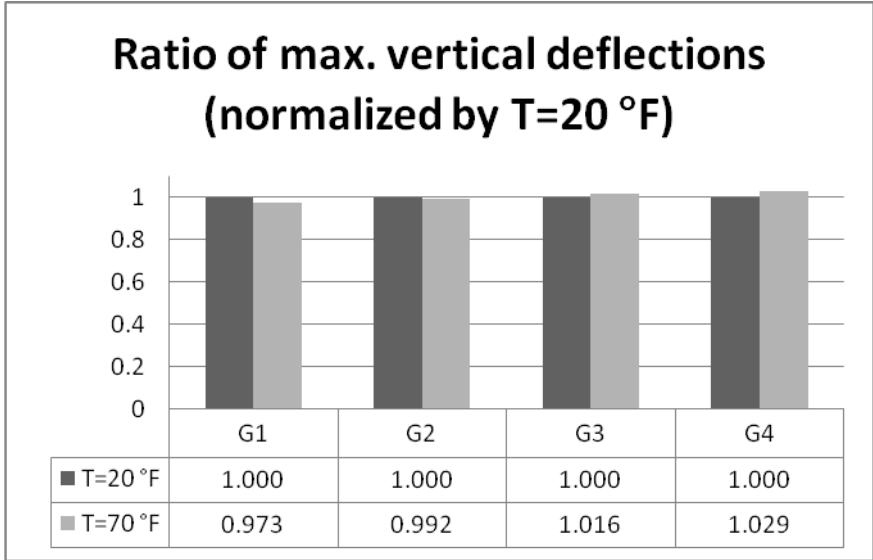


Figure 246: Ratio of Maximum Vertical Deflections for Bridge S5.

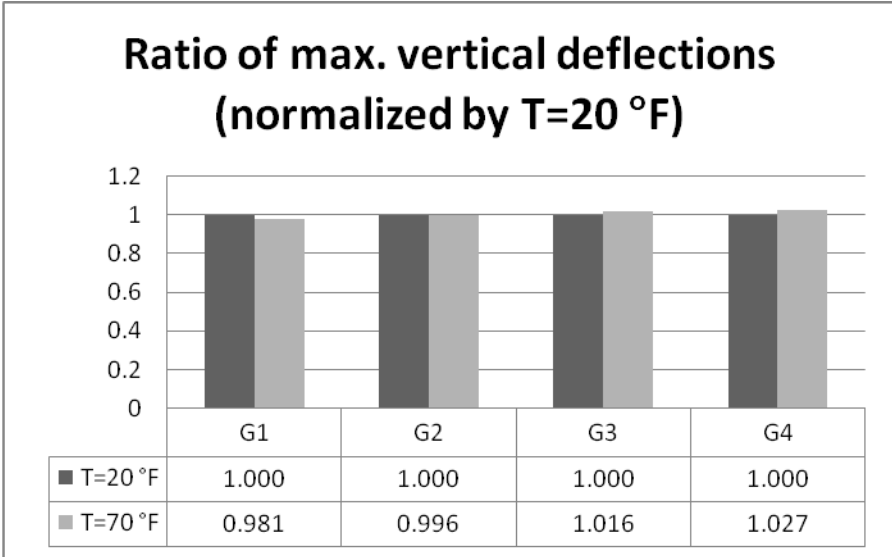


Figure 247: Ratio of Maximum Vertical Deflections for Bridge S6.

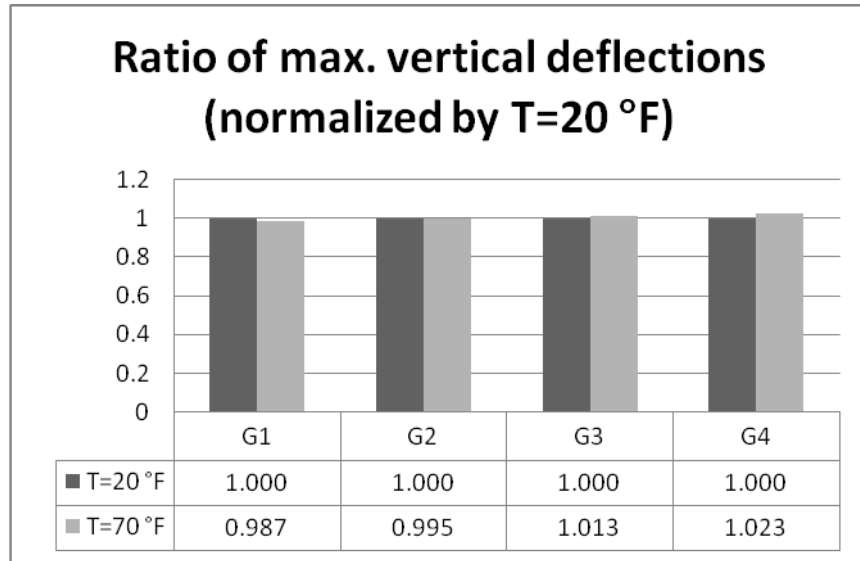


Figure 229: Ratio of Maximum Vertical Deflections for Bridge S7.

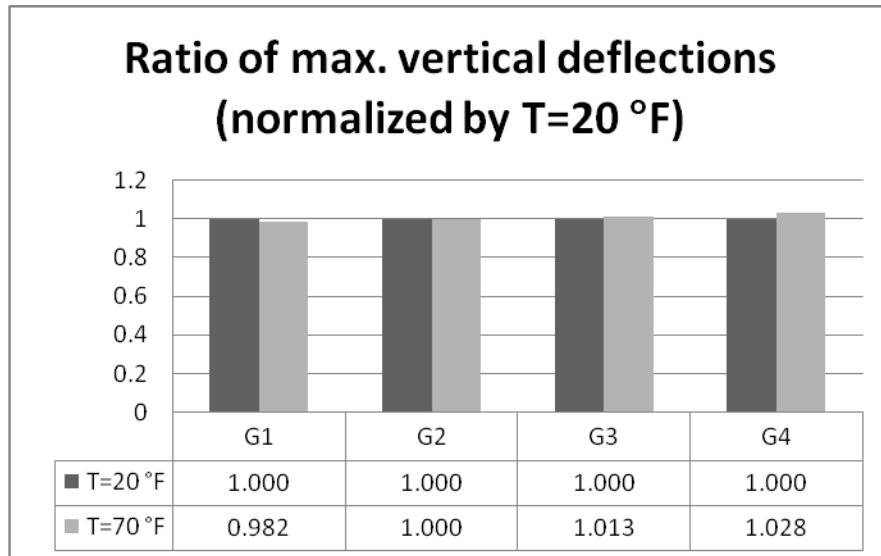


Figure 230: Ratio of Maximum Vertical Deflections for Bridge S8.

Ratio of max. vertical deflections (normalized by T=20 °F)

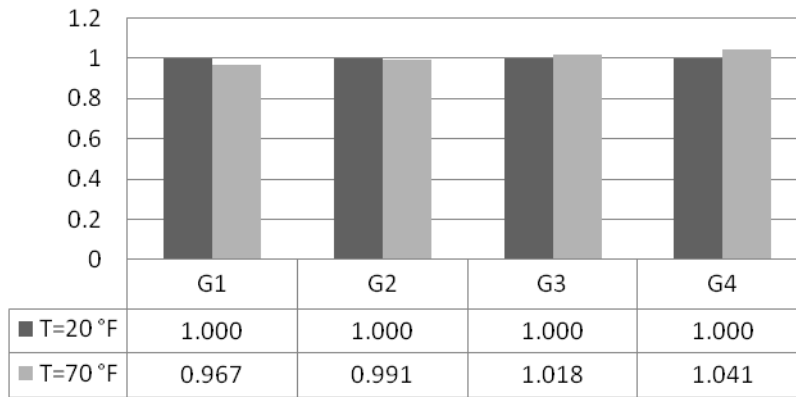


Figure 231: Ratio of Maximum Vertical Deflections for Bridge S9.

Ratio of max. vertical deflections (normalized by T=20 °F)

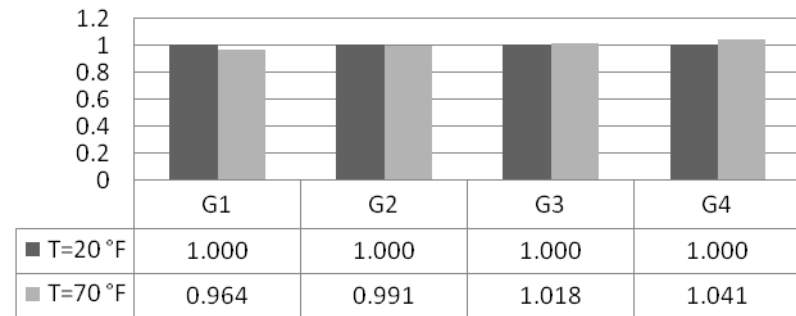


Figure 251: Ratio of Maximum Vertical Deflections for Bridge S10.

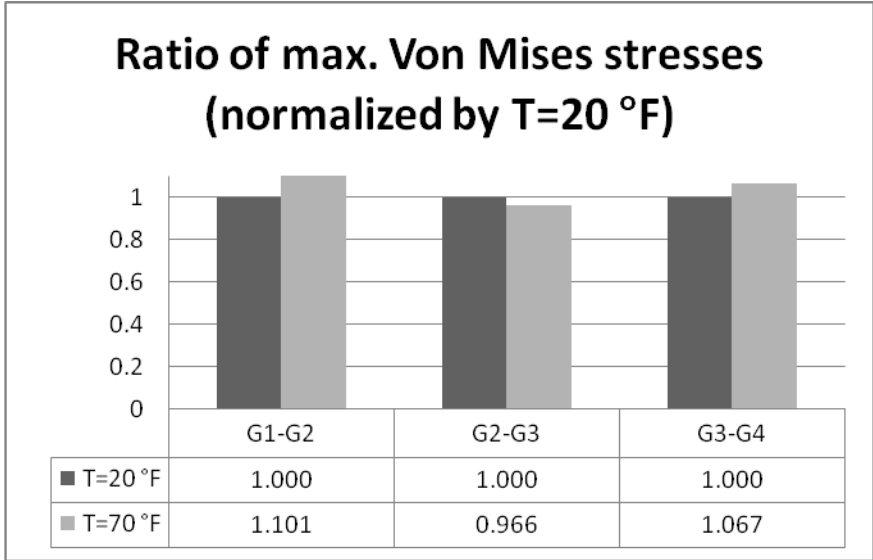


Figure 252: Ratio of Maximum Von Mises Stresses for Bridge S1.

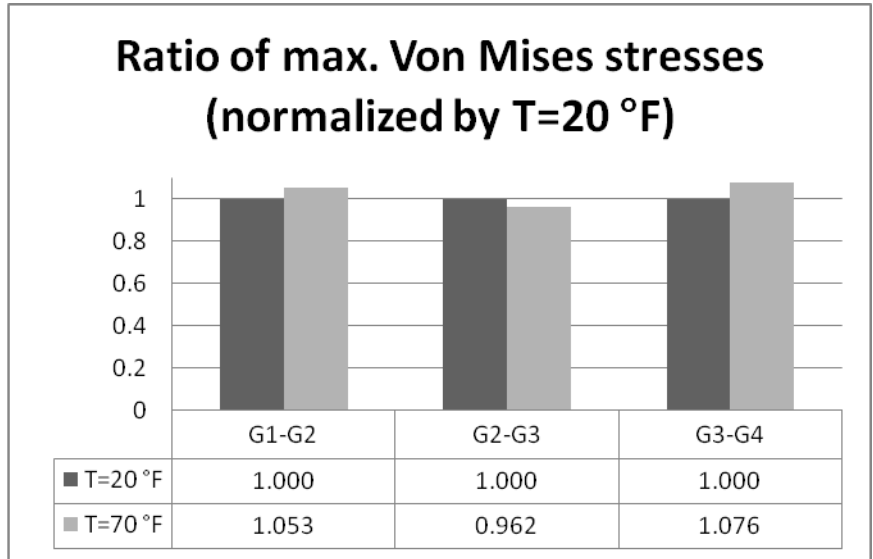


Figure 253: Ratio of Maximum Von Mises Stresses for Bridge S2.

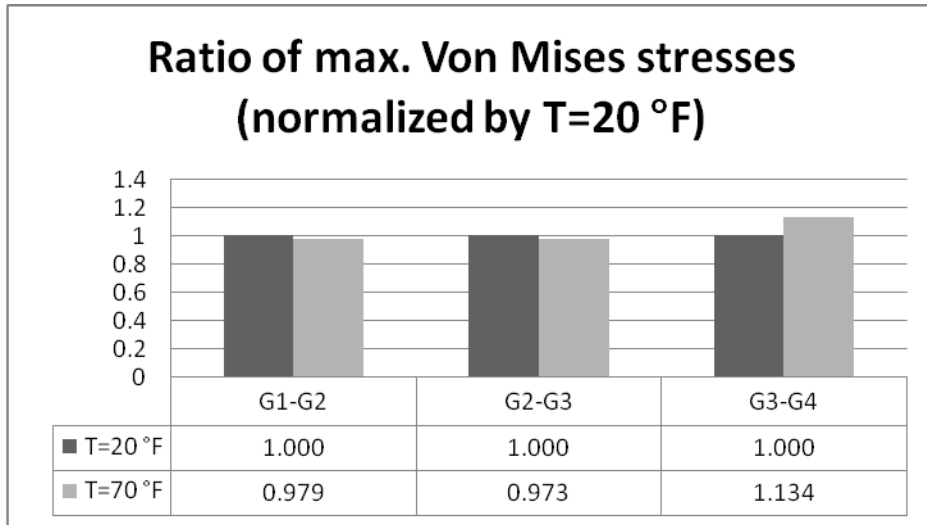


Figure 254: Ratio of Maximum Von Mises Stresses for Bridge S5.

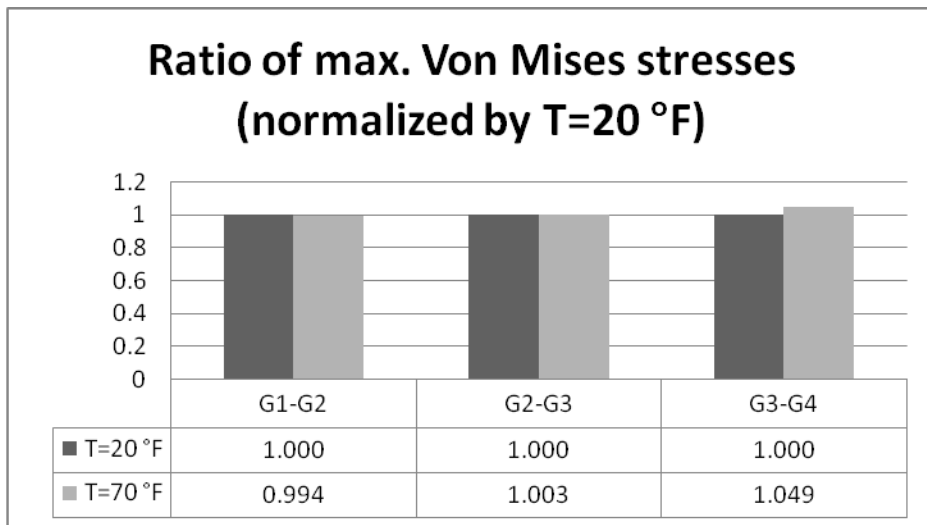


Figure 255: Ratio of Maximum Von Mises Stresses for Bridge S6.

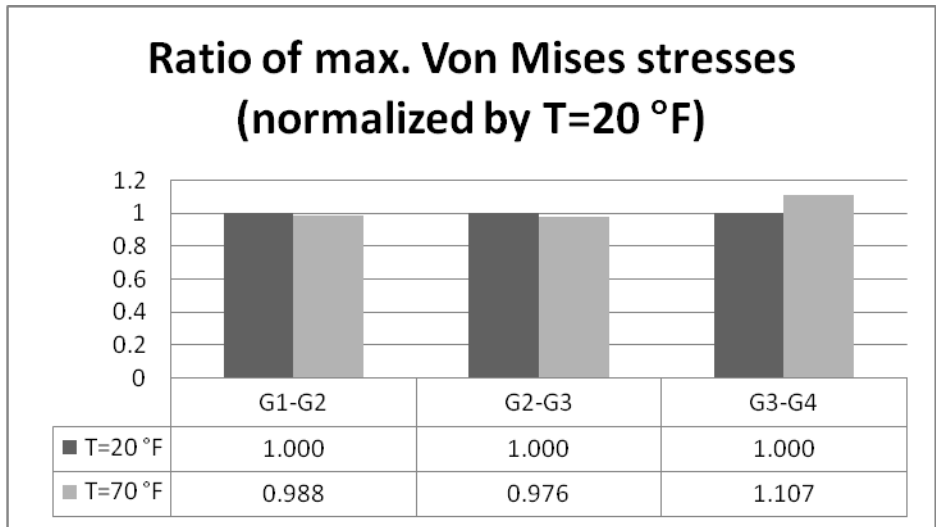


Figure 256: Ratio of Maximum Von Mises Stresses for Bridge S7.

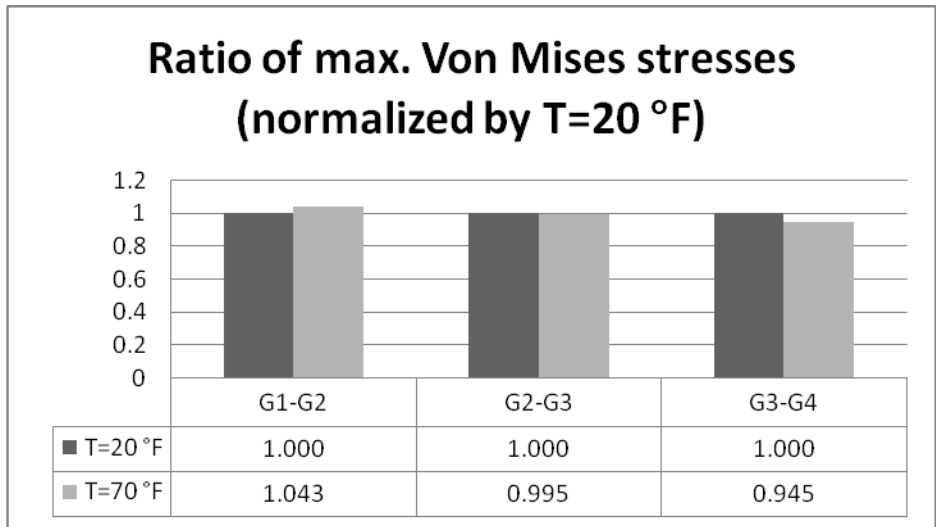


Figure 257: Ratio of Maximum Von Mises Stresses for Bridge S8.

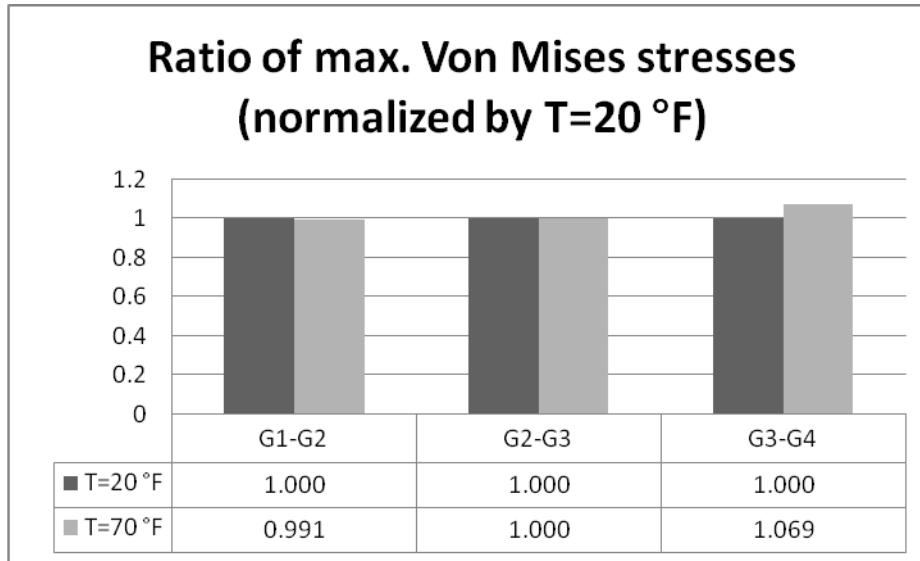


Figure 258: Ratio of Maximum Von Mises Stresses for Bridge S9.

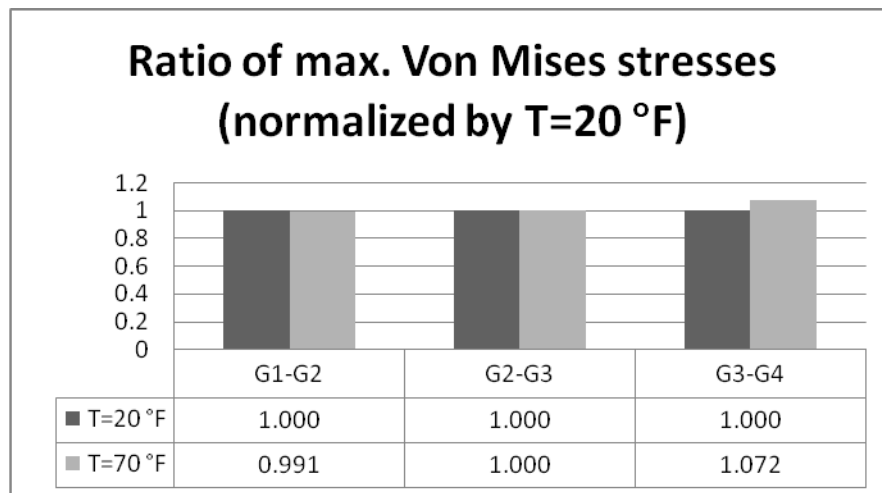


Figure 259: Ratio of Maximum Von Mises Stresses for Bridge S10.

5.7.2.3 Summary

This section examined the effects of temperature changes on curved and skewed bridge constructability during deck placement. In the analysis, temperature was increased by 50 °F after deck placement. Girder deflections and cross-frame stresses were examined after the temperature rise. Results showed minor changes in bridge deflections and stresses due to the temperature change. Hence, it was considered that temperature changes during construction had little impact on bridge constructability.

In summary, findings from the temperature change parametric studies for the curved and skewed bridges that were examined included:

- Curved
 - The applied temperature change did not have an appreciable impact on overall bridge deflections and stresses for all of the radii and cross-frame spacings studied.

- Skewed
 - The applied temperature change did not have an appreciable impact on overall bridge deflections and stresses for all of the skew angles and cross-frame spacings studied.

6 CONCLUSIONS

6.1 Project Overview

Summarized herein were research activities and findings in association with Work Order 009, “Guidelines for Analyzing Curved and Skewed Bridges and Designing Them for Construction.” As stated in the introduction, the project was divided into seven tasks:

1. Updated Literature Search
2. Data Acquisition System Maintenance
3. Numerical Modeling
4. Parametric Studies
5. Draft Final Report
6. Final Report
7. Invoice Submission

This report focused on Tasks 1 through 5, and due to earlier submittals related to Tasks 1 through 3 (Hiltunen et al. 2004; Linzell et al. 2003; Linzell et al. 2006; Linzell et al. 2008; Linzell et al. 2008), the bulk of this document summarizes the work completed and findings developed for Task 4. However, some information related to Task 2 is also provided.

The findings and the numerical modeling from the parametric studies are the basis for suggesting possible modifications to relevant PennDOT publications. Those publications are included in Appendix D of this report with suggested changes being shown in *italics*.

In-service structural response was tracked using instruments discussed in previous submittals to PennDOT. Using instruments that were in place on two bridges (Structure #'s 207 and 314), responses were tracked due to temperature changes after construction was completed. Data provided by these instruments for the examined time period did not indicate any obvious trends with respect to their global behavior.

The parametric studies that were completed focused on a group of representative curved and skewed steel bridge structures and numerically examined the influence of specific variables, as identified in the project scope, on behavior during construction. These items included: (1) web-plumbness; (2) temporary shoring placement and settlement effects; (3) cross-frame consistent detailing (i.e., applying the work by Chavel and Earls to other bridge geometries); (4) girder and cross-frame erection sequencing along the span and with respect to girder radius and the effects of “drop-in” erection; (5) solid plate diaphragms versus cross frames; and (6) global temperature change effects. Finite element models assisted with preliminary and final designs and with final, sequential analyses that focused on the influence of the above items on deformations and stress states at the completion of construction. Design and preliminary models were developed in SAP2000, with the final models used for the sequential analyses being developed in ABAQUS. Modeling decisions and approaches are summarized in previous submittals to PennDOT (Linzell et al. 2008). A superstructure modeling approach that consisted of representing the girder webs and concrete deck using shell elements, with beam elements representing other major components, such as the girder flanges and cross frames, was used. This modeling technique provided an acceptable compromise between reduced computation times provided by grillage models and increased accuracy provided by more sophisticated, and complicated, three-dimensional finite element models.

The final parametric studies were completed for a specified set of curved and skewed steel bridges, with bridge global geometries being obtained from a combination of statistical studies and PennDOT input. A total of 12 final curved bridge designs and 11 final skewed bridge designs were developed for the parametric studies. Information related to the final designs can be found in Table 3 and Table 4. In addition to these final structure studies, initial parametric studies that investigated the effects of erection sequencing on an additional, larger group of curved

bridges were completed prior to studying erection sequencing effects on the final curved bridge design group. Justifications for completing these initial studies and the bridges that were examined are discussed below.

6.2 Parametric Study Findings

Erection sequencing was the first parameter numerically studied using ABAQUS because the findings from that portion of the project influenced the remaining items that were examined. The study of the effects of erection sequencing began with initial examinations of a broad range of single- and two-span curved, I-girder structures and a single three-span, curved, I-girder structure. Various erection sequencing scenarios used in the initial studies were then applied to the final 12 curved bridges shown in Table 3 to reaffirm findings from the initial studies. Initial studies were not completed for the skewed structures, and erection sequencing scenarios recommended for the final curved structures were applied to the skewed structures in Table 4 to study their effects on construction response.

The initial studies examined a total of thirty single- and two-span bridges and a single three-span structure under the influence of the following erection sequencing parameters: (1) varying radii; (2) single-span structures and two-span structures with varying span ratios; (3) 4- and 5-girder cross sections; (4) different erection sequencing options that including erecting single girders and girders in pairs; (5) erecting the girders from inner to outer radius of curvature and from out to inner radius of curvature; and (6) the influence of temporary shoring. A summary of the initially examined single- and two-span bridges can be found in Figure 28. A framing plan of the single three-span structure that was initially examined is shown in Figure 59. These structures were statically analyzed in ABAQUS for the following construction scenarios: (1) paired-girder erection placing the interior girders first; (2) paired-girder erection placing the exterior girders first; (3) single-girder erection that placed the interior girder first; and (4) single-girder erection that placed the exterior girder first. “Paired” girder erection for the 5-girder bridges involved placing a single girder at some point during the process. Results from the initial group of analyses were examined statistically to identify preferred erection sequencing approaches, with preferred sequences being identified predominantly based on deflections, with vertical and radial deflections being of primary importance. Results from the initial studies indicated that, for the structures examined, the construction methods that initiated with the inner (lowest radius) girder are preferred, irrespective of number of spans, and that for bridges having more than two spans, paired inner erection methods are preferred. Results also indicated that, irrespective of span number and geometry, construction that initiates with a single outer girder is not recommended. In addition, it was observed from the results that bridge deflections were mainly controlled by R/L values, boundary conditions, and span lengths, but not by the “drop-in” effect. The observed rotations for sections prior to drop-in erection were small enough to allow for this erection approach should adequate control of the previously erected sections be provided.

The initial erection sequencing study findings were validated via additional investigations involving final curved and skewed designs. Vertical and radial deflections were the indexes used to evaluate the adequacy of the erection approaches that were applied to the selected final designs. Normalized deflections, consisting of maximum deflections from a given construction scenarios normalized with respect to maximums from the recommended preliminary study erection scenario (paired inner), were studied. Findings indicated that:

- Curved
 - Girder vertical deflections were decreased when paired-girder erection methods were used.
 - The paired inner erection was preferred for structures with severe curvature.
 - Drop-in erection would be an acceptable approach.
- Skewed
 - Erection methods examined herein did not show appreciable influence on skewed bridge behavior.
 - Drop-in erection would be an acceptable approach.

Studies of the effects of web out-of-plumbness on construction performance examined curved and skewed structures with a 1% imposed out-of-plumbness, the maximum permissible value for plate girders according to the Bridge Welding Code (AASHTO/AWS, 2004). The out-of-plumbness was introduced to the girder webs in a fashion that,

for the curved bridges, increased any anticipated twist in the girders and, for the skewed bridges, increased any anticipated global twisting during deck placement. Girder webs were intentionally tilted 1% of their depth along their entire length, with cross-frame geometries being modified accordingly. Static, sequential analysis was performed to examine the out-of-plumbness effects at each stage, with the paired inner erection method again being adopted since it was the recommended approach from the sequencing studies. Vertical and radial deflections were primarily compared, and at each stage the maximum girder vertical deflections and maximum radial deflections at splice locations were examined for the out-of-plumb cases, with those maximum deflections being normalized by the maximum deflections for the plumb web case. To examine out-of-plumbness effects on stresses, comparisons of maximum Von Mises stresses in the cross frames were also examined. Findings indicated that:

- Curved
 - Web out-of-plumbness did not cause appreciable bridge deflection and stress increases when the out-of-plumbness was within the limit (1%) specified in the Structural Welding Code (AWS, 2004).
 - Exceeding the 1% limit of the web out-of-plumbness can result in slightly higher vertical and lateral deformations and also stresses. However, the effects of horizontal curvature on these parameters are much larger than those from the web out-of-plumbness.
- Skewed
 - Web out-of-plumbness did not cause appreciable bridge deflection and stress increases when the out-of-plumbness was within the limit (1%) specified in the Structural Welding Code (AWS, 2004).
 - Exceeding the 1% limit of the web out-of-plumbness can result in slightly higher vertical deformations and stresses. However, the effects on lateral deformations are more pronounced. As a result, the effects of web-out-of plumbness, which could be beneficial to ensure web-plumb at the completion of construction, should be considered during the erection of structures having a skew less than 70°.

Temporary construction shoring placement was examined for curved and skewed final structures by applying the paired inner erection method to structures that were shored at: splice locations only; splice locations as well as at 0.4L of the span for exterior spans and and/or 0.5L for interior spans; and at 0.75L of the first span and at splice locations for the second span of the two-span bridges. In addition to studying the effects of these shoring placement schemes, the effects of support settlement in conjunction with the use of shoring was studied by examining critical curved and skewed structures in conjunction with three levels of support settlement, 0.001L, 0.002L, and 0.004L, where L is the span length between the abutment and pier, and having these settlement amounts occurring at either one shoring support or two support locations. Girder deformations and cross-frame Von Mises stresses were normalized against the web-plumb case and used to examine the shoring and settlement effects. Findings indicated that:

- Curved
 - While not shoring the superstructure during erection is certainly preferred from a cost-effectiveness standpoint, should shoring be deemed necessary during construction in addition to shoring at splice locations, placing one temporary support at 0.4L could significantly reduce girder deflections, leading to a more constructible condition.
 - When adding additional shoring at 0.4L was not feasible, placing one support at 0.75L between the abutment and splice location could reduce girder vertical deflections by more than 75% when compared to the deflections of placing one support at the splice location.
 - Attempts should be made to limit support settlement to less than 0.001L (L=span length) during construction to mitigate stress increases in bridge members.
 - Small differences were observed between one support settling and two supports settling.
- Skewed
 - While not shoring the superstructure during erection is certainly preferred from a cost-effectiveness standpoint, should shoring be deemed necessary during construction, in addition to shoring at splice locations, placing one temporary support at 0.4L could significantly reduce girder deflections, leading to a more constructible condition.

- When adding additional shoring at 0.4L was not feasible, placing one support at 0.75L between the abutment and splice location could reduce girder vertical deflections by more than 70% for the structures studied when compared to the deflections of placing one support at the splice location.
- Attempts should be made to limit support settlement to less than 0.001L (L=span length) during construction to mitigate stress increases in bridge members.
- Two supports settling had a larger impact on stresses than one support settling.

The effects of inconsistently detailing cross-frame members during construction, studied earlier by Chavel and Earls (2006), were re-examined for final curved and skewed bridge designs by numerically studying paired-inner erection methods with and without inconsistently detailed cross frames. Temperature changes were placed into cross-frame members to either shorten or lengthen those members to the anticipated geometric conditions that would result when the girders were detailed to be web-plumb under one construction condition (e.g. no load) and cross frames were mistakenly detailed to be web-plumb under another condition (e.g. full dead load). Initial models were created in SAP2000 to establish what the inconsistently detailed cross-frame lengths would be, then sequencing models were run in ABAQUS to study their effects. Again, normalized girder deformations and cross-frame Von Mises stresses were used as the primary methods to assess the detailing effects. Findings indicated that:

- Curved
 - Inconsistent cross-frame detailing increased vertical and radial deflections.
 - Cross-frame stresses were appreciably increased as a result of the locked-in stresses due to the inconsistent detailing. This increase was more pronounced for cross frames near the supports.
 - Irrespective of the radius and cross-frame spacing, inconsistent cross-frame detailing should be avoided for all curved structures to mitigate locked-in stresses and increased deformations. The effects of inconsistent detailing can be more pronounced in bridges with larger cross frame spacings.
- Skewed
 - Inconsistent cross-frame detailing did not have a crucial impact on girder vertical deflections.
 - Inconsistent cross-frame detailing increased lateral deflections.
 - Cross-frame stresses were appreciably increased as a result of the locked-in stresses due to inconsistent detailing. This increase was more pronounced for cross frames near the supports.
 - Irrespective of the skew and cross-frame spacing, inconsistent cross-frame detailing should be avoided for all skewed structures to mitigate locked-in stresses and increased deformations. The effects of inconsistent detailing can more pronounced in bridges with larger cross frame spacings.

The effects of replacing cross frames with diaphragms on construction behavior was examined via the study of three replacement scenarios: (1) diaphragms replacing cross frames at the abutments only, (2) diaphragms replacing cross frames at the abutments and piers, and (3) diaphragms replacing cross frames at the abutments, piers, and at mid-span. Paired-girder erection was used to study their effects, and the girder deformations and cross-frame Von Mises stresses, which were normalized against similar values for the case where no diaphragms were present, were again used to assess the effects on construction response. Findings indicated:

- Curved
 - Replacing cross frames with solid plate diaphragms did not severely affect bridge vertical and radial deflections and cross-frame stresses during construction, irrespective of the radius and cross-frame spacing.
 - Replacing cross frames with solid plate diaphragms at the abutment and pier locations for the curved bridges that were studied did not adversely affect or appreciably benefit their construction behavior. Nevertheless, using diaphragms at the mid-span locations can cause slightly higher deformations for the girders when compared to the use of cross frames at those locations.
- Skewed
 - Placing solid plate diaphragms in skewed bridges slightly increased deformations due to the self weight of the diaphragms, but did not severely affect cross-frame stresses.
 - Replacing cross frames with solid plate diaphragms at the abutment and pier locations for the skewed bridges did not adversely affect or appreciably benefit their construction behavior.

However, using diaphragms at the mid-span locations can cause slightly higher deformations for the girders when compared to the use of cross frames at those locations.

Temperature effects on construction response were studied by examining their influence on girder deflections and cross-frame stresses when a 50 °F temperature increase occurred during deck placement. Paired-girder erection was used, and values were normalized with respect to no temperature change occurring as the deck was placed. Findings indicated that:

- Curved
 - The applied temperature change did not have an appreciable impact on overall bridge deflections and stresses for all of the radii and cross-frame spacings studied.
- Skewed
 - The applied temperature change did not have an appreciable impact on overall bridge deflections and stresses for all of the skew angles and cross-frame spacings studied.

These findings are summarized in Table 34.

Table 34. Summary Table.

DM 4/ 408/ BD	Proposed Language	Report Section
DM4 Section 2, Index	Single Inner Erection - Erecting a single girder from inner radius to outer radius. Single Outer Erection - Erecting a single girder from outer radius to inner radius. Paired Inner Erection - Erecting two girders from inner radius to outer radius. Paired Outer Erection - Erecting two girders from outer radius to inner radius.	5.4
DM4 2.5.3.1P	Should the contractor deem that temporary falsework is necessary for the construction of curved and skewed steel bridges, the following guidelines should be used for its placement: <ul style="list-style-type: none"> • When temporary falsework is needed for a span, it shall be placed at locations to reduce splice rotations and girder vertical deflections.. • The stability of the structure supported by temporary falsework shall be evaluated. 	5.4
DM4 C2.5.3.1P	While using no temporary falsework is desirable from a cost-effectiveness perspective, should the designer and/or contractor deem that falsework is needed to ensure that a curved or skewed steel bridge is constructible, it should initially be placed near splice locations. When girder vertical deflections are still a concern, an additional temporary support should be placed as close as possible to the location of maximum vertical deflection of the span (approximately 0.4 L from an abutment, where L is the span length, for side spans and 0.5 L for intermediate spans) to reduce girder deflections. For the side spans, when adding multiple temporary supports is not feasible, placing one support near 0.75L from the abutments is suggested.	5.4

DM4 2.5.3.2P	<p>The following guidelines should be used for girder erection of horizontally curved steel I-girder structures:</p> <ul style="list-style-type: none"> • Should adequate crane capacity be available, paired girder erection approaches are preferred. • When the radius of the curved structure is less than 300 feet, it is recommended that girders be placed from inner radius to outer radius. • An analysis shall be performed to ensure that the structure is stable for all stages of construction and that supports necessary to maintain stability have been provided. <p>The following guidelines should be used for girder erection of skewed steel I-girder structures:</p> <ul style="list-style-type: none"> • An analysis shall be performed to ensure that the structure is stable for all stages of construction and that supports necessary to maintain stability have been provided. 	5.2
DM4 C2.5.3.2P	<p>Paired girder erection, as opposed to single erection, requires fewer temporary supports for the erected segments during all stages of construction. However for bridges with an odd number of girders, at least one girder line must be erected by itself.</p> <p>Girder erection from inner radius to outer radius, when compared to the opposite direction, can result in slightly smaller deformations for the girders for all stages of construction which, in turn, means the structure is more constructible. This effect is more pronounced in severely curved structures (i.e., radius less than 300 ft).</p> <p>Stability of partial and completed girders at various stages of erection is the responsibility of the contractor, as specified in Publication 408 Section 1050.3(c).</p> <p>For construction of straight skewed bridges, paired erection does require a smaller number of temporary supports but offers no other substantial benefits over a single erection approach with respect to deformations.</p>	5.2
DM4 Section 2, Reference	PennDOT Publication 408, Section 1050, "Steel Bridge Superstructure," 2007.	
DM4 Section 3, Index	Span Length - The distance between supports along the centerline of the girder web.	
DM4 3.12.8P	<p>When falsework is used, an analysis should be performed to check its settlement effects on response during construction. As a minimum, the following scenarios should be considered for the analysis:</p> <ul style="list-style-type: none"> • Settlement of single and multiple temporary supports . 	5.4

	<ul style="list-style-type: none"> • A minimum settlement of one thousandth of the span length should be used. 	
DM4 C4.6.1.2.1	The selected refined method of analysis for a structure curved in plan must provide an accurate prediction of behavior, both during construction and while in-service. While the method of analysis that is selected is at the discretion of the designer, a superstructure modeling technique that represents the girder webs and concrete deck using shell elements and other major superstructure components using beam elements provides an acceptable compromise between reduced computation times provided by grillage analogy models and increased accuracy provided by more sophisticated three-dimensional finite element models.	
DM4 C4.6.2.2.1	This does not mandate a 3-D analysis, but does mean a special analysis of the cross-frame must be provided in order to account for the differential deflections which occur across a cross-frame. This analysis should accurately account for cross frame member geometry and stiffness. Should a grillage analogy model be used, accurate representation of cross frame stiffness should be established via special analysis of representative frames. Should a more sophisticated 3-D analysis be used, models can be constructed following the technique recommended in C4.6.1.2.1 for structures curved in plan.	
DM4 6.7.4.1	Diaphragm members in horizontally curved and skewed bridges may be used at support locations.	5.6
DM4 C6.7.4.1	Diaphragm members in horizontally curved and skewed bridges may be used at support locations. When support lines are skewed less than 70 degrees, intermediate diaphragms or cross-frames shall be placed normal to the girders in contiguous or discontinuous lines. When cross frames and diaphragms are normal to web near skewed supports, adequate girder restraint shall be provided.	5.6
DM4 C6.7.4.1	Placement of cross frames parallel to the skew has been shown to induce significant localized lateral bending near support locations (AASHTO Subcommittee on Bridges & Structures, 2010).	
DM4 C6.7.4.1	Solid plate diaphragms can be used at support locations in horizontally curved and skewed bridges. Replacing cross frames with solid plate diaphragms at abutment and pier locations has been shown to not adversely affect or appreciably benefit deformations during construction. For other intermediate locations along the bridge spans, diaphragms may cause higher stresses and deformations in the bridge structures during construction when compared to the use of cross frames.	5.6

DM4 6.7.4.2	Cross frames and steel girders in curved and skewed bridges should both be detailed so that the webs are plumb under a specified loading condition.	5.5
DM4 C6.7.4.2	In curved and skewed bridges, cross-frame stresses can increase appreciably as a result of locked-in stresses caused by inconsistent detailing. This increase may be more pronounced in bridges with larger cross frame spacings and for cross frames near the bridge supports. For bridges with skew angles between 90° and 70°, develop shop drawings which detail all webs plumb when girders are erected and diaphragms connected. For curved bridges and skewed bridges with skew angles less than 70°, develop shop drawings and erection procedures which detail all webs plumb after the full dead load (self weight of all structural and non-structural components, not including weight of the future wearing surface) is applied. See Article 6.7.2 and BC-754, “Steel Diaphragms.”	5.5
DM4 6.10.3.2.5.1P	(f) Temperature changes as prescribed in 3.12.2.1.1.	5.7
DM4 C6.10.3.2.5.1P	The effects from temperature change on the curved and skewed bridges are mostly functions of the girder support conditions. When minimum required restraint necessary for girder(s) global stability (i.e., prevention of global buckling of the girder or collection of girders) is provided, the applied temperature change may not have an appreciable impact on overall bridge deflections and stresses.	5.7
DM4 Section 6, Reference	American Association of State Highway and Transportation Officials (AASHTO), Subcommittee on Bridges and Structures, Agenda Item 14, http://bridges.transportation.org/Pages/2010AgendaItems-SacramentoCA.aspx , 2010. PennDOT Bridge Construction Standards, BC-754, Steel Diaphragms. 2006.	
BD-620M	ADDITIONAL LATERAL STABILITY CRITERIA FOR SKEWED STEEL BRIDGES 6. CROSS FRAME INCONSISTENT DETAILING SHOULD BE AVOIDED. FOR BRIDGES WITH SKEW ANGLES BETWEEN 90° AND 70°, DEVELOP SHOP DRAWINGS WHICH DETAIL ALL WEBS PLUMB WHEN GIRDERS ARE ERECTED AND DIAPHRAGMS CONNECTED. FOR SKEWED BRIDGES WITH SKEW ANGLES LESS THAN 70°, DEVELOP SHOP DRAWINGS AND ERECTION PROCEDURES WHICH DETAIL ALL WEBS PLUMB AFTER THE FULL DEAD LOAD (SELF WEIGHT OF ALL STRUCTURAL AND NON-STRUCTURAL COMPONENTS, NOT INCLUDING WEIGHT OF THE FUTURE WEARING SURFACE) IS APPLIED.	5.5

	<p>ADDITIONAL LATERAL STABILITY CRITERIA FOR CURVED STEEL BRIDGES</p> <p>6. CROSS FRAME INCONSISTENT DETAILING SHOULD BE AVOIDED. FOR ALL CURVED BRIDGES DEVELOP SHOP DRAWINGS AND ERECTION PROCEDURES WHICH DETAIL ALL WEBS PLUMB AFTER THE FULL DEAD LOAD (SELF WEIGHT OF ALL STRUCTURAL AND NON-STRUCTURAL COMPONENTS, NOT INCLUDING WEIGHT OF THE FUTURE WEARING SURFACE) IS APPLIED.</p>	
408 Section 1050	<p>(c) Erection. References to Section of Division II, AASHTO Standard Specifications for Highway Bridges (date as indicated), and PennDOT Design Manual – Part 4 are identified by the abbreviation AASHTO or PennDOT DM4, followed by the section number, e.g., AASHTO 11.6.4.</p> <p>2. Falsework Design and Construction. AASHTO 11.2.2, 11.6.1, Section 105.03(c) and PennDOT DM4 2.5.3.1P.</p> <p>3. Erection Procedure. AASHTO 11.6.4 and Penn DOT DM4 6.10.3.2.5.1P.</p>	5.2 and 5.4

A recommended implementation plan for the findings from this study and subsequent suggested findings in Appendix D would consist of:

- PennDOT reviews the findings obtained from the project summarized herein and suggests corresponding modification to relevant PennDOT documents.
- PennDOT selects suggested revisions that the Department views as acceptable for inclusion in the PennDOT documents.
- PennDOT initiates the process to include those items in future publications.
- PennDOT reviews the findings from other relevant projects that will be completed after publication of this report for inclusion in future PennDOT documents. These projects include NCHRP Project 12-79. Suggested modifications from the present work that PennDOT views as acceptable can be integrated with any findings from the other relevant projects.
- Development and implementation by PennDOT of training tools to assist with implementation of any changes in relevant PennDOT documents.

7 REFERENCES

- American Association of State Highway and Transportation Officials. (2007). LRFD Design Specifications, Washington, D.C.
- American Association of State Highway and Transportation Officials. (2003). Guide Specifications for Horizontally Curved Steel Girder Highway Bridges, Washington, D.C.
- American Association of State Highway and Transportation Officials/American Welding Society, (2004). Structural Welding Code-Steel, 19th Edition, Miami, FL.
- Chavel, B.W. and Earls, C.J. (2006), “Construction of a Horizontally Curved Steel I-Girder Bridge. PartII: Inconsistent Detailing”, ASCE Journal of Bridge Engineering, Vol.11, (1), pp. 91–98.
- Hiltunen, D.R., Johnson, P.A., Laman, J.A., Linzell, D.G., Miller, A.C., Niezgoda, S.L., Scanlon, A., Schokker, A.J. and Tikalsky, P.J. (2004). Interstate 99 Research, Contract No. SPC 020S78, Pennsylvania Department of Transportation, October, 324 pp.
- Galambos, T.V., Hajjar, J.F., Leon, R.T., Huang, W-H, Pulver, B.E., and Rudie, B.J. (1996). “Stresses in Steel Curved Girder Bridges,” Minnesota Department of Transportation Report No. MN/RC – 96/28, August.
- Linzell, D.G., Laman, J.A., Bell, B., Bennett, A., Colon, J., Lobo, J., Norton, E. and Sabuwala, T. (2003). Prediction of Movement and Stresses in Curved and Skewed Bridges, University-Based Research, Education and Technology Transfer Program; Agreement No. 359704, Work Order 79. Final Report, Pennsylvania Department of Transportation, March, 192 pp.
- Linzell, D.G., Nadakuditi, V.P. and Nevling, D.L. (2006). Prediction of Movement and Stresses in Curved and Skewed Bridges, PennDOT/MAUTC Partnership, Work Order No. 2, Research Agreement No. 510401, Final Report, Pennsylvania Department of Transportation, September, 86 pp.
- Linzell, D.G., Seo, J. and Coughlin, A. (2008). Guidelines for Analyzing Curved and Skewed Bridges and Designing them for Construction: Updated Literature Search Report, The Thomas D. Larson Pennsylvania Transportation Institute Report No. PTI 2008-15, August, 31 pp.
- Linzell, D.G., Nevling, D.L., and Seo, J. (2008). Guidelines for Analyzing Curved and Skewed Bridges and Designing them for Construction: Numerical Modeling Report, The Thomas D. Larson Pennsylvania Transportation Institute Report No. PTI 2008-16, August, 57 pp.
- Mintab,(2007). Users Manuals; Version 15.1.20.0. Minitab, Inc., State College, Pa.
- National Weather Service, National Oceanic and Atmospheric Administration. <<http://www.nws.noaa.gov>>
- Pennsylvania Department of Transportation (2007). PennDOT Design Manual – Part 4, Structures (Publication 15M).

8 APPENDIX A

Updated Literature Search Report

**COMMONWEALTH OF PENNSYLVANIA
DEPARTMENT OF TRANSPORTATION**

PENNDOT RESEARCH



**GUIDELINES FOR ANALYZING CURVED AND SKEWED BRIDGES
AND DESIGNING THEM FOR CONSTRUCTION**

LITERATURE SEARCH REPORT

**Work Order No. PSU009
Intergovernmental Agreement, No. 510602**

August 15, 2008

By D. G. Linzell, J. Seo and A. Coughlin

PENNSSTATE



**The Thomas D. Larson
Pennsylvania Transportation Institute**

**The Pennsylvania State University
Transportation Research Building
University Park, PA 16802-4710
(814) 865-1891 www.pti.psu.edu**

GUIDELINES FOR ANALYZING CURVED AND SKEWED BRIDGES AND DESIGNING
THEM FOR CONSTRUCTION

LITERATURE SEARCH REPORT

Work Order No. PSU-009
Intergovernmental Agreement No. 510602

Prepared for

Bureau of Planning and Research
Commonwealth of Pennsylvania
Department of Transportation

By

Daniel G. Linzell, Ph.D., P.E.
Junwon Seo
Andrew Coughlin

The Thomas D. Larson Pennsylvania Transportation Institute
The Pennsylvania State University
Transportation Research Building
University Park, PA 16802-4710

December 15, 2008

PTI 2008-15

This work was sponsored by the Pennsylvania Department of Transportation and the U.S. Department of Transportation, Federal Highway Administration. The contents of this report reflect the views of the authors, who are responsible for the facts and the accuracy of the data presented herein. The contents do not necessarily reflect the official views or policies of either the Federal Highway Administration, U.S. Department of Transportation, or the Commonwealth of Pennsylvania at the time of publication. This report does not constitute a standard, specification, or regulation.

TABLE OF CONTENTS

8.1 INTRODUCTION	171
8.2 GENERAL DESIGN GUIDELINE AND LITERATURE SEARCH.....	171
8.3 PROPOSED DESIGN FOR CONSTRUCTION DOCUMENT TEMPLATE	176
REFERENCES	177

8.1 INTRODUCTION

The modern transportation industry encounters an increasing use of curved and skewed I-girder/beam bridges for a number of reasons. These types of bridges are becoming more common as highway infrastructure is increasingly rebuilt atop existing structures to handle increasing traffic volumes or new interchange geometries within the context of urban settings. In particular, curved I-girder/beam bridges have the ability to change direction within each span and thus are ideal structures for applications such as highway interchanges or to connect existing roadways where abutments cannot be relocated for physical or economic reasons. Additionally, specification of the curved structure, while generating more superstructure costs in terms of materials and engineering, actually reduces the structure's cost through the elimination of interior supports, significant deck overhangs, and expensive right-of-way acquisitions. Similarly, skewed I-girder/beam bridges are also useful when roadway alignment changes are not feasible or economical because of the topography of the site and also at particular areas where environmental impact is an issue.

However, curved and skewed I-girder/beam bridges tend to significantly deflect and rotate out of plane under the action of gravity. In particular, these bridge types of construction prove to be a challenge where each girder tends to rotate under its own weight and any additional load (e.g., concrete deck) applied perpendicular to the plane of curvature. Oftentimes, the construction of such bridges is more complex, and more detailed consideration of the construction process is required when compared to constructing corresponding straight steel I-girder bridges. As mentioned above, this is because unlike a straight steel I-girder, curved and skewed girder bridge construction must control not only the vertical displacement of the I-girders but also the out-of-plane displacements such that structural components, including cross frames, can be erected with limited difficulty. Therefore, varied construction strategies attempt to actively counteract the girders' tendency to deflect and rotate out of plumb.

To achieve better understanding of the effects of design, fabrication, and construction on the geometry and load distribution in a curved or skewed I girder/beam bridge system, further study on such bridges is required. Therefore, this project is intended to continue examination of the behavior of curved and skewed I-girder bridges during construction with the intention of developing criteria to assist the process. The specified objectives of this project are presented as follows:

- (1) Continue to develop and maintain acquisition capabilities for instruments on two structures in the I-99 corridor – #207, a horizontally curved, steel, I-girder bridge, and #314, a skewed, pre-stressed, concrete bridge.
- (2) Develop, examine, and reduce data produced from these structures as needed.
- (3) Continue examination of numerical model accuracy for curved and skewed steel I-girder bridges and select appropriate model types and software for continued application.
- (4) Extend numerical studies to examine prevalent issues affecting curved and skewed steel I-girder bridge behavior during construction.
- (5) Develop relevant guidelines for curved and skewed steel I-girder bridges during construction.

8.2 GENERAL DESIGN GUIDELINE AND LITERATURE SEARCH

This report serves as an addendum to literature searches completed in association with earlier projects funded by PennDOT. Resulting information can be found in reports published in association with those projects (Linzell et al. 2003; Hiltunen et al. 2004; Linzell et al. 2006) and, for horizontally curved steel bridges, in other publications (Zureick et al. 1994; Hall et al. 1999; Linzell et al. 2004; Kulicki et al. 2006). The focus of the literature search completed herein was to expand previous findings and to expand the body of the literature search to include specific items identified as additional focus areas by the sponsor during development of the current project scope.

Recent work completed in association with the construction response of curved steel bridges has been published in association with the Curved Steel Bridge Research Project (CSBRP) by the AASHTO/NSBA Steel Bridge Collaboration and by others. The recent research work has largely focused on revision of existing specifications (AASHTO 2005), development of model types and prototype software packages that can be used to predict construction response (Chang 2006; Chang and White 2006), publication of qualitative recommendations and representative plan sets to assist with the erection of steel structures (AASHTO/NSBA 2003, 2006), examination of cross frame detailing and erection decisions on final geometry at the completion of superstructure erection (Chavel and Earls 2006a, 2006b), study of lifting requirements for curved girder segments coupled with the development of strength and slenderness limits for non-composite curved I-girder flanges that account for web contributions (Madhavan 2006), examining web out-of-plumbness and resulting problems related to deck pour sequencing, cross bracing forces (Howell and Earls 2007), and examination of the effect of bearing type on curved steel bridge behavior (Samaan et al. 2002).

Recent research related to skewed bridge response during construction has been more limited and was largely summarized in past submittals (Linzell et al. 2003); however, revisions to existing specifications have also occurred (AASHTO 2005). Work by the AASHTO/NSBA Steel Bridge Collaboration above has also attempted to address skewed steel bridge construction issues in largely qualitative form, and other research has been published related to steel superstructure response during deck placement (Choo et al. 2005; Norton et al. 2003). A few studies related to bearing types and their influence on skewed steel bridge behavior have also been published (Samaan et al. 2002). More detailed information related to design guidelines research for curved and skewed I-girder/beam bridges is incorporated into Section 2.1, while more detailed information related to additional research in the additional focus areas is incorporated into Section 2.2.

8.2.1 General Design Provisions and Guidelines

For bridge designers in Pennsylvania, PennDOT language related to curved and skewed steel I-girder bridges is largely found in Sections 2, 3, 4, 6, and 14 of Part B of *PennDOT Publication 15M, Design Manual Part 4* (PennDOT 2007). These sections refer to and/or supplement similar sections in the *AASHTO LRFD Bridge Design Specifications* (AASHTO 2004), with Section 2 providing serviceability information, Section 3 general design information, Section 4 analysis information, Section 6 strength design information, and Section 14 bearing detailing information. As a result of the approach and the utilization of references to AASHTO, specific information related to construction is limited and qualitative in nature with specific mention of construction effects limited to consideration of uplift forces that could occur.

PennDOT Publication 408/2007 (PennDOT 2007) contains construction specifications for PennDOT projects with specific references to steel superstructures occurring in Section 1050. This section largely deals with bearing placement and tolerances with no specific differentiation between straight bridges and those of irregular geometry. Qualitative mention of erection procedures is also made, again with no differentiation between straight bridges and curved and skewed structures.

Research related to curved steel I-girder bridges has historically focused on in-service behavior and development of design criteria to address this response. Curved Steel Bridge Research Project (CSBRP) research in this area resulted in extensive changes in Section 6 of the *2005 Interim AASHTO LRFD Bridge Design Specifications* (AASHTO 2005) which were incorporated into *PennDOT Publication 15M, Design Manual Part 4* (PennDOT 2007). Until recently, work related to construction response of these structures was largely completed in association with I-99 corridor construction or via other research completed by the PI (Hiltunen et al. 2006; Linzell et al. 2002, 2004; Nevling et al. 2006; Zureick et al. 2000; Linzell 1999). However, since the submission of earlier I-99 corridor reports, there has been valuable research by others that examines construction response.

Ongoing work by the AASHTO/NSBA Steel Bridge Collaboration has resulted in the publication of a number of documents related to steel bridge construction. Of these documents, the *Guidelines for Design for Constructability*, the *Steel Bridge Erection Guide Specification*, and corresponding sample erection plans (AASHTO/NSBA 2003, 2006) contain the most specific references and guidance for curved steel I-girder bridge construction. While these

documents contain a large amount of valuable information relevant to the scope of this project, they are also largely qualitative in nature.

Previously discussed revisions to the *AASHTO LRFD Bridge Design Specifications* do include more information related to construction issues for curved steel I-girder bridges resulting from CSBRP work (AASHTO 2005), with designers being directed to pay close attention to deflection and stability issues during construction.

Research related to skewed steel bridge construction response has been much more limited, and historical work was summarized in previous submittals to PennDOT (Linzell et al. 2003). While the 2005 AASHTO Interims do discuss preferential cross frame placement schemes for steel superstructures as a function of skew angle and the need to address differential deflections during design, the most comprehensive recent publications attempting to address construction response are the aforementioned AASHTO/NSBA Steel Bridge Collaboration documents. In these documents, discussion of skewed construction aspects is also largely qualitative in nature and focuses on the effects of skew on superstructure deformations and how to counteract those effects and placement and orientation of cross frames in skewed superstructures.

8.2.2 Updated Literature Search

Topics that have been updated through the current literature search includes research focusing on the following areas as they relate to curved and skewed bridge construction behavior: (1) development of model types and prototype software packages; (2) web-plumbness; (3) bearing type and restraint; (4) cross frames behavior; (5) temporary shoring placement and settlement; and (6) global temperature change. Summaries of each topic are provided below.

8.2.2.1 Development of model types and prototype software packages

A number of modeling strategies for design and construction analysis of curved I-girder bridge systems ranging from modified line-girder analyses to finite element approaches have been recently published. Chang et al. (2006) conducted research on a representative full-scale composite curved I-girder bridge, tested at the FHWA Turner-Fairbank Highway Research Center (TFHRC) and utilized the bridge for assessment of different modeling approaches. The predictions of key lateral and vertical displacements, reactions, cross frame forces, and major-axis and flange lateral bending stresses were evaluated with respect to the test bridge. They discussed the efficacy of the various approaches. In addition, this research focused on the development and validation of a prototype software package that focuses on predicting construction response of curved steel I-girder bridge systems during girder erection and the deck pour. Coupled with the creation of this tool was the development of expanded 2D modeling approaches for curved I-girder bridges during construction. Topkaya and Williamson (2003) presented a variety of computational efforts related to predicting the behavior of horizontally curved trapezoidal steel girders during erection and before the concrete deck hardened to form a closed section. The program they developed, UTrap, was formulated based on the finite element method to account for construction sequencing and was designed to be computationally efficient and easy for bridge designers to use. It was reported that the developed software was able to accurately capture girder stresses during construction (Topkaya et al. 2003).

8.2.2.2 Effects of web-plumbness

In horizontally curved steel girder bridges, the girders have a tendency to deform out-of-plumb as they are put under vertical load because of load eccentricity with respect to the curved girder supports locations. In horizontally curved bridges with smaller radii of curvature and longer spans, web out-of-plumbness is a concern because it can increase stresses in girder flanges, cause fabrication problems with cross bracing and deck pouring, increase cross bracing forces, and create the perception of safety problems (Howell and Earls 2007). Flanges of curved girders have been shown to have stress increases as high as 23% due to vertical and lateral bending caused by out-of-plumbness. Vertical bending stresses can also increase in parts of the flanges because of added eccentricity from the neutral axis caused by the radii of curvature. Lateral bending results from a weak axis component of the vertical loads on an out-of-plumb girder. These effects should be included in any stress analysis of girders (AASHTO 2003).

Differential deflections and out-of-plumbness can cause problems with cross frame detailing; inconsistent detailing and geometric inconsistencies can result (Domalik et al. 2005), and increased cross frame forces can occur (Howell and Earls 2007). To alleviate this problem, one of several techniques can be used. The most common method used when web plumbness problems arise during fabrication is to impose outside forces by means of cranes and/or jacking to set the member in a position where the cross frame can be placed. This, however, can be costly, can impose stresses that the superstructure was not designed to carry, and at times may require forces above the capacity of the equipment used for construction (Chavel and Earls 2006b). As an alternative, the engineer of record can specify vertical and twist camber to result in a near plumb condition at a specified stage of construction (e.g., no load, steel self weight, full dead load) agreed upon by the steel fabricator (Chavel and Earls 2006b, AASHTO/NSBA 2003). In addition, some deflection problems have been shown to be mitigated by using a suitable erection sequence (Bell and Linzell 2007).

Safety perception problems can likely be mitigated by keeping the out-of-plumbness to a minimum when the bridge is in operation. Since its effect is very small after the deck hardens, care should be taken in the design stage to ensure that the girders will be near plumb after the deck is poured. This care should be taken especially in cases of long span and small radius of curvature combinations (Howell and Earls 2007).

While limited studies have attempted to examine the effects of web-plumbness on curved bridge construction behavior, there have been no reported studies on the effects of web-plumbness on skewed steel bridge behavior during construction.

8.2.2.3 Effects of bearing type and restraint

The type and arrangement of bearings for a bridge superstructure are important considerations in bridge design. For a curved continuous girder bridge, the support conditions for the bridge superstructure may significantly influence the distribution of maximum stresses, reactions, and shear forces, as well as the bridge's natural frequencies and mode shapes. However, current design practices in the U.S. recommend very few guidelines for bearing arrangements and types. A few papers related to bearing types for curved and skewed steel bridges have been published (Samaan et al. 2002; Tindal and Yoo, 2003).

Samaan et al. (2002) described an extensive study carried out using an experimentally calibrated finite element model in which curved, continuous prototype bridges were analyzed to determine their structural response. Six different types and arrangements of support bearings were studied to determine their effects on the maximum stress and reaction distributions, as well as on the natural frequencies of such bridges. The results were used to suggest the most favorable bearing arrangement and type.

Tindal and Yoo (2003) examined bearing effects on skewed steel highway bridges. Three bearing orientation cases, representative of current AASHTO LRFD design practices, were considered, and parametric studies were conducted. Hypothetical bridges were designed for a range of different span lengths, section depths, widths, and skews. Each bridge model was tested under all three bearing orientation case parameters, and the relative influence of each parameter on behavior was discussed.

8.2.2.4 Effects of cross frames

Because of the coupling action of the vertical bending and torsion, curved and skewed girders are subject to significant rotations. During construction, the noncomposite steel girder must support the wet concrete and steel weight in addition to other construction loads, such as the weight of screed, formwork, and other items. There have been large relative deflections observed between girders on curved and skewed girder bridges under steel selfweight and during deck placement that make it difficult to maintain the specified final cambers and superelevations and to form and key in the construction joints. Since it is not practical to increase the girder stiffness simply to minimize the relative deflections and rotations, either cross frames, lateral bracing, temporary shoring, or a combination of these items is considered. Because the cross frames are not only expensive but can adversely affect the fatigue behavior of the steel girder, the number of cross frames should be minimized (Norton et al. 2003).

However, there are currently few design guidelines available for intermediate cross frames in curved steel girder bridges. There have been a few publications related to cross frames' effects on curved bridges, with much of the focus being curved box girders (Memberg, 2002; Kim and Yoo, 2006). Memberg (2002) presented a procedure for the design of intermediate external diaphragms that recommended designing these members to carry forces that were more than ten times higher than those measured experimentally. Kim and Yoo (2006) evaluated the effects of cross frames on deck unevenness during construction by modeling hypothetical twin-box girder bridges using ABAQUS. A deck unevenness ratio was defined that quantified the degree of unintended deck slope caused by relative superstructure deflections and rotations. Additional relevant research associated with examinations of the influence of cross frame detailing and specific erection decisions on final superstructure geometry for a curved I-girder bridge has also been published (Chavel and Earls 2006a, 2006b). Findings from this work were used to emphasize the need for designers to explicitly specify the dead load state used to detail the curved superstructure to prevent fit-up problems during erection.

In addition, there have been a few papers related to cross frames' effects on skewed steel I-girder bridges (Azizinamini et al. 1995; Wang et al. 2008). Azizinamini et al. (1995) conducted analytical and experimental investigations on the influence that cross frames having different configurations had on load resisting capacity. Results indicated that for steel bridges with small skew, the presence of cross frames had little influence on behavior after construction. Cross frames were shown not only to be unnecessary after construction but were stated to be, to a degree, harmful as they tried to prevent the tendency of the girders to separate and consequently transferred restraining forces to the girder webs, which could cause fatigue cracking. Wang et al. (2008) outlined cross frame placement requirements for bridges with skewed supports when considering primarily stability; however, stiffness and strength were also addressed. Two orientations of the intermediate cross frame were considered, and as a result of this research, stability cross frame requirements for steel girders were presented as a function of support geometry and bracing orientation.

8.2.2.5 Temporary shoring placement and settlement

Many horizontally curved steel I-girder bridges utilize shoring during construction. It is often assumed that the bridge superstructure (girders and cross bracing) will be erected in a specified no-load condition. To achieve this, temporary shoring (or falsework) is implemented to control horizontal and vertical deflections during erection (Chavel and Earls 2006). Other erection procedures involve erecting the girders in pairs, with cross bracing being erected on the ground and then the pair being lifted into place. This can result in fewer horizontal and vertical alignment problems than single girder erection techniques, but shoring has been shown to further reduce alignment problems (Bell and Linzell 2007). When project constraints allow shoring to be utilized, it will likely provide a benefit by eliminating fit-up problems that can arise during construction. Hydraulic jacks mounted on the shoring can further correct any alignment problems that may arise during fabrication and deck pouring. Chavel and Earls (2006) have suggested that some misalignments during construction thought to be from girder deflections are in fact due to fabrication and detailing errors since finite element models were unable to replicate the misaligned response.

Publications related to shoring location or support settlement effects on curved and skewed structure construction response could not be identified.

8.2.2.6 Global temperature change during deck placement

Very little information exists about the effects that global temperature changes during deck placement have on steel bridge behavior be they straight, curved, or skewed bridges. NCHRP's Steel Bridge Erection Practices publication (2005) identifies horizontal and vertical deflections caused by temperature changes as a problem that several contractors have reported, but no solutions are given.

The research that exists has studied a skewed steel bridge for the purpose of validating finite element models. In the process of monitoring deflections and stresses induced into an actual bridge during placement of the deck, a finite element model showed reduced accuracy as the placement progressed throughout a single day. When thermal effects were added, model predictions improved significantly (Choo et al. 2005).

8.2.3 Summary

The latest general PennDOT and federal design provisions, along with updated research and work in additional specified areas related to curved and skewed bridge systems during construction, were summarized. Updates to general design provisions have occurred but have been largely qualitative in nature. Updates to already established curved and skewed bridge research areas related to construction have largely consisted of further examination and development of tools to accurately predict construction response. Additional topics that were included in the present literature search consisted of web out-of-plumbness, bearing type and restraint, cross frames; temporary shoring placement and settlement, as well as global temperature change and those topics as they related to curved and skewed bridge construction, had somewhat limited information available in the literature.

8.3 PROPOSED DESIGN FOR CONSTRUCTION DOCUMENT TEMPLATE

As discussed and included in the current project scope document, the format in which findings from this work would be presented would permit incorporation into relevant PennDOT specification documents should PennDOT feel that modifications suggested by Penn State personnel are warranted. As was discussed in the scope document, modifications will focus on: (1) Sections 2, 3, 4, and 6 within PennDOT Publication 15M, Design Manual Part 4 (PennDOT 2002); (2) Section 1050.3 in PennDOT Specifications Publication 408/2007 (PennDOT 2007); and PennDOT Standard Drawing Set BD-620M (PennDOT 2004). A proposed initial draft containing possible modifications to each of the aforementioned documents was included in the scope and is reproduced in the pages that follow. Additional suggestions for modifications as a result of research work that has occurred since initiation of the project have also been incorporated into the following pages. Any suggested modifications or changes to the initial draft document since initiation of the project are shown in ***12-Point font, in bold and italics***. It should be emphasized that all suggested modifications provided herein are preliminary and that extensive changes could occur as the project progresses.

8.4 REFERENCES

- AASHTO (2004). *AASHTO LRFD Bridge Design Specifications*. American Association of State Highway and Transportation Officials, Washington, D.C.
- AASHTO (2005). *2005 Interim AASHTO LRFD Bridge Design Specifications*. Customary U.S. Units. American Association of State Highway and Transportation Officials, Washington, D.C.
- AASHTO/NSBA Steel Bridge Collaboration (2003, 2006). *Guidelines for Design for Constructability G12.1*. American Association of State Highway and Transportation Officials, Washington, D.C.
- Azizinamini, A., Kathol, S., and Beacham, M. W. (1995). "Influence of Cross Frames on Load Resisting Capacity of Steel Girder Bridges," *Engineering Journal*, 32(3), 107-116.
- Bell, B. J., and Linzell, D. G. (2007). "Erection Procedure Effects on Deformations and Stresses in a Large Radius, Horizontally Curved, I-Girder Bridge." *J. Bridge Eng.*, 12(4), 467-476.
- Chang, C. J., White, D. W., Beshah, F. and Wright, W. (2006). "Design Analysis of Curved I-Girder Bridge Systems - An Assessment of Modeling Strategies," *Annual Proceedings, Structural Stability Research Council*, 349-369.
- Chang, C. J. (2006). "Construction Simulation of Curved Steel I-Girder Bridges," Thesis in Civil Engineering, Georgia Institute of Technology, Atlanta, GA, USA.
- Chavel, B. W., and Earls, C. J. (2006a). "Construction of a Horizontally Curved Steel I-Girder Bridge. Part I: Erection Sequence." *J. Bridge Eng.*, 11(1), 81-90.
- Chavel, B. W., and Earls, C. J. (2006b). "Construction of a Horizontally Curved Steel I-Girder Bridge. Part II: Inconsistent Detailing." *J. Bridge Eng.*, 11(1), 91-98.
- Choo, T, Linzell, D. G., Lee, J. I., and Swanson, J. A. (2005). "Response of a continuous, skewed, steel bridge during deck placement." *J. of Constructional Steel Research*, 61, 567-586.
- Dey, G. (2001). "Bridging the curve: Design and fabrication issues affecting economy and constructability," *Bridgeline*, 11(1). HDR Engineering, Omaha, NE.
- Domalik, D. E., Shura, J. F., and Linzell, D. G. (2005). "Design and Field Monitoring of Horizontally Curved Steel Plate Girder Bridge." *Transportation Research Record* 1928, Transportation Research Board, Washington, D.C., 83-91.
- Hall, D. H., Grubb M. A., and Yoo, C. H. (1999). *Improved Design Specifications for Horizontally Curved Steel Girder Highway Bridges*, National Cooperative Highway Research Program, Research Report 424, Transportation Research Board, Washington, D.C.
- Hiltunen, D. R., Johnson, P. A., Laman, J. A., Linzell, D. G., Miller, A. C., Niezgoda, S. L., Scanlon, A., Schokker, A. J., and Tikalsky, P. J. (2004). *Interstate 99 Research*, Final Report, Pennsylvania Transportation Institute, Report No. PTI 2005-02, October, 324 pp.
- Howell, T. D. (2006). "On the influence of web out of plumbness on horizontally curved steel I-girder bridge serviceability during construction," Thesis in Civil Engineering, Univ. of Pittsburgh, Pittsburgh, PA.
- Howell, T. D., and Earls, C. J. (2007). "Curved Steel I-Girder Bridge Response during Construction Loading: Effects of Web Plumbness," *Journal of Bridge Engineering*, 12(4), 485-493.

- Kim, K. S., and Yoo, C. H. (2006). "Effects of external bracing on horizontally curved box girder bridges during construction," *Engineering Structure*, 28 1650–1657.
- Kulicki, J. M., Wassef, W. G., Kleinhans, D. D., Yoo, C. H., Nowak, A. S. and Grubb, M. (2006). *Development of LRFD Specifications for Horizontally Curved Steel Girder Bridges*, National Cooperative Highway Research Program, Research Report 563, Transportation Research Board, Washington, D.C.
- Linzell, D. G. (1999). "Studies of a Full-Scale Horizontally Curved Steel I-Girder Bridge System under Self-Weight," Thesis in Civil Engineering, Georgia Institute of Technology, Atlanta, GA, USA.
- Linzell, D. G., Laman, J. A., Bell, B., Bennett, A., Colon, J., Lobo, J., Norton, E., and Sabuwala, T. (2003). *Prediction of Movement and Stresses in Curved and Skewed Bridges*, University-Based Research, Education and Technology Transfer Program; Agreement No. 359704, Work Order 79. Final Report, Pennsylvania Department of Transportation, March, 192 pp.
- Linzell, D. G., Hall, D. H., and White, D. W. (2004). "A Historical Perspective on Horizontally Curved I-Girder Bridge Design in the United States," *ASCE Journal of Bridge Engineering*, 9(3), 218-229.
- Linzell, D. G., Leon, R. T., and Zureick, A. H. (2004). "Experimental and Analytical Studies of a Horizontally Curved Steel I-Girder Bridge during Erection," *ASCE Journal of Bridge Engineering*, 9(6), 521-530.
- Linzell, D. G., Nadakuditi, V. P. and Nevling, D. L. (2006). *Prediction of Movement and Stresses in Curved and Skewed Bridges*, Final Report, Pennsylvania Transportation Institute, Report No. PTI 2007-05, November, 93 pp.
- Madhavan, M., and Davidson, J. S. (2004). "Elastic buckling of centerline-stiffened plates subjected to a linearly varying stress distribution." *Proceedings of the Twenty-second Southeastern Conference on Theoretical and Applied Mechanics*, August 15-17, Tuskegee Alabama.
- Memberg, M. A. (2002). "A design procedure for intermediate external diaphragms on curved steel trapezoidal box bridges," MS thesis. Austin (TX): University of Texas.
- NCHRP. (2005). *Steel Bridge Erection Practices*, National Cooperative Highway Research Board Synthesis 345, Transportation Research Board, Washington, D.C.
- Nevling, D., Linzell, D., and Laman, J. (2006). "Examination of Level of Analysis Accuracy for Curved I-Girder Bridges through Comparisons to Field Data," *ASCE Journal of Bridge Engineering*, 11(2), 160-168.
- Norton, E. K., Linzell, D. G., and Laman, J. A. (2003). "Examination of the Response of a Skewed Steel Bridge Superstructure During Deck Placement," *Transportation Research Record* 1845, 66-75.
- Pennsylvania Department of Transportation (2007), *Publication 408/2007*.
- Pennsylvania Department of Transportation (2004), *BD-620M, Standard, Steel Girder Bridges Lateral Bracing Criteria and Details*.
- Pennsylvania Department of Transportation (2004), *Publication 15M, Design Manual Part 4*.
- Samaan, M., Sennah, K., and Kennedy, J. B. (2002). "Positioning of bearings for curved continuous spread-box girder bridges," *Canadian Journal of Civil Engineering*, 29: 641–652.
- Tindal, T. T., and Yoo, C. H. (2003). "Thermal Effects on Skewed Steel Highway Bridges and Bearing Orientation," *J. Bridge Eng.*, 8(2), 57-65.
- Topkaya, C., and Williamson, E. B. (2003). "Development of computational software for analysis of curved girders under construction loads," *Computers and Structures* 81, 2087-2098.

Wang, L., and Helwig, T. A. (2008). "Stability Bracing Requirements for Steel Bridge Girders with Skewed Supports," *J. Bridge Eng.*, 13(2), 149-157.

Zureick, A., Naqib, R., and Yadlosky, J. M. (1994). *Curved Steel Bridge Research Project, Interim Report I: Synthesis*, HDR Engineering, Inc., Publication Number FHWA-RD-93-129, December.

Zureick, A., Linzell, D., Leon, R. T., and Burrell, J. (2000). "Curved Steel Bridges: Experimental and Analytical Studies," *Engineering Structures*, 22(2).

9 APPENDIX B

Numerical Modeling Report

**COMMONWEALTH OF PENNSYLVANIA
DEPARTMENT OF TRANSPORTATION**

PENNDOT RESEARCH



**GUIDELINES FOR ANALYZING CURVED AND SKEWED BRIDGES
AND DESIGNING THEM FOR CONSTRUCTION**

FINAL INTERIM REPORT: NUMERICAL MODELING

**Work Order No. PSU009
Intergovernmental Agreement, No. 510602**

September 9, 2009

By D. G. Linzell, D. L. Nevling and J. Seo

PENNSSTATE



**The Thomas D. Larson
Pennsylvania Transportation Institute**

**The Pennsylvania State University
Transportation Research Building
University Park, PA 16802-4710
(814) 865-1891 www.pti.psu.edu**

GUIDELINES FOR ANALYZING CURVED AND SKEWED BRIDGES AND DESIGNING
THEM FOR CONSTRUCTION

FINAL INTERIM REPORT: NUMERICAL MODELING

Work Order No. PSU-009
Intergovernmental Agreement No. 510602

Prepared for

Bureau of Planning and Research
Commonwealth of Pennsylvania
Department of Transportation

By

Daniel G. Linzell, Ph.D., P.E.
Deanna L. Nevling
Junwon Seo

The Thomas D. Larson Pennsylvania Transportation Institute
The Pennsylvania State University
Transportation Research Building
University Park, PA 16802-4710

September 9, 2009

PTI 2008-16

This work was sponsored by the Pennsylvania Department of Transportation and the U.S. Department of Transportation, Federal Highway Administration. The contents of this report reflect the views of the authors, who are responsible for the facts and the accuracy of the data presented herein. The contents do not necessarily reflect the official views or policies of either the Federal Highway Administration, U.S. Department of Transportation, or the Commonwealth of Pennsylvania at the time of publication. This report does not constitute a standard, specification, or regulation.

TABLE OF CONTENTS

9.1 INTRODUCTION	184
9.2 STRUCTURE DESCRIPTIONS	184
9.3 MODELING TECHNIQUES	196
9.4 COMPARISONS AND MODIFICATIONS	199
9.5 ADDITIONAL EVALUATIONS	222
9.6 CONCLUSIONS.....	233
9.7 REFERENCES	234

9.1 Introduction

This report summarizes modeling development and verification completed in association with Work Order 009, *Guidelines for Analyzing Curved and Skewed Bridges and Designing Them for Construction*. The work order is a continuation of earlier projects and information related to modeling efforts completed in association with those projects can be found in earlier reports (Linzell et al. 2003; Hiltunen et al. 2004; Linzell et al. 2006).

The intent of the modeling portion of the project is to further develop and select models to assist with parametric studies being completed in association with future project tasks. Findings from Task 1 (Literature Search) of the current project coupled with detailed analyses and accuracy evaluations for one curved bridge, Structure #207, were used to complete any additional major modifications required to improve model accuracy. The effectiveness of these modifications was further evaluated by comparing model predictions to information obtained during the construction of other curved and skewed bridges. The curved bridges include Structure #7A, a structure that was examined and summarized in past submittals to PennDOT (Linzell et al. 2003; Hiltunen et al. 2004; Linzell et al. 2006) and the I-79 Missing Ramps Bridge. The skewed structure is Structure #28, another bridge that was examined and summarized in past submittals to PennDOT (Linzell et al. 2003).

The sections that follow provide information on the structures that were modeled and discuss the modeling techniques examined with the current effort and with other efforts completed in association with this study. In addition, they summarize comparisons, modifications, and additional evaluations that were completed.

9.2 Structure Descriptions

As was discussed above, a total of four structures were utilized for model validation and modification. Structure descriptions and erection and instrumentation information are provided herein, and, if applicable, references are provided to previous PennDOT submittals containing additional information.

9.2.1 Structure #207

Structure #207 is the bridge that was used for the majority of the model validation and modification steps performed in association with this project. Additional discussion of the bridge design and erection is provided in past submittals to PennDOT (Linzell et al. 2003; Hiltunen et al. 2004; Linzell et al. 2006). A brief design, erection, and instrumentation summary is provided herein.

Structure #207 is located in Centre County, PA, at the intersection of Interstate 99 and United States Route 322 East. The two-span continuous bridge contains five singly-symmetric steel plate girders. It spans a total distance of 146.53 m (480.75 ft) with Span 1 measuring 65.38 m (214.50 ft) and Span 2 ranging 81.50 m (266.25 ft). The bridge centerline radius of curvature is 585 m (1921 ft), and the girders are spaced at 3.25 m (10.67 ft) center to center. Four field splices are located along the bridge.

All girder webs are 2.74 m (108.00 in) deep. Top and bottom flanges dimensions vary along the girder length. More detail on the girder dimensions at select locations and representative structural drawings can be found in previous PennDOT submittals (Linzell et al. 2006).

Structure #207 was constructed using a single girder erection procedure, working from interior girder (G5) toward exterior girder (G1). Span 1 was erected along with a portion of Span 2 (to Field Splice 3) prior to any girder placement within Span 2. The contractor utilized temporary shoring towers under G4 and G5 and tie-downs at the abutments and piers. Three cranes were used to place the girders, and a boom truck was used to place the cross-frames. Deadmen were affixed to G2 at the completion of erection to provide additional radial restraint prior to the deck pour. Bolts were installed throughout the process but were not tightened until all girders and cross-frames were in place. Superstructure erection took 10 days to complete. Initially, the contractor attempted to tighten bolted girder field splices by lifting a single girder splice at a time, which resulted in undesired movement of adjacent, tightened field splices. Therefore, all five girders

were lifted at a given field splice simultaneously using the temporary shoring towers, and this problem was mitigated. As tightening and aligning progressed, minor alignment problems (top of girder elevations) were observed, and two splices needed to be reassembled.

Placement of the 229-mm (9-ft), reinforced concrete deck was conducted in four stages. Deck reinforcement consisted of two epoxied rebar mats. Main reinforcing steel was oriented radially and consisted of #5 bars spaced 152 mm (6 in) on center. Transverse reinforcement consisted of #5 bars spaced at 279 mm (11") in positive moment regions, and #5 and #6 bars alternating at 127 mm (5") in the negative moment region. To minimize deck cracking in the negative moment regions, concrete in the positive moment region of Span 1 was placed first, followed by the positive moment region of Span 2. The negative moment region over the pier was poured during the third stage, with the blockouts at Abutments 1 and 2 poured during the final stage. A pump truck was used to deliver concrete onto the bridge, and a finishing machine and work bridges were used to place and finish concrete to the desired elevation and cross-slope. Each consecutive placement step was performed within two days of the previous step. Parapets were added after the entire deck had achieved 28-day strength. Additional detail on the erection process can be found in previous submittals to PennDOT (Linzell et al. 2003; Linzell et al. 2006).

Penn State University personnel instrumented the structure using a total of 65 vibrating wire strain gauges and 4 vibrating wire tiltmeters, and 10 laser targets were used to monitor the bridge during construction. The majority of the instruments were placed on the exterior girders and on cross-frames identified as critical elements in the curved system from preliminary analyses. Additional details on the preliminary analyses and the instrumentation can be found in previous submittals to PennDOT (Linzell et al. 2003; Hiltunen et al. 2004; Linzell et al. 2006).

9.2.2 Structure #7A

Structure #7A was used for some earlier model validation studies and, as such, is described in previous submittals to PennDOT (Linzell et al. 2003). A brief design, erection, and instrumentation summary is provided herein.

Structure #7A is one of two side-by-side horizontally curved composite steel I-girder bridges constructed at an I-99 interchange over Park Avenue in Centre County, Pennsylvania. It is a six-span structure whose cross-section consists of five singly symmetric plate girders spaced at 2.97 m (9.75 ft) with radii varying from 585.3 m to 597.2 m (1920 ft to 1959 ft). The girders are composed of stiffened web plates with a constant depth and thickness and flange plates of varying dimensions. Girders are braced radially using cross-frames made up of WT sections, and no lateral bracing system was included in the original construction plans.

The complete structure consists of 2 three-span continuous units spanning a total distance of 530.1 m (1739 ft) along the roadway's construction line. The eastern of these, which is the focus of this work, is composed of spans designated Spans 4, 5, and 6. More detail on the structure dimensions can be found in previous PennDOT submittals (Linzell et al. 2003).

A construction plan was prepared by the original contractor that called for erection of girders in pairs, with the single girder line having the highest radius of curvature being placed after the other four girder lines (two pairs) had been erected in a given span. Each girder pair was preassembled on the ground with cross-frames fully bolted and tightened, and the units were then raised incrementally from splice to splice.

Erection was initiated with placement of Span 4 steel, beginning at Pier 4 and working toward Pier 3. Prior to the erection phase, falsework was mounted to Pier 4 to support hydraulic jacks that stabilized and adjusted the system during construction to achieve the design "no-load" geometry prior to deck placement. Originally, construction was to be accomplished using four cranes, and no temporary shoring towers would be employed.

Halfway through erection of Span 4, twisting of G2 and G3 caused undesired deformations and made it impossible to continue without revising construction measures and/or adding bracing. The proposed

solution included implementing a single support tower in Span 4, which was placed approximately 36 m (118.11 ft) east of Pier 3 and would allow cranes to be released to resume erection. Complications continued to occur during the erection procedure, and upon completion of Span 4 and a cantilevered portion of Span 5, the superstructure was surveyed and shown to be severely out of lateral alignment from the intended “no-load” geometry, with horizontal misalignments of 274 mm (10.8 in) at Field Splice #11 in Span 4 and 351 mm (13.8 in) at Field Splice #14.

A second contractor was hired to realign the superstructure and complete the erection of the remaining spans. Once the design geometry of the erected portion of the bridge was attained, upper lateral bracing was inserted between the fascia and first interior girders, and steel placement continued using a revised plan that called for the erection of single girder lines rather than girder pairs, placing the girder line with the largest radius of curvature first and working inward. Furthermore, the revised scheme required the implementation of temporary support towers in all spans. More detail on the intended and final erection plans can be found in previous PennDOT submittals (Linzell et al. 2003).

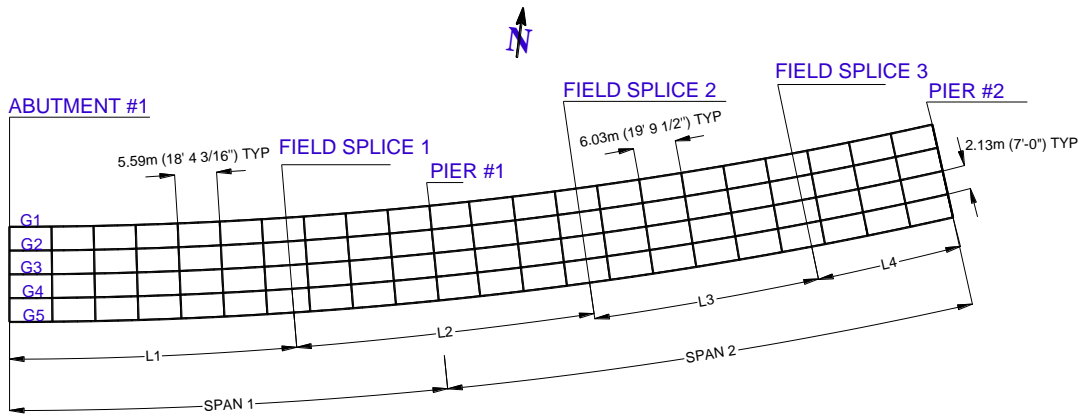
A limited field monitoring program was instituted during construction of Structure 7A. Data were collected during two phases of steel erection: (1) realignment of the previously erected portion in Span 4 and a portion of Span 5 and (2) completion of steel erection in Spans 5 and 6. Field survey data tracking deformations at various stages throughout both processes were collected by a third party. More detail on the instrumentation and data collection plans can be found in previous PennDOT submittals (Linzell et al. 2003).

9.2.3 Missing Ramps Bridge

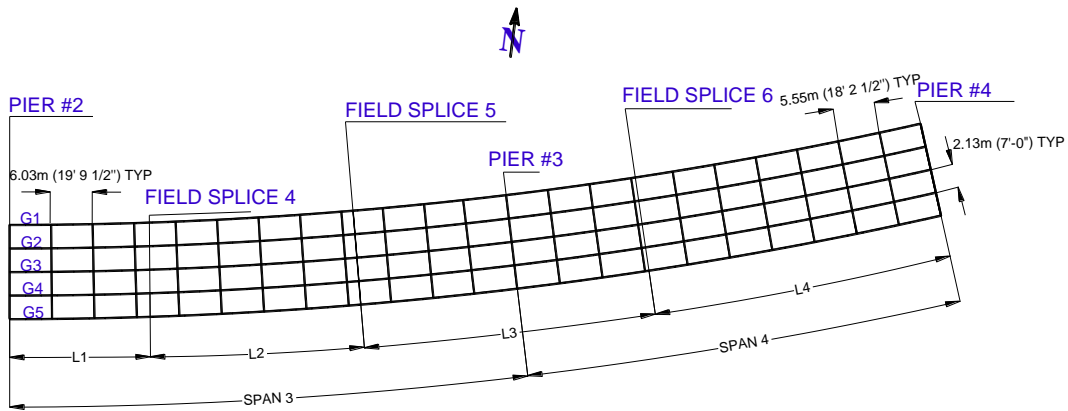
The Missing Ramps Bridge is a seven-span continuous composite steel plate girder bridge with a total length of 452.93 m (1486 ft). The superstructure utilizes five ASTM A709 Grade 50 singly symmetric steel plate girders that are 2.29 m (90 in) deep and spaced at 2.13 m (7 ft) center to center. Flange plate dimensions vary along the length of the girders. Spans 1, 2, 3, 4, 5, 6, and 7 measure 55.93 m (183 ft 6 in), 72.39 m (237 ft 6 in), 72.39 m (237 ft 6 in), 72.39 m (237 ft 6 in), 55.50 m (182 ft 1 in), 63.27 m (207 ft 7 in), 68.88 m (226 ft), and 63.7 m (209 ft) along the arc, respectively, and the radius of curvature to the center girder is 253.14 m (830 ft 6 in). Lateral bracing is provided using both X- and K-shaped cross-frames containing WT sections oriented radially along both spans. For shipping purposes, each girder consists of five sections that are bolted at 11 field splices. Table 35 provides some information on girder geometry. Figure 232 and Figure 233 detail plan views and typical superstructure cross-sections.

Table 35. Girder Lengths, Radii, and Field Splice Locations (see Figure 1).

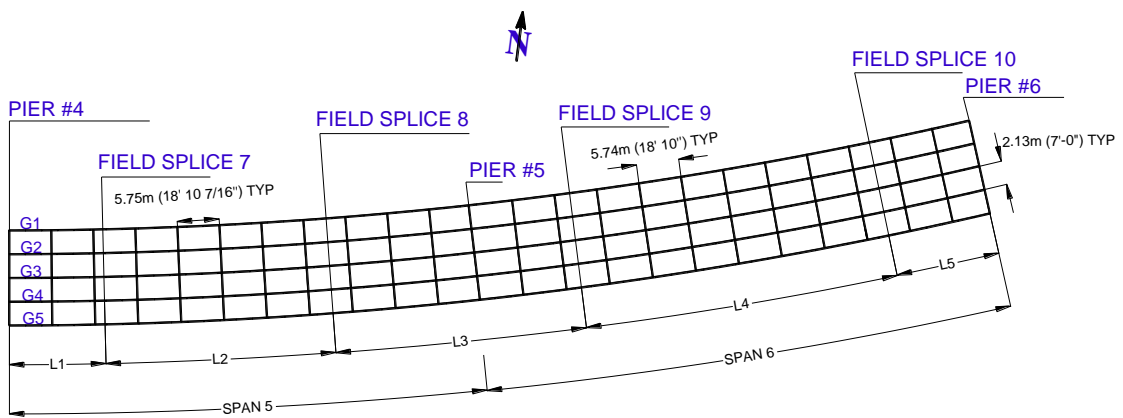
Span (1)	Girder ID (2)	Radius m (ft) (3)	L1 m (ft) (4)	L2 m (ft) (5)	L3 m (ft) (6)	L4 m (ft) (7)	L5 m (ft) (8)	First Span m (ft) (9)	Second Span m (ft) (10)	Total m (ft) (11)
1 and 2	G1	248.87 (816.50)	37.04 (121.52)	39.24 (128.75)	30.25 (99.24)	19.20 (63.00)	N/A N/A	54.69 (179.43)	70.79 (232.24)	125.48 (411.67)
	G2	251.00 (823.50)	37.51 (123.06)	39.24 (128.75)	30.85 (101.23)	19.20 (63.00)	N/A N/A	55.16 (180.97)	71.39 (234.23)	126.55 (415.20)
	G3	253.14 (830.50)	37.98 (124.59)	39.24 (128.75)	31.46 (103.22)	19.20 (63.00)	N/A N/A	55.63 (182.51)	71.98 (236.17)	127.61 (418.68)
	G4	255.27 (837.50)	38.44 (126.13)	39.24 (128.75)	32.07 (105.21)	19.20 (63.00)	N/A N/A	56.10 (184.05)	72.61 (238.21)	128.70 (422.26)
	G5	257.40 (844.50)	38.91 (127.67)	39.24 (128.75)	32.67 (107.20)	19.20 (63.00)	N/A N/A	56.57 (185.59)	73.21 (240.20)	129.78 (425.79)
3 and 4	G1	248.87 (816.50)	19.20 (63.00)	30.25 (99.24)	39.01 (128.00)	36.84 (120.85)	N/A N/A	70.79 (232.24)	54.26 (178.02)	125.05 (410.26)
	G2	251.00 (823.50)	19.20 (63.00)	30.85 (101.23)	39.01 (128.00)	37.30 (122.39)	N/A N/A	71.39 (234.23)	54.73 (179.56)	126.12 (413.79)
	G3	253.14 (830.50)	19.20 (63.00)	31.46 (103.22)	39.01 (128.00)	37.77 (123.93)	N/A N/A	71.98 (236.17)	55.20 (181.09)	127.18 (417.26)
	G4	255.27 (837.50)	19.20 (63.00)	32.07 (105.21)	39.01 (128.00)	38.24 (125.46)	N/A N/A	72.61 (238.21)	55.67 (182.63)	128.27 (420.84)
	G5	257.40 (844.50)	19.20 (63.00)	32.67 (107.20)	39.01 (128.00)	38.71 (127.01)	N/A N/A	73.21 (240.20)	56.14 (184.17)	129.35 (424.37)
5 and 6	G1	248.87 (816.50)	14.63 (48.00)	27.11 (88.95)	34.75 (114.00)	38.10 (124.99)	14.63 (48.00)	61.86 (202.95)	67.36 (220.99)	129.22 (423.94)
	G2	251.00 (823.50)	14.63 (48.00)	27.65 (90.70)	34.75 (114.00)	38.68 (126.89)	14.63 (48.00)	62.39 (204.70)	67.94 (222.89)	130.33 (427.59)
	G3	253.14 (830.50)	14.63 (48.00)	28.18 (92.46)	34.75 (114.00)	39.25 (128.78)	14.63 (48.00)	62.93 (206.46)	68.51 (224.78)	131.44 (431.24)
	G4	255.27 (837.50)	14.63 (48.00)	28.72 (94.21)	34.75 (114.00)	39.83 (130.68)	14.63 (48.00)	63.46 (208.21)	69.09 (226.68)	132.55 (434.89)
	G5	257.40 (844.50)	14.63 (48.00)	29.25 (95.96)	35.00 (114.83)	40.41 (132.57)	14.63 (48.00)	64.00 (209.96)	69.67 (228.57)	133.66 (438.53)
7	G1	248.87 (816.50)	24.38 (80.00)	38.90 (127.63)	N/A N/A	N/A N/A	N/A N/A	63.29 (207.63)	N/A N/A	63.29 (207.63)
	G2	251.00 (823.50)	24.38 (80.00)	39.15 (128.46)	N/A N/A	N/A N/A	N/A N/A	63.54 (208.46)	N/A N/A	63.54 (208.46)
	G3	253.14 (830.50)	24.38 (80.00)	39.41 (129.30)	N/A N/A	N/A N/A	N/A N/A	63.79 (209.30)	N/A N/A	63.79 (209.30)
	G4	255.27 (837.50)	24.38 (80.00)	39.66 (130.13)	N/A N/A	N/A N/A	N/A N/A	64.05 (210.13)	N/A N/A	64.05 (210.13)
	G5	257.40 (844.50)	24.38 (80.00)	39.92 (130.96)	N/A N/A	N/A N/A	N/A N/A	64.30 (210.96)	N/A N/A	64.30 (210.96)



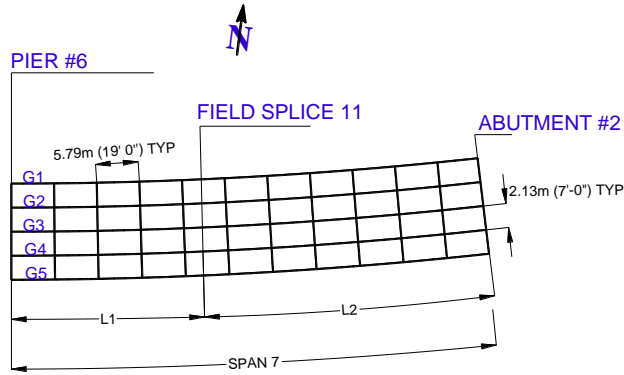
(a) Spans 1 and 2



(b) Spans 3 and 4

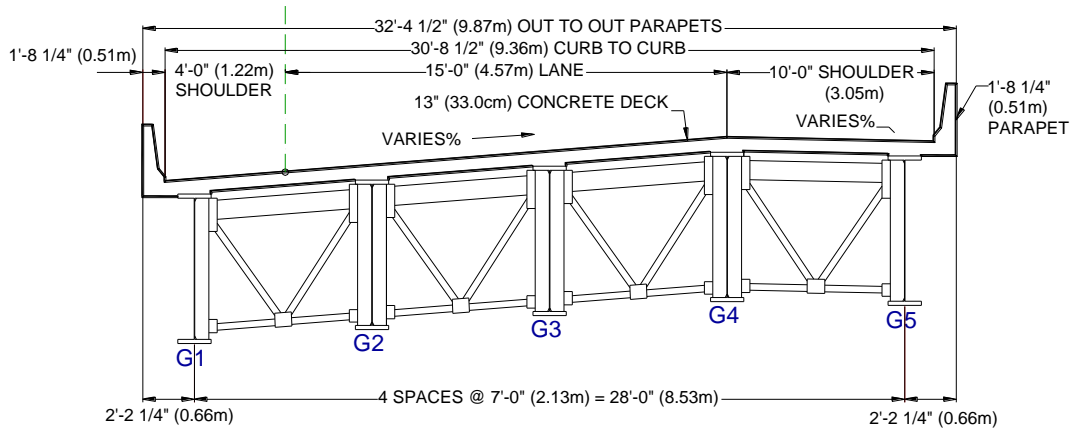


(c) Spans 5 and 6

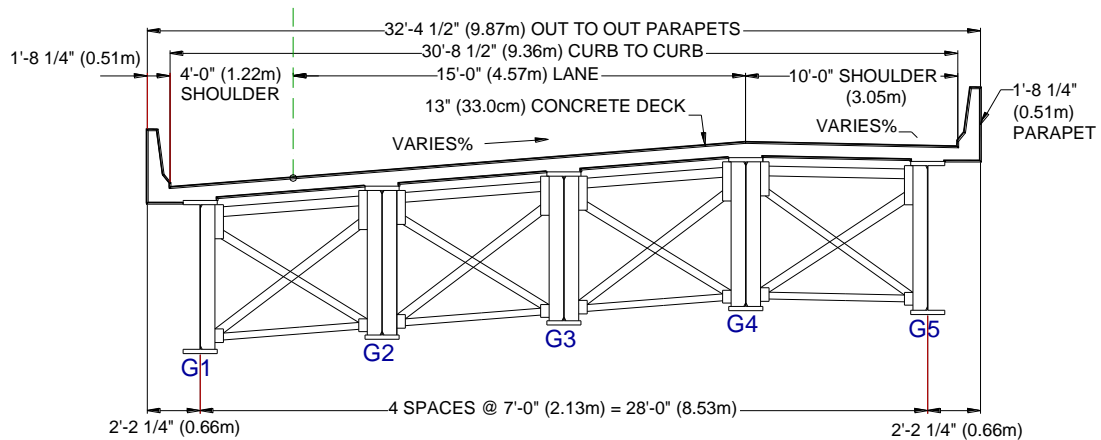


(d) Span 7

Figure 232. Plan Views, Missing Ramps Bridge.



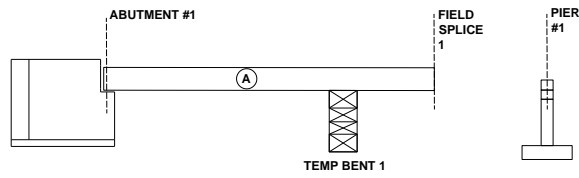
(a) End Section



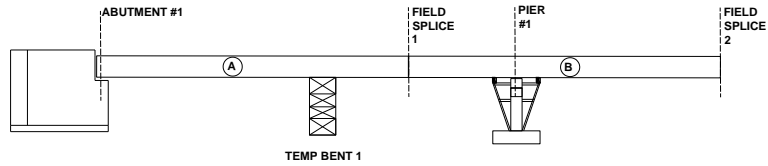
(b) Interior Section

Figure 233. Typical Cross-Sections, Missing Ramps Bridge.

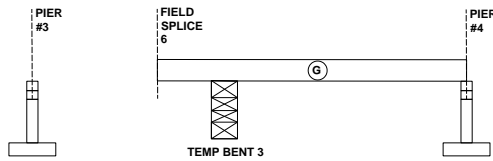
The Missing Ramps Bridge was constructed using a single girder erection procedure, working from either the exterior girder (G5) toward interior girder (G1) or from the interior girder toward the exterior girder, depending upon the location. A combination of cranes and temporary bents was used to lift and hold girder segments during the process. Due to the existence of an expansion joint over Pier 4, the girder erection sequence was separated into Units 1 and 2 as shown in Figure 234 and Figure 235, which re-create the planned sequence. The actual erection sequence initiated with Unit 2 and ended with Unit 1 with some modifications occurring during the initial stages of the Unit 2 erection. These modifications are detailed below.



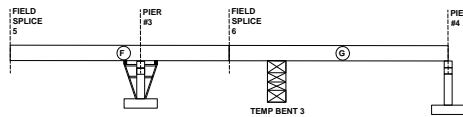
(a) Stage 1



(b) Stage 2



(c) Stage 3



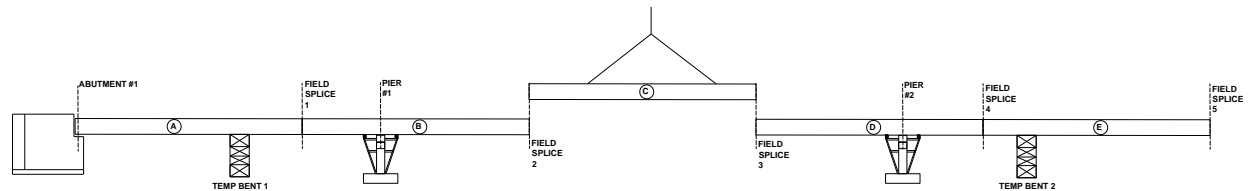
(d) Stage 4



(e) Stage 5



(e) Stage 6



(e) Stage 7

Figure 234. Unit 1, Girder Erection Details, Missing Ramps Bridge.

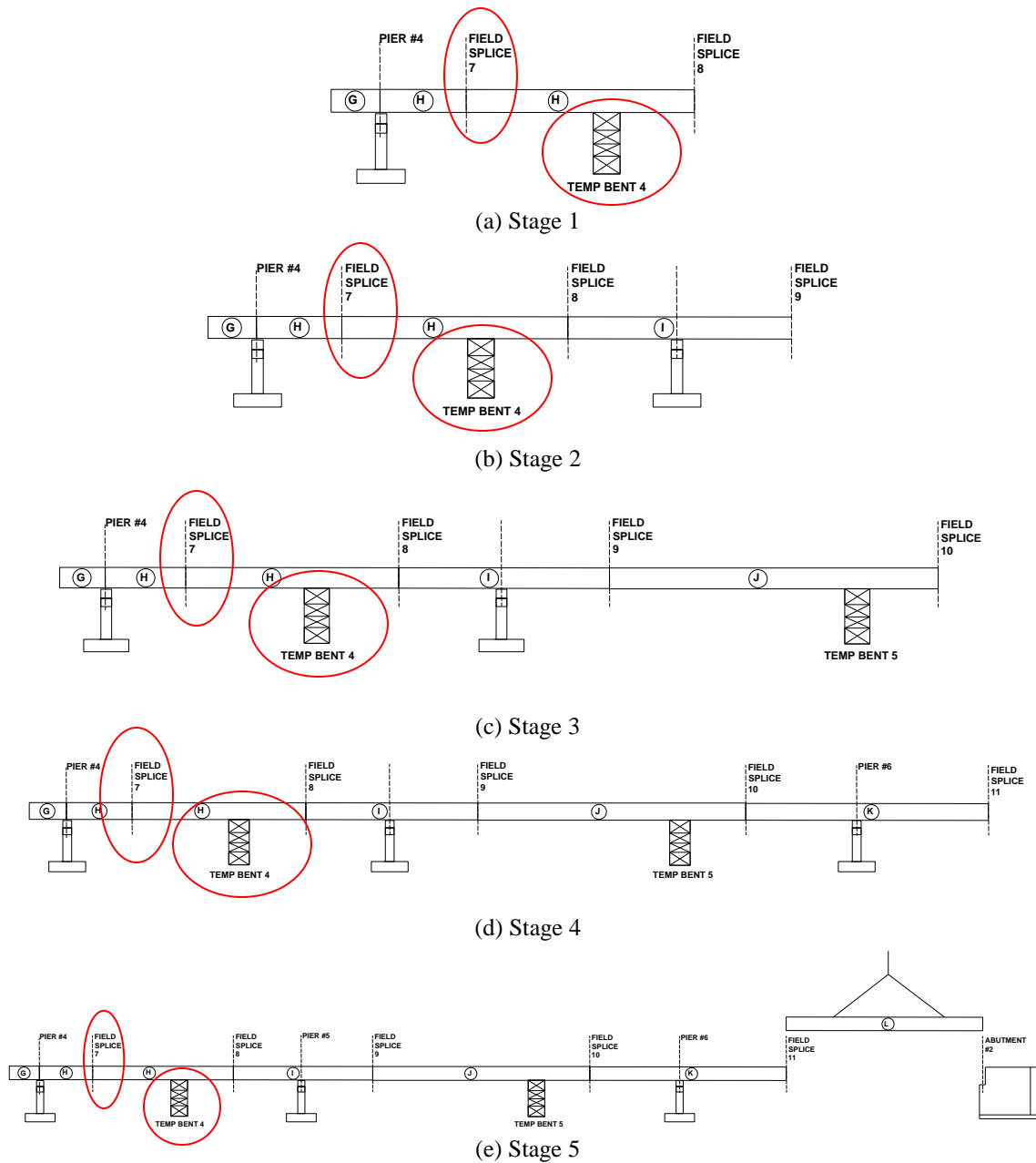


Figure 235. Unit 2, Girder Erection Details, Missing Ramps Bridge.

The girder erection schedule for Unit 1 involved 7 stages as shown in Figure 234. For Stage 1, Temporary Bent 1 was erected, and all bearings on Abutment 1 were configured. All bearings were blocked to prevent translation and movement in the longitudinal direction. Segment A was erected using an exterior girder (G5) toward interior girder (G1) procedure with cross-frames being fit between adjacent girders after they were erected. For Stage 2, all bearings on Pier 1 were configured, and an interior girder (G1) to exterior girder (G5) procedure was used, again with cross-frames fit between adjacent girders after their placement. For Stage 3, Temporary Bent 3 was erected, and bearings on Pier 4 were configured and blocked. Interior to exterior girder erection was used. For Stage 4, all bearings on Pier #3 were configured and an interior to exterior girder sequence was used. For Stage 5, Temporary Bent 2 was erected, and interior to exterior

girder erection was used. For Stage 6, bearings at Pier 2 were blocked, and interior to exterior erection was used. For Stage 7, the final Unit 1 stage, interior to exterior erection was used.

Unit 2 had five planned stages as shown in Figure 235. For Stage 1, the original planned procedure shown in the figure, which involved using a combination of cranes and Temporary Bent 4 to lift, position, and stabilize the girders, was replaced with a procedure that eliminated Bent 4 (circled in figure) and utilized cranes only. In addition, Field Splice 7 (circled in figure) was eliminated from those segments. All other erection tasks from the original plan, including configuring and blocking the Pier 4 bearings, erecting segments from exterior toward interior girder and fitting cross-frames between girders after they were in place, were followed. At the completion of Stage 1, it was decided to return to the original erection plan and utilize a combination of temporary shoring towers and cranes. Therefore, Stage 2 involved configuration and blocking of bearings at Pier #5 and interior to exterior girder erection as shown in Figure 235. For Stage 3, Temporary Bent 5 was built as originally planned, and girder segments were erected from interior toward exterior girder (G5). For Stage 4, bearings at Pier 6 were configured and blocked to prevent movement, and interior toward exterior girder erection was used. The final stage began with configuration and blocking of the Abutment 2 bearings and utilized interior to exterior girder erection.

In addition to cranes used to place the girders, a boom truck was used to install the cross-frames. Bolts were installed throughout the girder erection process but were not tightened until all girders and cross-frames were in place.

The deck placement sequence was also divided between Units 1 and 2. As shown in Figure 236, for Unit 1, deck in the positive moment regions (1 and 2) was placed first. To minimize deck cracking in the negative moment regions, region 3 over the piers was poured during the final stage. The approach is similar for Unit 2 shown in Figure 237, where deck in positive moment regions 4 and 5 was placed first followed by negative moment region 6 over the piers. A pump truck was used to deliver concrete to the bridge, and a finishing machine and work bridges were used to place and finish concrete to the desired elevation and cross-slope.

During girder erection, PennDOT personnel tracked girder web rotations at each cross-frame connection point. A number of measurements were taken, and each involved evaluating the amount of radial translation of the top of the girder web toward or away from the center of the curvature during girder erection. This information was used by Penn State personnel to assist with computer model validation as reported in the following sections.

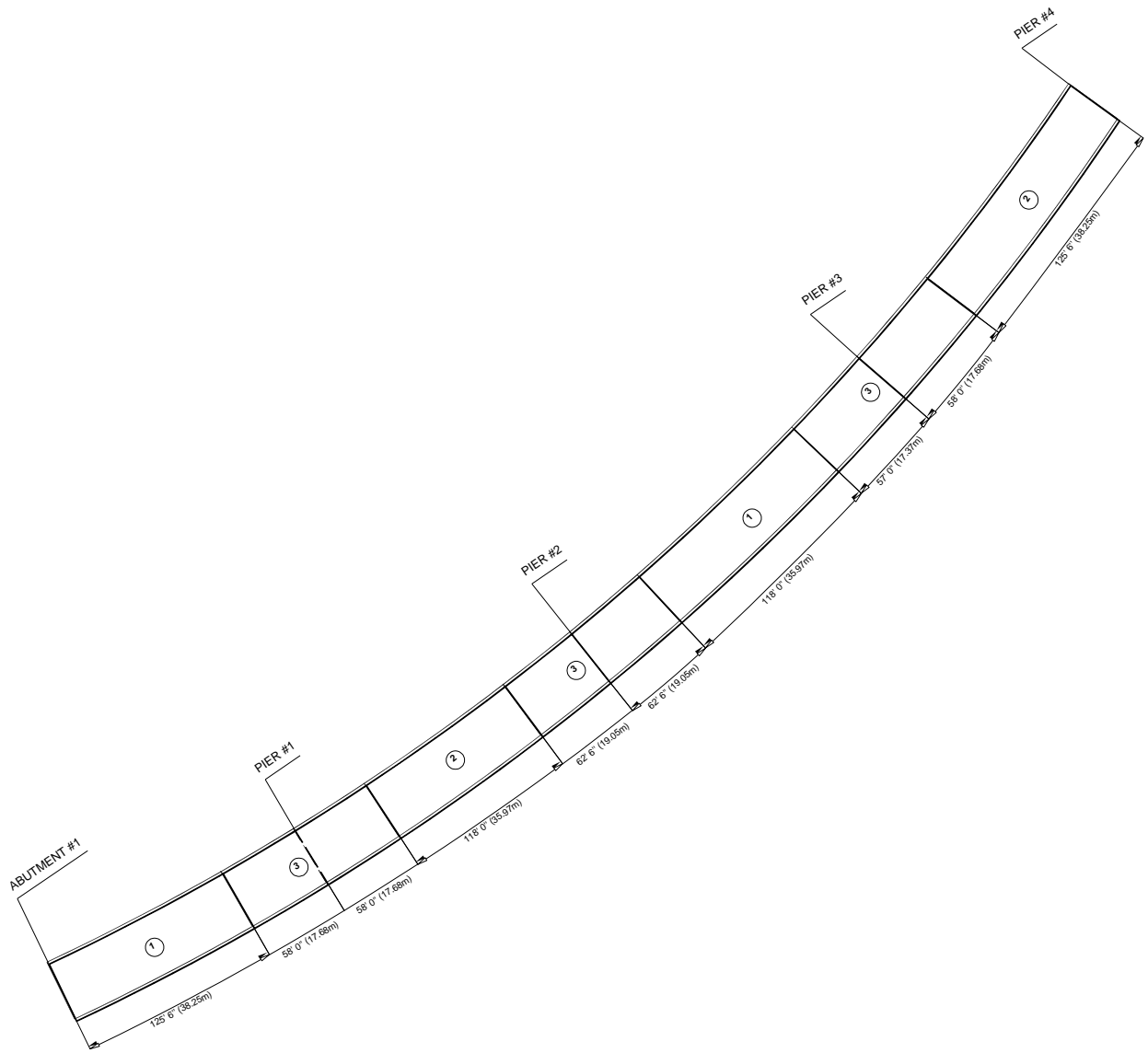


Figure 236. Unit 1 Deck Placement Sequence, Missing Ramps Bridge.

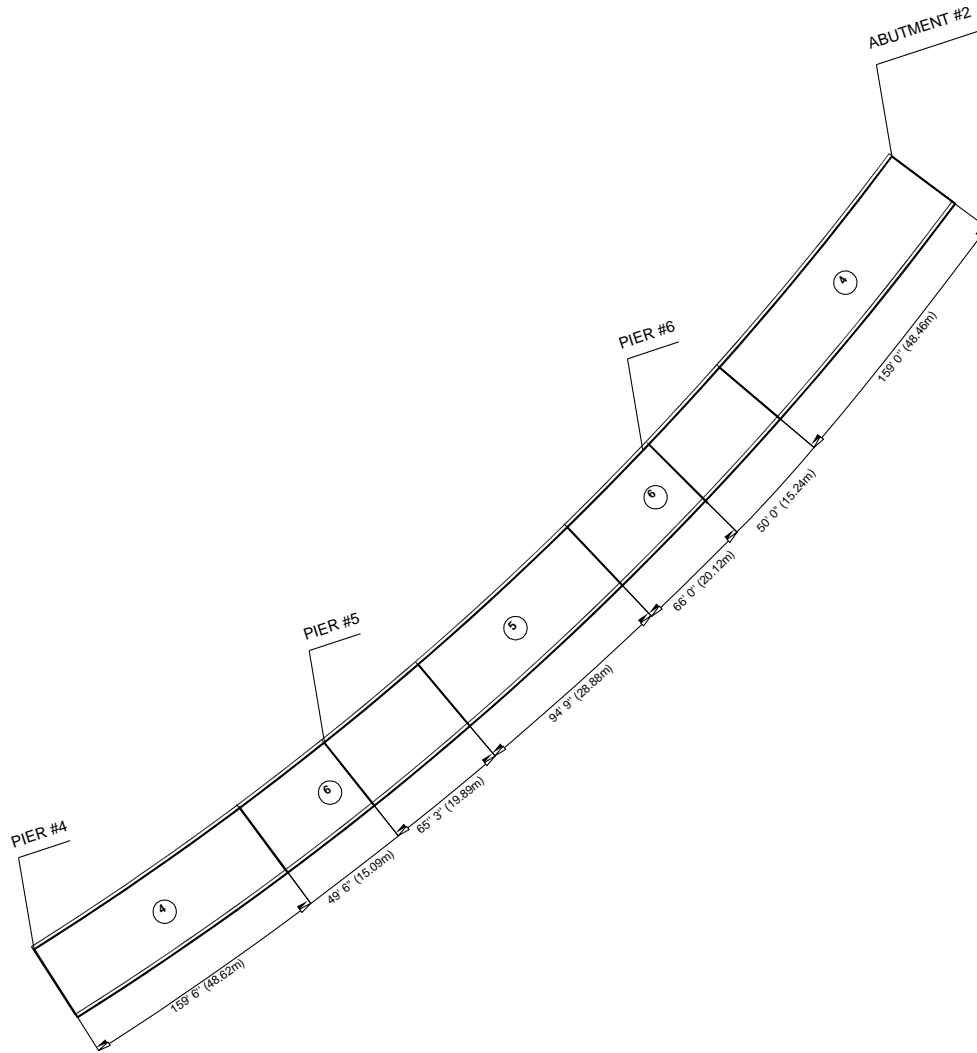


Figure 237. Unit 2 Deck Placement Sequence, Missing Ramps Bridge.

9.2.4 Structure #28

In similar fashion to Structure #7A, Structure #28 was used for some earlier model validation studies and, as such, is described in previous submittals to PennDOT (Linzell et al. 2003). A brief design, erection, and instrumentation summary is provided herein.

Structure #28 is a single-span composite steel-plate girder bridge located at an interchange between I-99 and Pennsylvania State Route 150. The bridge is 74.45 m (244 ft 3 in) in length with a skew of approximately 55 degrees. A total of seven girders are used to support the structure, with each girder being constructed using 17.5 mm by 2400 mm (11/16 in by 94 in) web plates and flange plates of varying dimensions. Girders are braced using “X” shaped cross-frames between the supports and “K” shaped cross-frames at the supports. Cross-frames are staggered near each abutment. The fascia girders (G1 and G7) and their adjacent interior girders (G2 and G6) are supported by non-guided expansion bearings at the abutments. Remaining girders utilize guided expansion bearings at the west abutment and fixed bearings at the east abutment. Additional details on structure dimensions can be found in previous PennDOT submittals (Linzell et al. 2003).

Girders were erected with web plates out of plumb at the abutments and at midspan. Girders were fabricated in the plumb position, and the cross-frames were used to force the webs out of plumb by an amount equal and opposite to the anticipated rotation after placement of the deck.

Concrete deck placement began at the east abutment and proceeded perpendicular to the centerline of the bridge using two screeds that were staggered to attempt to place wet concrete parallel to the skew. Screenshot rails were attached to G1, G4, and G7. More details on the erection and deck placement schemes can be found in previous PennDOT submittals (Linzell et al. 2003).

Structure #28 was monitored by Penn State personnel during the deck pour, which occurred overnight. Longitudinal strains and girder displacements were measured using strain transducers and linear variable differential transformers (LVDTs). Strain transducers attempted to measure strains in girder flanges and in individual cross-frame members at select locations and the LVDTs measuring lateral displacements of the girder webs at the abutments. Global geometric data were also collected from traditional surveys performed before and after the deck placement process and using a three-dimensional laser scanner system. Additional details on the instrumentation can be found in previous submittals to PennDOT (Linzell et al. 2003).

9.3 Modeling Techniques

This section details modeling techniques selected for the study. Included in this discussion are summaries of examined model construction approaches, including discretization levels, constitutive models, and support conditions, along with a discussion of analysis techniques. If applicable, references are provided to previous PennDOT submittals containing relevant information.

9.3.1 Model Construction

The types of models examined included variations of grillage (two-dimensional) finite element analysis approaches and variations of three-dimensional approaches that included a mix of line, shell, and solid elements. For certain model types, detailed discussion of their characteristics are provided in previous submittals to PennDOT, and, therefore, only brief summaries are provided herein.

9.3.1.1 Grillage (2D)

Grillage models used for predicting construction response were developed in SAP2000 in association with earlier model validation studies and, as such, are largely described in previous submittals to PennDOT (Linzell et al. 2006). Therefore, a brief summary is provided herein.

For these models, the steel superstructure was modeled as a true grillage; however, in an attempt to more accurately represent deck load distribution onto the steel superstructure, when the concrete deck was being placed, it was modeled using shell elements. As a result, the final model could not be called a true grillage as classically defined but was referred to as a “modified” grillage model. Composite action was simulated for stages that required it using rigid links. Design support conditions at the pier and abutments were idealized, and a self-weight function was used to apply all dead loads.

Nodes were placed at all cross-frame and flange transitions along the girder lines. Girders were modeled as straight frame members between these nodes, following common grillage modeling practice. All flange and web transitions were considered, as well as radial and tangential elevation changes. Intermediate stiffeners were not considered by the grillage model. K-shaped cross-frames were modeled as straight frame members and assigned equivalent stiffness values, again, following common grillage modeling practice. Geometric properties required for a typical cross-frame member were established by modeling a typical cross-frame and included strong and weak axis moments of inertia, vertical and horizontal shear areas, torsional constants, and an equivalent area for self-weight calculations. Material response was assumed to be elastic.

9.3.1.2 Full Shell (3D)

Full shell three-dimensional models used for predicting construction response were also developed in ABAQUS in association with earlier model validation studies and, as such, are largely described in previous submittals to PennDOT (Linzell et al. 2006). Therefore, a brief summary is provided herein.

ABAQUS S4R elements were used to model the flanges and webs of all girders with webs shells distributed in a fashion that maintained an element aspect ratio close to 1:1. Flange nodes corresponded to web nodes along the length of the girders. Flange element aspect ratios did not exceed 2:1. Radial cross-frame members between adjacent girders were assumed rigidly connected to the girder webs and were modeled using B31OS beam elements, with the diagonals and the top and bottom chords being modeled as separate members for each cross-frame. Girder web stiffeners were modeled using ABAQUS B31 beam elements. The slab was modeled using S4R shell elements, with slab elements having an aspect ratio of 2:1. All components of the model were assigned nominal material and geometric properties. Boundary conditions were input to match what was observed from the design plans, depending on the structure, during erection. Composite action was maintained for appropriate stages using rigid links. Loads consisted of bridge component dead loads.

9.3.1.3 Shell and Beam (3D)

Based on report results from earlier studies (discussed in the following sections) and published literature (Chavel and Earls 2006a, 2006b; Kim et al. 2005), the full shell three-dimensional models were modified slightly to reduce analysis time and provide an additional analysis approach that could be examined. A summary of these models, largely focusing on the modifications instituted when compared to the full shell models, is provided herein.

Girder webs were still modeled using ABAQUS S4R shell elements with webs shells distributed in a fashion that maintained a 1:1 element aspect ratio. Flange shell elements were replaced with ABAQUS B31 beam elements with flange nodes corresponding web nodes. The B31 beam element has 6 degrees of freedom and allows for transverse shear deformation. It can accurately model both vertical and lateral bending effects in the flanges. ABAQUS calculates stress values at 25 integration points within the B31 elements. Figure 238 shows the locations of the 25 integration points within a typical flange cross-section. Flanges were not offset from the girder web initially because of the large depth of the web 2743 mm (108 in) compared to the small average flange offset distance of 60 mm (2.3 in). The effect of this decision was examined and is discussed in the following sections. The stress values at the tips of the flanges can be used to calculate both the vertical and lateral bending of the flanges. Radial cross-frame members between adjacent girders and web stiffeners were still modeled using B31OS elements. The slab was still modeled using S4R shell elements with an aspect ratio of 2:1. Nominal material and geometric properties were again used, and boundary conditions matched design plans or observed erection conditions. Composite action was again maintained using rigid links. Loads again consisted of component dead loads. A typical cross-section with modeling details is shown in Figure 239.

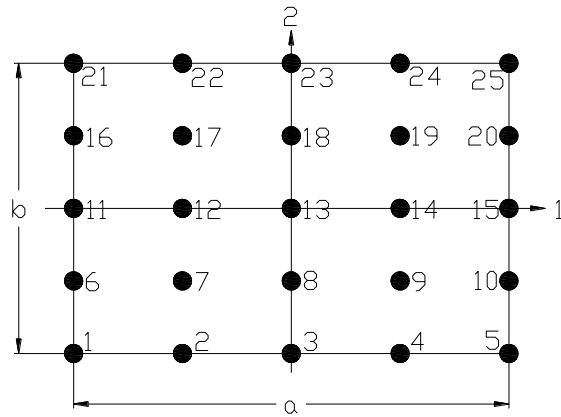
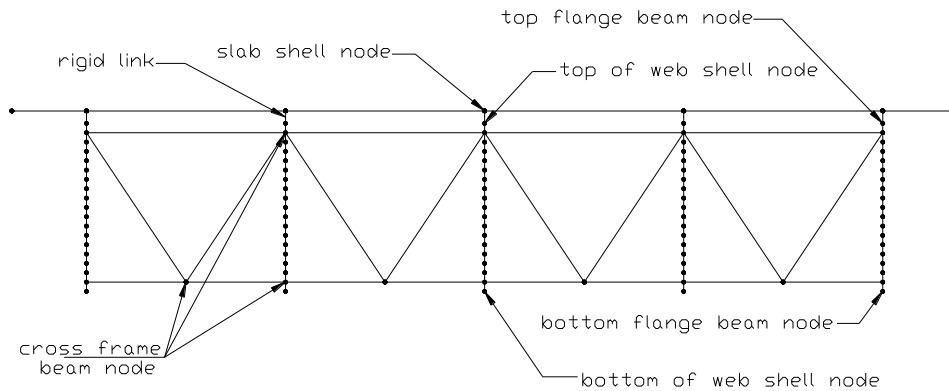


Figure 238. Representative B31 Flange Element.



Note: Stiffener beam nodes correspond to web shell node locations

Figure 239. Typical Cross-Section, Shell and Beam Model Construction.

9.3.1.4 Frame, Shell, Brick (3D)

Three-dimensional models containing a combination of frame, shell and brick elements and used for predicting construction response were also developed in ABAQUS in association with earlier model validation studies. Therefore, these models are largely described in previous submittals to PennDOT (Linzell et al. 2006), and a brief summary of these models, largely focusing on the modifications when compared to the full shell models, is provided herein.

Girder webs were, again, still modeled using ABAQUS S4R shell elements. Flanges were modeled using B31 elements with cross-frame members between adjacent girders and web stiffeners modeled using B31OS elements. The slab was modeled using ABAQUS C3D8R brick elements, which are eight-noded, reduced integration, linear brick elements. Composite action was maintained using rigid links. Nominal material and geometric properties were used with boundary conditions matching design plans or observed conditions. Loads consisted of component dead loads.

9.3.2 Analysis Techniques

As discussed in a previous submittal to PennDOT (Linzell et al. 2006), irrespective of the software used to complete the analysis and the type of model being examined, analyses proceeded using a number of stages

that applied the dead load of the structure in sequential steps based on the construction procedure. During each stage, elements corresponding to the components that were added or placed for that stage were added to the model's deformed shape, and the next analysis step was performed. All relevant information was retained from each stage and used as initial conditions for the next construction step.

9.4 Comparisons and Modifications

Previous submittals to PennDOT (Linzell et al. 2006) included comparisons between field data recorded during construction of Structure #207 and results from the (1) grillage, (2) full shell, and (3) frame, shell, and brick models. The reported information focused on stress change predictions during the construction process for this structure and, based upon these comparisons, were largely inconclusive regarding a preferred modeling technique. All models were shown to effectively predict trends recorded during construction, but accuracy varied for predicting stress changes at known locations for specific construction events. Prediction accuracy improved for events that occurred after slab placement was initiated, but, again, no definitive conclusions could be made regarding a preferred modeling scheme. Since no definitive conclusions were obtained from these studies, additional comparisons and modifications were completed to obtain clearer information regarding selecting a preferred analysis approach and software package for future tasks.

9.4.1 Comparisons – Structure #207

Primary comparisons were performed between the field data recorded during construction of Structure #207, the grillage model, and the shell and beam model. The shell and beam model was selected for comparison since it offered similar levels of accuracy to the other 3D models and improved computational efficiency.

Comparisons were completed for the construction stages listed in Table 36. Figure 240 shows a representative erection drawing for an early stage of construction. For the shell and beam model, the ABAQUS MODEL CHANGE command was used to assign zero stiffness to the elements that were not present during certain stages of construction. For example, for the first stage of the analysis, only the elements corresponding to Girders 4 and 5 from Abutment 1 to Field Splice 3 (black lines Figure 240) were capable of carrying load. The remaining elements in the model (gray lines in Figure 240) were assigned a zero stiffness value so that they did not influence sequential analysis results. The shell and beam model was initially run assuming small strain and small deformation response to establish a baseline of its performance.

Table 36. Structure #207 Examined Construction Stages.

Stage Number	Section Placed During Stage*
Stage 1	Girders 4 and 5 Abutment 1 to Field Splice 3
Stage 2	Girder 3 Abutment 1 to Field Splice 3
Stage 4	Girders 1 and 2 Abutment 1 to Field Splice 3
Stage 5	Girders 4 and 5 Field Splice 3 to Abutment 2
Stage 6	Girder 3 Field Splice 3 to Abutment 2
Stage 8	Girders 1 and 2 Field Splice 3 to Abutment 2
Stage 10	First Portion of Slab
Stage 11	Second Portion of Slab
Stage 12	Third and Final Portion of Slab

*Includes all relevant cross-frames and abutments

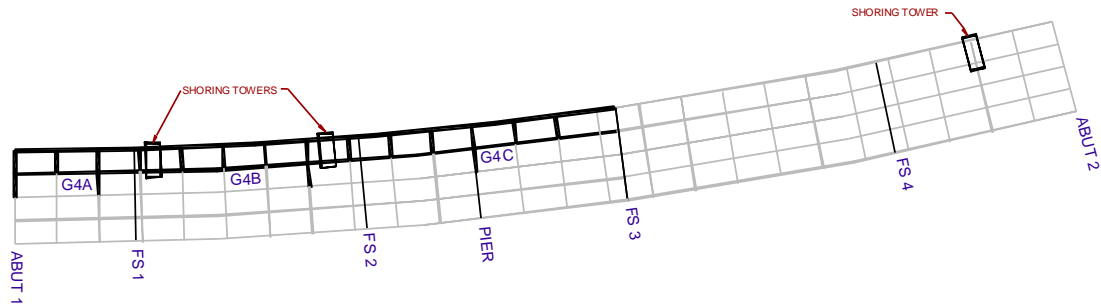


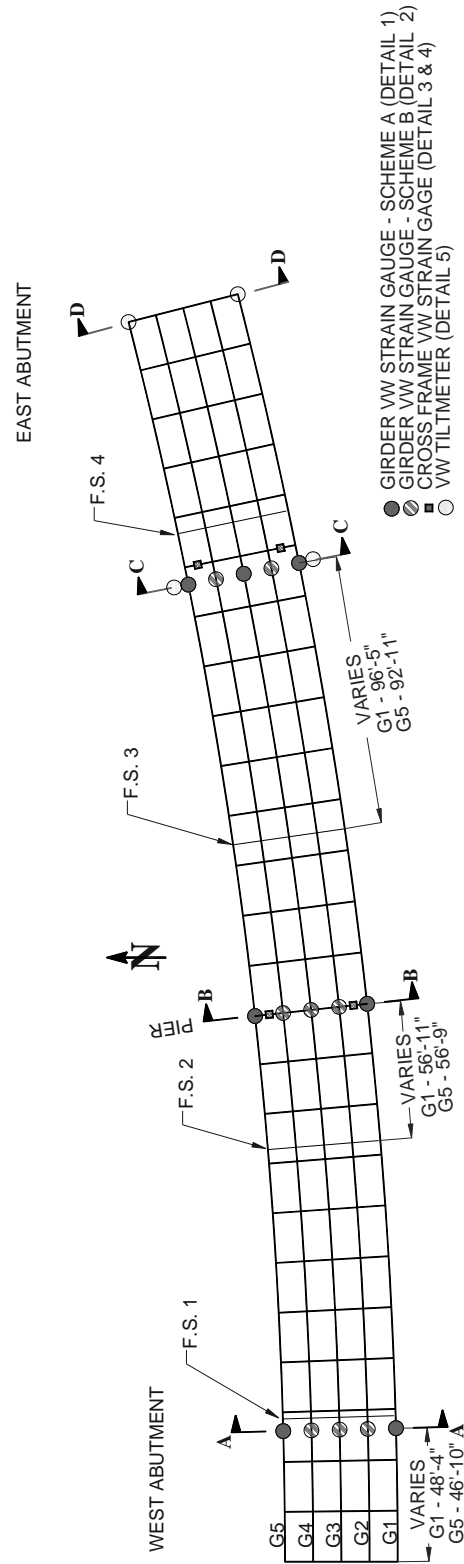
Figure 240. Structure #207 Construction Stage.

To establish a more definitive assessment of model accuracy when compared to field data comparisons during placement of the steel superstructure, examination of vertical and lateral bending moment distribution at locations corresponding to instrumented sections on Structure #207 was done. Examining moment distribution at select sections provides a more realistic picture of model accuracy for the entire structure at the completion of construction events when compared to comparison of single stress values at specific locations. During placement of the concrete deck, however, stresses at specific instrument locations had to again be examined because a number of girder top flange gauges on Structure #207 were damaged during the deck pour. In addition to the moment distribution and stress comparisons, vertical deformations predicted by the models were compared to those measured in the field.

9.4.1.1 Vertical Bending Moment Distribution – Superstructure Erection

Vertical bending moment distribution values from the computer models were calculated by summing all the girder vertical bending moments across a cross-section of the structure and then dividing each individual girder vertical bending moment value by the sum. A similar approach was used for the field data except that data started with strains at specific points rather than stresses. Methods for establishing moments for the computer and field data were outlined in previous submittals to PennDOT (Linzell et al. 2003; Linzell et al. 2006).

Representative vertical bending moment distribution plots will be presented and discussed herein. Results refer to stage numbers from Table 36, and sections refer to Figure 241. Representative calculations are provided in Appendix A.



BRIDGE S-207 - INSTRUMENT LOCATION PLAN

Figure 241. Structure #207 Instrumented Sections.

Figure 242 shows the vertical bending moment distribution results for Stage 6 Section B-B. Results for Girders 2 and 3 are not presented during this stage of construction because one or more of the instruments located on the Girder 2 and 3 flanges were malfunctioning during field testing. The figure shows that the ABAQUS three-dimensional model over-predicts the vertical bending moment distribution to Girders 1 and 5 when compared to field test results. The figure also shows that the ABAQUS three-dimensional finite element model predicts a smaller vertical bending moment distribution value for Girder 4 when compared to the field results. Figure 242 shows that the SAP2000 grillage model over-predicts the vertical bending moment distribution observed in the field for Girder 1 and under-predicts the vertical bending moment distribution observed in the field for Girders 4 and 5.

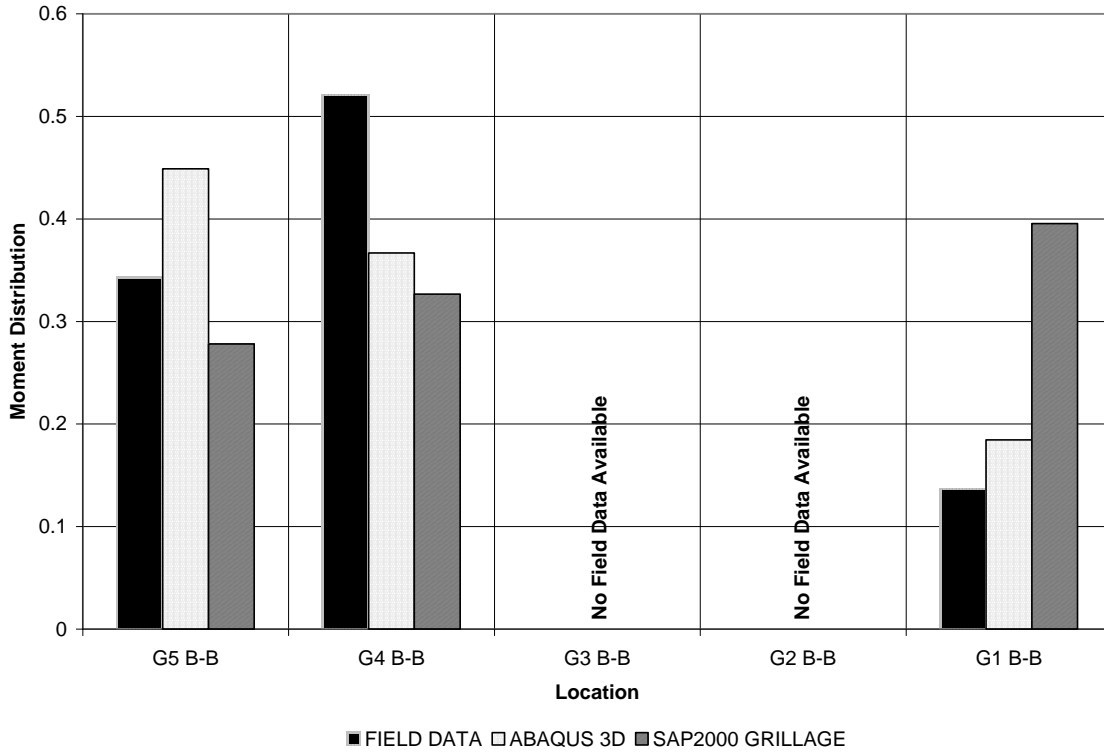


Figure 242. Stage 6 Vertical Bending Moment Distribution for Section B-B, Structure #207.

Figure 243 shows the vertical bending moment distribution comparisons for Stage 8b. Stage 8b represents the point in time when the entire steel superstructure had been erected and all the bolts had been tightened. The figure shows that the ABAQUS three-dimensional finite element model predicts a vertical bending moment distribution that is very similar to results obtained from the field. The SAP2000 grillage model did not predict vertical bending moment distribution as accurately.

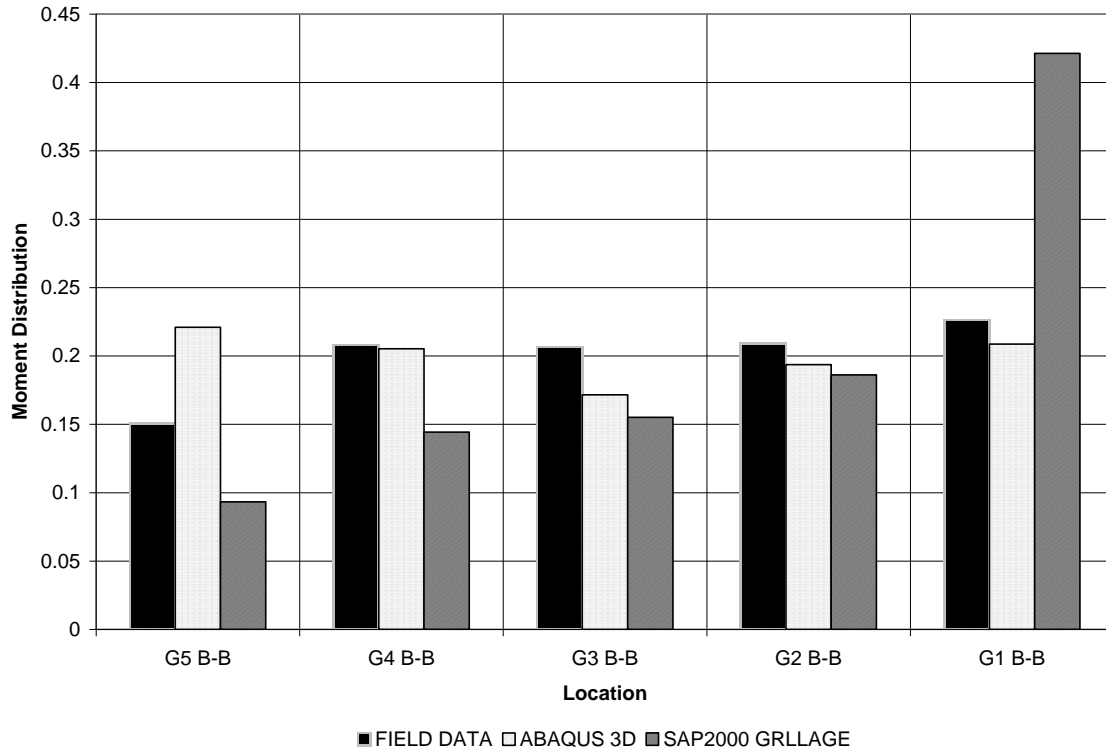


Figure 243. Stage 8b Vertical Bending Moment Distribution for Section B-B, Structure #207.

Figure 244 shows the vertical bending moment distribution results for Stage 5 Section C-C. Results are not presented for Girders 1, 2, and 3 because these sections are not in place during this stage of construction. It shows that the SAP2000 grillage model predicts the vertical bending moment distribution field behavior slightly better than the ABAQUS three-dimensional finite element model.

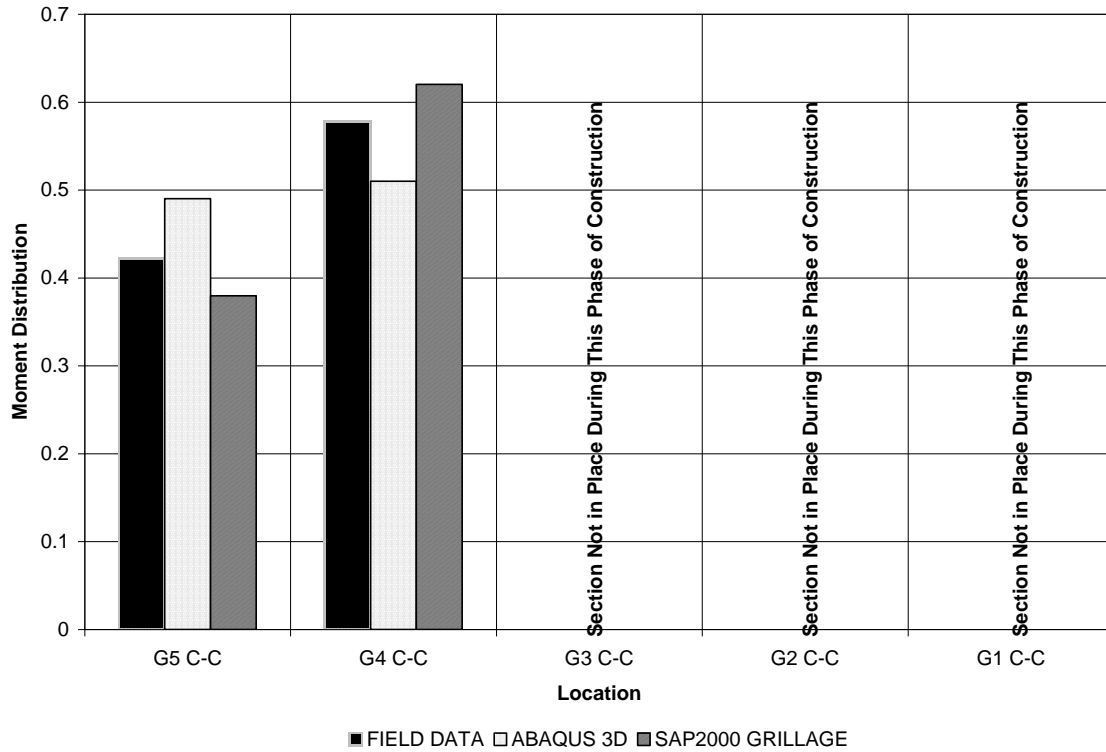


Figure 244. Stage 5 Vertical Bending Moment Distribution for Section C-C, Structure #207.

Figure 245 shows the vertical bending moment distribution results for Stage 6 Section C-C. Results are not presented for Girders 1 and 2 because these sections are not in place during this stage of construction. The ABAQUS three-dimensional finite element model over-predicts the vertical bending moment distribution values for Girders 4 and 5 when compared to the field test values and predicts smaller vertical bending moment distribution values for Girder 3 when compared to the field test results. The figure shows that the SAP2000 grillage model predicts a similar vertical bending moment distribution value for Girder 5 when compared to the field test results but that it over-predicts the vertical bending moment distribution value for Girder 4 and under-predicts the model vertical bending moment distribution value for Girder 3.

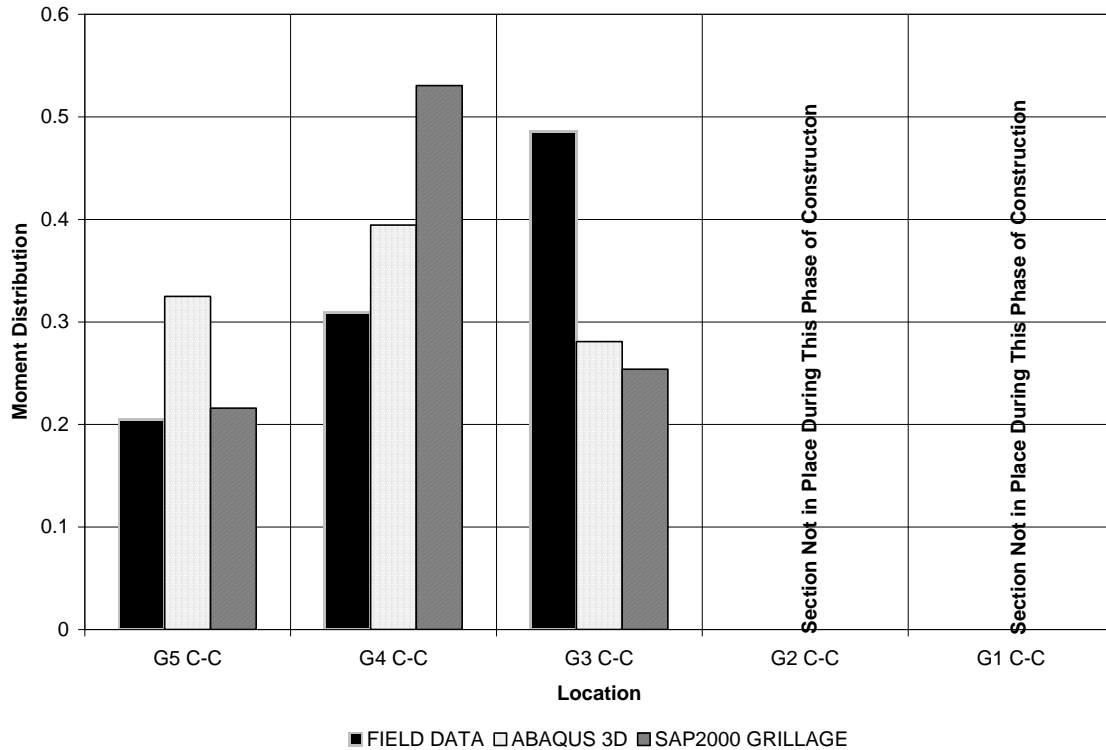


Figure 245. Stage 6 Vertical Bending Moment Distribution for Section C-C, Structure #207.

Figure 246 shows that neither the ABAQUS three-dimensional finite element model nor the SAP2000 grillage model predicts the vertical bending moment distribution values observed in the field for Stage 8b Section C-C. However, the ABAQUS three-dimensional finite element model predicts the general vertical bending moment distribution behavior observed in the field throughout the entire cross-section more accurately than the SAP2000 model.

The vertical bending moment distribution comparisons between the field data, the ABAQUS three-dimensional finite element model, and the SAP2000 grillage model provide conclusive evidence that the ABAQUS three-dimensional finite element model is more accurate than the SAP2000 grillage model in predicting the field vertical bending moment distribution behavior of the steel superstructure during erection.

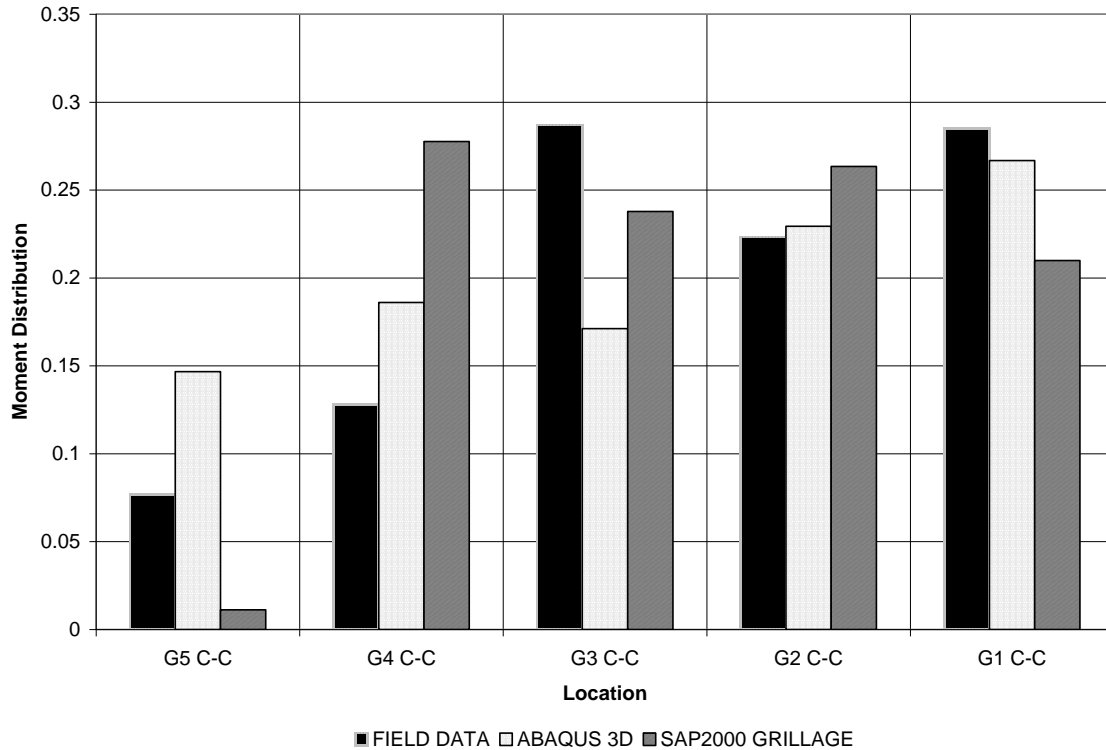


Figure 246. Stage 8b Vertical Bending Moment Distribution for Section C-C, Structure #207.

When the vertical bending moment distribution comparisons are examined to ascertain a preferred modeling method, the results can be interpreted as mixed. However, they do show an improvement for the ABAQUS 3D model when compared to the SAP2000 grillage model for predicting general distribution trends.

9.4.1.2 Lateral Bending Moment Distribution – Superstructure Erection

Lateral bending moment distributions were calculated using the same procedure that was followed for the vertical bending moment distribution calculations. Representative lateral bending moment distribution plots will be presented and discussed herein. Results refer to stage numbers from Table 36, and sections refer to Figure 241. Representative calculations are provided in Appendix A.

Figure 247 shows the lateral bending moment distribution for Stage 8b. The figure shows that neither the ABAQUS three-dimensional finite element nor the SAP2000 grillage model predicts the field lateral bending moment distribution for Section B-B well. The ABAQUS three-dimensional finite element model predicts similar lateral bending distribution values for Girders 1 and 4 but predicts significantly different values for G3 and G5. The figure also shows that the SAP2000 model predicts significantly different lateral moment distribution values for Girder 1, 3, 4, and 5 when compared to the field data.

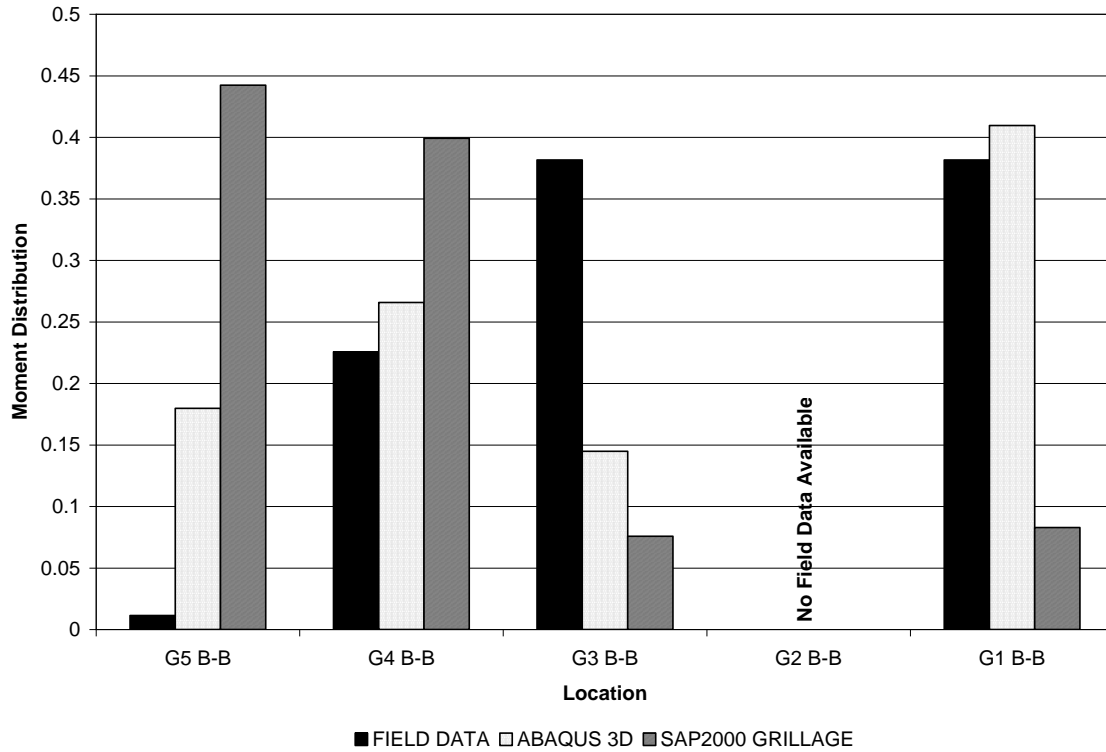


Figure 247. Stage 8b Lateral Bending Moment Distribution for Section B-B, Structure #207.

Figure 248 shows the lateral bending moment distribution results for Section C-C during Stage 8b of construction. The figure shows that the ABAQUS three-dimensional finite element model and the SAP2000 grillage model again do not predict the field lateral bending moment distribution accurately. There appears to be no pattern for discrepancies between the field lateral bending moment distribution values and those from the ABAQUS and the SAP2000 models.

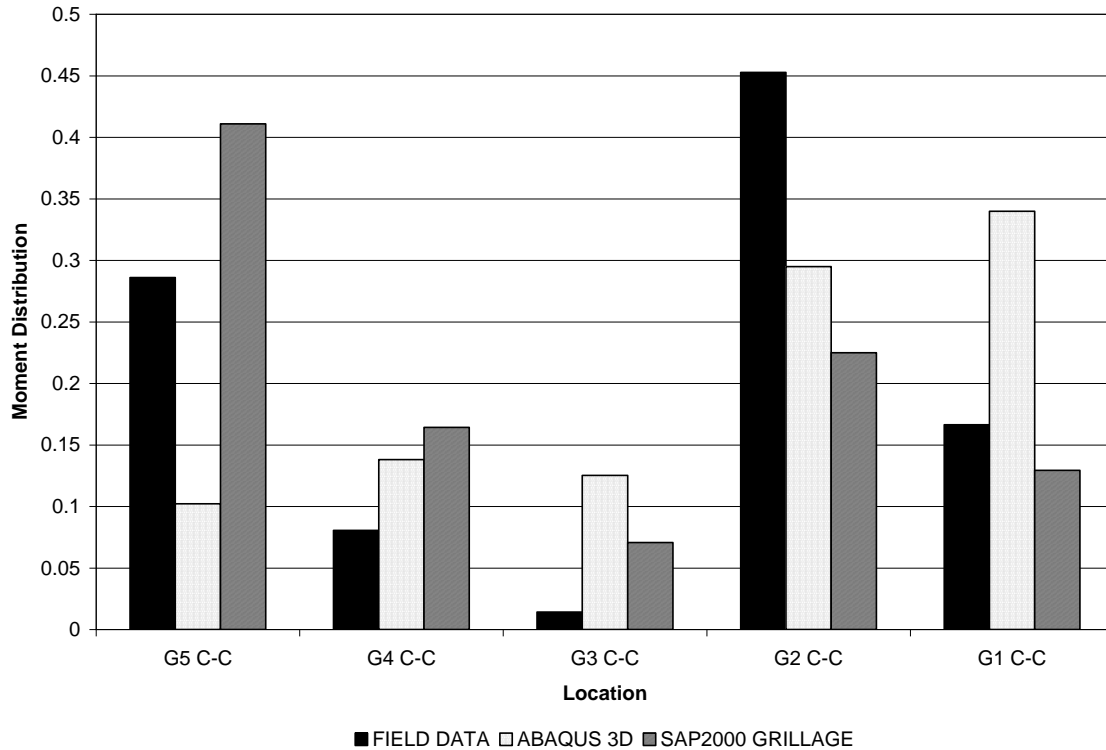


Figure 248. Stage 8b Lateral Bending Moment Distribution for Section C-C, Structure #207.

The figures above are representative plots of lateral bending moment distribution comparisons for the other stages of construction. These comparisons do not clearly identify which model more effectively predicts measured lateral bending moment behavior; in fact, neither the ABAQUS model nor the SAP2000 model effectively predicted lateral bending moment distributions observed in the field. However, it should be emphasized that lateral bending stresses for most construction stages were small compared to vertical bending stresses for those stages, and, as such, ineffective prediction of individual lateral bending stresses or the distribution of lateral bending stresses at a bridge cross-section cannot be construed as conclusive evidence that a modeling approach is ineffective.

9.4.1.3 Vertical Bending Stresses – Deck Pour

As stated earlier, comparisons during the deck pour had to be made by examining stress measurements at individual points because during the field test, a majority of the top flange strain gauges were damaged during the placement of the deck pans. Figure 249 shows the sequence of the deck placement used during construction. Stress comparisons will be presented for Deck Pour 1 (Stage 10), Deck Pour 2 (Stage 11), and Deck Pour 3 (Stage 12). Representative calculations are provided in Appendix A.

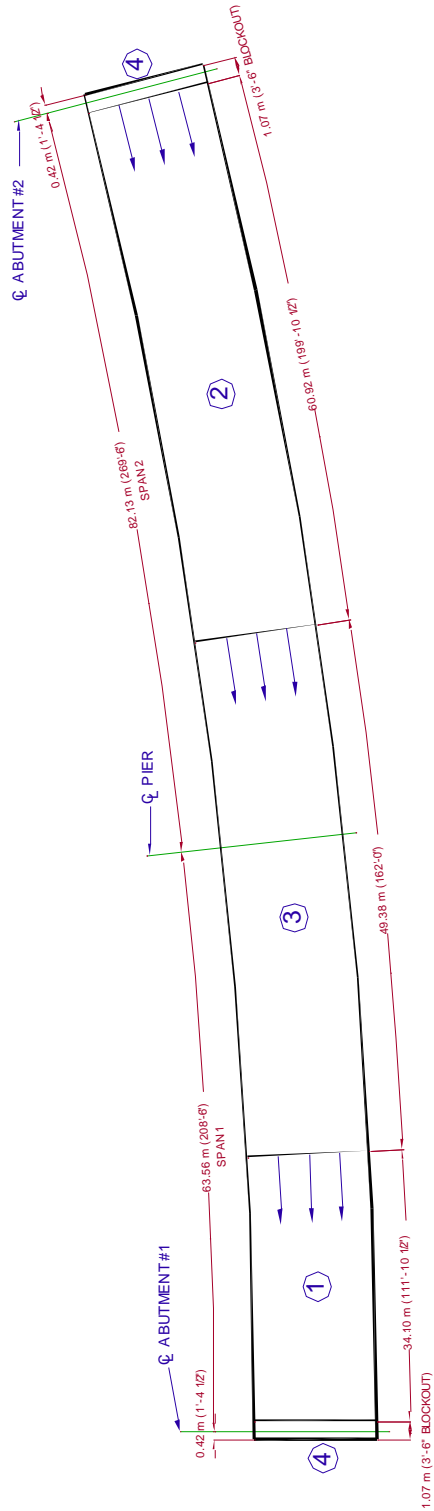


Figure 249. Deck Placement Sequence, Structure #207.

Figure 250 shows stress comparisons for Girder 1 bottom flange Section A-A. It shows that the ABAQUS three-dimensional model predicts smaller stress values than those observed in the field for all three stages

of the deck placement. The SAP2000 grillage model also under-predicts the stress values observed in the field for Girder 1 Section A-A for all three stages of deck placement.

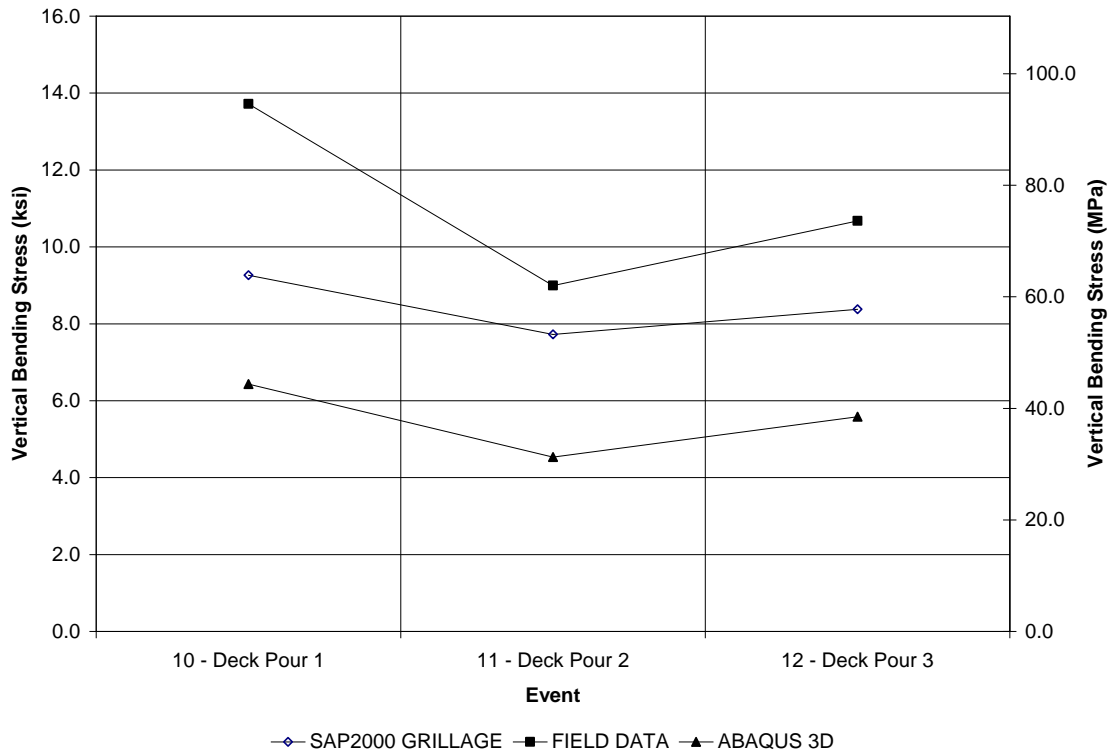


Figure 250. Stress Comparisons for Girder 1 Bottom Flange Section A-A, Structure #207.

Figure 251 shows stress comparisons for the bottom flange of Girder 1 Section B-B during placement of the concrete deck. It shows that the ABAQUS three-dimensional finite element model predicts stress very similar to those observed in the field for Girder 1, and it also shows that the SAP2000 model predicts larger stress values than those observed in the field for Girder 1 Section B-B.

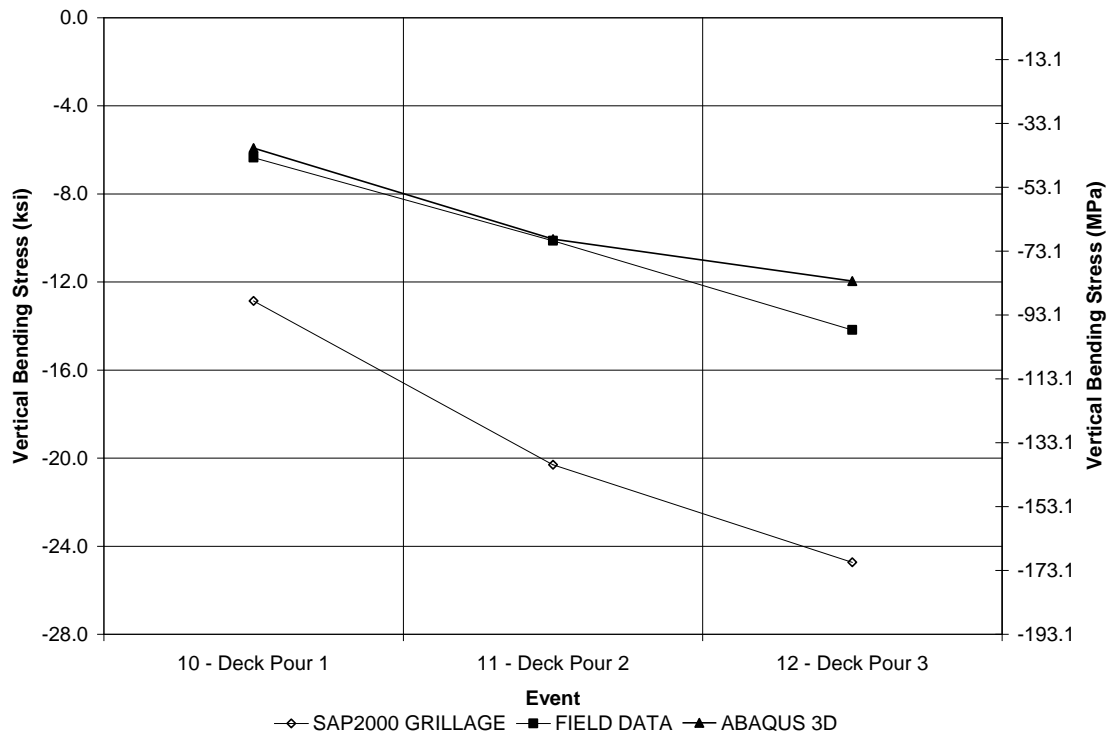


Figure 251. Stress Comparisons for Girder 1 Bottom Flange Section B-B, Structure #207.

Figure 252 shows stress comparisons for the top flange of Girder 3 Section B-B. It shows that the ABAQUS three-dimensional finite element model predicts stress values smaller than those observed in the field for the top flange of Girder 3 Section B-B, and the SAP2000 grillage model also predicts stress values smaller than those observed in the field for the top flange of Girder 3 Section B-B.

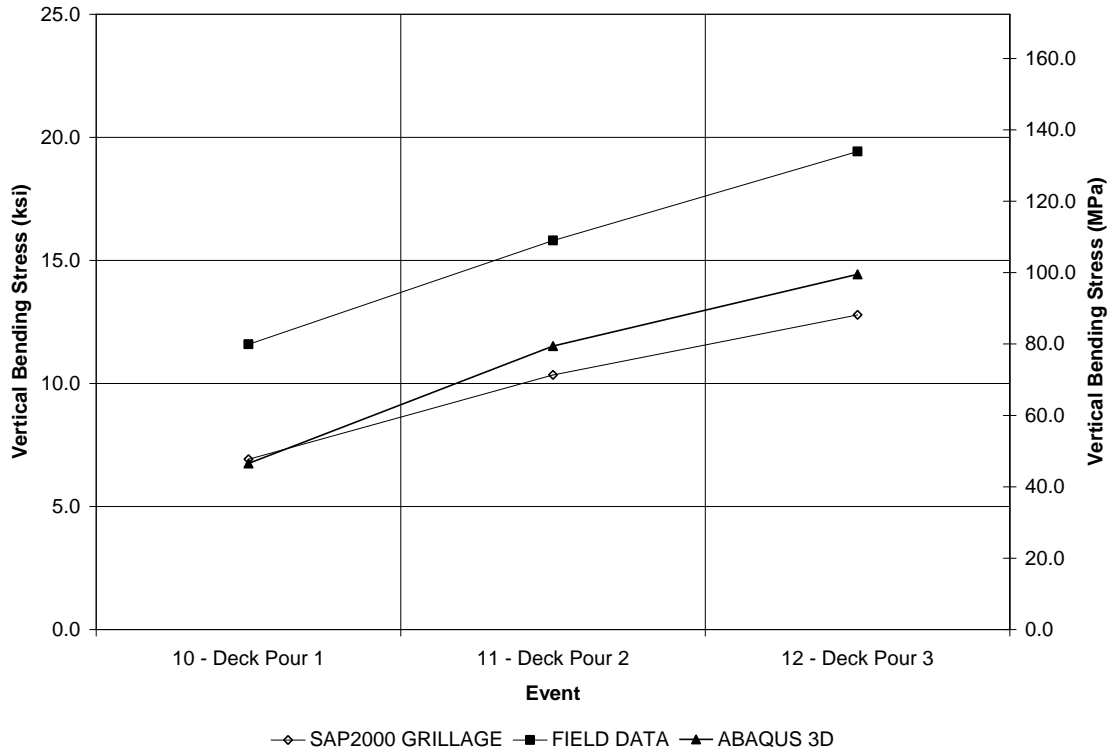


Figure 252. Stress Comparisons for Girder 3 Top Flange Section B-B, Structure #207.

The previously discussed figures show that for certain girder locations, both the ABAQUS three-dimensional finite element model and the SAP2000 grillage model accurately predict stress values observed in the field. However, for other locations, the predictions are not as accurate. These mixed results match those for earlier comparisons involving stress values at a single point and, as discussed earlier, cannot be construed as definitive information that can be used to select or reject one modeling approach over another. Since no conclusive evidence is provided using these comparisons, similar to what was found with earlier single-point stress comparisons, another global performance measure, such as structure deformations or moment distribution at a given cross-section as presented earlier, would be needed to assist with making a definitive model selection decision. Vertical deflections were selected as the global parameter to examine since extensive field data were available for the entire structure using a combination of tiltmeters and laser measurements. The next section contains deflection comparisons between the ABAQUS three-dimensional finite element model, the SAP2000 grillage model, and the field data.

9.4.1.4 Vertical Deflections – Deck Pour

This section contains deflection comparisons between the ABAQUS three-dimensional finite element model, the field data, and the SAP2000 grillage model. Deflection data obtained from the field test encompassed changes in deformations for all girders between erection of the entire steel superstructure and placement of the slab. Values from the computer models were obtained using sequential analyses that followed the same construction sequence. Figure 253 through Figure 257 show deflections for Girders 1 through 5, respectively.

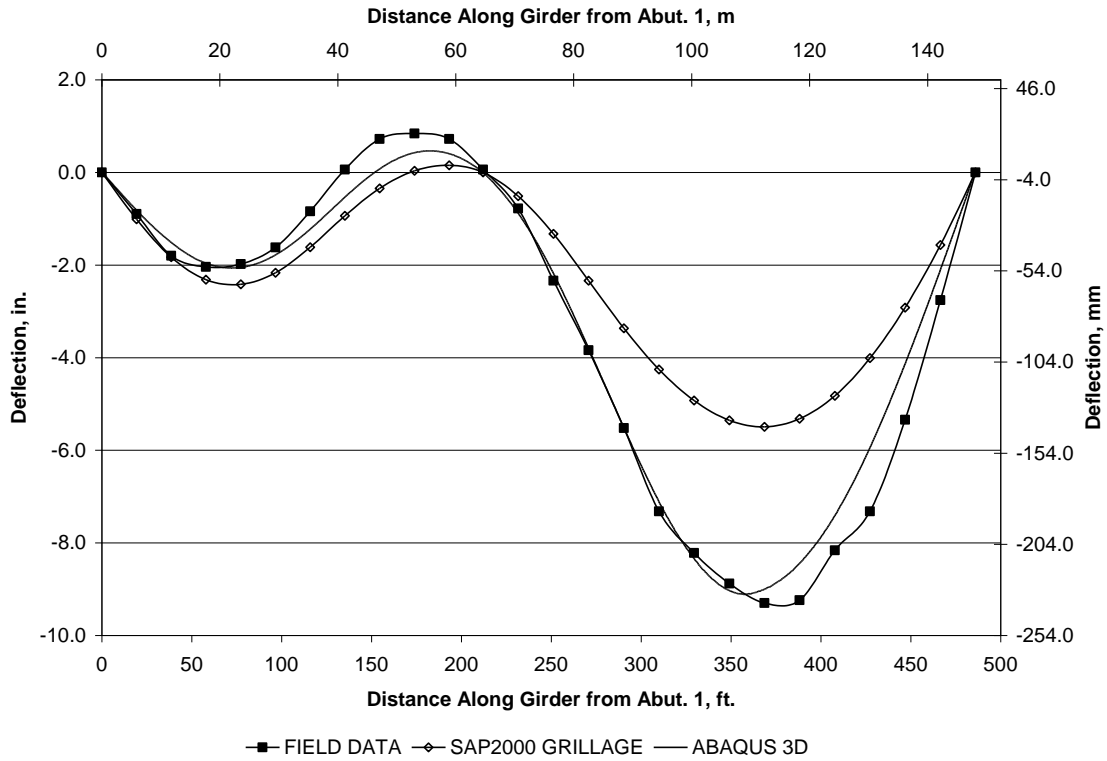


Figure 253. Change in Girder 1 Vertical Displacements between Erection of Entire Steel Superstructure and Placement of the Slab, Structure #207.

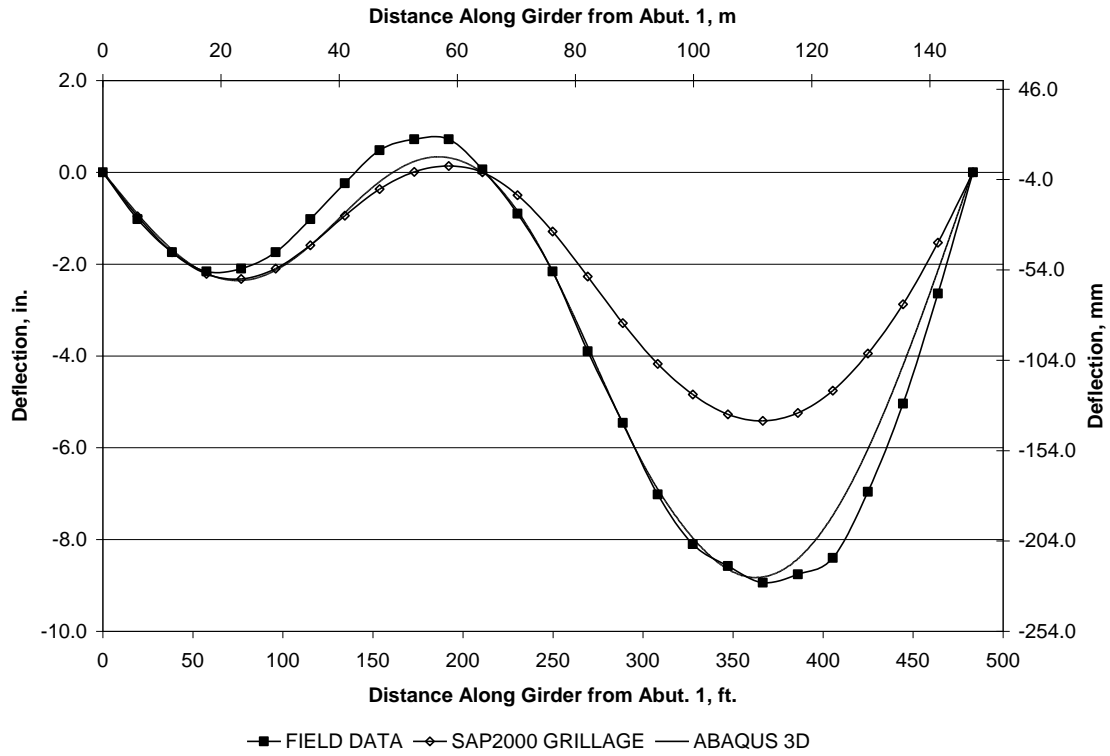


Figure 254. Change in Girder 2 Vertical Displacements between Erection of Entire Steel Superstructure and Placement of the Slab, Structure #207.

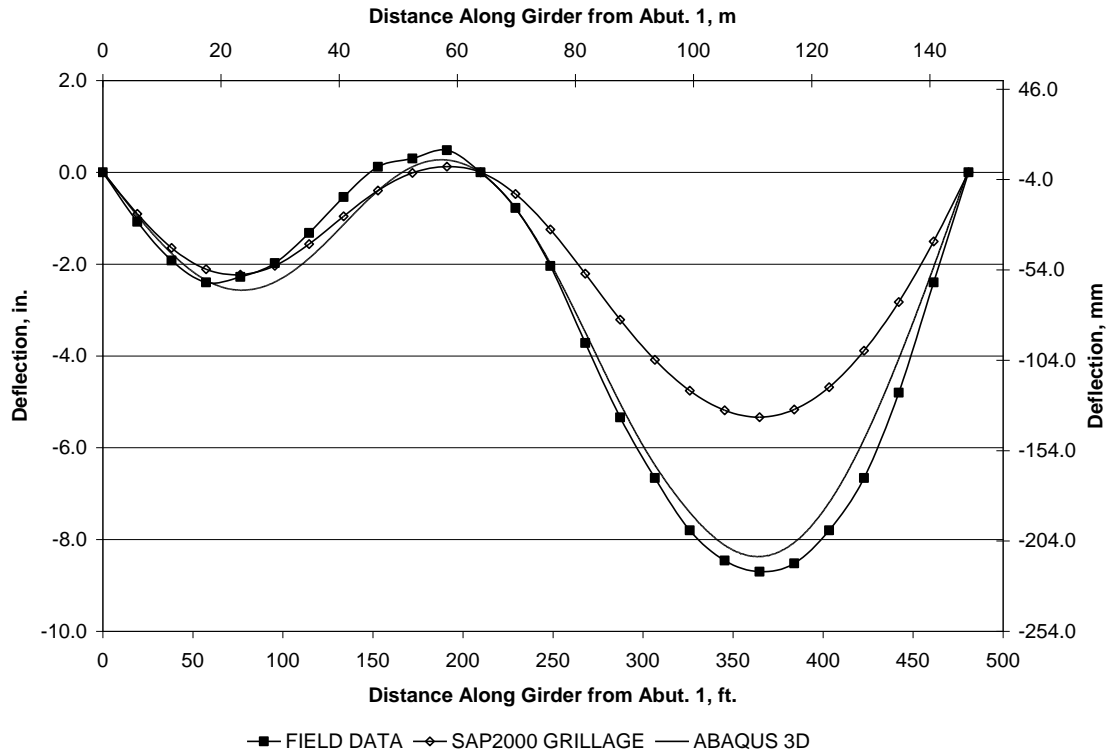


Figure 255. Change in Girder 3 Vertical Displacements between Erection of Entire Steel Superstructure and Placement of the Slab, Structure #207.

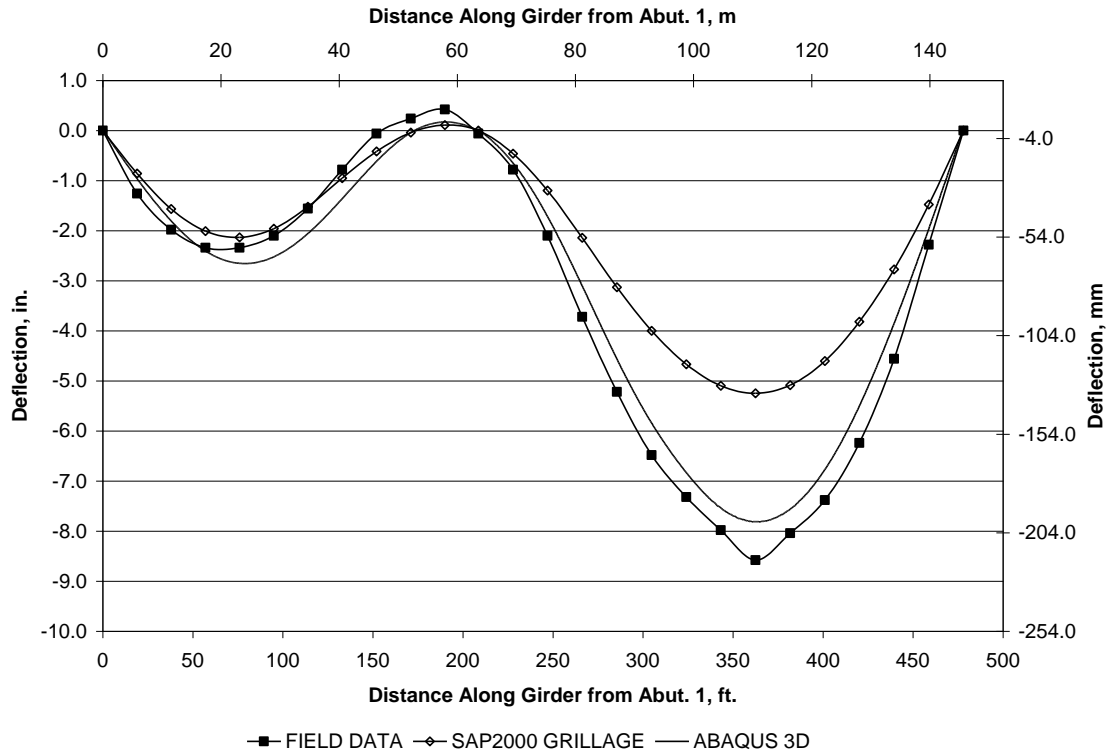


Figure 256. Change in Girder 4 Vertical Displacements between Erection of Entire Steel Superstructure and Placement of the Slab, Structure #207.

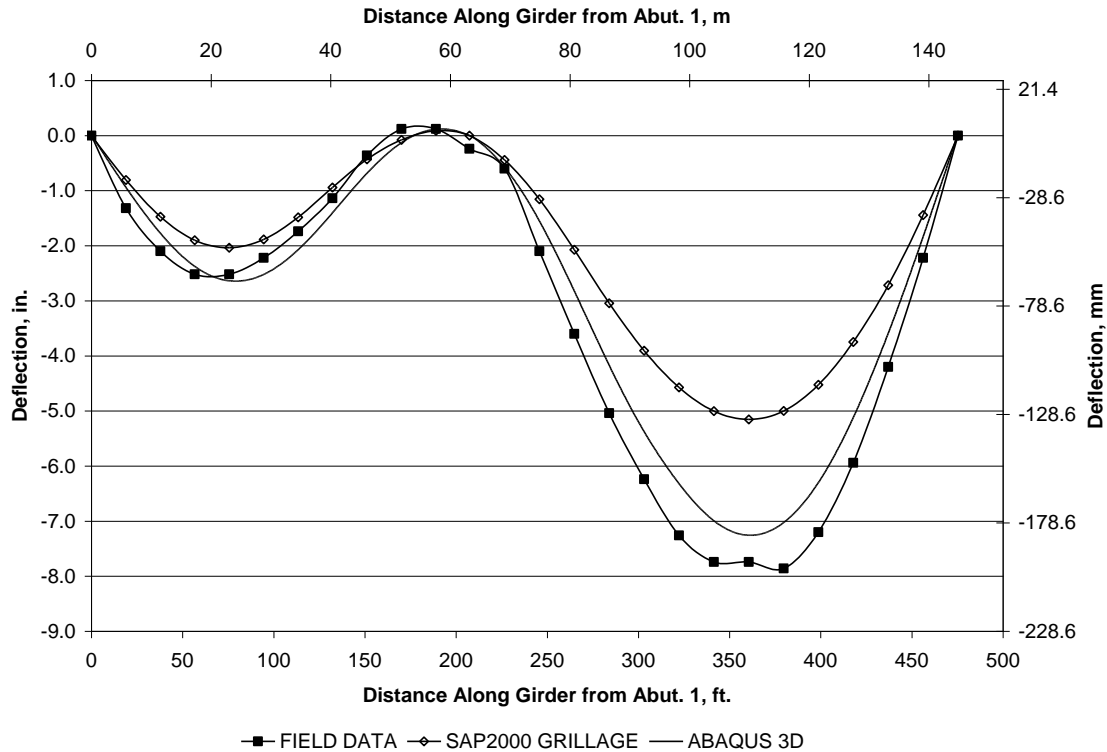


Figure 257. Change in Girder 5 Vertical Displacements between Erection of Entire Steel Superstructure and Placement of the Slab, Structure #207.

The figures show that both the SAP2000 grillage model and the ABAQUS three-dimensional finite element model predict the general behavior of girder vertical deflections observed in the field. However, the ABAQUS three-dimensional finite element model predicts the magnitude of the deflections of all of the girders more accurately than the SAP2000 grillage model when compared to field results. As a result of these comparisons, the ABAQUS shell and beam models were tentatively selected for use with future parametric studies.

9.4.2 Modifications

It was of interest to examine whether additional modifications to the selected modeling technique improved model accuracy. As discussed in previous submittal to PennDOT (Linzell et al. 2003; Linzell et al. 2006), earlier studies investigated the effects of certain parameter variations, such as boundary conditions, on results. Additional modifications that were explored included: (1) examining the effectiveness with which first-order displacement approaches selected for the previous comparisons predicted response for beams with greater horizontal curvature effects, (2) studying how changes in the sequential slab placement procedure used for the computer model affected results, and (3) examining how changes to the offset between the girder web and flanges elements affected results.

9.4.2.1 First-Order Displacements

The effectiveness of first-order displacement assumptions for predicting the response of beams having higher horizontal curvature influence was assessed using comparisons to experimental data from a study by Heins and Spates (1968). They conducted tests of a horizontally curved steel beam with a web depth of 177.8mm (7.0 in) and a thickness of 6.35mm (0.25 in). The flanges were 93.0 mm (3.7 in) by 10.0 mm (0.4 in). The beam was 9.1m (30.0 ft) long and had a radius of curvature of 15.2 m (50.0 ft). The ends of the girder were encased in concrete blocks to replicate fixed end conditions. The concrete blocks encased 0.5 m (1.5 ft) of each end of the girder, resulting in a clear span of 8.2 m (27.0 ft). The R/L ratio of the beam

was 1.85, indicating extreme curvature effects. The beam was tested under either a concentrated vertical load at midspan or a concentrated vertical load at its three-tenths point. The load in each case was 4448 N (1000 lb). It was instrumented with gauges to record deformations while under the test loads.

A three-dimensional finite element model of the test beam was created in ABAQUS following the shell and beam technique. The web was modeled using 7 S4R shell elements, with nodes along the girders placed at approximately 25 mm (1 in) intervals to keep the element aspect ratio as close to 1 as possible. The flanges were modeled using beam elements. Nodes along the ends of the beam were restrained from all movement to model the fixed support conditions. The beam was analyzed under two loading conditions: (1) concentrated load at midspan and (2) concentrated load at the three-tenths point.

Figure 258 and Figure 259 show representative deformation comparisons between test and computer model results. These comparisons indicate that using a first-order displacement approach does an effective job of predicting deformations, including rotations, for a beam with severe horizontal curvature. While rotations are not predicted with as much accuracy as vertical deflections, the fact that they are over-predicted by the model coupled with the small magnitude of the rotations that were measured supports using a first-order approach for future parametric studies.

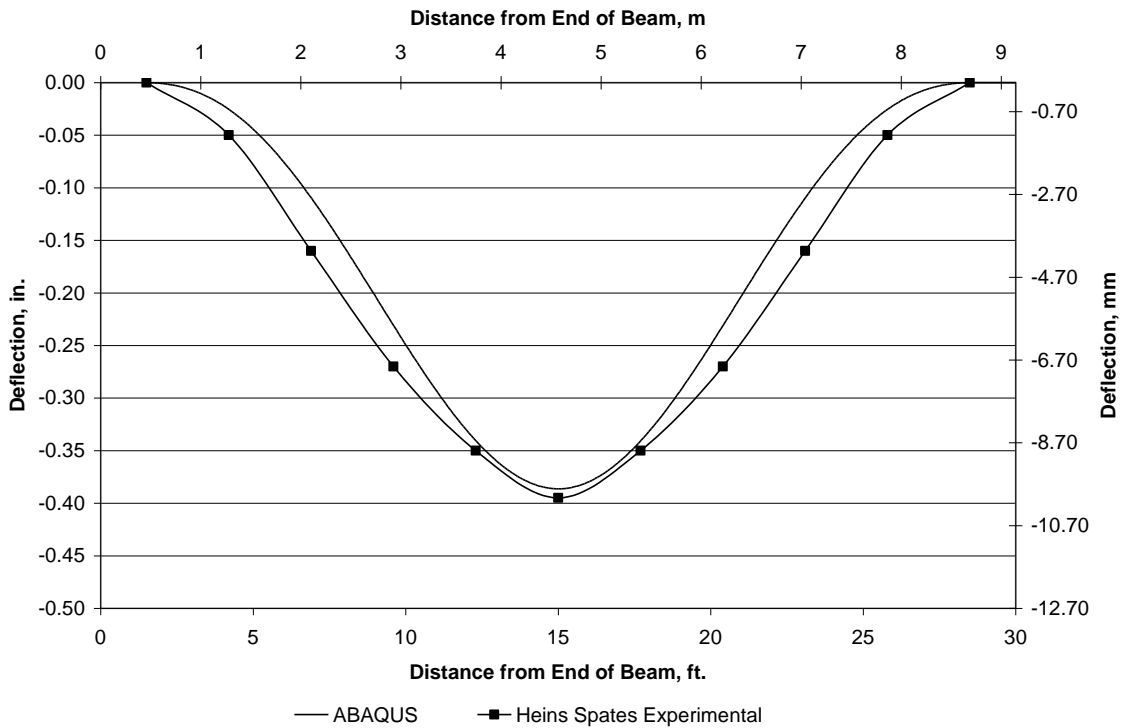


Figure 258. Vertical Deflection Comparison, Concentrated Load at Midspan, Heins and Spates (1968) Tests.

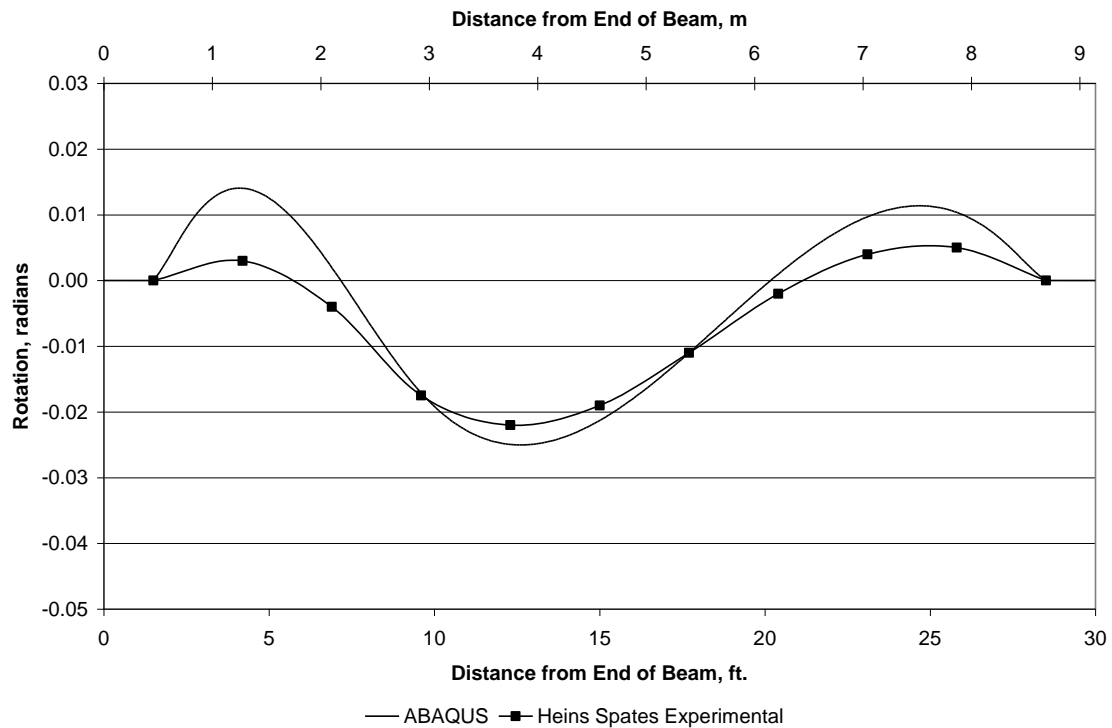


Figure 259. Rotation Comparison, Concentrated Load at Three-Tenths Point, Heins and Spates (1968) Tests.

9.4.2.2 Slab Placement

A modified technique for numerically placing the concrete slab was examined to determine its influence on results. The initial approach for adding deck concrete to the model involved placing each slab section in one step, thereby assuming that the concrete had achieved its full stiffness at the time of placement. To examine the influence of fresh concrete on computer results models were created that incorporated an additional step for each slab section that included slab shell elements with full weight but negligible stiffness. To simulate setting of the concrete a subsequent step that removed the “wet” concrete shells from the active list of elements in the model and added shells that had the full slab stiffness to the list of active elements.

To assess the influence of changing deck placement techniques on model results, final deformations predicted by each of the techniques were compared for Structure #207. Figure 260 and Figure 261 show representative final deflection results for Girder 1 for the original slab placement method (only one slab step per section placed) and the modified slab placement method (two steps per slab section placed). Only minor differences are shown, and as a result, the original technique was retained for future models due to a combination of its effectiveness and modeling efficiency.

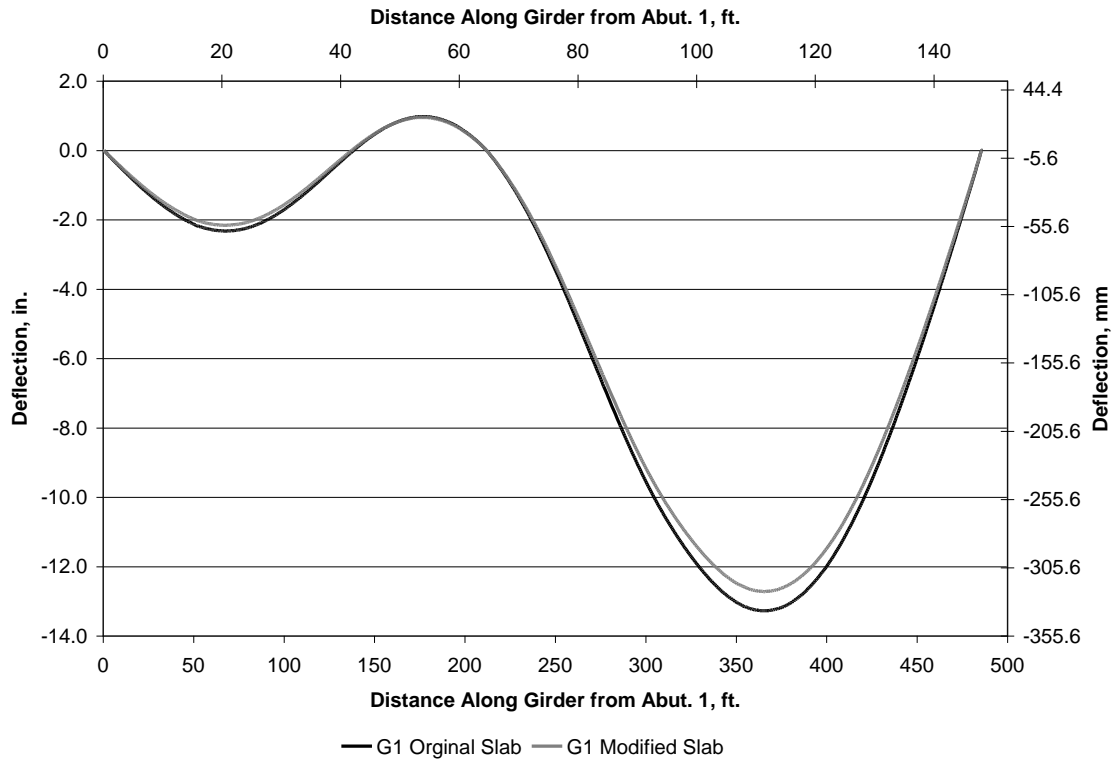


Figure 260. Vertical Deflection Comparisons, Original and Modified Slab Placement Techniques, Structure #207.

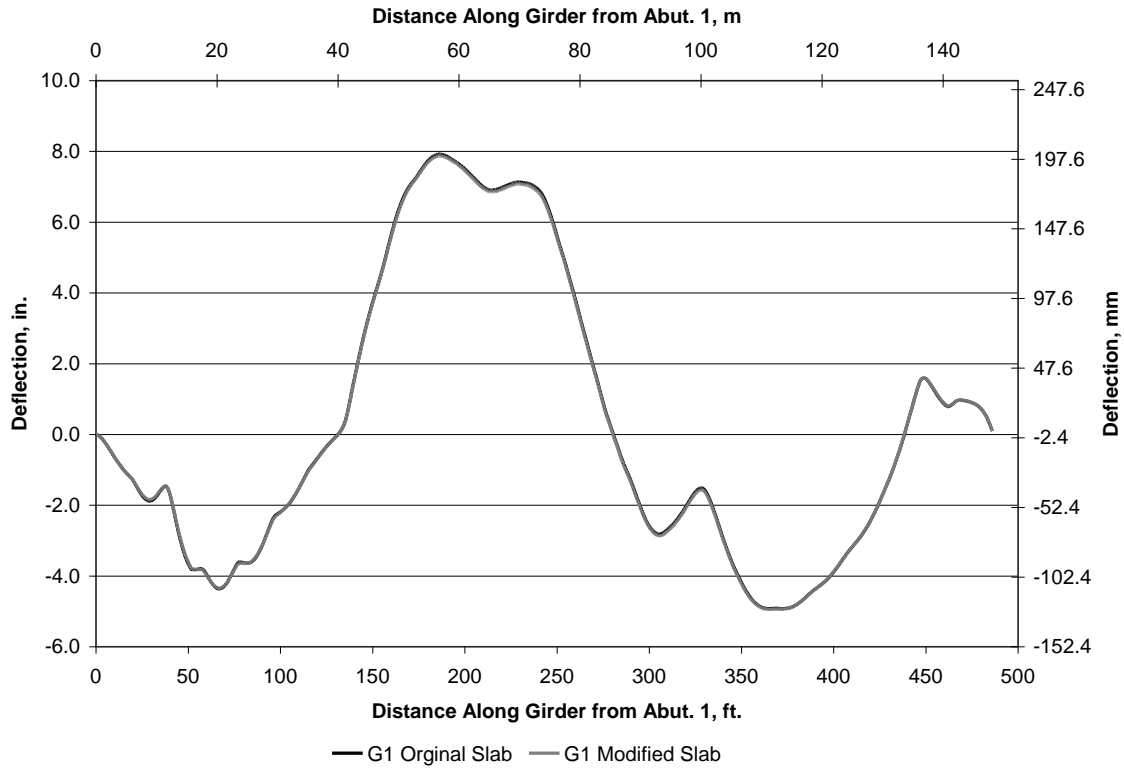


Figure 261. Radial Deflection Comparisons, Original and Modified Slab Placement Techniques, Structure #207.

9.4.2.3 Flange Offset

The original shell and beam models did not include flange offsets between the web shells and flange beam elements. A second model was created that incorporated flange nodes that were displaced a distance equal to half the thickness of the flange from the web shell nodes. Comparisons again occurred for Structure #207 and, in this case, improvement offered by including the offset via revised moment distribution comparisons during steel erection between the original ABAQUS finite element model, the ABAQUS model using flange offsets, the SAP2000 grillage model, and the field data were examined. A single representative comparison is shown in Figure 262, and it indicates that including flange offsets did not appreciably improve model accuracy. These results and those from earlier sections indicate that initial modeling assumptions for the shell and beam models were acceptable for the parametric studies.

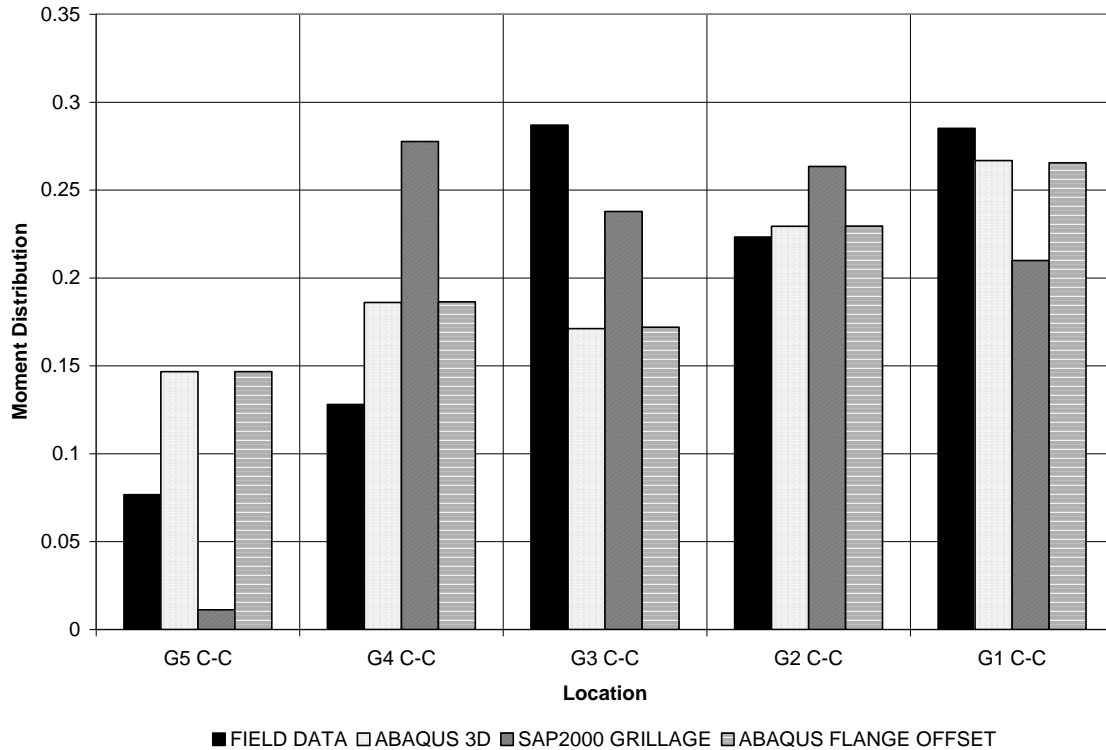


Figure 262. Stage 8b Vertical Bending Moment Distribution for Section C-C, Including Flange Offset, Structure #207.

9.5 Additional Evaluations

After recommendation of a modeling technique for future project tasks based on the comparisons and modification examination outlined previously, additional evaluation of the recommended technique occurred via comparisons to data recorded by Penn State personnel from other curved and skewed structures during construction. These structures included two curved plate girder bridges, Structure #7A and the I-79 Missing Ramps Bridge, and a single skewed plate girder structure, Structure #28. Evaluations that were completed and corresponding discussions are provided in the sections that follow.

9.5.1 Evaluations – Curved Bridges

As discussed in previous submittals to PennDOT (Linzell et al. 2003) and in previous sections, data for evaluating the effectiveness of the recommended model for predicting the response of Structure #7A and the Missing Ramps Bridge was collected during specific instances of the erection process, and, as such, limited comparisons are completed and discussed herein.

9.5.1.1 Structure #7A

Construction of the ABAQUS shell and beam model for Structure #7A followed the procedure discussed in previous sections. A view of the superstructure model, detailing element types and levels of discretization, is shown in Figure 263.

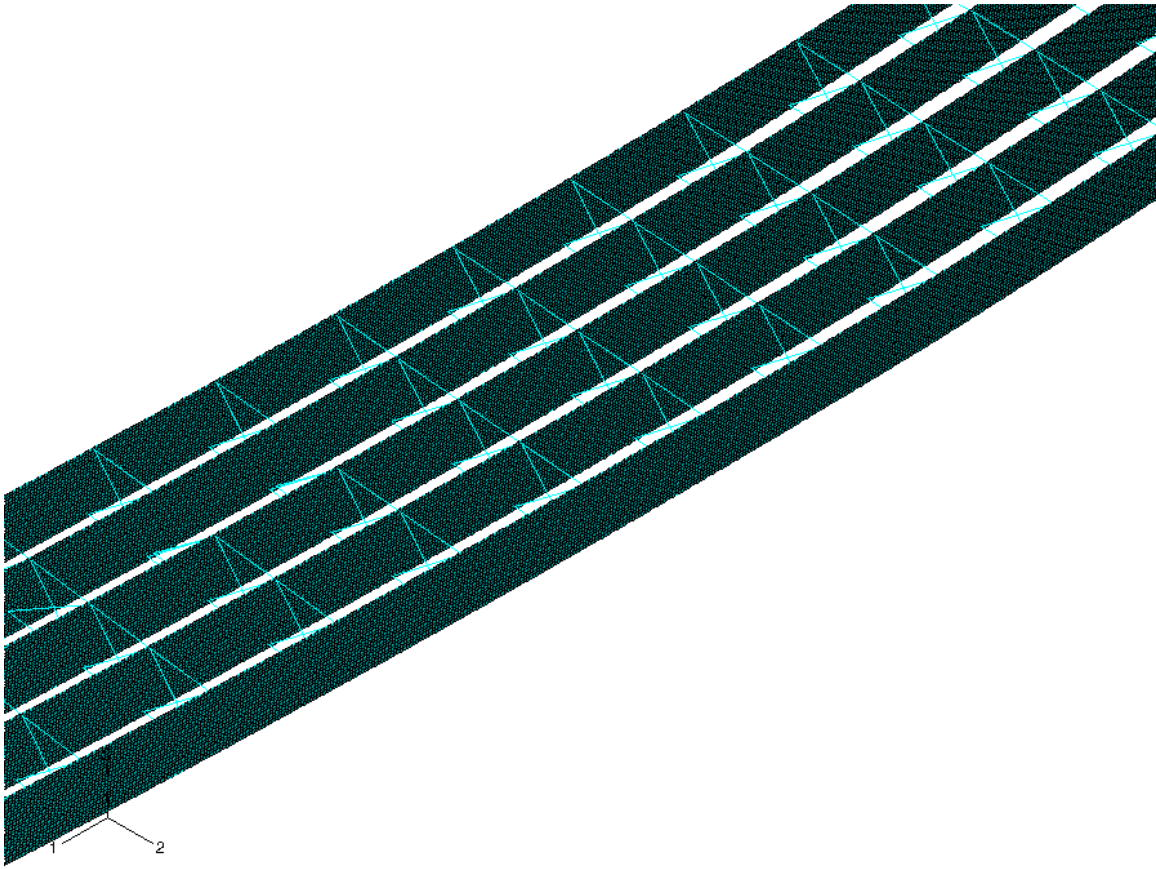


Figure 263. ABAQUS Model, Structure #7A.

As was discussed in earlier submittals to PennDOT (Linzell et al. 2003), deformation measurement surveys were taken during the realignment procedure by a third party. Representative comparisons between deformations recorded during these surveys and predictions from the ABAQUS models are shown in Figure 264 through Figure 268. These comparisons detail changes in vertical displacements during realignment of the superstructure in Spans 4 and 5 and indicate good agreement between measured and predicted values.

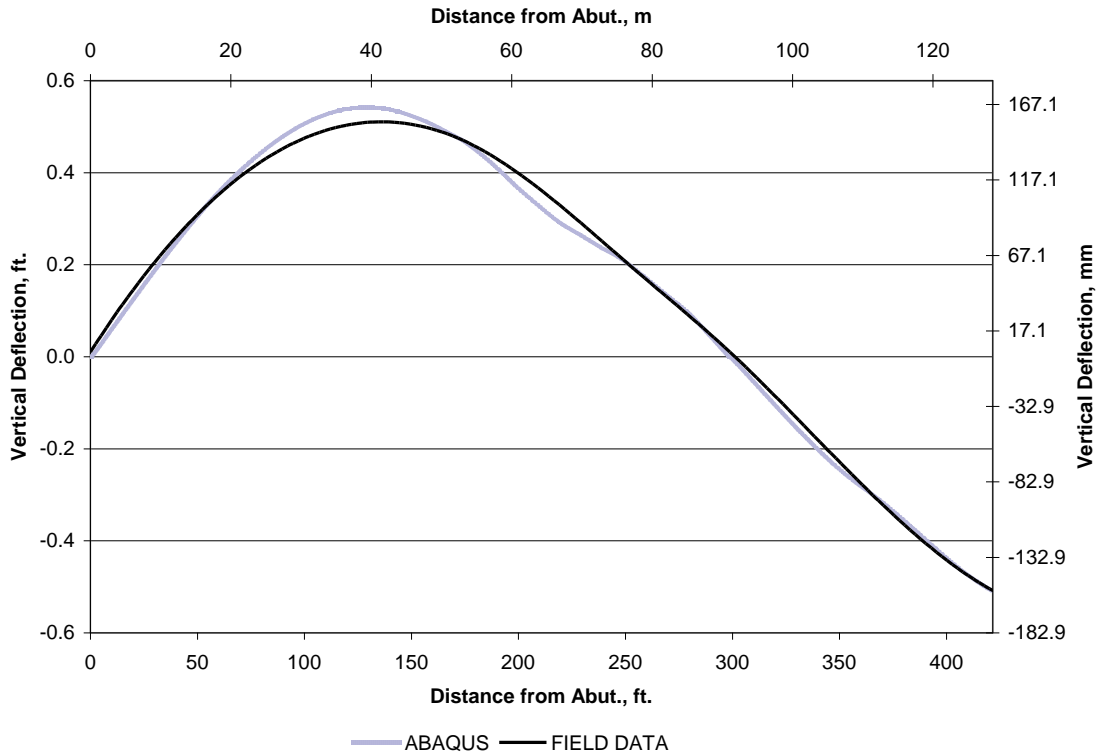


Figure 264. G1 Vertical Displacement Changes During Realignment of Spans 4 and 5, Structure #7A.

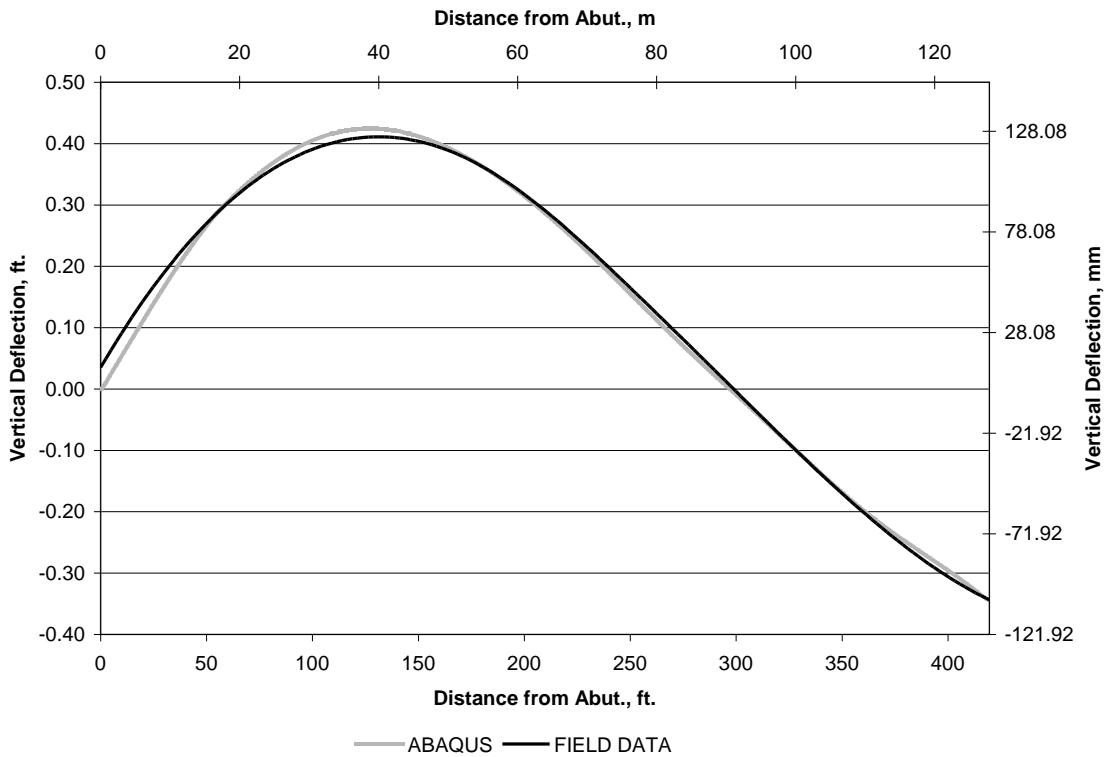


Figure 265. G2 Vertical Displacement Changes During Realignment of Spans 4 and 5, Structure #7A.

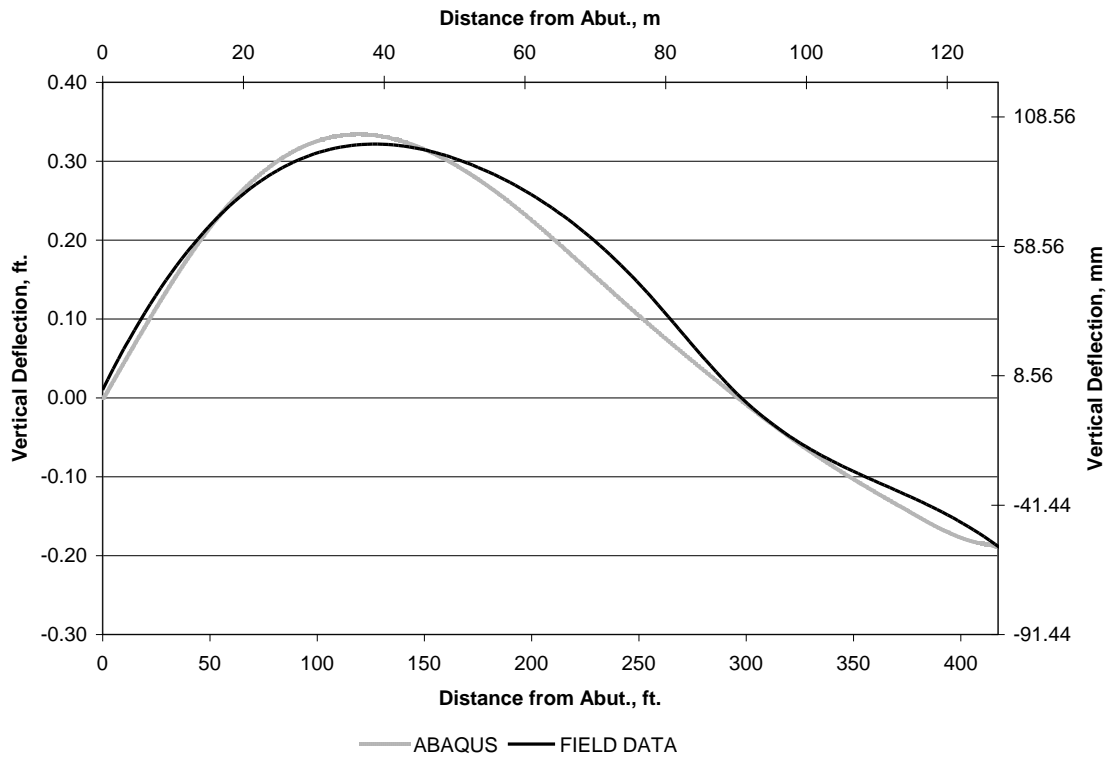


Figure 266. G3Vertical Displacement Changes During Realignment of Spans 4 and 5, Structure #7A.

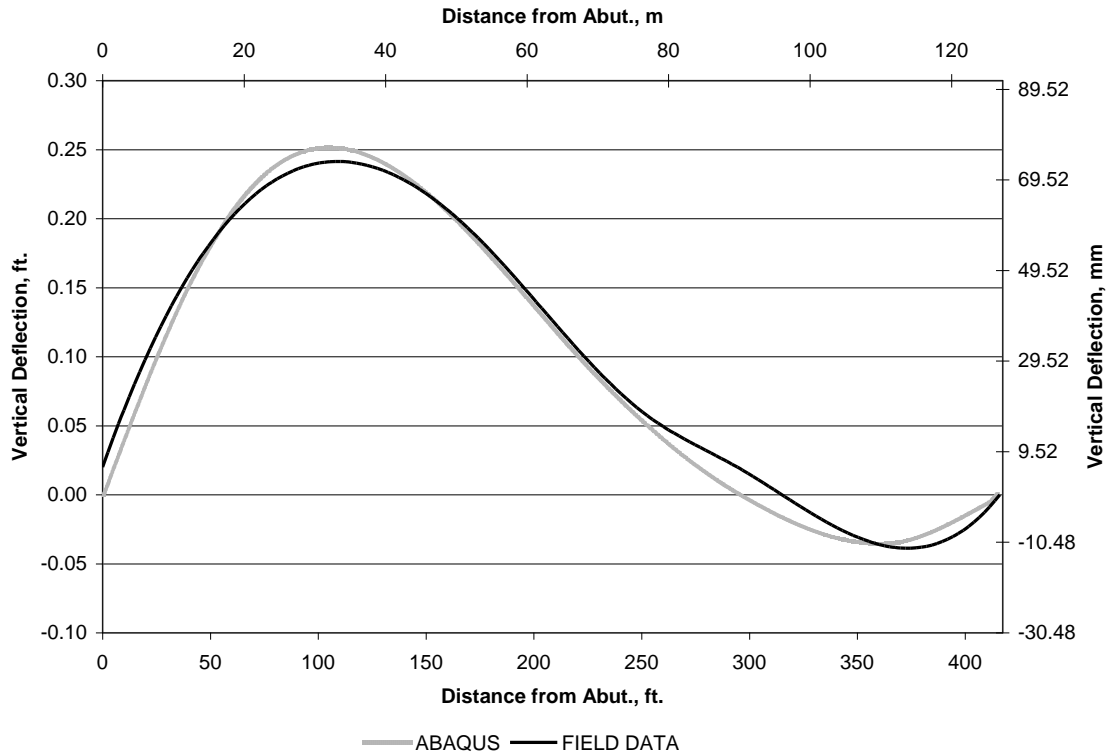


Figure 267. G4 Vertical Displacement Changes During Realignment of Spans 4 and 5, Structure #7A.

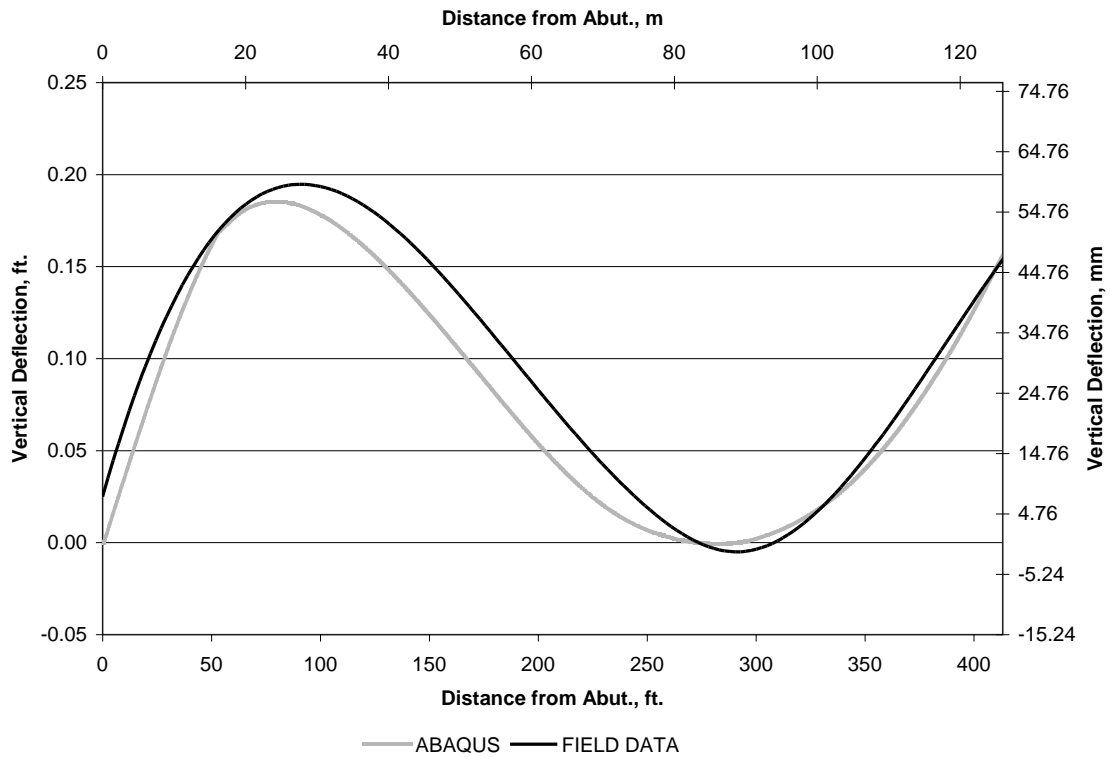


Figure 268. G5 Vertical Displacement Changes During Realignment of Spans 4 and 5, Structure #7A.

9.5.1.2 Missing Ramps Bridge

Construction of the ABAQUS shell and beam model for the Missing Ramps Bridge followed the procedure outlined and evaluated in the previous sections. A view of the steel superstructure model is shown in Figure 269. Figure 270 details cross-frame labels used for model evaluations.

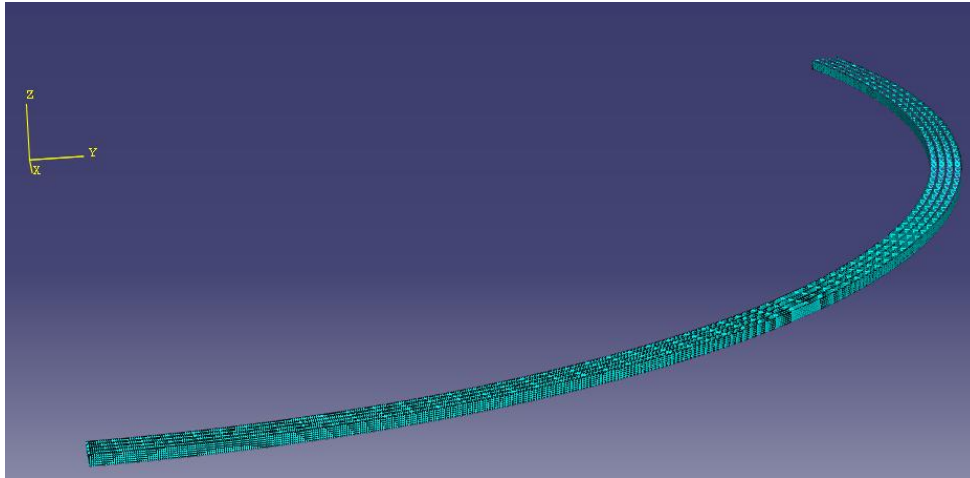


Figure 269. ABAQUS Model, Missing Ramps Bridge.

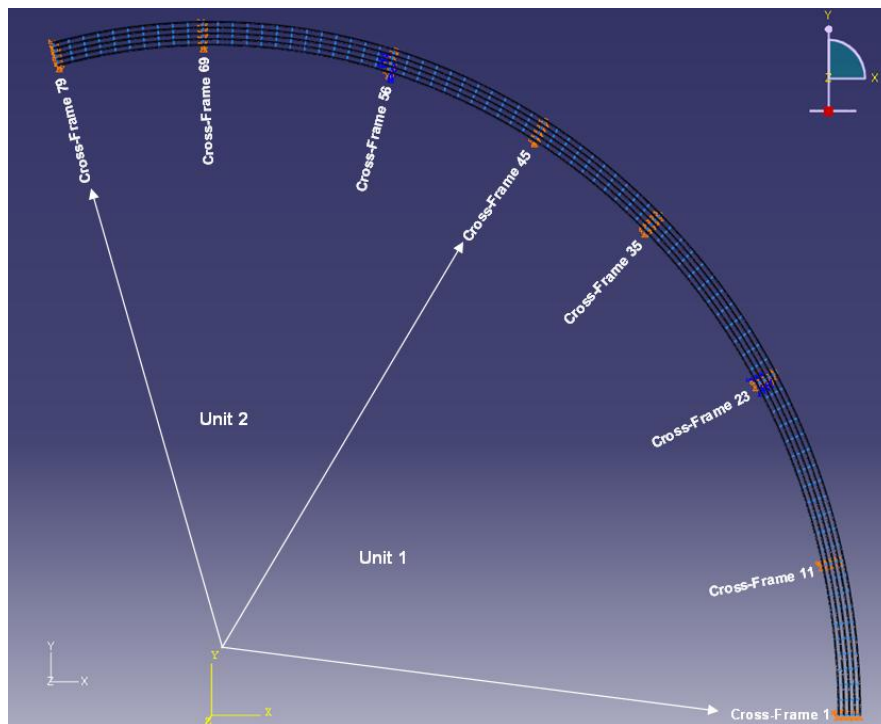


Figure 270. ABAQUS Model Detailing Cross-Frame Labels, Missing Ramps Bridge.

As was discussed in previous sections, PennDOT personnel measured girder rotations at cross-frame connection locations during construction of the steel superstructure by measuring radial translations at the web-top flange junction. Figure 271 through Figure 273 present representative comparisons between predicted and measured girder rotations at the completion of erection at select cross-frame locations. Comparisons are presented for Unit 1, followed by Unit 2. These comparisons show good agreement between predicted and measured lateral displacements at most girder locations and quite good prediction of girder movements at radial cross-sections through the bridge.

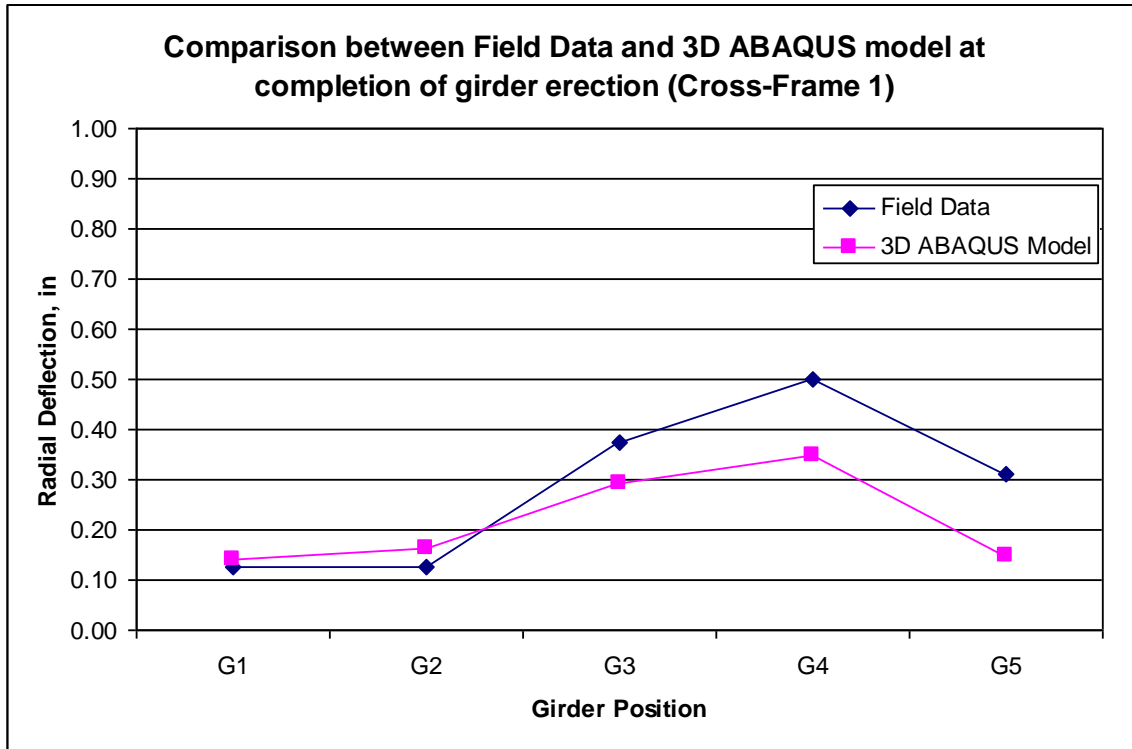


Figure 40. Girder Radial Translations at Web-Flange Junction, Cross-Frame 1, Completion of Unit 1 Girder Erection, Missing Ramps Bridge.

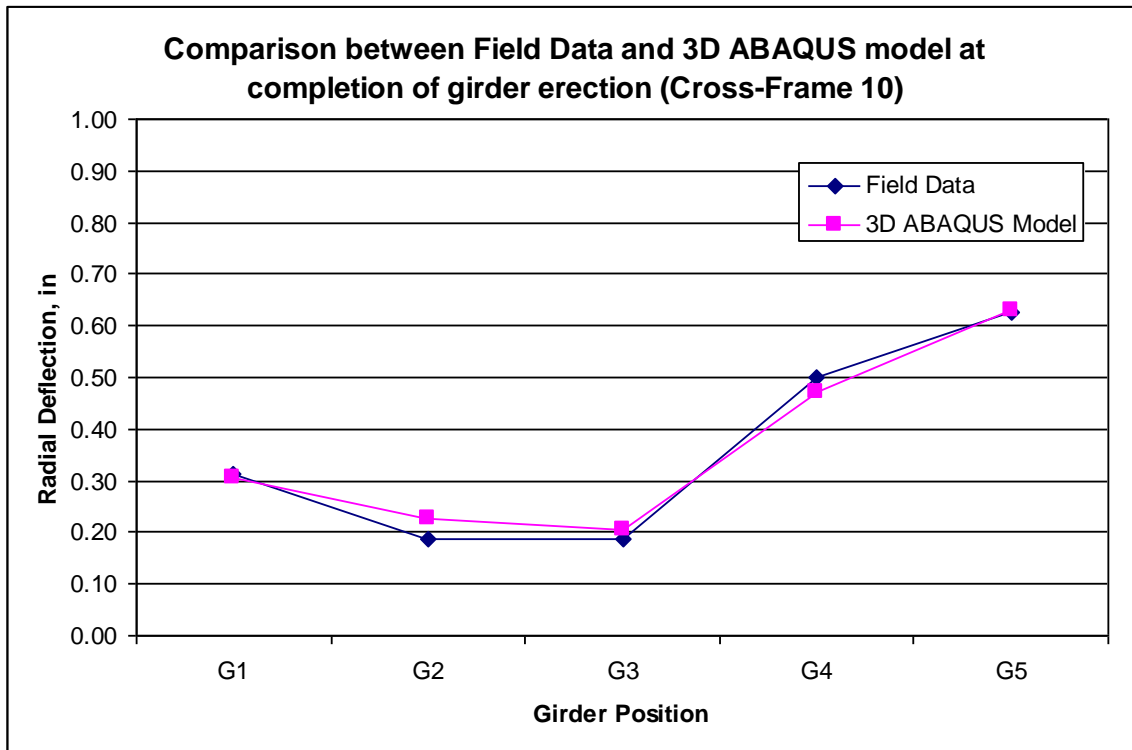


Figure 271. Girder Radial Translations at Web-Flange Junction, Cross-Frame 10, Completion of Unit 1 Girder Erection, Missing Ramps Bridge.

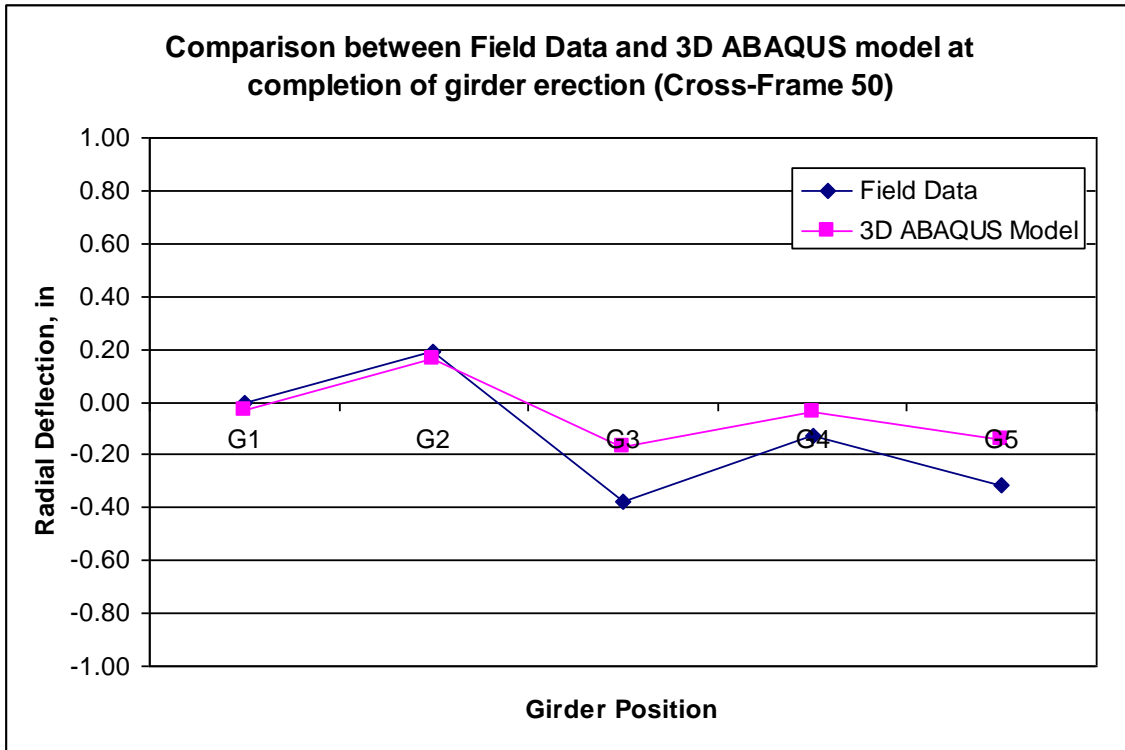


Figure 272. Girder Radial Translations at Web-Flange Junction, Cross-Frame 50, Completion of Unit 2 Girder Erection, Missing Ramps Bridge.

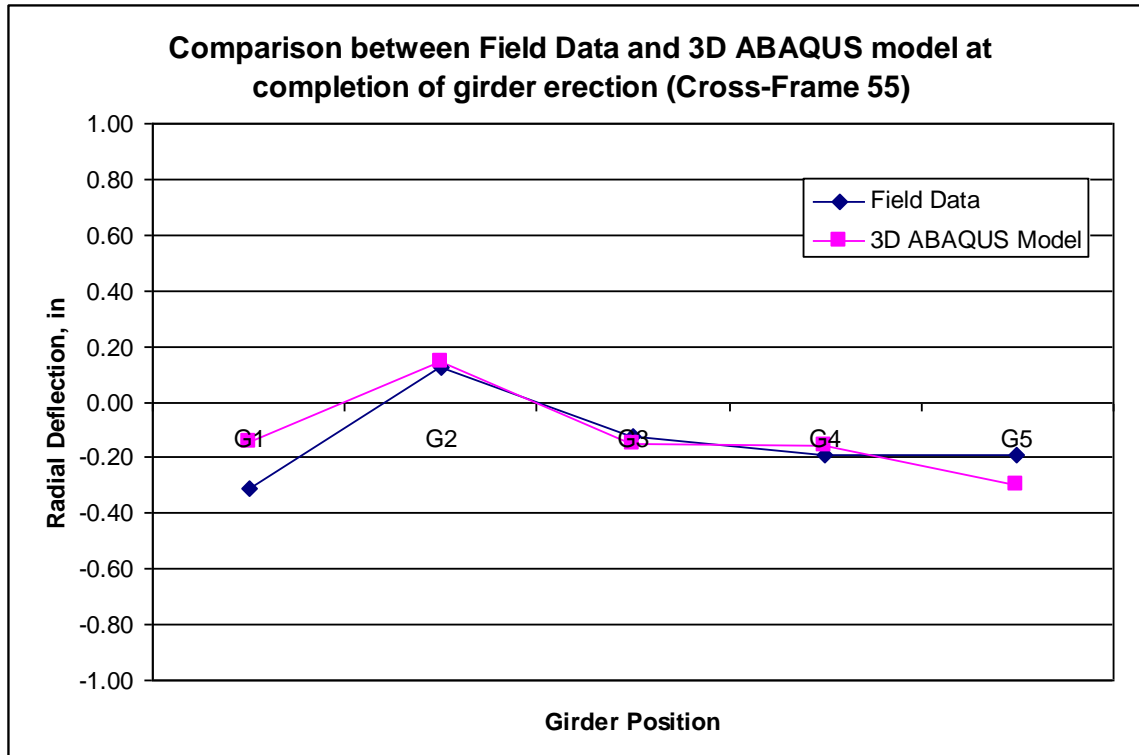


Figure 273. Girder Radial Translations at Web-Flange Junction, Cross-Frame 55, Completion of Unit 2 Girder Erection, Missing Ramps Bridge.

9.5.2 Evaluations – Skewed Bridge

As discussed in previous submittals to PennDOT, limited data that encompassed response of the structure during deck placement were collected for Structure #28. As a result, evaluations of model effectiveness consisted of examination of deformation predictions as the concrete deck was being placed.

9.5.2.1 Structure #28

Construction of the ABAQUS shell and beam model for Structure #28 followed the procedure outlined and evaluated in the previous sections. A view of the steel superstructure model is shown in Figure 274.

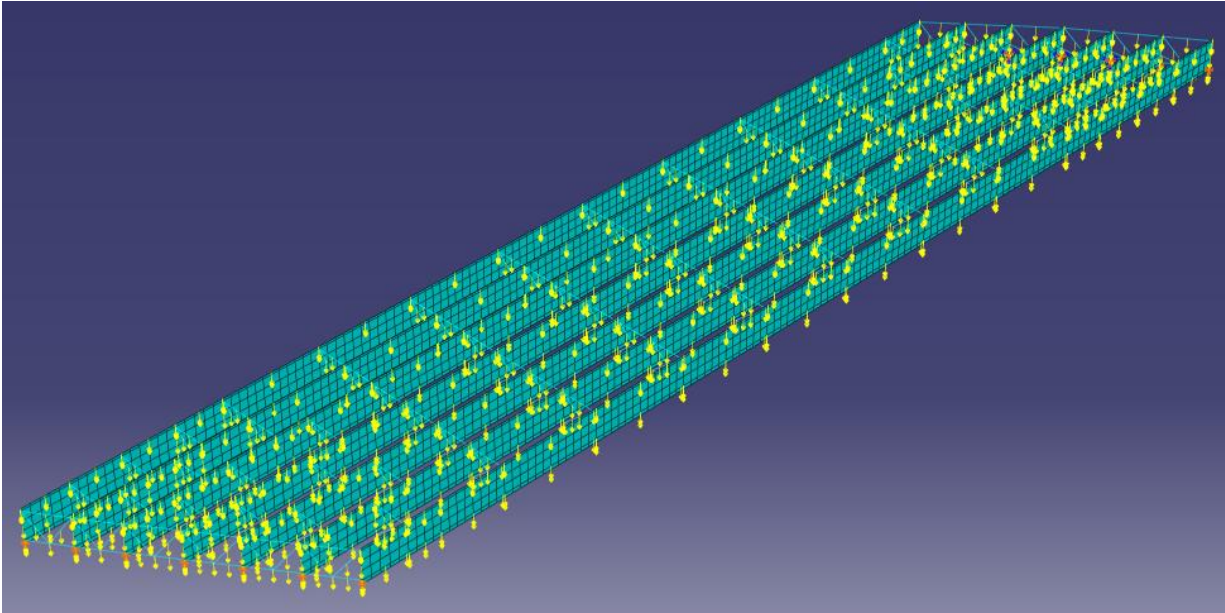


Figure 274. ABAQUS Model, Structure #28.

As was discussed in previous submittals to PennDOT (Linzell et al. 2003), the majority of the measurements taken during the deck pour were deformations. One set of deformation measurements involved tracking girder rotation at the abutments by measuring out-of-plane girder web displacement at its intersection with the top flange. Figure 275 details representative differences between final displacements at one (east) end of select girders and shows the effectiveness of the model for predicting those values. One additional set of measurements that was taken involved girder vertical displacements, and Figure 276 and Figure 277 show representative results for fascia girders G1 and G7. Again, the effectiveness of the model for predicting deformations is demonstrated.

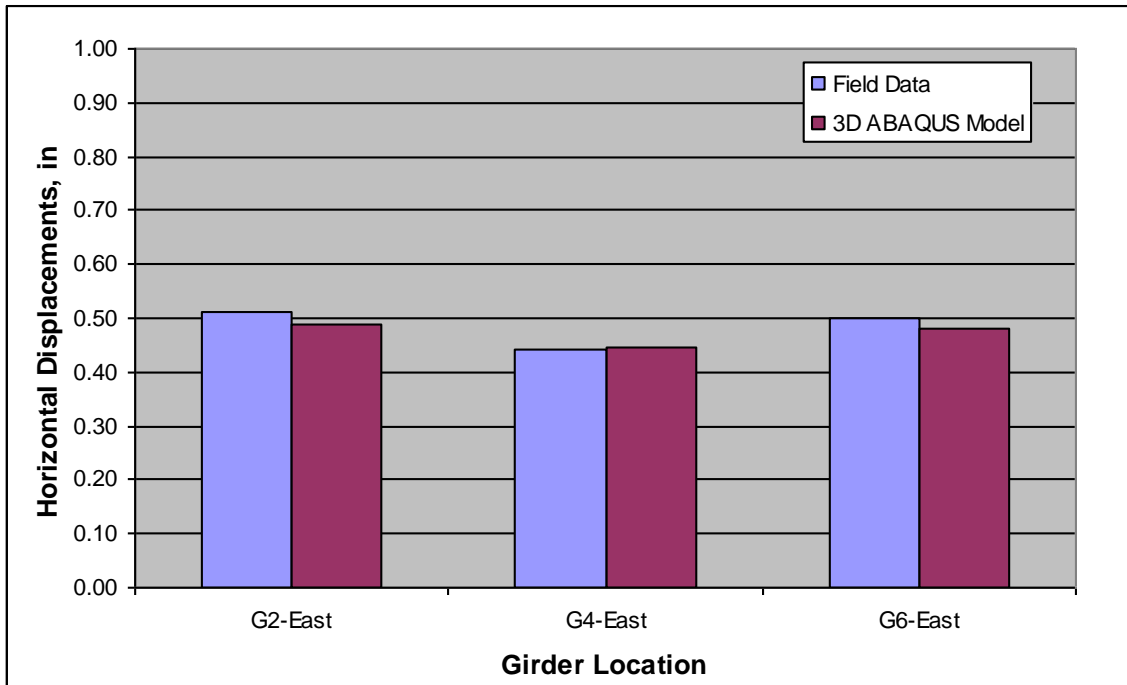


Figure 275. Girder Lateral Displacements, Completion of Deck Pour, Structure #28.

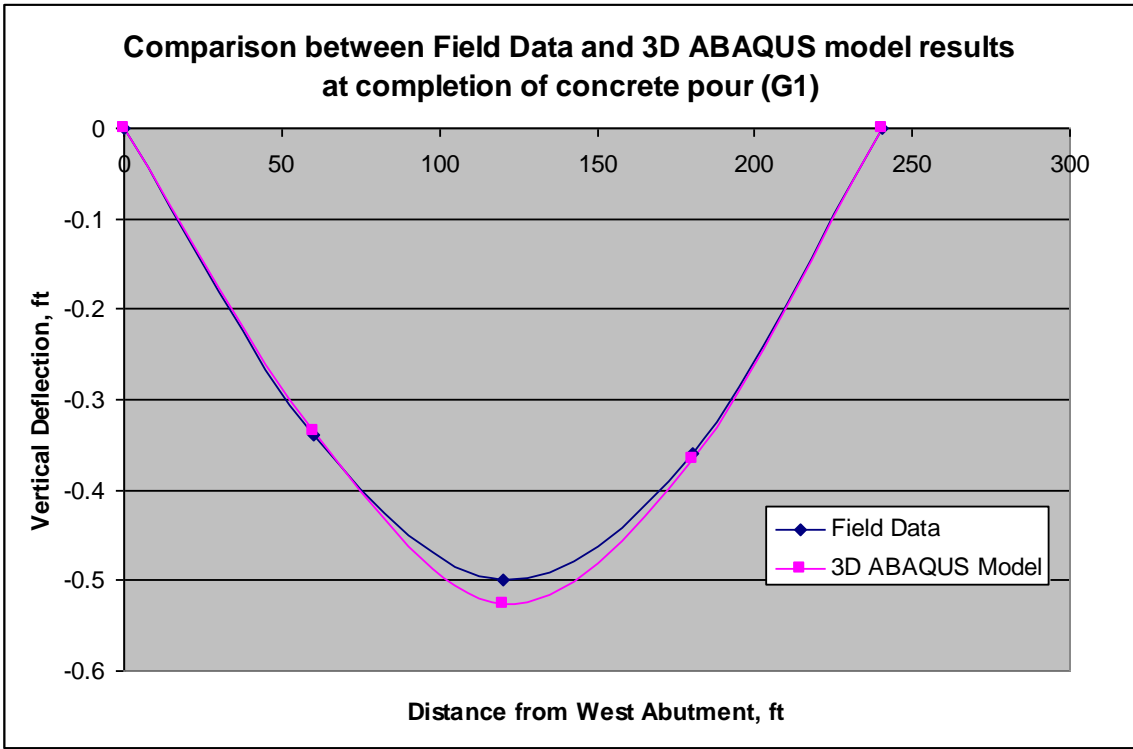


Figure 276. G1 Vertical Displacements, Completion of Deck Pour, Structure #28.

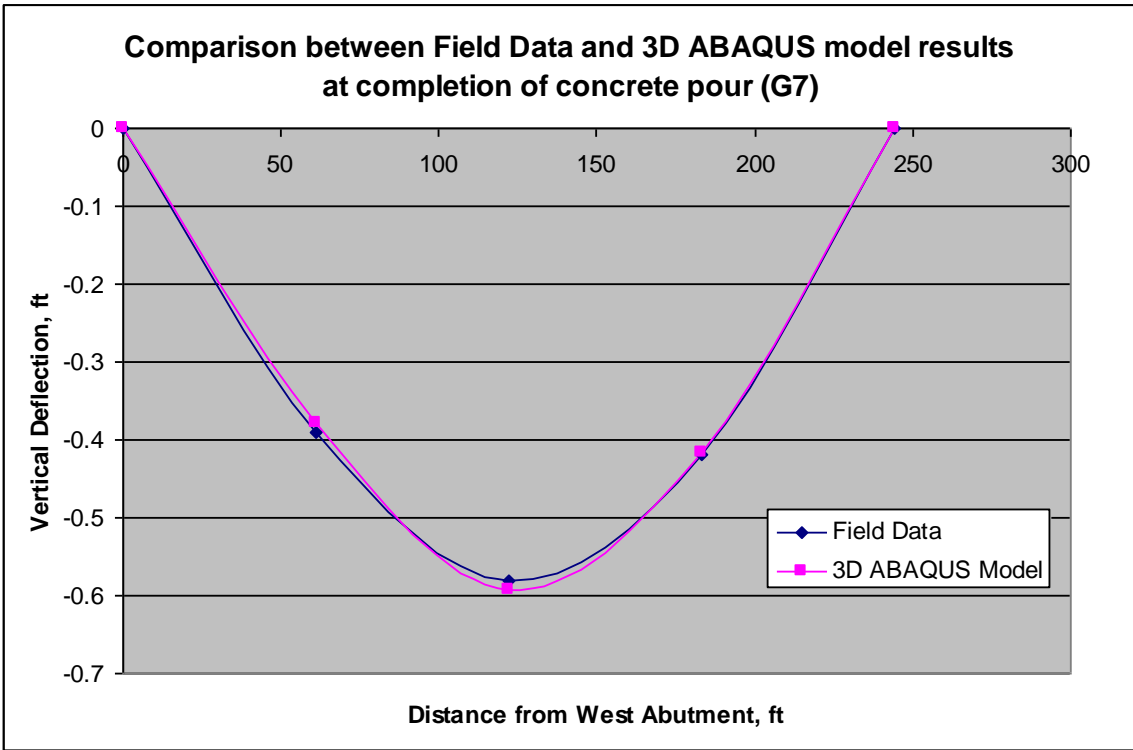


Figure 277. G7 Vertical Displacements, Completion of Deck Pour, Structure #28.

9.6 Conclusions

Summarized herein were modeling development and verification steps completed in association with Work Order 009, *Guidelines for Analyzing Curved and Skewed Bridges and Designing Them for Construction*. Contained within this report were sections that provided information on structures that were modeled, discussed modeling techniques that were examined, and explained comparisons, modifications, and evaluations that occurred to assist with selecting a model type to be used to complete future project tasks.

As a result of the work, a shell and beam model is recommended for future parametric studies. This model utilizes ABAQUS S4R shell elements for the girder webs with no offsets between the web and girder top and bottom flanges. ABAQUS B31 beam elements are used for girder flanges with cross-frame members and web stiffeners modeled using B31OS elements. The model is analyzed using a first-order deformation approach. When the deck pour is modeled, it is applied to the model using a single group of shell elements having hardened deck properties.

This type of model was selected because of:

- the computational efficiency and flexibility offered by an ABAQUS shell and beam model when compared to grillage models and three-dimensional finite element models involving purely shell elements to model the girder or a combination of shell and solid elements,
- its effectiveness for predicting deformations, variables that are of primary interest during erection, for various types of structures and at various instances during construction, and
- its similar to slightly improved level of accuracy for predicting bending moment distributions within curved structures when compared to grillage models or other three-dimensional models.

9.7 References

Chavel, B. W., and Earls, C. J. (2006a). "Construction of a Horizontally Curved Steel I-Girder Bridge. Part I: Erection Sequence." *J. Bridge Eng.*, 11(1), 81-90.

Chavel, B. W., and Earls, C. J. (2006b). "Construction of a Horizontally Curved Steel I-Girder Bridge. Part II: Inconsistent Detailing." *J. Bridge Eng.*, 11(1), 91-98.

Heins, C.P. and Spates, K.R. (1970), Behavior of Single Horizontally Curved Girder, Journal of the Structural Division, ASCE, 96(ST7), 1511-1529, USA.

Hiltunen, D.R., Johnson, P.A., Laman, J.A., Linzell, D.G., Miller, A.C., Niezgoda, S.L., Scanlon, A., Schokker, A.J. and Tikalsky, P.J. (2004), Interstate 99 Research, Contract No. SPC 020S78, Pennsylvania Department of Transportation, October, 324 pp.

Kim, Y.D., Jung, S.-K. and White, D.W. (2005), "Transverse Stiffener Requirements in Straight and Horizontally Curved Steel I-Girders," ASCE Journal of Bridge Engineering, 12(2), 174-183.

Linzell, D.G., Laman, J.A., Bell, B., Bennett, A., Colon, J., Lobo, J., Norton, E. and Sabuwala, T. (2003), Prediction of Movement and Stresses in Curved and Skewed Bridges, University-Based Research, Education and Technology Transfer Program; Agreement No. 359704, Work Order 79. Final Report, Pennsylvania Department of Transportation, March, 192 pp.

Linzell, D.G., Nadakuditi, V.P. and Nevling, D.L. (2006), Prediction of Movement and Stresses in Curved and Skewed Bridges, PennDOT/MAUTC Partnership, Work Order No. 2, Research Agreement No. 510401, Final Report, Pennsylvania Department of Transportation, September, 86 pp.

Appendix A – Representative Moment and Stress Calculations

Vertical Bending Moment Distribution Representative Calculations

Sample calculations: Use G5 Section B-B Stage 8b (see Table 36, Figure 241). Results shown in **BOLD**.

$\sigma_{tf} = \frac{ \sigma_{tffd} + \sigma_{bffd} }{d + t_{bf}} * t_{tf} + \sigma_{tffd}$	Equation 6
---	-------------------

where,

σ_{tf} = calculated top flange stress, ksi

σ_{tffd} = field data stress at bottom of top flange, ksi

σ_{bffd} = field data stress at bottom of bottom flange, ksi

t_{tf} = top flange thickness, in.

d = web depth, in.

t_{bf} = bottom flange thickness, in.

$\mathbf{4.40} = \frac{ 4.17 + -2.71 }{108 + 3.75} * 3.75 + 4.17$	Sample Equation 1
---	--------------------------

$M (k \cdot ft) = \frac{\sigma_{bffd} * I}{y_{bot} * 12}$	Equation 2
---	-------------------

where,

M (k-ft) = girder vertical bending moment, k-ft

I = moment of inertia, in.⁴

y_{bot} = distance to the neutral axis from bottom of the girder, in.

$\mathbf{-3847.7} = \frac{-2.71 * 725947.5}{42.56 * 12}$	Sample Equation 2
--	--------------------------

$M_{distG5} = \frac{M_{G5} (k \cdot ft)}{\sum M}$	Equation 3
---	-------------------

where,

M_{distG5} = vertical bending moment distribution to Girder 5

M_{G5} (k-ft) = Girder 5 vertical bending moment, k-ft

$\sum M$ (k-ft) = sum of the girder vertical bending moments at radial section, k-ft

$\mathbf{0.15} = \frac{-3847.7}{-25593.8}$	Sample Equation 3
--	--------------------------

The same equations and procedure was used for the ABAQUS and the SAP2000 girder vertical bending moment.

Lateral Bending Moment Distribution Representative Calculations

Sample calculations: Use G5 Section B-B Stage 8b (see Table 36, Figure 241). Results shown in **BOLD**.

$\sigma_{vbf} = \frac{\sigma_{ebf} + \sigma_{ibf}}{2}$	Equation 4
--	-------------------

where,

σ_{vbf} = bottom flange vertical bending stress, ksi

σ_{ebf} = bottom flange exterior tip vertical bending stress, ksi

σ_{ibf} = bottom flange interior tip vertical bending stress, ksi

$-3.51 = \frac{-3.43 + -3.59}{2}$	Sample Equation 4
-----------------------------------	--------------------------

$M_L (k \cdot ft) = \frac{ \sigma_{vbf} - \sigma_{ebf} * S}{12}$	Equation 5
---	-------------------

where,

M_L (k-ft) = bottom flange lateral bending moment, k-ft

S = weak axis section modulus of the bottom flange, in.³

$23.36 = \frac{ (-3.51 - -3.43) * 3658.67}{12}$	Sample Equation 5
--	--------------------------

$M_{LdistG5} = \frac{M_{LG5} (k \cdot ft)}{\sum M_L}$	Equation 6
---	-------------------

where,

$M_{LdistG5}$ = lateral bending moment distribution to Girder 5

M_{LG5} (k-ft) = Girder 5 lateral bending moment, k-ft

$\sum M_L$ (k-ft) = sum of the lateral bending moments at radial section, k-ft

$0.01 = \frac{23.36}{2057.53}$	Sample Equation 6
--------------------------------	--------------------------

The same equations and procedure was used for the ABAQUS and the SAP2000 girder lateral bending moment.

Vertical Bending Stresses During Slab Pour Representative Calculations

Sample calculations: Use G3 TF Section B-B Stage 10 (see Figure 249). Results shown in **BOLD**.

$\mu\epsilon = 0.391 * B * R_0$	Equation 7
---------------------------------	-------------------

where,

$\mu\epsilon$ = microstrain ($\mu\epsilon$)

B = batch gage factor

R_0 = reading from data-logger

$399.66 = 0.391 * 0.91 * 1123.24$	Sample Equation 8
-----------------------------------	--------------------------

$\sigma = \frac{\mu\epsilon * E}{1000000}$	Equation 9
--	-------------------

where,

σ = stress, ksi

$\mu\epsilon$ = microstrain ($\mu\epsilon$)

E = steel elastic modulus, ksi

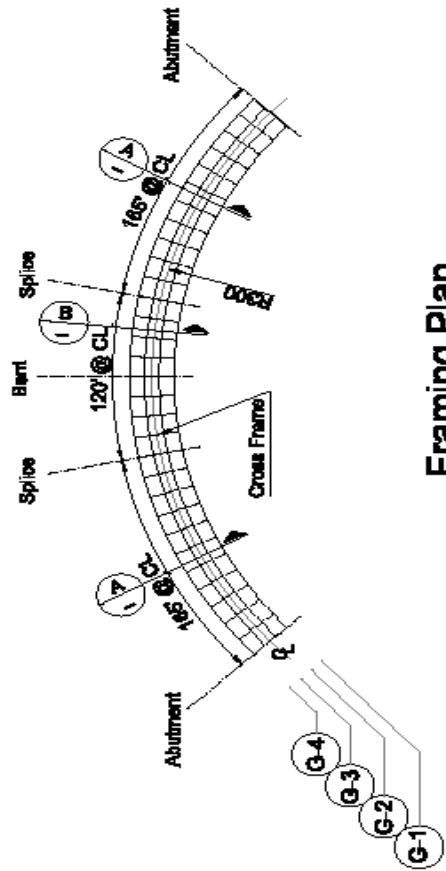
$11.59 = \frac{399.66 * 29000}{1000000}$	Sample Equation 10
--	---------------------------

10 APPENDIX C

Parametric Study Bridges

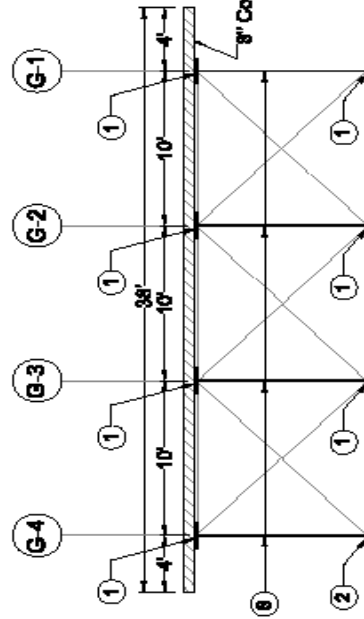
APPENDIX C-1

Curved Bridge Drawings

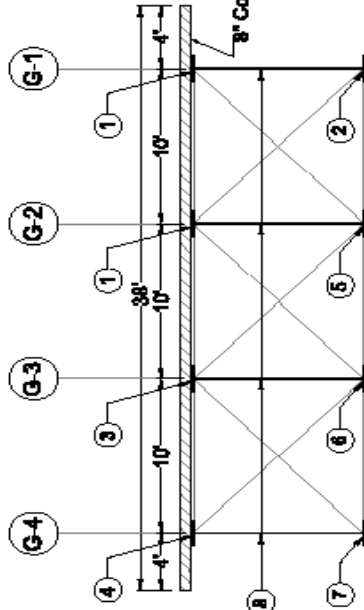


Framing Plan

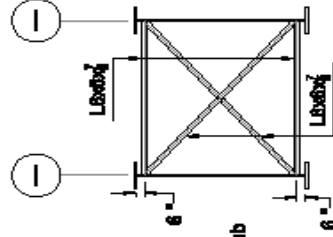
Bill of Material		
No.	Description	Slenderness
1	PL 1" x 20	Non-Compact Flange
2	PL 1 1/2" x 20	Compact Flange
3	PL 1 1/2" x 20	Compact Flange
4	PL 1 1/2" x 20	Compact Flange
5	PL 1 1/2" x 20	Compact Flange
6	PL 2 1/2" x 20	Compact Flange
7	PL 2 1/2" x 20	Compact Flange
8	PL 1/2" x 115	Non-Compact Web



Section A
Abut. - Splice



Section B
Splice - Splice



Cross Frame Detail

JOB NAME:

Bridge-C1

DATE:

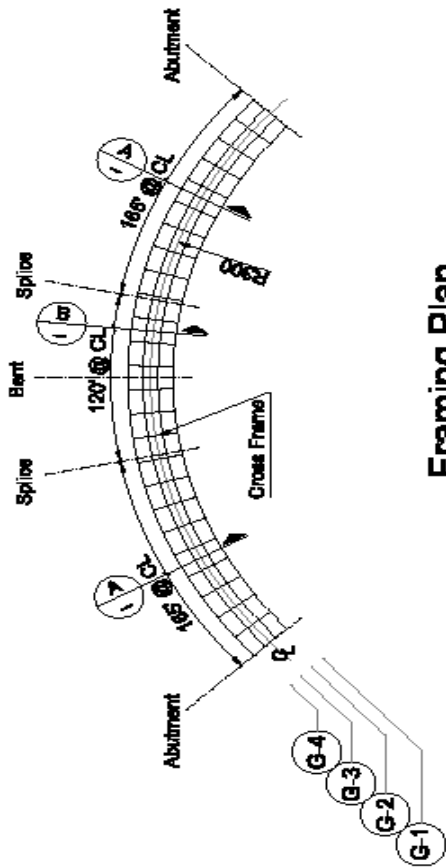
08-14-10

SHEET:

△

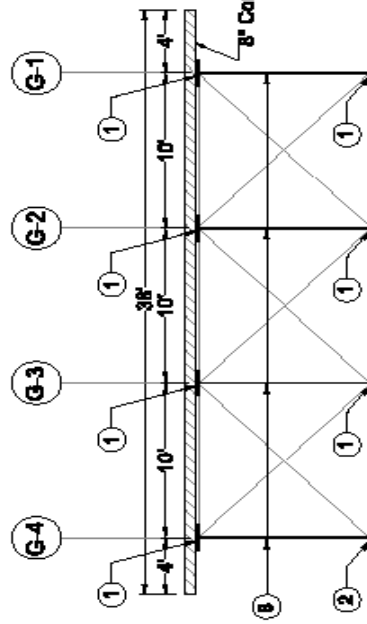
DESCRIPTION:

R=300 ft, Cross Frame Spacing= 10 ft, Girder Spacing= 10 ft, Span length= 220, 220 ft

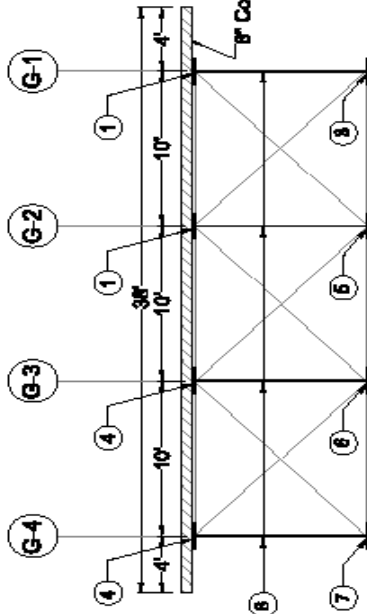


Framing Plan

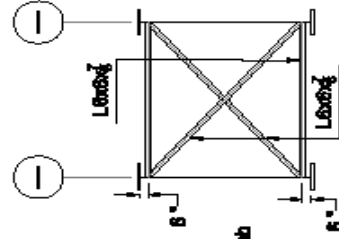
Bill of Material			
No.	Description	Quantity	Spans/Remarks
1	PL 1" x 20	1	Non-Compact Flange
2	PL 1 1/2" x 20	1	Compact Flange
3	PL 1 1/2" x 20	1	Compact Flange
4	PL 1 1/2" x 20	1	Compact Flange
5	PL 1 1/2" x 20	1	Compact Flange
6	PL 2 1/2" x 20	1	Compact Flange
7	PL 2 1/2" x 20	1	Compact Flange
8	PL 1/2" x 115	1	Non-Compact Web



Section A
Abut. - Splice

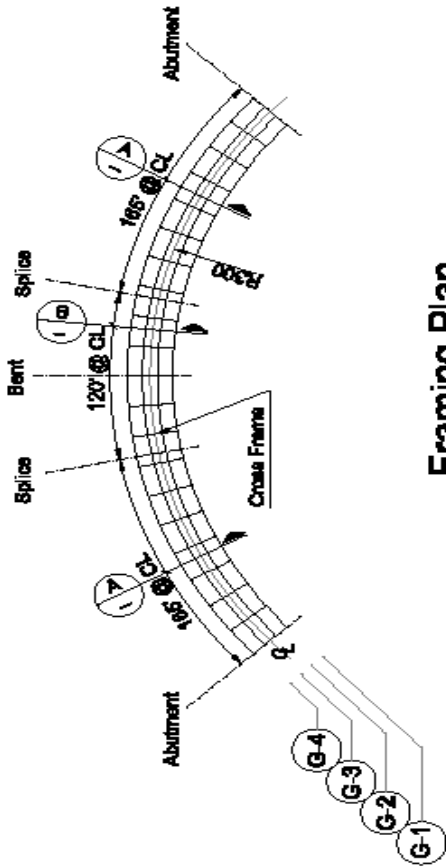


Section B
Splice - Splice



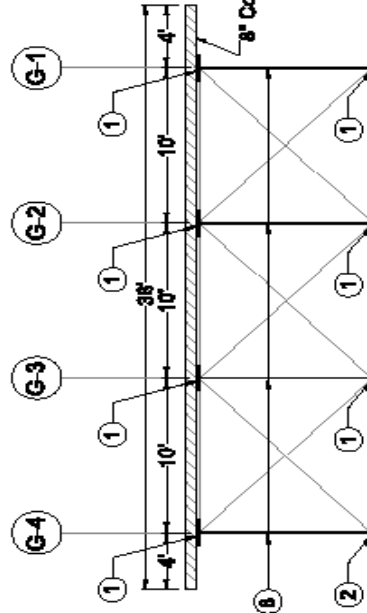
Cross Frame Detail

JOB NAME	DATE	SHEET
Bridge-C2	06-14-10	△
DESCRIPTION:		
R=300 ft, Cross Frame Spacing= 18 ft, Girder Spacing= 10 ft, Span length= 225,225 ft		

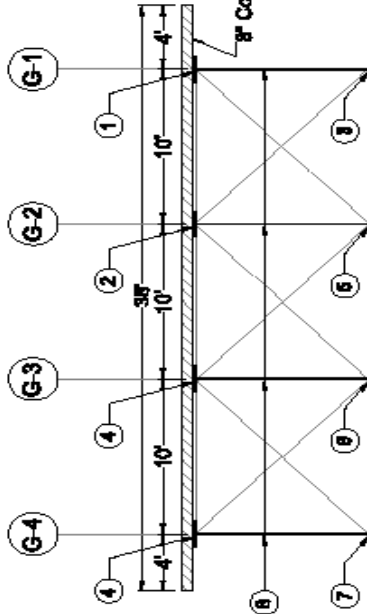


Framing Plan

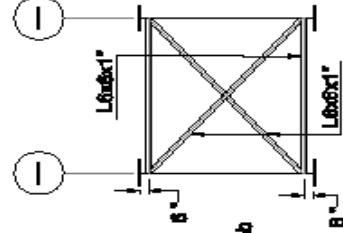
Bill of Material		
No.	Description	Slenderness
1	PL 1" x 20	Non-Compact Flange
2	PL 1 1/2" x 20	Compact Flange
3	PL 1 3/8" x 20	Compact Flange
4	PL 1 1/8" x 20	Compact Flange
5	PL 1 1/2" x 20	Compact Flange
6	PL 2 1/2" x 20	Compact Flange
7	PL 3" x 20	Compact Flange
8	PL 1/2" x 115	Non- Compact Web



Section A
Abut. - Splice

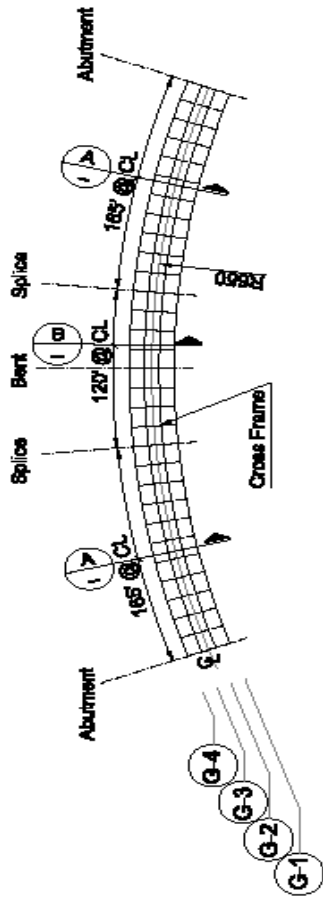


Section B
Splice - Splice



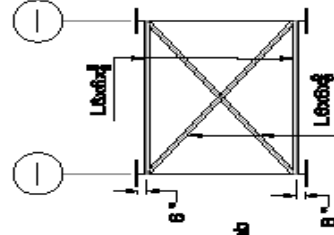
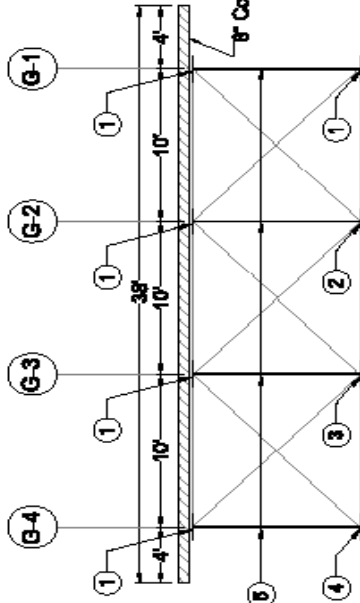
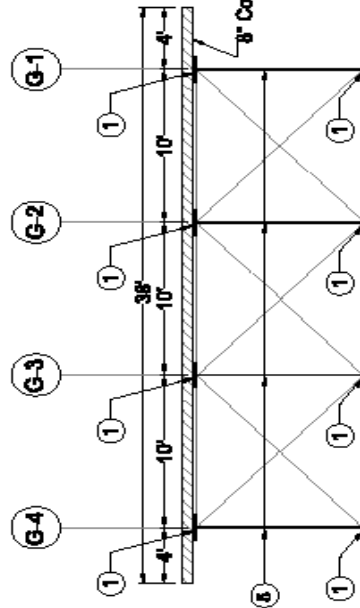
Cross Frame Detail

JOB NAME	DATE	SHEET
Bridge-C3	08-14-10	△
DESCRIPTION:		
R=300 ft, Cross Frame Spacing= 22.5 ft, Girder Spacing= 10 ft, Span length= 225,225 ft		



Framing Plan

Bill of Material		Slenderness
No.	Description	
1	PL 1" x 20	Non-Compact Flange
2	PL 1½" x 20	Compact Flange
3	PL 1½" x 20	Compact Flange
4	PL 2" x 20	Compact Flange
5	PL ½" x 115	Non-Compact Web

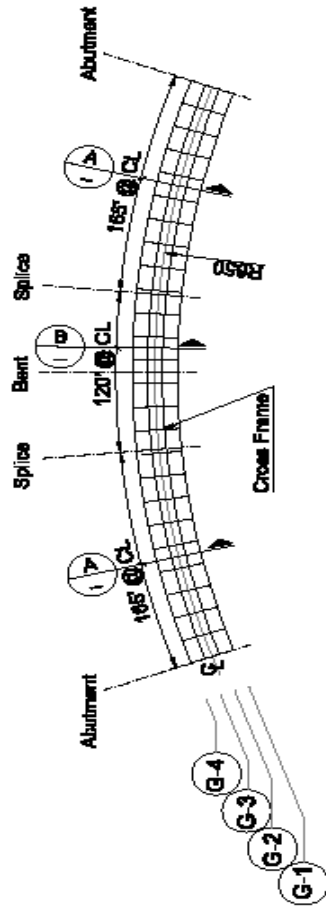


Section A
Abut. - Splice

Section B
Splice - Splice

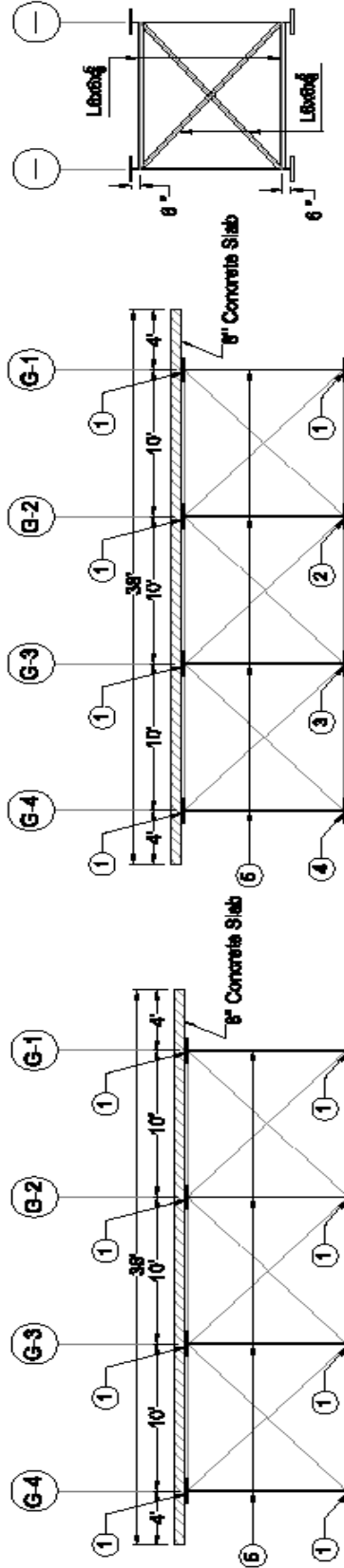
Cross Frame Detail

JOB NAME	DATE	SHEET
Bridge-C4	06-14-10	△
DESCRIPTION: R=660 ft, Cross Frame Spacing= 15 ft, Girder Spacing= 10 ft, Span length= 225, 225 ft		



Framing Plan

Bill of Material		
No.	Description	Slenderness
1	PL 1" x 20	Non-Compact Flange
2	PL 1½ x 20	Compact Flange
3	PL 1½ x 20	Compact Flange
4	PL 2" x 20	Compact Flange
5	PL ½ x 116	Non- Compact Web



Section A
Abut - Splice

Section B
Splice - Splice

Cross Frame Detail

JOB NAME:

Bridge-C5

DATE:

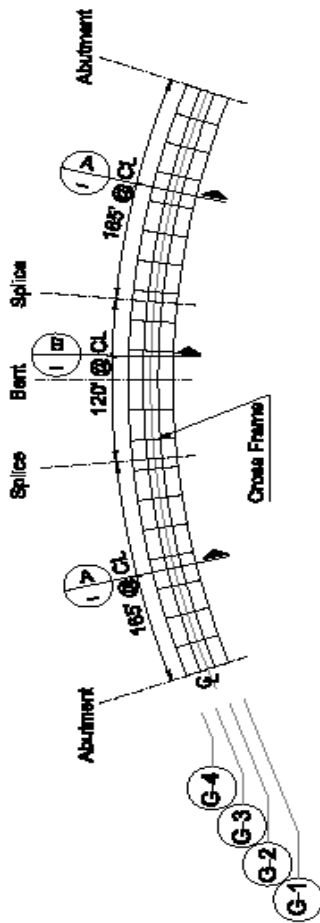
08-14-10

SHEET:

△

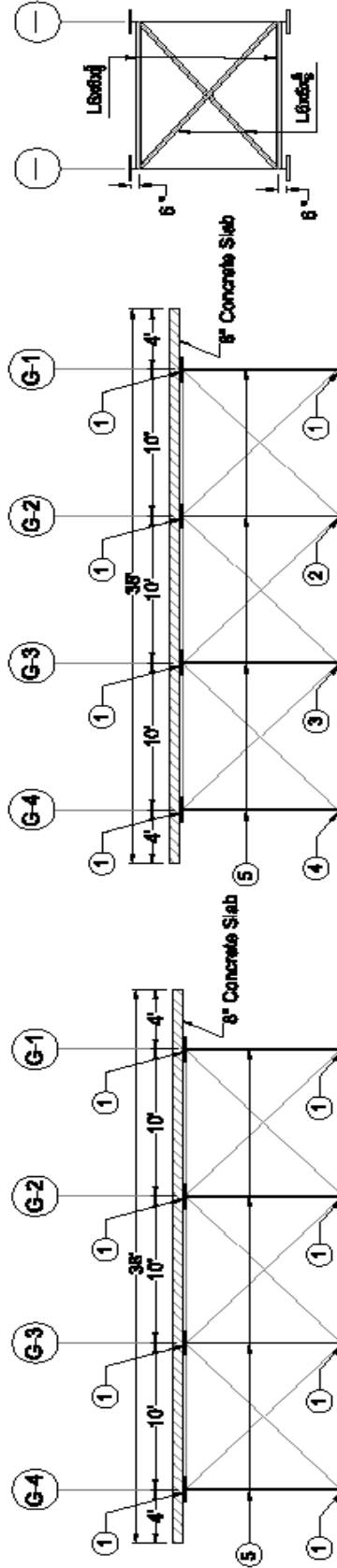
DESCRIPTION:

R=660 ft, Cross Frame Spacing= 18 ft, Girder Spacing= 10 ft, Span length= 228, 226 ft



Bill of Material		
No.	Description	Slenderness
1	PL 1" x 20	Non-Compact Flange
2	PL 1 1/2" x 20	Compact Flange
3	PL 1 1/2" x 20	Compact Flange
4	PL 2 1/2" x 20	Compact Flange
5	PL 7/8" x 115	Non-Compact Web

Framing Plan

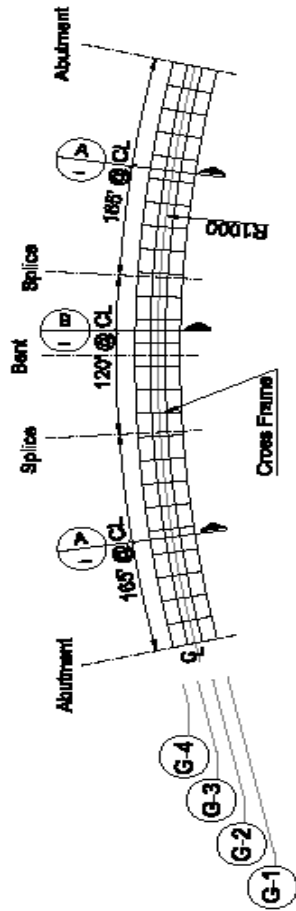


Section A
Abut. - Splice

Section B
Splice - Splice

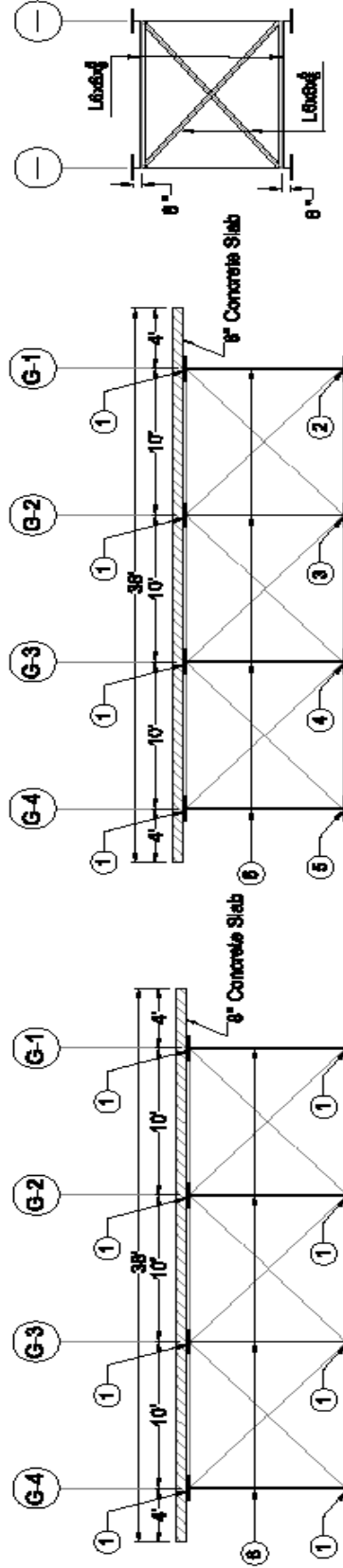
Cross Frame Detail

JOB NAME	DATE	SHEET
Bridge-C6	06-14-10	△
DESCRIPTION: R=600 ft, Cross Frame Spacing= 22.6 ft, Girder Spacing= 10 ft, Span length= 226,226 ft		



Bill of Material		
No.	Description	Slenderness
1	PL 1" x 20	Non-Compact Flange
2	PL 2" x 20	Compact Flange
3	PL 2½ x 20	Compact Flange
4	PL 2½ x 20	Compact Flange
5	PL 2½ x 20	Compact Flange
6	PL ½ x 110	Non- Compact Web

Framing Plan



Section A

Abut. - Splice

Section B

Splice - Splice

Cross Frame Detail

JOB NAME

Bridge-C8

DATE:

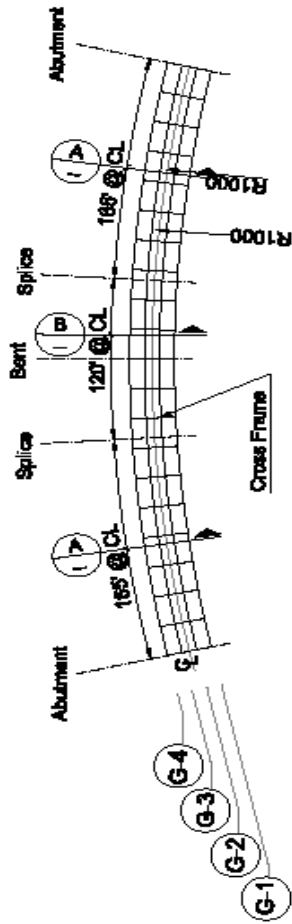
08-14-10

SHEET:

△

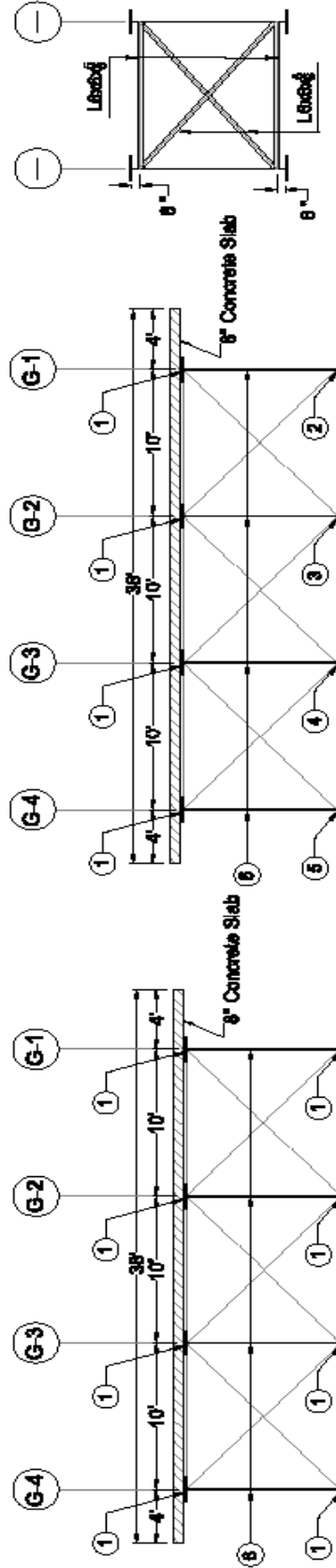
DESCRIPTION:

R=1000 ft, Cross Frame Spacing= 16 ft, Girder Spacing= 10 ft, Span length= 226, 226 ft.



Framing Plan

Bill of Material			
No.	Description	Quantity	Remarks
1	PL 1" x 20		Non-Compact Flange
2	PL 2" x 20		Compact Flange
3	PL 2 1/4" x 20		Compact Flange
4	PL 2 1/2" x 20		Compact Flange
5	PL 2 3/4" x 20		Compact Flange
6	PL 3/4" x 110		Non-Compact Web

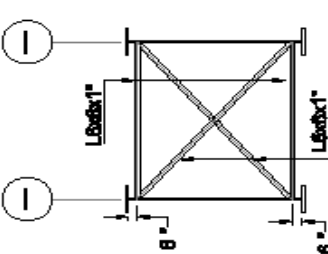
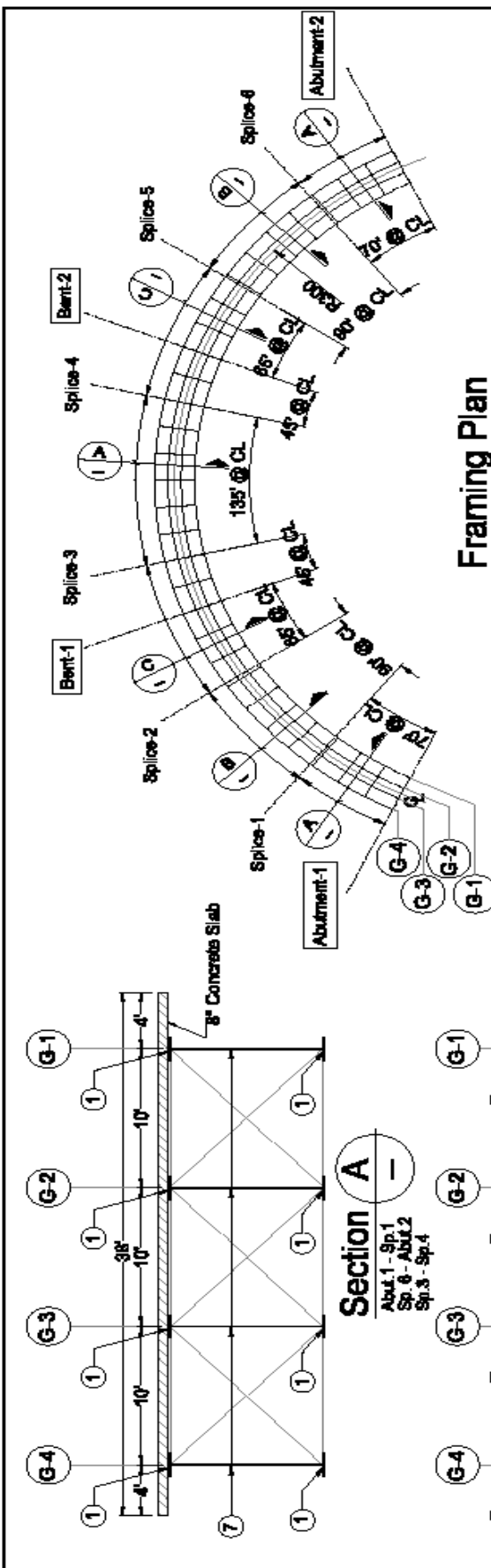


Section A
Abut. - Splice

Section B
Splice - Splice

Cross Frame Detail

JOB NAME	DATE	SHEET
Bridge-C9	08-14-10	△
DESCRIPTION: R=1000 ft, Cross Frame Spacing= 22.5 ft, Girder Spacing= 10 ft, Span length= 225.225 ft		



Bill of Material

No.	Description	Slenderness
1	PL 1" x 20	Non-Compact Flange
2	PL 1 1/2" x 20	Compact Flange
3	PL 1 3/4" x 20	Compact Flange
4	PL 1 3/4" x 20	Compact Flange
5	PL 1 3/4" x 20	Compact Flange
6	PL 2 1/2" x 20	Compact Flange
7	PL 1/2" x 116	Non-Compact Web

Cross Frame Detail

Section A
 Abut. 1 - Sp.1
 Sp. 6 - Abut.2
 Sp.3 - Sp.4

Section B
 Sp. 1 - Sp.2
 Sp.5 - Sp.6

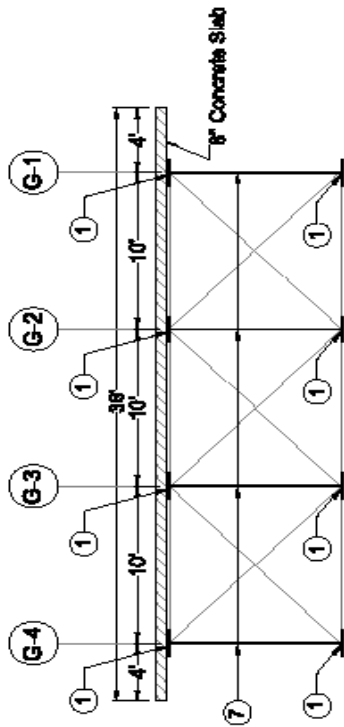
Section C
 Sp.2 - Sp.3
 Sp.4 - Sp.5

JOB NAME: **Bridge-C10**

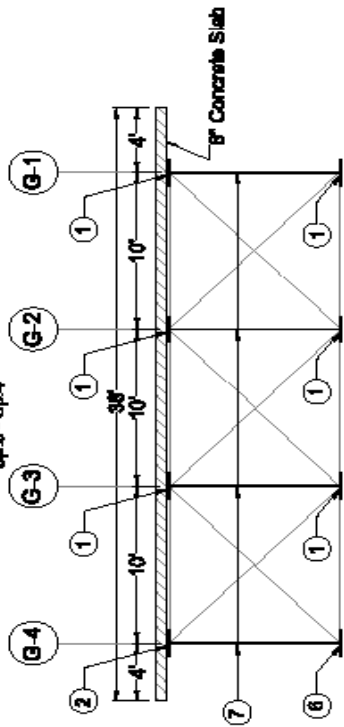
DATE: 06-14-10

SHEET: Δ

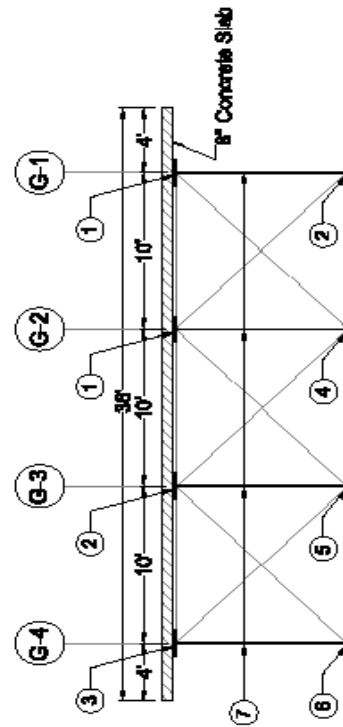
DESCRIPTION: R=300 ft, Cross Frame Spacing= 22.5 ft, Girder Spacing= 10 ft, Span length= 225, 225, 225 ft



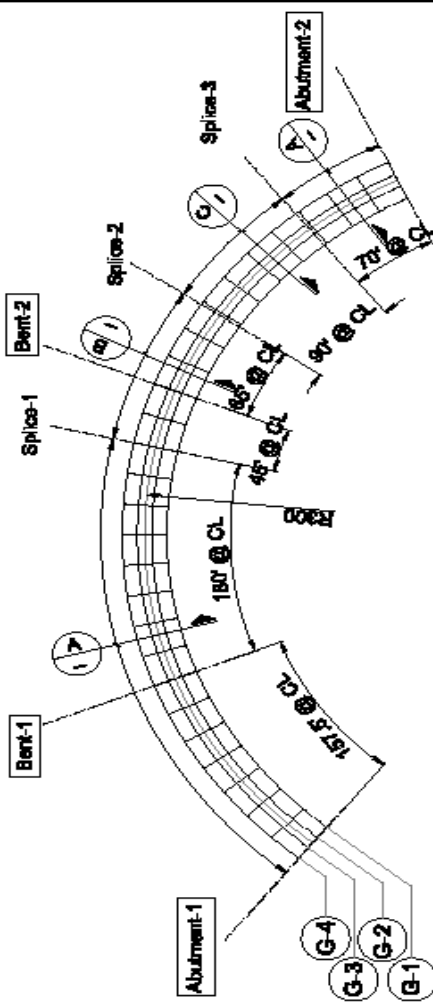
Section A
 Abut. 1 - Sp. 1
 Sp. 6 - Abut. 2
 Sp. 3 - Sp. 4



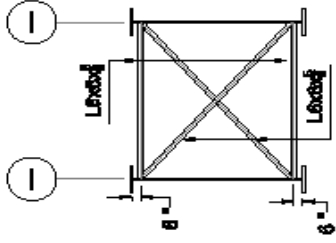
Section B
 Sp. 1 - Sp. 2
 Sp. 5 - Sp. 6



Section C
 Sp. 2 - Sp. 3
 Sp. 4 - Sp. 5



Framing Plan



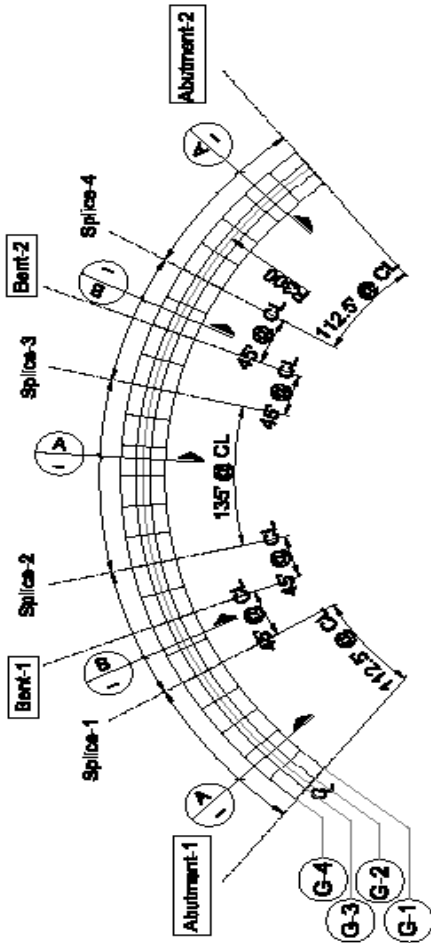
Cross Frame Detail

Bill of Material		
No.	Description	Slenderness
1	FL 1" x 20	Non-Compact Flange
2	PL 1/2" x 20	Compact Flange
3	PL 1/2" x 20	Compact Flange
4	PL 1/2" x 20	Compact Flange
5	PL 2/3" x 20	Compact Flange
6	PL 2/3" x 20	Compact Flange
7	PL 1/2" x 115	Non-Compact Web

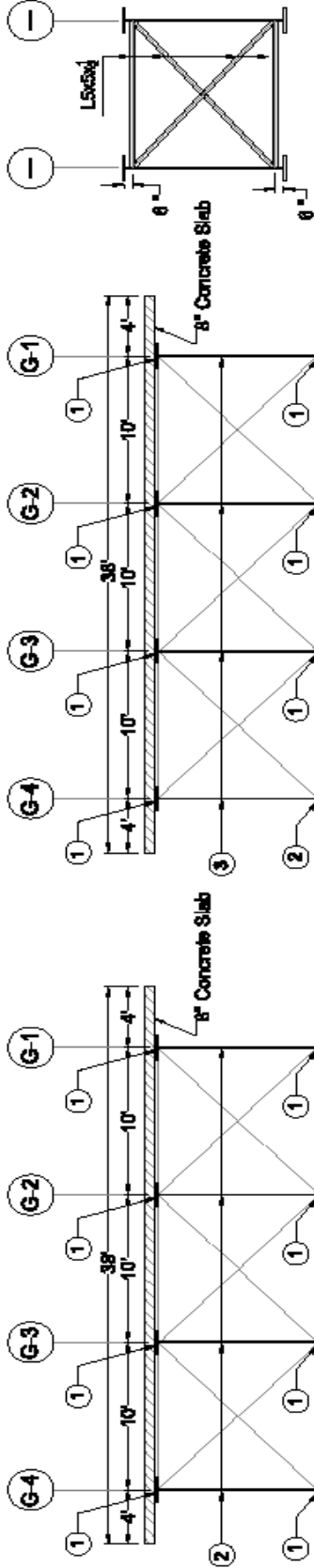
JOB NAME: **Bridge-C11** DATE: 06-14-10 SHEET: Δ

DESCRIPTION:
 R-300 ft, Cross Frame Spacing= 22.5 ft, Girder Spacing= 10 ft, Span length= 157.5, 215, 225 ft

Bill of Material		Slenderness
No.	Description	
1	PL 1" x 20	Non-Compact Flange
2	PL 1½" x 20	Compact Flange
3	PL ½" x 115	Non-Compact Web



Framing Plan



Cross Frame Detail

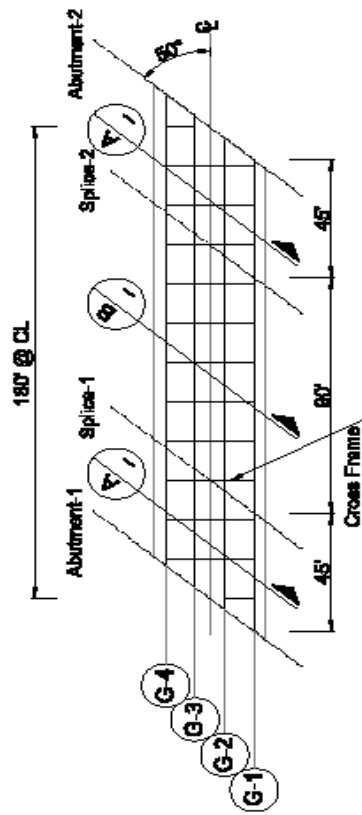
Section B
Sp.1 - Sp.2
Sp.5 - Sp.6

Section A
Abut.1 - Sp.1
Sp.6 - Abut.2
Sp.2 - Sp.3

JOB NAME:	Bridge-C12	DATE:	08-14-10	SHEET:	△
DESCRIPTION: R=300 ft, Cross Frame Spacing = 22.5 ft, Girder Spacing = 10 ft, Span length = 157.5, 225, 157.5 ft.					

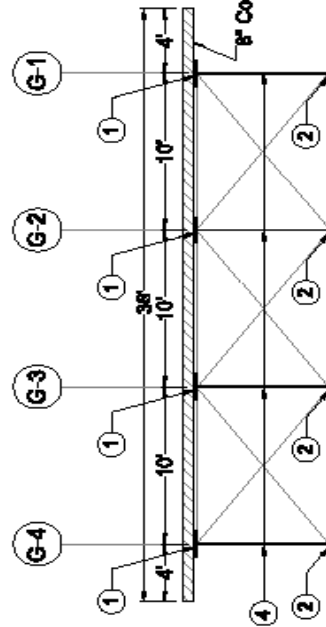
APPENDIX C-2

Skewed Bridge Drawings

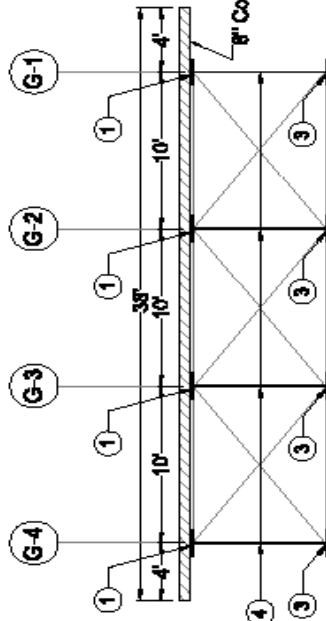


Framing Plan

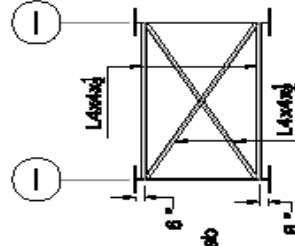
Bill of Material		
No.	Description	Slenderness
1	PL 1" x 20	Non-Compact Flange
2	PL 1 1/2" x 20	Compact Flange
3	PL 1 1/2" x 20	Compact Flange
4	PL 5/8" x 90	Slender Web



Section A
Abut 1 - Splice 1
Splice 2 - Abut 2



Section B
Splice 1 - Splice 2



Cross Frame Detail

JOB NAME:

Bridge-S1

DATE:

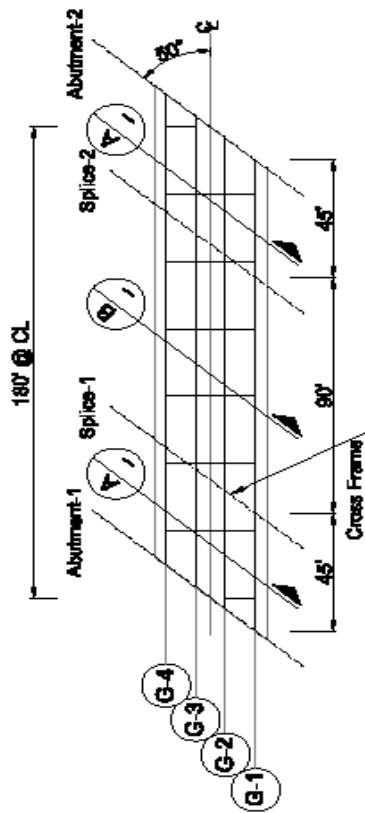
6-14-10

SHEET:

△

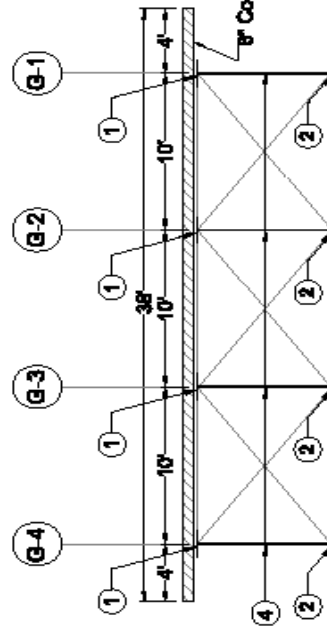
DESCRIPTION:

Skewness=50', Cross Frame Spacing= 15 ft, Girder Spacing= 10 ft, Span length= 180 ft

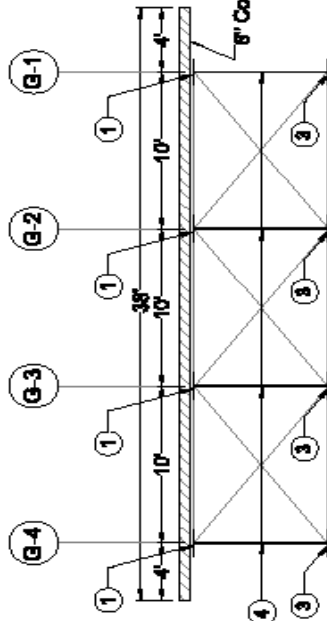


Framing Plan

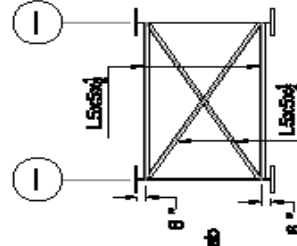
Bill of Material		Slenderness
No.	Description	
1	PL 1" x 20	Non-Compact Flange
2	PL 1½" x 20	Compact Flange
3	PL 1½" x 20	Compact Flange
4	PL ½" x 80	Slender Web



Section A
Abut.1 - Splice.1
Splice.2 - Abut.2



Section B
Splice.1 - Splice.2



Cross Frame Detail

JOB NAME:

Bridge-S2

DATE:

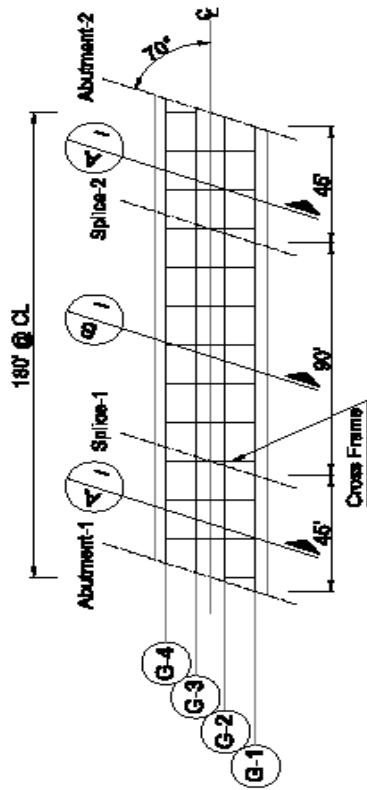
6-14-10

SHEET:

△

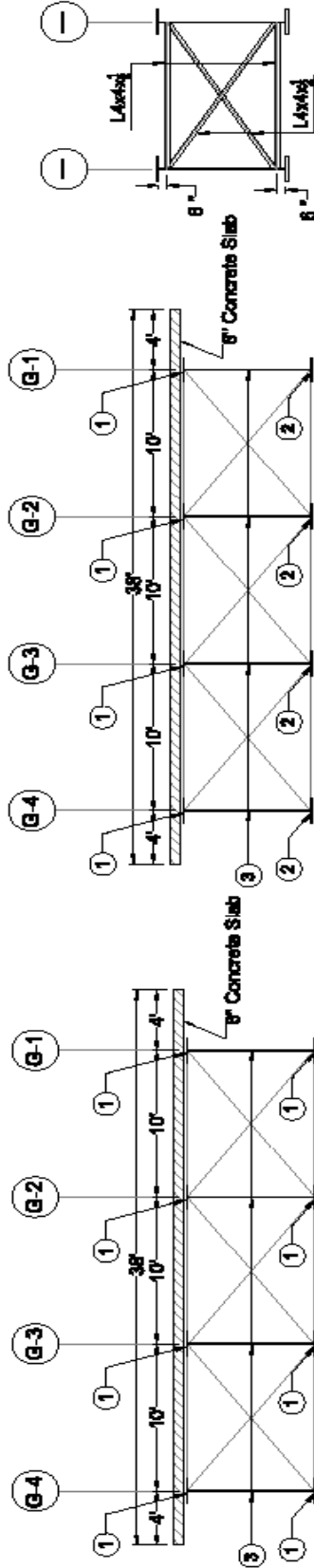
DESCRIPTION:

Skewness=50', Cross Frame Spacing= 25 @ 5', Girder Spacing= 10 ft, Span length= 180 ft



Bill of Material		
No.	Description	Slenderness
1	PL 1" x 20	Non-Compact Flange
2	PL 1 1/2" x 20	Compact Flange
3	PL 8" x 80	Slender Web

Framing Plan



Section A

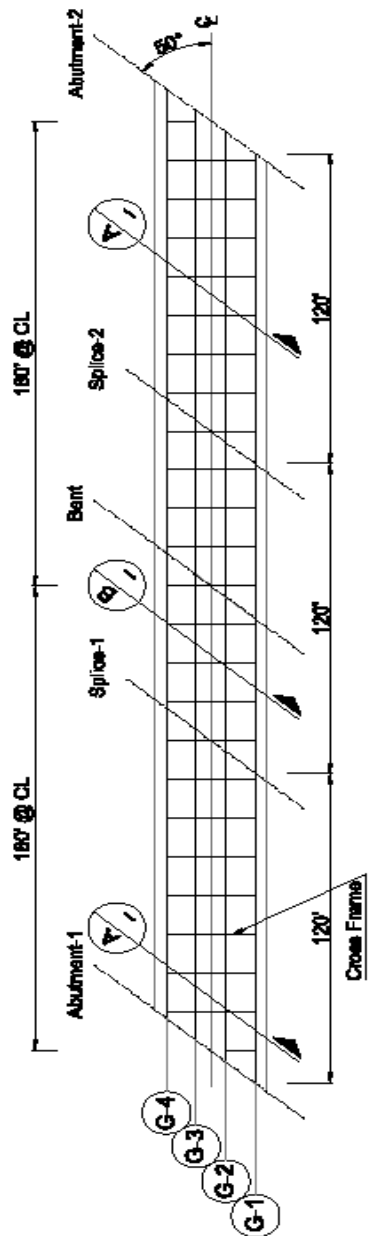
Abut 1 - Splice1
Splice2 - Abut.2

Section B

Splice1 - Splice2

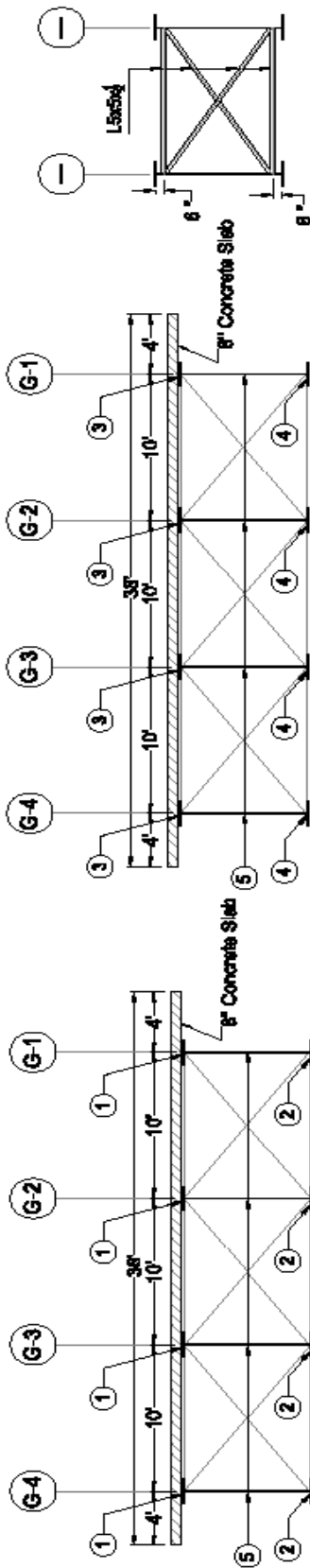
Cross Frame Detail

JOB NAME:	DATE:	SHEET:
Bridge-S3	6-14-10	△
DESCRIPTION: Skewness=70', Cross Frame Spacing= 15 ft, Girder Spacing= 10 ft, Span length= 180 ft		



Bill of Material		
No.	Description	Slenderness
1	PL 1" x 20	Non-Compact Flange
2	PL 1 1/2 x 20	Compact Flange
3	PL 1 1/2 x 20	Compact Flange
4	PL 2 1/2 x 20	Compact Flange
5	PL 1/2 x 80	Slender Web

Framing Plan

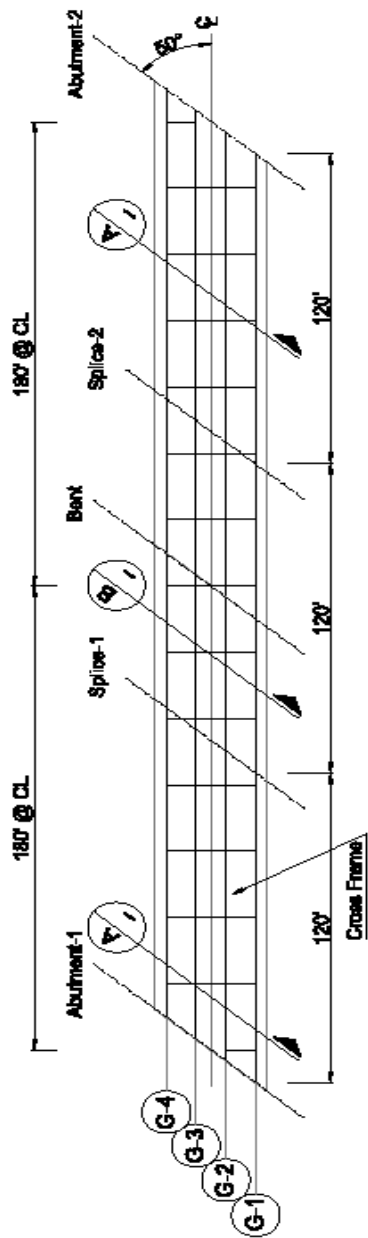


Section A
Abut 1 - Splice1
Splice2 - Abut.2

Section B
Splice1 - Splice2

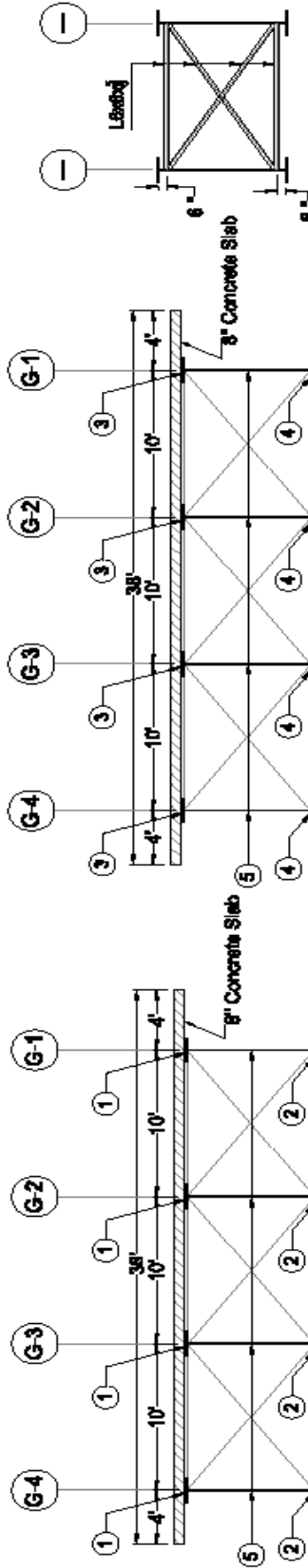
Cross Frame Detail

JOB NAME:	Bridge-S5	DATE:	6-14-10	SHEET:	△
DESCRIPTION:	Skewness=60', Cross Frame Spacing= 15 ft, Girder Spacing= 10 ft, Span length= 180,180 ft				



Bill of Material		
No.	Description	Slenderness
1	PL 1" x 20	Non-Compact Flange
2	PL 1½ x 20	Compact Flange
3	PL 1½ x 20	Compact Flange
4	PL 2½ x 20	Compact Flange
5	PL ½ x 80	Slender Web

Framing Plan

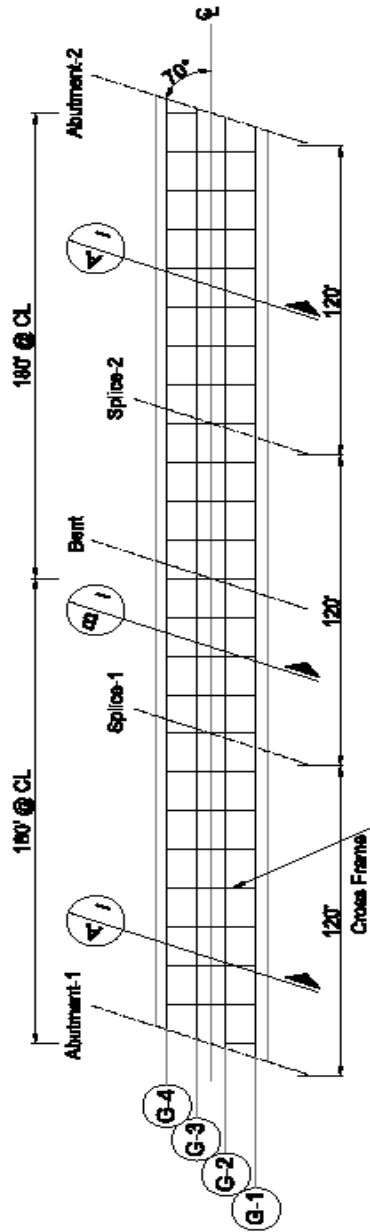


Cross Frame Detail

Section B
Splice-1 - Splice-2

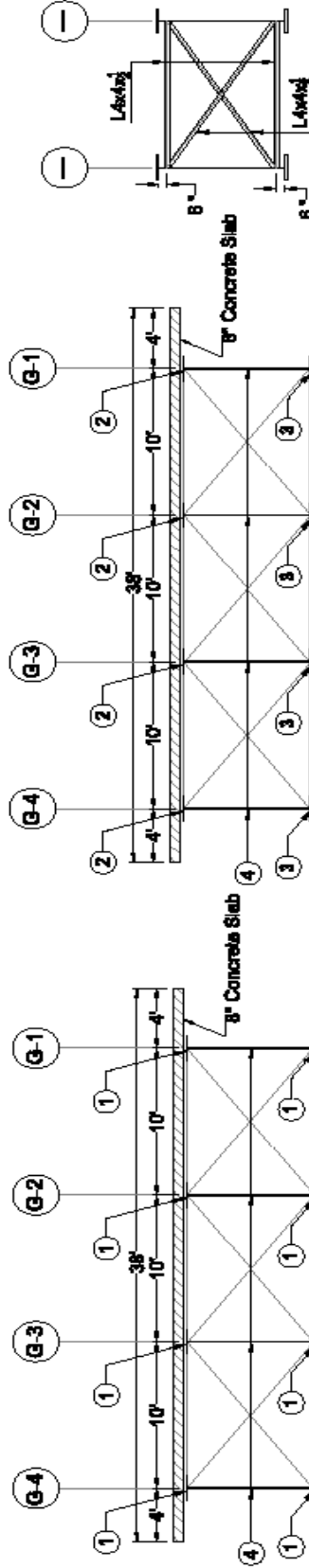
Section A
Abut-1 - Splice-1
Splice-2 - Abut-2

JOB NAME:	DATE:	SHEET:
Bridge-S6	8-14-10	△
DESCRIPTION: Skewness=50', Cross Frame Spacing= 25' & 5", Girder Spacing= 10 ft, Span length= 180, 180 ft		



Bill of Material		
No.	Description	Slenderness
1	PL 1" x 20	Non-Compact Flange
2	PL 1 1/2" x 20	Compact Flange
3	PL 2 1/2" x 20	Compact Flange
4	PL 3/4" x 80	Slender Web

Framing Plan

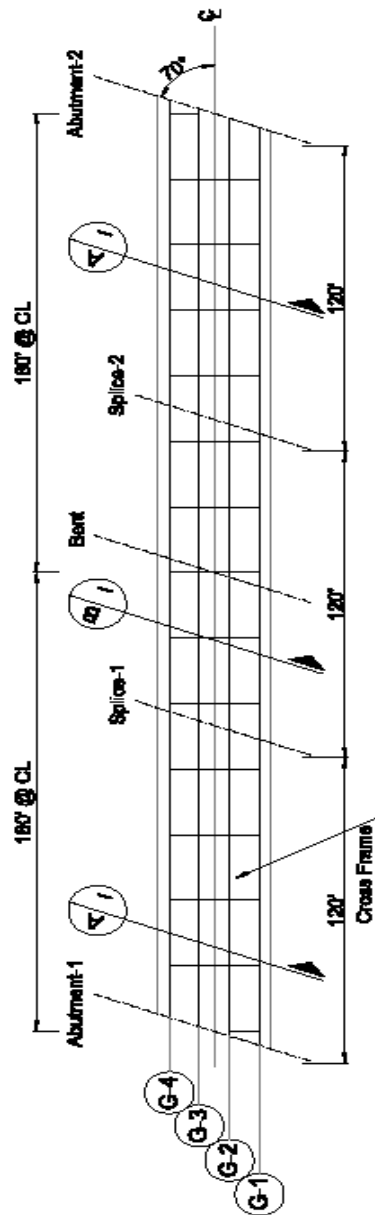


Cross Frame Detail

Section B
Splice1 - Splice2

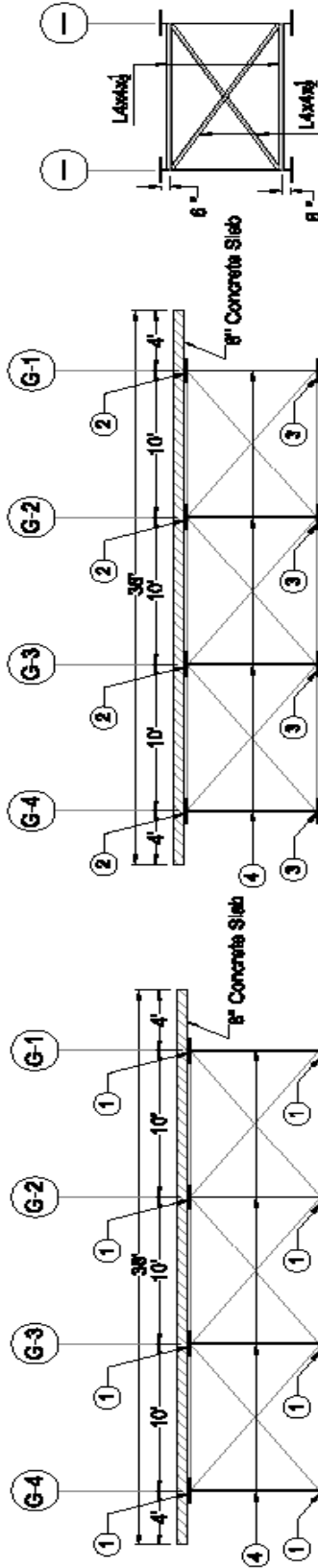
Section A
Abut.1 - Splice1
Splice2 - Abut.2

JOB NAME	DATE	SHEET
Bridge-S7	6-14-10	△
DESCRIPTION: Skewness=70', Cross Frame Spacing= 15 ft, Girder Spacing= 10 ft, Span length= 180,180 ft		



Bill of Material		
No.	Description	Slenderness
1	PL 1" x 20	Non-Compact Flange
2	PL 1½ x 20	Compact Flange
3	PL 2½ x 20	Compact Flange
4	PL ½ x 80	Slender Web

Framing Plan



Cross Frame Detail

Section A

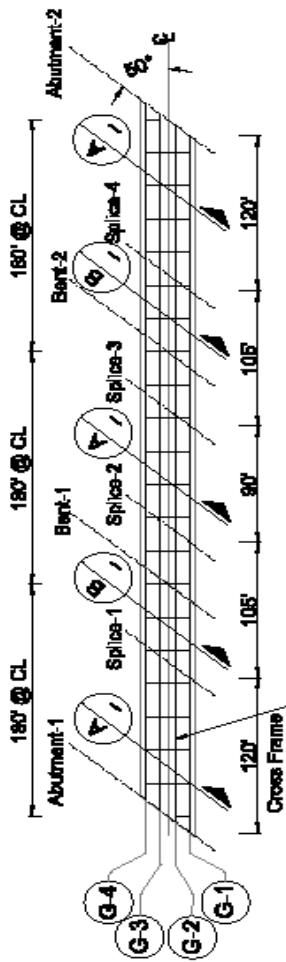
Abut.1 - Splice1
Splice2 - Abut.2

Section B

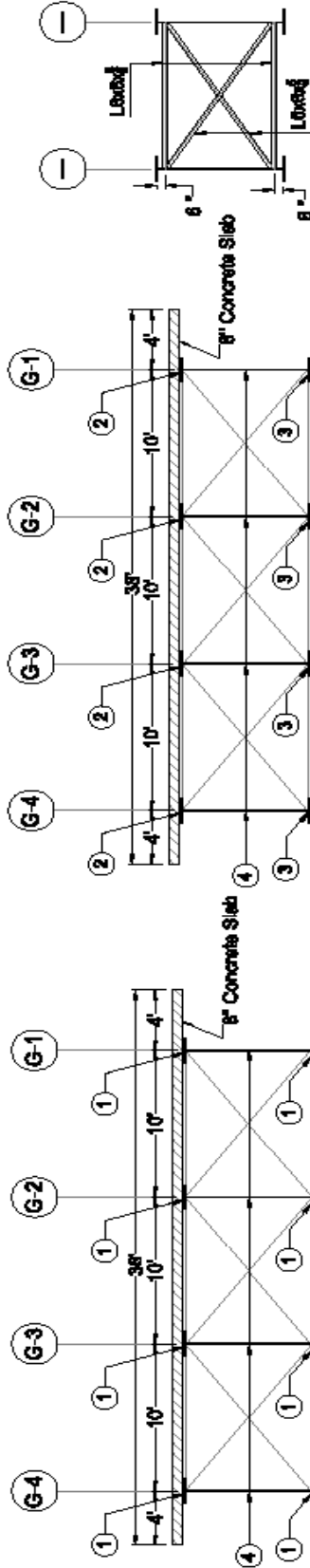
Splice1 - Splice2

JOB NAME:	Bridge-S8	DATE:	6-14-10	SHEET:	△
DESCRIPTION:	Slenderness=70, Cross Frame Spacing= 26' 8.6", Girder Spacing= 10 ft, Span length= 180, 180 ft				

Bill of Material		
No.	Description	Slenderness
1	PL 1" x 20	Non-Compact Flange
2	PL 1½" x 20	Compact Flange
3	PL 2½" x 20	Compact Flange
4	PL ½" x 90	Slender Web



Framing Plan

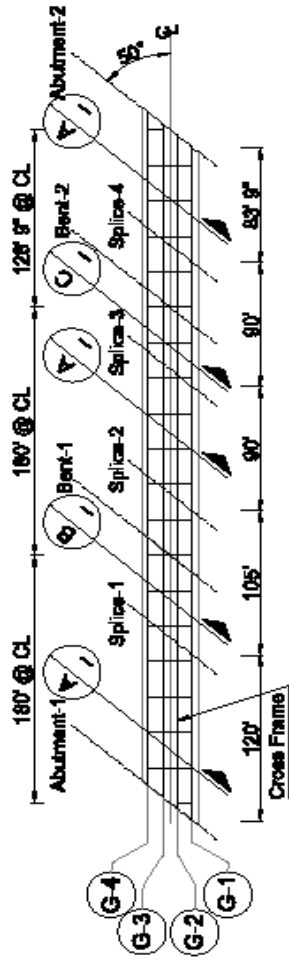


Cross Frame Detail

Section B
 Splice1 - Splice2
 Splice3 - Splice4

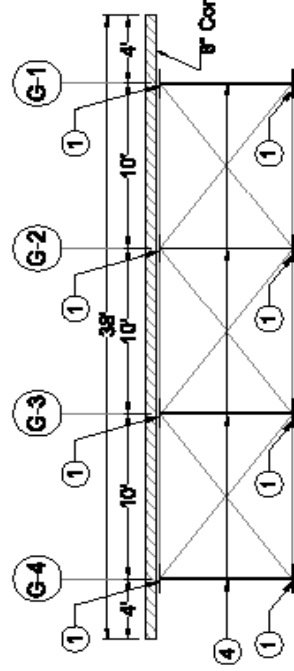
Section A
 Abut.1 - Splice1
 Splice4 - Abut.2
 Splice2 - Splice3

JOB NAME:	DATE:	SHEET:
Bridge-S9	6-14-10	△
DESCRIPTION: Span length= 160,180,180 ft Span Spacing= 10 ft, Girder Spacing= 25' & 6", Cross Frame Spacing= 10 ft, Span lengths= 160,180,180 ft		

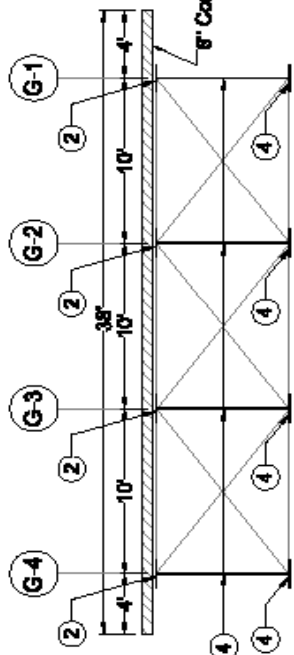


Framing Plan

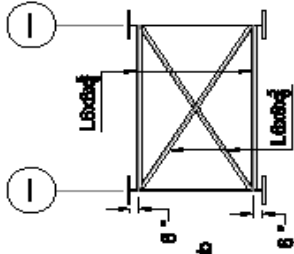
Bill of Material		
No.	Description	Slenderness
1	PL 1" x 20	Non-Compact Flange
2	PL 1½" x 20	Compact Flange
3	PL 1½" x 20	Compact Flange
4	PL 2½" x 20	Compact Flange
4	PL ½" x 90	Slender Web



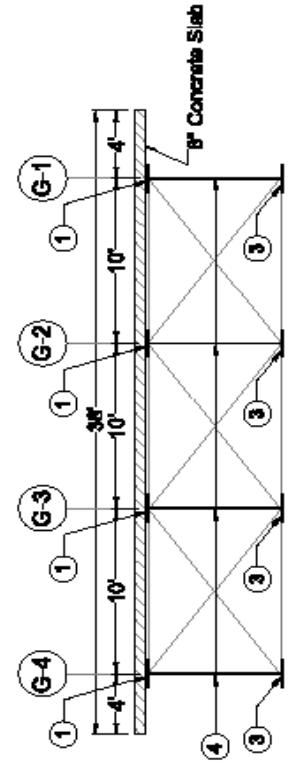
Section A
Abut 1 - Splice1
Splice2 - Abut 2



Section B
Splice1 - Splice2

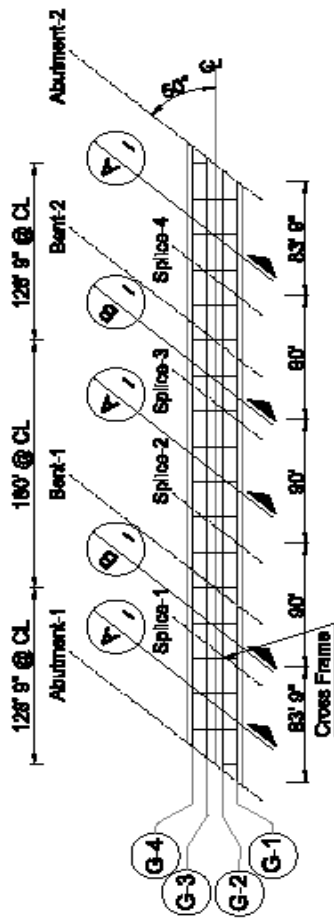


Cross Frame Detail



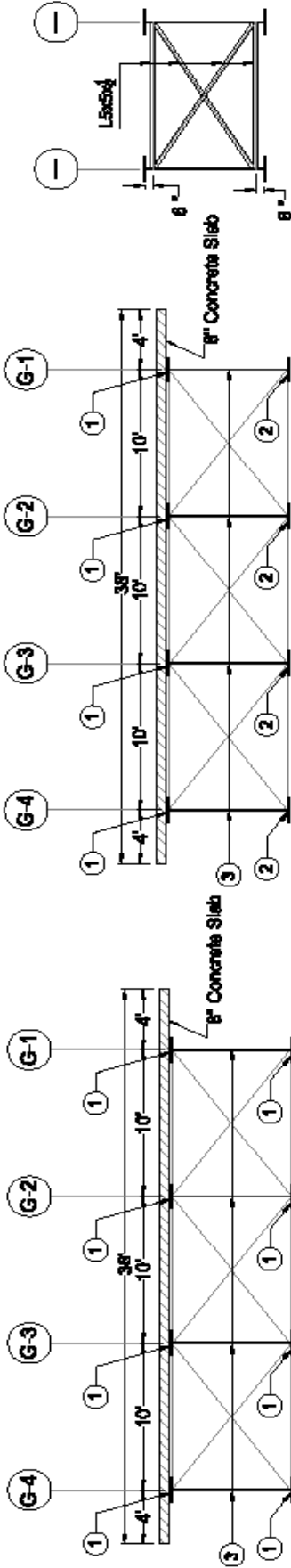
Section C
Abut 1 - Splice1
Splice2 - Abut 2

JOB NAME:	Bridge-S10	DATE:	6-14-10	SHEET:	△
DESCRIPTION: Skidness=50', Cross Frame Spacing= 25' & 6", Girder Spacing= 10 ft, Span lengths= 180', 180', 128' 7"					



Framing Plan

Bill of Material		
No.	Description	Slenderness
1	PL 1" x 20	Non-Compact Flange
2	PL 1/2" x 20	Compact Flange
3	PL 1/2" x 90	Slender Web



Section A

Abut. 1 - Splice 1
Splice 2 - Abut. 2
Splice 2 - Splice 3

Section B

Splice 1 - Splice 2
Splice 3 - Splice 4

Cross Frame Detail

JOB NAME:	Bridge-S11	DATE:	6-14-10	SHEET:	△
DESCRIPTION: Span length=128' 7", Span length= 128' 7", 128' 7" Slenderness=70', Cross Frame Spacing= 25' 8.6", Girder Spacing= 10 ft, Span length= 128' 7", 128' 7"					

11 APPENDIX D

PennDOT Documents

DESIGN MANUAL

PART 4

VOLUME 1

PART B: DESIGN SPECIFICATIONS

SECTION 2 - GENERAL DESIGN AND LOCATIONS FEATURES

SECTION 2 - TABLE OF CONTENTS

2.3 LOCATION FEATURES 1

2.3.2 Bridge Site Arrangement 1

2.3.2.2 TRAFFIC SAFETY 1

2.3.2.2.1 Protection of Structures 1

2.3.2.2.2 Protection of Users ii

2.3.2.2.3 Geometric Standards ii

2.3.3 Clearances ii

2.3.3.2 HIGHWAY VERTICAL ii

2.3.3.3 HIGHWAY HORIZONTAL iii

2.3.3.4 RAILROAD OVERPASS iii

2.5 DESIGN OBJECTIVES v

2.5.2 Serviceability vi

2.5.2.2 INSPECTABILITY vi

2.5.2.2.1P General vi

2.5.2.2.2P Inspection Walks vi

2.5.2.2.2aP General vi

2.5.2.2.2bP Design Live Load vii

2.5.2.2.2cP Geometry vii

2.5.2.2.2dP Connection to the Main Members vii

2.5.2.2.3P Inspectability for Enclosed Section vii

2.5.2.2.4P Girder Handrail vii

2.5.2.2.5P Sound Barriers vii

2.5.2.6 DEFORMATIONS vii

2.5.2.6.1 General vii

2.5.2.6.2 Criteria for Deflection viii

2.5.2.6.3 Criteria for Span-to-Depth Ratios ix

2.5.2.7 CONSIDERATION OF FUTURE WIDENING ix

2.5.2.7.1 Exterior Beams on Multi-Beam Bridges ix

2.5.3 Constructibility ix

2.5.3.1P FALSEWORK x

2.6 HYDROLOGY AND HYDRAULIC xii

2.6.6 Roadway Drainage xii

2.6.6.1 GENERAL xii

2.7P DESIGN DRAWINGS xiii

2.7.1P Moment and Shear Envelope Diagrams xiii

2.7.2P Major, Complex and Unusual Bridges xiv

2.7.2.1P LOAD DATA SHEET xiv

2.8P BRIDGE SECURITY xv

2.8.1P General xv

C3.1 SCOPE 1

3.3 NOTATION 1

3.3.1 General 1

3.4 LOAD FACTORS AND COMBINATIONS 1

3.4.1 Load Factors and Load Combinations 1

3.4.1.1P LOAD FACTORS AND COMBINATIONS FOR TYPICAL PENNDOT BRIDGE COMPONENTS 5

3.5 PERMANENT LOADS 19

3.5.1	Dead Loads: DC, DW and EV	19
3.5.1.1P	APPLICATION OF DEAD LOAD ON GIRDER AND BOX BEAM STRUCTURES	19
3.6	LIVE LOADS	19
3.6.1	Gravity Loads: LL, PL	19
3.6.1.1	VEHICULAR LIVE LOAD	19
3.6.1.1.2	Multiple Presence of Live Load	19
3.6.1.2	DESIGN VEHICULAR LIVE LOAD	20
3.6.1.2.1	General	20
3.6.1.2.3	Design Tandem	20
3.6.1.2.5	Tire Contact Area	20
3.6.1.2.6	Distribution of Wheel Loads through Earth Fills	21
3.6.1.2.7P	Design Permit Load	21
3.6.1.2.8P	Maximum Legal Load (ML-80)	22
3.6.1.3	APPLICATION OF DESIGN VEHICULAR LIVE LOADS	22
3.6.1.3.1	General	22
3.6.1.3.2	Loading for Live Load Deflection Evaluation	23
3.6.1.3.3	Design Loads for Decks, Deck Systems, and the Top Slab of Box Culverts	24
3.6.1.3.4	Deck Overhang Load	24
3.6.1.4	FATIGUE LOAD	25
3.6.1.4.2	Frequency	25
3.6.1.5	RAIL TRANSIT LOAD	25
3.6.1.5.1P	General	25
3.6.1.5.2P	Distribution of Rail Transit Loads Through Earth Fill	25
3.6.1.6	PEDESTRIAN LOADS	29
3.6.2	Dynamic Load Allowance: IM	29
3.6.2.1	GENERAL	29
3.6.2.1.1P	Components for which IM is Applicable	29
3.6.2.1.2P	Components for which IM is Not Applicable	29
3.6.2.2	BURIED COMPONENTS	30
3.6.2.3	WOOD COMPONENTS	30
3.6.4	Braking Force: BR	30
3.6.5	Vehicular Collision Force CT	31
3.6.5.3	Vehicular Collision with barriers	31
3.8	WIND LOAD: WL AND WS	31
3.8.1	Horizontal Wind Pressure	31
3.8.1.2	WIND PRESSURE ON STRUCTURES: WS	31
3.8.1.2.1	General	31
C3.8.1.2.2	Loads from Superstructures	32
3.8.3	Aeroelastic Instability	32
3.8.3.4	WIND TUNNEL TESTS	32
3.9	ICE LOADS: IC	32
3.9.1	General	32
3.9.5	Vertical Forces due to Ice Adhesion	32
3.10	EARTHQUAKE EFFECTS: EQ	33
C3.10.1	General	33
3.10.2	Acceleration Coefficient	34
3.10.7	Response Modification Factors	35
3.10.7.1	GENERAL	35
3.10.9	Calculation of Design Forces	35
3.10.9.2	SEISMIC ZONE 1	35
3.10.9.3	SEISMIC ZONE 2	36
3.10.9.5	LONGITUDINAL RESTRAINERS	37
3.11	EARTH PRESSURE: EH, ES, LS AND DD	37
3.11.1	General	37
3.11.3	Presence of Water	37
3.11.5	Earth Pressure: EH	37
C3.11.5.2	AT-REST PRESSURE COEFFICIENT, k_o	37
C3.11.5.3	ACTIVE PRESSURE COEFFICIENT, k_a	38
3.11.5.4	PASSIVE PRESSURE COEFFICIENT, k_p	38
3.11.5.5	EQUIVALENT-FLUID METHOD OF ESTIMATING EARTH PRESSURES	40

3.11.5.6P EARTH PRESSURE FOR NONGRAVITY CANTILEVER WALLS	41
3.11.5.7 APPARENT EARTH PRESSURES FOR ANCHORED WALLS	47
3.11.5.6.1P Cohesionless Soils.....	48
3.11.5.7.2P Cohesive Soils.....	51
3.11.5.7.2a <i>Stiff to Hard, Including Fissured Cohesive Soils</i>	51
3.11.5.6.2bP <i>Very Soft to Medium-Stiff Cohesive Soils</i>	52
3.11.6 Surcharge Loads: ES and LS.....	55
3.11.6.4 LIVE LOAD SURCHARGE: LS	55
3.12 FORCE EFFECTS DUE TO SUPERIMPOSED DEFORMATIONS: TU, TG, SH, CR, SE.....	56
3.12.2 Uniform Temperature	56
3.12.2.1.1 TEMPERATURE RANGES	56
3.12.7 Minimum Temperature Force for Fixed Substructures.....	57
3.13 FRICTION FORCES: FR.....	58
3.14 VESSEL COLLISION: CV	58
3.14.1 General	58
3.14.2 Owner's Responsibility.....	58
C3.14.15 Protection of Substructures	58
3.15P FORCE TRANSFER TO SUBSTRUCTURE.....	59
3.15.1P Longitudinal Force.....	59
3.15.1.2P FORCE TRANSFER TO SUBSTRUCTURE	59
3.15.1.3P EFFECTIVE LENGTH FOR SUPERSTRUCTURE FORCES	59
3.15.1.4P FORCE RESOLUTION TO SUBSTRUCTURE	59
3.15.2P Transverse Force.....	60
3.15.2.1P FORCE TRANSFER TO SUBSTRUCTURE	60
3.15.2.2P EFFECTIVE LENGTHS FOR SUPERSTRUCTURE FORCES.....	61
3.15.2.3P FORCE RESOLUTION TO SUBSTRUCTURE	61
3.15.2.4P DETERMINATION OF BEARING REACTIONS	61

[THIS PAGE IS INTENTIONALLY LEFT BLANK]

SPECIFICATIONS

COMMENTARY

2.3 LOCATION FEATURES

2.3.2 Bridge Site Arrangement

2.3.2.2 TRAFFIC SAFETY

2.3.2.2.1 Protection of Structures

The following shall supplement A2.3.2.2.1.

The minimum lateral clearance for locating substructure units for bridges over highways or railroads shall be as follows:

- (a) For bridges over a highway, refer to Design Manual Part 2, Chapter 4.4.C for the minimum horizontal clearance for locating substructure units.
- (b) For bridges over railroads, see D2.3.3.4.

SPECIFICATIONS

2.3.2.2.2 Protection of Users

The following shall replace the last paragraph of A2.3.2.2.2.

Sidewalks on bridges shall be protected by barriers unless approved by the Department.

2.3.2.2.3 Geometric Standards

The following shall replace the last sentence of A2.3.2.2.3.

For roadway geometry refer to Design Manual, Part 2. For bridge-mounted barriers, structure-mounted guide rail and other protective devices refer to appropriate Standard Drawings.

2.3.3 Clearances

2.3.3.2 HIGHWAY VERTICAL

The following shall replace the first sentence of the first paragraph of A2.3.3.2.

Refer to Design Manual, Part 2, for minimum vertical clearance for overhead bridges.

The following shall supplement A2.3.3.2.

Vertical clearance over the width of the roadway, including shoulders, shall be provided in accordance with Design Manual, Part 2, Chapter 2, Section 2.21, and as follows:

- For bridges over railroads, see D2.3.3.4.
- Minimum required vertical clearance shall preferably be maintained within the recovery area. In calculating actual vertical clearance under a beam splice, an allowance of 20 mm {3/4 in.}, plus the thickness of the outside flange splice plate, shall be made.
- Vertical clearance is to be measured at any high point on the outer edge shoulder. 30 mm {1 in.} will be deducted from the actual measurement for posting purposes to account for minor variations as proper location of measurement and jumping of traveling vehicles.
- For vertical sag under the bridge, ensure that the vertical clearance is measured from a chord between any two high points along the traveling direction to account for the maximum truck length permitted on the road.

For prestressed concrete beams, do not take credit for beam camber in determining actual vertical clearance,

COMMENTARY

C2.3.2.2.2

The following shall replace the last paragraph of AC2.3.2.2.2.

An example where the Department may waive the sidewalk barrier requirement would be in an urban environment where a curbed approach walkways exists and the posted vehicular speed is less than or equal to 50 km/hr {30 mph}.

SPECIFICATIONS

COMMENTARY

unless the beam is cast or assembled specifically to provide vertical curvature of the bottom of the beam.

2.3.3.3 HIGHWAY HORIZONTAL

The following shall supplement the first paragraph of A2.3.3.3.

Refer to Design Manual, Part 2, for additional details on bridge widths, including criteria for bridges on Very Low Volume Roads.

2.3.3.4 RAILROAD OVERPASS

The following shall supplement A2.3.3.4. Pennsylvania Public Utility Commission (PUC) has jurisdiction on railroad overpass clearances.

Refer to Design Manual, Part 1A, Chapter 7, Section 12, for additional details where railroad are overpassed by a highway structure.

Structures carrying railroad tracks shall be designed according to AREMA specifications and the modifications adopted by the railroad system involved.

For structures carrying highways over railroad tracks, the minimum horizontal clearance, specified and provided, from the centerline of track shall be in accordance with Publication 371 and/or Railroad Form D-4279 to face of abutment or pier and shall be shown on the drawings. A 5500 mm {18'-0"} lateral clearance from the centerline of track shall be provided for off-track equipment on one side if requested by the railroad. Class 1 (major) railroads may require additional lateral clearance depending upon the need for drainage ditches and the roadway for off-track equipment. If track and abutment or piers are skewed relative to each other, horizontal clearances to the extremities of the structure shall also be shown. If the track is on a curve within 24 400 mm {80 ft.} of the crossing, additional horizontal clearance is required to compensate for the curve (refer to AREMA, Volume 2, Chapter 28). If a railroad requests clearance in excess of the above, complete justification of this request shall be provided. The agreement on the lateral and vertical clearances shall be reached with the operating railroad, or the determination from the PUC shall be secured prior to submitting for TS&L approval.

The minimum vertical clearance over the top of rail shall be in accordance with Publication 371 and/or Railroad Form D-4279 and shall be shown for each track on the drawings. If track and abutments or piers are skewed relative to each other, vertical clearances to the extremities of the structure should also be shown. Approval for any exception to the above minimum clearance over railroad tracks shall be secured from the operating railroad company or the PUC prior to submitting for TS&L approval.

To provide for a drainage ditch parallel to track, the elevation of the top of footings adjacent to track shall be at least 1100 mm {3'-6"} below the elevation of the top of rail,

SPECIFICATIONS

COMMENTARY

unless rock is encountered.

The edge of footing shall be at least 2200 mm {7 ft.} from the centerline of adjacent track.

If pier bents are used between 5480 mm {18 ft.} and 7620 {25 ft.} from the centerline of tracks, columns shall be protected by crash walls at least 760 mm {2'-6"} thick, which shall extend 3048 mm {10 ft.} above the top of rail and 1828 mm {6 ft.} for single column or 762 mm {2'-6"} for multi-column bents beyond the outside face of outside columns. The crash wall shall rest upon the column footings, extend 152 mm {6 in.} from the face of columns adjacent to traffic, and shall connect all columns in a pier bent. Solid piers with a minimum thickness of 760 mm {2'-6"} and a length of 6100 mm {20 ft.}, single column piers of minimum 1220 mm x 3800 mm {4'-0" x 12'-6"} dimensions or any solid pier sections with equivalent cross sections and minimum 760 mm {2'-6"} thickness negate the need to provide crash walls. Reinforcement to be designed in accordance with A3.6.5.2, but not less than horizontal bars of No. 19 at 300 mm {No. 6 at 12 in.} each face, and vertical stirrups of No. 13 at 300 mm {No. 4 at 12 in.}. Crash walls meeting the same dimension and reinforcement requirements as above shall also be provided in front of prefabricated walls.

Bridge scuppers shall not drain onto railroad tracks. Provision shall be made to direct surface water from the bridge area into an adequate drainage facility along the railroad track, in which case drainage approval by the railroad company is required prior to submission of final plans.

Safety provisions required during excavation in the vicinity of railroad tracks and substructures shall be in accordance with the Special Provision "Maintenance and Protection of Railroad Traffic".

Sheet piling used during excavation for protection of railroad tracks and substructure shall be designed according to AREMA specifications and shall be subject to approval by the railroad company. The use of caisson footings shall be evaluated in lieu of sheet piling and deep foundation.

Complete details of temporary track(s) or a temporary railroad bridge to be constructed by the Department's contractor shall be shown on the design drawings. Applicable railroad design standards or design drawings shall be referred to or duplicated on the design drawings.

For highway structures with sidewalks, protective fencing shall be provided on all structures crossing over railroads. The protective fence shall extend at least 2440 mm {8 ft.} from top of sidewalk or driving surface adjacent to the barrier wall. The fence may be placed on top of the barrier wall.

All railroad clearances shall be based on the railroad's current design criteria.

For electrified railroad tracks, these additional requirements apply:

- If a railroad is electrified, it shall be so noted on the

SPECIFICATIONS

COMMENTARY

preliminary plans submitted for type, size and location approval.

- Protective barrier shall be provided on spans or on part of spans for structures over electrified railroads, as directed by the railroad company. Generally, the protective barrier shall extend at least 3100 mm {10 ft.} beyond the point at which any electrified railroad wire passes under the bridge. However, in no case shall the end of the protective barrier be less than 3100 mm {10 ft.} from the wire measured in a horizontal plane and normal to the wire outside of the limit of the bridge, and less than 1900 mm {6 ft.} from the wire within the limit of the bridge.
- Details of protective barriers are shown on Standard Drawing BC-711M. If conditions warrant or if directed by the railroad company, details shall be modified. Such modifications shall be shown on the design drawings.
- All open or expansion joints in the concrete portion of barriers, divisors, sidewalks, and curbs within the limits of the barrier shall be covered or closed with joint materials. Details of such joints shall be shown on the design drawings.
- In the case of bridges crossing electrified railroad tracks, the details of catenary attachments and their locations, if attached or pertinent to the structure, shall be shown on the plans. Consideration shall be given to realign the catenary by installing support columns on each side of the bridge to avoid catenary attachments to the bridge. Normally, ground cable attachments, cables, miscellaneous materials, etc. are supplied by the contractor and are installed by the railroad. A separate block identifying materials required, description of materials, railroad reference number for materials, and party responsible for providing or installing materials shall be shown on the plans. Approval of grounding plans shall be obtained from the railroad concurrently with approval of the structure drawings.

Where the PUC has jurisdiction over the structure involved, PUC Docket Number, either A.____ or C.____ (A stands for Application and C stands for complaint) shall be shown on the first sheet of the design drawings (S-drawings) above the title block, after the PUC has approved the plans.

The responsible designer shall add the PUC Docket Number on all plans, and the District shall add the PUC Docket Number in BMS where the PUC has jurisdiction over the structure involved.

Where applicable, the USDOT/AAR number of the existing structure shall be shown on the first sheet of the design drawings.

2.5 DESIGN OBJECTIVES

SPECIFICATIONS

COMMENTARY

2.5.2 Serviceability

2.5.2.2 INSPECTABILITY

D2.5.2.2.1P, D2.5.2.2.2P, D2.5.2.2.3P and D2.5.2.2.4P shall replace A2.5.2.2.

2.5.2.2.1P General

Inspection and maintenance instructions and requirements for critical details shall be stipulated on the plans. The plans shall also include reference to the method of access for inspection of the subject details.

It is necessary to have adequate means of access for bridge safety inspection. Review bridge designs for inspectability at TS&L, final design and construction stages. PP3.6.6 provides information for checking a structures inspectability with PennDOT's underbridge crane.

For special bridge conditions, the inspectability shall be as determined by the Chief Bridge Engineer.

2.5.2.2.2P Inspection Walks

2.5.2.2.2aP *General*

Unless approved otherwise, inspection walks shall be provided for long bridges (over 300 000 mm {1,000 ft.}) which cannot be readily inspected using inspection crane or which are otherwise inaccessible from underneath. Generally, inspection walks are required under the following conditions:

- Bridge width over 18 000 mm {60 ft.}, inaccessible from underneath
- Superstructure depth over 3500 mm {11.5 ft.}, including beams, barrier, railing or fencing, and noise walls, inaccessible from underneath
- High bridge underclearance (in excess of 9000 mm {30 ft.}), particularly for bridges over large rivers

SPECIFICATIONS

COMMENTARY

2.5.2.2.2bP Design Live Load

A minimum design live load of 3.8 kN/m² {80 psf} shall be used.

2.5.2.2.2cP Geometry

The minimum width shall be 1200 mm {4 ft.}. The minimum overhead clearance shall be 1800 mm {6 ft.}. Toe guard protection and railing shall be provided if the walk is not protected by the girders. The walk shall be secured against vandalism and shall not provide entrance to the general public. The entrances shall be locked or secured against access. Provision shall be made to cross from one bay to the next, generally at pier locations for at least one person, 1800 mm {6 ft.} in height, carrying tools and equipment.

2.5.2.2.2dP Connection to the Main Members

Generally, a bolted or threaded insert type of connection shall be provided to secure the walks in position. Lock washers or another positive connection device shall be specified to protect the connection from being loosened due to bridge vibration.

2.5.2.2.3P Inspectability for Enclosed Section

Vent holes and large size (600 mm by 900 mm {2 ft. by 3 ft.} minimum and 900 mm by 1200 mm {3 ft. by 4 ft.} desirable opening) inspection hatches shall be provided for large-span box structures; provision for lighting, cross ventilation, and steps shall be made where required. Large box sections shall have a coat of white paint on the interior.

2.5.2.2.4P Girder Handrail

Where other inspection facilities are not provided, handrails shall be attached to the web of steel girders greater than 1800 mm {72 in.} in depth.

2.5.2.2.5P Sound Barriers

Sound barriers shall be designed and detailed to maintain bridge inspectability. For special conditions, the inspectability shall be determined by the Chief Bridge Engineer.

2.5.2.6 DEFORMATIONS

2.5.2.6.1 General

The following shall replace A2.5.2.6.1.
Bridges shall be designed to avoid undesirable structural or psychological effects due to their deformations.

C2.5.2.6.1

The following shall replace AC2.5.2.6.1.
Service load deformations may cause deterioration of wearing surfaces and local cracking in concrete slabs and in metal bridges which could impair serviceability and

SPECIFICATIONS

2.5.2.6.2 Criteria for Deflection

The following shall replace A2.5.2.6.2.

In applying criteria for deflection, the vehicular load shall include the dynamic load allowance.

To control deflections of structures, the following principles shall apply:

- when investigating the maximum absolute deflection, all design lanes should be loaded, and all supporting components should be assumed to deflect equally,
- for composite design, the design cross-section should include the entire width of the roadway, neglecting any stiffness contribution by barrier, railing or other secondary members of the bridge,
- when investigating maximum relative displacements, the number and position of loaded lanes should be selected to provide the worst differential effect,
- the live load portion of Load Combination Service I of Table A3.4.1-1 should be used, including the dynamic load allowance, IM
- the live load shall be taken from D3.6.1.3.2,
- the provisions of A3.6.1.1.2 should apply,
- for skewed bridges, a normal cross-section may be used; for curved and curved skewed bridges a radial cross-section may be used.

The following deflection limits shall be used for steel, aluminum and/or concrete construction:

- vehicular load, general..... Span/800
- vehicular and/or pedestrian loads Span/1000
- vehicular load on cantilever arms Span/300
- vehicular and/or pedestrian loads on cantilever arms..... Span/375

For steel I-shaped beams and girders, the provisions of A6.10.4 and A6.11.4, respectively, regarding the control of permanent deflections through flange stress controls, shall apply.

The following deflection limits shall be used for wood construction:

- vehicular load, general..... Span/425

COMMENTARY

durability, even if self limiting and not a potential source of collapse.

C2.5.2.6.2

The following shall replace AC2.5.2.6.2.

For a multi-beam bridge, this is equivalent to saying that the distribution factor for deflection is equal to the number of lanes divided by the number of beams.

The weight of barrier, railing or other secondary members shall be included for deflection and design. Only the stiffness of these items should be neglected.

From a structural viewpoint, large deflections in wood components cause fasteners to loosen and brittle materials, such as asphalt pavement, to crack and break. In addition, members that sag below a level plane present a poor

SPECIFICATIONS

- vehicular and/or pedestrian loads Span/800
- vehicular load on wood planks and panels: extreme relative deflection between adjacent edges..... 2.5 mm { 1/8 in. }

The following provisions shall apply to orthotropic plate decks:

- vehicular load on deck plate Span/300
- vehicular load on ribs of orthotropic metal decks Span/1000
- vehicular load on ribs of orthotropic metal decks: extreme relative deflection between adjacent ribs..... 2.5 mm { 1/8 in. }

2.5.2.6.3 Criteria for Span-to-Depth Ratios

The following shall replace the first paragraph of A2.5.2.6.3.

Structures or components of structures shall satisfy the span-to-depth ratios given in Table A2.5.2.6.3-1

where:

S = slab span length (mm) {ft}

L = span length (mm) {ft}

Concrete decks on multi-girder-type bridges shall satisfy the span-to-depth ratios in Table A1 with the heading "Slabs".

2.5.2.7 CONSIDERATION OF FUTURE WIDENING

2.5.2.7.1 Exterior Beams on Multi-Beam Bridges

The following shall replace A2.5.2.7.1.

The load carrying capacity of exterior beams shall not be less than the load carrying capacity of an interior beam, unless specifically approved by the Chief Bridge Engineer.

2.5.3 Constructibility

The following shall supplement A2.5.3.

An acceptable slab placement sequence shall be shown in the contract plans. Figure 1 illustrates the format to be used. The actual sequence shall be determined from an erection analysis (see D6.10.3.2.4P) for the specific structure in question. For steel girder structures and prestressed beams made continuous for live load, see D6.10.3.2.4P and D5.14.1.2.7fP, respectively, for additional requirements concerning slab placement sequence. The

COMMENTARY

appearance and can give the public a perception of structural inadequacy. Deflections from moving vehicle loads also produce vertical movement and vibrations that annoy motorists and alarm pedestrians, Ritter (1990).

Excessive deformation can cause premature deterioration of the wearing surface and affect the performance of fasteners, but limits on the latter have not yet been established.

The intent of the relative deflection criterion is to protect the wearing surface from debonding and fracturing due to excessive flexing of the deck. The restriction on relative rib displacement may be revised or removed when more data is available to formulate appropriate requirements as function of thickness and physical properties of the wearing surface employed.

C2.5.2.7.1

The following shall supplement A2.5.2.7.1.

The stiffness of the interior and exterior beams should be relatively equal.

C2.5.3

The two-curing day waiting period between pours in adjacent continuous spans is for crack control. Studies have shown that longer waiting periods have no significant effect on cracking, primarily because shrinkage is the dominating factor in cracking. The two-curing day period between adjacent pours in the same span will provide enough strength gain to introduce composite action and will increase the stability of the girder over the length of the previous

SPECIFICATIONS

COMMENTARY

required curing strength (if any) of the concrete of a previous placement segment shall be designated as appropriate. Instead of specifying a curing strength of the concrete, a time delay (if any) between placements may be designated, as appropriate. A minimum waiting period of two curing days between positive moment region placements in immediately adjacent continuous spans and between adjacent positive moment placements in the same span shall be specified in the contract plans. A minimum waiting period between other placements need not be specified if analysis suggests that it is unnecessary.

pour.

3	7	4	8	6	2	6	9	5	1	5	9	6	2	6	8	4	7	3
+M	-M	+M	-M	+M		-M		+M	-M		+M	-M		+M	-M	+M	-M	+M
Ω	Ω	Ω		△				△		Ω		Ω		Ω				

Two days must elapse between Pours 1 and 2; 3 and 4; 5 and 6.

SLAB REPLACEMENT SEQUENCE

+M DENOTES POSITIVE MOMENT
 -M DENOTES NEGATIVE MOMENT

NOTE: The Contractor may use an alternative slab placement sequence if the provisions in the DM-4, Section 2 (D2.5.3) are met.

Figure 2.5.3-1 - Example of Slab Placement Sequence for Contract Plans

The Contractor may use an alternate slab placement sequence if the following provisions are met:

- The Contractor shall submit to the Department a revised slab placement sequence with support calculations and computer stress analysis. The revised slab placement sequence shall meet the requirements of which the original slab placement sequence were based on.
- The Department will review and approve calculations.
- The Contractor shall receive written approval prior to the use of the revised slab placement sequence and/or camber values.
- All costs for the development and approval of the revised slab placement sequence and camber values shall be borne by the Contractor.
- The Department will be the sole judge of the acceptability of the revised slab placement sequence and camber values.

2.5.3.1P FALSEWORK

C2.5.3.1P

SPECIFICATIONS

Composite beams shall be designed with no intermediate falsework during placing and curing of the concrete deck.

When falsework is used on a project, it shall be designed for the following items, but not limited to:

- vertical loads,
- horizontal loads,
- differential settlement forces,
- unbalanced temporary loadings (e.g., staged construction), and
- errant highway vehicles.

The following guidelines should be used for the approval of the falsework:

- Every bridge on a project should receive a separate falsework design analysis.
- In the event falsework is moved from one bridge to another, it should be thoroughly inspected for structural damage and plumbness to ensure that all members are in place and properly aligned and corrected.
- Ensure that the requirement of Publication 408, Section 105.02(c), “all drawings for load bearing falsework submissions are to be signed and sealed by a Professional Engineer, registered in the Commonwealth of Pennsylvania”, is fully enforced.
- During the falsework review, make sure that it is designed to handle vertical and horizontal loading and to contain enough redundancy to prevent a failure in the entire system. Vertical loading and differential settlement forces, and horizontal lateral and longitudinal forces should be taken into account. Unbalanced temporary loading caused by the placement sequence, should also be considered.
- If an unfortunate event occurs due to the failure of the falsework, preserve and document the in-place failure and assign investigation responsibilities to qualified impartial parties.
- If service load design is used, designers may increase the allowable basic unit stress by 25% for temporary falsework.

Should the contractor deem that temporary falsework is necessary for the construction of curved and skewed steel

COMMENTARY

For overhang bracket requirements see D6.10.3.2.4.2P.

Refer to Appendix P for guidance on jacking and supporting the superstructure.

For purposes of these guidelines, temporary falsework is defined as falsework constructed for no more than one construction season.

While using no temporary falsework is desirable from a cost-effectiveness perspective, should the designer and/or

SPECIFICATIONS

bridges, the following guidelines should be used for its placement:

- *When temporary falsework is needed for a span, it shall be placed at locations to reduce splice rotations and girder vertical deflections.*

The stability of the structure supported by temporary falsework shall be evaluated.

2.5.3.2P GIRDER ERECTION SEQUENCE

The following guidelines should be used for the girder erection sequence for horizontally curved steel I-girder structures:

- *Should adequate crane capacity be available, paired girder erection approaches are preferred.*
- *When the radius of the curved structure is less than 300 feet, it is recommended that girders be placed from inner radius to outer radius.*
- *An analysis shall be performed to ensure that the structure is stable for all stages of construction and that supports necessary to maintain stability have been provided.*

The following guidelines should be used for the girder erection sequence for skewed steel I-girder structures:

- *An analysis shall be performed to ensure that the structure is stable for all stages of construction and that supports necessary to maintain stability have been provided.*

2.6 HYDROLOGY AND HYDRAULIC

2.6.6 Roadway Drainage

2.6.6.1 GENERAL

The following shall supplement A2.6.6.1.

Dimensions for the deck cross slopes shall be shown in the same manner as indicated on the roadway plans (e.g., 2%). The water table cross slope on bridge decks which are not superelevated shall be sloped toward the curb or median. The rate of slope shall be 4% for water table widths of 1800 mm {6 ft.} or less, and 3% for water table widths over 1800 mm {6 ft.}. On superelevated decks, the water table on the high side shall be as specified in Design Manual, Part 2. On the low side, the water table shall slope in the

COMMENTARY

contractor deem that falsework is needed to ensure that a curved or skewed steel bridge is constructible, it should initially be placed near splice locations. When girder vertical deflections are still a concern, an additional temporary support should be placed as close as possible to the location of maximum vertical deflection of the span (approximately 0.4 L from an abutment, where L is the span length, for side spans and 0.5 L for intermediate spans) to reduce girder deflections. For the side spans, when adding multiple temporary supports is not feasible, placing one support near 0.75L from the abutments is suggested.

C2.5.3.2P

Paired girder erection, as opposed to single erection, requires fewer temporary supports for the erected segments during all stages of construction. However for bridges with an odd number of girders, at least one girder line must be erected by itself.

Girder erection from inner radius to outer radius, when compared to the opposite direction, can result in slightly smaller deformations for the girders for all stages of construction which, in turn, means the structure is more constructible. This effect is more pronounced in severely curved structures (i.e., radius less than 300 ft).

Stability, which refers to the prevention of excessive deformations and the possibility of buckling, of partial and completed girders at various stages of erection, is the responsibility of the contractor as specified in Publication 408 Section 1050.3(c).

For construction of straight skewed bridges, paired erection does require a smaller number of temporary supports but offers no other substantial benefits over a single erection approach with respect to deformations.

SPECIFICATIONS

COMMENTARY

same direction and magnitude as the adjacent lane, but not less than 4% for water table widths of 1800 mm {6 ft.} or less, nor less than 3% for water table widths over 1800 mm {6 ft.}. On a superelevated bridge with a paved median, adjustment of the grades of adjacent roadways may be required to equalize the height of the divisor or median barrier.

2.7P DESIGN DRAWINGS**2.7.1P Moment and Shear Envelope Diagrams**

For simple span bridges, the contract plans shall contain a table of following items:

- (1) Maximum non-composite dead load moment
- (2) Maximum composite dead load moment (including future wearing surface)
- (3) Maximum live load plus impact moment for PHL-93 and P-82 loading conditions
- (4) Maximum non-composite dead load shear
- (5) Maximum composite dead load shear (including future wearing surface)
- (6) Maximum live load plus impact shear for PHL-93 and P-82 loading conditions
- (7) Composite and non-composite section properties at resisting sections

For multiple span continuous bridges, as a minimum, the contract plans shall contain a diagrammatic presentation of the following on a per-girder basis:

- (1) Non-composite dead load moment diagram
- (2) Composite dead load moment diagram (including future wearing surface)
- (3) Separate positive and negative live load plus impact moment envelope for PHL-93 and P-82 loading conditions
- (4) Summation of (1) and (2)
- (5) Non-composite dead load shear diagram
- (6) Composite dead load shear diagram (including future wearing surface)
- (7) Separate positive and negative live load plus impact shear envelope for PHL-93 and P-82

SPECIFICATIONS

COMMENTARY

loading conditions

- (8) Summation of (5) and (6)
- (9) Composite and non-composite section properties at the resisting sections

The data to construct this presentation shall not have load factors applied.

Also, a table of reactions shall be provided for total dead load, and positive and negative live load, plus impact without load factors applied.

2.7.2P Major, Complex and Unusual Bridges

2.7.2.1P LOAD DATA SHEET

For the new design of major, complex and unusual bridges, additional information shall be included on the design drawings for typical common components such as bearings, floorbeams, and stringers. For these items as a minimum, the contractor plans shall contain a tabular presentation of the following:

- Bearings
 - (a) Vertical Force
 - 1. Total Dead Load
 - 2. Live Load plus Impact
 - 3. Summation of 1. and 2.
 - (b) Transverse Force Wind Load
 - (c) Longitudinal Force
 - 1. Wind Load
 - 2. Traction Load
 - 3. Friction Load
- Truss Members
 - (a) Axial Force
 - 1. Total Dead Load
 - 2. Live Load plus Impact
 - 3. Summation of 1. and 2.
 - (b) Bending Moment
 - 1. Total Dead Load
 - 2. Live Load plus Impact
 - 3. Summation of 1. and 2.
 - (c) Section Properties

SPECIFICATIONS

COMMENTARY

1. Gross Area
2. Net Area
3. Section Modulus

- Floorbeam

Provide the same type of information as required in D2.7.1P for girders.

- Stringers

Provide the same type of information as required in D2.7.1P for girders.

The data for this tabular presentation shall not have load factors applied.

2.8P BRIDGE SECURITY

2.8.1P General

For the purpose of this section bridges deemed important shall include (1) new singular bridges of total replacement value exceeding \$100 million or (2) new or existing bridges identified as critical by the Department's Emergency Transportation Operations Section.

A risk management approach shall be utilized to assess structural vulnerability and countermeasures. A threat based component level analysis shall be conducted considering a full range of threats. FHWA's workshop methodology or other BQAD approved methodology shall be used.

The results of such processes and included design/mitigation criteria and features shall be considered sensitive project information that is protected by restricted access. Contract documents shall not include reference to any security standard, design capability, or other information that might provide knowledge of bridge resistance.

For all bridges, restrict access to doors/hatches by using locks or by making inaccessible except by special mobile equipment, such as snooper, man lift, etc. In cellular structures, avoid vent hole diameters larger than 2 inches when holes are in easy reach. Avoid nooks and areas that allow for concealed access and create a confined pressure effect. If these details are unavoidable consideration should be given to barring access.

SPECIFICATIONS

COMMENTARY

PENNSYLVANIA DEPARTMENT OF TRANSPORTATION
DESIGN MANUAL

PART 4

VOLUME 1

PART B: DESIGN SPECIFICATIONS

SECTION 3 – LOADS AND LOAD FACTORS

SECTION 3 - TABLE OF CONTENTS

2.3 LOCATION FEATURES	1
2.3.2 Bridge Site Arrangement	1
2.3.2.2 TRAFFIC SAFETY	1
2.3.2.2.1 Protection of Structures	1
2.3.2.2.2 Protection of Users	ii
2.3.2.2.3 Geometric Standards	ii
2.3.3 Clearances	ii
2.3.3.2 HIGHWAY VERTICAL	ii
2.3.3.3 HIGHWAY HORIZONTAL	iii
2.3.3.4 RAILROAD OVERPASS	iii
2.5 DESIGN OBJECTIVES	v
2.5.2 Serviceability	vi
2.5.2.2 INSPECTABILITY	vi
2.5.2.2.1P General	vi
2.5.2.2.2P Inspection Walks	vi
2.5.2.2.2aP General	vii
2.5.2.2.2bP Design Live Load	vii
2.5.2.2.2cP Geometry	vii
2.5.2.2.2dP Connection to the Main Members	vii
2.5.2.2.3P Inspectability for Enclosed Section	vii
2.5.2.2.4P Girder Handrail	vii
2.5.2.2.5P Sound Barriers	vii
2.5.2.6 DEFORMATIONS	vii
2.5.2.6.1 General	vii
2.5.2.6.2 Criteria for Deflection	viii
2.5.2.6.3 Criteria for Span-to-Depth Ratios	ix
2.5.2.7 CONSIDERATION OF FUTURE WIDENING	ix
2.5.2.7.1 Exterior Beams on Multi-Beam Bridges	ix
2.5.3 Constructibility	ix
2.5.3.1P FALSEWORK	x
2.6 HYDROLOGY AND HYDRAULIC	xii
2.6.6 Roadway Drainage	xii
2.6.6.1 GENERAL	xii
2.7P DESIGN DRAWINGS	xiii
2.7.1P Moment and Shear Envelope Diagrams	xiii
2.7.2P Major, Complex and Unusual Bridges	xiv
2.7.2.1P LOAD DATA SHEET	xiv
2.8P BRIDGE SECURITY	xv
2.8.1P General	xv
C3.1 SCOPE	1
3.3 NOTATION	1
3.3.1 General	1
3.4 LOAD FACTORS AND COMBINATIONS	1

SPECIFICATIONS

COMMENTARY

3.4.1 Load Factors and Load Combinations	1
3.4.1.1P LOAD FACTORS AND COMBINATIONS FOR TYPICAL PENNDOT BRIDGE COMPONENTS	5
3.5 PERMANENT LOADS	19
3.5.1 Dead Loads: DC, DW and EV	19
3.5.1.1P APPLICATION OF DEAD LOAD ON GIRDER AND BOX BEAM STRUCTURES	19
3.6 LIVE LOADS.....	19
3.6.1 Gravity Loads: LL, PL.....	19
3.6.1.1 VEHICULAR LIVE LOAD	19
3.6.1.1.2 Multiple Presence of Live Load	19
3.6.1.2 DESIGN VEHICULAR LIVE LOAD	20
3.6.1.2.1 General	20
3.6.1.2.3 Design Tandem.....	20
3.6.1.2.5 Tire Contact Area	20
3.6.1.2.6 Distribution of Wheel Loads through Earth Fills	21
3.6.1.2.7P Design Permit Load.....	21
3.6.1.2.8P Maximum Legal Load (ML-80).....	22
3.6.1.3 APPLICATION OF DESIGN VEHICULAR LIVE LOADS	22
3.6.1.3.1 General	22
3.6.1.3.2 Loading for Live Load Deflection Evaluation.....	23
3.6.1.3.3 Design Loads for Decks, Deck Systems, and the Top Slab of Box Culverts	24
3.6.1.3.4 Deck Overhang Load.....	24
3.6.1.4 FATIGUE LOAD	25
3.6.1.4.2 Frequency	25
3.6.1.5 RAIL TRANSIT LOAD	25
3.6.1.5.1P General.....	25
3.6.1.5.2P Distribution of Rail Transit Loads Through Earth Fill	25
3.6.1.6 PEDESTRIAN LOADS	29
3.6.2 Dynamic Load Allowance: IM.....	29
3.6.2.1 GENERAL	29
3.6.2.1.1P Components for which IM is Applicable	29
3.6.2.1.2P Components for which IM is Not Applicable	29
3.6.2.2 BURIED COMPONENTS	30
3.6.2.3 WOOD COMPONENTS.....	30
3.6.4 Braking Force: BR.....	30
3.6.5 Vehicular Collision Force CT	31
3.6.5.3 Vehicular Collision with barriers.....	31
3.8 WIND LOAD: WL AND WS.....	31
3.8.1 Horizontal Wind Pressure.....	31
3.8.1.2 WIND PRESSURE ON STRUCTURES: WS	31
3.8.1.2.1 General	31
C3.8.1.2.2 Loads from Superstructures	32
3.8.3 Aeroelastic Instability.....	32
3.8.3.4 WIND TUNNEL TESTS.....	32
3.9 ICE LOADS: IC.....	32
3.9.1 General	32
3.9.5 Vertical Forces due to Ice Adhesion.....	32
3.10 EARTHQUAKE EFFECTS: EQ.....	33
C3.10.1 General.....	33
3.10.2 Acceleration Coefficient	34
3.10.7 Response Modification Factors.....	35
3.10.7.1 GENERAL	35
3.10.9 Calculation of Design Forces	35
3.10.9.2 SEISMIC ZONE 1.....	35
3.10.9.3 SEISMIC ZONE 2.....	36
3.10.9.5 LONGITUDINAL RESTRAINERS	37
3.11 EARTH PRESSURE: EH, ES, LS AND DD	37

SPECIFICATIONS

COMMENTARY

3.11.1 General 37

3.11.3 Presence of Water 37

3.11.5 Earth Pressure: EH 37

 C3.11.5.2 AT-REST PRESSURE COEFFICIENT, k_o 37

 C3.11.5.3 ACTIVE PRESSURE COEFFICIENT, k_a 38

 3.11.5.4 PASSIVE PRESSURE COEFFICIENT, k_p 38

 3.11.5.5 EQUIVALENT-FLUID METHOD OF ESTIMATING EARTH PRESSURES 40

 3.11.5.6P EARTH PRESSURE FOR NONGRAVITY CANTILEVER WALLS 41

 3.11.5.7 APPARENT EARTH PRESSURES FOR ANCHORED WALLS 47

 3.11.5.6.1P Cohesionless Soils..... 48

 3.11.5.7.2P Cohesive Soils..... 51

 3.11.5.7.2a *Stiff to Hard, Including Fissured Cohesive Soils* 51

 3.11.5.6.2bP *Very Soft to Medium-Stiff Cohesive Soils*..... 52

3.11.6 Surcharge Loads: ES and LS..... 55

 3.11.6.4 LIVE LOAD SURCHARGE: LS 55

3.12 FORCE EFFECTS DUE TO SUPERIMPOSED DEFORMATIONS: TU, TG, SH, CR, SE..... 56

3.12.2 Uniform Temperature 56

 3.12.2.1.1 TEMPERATURE RANGES 56

3.12.7 Minimum Temperature Force for Fixed Substructures..... 57

3.13 FRICTION FORCES: FR..... 58

3.14 VESSEL COLLISION: CV 58

3.14.1 General 58

3.14.2 Owner's Responsibility..... 58

C3.14.15 Protection of Substructures 58

3.15P FORCE TRANSFER TO SUBSTRUCTURE..... 59

3.15.1P Longitudinal Force 59

 3.15.1.2P FORCE TRANSFER TO SUBSTRUCTURE 59

 3.15.1.3P EFFECTIVE LENGTH FOR SUPERSTRUCTURE FORCES 59

 3.15.1.4P FORCE RESOLUTION TO SUBSTRUCTURE 59

3.15.2P Transverse Force 60

 3.15.2.1P FORCE TRANSFER TO SUBSTRUCTURE 60

 3.15.2.2P EFFECTIVE LENGTHS FOR SUPERSTRUCTURE FORCES..... 61

 3.15.2.3P FORCE RESOLUTION TO SUBSTRUCTURE 61

 3.15.2.4P DETERMINATION OF BEARING REACTIONS 61

SPECIFICATIONS

COMMENTARY

[THIS PAGE IS INTENTIONALLY LEFT BLANK]

SPECIFICATIONS

COMMENTARY

C3.1 SCOPE

The following shall supplement the second paragraph of AC3.1.

Before any test results are used in the design of a structure, the tests and the test results must be approved by the Chief Bridge Engineer

3.3 NOTATION**3.3.1 General**

The following shall supplement A3.3.1

- B = Vertical element width (mm) {ft} (3.11.5.6)
 C = Pressure coefficient for loads applied on a subgrade (dim) (3.6.1.5.2P)
 D = Depth of embedment of discrete and continuous vertical wall elements (mm) {ft} (3.11.5.6); width of uniformly loaded area (mm) {ft} (3.6.1.5.2P)
 F = Fictitious force applied at bottom of embedded continuous vertical wall element to provide horizontal force equilibrium for simplified earth pressure distributions (N/mm) {kip/ft} (3.11.5.6)
 I_f = Impact factor (dim) (3.6.1.5.2P)
 k_p = Passive coefficient of lateral earth pressure (dim) (3.11.5.6)
 ℓ = Spacing between vertical wall elements (c/c) (mm) {ft} (3.11.5.6)
 M = Length of uniformly loaded area (mm) {ft} (3.6.1.5.2P)
 M = constant used in calculating active earth pressure coefficient in certain conditions (dim) (3.11.5.6.2bP)
 P_a = Active resistance per vertical wall element (N) {kips}
 P_a = Active earth pressure per unit length of wall (N/mm) {kip/ft} (3.11.5.6)
 P_o = Intensity of the distributed load at the bottom of the railroad ties (MPa) {ksi} (3.6.1.5.2P)
 P_p = Passive resistance per vertical wall element (N) {kips}
 P_p = Passive earth pressure per unit length of wall (N/mm) {kip/ft} (3.11.5.6)
 S_m = Shear strength of rock mass (MPa) {ksf} (3.11.5.6)
 S_u = Undrained shear strength of cohesive soil (MPa) {ksf} (3.11.5.6)
 W_1 = Live load on structure from railroad loading (N/mm) {kip/ft} (3.6.1.5.2P)
 B = Ground surface slope behind wall {+ for slope up from wall; - for slope down from wall} (DEG) (3.11.5.6)
 β' = Ground surface slope in front of wall {+ for slope up from wall; - for slope down from wall} (DEG) (3.11.5.6)

3.4 LOAD FACTORS AND COMBINATIONS**3.4.1 Load Factors and Load Combinations**

The following shall replace Strength II description in A3.4.1.

- Strength II - Load combination relating to the Design Permit Load (P-82) use of the bridge. This load combination only applies to the superstructure, except for pier caps which support a superstructure with a span length greater than 20 000 mm {65 ft.}. Bearings, (including uplift check), substructure and foundation need not be designed for this load combination. For

C3.4.1

The following shall replace Strength II commentary in AC3.4.1.

In design, the use of distribution factors in D4.6.2.2 and A4.6.2.2 represents that the P-82 is in all design lanes.

The method for rating takes into account that the P-82 is in one lane and the other lanes are occupied by the vehicular live load.

In AC3.4.1, the commentary for Strength II states that "For bridges longer than the permit vehicle, the presence of the design lane load, preceding and following the permit load in its lane, should be considered." A study done for the

SPECIFICATIONS

COMMENTARY

design, the distribution factors given in D4.6.2.2 and A4.6.2.2 shall be used.

For the rating of existing bridges with Strength II criteria, the following equation may be used to determine Strength II live load moments and shear:

$$FR_T = FR_{P-82} \left(\frac{g_1}{1.2} \right) + FR_{PHL-93} \left(g - \frac{g_1}{1.2} \right)$$

where:

FR_T = total force response, moment or shear

FR_{P-82} = P-82 force response, moment or shear

FR_{PHL-93} = PHL-93 force response, moment or shear

g_1 = single lane distribution factor, moment or shear

g = multi-lane distribution factor, moment or shear

FR_T need not be taken greater than $FR_{P-82(g)}$.

The following shall supplement A3.4.1.

- STRENGTH IP - Load combination relating to the pedestrian load and a reduced vehicular live load.
- STRENGTH VI - Load combination relating to the design of piers which includes ice and wind load acting together.
- EXTREME EVENT III - Load combination relating to the failure of one element of a component without the failure of the component.
- EXTREME EVENT IV - Load combination relating to the failure of one component without the collapse of the structure.

The conditions for which Extreme Event III and IV are to be investigated are given in D1.3.4.

Department showed that the P-82 with the interrupted lane load only controls for moments in a small range of spans and is only maximum of 2% above the PHL-93 loading. For shear, the maximum difference between the PHL-93 and P-82 with lane load was 7.5% with P-82 and lane load being greater than PHL-93. The Department concluded that this difference was acceptable because the study considered all the lanes loaded with the P-82. Therefore, the P-82 loading need not be considered with a partial lane load.

The following shall supplement AC3.4.1.

Extreme Events III and IV are uncalibrated load combinations. They are intended to force consideration of the safety of damaged structures.

For this extreme event, a 3-D analysis is required. The objective of this analysis is survival of the bridge (i.e., the bridge may have large permanent deflections, but it has not collapsed).

SPECIFICATIONS

COMMENTARY

Table 3.4.1P-1 - Additional PennDOT Load Combinations and Load Factors

Load Combination Limit State	DC DD DW EH EV ES	LL IM CE BR PL LS	WA	WS	WL	FR	TU CR SH	TG	SE	Use One of These at a Time			
										EQ	IC	CT	CV
STRENGTH IP	γ_p	*	-	-	-	-	-	-	-	-	-	-	-
STRENGTH VI	γ_p	-	1.25	1.25	-	-	-	-	-	-	1.25	-	-
EXTREME EVENT III	γ_p	γ'_{LL}	-	-	-	-	-	-	-	-	-	-	-
EXTREME EVENT IV	γ'_p	γ'_{LL}	-	-	-	-	-	-	-	-	-	-	-
* $\gamma_{LL} = 1.35, \gamma_{PL} = 1.75$													

Table 3.4.1P-2 - Load Factor for Live Load for Extreme III and IV, γ'_{LL}

Case	III	IV
	γ'_{LL}	γ'_{LL}
PHL-93 Loading – all applicable lanes	1.30	1.15
Permit load in governing lane with PHL-93 in other applicable lanes	1.10	1.05

Table 3.4.1P-3 - Load Factors for Permanent Loads for Extreme Event IV, γ'_p

Type of Load	Load Factor	
	Maximum	Minimum
DC: Component and Attachments	1.05	0.95
DW: Wearing Surfaces and Utilities	1.05	0.90

Unless otherwise specified, interaction of force effects shall be accounted for by selecting load factors which maximize and minimize each of the force effects one at a time with the same load factors used to compute the associated force effect.

As an example for a design which involves the interaction of moment and axial force, the following four design cases would be investigated:

- select the load factors which maximize moment and use these load factors in determining axial force
- select the load factors which minimize moment and use these load factors in determining axial force
- select the load factors which maximize axial force and use these load factors in determining moment

SPECIFICATIONS

COMMENTARY

- select the load factors which minimize axial force and use these load factors in determining moment.

Due to the nature of force interaction, the absolute worst case may not necessarily be that for which one of the force effects is maximized, but an intermediate case. However, the difference between the absolute worst case and the design cases presented here are believed to be within the tolerance of the design process. Therefore, as a reasonable interpretation of the specification, maximum and minimum force effects taken in conjunction with associated force effects for interaction are to be considered. If the Engineer believes that an intermediate case will govern to an appreciable degree, the Engineer shall notify the Chief Bridge Engineer. Then, the Chief Bridge Engineer will determine if intermediate cases shall be investigated.

For MSE wall designs, D11.10.5.2 and D11.10.6.2 state when to apply maximum and minimum EH and EV.

The following shall supplement the sixth paragraph of A3.4.1 relating to TU, CR and SH.

The larger load factor shall be used to determine the final length of the member. The smaller load factor shall be used in determining force effects, such as creep and shrinkage effects in pier caps and columns.

The following shall replace the ninth paragraph of A3.4.1 relating to γ_{TG} and γ_{SE} .

For the application of temperature gradient see D3.12.3. The load factor for settlement γ_{SE} shall be determined on a project-specific basis.

The following shall replace the eleventh paragraph of A3.4.1 relating to γ_{EQ} .

The load factor γ_{EQ} for live load for the Extreme Event-I limit state shall be taken as 0.0.

The following shall supplement A3.4.1 for the design of box culverts.

Lateral earth pressures for box culverts shall be computed using the equivalent fluid method given in A3.11.5.5 and D3.11.5.5, and appropriate load factors, EH, as given in Table 3.4.1-2, for horizontal earth pressures.

To maximize the load effect, the maximum at-rest load factor shall be used with the maximum equivalent fluid weight from Table D3.11.5.5-2, and the minimum at-rest load factor shall be used with the minimum equivalent fluid weight. In addition, a 50% reduction in both maximum and minimum unfactored lateral earth pressures, EH and ES, shall be considered for determining the maximum positive moment in the top slab of the culvert, as specified in A3.11.7.

In Table A3.4.1-2, the first bulleted item under EV: Vertical Earth Pressure, “Retaining Structures”, shall be changed to “Retaining Walls and Abutments”.

The Department is currently using $\gamma_{EQ} = 0.0$ in accordance with numerous past years of AASHTO practice. We will continue to use $\gamma_{EQ} = 0.0$ until further work is completed justifying a different value.

The following shall supplement AC3.4.1 for the design of box culverts.

Rigid frame action of box culvert structures is assumed to result in relatively small movements as compared to that of a retaining wall or abutment-type structure, thus, an at-rest condition is assumed.

SPECIFICATIONS

COMMENTARY

3.4.1.1P LOAD FACTORS AND COMBINATIONS FOR TYPICAL PENNDOT BRIDGE COMPONENTS

Tables 1 through 6 provide the load factors with the corresponding limit state condition for the following typical PennDOT bridge components:

- steel girders (Table 1)
- prestressed girders (Table 2)
- abutment/retaining walls (Table 3)
- box culverts (Table 4)
- steel floorbeams (Table 5)
- steel trusses (Table 6)

Tables 1, 2, 4, 5 and 6 also include information for rating these components. (Rating are not typically done for abutment/retaining walls.)

C3.4.1.1P

The design live load vehicle in the fatigue load combination designated as HS20-9.0 refers to an HS20 truck with a fixed 9 meter {30 ft.} rear axle spacing.

Table D3.4.1.1P-1 - Load Factors and Live Load Vehicles for Steel Girders

	Load Combination												
	STR I	STR IP ⁸	STR IA ⁶	STR II	STR III	STR IV ¹	STR V	SERV II	SERV IIA ⁶	SERV IIB	FATIGUE ²	DEFL ²	CONST/ UNCURED SLAB ⁹
γ_{DC} ³	1.25, 0.90	1.25, 0.90	1.25, 0.90	1.25, 0.90	1.25, 0.90	1.5	1.25, 0.90	1.00	1.00	1.00	---	---	1.25
γ_{DW} ⁴	1.50, 0.65	1.50, 0.65	1.50, 0.65	1.50, 0.65	1.50, 0.65	1.50, 0.65	1.50, 0.65	1.00	1.00	1.00	---	---	1.50, 0.65
γ_{LL}	1.75	1.35	1.10	1.35	---	---	1.35	1.30	1.00	1.00	0.75	1.00	1.50
γ_{PL}	---	1.75	---	---	---	---	---	---	---	---	---	---	---
γ_{WS}	---	---	---	---	1.40	---	0.40	---	---	---	---	---	1.25
Design LL Veh. ⁷	PHL-93	PHL-93	PHL-93	Permi t (P-82)	---	---	PHL-93	PHL-93	PHL-93	Permi t (P-82)	HS20-9.0	PennDOT Defl. Trk.	User Def.
Rating Veh.	Rating Applicability: I = Inventory, O = Operating												
PHL-93	I	I	O	---	---	---	---	I	O	---	---	---	---
P-82	---	---	---	O	---	---	---	---	---	O	---	---	---
ML-80	I	I	---	O	---	---	---	I	O	---	---	---	---
HS20	I	I	---	O	---	---	---	I	O	---	---	---	---
H20	I	I	---	O	---	---	---	I	O	---	---	---	---
Spec. Veh.	I	I	---	O	---	---	---	I	O	---	---	---	---

Table D3.4.1.1P-1 - Load Factors and Live Load Vehicles for Steel Girders (Continued)

Notes:

¹Applicable when DL/LL ratio exceeds 7.0

²A load factor of unity is applied to permanent loads for the fatigue and deflection limit state only when specified

³DC load factor also used for barrier loads

⁴DW load factor also used for utility loads

⁵All loads applied to non-composite section for non-composite girders (Live loads are applied to the n section for steel)

⁶Load combination for rating only

⁷This row lists the typical design vehicle to be used for each load combination

⁸The reduced load factor for LL with PL (see D3.4.1)

⁹Design live load N/A for uncured slab check

Permanent Loads for Girder Programs		Section Properties ⁵	
Load	Steel		Steel
DC1	γ_{GR}	Girder	Nc
	γ_{SLAB}	Slab	nc
	γ_{SLAB}	Haunch	nc
DC2	γ_{DC2}	Barrier	3n
DW	γ_{FWS}	FWS	3n

Table D3.4.1.1P-2 - Load Factors and Live Load Vehicles for Prestressed Concrete Girders

	Load Combination											
	STR I	STR IP ⁸	STR IA ⁶	STR II	SERV I (P/S compr. chk.)		SERV III (P/S tension chk.)		SERV IIIA (M _r @ 0.9 f _y chk.)	SERV IIIB (PennDOT-cracking chk.)	FATIGUE ¹	DEFL ¹
					w/o PL	with PL	w/o PL	with PL				
γ_{DC} ²	1.25, 0.90	1.25, 0.90	1.25, 0.90	1.25, 0.90	1.00	1.00	1.00	1.00	1.00	1.00	---	---
γ_{DW} ³	1.50, 0.65	1.50, 0.65	1.50, 0.65	1.50, 0.65	1.00	1.00	1.00	1.00	1.00	1.00	---	---
γ_{LL}	1.75	1.35	1.10	1.35	1.00	0.80	0.80 ⁴	0.65 ⁹	1.00	1.00	0.75	1.00
γ_{PL}	—	1.75	---	---	---	1.00	---	1.00	---	---	---	---
$\gamma_{CR,SH}$	0.5	0.5	0.5	0.5	1.00	1.00	1.00	1.00	---	---	---	---
Design LL Veh. ⁷	PHL-93	PHL-93	PHL-93	Permit (P-82)	PHL-93		PHL-93		Controlling PHL-93 or P-82	Controlling PHL-93 or P-82	HS20-9.0	PennDOT Defl. Trk.
Rating Vehicle	Rating Applicability: I = Inventory, O = Operating											
PHL-93	I	I	O	---	I	I	O	---	---	---	---	---
P-82	---	---	---	O	---	---	O	---	---	---	---	---
ML-80	I	I	---	O	I	I	O	---	---	---	---	---
HS20	I	I	---	O	I	I	O	---	---	---	---	---
H20	I	I	---	O	I	I	O	---	---	---	---	---
Spec. Veh.	I	I	---	O	I	I	O	---	---	---	---	---

Table D3.4.1.1P-2 - Load Factors and Live Load Vehicles for Prestressed Concrete Girders (Continued)

Notes:

¹A load factor of unity is applied to permanent loads for the fatigue and deflection limit state only when specified

²DC load factor also used for barrier loads

³DW load factor also used for utility loads

⁴For rating vehicles, the live load for Service III is to be taken as 1.0 ($\gamma = 0.80$ for PHL-93 only)

⁵All loads applied to non-composite section for non-composite girders

(Live loads are applied to the n section for P/S composite girders. For P/S, live load stresses can be based on transformed strands)

⁶Load combination for rating only

⁷This row lists the typical design vehicle to be used for each load combination

⁸The reduced load factor for LL with PL (see D3.4.1)

⁹For rating vehicles (other than PHL-93), the live load factor for Service III is to be taken as 0.80 for the pedestrian load case

Permanent Loads for Girder Programs		Section Properties ⁵	
Load	P/S		P/S
DC1	γ_{GIR}	Girder	nc
	γ_{SLAB}	Slab	nc
	γ_{SLAB}	Haunch	nc
	γ_{ID}	Int. Dia.	nc
	γ_{ED}	Ext. Dia.	nc
DC2	γ_{DC2}	Barrier	n
DW	γ_{FWS}	FWS	n

Table D3.4.1.1P-3 - Load Factors and Live Load Vehicles for Abutment/Retaining Walls

	Load Combination									
	SERV I	STR I	STR IP	STR II	STR III	STR V	EXTREME I ²	EXTREME II ³	Min. γ for Const. Case (Strength) ⁵	γ for consolidation/secondary settlement
γ_{DC}	1.00	1.25, 0.90	1.25, 0.90	1.25, 0.90	1.25, 0.90	1.25, 0.90	1.25, 0.90	1.25, 0.90	1.25, 0.90	1.00
γ_{DW}	1.00	1.50, 0.65	1.50, 0.65	1.50, 0.65	1.50, 0.65	1.50, 0.65	1.50, 0.65	0.00	---	1.00
γ_{EV}	1.00	γ_{EV}	γ_{EV}	γ_{EV}	γ_{EV}	γ_{EV}	γ_{EV}	γ_{EV}	γ_{EV}	1.00
γ_{EH}	1.00	γ_{EH}	γ_{EH}	γ_{EH}	γ_{EH}	γ_{EH}	0.00	γ_{EH}	γ_{EH}	1.00
γ_{ES}^4	1.00	1.50	1.50	1.50	1.50	1.50	1.50	1.50	1.50	1.00
γ_{LS}^4	1.00	1.75	1.35	1.35	0.00	1.35	γ_{EQ}	0.50	1.50	0.00
γ_{LLIM}^1	1.00, 0	1.75, 0	1.35, 0	1.35, 0	0.00	1.35, 0	$\gamma_{EQ}, 0$	0.00	---	0.00
γ_{PL}	0.00	0.00	1.75, 0.00	0.00	0.00	0.00	0.00	0.00	---	0.00
γ_{WS}	0.3	0.00	0.00	0.00	1.40	0.40	0.00	0.00	---	0.00
γ_{WL}	1.0	0.00	0.00	0.00	0.00	1.0	0.00	0.00	---	0.00
γ_{WA}	1.0	1.0	1.0	1.0	1.0	1.0	1.0	1.0	1.0	1.0
γ_{BR}	1.0	1.75	1.35	1.35	0.00	1.35	γ_{EQ}	0.00	---	0.00
γ_{CE}	1.0	1.75	1.35	1.35	0.00	1.35	γ_{EQ}	0.00	---	0.00
γ_{FR}	1.0	1.0	1.0	1.0	1.0	1.0	1.0	1.0	---	0.00
γ_{TU}	1.0	0.5	0.5	0.5	0.5	0.5	0.00	0.00	---	0.00
γ_{EQ}	0.00	0.00	0.00	0.00	0.00	0.00	1.0	0.00	---	0.00
γ_{CT}	0.00	0.00	0.00	0.00	0.00	0.00	0.00	1.0	---	0.00
Design LL Vehicle	PHL-93	PHL-93	PHL-93	P-82	---	---	PHL-93	---	---	—

Table D3.4.1.1P-3 - Load Factors and Live Load Vehicles for Abutment/Retaining Walls (Continued)

Notes:

¹For a negative reaction on an abutment (uplift), use the maximum load factor

²For the seismic load case, EH loads (normal lateral earth pressure) replaced by EQ soil loads. γ_{EQ} for live loads = 0.0.

³Parapet collision force, CT.

⁴All lateral loads and their vertical components are maximized.

⁵For evaluation of the temporary construction stages using the Strength Limit states (see D11.6.1.2), use the greater of the γ noted under Construction Case column or under the given Strength Limit State column.

	Abutment/Retaining Wall Earth Load Factors	
	Maximum	Minimum
γ_{EV}	1.35	1.00
γ_{EH}	1.50	(4)

Table D3.4.1.1P-4 - Load Factors and Live Load Vehicles for Box Culverts

	Load Combination					
	SERV I	STR I	STR IA	STR II	FATIGUE ¹	Min. γ for Const. Case (Strength) ⁴
γ_{DC}	1.00	1.25, 0.90	1.25, 0.90	1.25, 0.90	---	1.25, 0.90
γ_{DW}	1.00	1.50, 0.65	1.50, 0.65	1.50, 0.65	---	---
γ_{EV}	1.00	γ_{EV}	γ_{EV}	γ_{EV}	—	γ_{EV}
γ_{EH}	1.00	γ_{EH}	γ_{EH}	γ_{EH}	—	γ_{EH}
γ_{ES}^3	1.00	1.50, 0.75	1.50, 0.75	1.50, 0.75	---	1.50, 0.75
γ_{LS}	1.00, 0	1.75, 0	1.10, 0	1.35, 0	---	1.50, 0
γ_{LLIM}	1.00, 0	1.75, 0	1.10, 0	1.35, 0	0.75	---
Design LL Vehicle	PHL-93	PHL-93	PHL-93	P-82	HS20-9.0	---
Rating Vehicle ²	Rating Applicability: I = Inventory, O = Operating					
PHL-93	---	I	O	---	---	---
P-82	---	---	---	O	---	---
ML-80	---	I	---	O	---	---
HS20	---	I	---	O	---	---
H20	---	I	---	O	---	---
Spec. Veh.	—	I	---	O	---	---

Notes:

¹Fatigue load factor should be factored by PTF. A load factor of unity is applied to permanent loads for the fatigue limit state only when specified.

²Rating applicable for box culverts only

³Minimum ES of 0.50 applies for top slabs of box culverts

⁴See A3.4.2, Load Factors for Construction Loads

	Box Culvert Earth Load Factors	
	Maximum	Minimum
γ_{EV}	1.30	0.90
γ_{EH}	1.35	0.90*
*Use 0.50 minimum for culvert top slab		

Table D3.4.1.1P-5 - Load Factors and Live Load Vehicles for Steel Floorbeams

	Load Combination											
	STR I	STR IP ⁷	STR IA ⁵	STR II	STR III	STR V	SERV II	SERV IIA ⁵	SERV IIB	FATIGUE ¹	DEFL ¹	CONST/ UNCURED SLAB ⁸
γ_{DC} ²	1.25, 0.90	1.25, 0.90	1.25, 0.90	1.25, 0.90	1.25, 0.90	1.25, 0.90	1.00	1.00	1.00	---	---	1.25
γ_{DW} ³	1.50, 0.65	1.50, 0.65	1.50, 0.65	1.50, 0.65	1.50, 0.65	1.50, 0.65	1.00	1.00	1.00	---	---	1.50, 0.65
γ_{LL}	1.75	1.35	1.10	1.35	---	1.35	1.30	1.00	1.00	0.75	1.00	1.50
γ_{PL}	---	1.75	---	---	---	---	---	---	---	---	---	---
γ_{WS}	---	---	---	---	1.40	0.40	---	---	---	---	---	1.25
Design LL Veh. ⁶	PHL-93	PHL-93	PHL-93	Permit (P-82)	---	PHL-93	PHL-93	PHL-93	Permit (P-82)	HS20-9.0	PennDOT Defl. Trk.	User Def.
Rating Veh.	Rating Applicability: I = Inventory, O = Operating											
PHL-93	I	I	O	---	---	---	I	O	---	---	---	---
P-82	---	---	---	O	---	---	---	---	O	---	---	---
ML-80	I	I	---	O	---	---	I	O	---	---	---	---
HS20	I	I	---	O	---	---	I	O	---	---	---	---
H20	I	I	---	O	---	---	I	O	---	---	---	---
Spec. Veh.	I	I	---	O	---	---	I	O	---	---	---	---

Table D3.4.1.1P-5 - Load Factors and Live Load Vehicles for Steel Floorbeams (Continued)

Notes:

- ¹A load factor of unity is applied to permanent loads for the fatigue and deflection limit state only when specified
- ²DC load factor also used for barrier loads, sidewalk, median barrier, railings, etc.
- ³DW load factor also used for utility loads
- ⁴All loads applied to non-composite section for non-composite floorbeams (Live loads are applied to the n section for steel)
- ⁵Load combination for rating only
- ⁶This row lists the typical design vehicle to be used for each load combination
- ⁷The reduced load factor for LL with PL (see D3.4.1)
- ⁸Live load N/A for uncured slab check

Permanent Loads for Floorbeam Programs		Section Properties ⁴	
Load	Steel		Steel
DC1	γ_{FLBM} γ_{SLAB} γ_{SLAB}	Floorbeam Slab Haunch	Nc nc nc
DC2	γ_{DC2}	Barrier, Sidewalk, Median Barrier, Railings, etc.	3n
DW	γ_{FWS}	FWS	3n

Table D3.4.1.1P-6 - Load Factors and Live Load Vehicles for Steel Trusses

	Load Combination														
	STR I	STR IP ⁸	STR IA ⁵	STR II	STR III	STR IV ¹	STR V	EXT. EVEN T III	EXT. EVEN T IV	SERV II	SERV IIA ⁵	SERV IIB	FATIGUE ²	DEFL ²	CONST
γ_{DC} ³	1.25, 0.90	1.25, 0.90	1.25, 0.90	1.25, 0.90	1.25, 0.90	1.5	1.25, 0.90	1.25, 0.90	1.05, 0.95	1.00	1.00	1.00	---	---	1.25
γ_{DW} ⁴	1.50, 0.65	1.50, 0.65	1.50, 0.65	1.50, 0.65	1.50, 0.65	1.50, 0.65	1.50, 0.65	1.50, 0.65	1.05, 0.90	1.00	1.00	1.00	---	---	1.50, 0.65
γ_{LL}	1.75	1.35	1.10	1.35	---	---	1.35	1.30	1.15	1.30	1.00	1.00	0.75	1.00	1.50
γ_{PL}	---	1.75	---	---	---	---	---	1.10	1.05	---	---	---	---	---	---
γ_{ws}	---	---	---	---	1.40	---	0.40	---	---	---	---	---	---	---	1.25
Design LL Veh. ⁶	PHL-93	PHL-93	PHL-93	Permit (P-82)	---	---	PHL-93	PHL-93 P-82	PHL-93, P-82	PHL-93	PHL-93	Permit (P-82)	HS20-9.0	PennDOT Defl. Trk.	User Def.
Rating Veh.	Rating Applicability: I = Inventory, O = Operating														
PHL-93	I	I	O	---	---	---	---	---	---	I	O	---	---	---	---
P-82	---	---	---	O	---	---	---	---	---	---	---	O	---	---	---
ML-80	I	I	---	O	---	---	---	---	---	I	O	---	---	---	---
HS20	I	I	---	O	---	---	---	---	---	I	O	---	---	---	---
H20	I	I	---	O	---	---	---	---	---	I	O	---	---	---	---
Spec. Veh.	I	I	---	O	---	---	---	---	---	I	O	---	---	---	---

Table D3.4.1.1P-6 - Load Factors and Live Load Vehicles for Steel Trusses (Continued)

Notes:

¹Applicable when DL/LL ratio exceeds 7.0

²A load factor of unity is applied to permanent loads for the fatigue and deflection limit state only when specified

³DC load factor also used for barrier loads, sidewalk, median barrier, railings, deck, stringers, truss floorbeams, wind and lateral bracing, etc.

⁴DW load factor also used for utility loads

⁵Load combination for rating only

⁶This row lists the typical design vehicle to be used for each load combination

⁷The reduced load factor for LL with PL (see D3.4.1)

SPECIFICATION

3.5 PERMANENT LOADS**3.5.1 Dead Loads: DC, DW and EV**

The following shall supplement A3.5.1.

The acceleration due to gravity (g) shall be taken as 9.81 m/s^2 for use in determining force effects from mass.

In addition to the weight of the deck slab, the design dead load shall include provisions for a future wearing surface with a surface area density of 150 kg/m^2 {0.030 ksf} on the deck slab between the curbs. This load shall be considered for all deck slabs, including decks with a bituminous wearing surface, but not for structures under fill. For decks formed using permanent metal deck forms, an additional dead load shall be included based on a surface density of 75 kg/m^2 {0.015 ksf} which takes into account the weight of the form, plus the weight of the concrete in the valleys of the forms.

In Table A3.5.1-1, replace the low density concrete value of 1775 kg/m^3 {0.110 kcf} with 1840 kg/m^3 {0.115 kcf}. Also in Table A3.5.1-1, delete the "sand-low-density" concrete value. For use of low density concrete with densities different than 1840 kg/m^3 {0.115 kcf}, see D5.4.2.1 and DC5.4.2.1.

3.5.1.1P APPLICATION OF DEAD LOAD ON GIRDER AND BOX BEAM STRUCTURES

The provisions in this article apply to superstructure types, a, b, c, f, g, h, k and l given in Table A4.6.2.2.1-1.

For composite adjacent and spread beams, the barrier (single barrier) load shall be equally distributed to the nearest three and two beams, respectively, when the barriers are placed after slab has hardened.

The dead load of items, such as fencing and sound barriers, if placed after the slab has hardened, shall be distributed to girder as described above.

Sidewalk dead load shall be distributed to a girder using the lever rule.

For noncomposite girders, the barrier load shall be distributed solely to the fascia girder.

The future wearing surface shall be distributed equally among all girders.

3.6 LIVE LOADS**3.6.1 Gravity Loads: LL, PL****3.6.1.1 VEHICULAR LIVE LOAD****3.6.1.1.2 Multiple Presence of Live Load**

Delete the last sentence of the second paragraph of A3.6.1.1.2.

COMMENTARY

C3.5.1

The following shall supplement AC3.5.1.

The normal density concrete and low density concrete with densities of 2400 kg/m^3 {0.150 kcf} and 1840 kg/m^3 {0.115 kcf} respectively include an allowance for reinforcement in the calculation of the density.

For concrete deck slabs, provisions must be made in the design for the addition of a bituminous wearing surface at some future time. Even in cases where the initial design includes a bituminous surface, provision must be made for an additional future wearing surface since the original bituminous material is not always stripped off before the new surface is added.

For structures under fill, the additional dead load associated with a future wearing surface is insignificant when compared with other contributions to the dead load. Therefore, in this case, no allowance for future wearing surface is necessary.

It is recognized that permanent metal deck forms are available for which the surface density is less than 75 kg/m^2 {0.015 ksf}; however, the minimum design load should be retained at this level. Lightweight forms may be advantageous in certain situations, such as rehabilitation, and should be evaluated on a case-by-case basis.

C3.6.1.1.2

Delete the third through seventh paragraphs of AC3.6.1.1.2.

SPECIFICATION

COMMENTARY

3.6.1.2 DESIGN VEHICULAR LIVE LOAD

3.6.1.2.1 General

The following shall replace the first paragraph of A3.6.1.2.1.

The vehicular live loading on the roadways of bridges or incidental structures, designated PHL-93, shall consist of a combination of the:

- design truck or design tandem, and
- design lane load,

as given in A3.6.1.2 and D3.6.1.2.

3.6.1.2.3 Design Tandem

Modify A3.6.1.2.3 so that weight of each axle is increased from 110 kN to 140 kN {25 kips to 31.25 kips}.

C3.6.1.2.1

The following shall supplement AC3.6.1.2.1.

At this time, the Department makes no exceptions to the requirements for application of PHL-93 vehicular live load for bridges on low volume roads.

C3.6.1.2.5

The following shall supplement AC3.6.1.2.5.

The area load applies only to the design truck and tandem. For other design vehicles, the tire contact area should be determined by the engineer.

As a guideline for other truck loads, the tire area in mm² {in²} may be calculated from the following dimensions:

Metric Units:

$$\text{Tire width} = P/0.142$$

$$\text{Tire length} = 165\gamma(1+IM/100)$$

U.S. Customary Units:

$$\text{Tire width} = P/0.8$$

$$\text{Tire length} = 6.4\gamma(1+IM/100)$$

where:

γ = load factor, as given in A3.4.1 and D3.4.1, except for buried structures where the load factor shall be 1.35

IM = dynamic load allowance percent

P = wheel load
 = 72.5 kN {16 kips} for the design truck, 70 kN {15.625 kips} for the design tandem and 60 kN {13.5 kips} for the P-82

SPECIFICATION

COMMENTARY

3.6.1.2.6 Distribution of Wheel Loads through Earth Fills

The following shall replace the first paragraph of A3.6.1.2.6.

Where the depth of fill is less than 600 mm {2 ft.}, live loads shall be distributed to the top slabs of culverts as specified in D4.6.2.12P.

The following shall replace the second paragraph of A3.6.1.2.6.

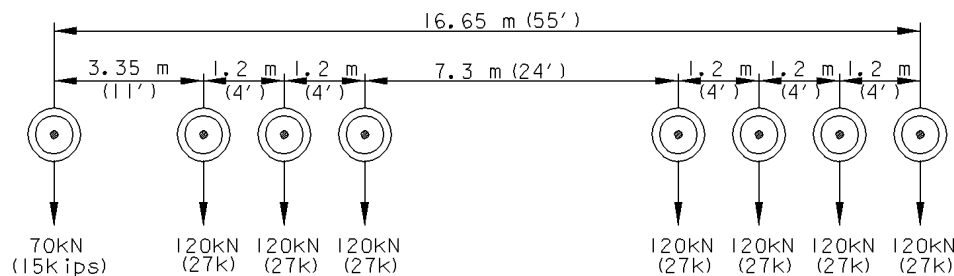
In lieu of a more precise analysis, or the use of other acceptable approximate methods of load distribution permitted in Section 12, where the depth of fill is 600 mm {2 ft.} or greater, wheel loads may be considered to be uniformly distributed over a rectangular area with sides equal to the dimension of the tire contact area, as specified in A3.6.1.2.5, and increased by either 1.15 times the depth of the fill in select granular backfill, or the depth of the fill in all other cases. The provisions of A3.6.1.1.2 and A3.6.1.3 shall apply.

The following shall replace the last paragraph of A3.6.1.2.6.

Where live load and impact moment in concrete slabs, based on the distribution of wheel load through earth fills, exceeds the live load and impact moment calculated according to A4.6.2.1 and D4.6.3.2, the latter moment shall be used.

3.6.1.2.7P Design Permit Load (P-82)

The weights and spacings of axles and wheels for the Permit Load (P-82) shall be as specified in Figure 1. A dynamic load allowance shall be considered as specified in D3.6.2 and A3.6.2.



NOTE: P-82 width is the same as the Design Truck.
 Transverse wheel location is the same as Design Truck.

C3.6.1.2.6

The following shall supplement AC3.6.1.2.6.

Traditionally, the effect of fills less than 600 mm {2 ft.} deep on live load has been ignored. Research (McGrath, et al. 2004) has shown that in design of box sections allowing distribution of live load through fill in the direction parallel to the span provides a more accurate design model to predict moment, thrust, and shear forces. Provisions in D4.6.2.12P provide a means to address the effect of shallow fills.

SPECIFICATION

COMMENTARY

Figure 3.6.1.2.7P-1 - Pennsylvania Permit Load (P-82) 910 kN {102 tons}, 8 Axle

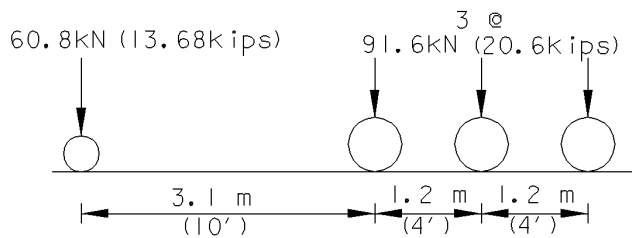
Axles which do not contribute to the extreme force effect under consideration shall be neglected.

For multi-girder superstructures design, the permit load shall be in one lane or in multiple lanes whichever is the controlling case.

For superstructure with girder-floorbeam-stringer systems and substructure components designs, the permit load shall be in one lane or in one lane with PHL-93 loading in adjacent lanes, whichever is the controlling case.

3.6.1.2.8P Maximum Legal Load (ML-80)

The weights and spacings of axles and wheels for the Maximum Legal Load (ML-80) shall be as specified in Figure 1. The ML-80 truck is used for rating.



NOTE: ML-80 width is the same as the design truck.
Transverse wheel location is the same as design truck.

Figure 3.6.1.2.8P-1 - Pennsylvania Maximum Legal Load (ML-80) 335.7 kN {37.74 tons}, 4 Axle

3.6.1.3 APPLICATION OF DESIGN VEHICULAR LIVE LOADS

3.6.1.3.1 General

The following shall replace A3.6.1.3.1.

Unless otherwise specified, the extreme force effect shall be taken as the larger of the following:

- the effect of the design tandem combined with the effect of the design lane load, or
- the effect of one design truck with the variable axle spacing specified in A3.6.1.2.2, combined with the effect of the design lane load, and
- for the negative moment between points of dead load contraflexure, the effect of two design trucks spaced a minimum of 15 000 mm {50 ft.} between the lead axle of one truck and the rear axle of the other truck,

C3.6.1.2.8P

The ML-80 is not considered a notional load. Therefore, all of the axles shall be considered when determining force effects.

C3.6.1.3.1

Delete the second and third sentences of the third paragraph of AC3.6.1.3.1.

The following shall supplement AC3.6.1.3.1.

The BXLRFD program does not consider the effect of two design trucks, since the minimum distance between the two design trucks is 15 000 mm {50 ft.} which is at the upper limit of a twin cell culvert. The effects of two tandems are considered for a twin cell box culvert in the BXLRFD program.

SPECIFICATION

combined with the effect of the design lane load; the distance between the 145 kN {32 kips} axles of each truck shall be taken as 4300 mm {14 ft.}.

For the reaction at interior piers only, 90% of the effect of two design trucks spaced a minimum of 15 000 mm {50 ft.} between the lead axle of one truck and the rear axle of the other truck, combined with 90% of the effect of the design lane load. The distance between the 145 kN {32 kips} axles of each truck shall be taken as 4300 mm {14 ft.}.

- For the negative moment between points of dead load contraflexure, the effect of two tandems with axle weights of 110 kN {25 kips} spaced from 8000 mm to 12 000 mm {26 ft. to 40 ft.} apart, combined with the effect of the design lane load.

For the reaction at interior piers only, 100% of the effect of two tandems with axle weights of 110 kN {25 kips} spaced from 8000 mm to 12 000 mm {26 ft. to 40 ft.} apart combined with the effect of the design lane load.

Axles which do not contribute to the extreme force effect under consideration shall be neglected.

Both the design lanes and the position of the 3000 mm {10 ft.} loaded width in each lane shall be positioned to produce extreme force effects. The design truck or tandem shall be positioned transversely such that the center of any wheel load is not closer than:

- for the design of the deck overhang - 300 mm {1 ft.} from the face of the curb or railing, and
- for the design of all other components - 600 mm {2 ft.} from the edge of the design lane.

Unless otherwise specified, the lengths of design lanes, or parts thereof, which contribute to the extreme force effect under consideration, shall be loaded with the design lane load.

3.6.1.3.2 Loading for Live Load Deflection Evaluation

The following shall replace A3.6.1.3.2.

The deflection should be taken as 125% of the larger of:

- that resulting from the effect of one design truck with the variable axle spacing specified in A3.6.1.2.2,
- that resulting from the effect of 25% of one design truck with the variable axle spacing specified in A3.6.1.2.2, combined with the effect of the design lane.

COMMENTARY

C3.6.1.3.2

The following shall replace AC3.6.1.3.2.

The LRFD live load deflection criteria was developed such that deflections would be roughly equivalent to those produced by a HS20 vehicle. A 25% increase is specified to be consistent with the Department's past use of the HS25 vehicle for computing deflections.

SPECIFICATION

3.6.1.3.3 Design Loads for Decks, Deck Systems, and the Top Slab of Box Culverts

Replace the three bullets of the second paragraph of A3.6.1.3.3 with the following.

- Where the slab spans primarily in the transverse direction, only the axles of the design truck of A3.6.1.2.2 or design tandem of D3.6.1.2.3 shall be applied to the deck slab or top slab of box culverts.
- Where the slab spans primarily in the longitudinal direction:
 - For top slabs of box culverts of all spans and for all other cases, including slab-type bridges where the span does not exceed 4600 mm {15.0 ft.}, only the axle loads of the design truck or design tandem of A3.6.1.2.2 and D3.6.1.2.3, respectively, shall be applied.
 - For all other cases, including slab-type bridges (excluding top slabs of box culverts) where the span exceeds 4600 mm {15.0 ft.}, all of the load shall be applied.

Replace the third paragraph of A3.6.1.3.3 with the following:

Where the refined methods are used to analyze decks, force effects shall be determined on the following basis:

- Where the slab spans primarily in the transverse direction, only the axles of the design truck of A3.6.1.2.2 or design tandem of D3.6.1.2.3 shall be applied to the deck slab.
- Where the slab spans primarily in the longitudinal direction (including slab-type bridges), all of the loads specified in D3.6.1.2 shall be applied.

3.6.1.3.4 Deck Overhang Load

The following shall replace A3.6.1.3.4.

The deck overhang load shall be as given in D3.6.1.3.1.

Also, the ultimate strength of the deck section shall be greater than the ultimate strength of the barrier, see Section A13 and its Appendix. Horizontal loads on the overhang resulting from vehicle collision with barriers shall be in accordance with the provisions of Section A13 and its Appendix.

COMMENTARY

C3.6.1.3.3

Add the following after the second paragraph of AC3.6.1.3.3.

The design truck and tandem without the lane load and with a multiple presence factor of 1.2 results in factored force effects that are similar to the factored force effects using the Standard Specification for typical span ranges of box culverts.

C3.6.1.3.4

The following shall replace AC3.6.1.3.4.

The deck overhang slab provided in BD-601M has been designed for the vertical design loads (D3.6.1.3.1) or a strength greater than the applied forces transmitted to the overhang when the barrier is subjected to the maximum collision force it can resist (Section A13) whichever is greater. The ultimate strength of the barrier used in the design of the overhang was based on the Department's Typical Barrier (see Standard Drawing BD-601M) which placed greater demand on the deck overhang than the other Department barriers.

SPECIFICATION

COMMENTARY

3.6.1.4 FATIGUE LOAD

3.6.1.4.2 Frequency

The following shall replace Table A3.6.1.4.2-1.

Table 3.6.1.4.2-1 – Fraction of Truck Traffic in a Single Lane, p

Number of Lanes Available to Trucks	p
1	1.00
2 or more	0.85

3.6.1.5 RAIL TRANSIT LOAD

3.6.1.5.1P General

Live loads for rail traffic shall use a combination of axle loads and axle spacings represented by the Cooper E80 loading, as shown in Figure 1.

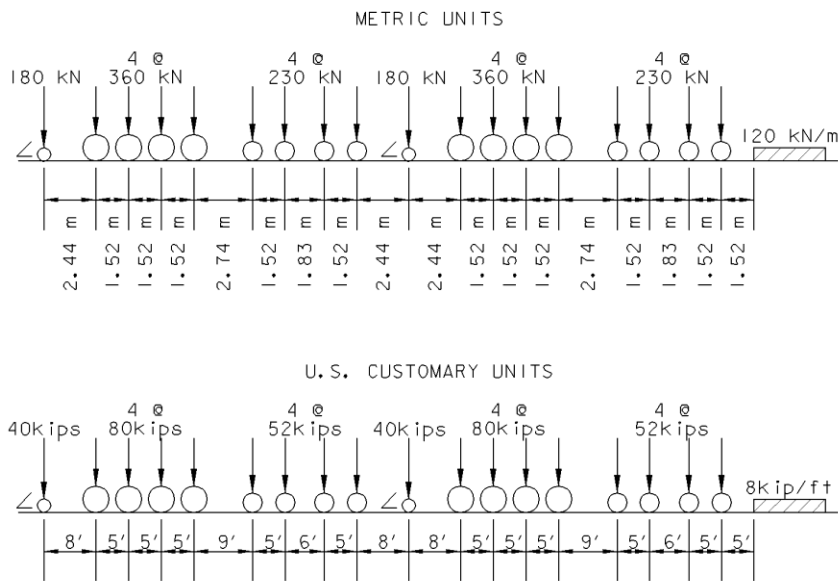


Figure 3.6.1.5.1P-1 - Wheel Spacing for Cooper E80 Design Loading (Load/Axle)

3.6.1.5.2P Distribution of Rail Transit Loads Through Earth Fill

The load intensity, W_1 , on a buried structure due to rail transit loading shall be determined using the following relationship:

SPECIFICATION

COMMENTARY

$$W_1 = C P_o B_c (1 + I_f) \quad (3.6.1.5.2P-1)$$

Refer to Table 1 for values of C. The series of axle loads and spacing shall be converted into a uniform load at the bottom of the railroad ties. The loading, P_o , at the base of the ties shall be represented by a ground pressure of 97 MPa {2025 ksf}, which represents the locomotive drive-wheel (four at 360 kN {80 kips}) loading distributed over an area 2400 mm by 6100 mm {8 ft. by 20 ft.} and a track structure loading of 3 kN/m {0.2 kip/ft}. The impact factor, I_f , shall range from 40% at zero cover to 0% at 3000 mm {10 ft.} of cover.

The live load and the dead load, including the impact factor, for a Cooper E80 loading can be determined from Figure 1. To obtain the live load per linear meter, multiply the unit load from Figure 1 by the outside horizontal span of the pipe, B_c .

DM-4, Section 3 – Loads and Load Factors

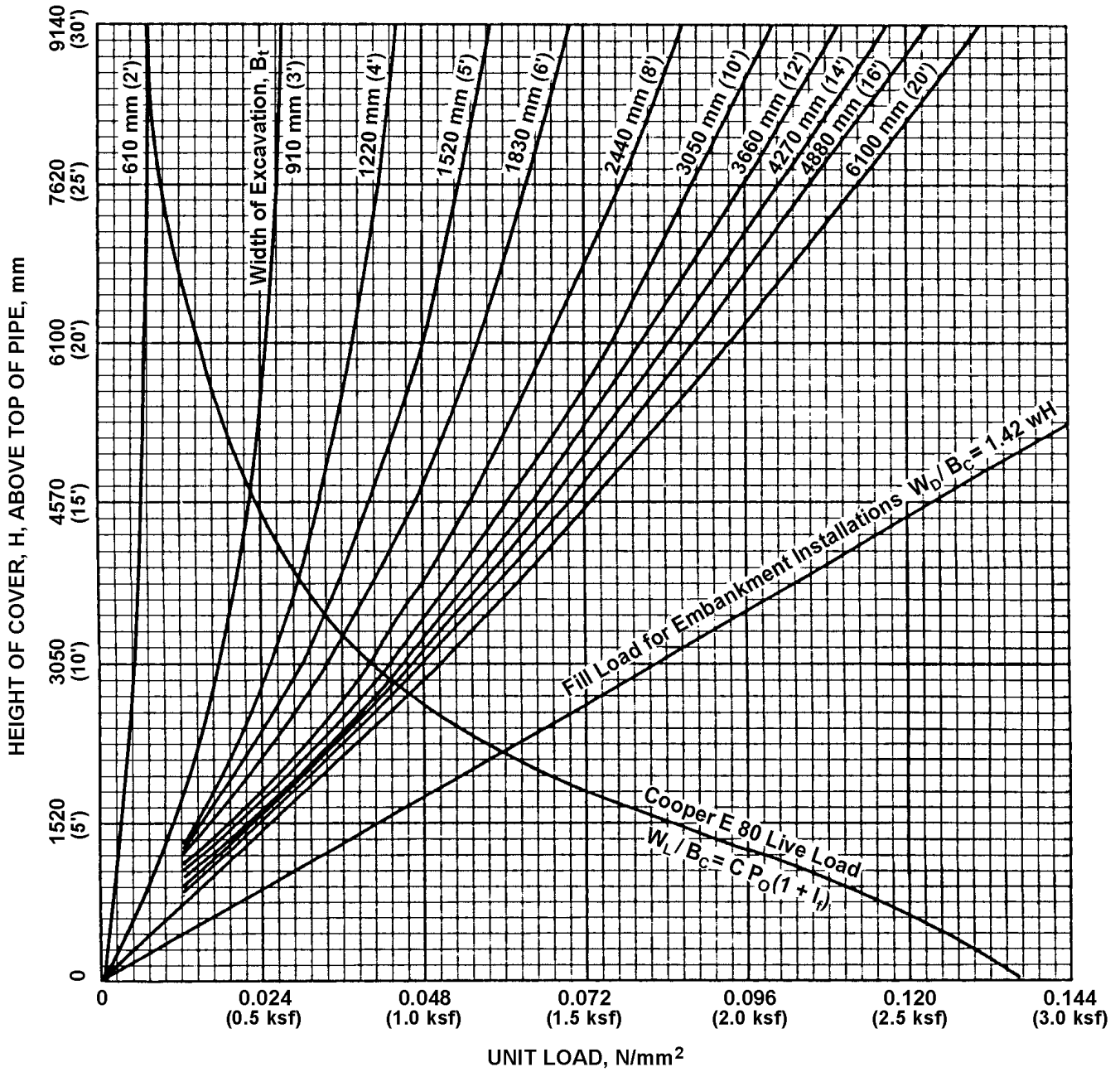
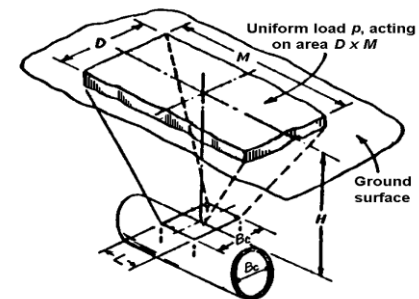


Figure 3.6.1.5.2P-1 - Live and Dead Loads on Pipe Installed Under Railroads (ACPA, 1981)

Table 3.6.1.5.2P-1 - Values of Load Coefficient (C) for Concentrated and Distributed Superimposed Loads Vertically Centered Over Culvert (ASCE, 1969)

$\frac{D}{2H}$ or $\frac{B_c}{2H}$	$\frac{M}{2H}$ or $\frac{L}{2H}$													
	0.1	0.2	0.3	0.4	0.5	0.6	0.7	0.8	0.9	1.0	1.2	1.5	2.0	5.0
0.1	0.019	0.037	0.053	0.067	0.079	0.089	0.097	0.103	0.108	0.112	0.117	0.121	0.121	0.128
0.2	0.037	0.072	0.103	0.131	0.155	0.174	0.189	0.202	0.211	0.219	0.229	0.238	0.211	0.218
0.3	0.053	0.103	0.149	0.190	0.221	0.252	0.274	0.292	0.306	0.318	0.333	0.345	0.355	0.360
0.4	0.067	0.131	0.190	0.241	0.281	0.320	0.349	0.373	0.391	0.405	0.425	0.440	0.454	0.460
0.5	0.079	0.155	0.224	0.284	0.336	0.379	0.414	0.441	0.463	0.484	0.505	0.525	0.540	0.548
0.6	0.089	0.171	0.252	0.320	0.379	0.428	0.467	0.499	0.524	0.544	0.572	0.596	0.613	0.624
0.7	0.097	0.189	0.274	0.349	0.414	0.467	0.511	0.516	0.584	0.597	0.628	0.650	0.674	0.688
0.8	0.103	0.202	0.292	0.373	0.441	0.499	0.546	0.581	0.615	0.639	0.674	0.703	0.725	0.740
0.9	0.108	0.211	0.306	0.391	0.463	0.524	0.574	0.615	0.647	0.673	0.711	0.742	0.766	0.784
1.0	0.112	0.219	0.318	0.405	0.481	0.544	0.597	0.639	0.673	0.701	0.740	0.774	0.800	0.816
1.2	0.117	0.229	0.333	0.425	0.505	0.572	0.628	0.674	0.711	0.740	0.783	0.820	0.819	0.868
1.5	0.121	0.238	0.345	0.440	0.525	0.596	0.650	0.703	0.742	0.774	0.820	0.861	0.891	0.916
2.0	0.121	0.211	0.355	0.454	0.540	0.613	0.674	0.725	0.766	0.800	0.819	0.894	0.930	0.956

*Influence coefficients for solution of Holl's and Newmark's integration of the Boussinesq equation for vertical stress



SPECIFICATIONS

COMMENTARY

3.6.1.6 PEDESTRIAN LOADS

The following shall supplement A3.6.1.6.

The pedestrian load is distributed using the lever rule.

When pedestrian loads are to be considered, two loading conditions shall be considered. The first loading condition assumes that the sidewalk is not present (i.e., an extended roadway surface and barrier would replace the sidewalk area) and the bridge is used for vehicular live load only. Under the second loading condition, the pedestrian load is present and the vehicular live load is factored at a reduced level. The Strength IP load combination was developed for the second loading condition.

3.6.2 Dynamic Load Allowance: IM

3.6.2.1 GENERAL

The following shall supplement A3.6.2.1.

For permit loads, the static effect of the P-82 shall be increased by a percentage not to exceed $IM = 20\%$.

IM for deck design = 50%

The second to last paragraph in A3.6.2.1 which begins "Dynamic load allowance need not..." shall be deleted.

3.6.2.1.1P Components for which IM is Applicable

The following components shall have the IM factor included in the design:

- all superstructure components including deck and deck joints
- pier caps and shafts
- backwalls and pedestals of abutments
- bearings, except for plain and reinforced elastomeric bearings

For buried components covered in D12 and A12, see D3.6.2.2. For wood component, see D3.6.2.3.

3.6.2.1.2P Components for which IM is Not Applicable

The following components shall not have the IM factor included in the design:

- retaining walls not subject to vertical reactions from the superstructure, including MSE walls
- foundation components which are entirely below

C3.6.2.1

Irregularities in decks such as potholes can result in large localized impact effects. As a result, PennDOT requires that the impact for decks be increased from 33% to 50% for decks. Other elements of the bridge structure should not be greatly affected by high localized impact due to dampening. The combination of 50% impact, the design truck (former HS20 truck) and LRFD deck design criteria will produce deck designs comparable to 30% impact, HS25 and past AASHTO deck design criteria.

C3.6.2.1.2P

The PAPIER program carries the live loads from the pier cap through to the footing without the removal of the effect of the dynamic load allowance (IM) input by the user. This provides a consistent mathematical model throughout the structure, where the moments, shears, and axial forces at the bottom of the column are equal to those at the top of the footing of the pier.

SPECIFICATIONS

COMMENTARY

ground level, including footings (except for frame and box culverts where IM is applicable as per A3.6.2.2), piles, caissons and pedestals

- abutment stems
- plain and reinforced elastomeric bearings
- buried components with 2400 mm {8 ft.} or greater fill above them (see A3.6.2.2)

The pedestrian load shall not have the IM factor applied.

3.6.2.2 BURIED COMPONENTS

The following shall replace A3.6.2.2.

The dynamic load allowance for culverts and other buried structures covered by Section 12, in percent, shall be taken as:

Metric Units:

$$IM = 40 (1.0 - 4.1 \times 10^{-4} D_E) \geq 0\% \quad (3.6.2.2-1)$$

U.S. Customary Units:

$$IM = 40 (1.0 - 0.125 D_E) \geq 0\%$$

where:

D_E = the minimum depth of earth cover above the structure (mm) {ft.}

Dynamic load allowance shall not be applied to foundation pressures.

3.6.2.3 WOOD COMPONENTS

C3.6.2.3

The following shall replace A3.6.2.3.

For wood bridges and wood components of bridges, the dynamic load allowance specified in A3.6.2.1 may be reduced to 50 percent of the values specified for IM in Table A3.6.2.1-1.

Delete the second sentence of CA3.6.2.3.

3.6.4 Braking Force: BR**C3.6.4**

The following shall supplement A3.6.4.

Dynamic load allowance is not applied to the braking force.

The following shall supplement CA3.6.4.

LRFD analysis of the capacity of existing substructure units on shorter span bridges may become problematic. Use of the original design braking force, requiring approval of the Chief Bridge Engineer, may be warranted for analysis of these older structures.

SPECIFICATIONS

COMMENTARY

Braking Force Factor Tables previously included in DM-4 have been deleted since AASHTO 3rd edition added lane loading.

The AASHTO 2nd edition used only axle loads, thus Braking Force Factor was developed.

3.6.5 Vehicular Collision Force CT

3.6.5.3 Vehicular Collision with barriers

The following shall supplement A3.6.5.3.

For transverse vehicular collision loading transferred to the substructure for u-wings and retaining walls, use a load of 45 kN {10 kip} acting over 1.5 m {5 ft} length applied at a distance equal to the height of the concrete barrier above the top of the wall.

3.8 WIND LOAD: WL AND WS

3.8.1 Horizontal Wind Pressure

3.8.1.2 WIND PRESSURE ON STRUCTURES: WS

3.8.1.2.1 General

C3.6.5.3

The following shall supplement AC3.6.5.3.

The transverse vehicular collision loading of 45 kN {10 kip} acting over 1.5 m {5 ft} may be distributed down to the footing at a 1:1 slope. Adjacent to open joints, this load may only be distributed in one direction which will usually be the controlling condition. Distributing the load in one direction is conservative for footing designs, since the footings are continuous at open joints.

C3.8.1.2.1

SPECIFICATIONS

COMMENTARY

3.8.3 Aeroelastic Instability**3.8.3.4 WIND TUNNEL TESTS**

The following shall replace A3.8.3.4.

If approved by the Chief Bridge Engineer, representative wind tunnel tests may be used to satisfy the requirements of A3.8.3.2 and A3.8.3.3.

3.9 ICE LOADS: IC**3.9.1 General**

The following shall supplement A3.9.1.

The forces due to ice shall be applied at the average elevation of the highest expected water elevation and the normal water elevation.

3.9.5 Vertical Forces due to Ice Adhesion

The following shall replace A3.9.5.

The vertical force on a bridge pier due to rapid water level fluctuation shall be taken as:

Metric Units:

- for a circular pier, in N:
 $0.3 t^2 + 0.0169 R t^{1.25}$
- for an oblong pier, in N:
 $0.3 t^2 + 0.0169 R t^{1.25} + 2.3 \times 10^{-3} L t^{1.25}$

U.S. Customary Units:

- for a circular pier, in kips:
 $6.27 t^2 + 1.48 R t^{1.25}$
- for an oblong pier, in kips:
 $6.27 t^2 + 1.48 R t^{1.25} + 0.2 L t^{1.25}$

where:

The following shall replace the last paragraph of AC3.8.1.2.1.

If approved by the Chief Bridge Engineer, wind tunnel tests may be used to provide more precise estimates of wind pressures. Such testing should be considered where wind is a major design load.

C3.8.1.2.2

The following shall supplement AC3.8.1.2.2.

The columns referenced in A3.8.1.2.2 are columns in arch bridges not columns in substructure units.

C3.9.1

The following shall supplement AC3.9.1.

The PAPIER program uses a default ice thickness of 150 mm {6 in.} and a default ice crushing strength of 2.75 MPa {58 ksf}.

C3.9.5

Delete AC3.9.5.

SPECIFICATIONS

- t = ice thickness (mm) {ft.}
- R = radius of circular pier (mm) {ft.} or approximated end of oblong pier
- L = perimeter of pier excluding half circles at ends of oblong pier (mm) {ft.}

3.10 EARTHQUAKE EFFECTS: EQ

COMMENTARY

C3.10.1 General

The following shall supplement AC3.10.1.

Minimize bridge skew as much as and whenever possible. It is well known that skewed structures perform poorly in seismic events when compared to the performance of normal or non-skewed structures.

These specifications present seismic design and construction requirements applicable to the majority of highway bridges to be constructed in the United States. Bridges not covered by these provisions probably constitute 5 to 15 percent of the total number of bridges designed.

The Project Engineering Panel (PEP) of the Applied Technology Council (ATC) has decided that special seismic design provisions are not required for buried structures. It was recognized by the PEP, however, that this decision may need to be reconsidered as more research data on the seismic performance of this type of structure become available.

These specifications specify minimum requirements. More sophisticated design or analysis techniques may be utilized if deemed appropriate by the Design Engineer.

For bridge types not covered by these specifications, the following factors should be considered.

- (a) The recommended elastic design force levels of the specifications should be applicable because force levels are largely independent of the type of bridge structure. It should be noted that the elastic design force levels of the specifications are part of a design philosophy described in Chapter 1 of FHWA Research Report FHWA-IP-87-6. The appropriateness of both the design force levels and the design philosophy must be assessed before they are used for bridges that are not covered by these specifications.
- (b) A multi-mode dynamic analysis should be considered, as specified in A4.7.4.3.3
- (c) Design displacements are as important as design forces; when possible, the design methodology should consider displacements arising from the effects discussed in DC4.7.4.4.

SPECIFICATIONS

COMMENTARY

- (d) If a design methodology similar to that used in these specifications is deemed desirable, the design requirements contained herein should be used to ensure compliance with the design philosophy.

Use caution when referencing the flowcharts contained in the Appendix to A3. They reference AASHTO LRFD Specifications which may be modified by the Design Manual, Part 4.

3.10.2 Acceleration Coefficient

The following shall replace A3.10.2.

The acceleration coefficient, A , to be used in the application of these provisions shall be determined from the County designations given in Figure 1.

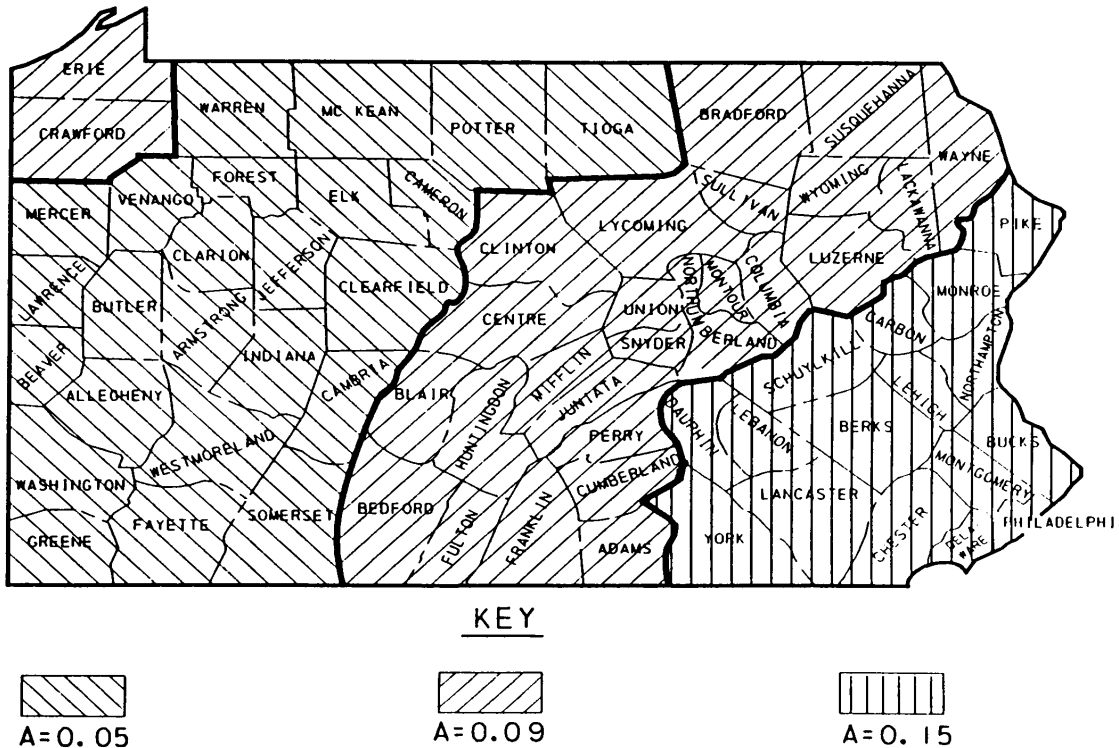


Figure 3.10.2-1 - Acceleration Coefficients for Pennsylvania Counties

3.10.7 Response Modification Factors

3.10.7.1 GENERAL

The following shall replace the first paragraph of A3.10.7.1.

Do not apply the response modification factors to single span structures or to structures in Seismic Zone 1.

The use of R-factors requires the reinforcing details meet the requirements of this document and the LRFD Specifications for consideration of structural ductility. All R-factors from Table A3.10.7.1-1 must be reduced to 1.0 if the details do not meet the specification requirements, unless tests have been done to indicate otherwise.

3.10.9 Calculation of Design Forces

3.10.9.2 SEISMIC ZONE 1

C3.10.9.2

The following shall supplement AC3.10.9.2.
 Prior to the redesign phase of the PEP project, the PEP thought that the design of connections for wind forces would be satisfactory for anticipated seismic forces for bridges in Seismic Zone 1. However, when the magnitude of the wind and seismic forces were compared for six bridges, it was found in almost all cases that, for an

SPECIFICATIONS

3.10.9.3 SEISMIC ZONE 2

COMMENTARY

acceleration coefficient of 0.10, seismic forces were greater than wind forces. In some cases the difference was significant. Hence it was deemed necessary to include the requirement of this section for the design of the connections. The requirement is simple and somewhat conservative, especially for more flexible bridges, since the forces are based on the maximum elastic response coefficient. If the design forces are difficult to accommodate, it is recommended that Seismic Zone 2 analysis and design procedures be used.

C3.10.9.3

The following shall supplement AC3.10.9.3.

The seismic design forces specified for bridges in Seismic Zone 2 are intended to be relatively simple, but consistent with the overall design concepts and methodology. Inherent in any simplification of a design procedure, however, is a degree of conservatism; for Seismic Zone 2 this occurs in the determination of the design forces for the foundations and connections to columns. If these forces appear to be excessive, more refined methods may be used. An acceptable approach would be to use the methods suggested for Seismic Zones 3 and 4 in the LRFD Specifications. For such a refinement, the foundations and connections to columns are designed for the maximum forces that a column can transmit to these components. In some cases, these may be considerably less than the design forces specified in this section.

This section specifies the design forces for the structural components of the bridge. In the first step, the elastic forces of Load Cases 1 and 2 of A3.10.8 are divided by the appropriate R-factors of A3.10.7. These forces are combined with those from other loads in load combination, Extreme Event I. Each component shall be designed to resist two seismic load combinations, one including Load Case 1 and the other including Load Case 2. Each load case incorporates different proportions of bi-directional seismic loading. This may be important for some components (e.g., bi-axial design of columns) and unimportant for others. In the design loads for each component, the sign of the seismic forces and moments obtained from A3.10.8 can be taken as either positive or negative. The sign of the seismic force or moment that gives the maximum magnitude for the design force (either positive or negative) shall be used.

This section also specifies the design forces for foundations which include the footings, pile caps, and piles. The design forces are essentially twice the seismic design forces of the columns. This will generally be conservative and was adopted to simplify the design procedure for bridges in Seismic Zone 2. However, if seismic forces do not govern the design of columns and piers, there is a possibility that during an earthquake the foundations will be subjected to forces larger than the design forces. This will occur if the columns remain elastic throughout the duration

SPECIFICATIONS

3.10.9.5 LONGITUDINAL RESTRAINERS

The following shall supplement A3.10.9.5.

Restrainers may only be used with the prior approval of the Chief Bridge Engineer.

3.11 EARTH PRESSURE: EH, ES, LS AND DD**3.11.1 General**

The following shall supplement A3.11.1.

Both the vertical and horizontal components of an inclined lateral earth pressure shall be considered for application of load and load factors.

3.11.3 Presence of Water

The following shall supplement A3.11.3.

Walls along a stream or river shall be designed for a minimum differential water pressure due to a 1000 mm {3'-0"} head of water in the backfill soil above the weephole inverts.

3.11.5 Earth Pressure: EH

COMMENTARY

of the seismic ground motion. Thus, for essential bridges in Seismic Zone 2, consideration should be given to the use of more refined methods in the design of the foundation. An acceptable approach would be to use the methods suggested for Seismic Zones 3 and 4 in the LRFD Specifications. It should be noted that ultimate soil and pile strengths are to be used with the specified foundation seismic design forces.

C3.11.3

The following shall supplement AC3.11.3.

Evaluation of water pressures and seepage forces is critical in the design of retaining walls because water pressures and seepage forces are the most common causes of retaining wall failure. Seepage forces and water pressures affect the stability of retaining walls by:

- Increasing the weight of soil behind the wall through saturation, thereby increasing the driving soil pressure
- Decreasing the effective weight of soil in front of the wall through upward seepage forces, thereby reducing the resisting soil pressure
- Decreasing the effective stress (normal force) on the wall foundation due to wall weight through uplift, thereby reducing sliding resistance and resistance to overturning.

C3.11.5.2 AT-REST PRESSURE COEFFICIENT, k_0

The following shall supplement AC3.11.5.2.

At-rest earth pressures are usually limited to bridge abutments to which superstructures are fixed prior to backfilling (e.g., framed bridges) or to cantilevered walls where the heel is restrained and the base/stem connection prevents rotation of the stem.

SPECIFICATIONS

COMMENTARY

C3.11.5.3 ACTIVE PRESSURE COEFFICIENT, k_a

The following shall supplement AC3.11.5.3.

The differences between the Coulomb Theory currently specified, and the Rankine Theory specified in the past is illustrated in Figure C1. The Rankine theory is the basis of the equivalent fluid method of A3.11.5.5 and the design procedures for mechanically stabilized earth walls.

Gravity and semi-gravity walls usually deflect a sufficient amount during backfilling to develop an active state of stress in the retained soil. This also is true of cantilevered and counterfort walls unless the heel is tied down or otherwise restrained and the base/stem connection prevents sufficient rotation of the stem to develop an active state of stress in the soil.

Wall movements cause the development of friction between the wall and the soil in contact with the wall. This resulting frictional force has the effect of inclining the earth pressure resultant on the wall, whereas the resultant would be normal to the wall in the case of no friction. The angle of inclination of the earth pressure resultant with respect to a line normal to the wall is called the angle of wall friction (δ).

3.11.5.4 PASSIVE PRESSURE COEFFICIENT, k_p

The following shall replace Figures A3.11.5.4-1 and A3.11.5.4-2.

SPECIFICATIONS

COMMENTARY

REDUCTION FACTOR (R) OF k_p FOR VARIOUS RATIOS OF $-\delta/\phi$									
ϕ	δ/ϕ	-0.7	-0.6	-0.5	-0.4	-0.3	-0.2	-0.1	0.0
10		.978	.962	.946	.929	.912	.898	.881	.864
15		.961	.934	.907	.881	.854	.830	.803	.775
20		.939	.901	.862	.824	.787	.752	.716	.678
25		.912	.860	.808	.759	.711	.666	.620	.574
30		.878	.811	.746	.686	.627	.574	.520	.467
35		.836	.752	.674	.603	.536	.475	.417	.362
40		.783	.682	.592	.512	.439	.375	.316	.262
45		.718	.600	.500	.414	.339	.339	.221	.174

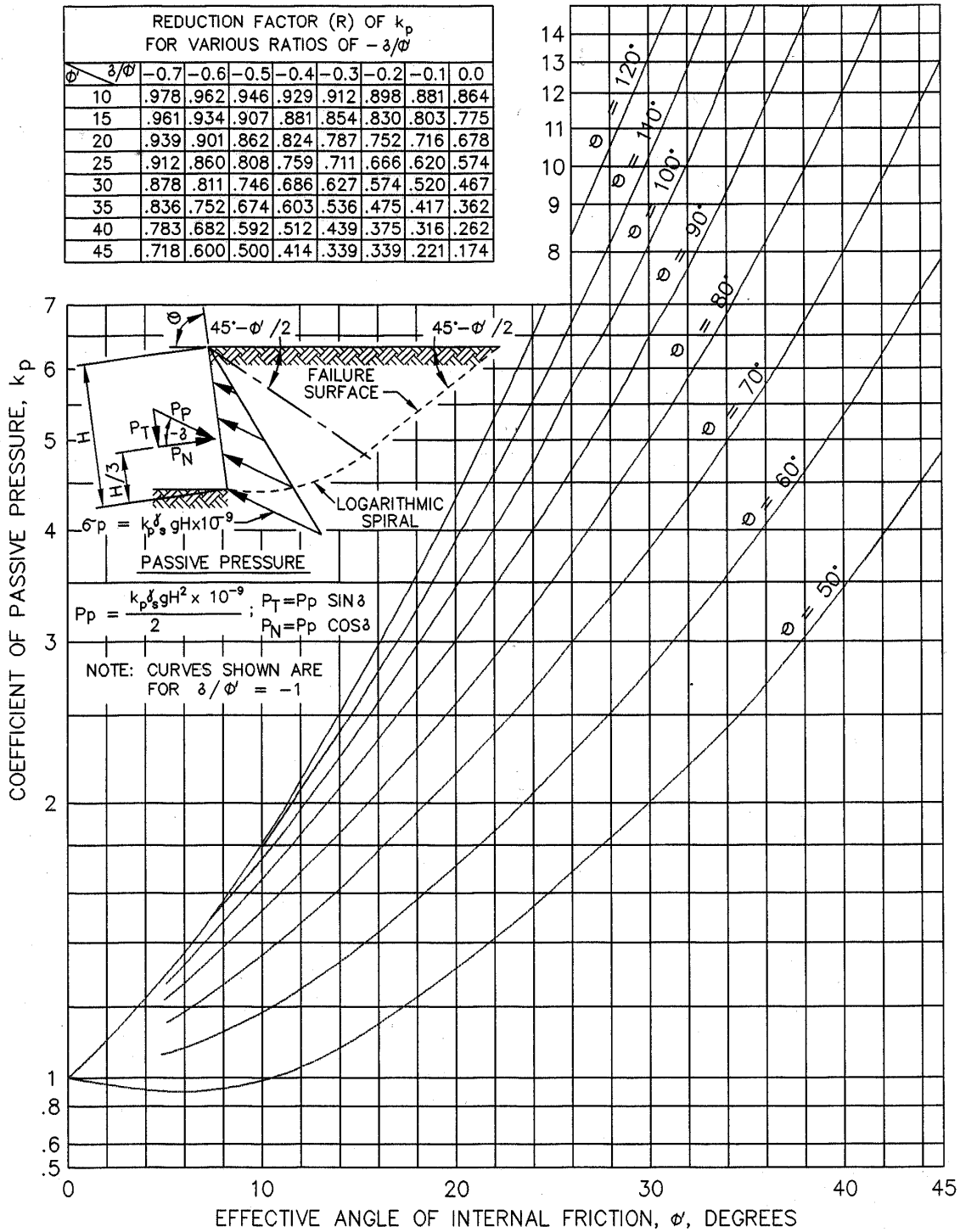


Figure 3.11.5.4-1 - Computational Procedures for Passive Earth Pressure for Sloping Wall with Horizontal Backfill

SPECIFICATIONS

COMMENTARY

REDUCTION FACTOR (R) OF k_p FOR VARIOUS RATIOS OF $-\beta/\phi$									
ϕ	β/ϕ	-0.7	-0.6	-0.5	-0.4	-0.3	-0.2	-0.1	0.0
10		.978	.962	.946	.929	.912	.898	.881	.864
15		.961	.934	.907	.881	.854	.830	.803	.775
20		.939	.901	.862	.824	.787	.752	.716	.678
25		.912	.860	.808	.759	.711	.666	.620	.574
30		.878	.811	.746	.686	.627	.574	.520	.467
35		.836	.752	.674	.603	.536	.475	.417	.362
40		.783	.682	.592	.512	.439	.375	.316	.262
45		.718	.600	.500	.414	.339	.271	.221	.174

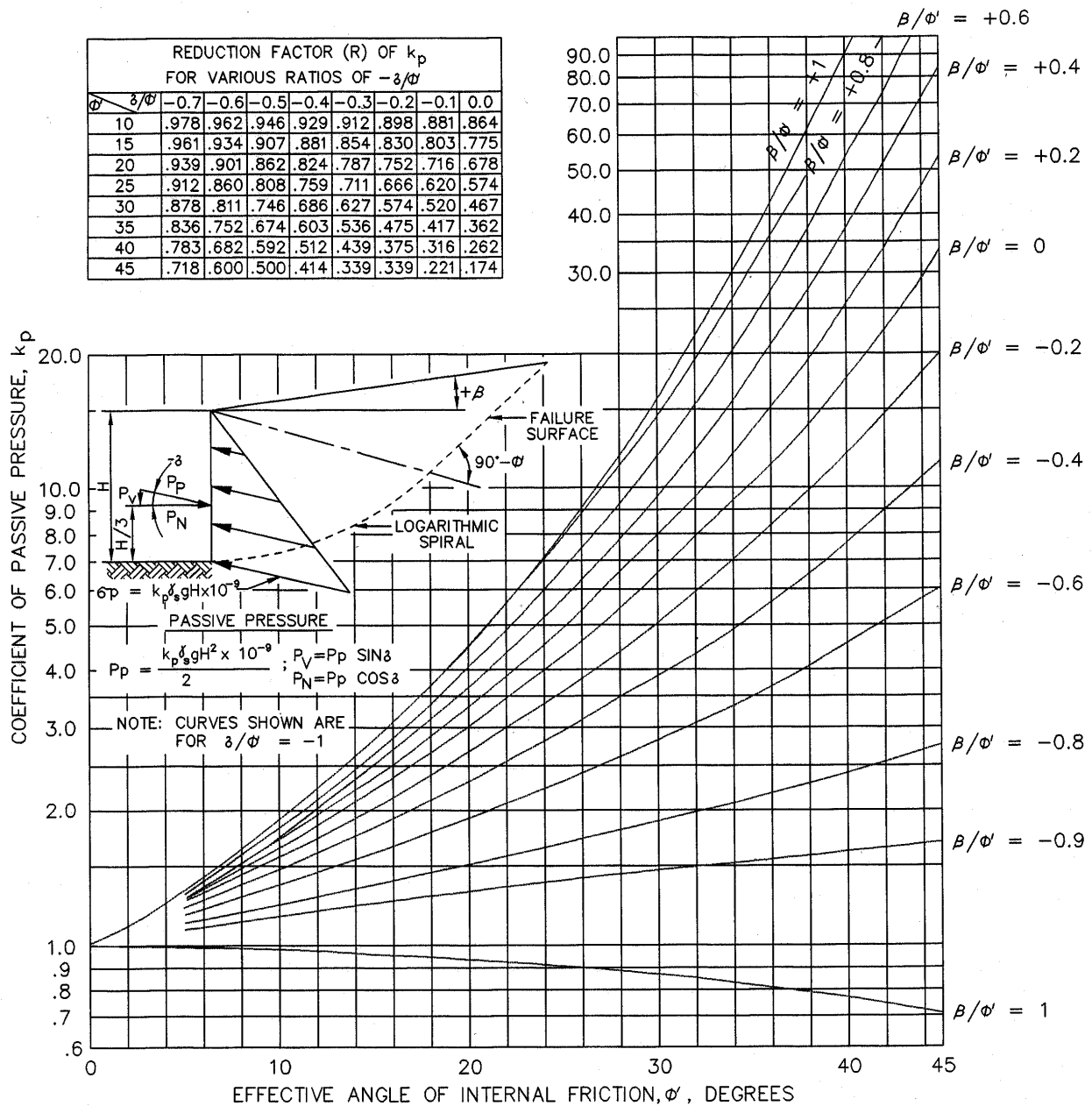


Figure 3.11.5.4-2 - Computational Procedures for Passive Earth Pressure for Vertical Wall With Sloping Backfill

3.11.5.5 EQUIVALENT-FLUID METHOD OF ESTIMATING EARTH PRESSURES C3.11.5.5

The following shall supplement A3.11.5.5.

Cohesionless soils with a maximum fines content of 5% by weight shall be used for backfill. This criteria can be met by backfilling with AASHTO No. 57 or the Department's open graded subbase (OGS) in conformance with Publication 408, Section 703.

For yielding walls backfilled with these materials, the design earth pressure at any depth shall be defined as

In the fifth paragraph of AC3.11.5.5, remove the reference to Figure AC3.11.5.3-1.

The following shall supplement AC3.11.5.5.

Soils with more than 5% fines shall be avoided as backfill because of their low permeability and potential frost susceptibility.

For design, the Department's open graded subbase (OGS) shall have the following assumed properties:

SPECIFICATIONS

increasing at a rate of 5.5×10^{-6} MPa/mm {0.035 ksf/ft}, plus the live load surcharge from A3.11.6.2 and D3.11.6.2.

For unyielding walls, restrained abutments (e.g., backfilled after superstructure erection), at-rest earth pressure, increasing at 8.0×10^{-6} MPa/mm {0.05 ksf/ft}, plus the live load surcharge from A3.11.6.2 and D3.11.6.2, shall be used.

The following shall supplement A3.11.5.5 for the design of box culverts.

For box culverts, equivalent fluid density shall be taken as specified in Table 2.

Table 3.11.5.5-2 - Equivalent Fluid Densities for Box Culverts

	Metric Units		U.S. Customary Units	
	Level Backfill 1 (kg/m ³)	Backfill with $\beta=25^\circ$ (kg/m ³)	Level Backfill (kcf)	Backfill with $\beta=25^\circ$ (kcf)
Minimum	720	880	0.045	0.055
Maximum	1120	1280	0.070	0.080

These equivalent fluid densities along with the appropriate maximum and minimum load factors shall be selected to produce the extreme force effects.

3.11.5.6 EARTH PRESSURE FOR NONGRAVITY CANTILEVER WALLS

For permanent walls, the simplified earth pressure distributions shown in Figures 1 and 2, or other suitable earth pressure distributions, may be used. If walls will support or are supported by cohesive soils for temporary applications, walls may be designed based on total stress methods of analysis and undrained shear strength parameters. For this latter case, the simplified earth pressure distributions shown in Figures 3 and 4, or other approved earth pressure distributions, may be used with the following restrictions:

- The ratio of overburden pressure to undrained shear strength (i.e., stability number $N = 10^{-9}\gamma H/c$ {U.S. Customary Units: $N = \gamma H/c$ }) must be < 3 .
- The active earth pressure shall not be less than 0.25 times the effective overburden pressure at any depth, or 5.5×10^{-6} MPa/mm {0.035 ksf/ft} of wall height, whichever is greater.

For temporary walls with discrete vertical elements

COMMENTARY

- moist density = 1920 kg/m^3 {0.120 kcf}
- saturated density = 2160 kg/m^3 {0.135 kcf}
- angle of internal friction = 30°

The following shall supplement AC3.11.5.5 for the design of box culverts.

Two soil types were selected for design to reflect potential lateral at-rest earth pressures for box culverts, considering construction practice and soil variability in Pennsylvania. The engineered backfill required for a distance of only 300 mm {1 ft.} from the face of the culvert wall is not sufficient to reduce lateral earth pressures to levels that would be expected for abutments and retaining walls for which more detailed backfill requirements are specified. Lateral earth pressures resulting from the factored load combinations, specified in this article, A3.4.1 and D3.4.1 compare closely with past DM-4 practice.

Although the equivalent fluid weights given in Table 1 correspond to those for "Dense Sand or Gravel" and "Compacted Lean Clay", backfill material shall be in conformance with the requirements given in Publication 408 and the contract documents. Equivalent fluid weights specified herein are for design only. Values of the equivalent fluid pressure for a sloping backfill are provided for the rare case in which the culvert is parallel to the roadway. In such a case, consideration should be given to sliding as a result of the imbalance of lateral loads.

C3.11.5.6

Nongravity cantilevered walls temporarily supporting or supported by cohesive soils are subject to excessive lateral deformation if the undrained soil shear strength is low compared to the shear stresses. Therefore, use of these walls should be limited to soils of adequate strength as represented by the stability number ($N = 10^{-9}\gamma H/c$) {U.S. Customary Units: $N = \gamma H/c$ }.

Base movements in the soil in front of a wall become significant for values of N of about 3 to 4, and a base failure can occur when N exceeds about 5 to 6, Terzaghi and Peck (1967).

SPECIFICATIONS

COMMENTARY

embedded in granular soil or rock, Figure 1 may be used to determine passive resistance and Figure 3 may be used to determine the active earth pressure due to the retained soil.

METRIC UNITS

U. S. CUSTOMARY UNITS

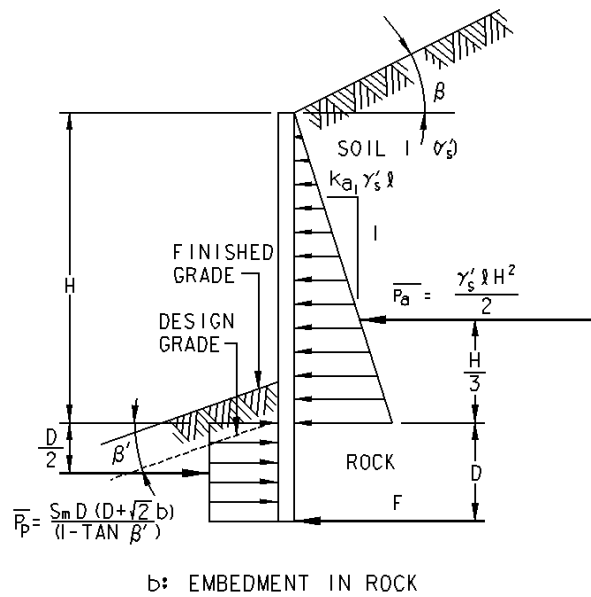
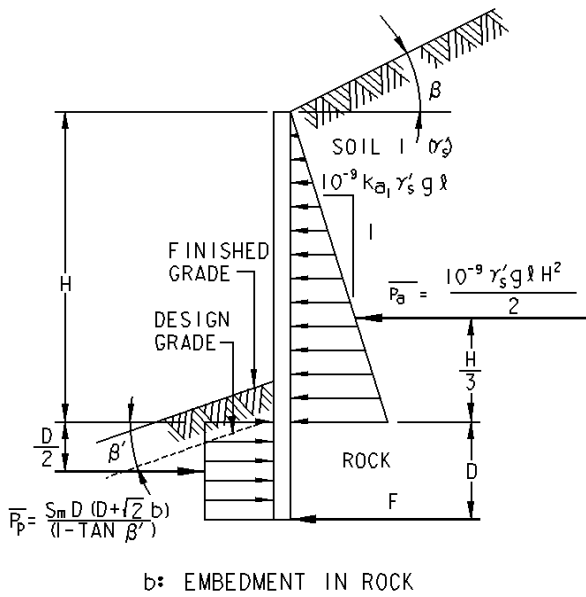
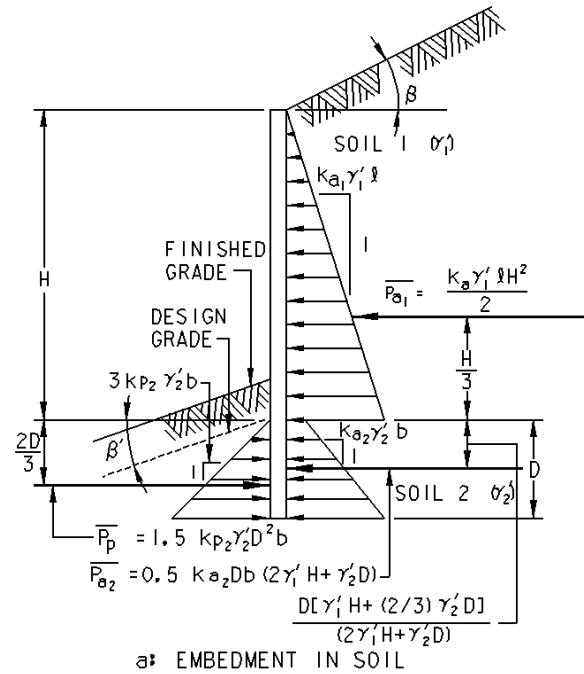
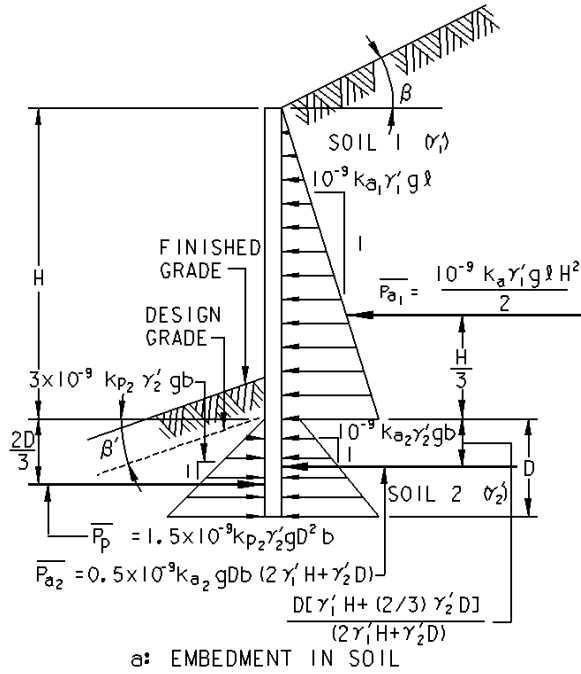


Figure 3.11.5.6-1 - Simplified Earth Pressure Distributions for Permanent Nongravity Cantilevered Walls with Discrete Vertical Wall Elements

SPECIFICATIONS

COMMENTARY

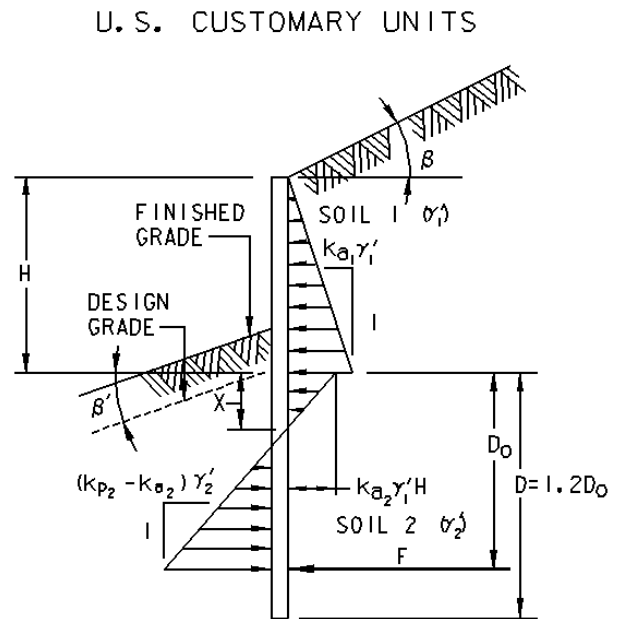
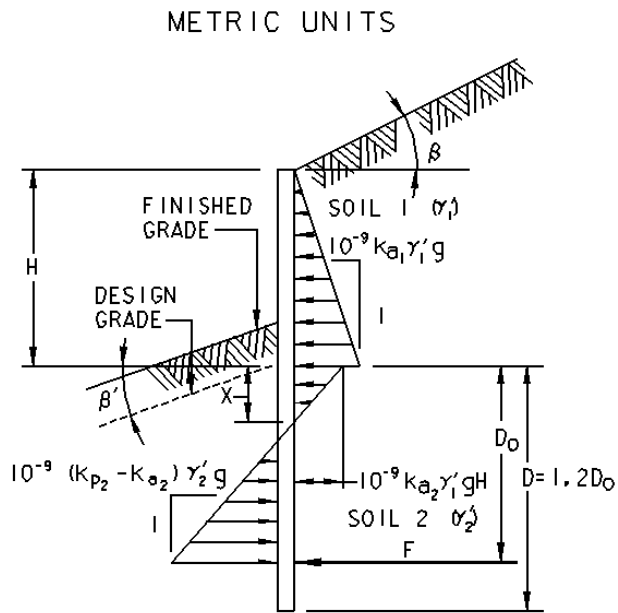


Figure 3.11.5.6-2 - Simplified Earth Pressure Distributions for Permanent Nongravity Cantilevered Walls with Continuous Vertical Wall Elements modified after Teng (1962)

SPECIFICATIONS

COMMENTARY

METRIC UNITS

U. S. CUSTOMARY UNITS

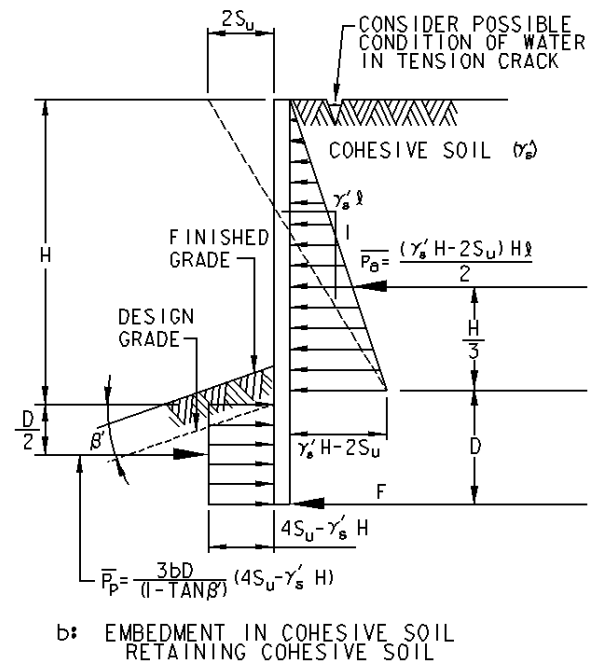
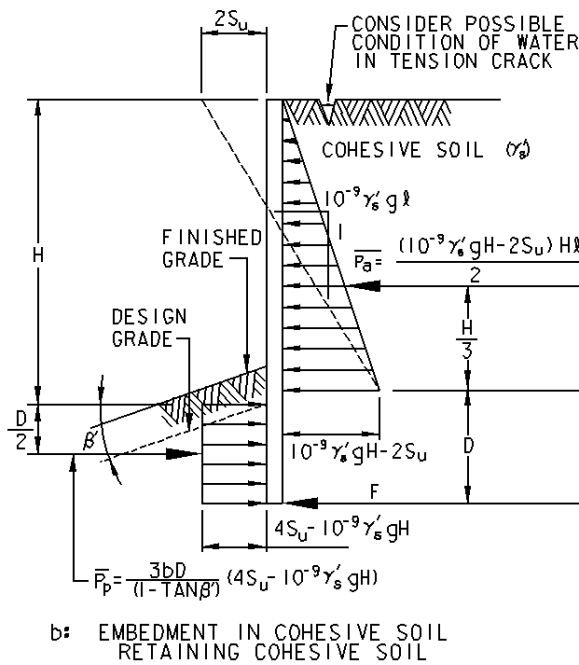
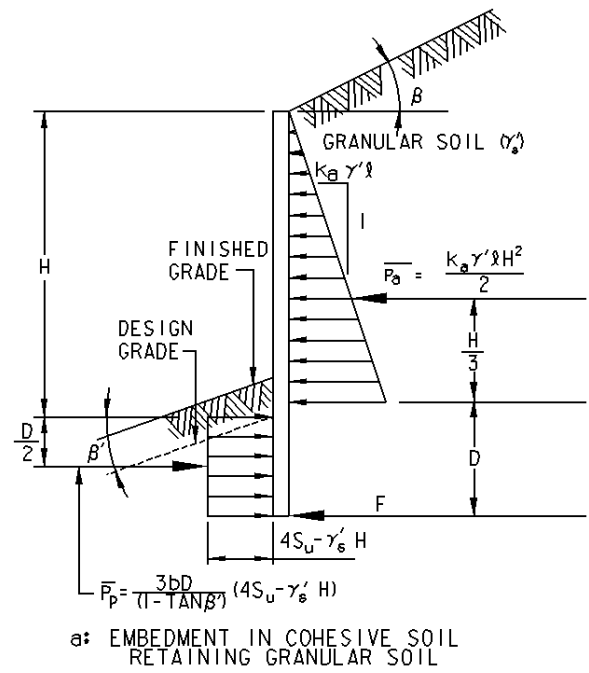
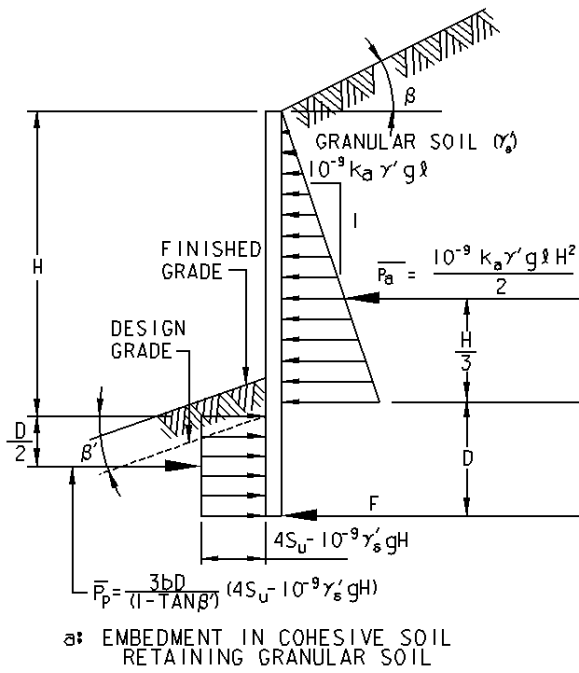
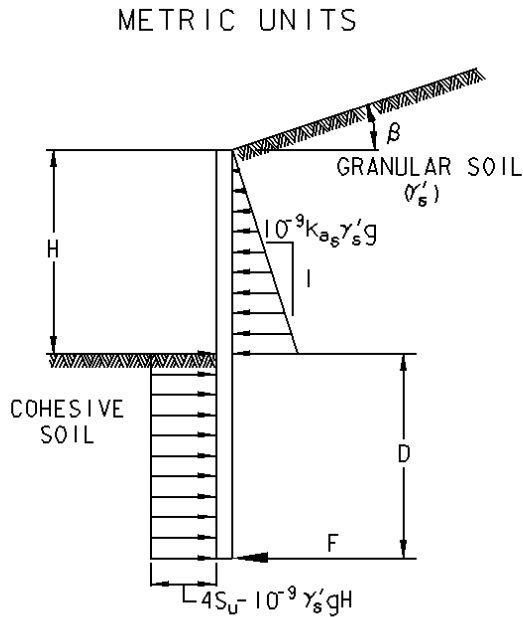


Figure 3.11.5.6-3 - Simplified Earth Pressure Distributions for Temporary Nongravity Cantilevered Walls with Discrete Vertical Wall Elements

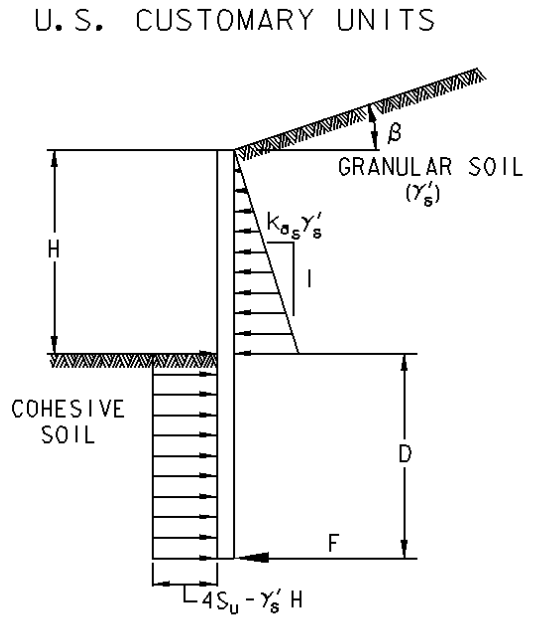
SPECIFICATIONS

COMMENTARY



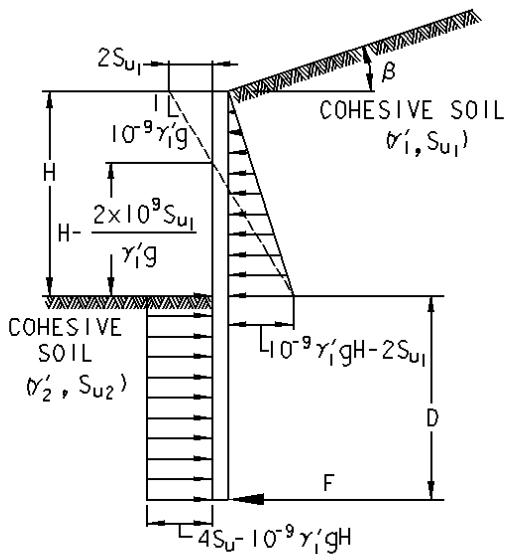
a: EMBEDMENT IN COHESIVE SOIL
RETAINING GRANULAR SOIL

NOTE: FOR WALLS EMBEDDED IN GRANULAR SOIL, REFER TO FIGURE 3.11.5.9P-2 AND USE ABOVE DIAGRAM FOR RETAINED COHESIVE SOIL WHEN APPROPRIATE.

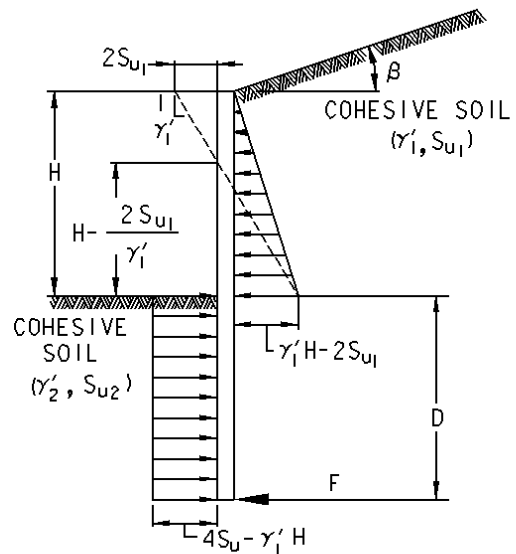


a: EMBEDMENT IN COHESIVE SOIL
RETAINING GRANULAR SOIL

NOTE: FOR WALLS EMBEDDED IN GRANULAR SOIL, REFER TO FIGURE 3.11.5.9P-2 AND USE ABOVE DIAGRAM FOR RETAINED COHESIVE SOIL WHEN APPROPRIATE.



b: EMBEDMENT IN COHESIVE SOIL
RETAINING COHESIVE SOIL



b: EMBEDMENT IN COHESIVE SOIL
RETAINING COHESIVE SOIL

Figure 3.11.5.6-4 - Simplified Earth Pressure Distributions for Temporary Nongravity Cantilevered Walls with Continuous Vertical Wall Elements modified after Teng (1962)

SPECIFICATIONS

Where discrete vertical wall elements are used for support, the width of each vertical element shall be assumed to equal the width of the flange or diameter of the element for driven sections and the diameter of the concrete-filled hole for sections encased in concrete.

The magnitude and location of resultant loads and resisting forces for permanent walls with discrete vertical elements embedded in soil and rock for lateral support may be determined using the earth pressure distributions presented in Figures 1 and 3. The procedure for determining the resultant passive resistance of a vertical element embedded in soil assumes the net passive resistance is mobilized across a maximum of three times the element width or diameter (reduced, if necessary, to account for soft clay, or discontinuities in the embedded depth of soil or rock) and that the active pressure below the facing elements acts only on the actual vertical element width. For the embedded portion of a wall with discrete vertical elements, the net passive resistance shall not be taken greater than that for continuous embedded vertical elements as determined using Figure 2 for permanent walls and Figure 4 for temporary walls.

The magnitude and location of resultant loads and resisting forces for permanent walls with continuous vertical elements may be determined using the earth pressure distributions presented in Figure 2 for permanent walls and Figure 4 for temporary walls.

Some portion of the embedded depth below finished grade, noted as β' in Figures 1-3, (usually 900 mm {3 ft.} for an element in soil, and 300 mm {1 ft.} for an element in rock) is ineffective in providing passive lateral support.

In developing the design lateral pressure, the lateral pressure due to water, live load surcharge, permanent point and line surcharge loads, backfill compaction, or other types of surcharge loads shall be added to the lateral earth pressure.

3.11.5.7 APPARENT EARTH PRESSURES FOR ANCHORED WALLS

COMMENTARY

In Figures 1 and 3, the width of discrete vertical wall elements effective in mobilizing the passive resistance of the soil is based on a method of analysis by Broms (1964a and 1964b) for single vertical piles embedded in cohesive or cohesionless soil and assumes a vertical element. The effective width for passive resistance of three times the element width (b) is due to the arching action in soil and side shear on resisting rock wedges. The maximum width of 3b can be used when material in which the vertical element is embedded is intact. This width shall be reduced if planes or zones of weakness would prevent mobilization of resistance through this entire width. If the element is embedded in soft clay having a stability number less than 3, soil arching will not occur and the actual width shall be used as the effective width for passive resistance. Where a vertical element is embedded in rock (Figure 1b), the passive resistance of the rock is assumed to develop through the shear failure of a rock wedge equal in width to the vertical element (b) and defined by a plane extending upward from the base of the element at an angle of 45°.

The upper 600 to 900 mm {2 to 3 ft.} of the discrete embedded vertical element in soil, or 300 mm {1 ft.} in rock, is typically assumed ineffective in mobilizing passive resistance to account for the effects of freezing and thawing, weathering or other shallow ground disturbance (e.g., utility excavations or pavement replacement in front of the wall).

C3.11.5.7

SPECIFICATIONS

The following shall replace A3.11.5.7:

For anchored walls constructed from the top down, the earth pressure may be estimated in accordance with Articles D3.11.5.7.1 or D3.11.5.7.2.

3.11.5.7.1 Cohesionless Soils

The following shall supplement A3.11.5.7.1:

The apparent earth pressure distribution for temporary and permanent anchored walls constructed from the top down and supporting cohesionless soil may be determined using Figures 1(a) and 1(b). Water pressures and surcharge pressures, if applicable, should be added explicitly to the diagrams to evaluate the total lateral load acting on the wall. Determine geostatic water pressure on the wall using the maximum expected water table differential between excavation interior and exterior, based on borings or other information.

In both Figures 1(a) and 1(b), calculate the maximum pressure ordinate p as indicated in the figures.

The earth pressure total load P_a per unit length of wall may then be calculated from the area of the apparent earth pressure distribution diagram as:

Metric Units:

$$P_a = 0.65k_a\gamma'_s gH^2(10^{-9}) \quad (3.11.5.7.1-3)$$

U.S. Customary Units:

$$P_a = 0.65k_a\gamma'_s H^2$$

where:

P_a = total earth pressure load per unit length of wall
(N/mm of wall) {kip/ft of wall}

k_a = active earth pressure coefficient (dim)
= $\tan^2(45-\phi_f/2)$ for $\beta=0$
use Equation A3.11.5.3-1 for $\beta \neq 0$

γ'_s = effective unit weight of soil (kg/m^3) {kcf}

COMMENTARY

The following shall supplement the first paragraph of AC3.11.5.7.

The earth pressure diagrams used herein are primarily intended for use in homogeneous soils. They should not be used indiscriminately in stratified or relatively non-homogeneous soil layers; engineering judgment must be used in these cases.

When anchors, especially those near the top of the wall, are tensioned to loads in excess of those estimated using the apparent pressure diagrams, it is possible that the wall could be displaced back into the soil mass, resulting in undesirable deflections or a passive failure of the retained soil. It is important to remember that anchored walls are flexible and that they derive their satisfactory performance from a match between the soil pressure and the wall-anchor loads.

C3.11.5.7.1P

Anchored walls are typically constructed with free-draining material placed immediately behind the lagging, and therefore geostatic water pressure on the wall would not be of concern. However, there may be conditions of a permanent water table behind the wall where geostatic water pressure needs to be considered.

SPECIFICATIONS**COMMENTARY**

H = total excavation depth (mm) {ft.}

H_1 = distance from ground surface to uppermost ground anchor (mm) {ft.}

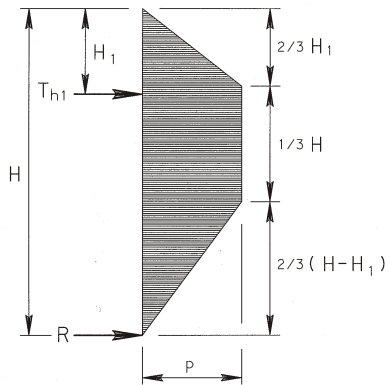
H_{n+1} = distance from base of excavation to lowermost ground anchor (mm) {ft.}

T_{hi} = horizontal load in anchor i (N/mm of wall) {kip/ft of wall}

R = reaction force to be resisted by subgrade (i.e., below base of excavation) (N/mm of wall) {kip/ft of wall}

SPECIFICATIONS

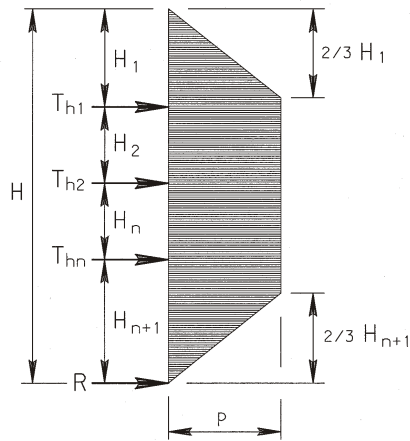
COMMENTARY



$$P = \frac{\text{TOTAL LOAD}}{2/3 H} \approx K_A \gamma_S^1 H (\text{u.s.})$$

(a) WALLS WITH ONE LEVEL OF GROUND ANCHORS

Figure 3.11.5.7.1-1(a) – Apparent Earth Pressure Distribution for Anchored Walls Constructed from the top down in Cohesionless Soils



$$P = \frac{\text{TOTAL LOAD}}{H - 1/3 H_1 - 1/3 H_{n+1}}$$

(b) WALLS WITH MULTIPLE LEVELS OF GROUND ANCHORS

Figure 3.11.5.7.1-1(b) – Apparent Earth Pressure Distribution for Anchored Walls Constructed from the top down in Cohesionless Soils

SPECIFICATIONS

COMMENTARY

3.11.5.7.2 Cohesive Soils

C3.11.5.7.2P

The following shall replace A3.11.5.7.2:

The apparent earth pressure distribution for cohesive soils is related to the stability number, N_s , which is defined as:

Cohesive soils with a stability number $N_s \leq 4$ are to be considered to be stiff to hard in consistency. Cohesive soils with a stability number $N_s > 4$ are to be considered very soft to medium-stiff in consistency

Metric Units:

$$N_s = \frac{\gamma_s H (10^{-9})}{S_u} \quad (3.11.5.7.2-1)$$

U.S. Customary Units:

$$N_s = \frac{\gamma_s H}{S_u}$$

where:

N_s = stability number (dim)

γ_s = total unit weight of soil (kg/m^3) {kcf}

H = total excavation depth (mm) {ft.}

S_u = average undrained shear strength of soil (MPa) {ksf}

Use the undrained shear strength of the soil through which the excavation extends.

3.11.5.7.2a Stiff to Hard, Including Fissured Cohesive Soils

C3.11.5.7.2a

The following shall replace A3.11.5.7.2a:

The apparent earth pressure distribution for temporary anchored walls constructed from the top down and supporting stiff to hard cohesive soils ($N_s \leq 4$) including fissured clays, where temporary conditions are of a controlled short duration and for which there is no available free water, may be determined using Figures 3.11.5.7.1-1(a) and 3.11.5.7.1-1(b). The identified terms remain the same, except that the maximum pressure ordinate of the diagram p shall be calculated as:

The following shall supplement AC3.11.5.7.2:

Metric Units:

$$p = 0.2\gamma_s gH \left(10^{-9} \right) \text{ to } 0.4\gamma_s gH \left(10^{-9} \right) \quad (3.11.5.7.2a-1)$$

U.S. Customary Units:

$$p = 0.2\gamma_s H \text{ to } 0.4\gamma_s H$$

SPECIFICATIONS

COMMENTARY

where:

p = maximum pressure ordinate (MPa) {ksf}

γ_s = total unit weight of soil (kg/m^3) {kcf}

H = total depth of excavation (mm) {ft.}

Surcharge pressures, if applicable, should be added explicitly to the diagrams to evaluate the total lateral load acting on the wall.

For other temporary conditions and for permanent conditions, calculate the earth pressure resultant using the maximum pressure ordinate obtained by either Equation 1 or Equation 3.11.5.7.1-1 with a value of k_a based on the drained friction angle of the clay. For any case, surcharge pressures, if applicable, should be added explicitly to the diagrams to evaluate the total lateral load acting on the wall. For conditions where there is available free water, determine geostatic water pressure on the wall using the maximum expected water table differential between excavation interior and exterior, based on borings or other information.

For permanent walls, the distribution (permanent or temporary) resulting in the maximum total force shall be used for design.

Alternatively, in fissured clays the apparent earth pressure diagram may be based upon previous successful experience with excavations constructed in similar soils. This is because earth pressures in these soils are most influenced by degree of fissuring or jointing in the clay and the potential reduction in strength with time, not necessarily the shear strength of the intact clay.

3.11.5.7.2b Very Soft to Medium-Stiff Cohesive Soils

The following shall replace A3.11.5.7.2b:

The apparent earth pressure distribution for temporary and permanent anchored walls constructed from the top down and supporting soft to medium-stiff cohesive soils may be determined using Figure 1. Soft to medium-stiff cohesive soils are those with a stability number $N_s > 4$.

There may be conditions of a permanent water table behind the wall where geostatic water pressure needs to be considered.

SPECIFICATIONS

COMMENTARY

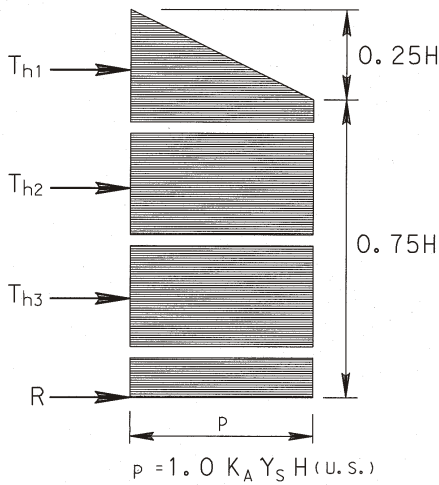


Figure 3.11.5.7.2b-1 - Apparent Earth Pressure Distribution for Anchored Walls Constructed from the top down in Soft to Medium-Stiff Cohesive Soils

Calculate the maximum pressure ordinate of the diagram p as:

Metric Units:

$$p = 0.4 k_a \gamma_s g H (10^{-9}) \quad (3.11.5.7.2b-1)$$

U.S. Customary Units:

$$p = 0.4 k_a \gamma_s H$$

where:

$$k_a = 0.22 \text{ for } 4 \leq N_s < 5.14$$

or

Metric Units:

$$k_a = 1 - m \frac{4 S_u}{\gamma_s g H (10^{-9})} \quad (3.11.5.7.2b-2)$$

U.S. Customary Units:

$$k_a = 1 - m \frac{4 S_u}{\gamma_s H}$$

for $N_s \geq 5.14$, and using $m = 0.4$

SPECIFICATIONS

COMMENTARY

Additionally, if $N_s \geq 6$ and the excavation is underlain by soft clay, calculate k_a by Equation 2 and Equation 3 below, and use the larger of the 2 k_a values in Equation 1 to calculate the maximum pressure ordinate.

Metric Units:

$$k_a = \max \left\{ \frac{4S_u}{\gamma_s H (10^{-9})} \frac{2\sqrt{2}d}{H} \left[\frac{\Delta H}{H} a - \frac{S_{ub}}{\gamma_s H (10^{-9})} b \right] \right.$$

U.S. Customary Units:

$$k_a = \max \left\{ \frac{4S_u}{\gamma_s H} \frac{2\sqrt{2}d}{H} \left[\frac{\Delta H}{H} a - \frac{S_{ub}}{\gamma_s H} b \right] \right.$$

where

$$a = \frac{H - \Delta H}{(2 - x)\sqrt{2}d} \text{ (dim)}$$

$$b = 5.14 \frac{2S_u \Delta H}{\sqrt{2}S_{ub}d} \text{ (dim)}$$

S_u = undrained shear strength of retained soil (MPa) {ksf}

S_{ub} = undrained shear strength of soil providing bearing resistance (MPa) {ksf}

d = depth of the potential base failure surface below the base of excavation (mm) {ft.}

γ_s = total unit weight of retained soil (kg/m^3) {kcf}

ΔH = depth of unloading at ground surface, if any (mm) {ft.}

X = length of unloading at top of anchored wall excavation, if any (mm) {ft.}

The value of d is taken as the thickness of soft to medium-stiff cohesive soil below the excavation base up to a maximum value of $B_c \sqrt{2}$, where B_c is the excavation width.

In any case, surcharge pressures, if applicable, should be added explicitly to the diagrams to evaluate the total lateral load acting on the wall. For conditions where there is available free water, determine geostatic water pressure on the wall using the maximum expected water table differential between excavation interior and exterior, based

There may be conditions of a permanent water table behind the wall where geostatic water pressure needs to be considered.

SPECIFICATIONS

COMMENTARY

on borings or other information.

3.11.5.8 EARTH PRESSURES FOR MECHANICALLY STABILIZED EARTH WALLS

3.11.5.8.1 General

The following shall replace the definition of k_a in A3.11.5.8.1:

k_a = active earth pressure coefficient specified herein

The following shall supplement A3.11.5.8.1:

Lateral earth pressure coefficients for MSE walls may be determined as follows:

- for a horizontal or sloping backfill surface, as shown in Figures A3.11.5.8.1-1 and A3.11.5.8.1-2, active earth pressure coefficient, k_a , in determining safety against soil failure may be taken as:

$$k_a = \cos \frac{\cos \beta \sqrt{\cos^2 \beta - e \sin^2 \beta}}{\cos \beta \sqrt{\cos^2 \beta - e \sin^2 \beta}} \quad (3.11.5.8.1-2)$$

β = slope of backfill behind wall (DEG)

ϕ_f = internal friction angle of backfill soil (DEG)

- for a broken back backfill surface, the active earth pressure coefficient, k_a , for evaluation of safety against soil failure may be taken as:

Error! Objects cannot be created from editing field
(3.11.5.8.1-3)

codes.

where:

B = notional slope of backfill behind wall as shown in Figure A3.11.5.8.1-3 (DEG)

ϕ_f = internal friction angle (DEG)

- active earth pressure coefficient, k_a , for determining safety against structural failure:

$$k_a = \tan^2 45^\circ - \frac{f}{2} \quad (3.11.5.8.1-4)$$

3.11.6 Surcharge Loads: ES and LS

3.11.6.4 LIVE LOAD SURCHARGE: LS

C3.11.6.4

SPECIFICATIONS

COMMENTARY

The following shall replace Table A3.11.6.4-1.

Table 3.11.6.4-1 - Equivalent Height of Soil for Vehicular Loading – Abutment

Metric Units		U.S. Customary Units	
Wall Height (mm)	H _{eq} (mm)	Wall Height (ft)	H _{eq} (ft)
≤ 1500	1200	≤ 5.0	4.0
≥ 3000	900	≥ 10.0	3.0

The following shall supplement A3.11.6.4.

The minimum design surcharge values for abutments in Table 1 are intended to account for normal traffic live loads and do not address the effects of backfill compaction. Refer to A3.11.2 to determine the effects of backfill compaction. For retaining walls, use Table 2.

Table 3.11.6.4-2 - Equivalent Height of Soil (h_{eq}) for Vehicular Loading - Retaining Walls

Metric Units			U.S. Customary Units		
Wall Height (mm)	Distance from back face of wall to the wheel line		Wall Height (ft)	Distance from back face of wall to the wheel line	
	0.0mm	300mm		0.0 ft	1 ft
≤ 1500	1500	900	≤ 5.0	5.0	3.0
3000	1050	900	10.0	3.5	3.0
≥ 4000	900	900	≥ 13.0	3.0	3.0

For box culverts, use 900 mm {3.0 ft} where live load effects are considered.

3.12 FORCE EFFECTS DUE TO SUPERIMPOSED DEFORMATIONS: TU, TG, SH, CR, SE

3.12.2 Uniform Temperature

3.12.2.1.1 TEMPERATURE RANGES

The following shall replace A3.12.2.1.1.

Provision shall be made for forces and movements resulting from variations in temperature. The range of temperature with respect to the normal erection temperature of 20° C {68° F} shall be as given in Table 1.

Delete the third paragraph of AC3.11.6.4.

The following shall supplement AC3.11.6.4.

In the development of this specification, the Department had a comparison made between their past abutment and retaining wall service load design method and the LRFD method. With minor modifications contained in this specification, the LRFD method gave similar results to the Department's past design method with one exception. For walls less than 1500 mm {5 ft.} in height on poor soils, the LRFD method may require base width significantly larger than past designs. Since the Department has not experienced problems with short headwalls for pipe culverts, the Standard Drawings may be used for headwalls for pipe culverts.

In Table D.3.11.6.4-2, the distance from back face of wall to edge of traveled way of 0.0 mm {0 ft} corresponds to placement of a point wheel load 600 mm {2 ft} from the back face of the wall. For the case of the uniformly distributed lane load, the 0.0 mm {0 ft} distance corresponds to the edge of the 3000 mm {10 ft} wide traffic lane.

C3.12.2.1

The following shall supplement AC3.12.2.1.1.

The inclusion of an additional temperature fall of 32° C is based on a Departmental study conducted in District 3-0. It was determined that the fixity at the connections of continuous spans produces a frame-type action that induces additional forces.

SPECIFICATIONS

COMMENTARY

Table 3.12.2.1.1-1 – Procedure A Temperature Ranges

Material	Metric Units		U.S. Customary Units	
	Temperature Rise	Temperature Fall	Temperature Rise	Temperature Fall
Steel or Aluminum Structures	23° C	43° C	42° F	78° F
Concrete Structures	18° C	32° C	32° F	58° F
Wood Structures	4° C	8° C	7° F	14° F
Bearings (Prestressed Concrete Structures) Temp. Range	Neoprene	Other	Neoprene	Other
	45° C	64° C	80° F	116° F
Bearings (Steel or Aluminum Structures) Temp. Range	56° C	86° C	100° F	156° F

For the design of integral abutments, the temperature range given for bearings shall be used.

3.12.3 Temperature Gradient

The following shall supplement A3.12.3.

The load factor for temperature gradient shall be taken as zero for those bridges which can be analyzed by the approximate methods given in A4.6.2 and D4.6.2, and are of Type a, b (only precast P/S concrete box girders), e, f, g, h, j, k and l as given in Table A4.6.2.2.1-1.

For Pennsylvania bridges other than those listed above, the Zone 3 data shall be used as given in Table A3.12.3-1.

3.12.7P Minimum Temperature Force for Fixed Substructures

When neoprene bearings are used, the fixed substructure unit(s) shall consider a thermal force equal to the largest thermal force from the largest expansion bearing substructure unit or utilize the results of an equilibrium analysis, whichever is larger.

3.12.8P Temporary Support Settlement For Curved and Skewed Bridges During Construction

When a temporary falsework is used, an analysis should be performed to check its settlement effects on member response during construction. As a minimum, the following scenarios should be considered for the analysis:

- *Settlement of single and multiple temporary supports.*
- *A minimum settlement of one thousandth of the span length should be used.*

C3.12.3

The following shall supplement AC3.12.3.

Pennsylvania has not experienced any temperature gradient-related problems in their typical multi-girder bridges. Therefore, as suggested in AC3.12.3, the Department's experience with typical multi-girder bridges has led them to exclude the temperature gradient load condition for these types of bridges.

C3.12.7P

This provision insures that fixed substructures are designed for a minimal thermal force even if an equilibrium analysis indicates no thermal forces are present. This is similar to the forces applied to steel bearings considering frozen bearings.

C3.13

The following shall replace AC3.13.

Low and high friction coefficients may be obtained from standard textbooks. If so warranted and approved by the Chief Bridge Engineer, the values may be determined by physical tests, especially if the surfaces are expected to be roughened in service.

When a force is transmitted from the superstructure to the substructure through a sliding bearing, the force applied to the substructure is considered a frictional force. However, forces transmitted, via a non-sliding bearing such as an elastomeric bearing, are factored by the appropriate load factor for the driving effect, such as TU.

SPECIFICATIONS

COMMENTARY

3.13 FRICTION FORCES: FR

The following shall supplement A3.13.

Friction force acts parallel to the direction of movement and is assumed to act at the bearing elevation at each expansion bearing, with due consideration given to the reactions that must develop at the fixed bearings to satisfy equilibrium. See A14.6.3.1 for horizontal forces.

Consideration of frozen expansion bearings and variation of friction is provided assuming the largest pier or abutment DL reaction times the applicable friction coefficient acts at the fixed pier or utilize the results of an equilibrium analysis, whichever is larger.

3.14 VESSEL COLLISION: CV**3.14.1 General**

The following shall supplement A3.14.1.

The vessel collision provisions provided in A3.14 and D3.14 shall only be used in the substructure design of bridges which cross a navigable waterway. The Department defines a navigable waterway as those waterways which:

- presently support commercial barge and/or ship traffic, and
- have supported commercial barge and/or ship traffic within the past 20 years.
- There is some reason to believe that the waterway will support commercial barge and/or ship traffic in the future.

3.14.2 Owner's Responsibility

The following shall replace A3.14.2.

When the vessel collision provisions are applicable according to D3.14.1, the designer must submit at the Type, Size and Location stage the following information for review by the Department:

- vessel traffic density in the waterway
- design velocity of vessels for the bridge
- suggested degree of damage that the bridge components, including protective systems are allowed to sustain

C3.14.1

The following shall supplement AC3.14.1.

For the vast majority of bridges over waterways in Pennsylvania, the vessel collision provisions will not be applicable.

The vessel collision provisions will most likely be applicable for bridges over the following waterways:

- lower portions of Delaware River
- lower portions of Schuylkill River
- lower portions of Allegheny River
- lower portions of Monongahela River
- Ohio River

C3.14.15 Protection of Substructures

SPECIFICATIONS

COMMENTARY

The following shall supplement AC3.14.15.
Any testing for protection systems of substructures must be approved by the Chief Bridge Engineer.

3.15P FORCE TRANSFER TO SUBSTRUCTURE

3.15.1P Longitudinal Force

3.15.1.2P FORCE TRANSFER TO SUBSTRUCTURE

Longitudinal forces, except friction (see D3.13), shall be carried only by fixed bearings.

3.15.1.3P EFFECTIVE LENGTH FOR SUPERSTRUCTURE FORCES

Longitudinal forces transmitted to the substructure from the superstructure shall be calculated using the center-to-center bearing length of superstructure restrained by fixed bearings. In the case of consecutively fixed piers, forces to the substructure shall be determined with due consideration to the relative stiffness of the piers.

3.15.1.4P FORCE RESOLUTION TO SUBSTRUCTURE

Longitudinal forces from the superstructure shall be directly applied at the bearings and shall be resolved in the directions perpendicular and parallel to the substructure, as shown in Figure 1. For frame analysis of the substructure, an equivalent parallel component shall be used, as shown in Figure 2.

For structures on a sloping grade with an inclined bearing plate, the reaction component parallel to the grade (longitudinal force) shall be considered.

SPECIFICATIONS

COMMENTARY

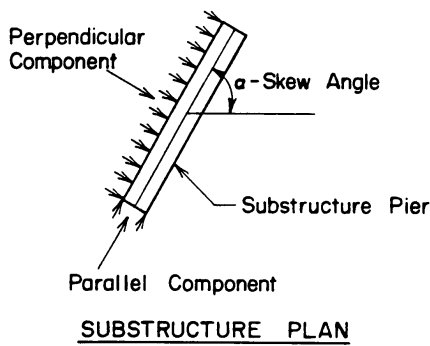
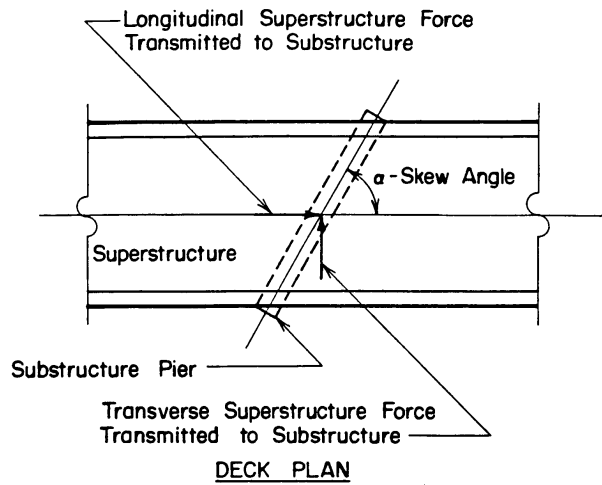


Figure 3.15.1.4P-1 - Force Resolution to Substructure

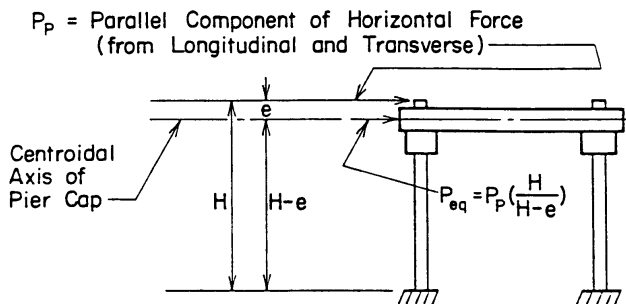


Figure 3.15.1.4P-2 - Equivalent Force for Frame Analysis of Substructure

3.15.2P Transverse Force

3.15.2.1P FORCE TRANSFER TO SUBSTRUCTURE

The transverse forces applied to the superstructure must be resisted by the bearings.

3.15.2.2P EFFECTIVE LENGTHS FOR

SPECIFICATIONS

COMMENTARY

SUPERSTRUCTURE FORCES

Unless a more rational method of analysis is used, transverse forces acting on a superstructure shall be transmitted to the bearings using the following span lengths:

Continuous Spans	Piers	Average of the two adjacent spans
	Abutments	One-half of the end span
Simple Spans		One-half of the span

3.15.2.3P FORCE RESOLUTION TO SUBSTRUCTURE

Transverse forces from the superstructure shall be resolved in the directions perpendicular and parallel to the substructure, as shown in Figure D3.15.1.4P-1.

3.15.2.4P DETERMINATION OF BEARING REACTIONS

The effect of the transverse force applied at the elevation specified for that force shall be taken into account in determining the vertical reactions at the bearings (see Figure 1).

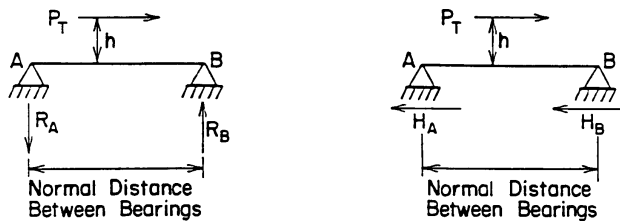
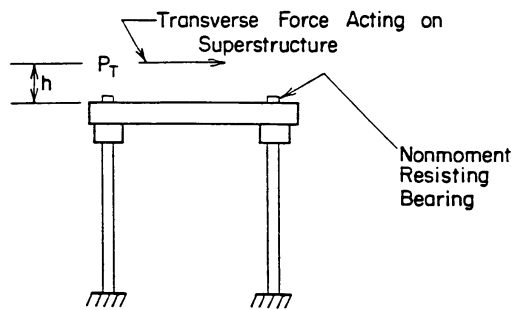


Figure 3.15.2.4P-1 - Bearing Reactions

REFERENCES

American Concrete Pipe Association (ACPA), Concrete Pipe Handbook, Vienna, VA, 435 p., 1981

American Society of Civil Engineers (ASCE), Design and Construction of Sanitary and Storm Sewer, prepared by a joint committee of the ASCE and the Water Pollution Control Federation (WPCF), ASCE - Manuals and Reports of Engineering Practice - No. 37 (WPCF Manual of Practice No. 9), 1969, 350 p.

Broms, B. B., "Lateral Resistance of Piles in Cohesive Soils", Journal of Soil Mechanics and Foundation Engineering Division, ASCE, Vol. 90, No. SM2, pp. 27-64, 1964a.

Broms, B. B., "Lateral Resistance of Piles in Cohesive Soils", Journal of Soil Mechanics and Foundation Engineering Division, ASCE, Vol. 90, No. SM3, pp. 123-156, 1964b.

Teng, W. C., "Foundation Design", Prentice-Hall, Englewood Cliffs, New Jersey, 466 pp., 1962

PENNSYLVANIA DEPARTMENT OF TRANSPORTATION
DESIGN MANUAL

PART 4

VOLUME 1
PART B: DESIGN SPECIFICATIONS

SECTION 4 - STRUCTURAL ANALYSIS AND EVALUATION

SECTION 4 - TABLE OF CONTENTS

4.1 SCOPE	B.4 - 1
4.2 DEFINITIONS	B.4 - 1
4.4 ACCEPTABLE METHODS OF STRUCTURAL ANALYSIS	B.4 - 1
4.5 MATHEMATICAL MODELING	B.4 - 2
4.5.1 General	B.4 - 2
4.5.2 Structural Material Behavior	B.4 - 2
4.5.2.2 ELASTIC BEHAVIOR	B.4 - 2
4.5.2.3 INELASTIC BEHAVIOR	B.4 - 3
4.6 STATIC ANALYSIS	B.4 - 3
4.6.1 Influence of Plan Geometry	B.4 - 3
4.6.1.2 STRUCTURES CURVED IN PLAN	B.4 - 3
4.6.1.2.1 General	B.4 - 3
4.6.2 Approximate Methods of Analysis	B.4 - 3
4.6.2.1 DECKS	B.4 - 3
4.6.2.1.3 Width of Equivalent Interior Strips	B.4 - 3
C4.6.2.1.6 Calculation of Force Effects.....	B.4 - 3
4.6.2.1.8 Live Load Distribution on Fully Filled and Partially Filled Grids	B.4 - 3
4.6.2.1.9 Inelastic Analysis	B.4 - 4
4.6.2.2 BEAM-SLAB BRIDGES	B.4 - 4
4.6.2.2.1 Application	B.4 - 4
4.6.2.2.2 Distribution Factor Method for Moment and Shear	B.4 - 8
4.6.2.2.2a Interior Beams with Wood Decks	B.4 - 8
4.6.2.2.2b Interior Beams with Concrete Decks	B.4 - 8
4.6.2.2.2e Skewed Bridges.....	B.4 - 13
4.6.2.2.3 Distribution Factor Method for Shear	B.4 - 13
4.6.2.2.3a Interior Beams.....	B.4 - 13
4.6.2.3 EQUIVALENT STRIP WIDTHS FOR SLAB-TYPE BRIDGES	B.4 - 19
4.6.2.5 EFFECTIVE LENGTH FACTOR, K.....	B.4 - 19
4.6.2.6.1 General	B.4 - 20
4.6.2.10P GIRDER - FLOORBEAM - STRINGER BRIDGES	B.4 - 21
4.6.2.10.1P Girder Live Load Distribution Factors	B.4 - 21
4.6.2.10.2P Stringer Live Load Distribution Factors.....	B.4 - 21
4.6.2.10.3P Floorbeam Live Load Distribution Factors	B.4 - 21
4.6.2.10.3aP Floorbeams with the Top Flange not Directly Supporting the Deck	B.4 - 21
4.6.2.10.3bP Floorbeams with the Top Flange Directly Supporting the Deck	B.4 - 21
4.6.2.11P DISTRIBUTION OF LOAD FROM THE SUPERSTRUCTURE TO THE SUBSTRUCTURE....	B.4 - 21
4.6.2.12P EQUIVALENT STRIP WIDTHS FOR BOX CULVERTS.....	B.4 - 22
4.6.2.12.1P General	B.4 - 22
4.6.2.12.2P Case 1: Traffic Travels Parallel to Span.....	B.4 - 22
4.6.2.12.3P Case 2: Traffic Travels Perpendicular to Span.....	B.4 - 22
4.6.2.12.4P Precast Box Culverts	B.4 - 23
4.6.3 Refined Methods of Analysis	B.4 - 24
4.6.3.1 GENERAL	B.4 - 24
4.6.3.2 DECKS.....	B.4 - 24
4.6.3.2.3 Orthotropic Plate Model	B.4 - 24
4.6.3.3 BEAM-SLAB BRIDGES	B.4 - 24

4.6.4 Redistribution of Negative Moments in Continuous Beam Bridges	B.4 - 36
4.6.4.1 GENERAL	B.4 - 36
4.6.4.2 REFINED METHOD	B.4 - 36
4.6.4.3 APPROXIMATE PROCEDURE	B.4 - 36
4.7 DYNAMIC ANALYSIS	B.4 - 36
4.7.1 Basic Requirements of Structural Dynamics	B.4 - 36
C4.7.1.4 DAMPING.....	B.4 - 36
4.7.2 Elastic Dynamic Responses	B.4 - 36
4.7.2.2 WIND-INDUCED VIBRATION	B.4 - 36
4.7.2.2.1 Wind Velocities.....	B.4 - 36
4.7.4 Analysis for Earthquake Loads	B.4 - 36
4.7.4.3 MULTI-SPAN BRIDGES	B.4 - 36
4.7.4.3.1 Selection of Method	B.4 - 36
4.7.4.3.5P Determination of Elastic Forces and Displacements	B.4 - 37
4.7.4.4 MINIMUM DISPLACEMENT REQUIREMENTS	B.4 - 37
4.7.4.5P BASE ISOLATION DESIGN	B.4 - 38
4.7.4.5.1P General	B.4 - 38
4.7.4.5.2P Statically Equivalent Seismic Force and Coefficient	B.4 - 43
4.7.4.5.3P Requirements for Elastic Force Determination	B.4 - 45
4.7.4.5.4P Design Displacement for Other Loads	B.4 - 46
4.7.4.5.5P Design Forces for Seismic Zone 1	B.4 - 46
4.7.4.5.6P Design Forces for Seismic Zone 2	B.4 - 46
4.7.4.5.7P Substructure Design Requirements	B.4 - 46
4.7.4.5.7.1P <i>Foundations and Abutments</i>	B.4 - 46
4.7.4.5.7.2P <i>Columns, Footings and Connections</i>	B.4 - 46
4.7.4.5.7.2aP <u>Structural Steel</u>	B.4 - 46
4.7.4.5.7.2bP <u>Reinforced Concrete</u>	B.4 - 46
4.8 ANALYSIS BY PHYSICAL MODELS	B.4 - 47
4.8.2 Bridge Testing	B.4 - 47

SPECIFICATIONS

COMMENTARY

4.1 SCOPE

The following shall replace the last paragraph of A4.1.
 Bridge structures shall be analyzed elastically, except as noted herein. An inelastic analysis of bridge structures may only be used for Extreme Event Limit States with the approval of the Chief Bridge Engineer.

C4.1

Delete the last sentence of the last paragraph of AC4.1.

4.2 DEFINITIONS

The following shall supplement A4.2.

Automatic Mesh Generator - Program or subprogram which creates the layout (arrangement of nodes and elements) of a model for the user if certain basic information is provided.

Influence Surface - Curved surface on which the ordinate is the value of the function (shear, moment, reaction, etc.) when a unit load is placed at the ordinate for a member location (centerline of a girder, support, etc.).

Influence Surface Loader - Computer program or portion of a computer program which calculates and maximizes the value of a function (shear, moment, reaction, deflection, etc.) by using the influence surface for that function.

Line Girder Analysis - Analysis of a bridge in which each girder is removed and analyzed as a single non-interacting element.

Loading Algorithm - Methodology used by the influence surface loader to calculate the moments, shear, etc.

PEP - Project Engineering Panel of Applied Technology Council

Refined Analysis - Analysis according to A4.6.3 and D4.6.3.

Shear Lag - Nonuniform stress pattern due to ineffective transmission of shear.

Skew Angle - Angular measurement between the base line of the bridge and centerline of the pier; a 90° skew angle defining a right bridge.

St. Venant Torsion - Uniform torsion resulting in no deformation of the cross-section.

Three-Dimensional Finite Element Analysis - Analysis in which a three-dimensional continuum is modeled as an assemblage of discrete elements in three-dimensional space.

Warping Torsion - Nonuniform torsion resulting in warping of the cross-section.

4.4 ACCEPTABLE METHODS OF STRUCTURAL ANALYSIS

The following shall supplement A4.4.

The designer shall also follow the requirements in PP1.4 in regards to computer programs.

Any computer program for the "3D or refined" analysis of girder bridges which has not been reviewed by the Department shall be submitted to, and approved by, the Chief Bridge Engineer prior to its use. A sample bridge(s) selected by the Department is to be modeled with the program so that the Department can make comparisons between its reviewed programs and the proposed program.

SPECIFICATIONS

COMMENTARY

Computer programs for the analysis of girder bridges approved for use (on LFD design projects) are listed in Appendix J. Only the version of a program listed in Appendix J has been tested and approved. If any changes and/or modifications have been made to a program since its approval date, then re-approval of the program is required. The approval of these programs is subject to the following conditions and limitations:

1. While certain software packages provide design optimization and/or code compliance checks, these aspects were not included in the review and approval process. Acceptance has been based solely upon the review of generalized design forces (moments, shears, reactions, etc.), as calculated by the software.
2. Acceptance of a software package by the Department does not affect the responsibility of the user for the proper application of the software and interpretation of its results. The acceptance of a software package does not constitute an endorsement nor does it relieve the vendor and the designer from their responsibility for accurate, technically correct and sound engineering results and services to the Department.
3. The Department's acceptance does not constitute any form of implied warranty, including warranty of merchantability and fitness for a particular purpose. The Commonwealth makes no warranty or representation, either expressed or implied, with respect to this software or accompanying documentation, including their quality performance, merchantability, or fitness for a particular purpose. In addition, the Commonwealth will not be liable for any direct, indirect, special, incidental, or consequential damages arising out of the use, inability to use, or any defect in the software or any accompanying documentation.

4.5 MATHEMATICAL MODELING

4.5.1 General

The following shall replace the second paragraph of A4.5.1.

Barriers shall not be considered in the calculation of the structural stiffness nor structural resistance of a structure.

The following shall supplement A4.5.1.

Centerline distances shall be used in the analysis of continuous frames, such as boxes, arches and pier bents.

4.5.2 Structural Material Behavior

4.5.2.2 ELASTIC BEHAVIOR

The following shall supplement A4.5.2.2.

For simple and continuous spans, composite stiffness

SPECIFICATIONS

COMMENTARY

shall be used if a concrete deck is used.

4.5.2.3 INELASTIC BEHAVIOR

The following shall replace the first sentence of the second paragraph of A4.5.2.3.

The inelastic model shall be based either upon the results of physical tests or upon a representation of load deformation behavior which is validated by tests, but either method must be approved by the Chief Bridge Engineer.

4.6 STATIC ANALYSIS

4.6.1 Influence of Plan Geometry

4.6.1.2 STRUCTURES CURVED IN PLAN

4.6.1.2.1 General

The following shall supplement A4.6.1.2.1.

Bridges which have kinked girders shall use the provisions of A4.6.1.2.1 to determine if they are to be considered curved.

For the design of horizontally curved steel girder highway bridges, a load and resistance factor design is required. A load factor design may also be permitted if requested at TS&L stage. For a load factor design, use the AASHTO, Guide Specification for Horizontally Curved Highway Bridges, AASHTO, Standard Specifications for Highway Bridges, and the 1993 Design Manual, Part 4. The force effects (i.e., moments, shear, reacting, etc.) for the curved bridge shall be determined using a refined method of analysis. (Please note that the above-referenced LFD documents are in U. S. Customary Units.)

4.6.2 Approximate Methods of Analysis

4.6.2.1 DECKS

4.6.2.1.3 Width of Equivalent Interior Strips

In Table A4.6.2.1.3-1 replace the entry for wood planks as follows:

The width of a primary wood plank strip spanning parallel to traffic shall be taken as 510 mm {20 in.}. The width of a primary wood plank strip spanning perpendicular to traffic shall be taken as the plank width, but not less than 250 mm {10 in.}.

4.6.2.1.8 Live Load Distribution on Fully Filled and Partially Filled Grids

The following shall replace A4.6.2.1.8.
Design in accordance with Tables per BD-604M.

C4.6.1.2.1

The selected refined method of analysis for a structure curved in plan must provide an accurate prediction of behavior, both during construction and while in-service. While the method of analysis that is selected is at the discretion of the designer, a superstructure modeling technique that represents the girder webs and concrete deck using shell elements and other major superstructure components using beam elements provides an acceptable compromise between reduced computation times provided by grillage analogy models and increased accuracy provided by more sophisticated three-dimensional finite element models.

C4.6.2.1.6 Calculation of Force Effects

Delete the first paragraph of AC4.6.2.1.6.

SPECIFICATIONS

COMMENTARY

The stiffness ratio, D, shall be taken as:

- for fully filled grids with at least 40 mm {1 1/2 in.} monolithic overfill2.0
- for all other fully filled grids2.5
- for partially filled grids with at least 40 mm {1 1/2 in.} monolithic overfill8.0
- for all other partially filled grid10.0

When approved by the Chief Bridge Engineer, the stiffness ratio, D, determined from test results may be used.

4.6.2.1.9 Inelastic Analysis

The following shall replace A4.6.2.1.9

The inelastic finite element analysis or yield line analysis are not permitted unless specifically approved by the Chief Bridge Engineer. If approved, this type of analysis is to be only used for Extreme Event Limit State.

4.6.2.2 BEAM-SLAB BRIDGES

4.6.2.2.1 Application

The following shall replace the third paragraph of A4.6.2.2.1.

For any variables exceeding the range of applicability, as specified in A4.6.2.2 and D4.6.2.2, the Chief Bridge Engineer must approve the method for determining the distribution factors.

The following shall supplement A4.6.2.2.1.

The articles in this section which provide approximate distribution factors are not applicable for bridges which are considered curved as defined in A4.6.1.2.1 and D4.6.1.2.1. For curved bridges, a refined method of analysis, as defined in A4.6.3 and D4.6.3, is required.

Additional requirements for skewed structures must be considered as follows:

- Apply the skew adjustment factors as given in A4.6.2.2.3c and D4.6.2.2.3c on all skewed structures as a minimum.
- Steel structures with a skew angle less than 70° require an additional check against uplift at the acute corners.
- Concrete structures with a skew angle less than 45° require an additional check against uplift at the acute corners.
- The design of bearings for bridges with skew angles less than 70° require consideration of out-of-plane rotations.

C4.6.2.2.1

The following shall replace the fifth sentence of the twelfth paragraph of AC4.6.2.2.1.

The use of transverse mild steel rods secured by nuts, or similar unstressed dowels should not be considered sufficient to achieve full transverse flexural continuity unless demonstrated by test or experience and approved by the Chief Bridge Engineer.

The following shall supplement AC4.6.2.2.1.

AASHTO provides consideration of skew angle by way of moment and shear correction factors. PennDOT agrees with the application of the shear correction factors. PennDOT has decided not to take advantage of the reduction in load distribution factors for moment. However, these factors do not adequately address problems due to out-of-plane rotations, uplift, or cross-frame forces. The provisions in this section are meant to be applied to account for these items. Note that uplift on concrete structures is not considered as critical as that on steel structures.

During routine bridge inspections, the Department has found many occurrences of buckled cross-frame members and poor bearing performance on skewed structures. The Department has found from refined analyses that cross-frames in skewed structures are potentially subjected to higher force levels than cross-frames in normal (90°) structures. This does not mandate a 3-D analysis, but does

SPECIFICATIONS

- Steel structures with skew angles less than 70° require a special cross-frame design and the cross-frame members must be considered as main load carrying members.

Table 1 describes how the term L (length) shall be determined for use in the live load distribution factor equations given in A4.6.2.2.2, A4.6.2.2.3, D4.6.2.2.2 and D4.6.2.2.3.

COMMENTARY

mean a special analysis of the cross-frame must be provided in order to account for the differential deflections which occur across a cross-frame. *This analysis should accurately account for cross frame member geometry and stiffness. Should a grillage analogy model be used, accurate representation of cross frame stiffness should be established via special analysis of representative frames. Should a more sophisticated 3-D analysis be used, models can be constructed following the technique recommended in C4.6.1.2.1 for structures curved in plan.*

A crude or approximate uplift check can be made using the second term of the adjustment factor as an estimate of negative live load reaction potential. Comparing the negative reaction with the dead load reaction will provide an estimate of the potential for uplift. The engineer must use engineering judgement regarding the applicability of this method.

An acute corner is defined as the corner of the structure where the angle formed by intersection of edge of the deck and the centerline of bearings is less than 90° .

Proper consideration of out-of-plane rotations during the bearing design is also required. Normally out of plane rotations will require multi-rotational bearings.

This method incorporated in this manual for determining L seems to be appropriate for the level of sophistication of the distribution factors. As additional knowledge is gained on this subject, this method for determining L may be modified.

SPECIFICATIONS

COMMENTARY

Table 4.6.2.2.1-1 - L for Use in Live Load Distribution Factor Equations

CONDITION	FORCE EFFECT	L (mm) {ft.}
A	Positive Moment	The length of the span for which moment is being calculated.
B	Negative Moment - End spans of continuous spans, from end to point of dead load contraflexure	The length of the span for which moment is being calculated.
C	Negative Moment - Near interior supports of continuous spans, from point of dead load contraflexure to point of dead load contraflexure	The average length of the two adjacent spans.
D	Negative Moment - Interior spans of continuous spans, from point of dead load contraflexure to point of dead load contraflexure	The length of the span for which moment is being calculated.
E	Shear	The length of the span for which shear is being calculated.
F	Exterior Reaction	The length of the exterior span.
G	Interior Reaction of Continuous Span	The average length of the two adjacent spans.

Figure 1 provides a graphical representation of the information given in Table 1.

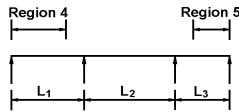
L for use in Live Load Distribution Factor Equations

Condition A



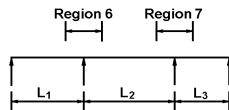
For Positive Moment Distribution Factors in Regions 1, 2 & 3, L_1 , L_2 & L_3 would be used in the Distribution Factor Equations respectively.

Condition B



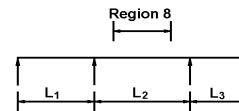
For Negative Moment Distribution Factors in Region 4 & 5, L_1 & L_3 would be used in the Distribution Factor Equations respectively.

Condition C



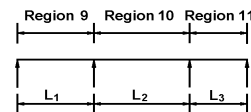
For Negative Moment Distribution Factors in Regions 6 & 7, $\frac{L_1 + L_2}{2}$ & $\frac{L_2 + L_3}{2}$ would be used in the Distribution Factor Equations respectively.

Condition D



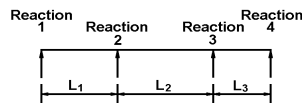
For the Negative Moment Distribution Factor in Region 8, L_2 would be used in the Distribution Factor Equations.

Condition E



For Shear Distribution Factors in Regions 9, 10 & 11, L_1 , L_2 & L_3 would be used in the Distribution Factor Equations respectively.

Condition F & G



For Reaction Distribution Factors for Reactions 1, 2, 3 & 4, L_1 , $\frac{L_1 + L_2}{2}$, $\frac{L_2 + L_3}{2}$ & L_3 would be used in the Distribution Factor Equations respectively.

Figure 4.6.2.2.1-1 - L for use in Live Load Distribution Factor Equations

DM-4, Section 4 – Structural Analysis and Evaluation

SPECIFICATIONS

In the rare occasion when the continuous span arrangement is such that an interior span does not have any positive dead load moment (i.e., no dead load points of contraflexure), the region of negative moment near the interior supports would be increased to the centerline of the span, and the L used in determining the live load distribution factors would be the average of the two adjacent spans.

4.6.2.2.2 Distribution Factor Method for Moment and Shear

4.6.2.2.2a Interior Beams with Wood Decks

The following shall supplement A4.6.2.2.2a.

The distribution factors given in Table A4.6.2.2.2a-1 for Glued Laminated Panels on Glued Laminated Stringers are applicable for panels with a 150 mm {6 in.} minimum nominal thickness.

4.6.2.2.2b Interior Beams with Concrete Decks

The following shall replace the second paragraph of A4.6.2.2.2b.

For preliminary design, the terms $K_g/(Lt^3)$ { $K_g/(12Lt^3)$ } in Table 1 shall be taken as 1.0 for non-composite beams.

The following shall replace Table A4.6.2.2.2b-1.

COMMENTARY

C4.6.2.2.2b

The following shall supplement AC4.6.2.2.2b.

In Table A4.6.2.2.2b-1, in the Category "Concrete Beams used in Multi-Beam Decks", the cross-section, Type g (from Table A4.6.2.2.1-1), with option "if sufficiently connected to act as a unit" has been removed from Table D4.6.2.2.2b-1. This option has been removed because it has been difficult to provide enough post-tensioning for the composite box beams to act as a unit.

Table 4.6.2.2.2b-1 – Distribution of Live Loads Per Lane for Moment in Interior Beams

Metric Units			
Type of Beams	Applicable Cross-Section from Table A4.6.2.2.1-1	Distribution Factors	Range of Applicability
Wood Deck on Wood or Steel Beams	a, l	See Table A4.6.2.2.2a-1	
Concrete Deck on Wood Beams	l	One Design Lane Loaded: S/3700 Two or More Design Lanes Loaded: S/3000	S ≤ 1800
Concrete Deck, Filled Grid, or Partially Filled Grid on Steel or Concrete Beams: Concrete T-Beams, T- and Double T-Sections	a, e, k	One Design Lane Loaded: $0.06 + \left(\frac{S}{2930}\right)^{1.0} \left(\frac{S}{L}\right)^{0.2} \left(\frac{K_g}{Lt_s^3}\right)^{0.1}$	1100 ≤ S ≤ 4900 110 ≤ t _s ≤ 300 6000 ≤ L ≤ 152 000 If L > 73 000, use L = 73 000 4 × 10 ⁹ ≤ K _g ≤ 3.2 × 10 ¹² N _b ≥ 4
	i, j if sufficiently connected to act as a unit	Two or More Design Lanes Loaded: $0.075 + \left(\frac{S}{3350}\right)^{1.0} \left(\frac{S}{L}\right)^{0.08} \left(\frac{K_g}{Lt_s^3}\right)^{0.1}$	
		Use lesser of the above or Lever Rule	
Cast-in-Place Concrete Multicell Box	d	One Design Lane Loaded: $\left(1.75 + \frac{S}{1100}\right) \left(\frac{300}{L}\right)^{0.35} \left(\frac{1}{N_c}\right)^{0.45} \geq \frac{S}{6400}$ Two or More Design Lanes Loaded: $\left(\frac{13}{N_c}\right)^{0.3} \left(\frac{S}{430}\right) \left(\frac{1}{L}\right)^{0.25}$	2100 ≤ S ≤ 4000 18 000 ≤ L ≤ 152 000 If L > 73 000, use L = 73 000 N _c ≥ 3 If N _c > 8 use N _c = 8 For two or more design lanes loaded If L > 427 000/N _c , use L = 427 000/N _c
Concrete Deck on Concrete Spread Box Beams	b, c	One Design Lane Loaded $\left(\frac{S}{910}\right)^{0.35} \left(\frac{Sd}{L^2}\right)^{0.25}$ Two or More Design Lanes Loaded: $\left(\frac{S}{1900}\right)^{0.6} \left(\frac{Sd}{L^2}\right)^{0.125}$	1800 ≤ S ≤ 5500 6000 ≤ L ≤ 152 000 If L > 43 000, use L = 43 000 430 ≤ d ≤ 1700 N _b ≥ 3
		Use Lever Rule	S > 5500

Table 4.6.2.2b-1 – Distribution of Live Loads Per Lane for Moment in Interior Beams (Continued)

Metric Units																
Type of Beams	Applicable Cross-Section From Table A4.6.2.2.1-1	Distribution Factors	Range of Applicability													
Concrete Beams used in Multi-Beam Decks	f	One Design Lane Loaded: $k \left(\frac{b}{2.8L} \right)^{0.5} \left(\frac{I}{J} \right)^{0.25}$ where : $k = 2.5(N_b)^{0.2} \geq 1.5$	$900 \leq b \leq 1500$ $6000 \leq L \leq 152\ 000$ If $L > 37\ 000$, use $L = 37\ 000$ $5 \leq N_b \leq 20$													
	g if sufficiently connected to act as a unit	Two or More Design Lanes Loaded: $k \left(\frac{b}{7600} \right)^{0.6} \left(\frac{b}{L} \right)^{0.2} \left(\frac{I}{J} \right)^{0.06} \left(\frac{5.66}{L^{0.15}} \right)^{\frac{N_b}{15}}$	$900 \leq b \leq 1500$ $6000 \leq L \leq 152\ 000$ $5 \leq N_b \leq 20$ If $N_b > 12$, use $N_b = 12$													
Steel Grids on Steel Beams	h	Regardless of Number of Loaded Lanes: S/D where: $C = K(W/L)$														
	g, i, j if connected only enough to prevent relative vertical displacement at the interface	$D = 300[11.5 - N_L + 1.4N_L(1 - 0.2C)^2]$ when $C \leq 5$ $D = 300\{11.5 - N_L\}$ when $C > 5$ $K = \sqrt{\frac{(1 + \mu)I}{J}}$ <p>For preliminary design, the following values of K may be used:</p> <table style="width: 100%; border: none;"> <thead> <tr> <th style="text-align: left;"><u>Beam Type</u></th> <th style="text-align: left;"><u>K</u></th> </tr> </thead> <tbody> <tr> <td>Non-voided rectangular beams</td> <td>0.7</td> </tr> <tr> <td>Rectangular beams with circular voids</td> <td>0.8</td> </tr> <tr> <td>Box section beams</td> <td>1.0</td> </tr> <tr> <td>Channel beams</td> <td>2.2</td> </tr> <tr> <td>T-beam</td> <td>2.0</td> </tr> <tr> <td>Double T-beam</td> <td>2.0</td> </tr> </tbody> </table>	<u>Beam Type</u>	<u>K</u>	Non-voided rectangular beams	0.7	Rectangular beams with circular voids	0.8	Box section beams	1.0	Channel beams	2.2	T-beam	2.0	Double T-beam	2.0
<u>Beam Type</u>	<u>K</u>															
Non-voided rectangular beams	0.7															
Rectangular beams with circular voids	0.8															
Box section beams	1.0															
Channel beams	2.2															
T-beam	2.0															
Double T-beam	2.0															
Steel Grids on Steel Beams	a	One Design Lane Loaded: S/2300 If $t_g < 100$ mm S/3050 If $t_g \geq 100$ mm Two or More Design Lanes Loaded: S/2400 If $t_g < 100$ mm S/3050 If $t_g \geq 100$ mm	$S_g \leq 1800$ mm $S_g \leq 1800$ mm													
Concrete deck on Multiple Steel Box Girders	b, c	Regardless of Number of Loaded Lanes: $0.05 + 0.85 \frac{N_L}{N_b} + \frac{0.425}{N_L}$	$0.5 \leq \frac{N_L}{N_b} \leq 1.5$													

Table 4.6.2.2b-1 – Distribution of Live Loads Per Lane for Moment in Interior Beams (Continued)

U.S. Customary Units			
Type of Beams	Applicable Cross-Section from Table A4.6.2.2.1-1	Distribution Factors	Range of Applicability
Wood Deck on Wood or Steel Beams	a, l	See Table A4.6.2.2.2a-1	
Concrete Deck on Wood Beams	l	One Design Lane Loaded: S/12 Two or More Design Lanes Loaded: S/10	S ≤ 6.0'
Concrete Deck, Filled Grid, or Partially Filled Grid on Steel or Concrete Beams; Concrete T-Beams, T- and Double T-Sections	a, e, k	One Design Lane Loaded: $0.06 + \left(\frac{S}{9.6}\right)^{1.0} \left(\frac{S}{L}\right)^{0.2} \left(\frac{K_g}{12Lt_s^3}\right)^{0.1}$ Two or More Design Lanes Loaded:	3.5' ≤ S ≤ 16.0' 4 1/2" ≤ t _s ≤ 12" 20' ≤ L ≤ 500' If L > 240', use L = 240' 10,000 in ⁴ ≤ K _g ≤ 7,600,000 in ⁴ N _b ≥ 4
	i, j If sufficiently connected to act as a unit	$0.075 + \left(\frac{S}{11}\right)^{1.0} \left(\frac{S}{L}\right)^{0.08} \left(\frac{K_g}{12Lt_s^3}\right)^{0.1}$	
	Use lesser of the above or Lever Rule		
Cast-in-Place Concrete Multicell Box	d	One Design Lane Loaded: $\left(1.75 + \frac{S}{3.6}\right) \left(\frac{1}{L}\right)^{0.35} \left(\frac{1}{N_c}\right)^{0.45} \geq \frac{S}{21}$ Two or More Design Lanes Loaded: $\left(\frac{13}{N_c}\right)^{0.3} \left(\frac{S}{5.8}\right) \left(\frac{1}{L}\right)^{0.25}$	7.0' ≤ S ≤ 13.0' 60' ≤ L ≤ 500' If L > 240', use L = 240' N _c ≥ 3 If N _c > 8 use N _c = 8 For two or more design lanes loaded If L > 1400/N _c , use L = 1400/N _c
Concrete Deck on Concrete Spread Box Beams	b, c	One Design Lane Loaded: $\left(\frac{S}{3.0}\right)^{0.35} \left(\frac{Sd}{12L^2}\right)^{0.25}$ Two or More Design Lanes Loaded: $\left(\frac{S}{6.3}\right)^{0.6} \left(\frac{Sd}{12L^2}\right)^{0.125}$	6.0' ≤ S ≤ 18.0' 20' ≤ L ≤ 500' If L > 140', use L = 140' 17" ≤ d ≤ 66" N _b ≥ 3
		Use Lever Rule	S ≥ 18.0'

Table 4.6.2.2b-1 – Distribution of Live Loads Per Lane for Moment in Interior Beams (Continued)

U.S. Customary Units															
Type of Beams	Applicable Cross-Section from Table A4.6.2.2.1-1	Distribution Factors	Range of Applicability												
Concrete Beams used in Multi-Beam Decks	f	One Design Lane Loaded: $k \left(\frac{b}{33.3L} \right)^{0.5} \left(\frac{I}{J} \right)^{0.25}$ where: $k = 2.5(N_b)^{-0.2} \geq 1.5$	$35" \leq b \leq 60"$ $20' \leq L \leq 500'$ If $L > 120'$, use $L = 120'$ $5 \leq N_b \leq 20$												
	g if sufficiently connected to act as a unit	Two or More Design Lanes Loaded: $k \left(\frac{b}{305} \right)^{0.6} \left(\frac{b}{12L} \right)^{0.2} \left(\frac{I}{J} \right)^{0.06} \left(\frac{2.4}{L^{0.15}} \right)^{\frac{N_b}{15}}$	$35" \leq b \leq 60"$ $20' \leq L \leq 500'$ $5 \leq N_b \leq 20$ If $N_b > 12$, use $N_b = 12$												
	h	Regardless of Number of Loaded Lanes: S/D where: $C = K(W/L)$													
	g, i, j if connected only enough to prevent relative vertical displacement at the interface	$D = 11.5 - N_L + 1.4N_L(1 - 0.2C)^2$ When $C \leq 5$ $D = 11.5 - N_L$ when $C > 5$ $K = \sqrt{\frac{(1 + \mu)I}{J}}$ for preliminary design, the following values of K may be used: <table style="margin-left: auto; margin-right: auto; border-collapse: collapse;"> <thead> <tr> <th style="text-align: left;"><u>Beam Type</u></th> <th style="text-align: left;"><u>K</u></th> </tr> </thead> <tbody> <tr> <td>Non-voided rectangular beams</td> <td>0.7</td> </tr> <tr> <td>Rectangular beams with circular voids</td> <td>0.8</td> </tr> <tr> <td>Box section beams</td> <td>1.0</td> </tr> <tr> <td>Channel beams</td> <td>2.2</td> </tr> <tr> <td>T-beam</td> <td>2.0</td> </tr> <tr> <td>Double T-beam</td> <td>2.0</td> </tr> </tbody> </table>		<u>Beam Type</u>	<u>K</u>	Non-voided rectangular beams	0.7	Rectangular beams with circular voids	0.8	Box section beams	1.0	Channel beams	2.2	T-beam	2.0
<u>Beam Type</u>	<u>K</u>														
Non-voided rectangular beams	0.7														
Rectangular beams with circular voids	0.8														
Box section beams	1.0														
Channel beams	2.2														
T-beam	2.0														
Double T-beam	2.0														
Steel Grids on Steel Beams	a	One Design Lane Loaded: $S/7.5'$ If $t_g < 4"$ $S/10.0'$ If $t_g \geq 4"$	$S \leq 6.0'$												
		Two or More Design Lanes Loaded: $S/8.0'$ If $t_g < 4"$ $S/10.0'$ If $t_g \geq 4"$	$S \leq 6.0'$												
Concrete deck on Multiple Steel Box Girders	b, c	Regardless of Number of Loaded Lanes: $0.05 + 0.85 \frac{N_L}{N_b} + \frac{0.425}{N_L}$	$0.5 \leq \frac{N_L}{N_b} \leq 1.5$												

SPECIFICATIONS

COMMENTARY

4.6.2.2d *Exterior Beams*

C4.6.2.2d

The following shall supplement AC4.6.2.2d.
The value of d_e is to be computed using the midpoint of the exterior web.

4.6.2.2e *Skewed Bridges*

C4.6.2.2e

Delete A4.6.2.2e.

The following shall replace AC4.6.2.2e.
PennDOT has decided not to take advantage of the reduction in load distribution factors for moment in longitudinal beams on skewed supports.

4.6.2.2.3 Distribution Factor Method for Shear

4.6.2.2.3a *Interior Beams*

The following shall replace the second sentence of Paragraph 1 in A4.6.2.2.3a.

For interior beams not listed in Table 1, lateral distribution of axle load shall be determined by lever rule.

The following shall replace Table A4.6.2.2.3a-1.

DM-4, Section 4 – Structural Analysis and Evaluation

Table 4.6.2.2.3a-1 – Distribution of Live Loads Per Lane for Shear in Interior Beams

Metric Units				
Type of Superstructure	Applicable Cross-Section from Table A4.6.2.2.1-1	One Design Lane Loaded	Two or More Design Lanes Loaded	Range of Applicability
Wood Deck on Wood or Steel Beams	See Table A4.6.2.2.2a-1			
Concrete Deck on Wood Beams	l	Lever Rule	Lever Rule	N/A
Concrete Deck, Filled Grid, or Partially Filled Grid on Steel or Concrete Beams; Concrete T-Beams, T- and Double T-Sections	a, e, k	$0.36 + \frac{S}{7600}$	$0.2 + \frac{S}{3600} - \left(\frac{S}{10\,700}\right)^2$	1100 ≤ S ≤ 4900 6000 ≤ L ≤ 152 000 If L > 73 000, use L = 73 000 110 ≤ t _s ≤ 300 N _b ≥ 4
	I, j if sufficiently connected to act as a unit	Lever Rule	Lever Rule	N _b = 3
Cast-in-Place Concrete Multicell Box	d	$\left(\frac{S}{2900}\right)^{0.6} \left(\frac{d}{L}\right)^{0.1}$	$\left(\frac{S}{2200}\right)^{0.9} \left(\frac{d}{L}\right)^{0.1}$	1800 ≤ S ≤ 4000 6000 ≤ L ≤ 152 000 890 ≤ d ≤ 2800 N _c ≥ 3
Concrete Deck on Concrete Spread Box Beams	b, c	$\left(\frac{S}{3050}\right)^{0.6} \left(\frac{d}{L}\right)^{0.1}$	$\left(\frac{S}{2250}\right)^{0.8} \left(\frac{d}{L}\right)^{0.1}$	1800 ≤ S ≤ 5500 6000 ≤ L ≤ 152 000 If L > 43 000, use L = 43 000 430 ≤ d ≤ 1700 N _b ≥ 3
		Lever Rule	Lever Rule	S > 5500
Concrete Box Beams Used in Multi-Beam Decks	f, g	$0.70 \left(\frac{b}{L}\right)^{0.15} \left(\frac{I}{J}\right)^{0.05}$	$\left(\frac{b}{4000}\right)^{0.4} \left(\frac{b}{L}\right)^{0.1} \left(\frac{I}{J}\right)^{0.05}$	900 ≤ b ≤ 1500 6000 ≤ L ≤ 152 000 If L > 37 000, use L = 37 000 5 ≤ N _b ≤ 20 6.8x10 ⁹ ≤ J ≤ 3.75x10 ¹¹ 2.1x10 ⁹ ≤ I ≤ 3.75x10 ¹¹
Concrete Beams Other Than Box Beams Used in Multi-Beam Decks	H	Lever Rule	Lever Rule	N/A
	i, j if connected only enough to prevent relative vertical displacement at the interface			
Steel Grid Deck on Steel Beams	a	Lever Rule	Lever Rule	N/A
Concrete Deck on Multiple Steel Box Beams	b, c	As specified in Table D4.6.2.2.2b-1		

DM-4, Section 4 – Structural Analysis and Evaluation

Table 4.6.2.2.3a-1 – Distribution of Live Loads Per Lane for Shear in Interior Beams (Continued)

U.S. Customary Units				
Type of Superstructure	Applicable Cross-Section from Table A4.6.2.2.1-1	One Design Lane Loaded	Two or More Design Lanes Loaded	Range of Applicability
Wood Deck on Wood or Steel Beams	See Table A4.6.2.2.2a-1			
Concrete Deck on Wood Beams	l	Lever Rule	Lever Rule	N/A
Concrete Deck, Filled Grid, or Partially Filled Grid on Steel or Concrete Beams; Concrete T-Beams, T- and Double T-Sections	a, e, k	$0.36 + \frac{S}{25}$	$0.2 + \frac{S}{12} - \left(\frac{S}{35}\right)^2$	$3.5' \leq S \leq 16.0'$ $20' \leq L \leq 500'$ If $L > 240'$, use $L = 240'$ $4 \frac{1}{2}'' \leq t_s \leq 12''$ $N_b \geq 4$
	i, j If sufficiently connected to act as a unit			
Cast-in-Place Concrete Multicell Box	d	$\left(\frac{S}{9.5}\right)^{0.6} \left(\frac{d}{12L}\right)^{0.1}$	$\left(\frac{S}{7.3}\right)^{0.9} \left(\frac{d}{12L}\right)^{0.1}$	$6.0' \leq S \leq 13.0'$ $20' \leq L \leq 500'$ $35'' \leq d \leq 110''$ $N_c \geq 3$
Concrete Deck on Concrete Spread Box Beams	b, c	$\left(\frac{S}{10}\right)^{0.6} \left(\frac{d}{12L}\right)^{0.1}$	$\left(\frac{S}{7.4}\right)^{0.8} \left(\frac{d}{12L}\right)^{0.1}$	$6.0' \leq S \leq 18.0'$ $20' \leq L \leq 500'$ If $L > 140'$, use $L = 140'$ $17'' \leq d \leq 66''$ $N_b \geq 3$
		Lever Rule	Lever Rule	$S > 18.0'$
Concrete Box Beams Used in Multi-Beam Decks	f, g	$\left(\frac{b}{130L}\right)^{0.15} \left(\frac{l}{J}\right)^{0.05}$	$\left(\frac{b}{156}\right)^{0.4} \left(\frac{b}{12L}\right)^{0.1} \left(\frac{l}{J}\right)^{0.05}$	$35'' \leq b \leq 60''$ $20' \leq L \leq 500'$ If $L > 120'$, use $L = 120'$ $5 \leq N_b \leq 20$ $16,500 \text{ in}^4 \leq J \leq 900,000 \text{ in}^4$ $5,000 \text{ in}^4 \leq I \leq 900,000 \text{ in}^4$
Concrete Beams Other Than Box Beams Used in Multi-Beam Decks	h	Lever Rule	Lever Rule	N/A
	i, j if connected only enough to prevent relative vertical displacement at the interface			
Steel Grid Deck on Steel Beams	a	Lever Rule	Lever Rule	N/A
Concrete Deck on Multiple Steel Box Beams	b, c	As specified in Table D4.6.2.2.2b-1		

SPECIFICATIONS

4.6.2.2.3c Skewed Bridges

The following shall replace the second paragraph of A4.6.2.2.3c.

In determining end shear for beams other than prestressed concrete adjacent box beams, the shear skew adjustment factor shall be applied to the shear distribution factor of exterior beams at the obtuse corners for a distance of one-half the span length (see Figure 1).

In determining end shear for prestressed concrete adjacent box beams, the shear skew adjustment factor shall be applied to the shear distribution factors for all the beams which are on a skew (see Figure 1).

COMMENTARY

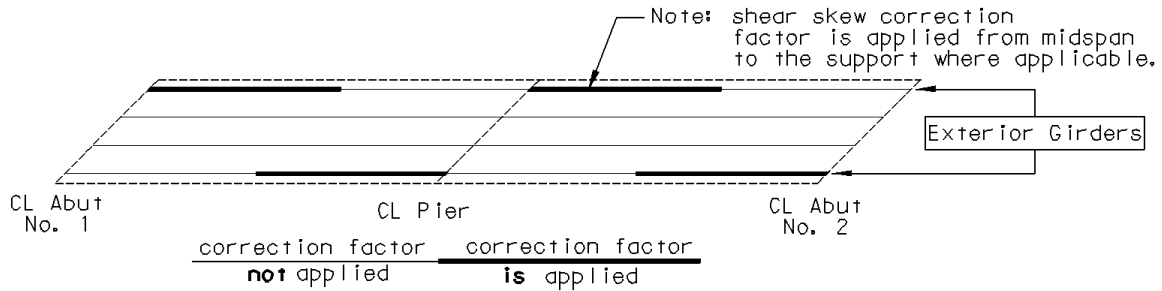
C4.6.2.2.3c.

The following shall supplement AC4.6.2.2.3c.

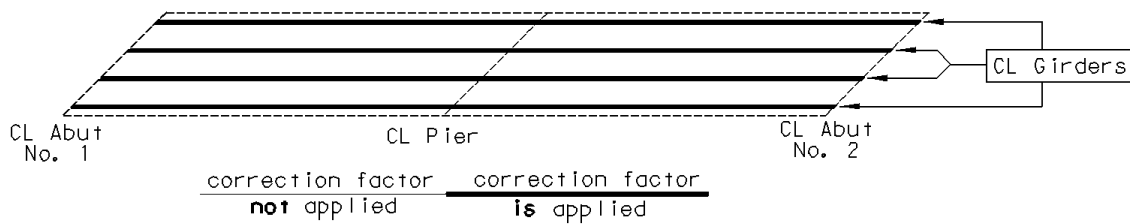
When structures have multiple skew angles, the smallest applicable skew angle associated with that girder should be used in calculation of shear correction factors.

Steel and P/S I-Beams and P/S Spread Box Beams:

Shear skew correction factor is to be applied to the shear at the ends of exterior beams at the obtuse corner (up to mid-span, where applicable).



P/S Adjacent Box Beams:



Note: The examples shown are based on the assumption that the girder is continuous over the pier. If such is not the case (i.e. at an expansion bearing), the correction factor would be applied at the simple end in a similar manner to which it was applied at the abutment.

Figure 4.6.2.2.3c-1 - Application of Shear Correction Factor for End Shear

In determining end reactions of continuous beams (such as reactions at abutments) for beams other than prestressed concrete adjacent box beams, the shear skew adjustment factor shall be applied to the shear distribution factor of exterior beams at the obtuse corners (see Figure 2).

In determining end reactions of continuous beams (such as reactions at abutments) for prestressed concrete adjacent box beams, the shear skew adjustment factor shall be

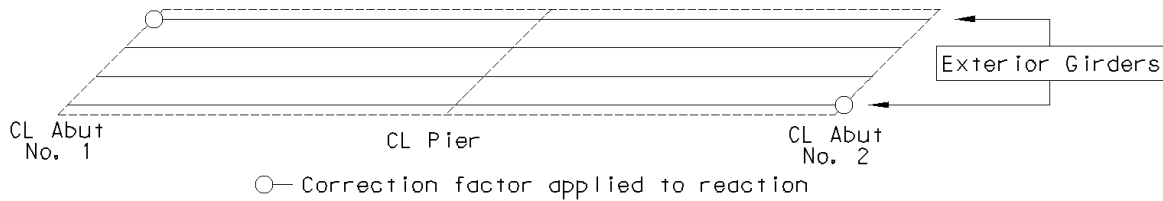
SPECIFICATIONS

COMMENTARY

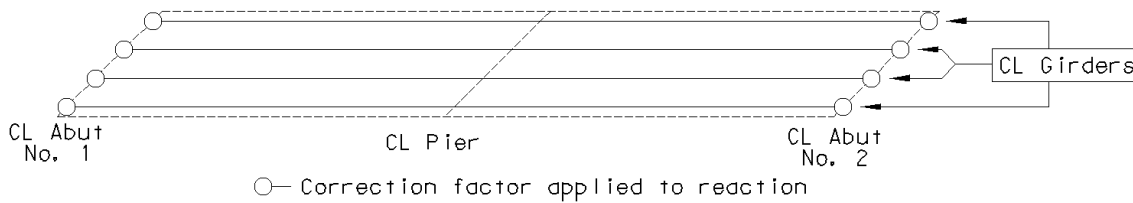
applied to the shear distribution factors for all the beams which are on a skew (see Figure 2).

Steel and P/S I-Beams and P/S Spread Box Beams:

Shear skew correction factor is to be applied to exterior girder reactions at the obtuse corner of simple-end reactions. It is not applied at continuous reactions such as pier reactions.



P/S Adjacent Box Beams:



Note: The examples shown are based on the assumption that the girder is continuous over the pier. If such is not the case (i.e. at an expansion bearing), the correction factor would be applied at the simple end in a similar manner to which it was applied at the abutment.

Figure 4.6.2.2.3c-2 - Application of Shear Skew Correction Factor for End Reactions

SPECIFICATIONS

COMMENTARY

The following shall replace Table A4.6.2.2.3c-1.

Table 4.6.2.2.3c-1 - Correction Factors for Load Distribution Factors for Support Shear of the Obtuse Corner

Metric Units			
Type of Superstructure	Applicable Cross-Section from Table 4.6.2.2.1-1	Correction Factor	Range of Applicability
Concrete Deck, Filled Grid, or Partially Filled Grid on Steel or Concrete Beams; Concrete T-Beams, T- and Double T-Section	a, e, k and also i, j if sufficiently connected to act as a unit	$1.0 - 0.20 \left(\frac{L t_s^3}{K_g} \right)^{0.3} \tan \theta$	$30^\circ \leq \theta \leq 90^\circ$ $1100 \leq S \leq 4900$ $6000 \leq L \leq 152\ 000$ If $L > 73\ 000$, use $L = 73\ 000$ $N_b \geq 4$
Cast-in-Place Concrete Multicell Box	d	$1.0 - \left[0.25 - \frac{L}{70d} \right] \tan \theta$	$30^\circ \leq \theta \leq 90^\circ$ $1800 < S \leq 4000$ $6000 \leq L \leq 152\ 000$ If $L > 73\ 000$, use $L = 73\ 000$ $900 \leq d \leq 2700$ $N_b \geq 3$
Concrete Deck on Spread Concrete Box Beams	b, c	$1.0 - \frac{\sqrt{Ld}}{6S} \tan \theta$	$30^\circ \leq \theta \leq 90^\circ$ $1800 \leq S \leq 3500$ If $S > 3500$, use $S = 3500$ $6000 \leq L \leq 152\ 000$ If $L > 43\ 000$, use $L = 43\ 000$ $430 \leq d \leq 1700$ $N_b \geq 3$
Concrete Box Beams Used in Multibeam Decks	f, g	$1.0 - \frac{L \sqrt{\tan \theta}}{90d}$	$30^\circ \leq \theta \leq 90^\circ$ $6000 \leq L \leq 152\ 000$ If $L > 37\ 000$, use $L = 37\ 000$ $305 \leq d \leq 1700$ $900 \leq b \leq 1500$ $5 \leq N_b \leq 20$

Table 4.6.2.2.3c-1 - Correction Factors for Load Distribution Factors for Support Shear of the Obtuse Corner (Continued)

U.S. Customary Units			
Type of Superstructure	Applicable Cross-Section from Table 4.6.2.2.1-1	Correction Factor	Range of Applicability
Concrete Deck, Filled Grid, or Partially Filled Grid on Steel or Concrete Beams; Concrete T-Beams, T- and Double T-Section	a, e, k and also i, j if sufficiently connected to act as a unit	$1.0 - 0.20 \left(\frac{12 L t_s^3}{K_g} \tan \theta \right)^{0.3}$	$30^\circ \leq \theta \leq 90^\circ$ $3.5' \leq S \leq 16.0'$ $20' \leq L \leq 500'$ If $L > 240'$, use $L = 240'$ $N_b \geq 4$
Cast-in-Place Concrete Multicell Box	d	$1.0 - \left[0.25 - \frac{12 L}{70 d} \tan \theta \right]$	$30^\circ \leq \theta \leq 90^\circ$ $6.0' < S \leq 13.0'$ $20' \leq L \leq 500'$ If $L > 240'$, use $L = 240'$ $35'' \leq d \leq 110''$ $N_b \geq 3$
Concrete Deck on Spread Concrete Box Beams	b, c	$1.0 - \frac{\sqrt{Ld}}{6S} \tan \theta$	$30^\circ \leq \theta \leq 90^\circ$ $6.0' \leq S \leq 11.5'$ If $S > 11.5'$, use $S = 11.5'$ $20' \leq L \leq 500'$ If $L > 140'$, use $L = 140'$ $17'' \leq d \leq 66''$ $N_b \geq 3$
Concrete Box Beams Used in Multibeam Decks	f, g	$1.0 - \frac{12 L}{90 d} \sqrt{\tan \theta}$	$30^\circ \leq \theta \leq 90^\circ$ $20' \leq L \leq 500'$ If $L > 120'$, use $L = 120'$ $17'' \leq d \leq 66''$ $35'' \leq b \leq 60''$ $5 \leq N_b \leq 20$

4.6.2.3 EQUIVALENT STRIP WIDTHS FOR SLAB-TYPE BRIDGES

The following shall replace the first paragraph of A4.6.2.3.

This article shall be applied to the types of cross-sections which are shown schematically in Table 1. For the purpose of this article, cast-in-place voided slab bridges may be considered as slab bridges.

4.6.2.5 EFFECTIVE LENGTH FACTOR, K

The following shall supplement A4.6.2.5.

For Extreme Event I, Seismic Loading, the effective length factor, K, in the plane of bending may be assumed to be unity in the calculation of λ .

SPECIFICATIONS

COMMENTARY

4.6.2.6 EFFECTIVE FLANGE WIDTH

4.6.2.6.1 General

The following shall replace the last two sentences of the first paragraph.

For the calculation of live load deflections, where required, the provisions of D2.5.2.6.2 shall apply.

C4.6.2.6.1

The following shall supplement AC4.6.2.6.1.

For typical continuous span bridges, the effective span length may be taken as the distance between points of dead load contraflexure, and can be approximated as shown in Table 1 below:

Table C4.6.2.6.1-1 - Approximate Effective Span Lengths for Computing Effective Slab Width of Continuous Span Bridges

Positive Flexure Regions		Negative Flexure Regions		
Exterior Span	Interior Span	Support Not Adjacent to Exterior Span	For Two-Span Girder	Support Adjacent to Exterior Span
$0.7 L_E$	$0.5 L_I$	$0.25 L_{I1} + 0.25 L_{I2}$	$0.3 L_{E1} + 0.3 L_{E2}$	$0.30 L_E + 0.25 L_I$

Where L_I and L_E represent interior and exterior span lengths, respectively. This approximation is only applicable for the purpose of computing effective span lengths to be used in the determination of the effective slab width. The approximation is based on assumed points of dead load contraflexure for balanced span lengths. In cases where this simplification is not valid, i.e., the spans are not balanced, a more rigorous estimation of the effective span length should be made by determining the actual points of dead load contraflexure. Because of the effective slab width affects the section properties to be used in the girder dead load analysis, an iterative procedure may be required to determine the appropriate values. In such cases, a 5% tolerance is allowed on the effective slab width, b_s .

Where the cross-section of the web or top flange changes over a flexural region, the minimum top flange width or web thickness within that region may be used in the calculation of the effective slab width.

Following the determination of the actual points of dead load contraflexure by the continuous beam analysis, the designer should compute the effective slab width in accordance with A4.6.2.6.1 based on the true effective span length. If the effective span length controls the calculation of b_s , the calculated value should be compared to the previously computed value to determine whether it is within the allowed tolerance. The effective span length will typically control the calculation of b_s only for short-spans having large girder spacings.

For steel girders, an acceptable approximation of the permanent load inflection points is the non-composite dead load contraflexure points based on the non-composite

SPECIFICATIONS

4.6.2.10P GIRDER - FLOORBEAM - STRINGER BRIDGES

4.6.2.10.1P Girder Live Load Distribution Factors

Girder live load distribution factors shall be calculated on the assumption that deck acts as a simple span between the girders or deck acts as beam with overhang for exterior girders (i.e., this assumes the stringers and floorbeams are not present).

4.6.2.10.2P Stringer Live Load Distribution Factors

Stringer live load distribution factors shall be based on D4.6.2.2 and A4.6.2.2.

4.6.2.10.3P Floorbeam Live Load Distribution Factors

4.6.2.10.3aP Floorbeams with the Top Flange not Directly Supporting the Deck

For floorbeams with the top flange not directly supporting the deck, the longitudinal reaction of design live load is determined and then these loads are moved transversely along the floorbeam to produce the maximum force effect assuming the stringers are not present.

4.6.2.10.3bP Floorbeams with the Top Flange Directly Supporting the Deck

For floorbeams with the top flange directly supporting the deck, the floorbeam distribution shall be calculated as given in A4.6.2.2.

4.6.2.11P DISTRIBUTION OF LOAD FROM THE SUPERSTRUCTURE TO THE SUBSTRUCTURE

In order to determine girder reactions (which are used as loads for the substructure design), the deck is assumed to act as a simple beam between interior girders and as a cantilever beam for the exterior girder and the first interior girder.

In the calculation of live load girder reactions, the design vehicle shall be assumed to spread uniformly over 3000 mm {10 ft.} (i.e., not two separate wheel loads).

COMMENTARY

section properties.

For prestressed concrete girders, an acceptable approximation of the permanent load inflection points is the composite dead load contraflexure points based on the composite (3n) section properties.

C4.6.2.11P

For abutments designed on a per meter basis, an acceptable alternate method of distribution would be to divide the sum total of all the loads applied to the abutment (for each limit state) by the abutment front face width. When using the above approach, the live load contribution may be obtained by determining the live load effect for one lane of loading and multiplying that effect by the number of design lanes.

SPECIFICATIONS

4.6.2.12P EQUIVALENT STRIP WIDTHS FOR BOX CULVERTS

4.6.2.12.1P General

This article shall be applied to box culverts with depths of fill less than 600 mm {2.0 ft}.

4.6.2.12.2P Case 1: Traffic Travels Parallel to Span

When traffic travels primarily parallel to the span, culverts shall be analyzed for a single loaded lane with the single lane multiple presence factor.

The axle load shall be distributed to the top slab for determining moment, thrust, and shear as follows:

- Perpendicular to the span:

Metric Units:

$$E = 2440 + 0.12 S \quad (4.6.2.12.2P-1)$$

U.S. Customary Units:

$$E = 96 + 1.44 S$$

- Parallel to the span:

$$E_{span} = LT + LLDF (H) \quad (4.6.2.12.2P-2)$$

where:

E = equivalent distribution width perpendicular to span (mm){in.}

S = clear span (mm) {ft.}

E_{span} = equivalent distribution length parallel to span (mm) {in.}

LT = length of tire contact area parallel to span, as specified in D3.6.1.2.5 (mm) {in.}

LLDF = factor for distribution of live load with depth of fill, 1.00, as specified in D3.6.1.2.6

H = depth of fill from top of culvert to top of pavement (mm) {in.}

4.6.2.12.3P Case 2: Traffic Travels Perpendicular to Span

When traffic travels perpendicular to the span, distribute live load to the top slab using the equations in

COMMENTARY

C4.6.2.12.1P

Design for depths of fill of 600 mm {2.0 ft} or greater are covered in D3.6.1.2.6

C4.6.2.12.2P

Culverts are designed under the provisions of Section D12. Box culverts are normally analyzed as two-dimensional frames. Equivalent strip widths are used to simplify the analysis of the three-dimensional response to live loads. Equations 1 and 2 are based on research (McGrath et al., 2004) that investigated the forces in box culverts with spans up to 7300 mm {24 ft}.

The distribution widths are based on distribution of shear forces. Distributions widths for positive and negative moments are wider; however, using the narrower width in combination with a single lane multiple presence factor provides designs adequate for multiple loaded lanes for all force effects.

Although past practice has been to ignore the distribution of live load with depth of fill, consideration of this effect, as presented in Equation 2, produces a more accurate model of the changes in design forces with increasing depth of fill. The increased load length parallel to the span, as allowed by Equation 2, may be conservatively neglected in design. For the BXLRFD computer program, Equation 2 has been ignored.

C4.6.2.12.3P

Culverts with traffic traveling perpendicular to the span can have two or more trucks on the same design strip at the

SPECIFICATIONS

A4.6.2.1 for concrete decks with primary strips perpendicular to the direction of traffic.

4.6.2.12.4P Precast Box Culverts

For precast box culverts, the distribution width computed with Equation 4.6.2.12.2P-1 shall not exceed the length between two adjacent joints without a means of shear transfer across the joint. Additionally, if no means of shear transfer is provided, the section ends shall be designed as an edge beam in accordance with the provisions of A4.6.2.1.4b.

Shear transfer may be provided by pavement, soil backfill, or a physical connection between adjacent sections.

COMMENTARY

same time. This must be considered, with appropriate multiple presence factor, in analysis of the culvert structural response.

C4.6.2.12.4P

Precast box culverts manufactured in accordance with AASHTO Materials Specification M273 are often installed with joints that do not provide a means of direct shear transfer across the joints of adjacent sections under service load conditions. This practice is based on research (James, 1984, Frederick, et al., 1988) that showed small deflections and strains under wheel loads with no earth cover, due primarily to the fact that the sections were designed as cracked sections but do not crack under service loading. While there are no known service issues with installation of standard box sections without means of shear transfer across joints, analysis (McGrath et al., 2004) shows that stresses are substantially higher when a box culvert is subjected to a live load at a free edge than when loaded away from a free edge.

Most shallow cover box culvert applications have some fill or a pavement that likely provide sufficient shear transfer to distribute live load to adjacent box sections without shear keys to avoid higher stresses due to edge loading. States and design agencies that utilize grouted shear keys, pavement or systems whose function is to transfer shear across joints may use past performance of these connections and/or materials as a basis for providing adequate shear transfer. Otherwise, for applications with zero depth of cover, and no pavement, soil, or other means of shear transfer such as shear keys, designers should design the culvert section for the specified reduced distribution widths. The use of post-tensioning in accordance with the BC Standard Drawings in conjunction with a cast-in-place slab or bituminous pavement is considered sufficient to provide adequate shear transfer between adjacent culvert sections.

SPECIFICATIONS

COMMENTARY

4.6.3 Refined Methods of Analysis

4.6.3.1 GENERAL

The following shall replace the second paragraph of A4.6.3.1.

Barriers shall not be considered in the calculation of the structural stiffness nor structural resistance of a structure.

The following shall supplement A4.6.3.1.

When a refined method of analysis is performed for beam-slab bridges other than those bridges defined in D4.6.1.2.1 and D4.6.2.2.1 (which must use a refined method analysis), the beams must have capacity not less than if it were designed using the approximate method of analysis given in A4.6.2.2.1 and D4.6.2.2.1.

4.6.3.2 DECKS

4.6.3.2.3 Orthotropic Plate Model

The following shall replace A4.6.3.2.3.

In orthotropic plate modeling, the flexural rigidity of the elements may be uniformly distributed along the cross-section of the deck. Where the torsional stiffness of the deck is not contributed solely by a solid plate of uniform thickness, the torsional rigidity should be established by physical testing, three-dimensional analysis, or generally accepted and verified approximations, and shall be approved by the Chief Bridge Engineer.

4.6.3.3 BEAM-SLAB BRIDGES

The following shall supplement A4.6.3.3.

When a refined method of analysis is performed, the live load force effects carried by each girder may be computed by the techniques listed below in order of decreasing sophistication:

- Three-dimensional finite element method, and
- Two-dimensional grillage analogy

With a two-dimensional grillage analogy or a three-dimensional finite element method, the rating of a bridge is not as straightforward as when the A4.6.2.2 or D4.6.2.2 is used. A refined method of analysis more closely represents the fact that the distribution of live loads on a bridge is not described by a constant distribution factor. When a refined method of analysis is used in the design, a table of live load distribution factors (based on design truck of the PHL-93) for girder maximum positive and negative moments and shear in each span shall be provided on the contract plans to aid in future ratings of the bridge. The live load distribution factor shall be in the form of a ratio of the force effect from the refined method of analysis caused by the design truck of the PHL-93 in that lane, divided by the force effect obtained

C4.6.3.1

Delete the second paragraph of AC4.6.3.1.

C4.6.3.3

The following shall supplement the bulleted list of AC4.6.3.3.

- If the program being used allows only for nodal loads, concentrated loads shall be distributed to adjacent nodes by simple statics. If the spacing of girders significantly exceeds 2400 mm {8 ft.}, it is preferable to place intermediate nodes on the transverse members to model load distribution more accurately.
- The framing of members at bearings is very important. Nodes at bearings should not be artificially restrained through the enforcement of fixed support conditions for other than vertical transitional support at all bearings, and longitudinal and transverse transitional support where the detailing dictates. This provision is critical to proper modeling of bridges with significant skew.
- The warping stiffness of girders is difficult to model, unless a warping (not St. Venant torsional) degree of freedom is explicitly provided by the computer program. As an approximation, the dead load moment diagram and live load moment envelope may be converted to a uniform flange bending (i.e., bimoment)

SPECIFICATIONS

from application of one design truck of the PHL-93 acting on a single, isolated girder. The commentary provides an example table of live load distribution factors.

Two other areas which must be considered for future ratings of bridges designed with refined method analysis are cross-frame forces and uplift at reactions. Therefore, at Type, Size and Location submission, the designer must include (for approval by the Chief Bridge Engineer) a proposed simplified method for rating a special vehicle for the controlling cross-frame member and uplift reaction condition.

When a grillage analogy or finite element model is implemented, the preferred procedure is the generation and subsequent loading of an influence surface to produce maximum effect. The influence surface shall be loaded to maximize positive and negative design values (moments, shear, diaphragm forces, etc.) for all critical points along the bridge. This process is analogous to the classical use of influence lines. The provisions of A3.6.1.1.2 shall apply to the loading method described above. It is also acceptable, though less rigorous and economical, to apply distribution factors from D4.6.2.2.2 to each girder in a grid system and allow the grid or finite element analysis to more accurately determine the load distribution to interior and exterior beams, and to account for the influences of skew and curvature, if present. The latter procedure is less preferred than the former procedure since uneconomical designs may result.

It is expressly *not* acceptable to load a grid or finite element model with the number of design lanes of live load given in A3.6.1.1.1, without simultaneously positioning the loads longitudinally and transversely to maximize and minimize each design moment, shear, diaphragm load (curved and/or skewed bridges), and reaction. Except in the most obvious cases (e.g., bridges that are essentially right and straight), the transverse and longitudinal position of live load which produces the critical design condition should be determined by the use of influence surfaces.

COMMENTARY

loading by the approximation below:

$$W = \frac{\sum M}{Rd}$$

where:

ΣM = total primary moment (N·mm) per mm
{k in/ft}

R = radius (mm) {ft.}

d = girder depth (mm) {in.}

This load may be applied to the flange and assumed to be reacted by the diaphragms and slab, as appropriate, analogous to a continuous beam on simple supports. If a warping degree of freedom or some approximate method of calculating warping stress is not included in the program, it will be necessary to combine the loads calculated according to the above method with the loads produced from diaphragms.

- If grid or finite element methods are used to determine dead load forces, then the structure, including diaphragms, must be cambered in accordance with the computer analysis. If some cambering other than that corresponding to the opposite of the natural dead load deflection is anticipated (e.g., cambering for more efficient dead load distribution), it must be reflected in the computer modeling.

The following shall supplement AC4.6.3.3.

Special care shall be exercised in modeling, analysis and interpretation of the results of two- and three-dimensional procedures. AC4.6.3.3 and this commentary provide guidelines. The designer is responsible for the correct application of advanced analysis methods and is advised that various commercial and generic computer programs can report significantly different results for various combinations of skew and/or curvature.

Figure C1 provides an example of a table for live load distribution factors which shall be included on the contract drawings. Since the figure provides only example tables, the table used on the contract drawings shall be developed for the specific structure in question.

When a refined method of analysis is used to design a bridge, the table of live load distribution factors shall be the basis for future ratings of the bridge. In order to provide a realistic rating in the absence of such a table, the rating of the bridge would require modeling the bridge by means of an analysis method similar to the one used in the original design. The live load distribution factors given in D4.6.2.2.2 should not be used for the rating, since they would generally provide an unduly conservative rating or, in a few cases, an unconservative rating.

SPECIFICATIONS

COMMENTARY

Girder 1-Moment Distribution Factors*						
Location	Positive Moment Distribution Factors			Negative Moment Distribution Factors		
	1 Lane	2 Lanes	N Lanes	1 Lane	2 Lanes	N Lanes
Span 1				–	–	–
Interior Support 1	–	–	–			
Span 2				–	–	–
Interior Support 2	–	–	–			
Span N				–	–	–
Interior Support N	–	–	–			

Girder 1 – Shear Distribution Factors*			
Location	1 Lane	2 Lanes	N Lanes

*These tables shall be repeated for each girder

Figure C4.6.3.3-1 - Example of Live Load Distribution Factor Tables

A live load distribution factor developed for the design truck may be used for permit and rating vehicles. When the bridge or the vehicle or both are unusual, an analysis should be made to justify the use of an design truck distribution factor for other types of vehicles.

One possible way to develop a simplified method for rating for cross-frame members would be to develop a table of ratings for PHL-93, P-82, ML-80, HS20 and H20 for 1 up to N lanes loaded at the time of original design. When a future rating of a special vehicle is required, the engineer could develop an approximate rating by interpolating among these vehicles used to develop the table.

A similar approach could be used for the uplift reaction condition. A table of uplift reactions for PHL-93, P-82, ML-80, HS20 and H20 for 1 up to N lanes loaded could be developed at the time of original design. When a future rating of a special vehicle is required, the engineer could develop an approximate uplift reaction by interpolating among these vehicles used to develop the table. Next, this uplift reaction could be in computing a rating.

Some programs use an influence surface loading technique that evaluates numbers of lanes of loading with

SPECIFICATIONS

COMMENTARY

appropriate multi-presence reduction factors. Other procedures apply the distribution factors given in D4.6.2.2.2 to each girder in a grid of girders and diaphragms and allow a grid analysis to evaluate the effects of skew, curvature, and the tendency for load to gravitate toward the exterior stringers, but they do not necessarily take advantage of the fact that the true distribution factor is often less than those given in D4.6.2.2.2 and typically is not constant for all effects (moment, shear, deflection, etc.) or locations along the bridge.

In 1986, the Department conducted a parametric study of steel girder bridges to compare the results obtained from these programs for a variety of combinations of skew and curvature. This parametric study could not cover all cases that might be encountered by designers, but did reveal some trends and comparative data which form the basis of a report titled "Review of Computer Programs for the Analysis of Girder Bridges", January 1989. Since 1986, many of the programs used in this study have been changed and/or updated. Therefore, some of the report's comparisons and observations may have lost their relevancy. For a copy of this report, contact the Chief Bridge Engineer's office.

The modeling of diaphragms and boundary conditions at supports and bearings is vital to obtaining the proper results from some of these sophisticated programs. The burden of correctly handling these factors rests squarely upon the shoulders of the designer. Consider the following example, which shows how a very small modeling error produces very erroneous results.

The framing plan shown in Figure C2 represents a real bridge that was designed using a grid-type approach. The designer had a good model for this structure, except that the rotational degree of freedom corresponding to the global x-axis at all of the bearings was fixed. This did not allow the diaphragms at the piers and abutments to respond correctly to the imposed loadings and deformations, and also had the effect, by virtue of vector resolution between global and local systems, of producing artificially stiff ends on the girders.

This incorrect boundary assumption altered both the dead load and live load forces. The effect of this on the dead load reactions obtained at the abutments and piers was dramatic. A modest uplift was reported at the near abutment dead load reaction for Girder 1, and a very substantial uplift was reported at the far abutment dead load reaction for Girder 5. This is shown in the table in Figure C2, as is a moment diagram for noncomposite dead loads which reflects the incorrect dead load reactions. Also shown are the correct dead load reactions which were determined when the structure was modeled using the generic STRESS computer program, with proper boundary conditions at the supports. In this case, a positive dead load reaction was found at all bearings, and a significantly different moment diagram for noncomposite dead load also resulted. Finally, the reaction table shows a set of incorrect dead load reactions obtained with STRESS when same error in

SPECIFICATIONS

COMMENTARY

boundary conditions was made to confirm the significance of proper modeling. The correct and incorrect dead load moment diagrams also are shown in Figure C2.

The differences in the degrees of freedom at the lines of support on this structure were also investigated, utilizing a relatively complete three-dimensional finite element analysis and the SAPIV computer program. The model is illustrated in Figure C3, which shows how the deck slab, girders and cross-frames were modeled in their proper relative positions in cross-section by means of rigid linking members. Also shown in this figure is a comparison of the dead load reactions obtained from STRESS and from SAPIV by applying all the noncomposite dead loads in a single loading. The agreement between these reactions is excellent.

In order to verify that the order of pouring the deck slab units would not contribute to an uplift situation, the pouring sequence was replicated in a three-dimensional SAPIV analysis. The results of the analysis of the three stages of the pouring sequence are shown in Figure C3, as well as the total accumulated load at the end of the pour. A comparison of the sequential loading with the application of a single loading of noncomposite dead load also showed relatively good agreement.

There are cases in which dead load uplift at the reactions due to skew and/or curvature is possible. The simple span bridge featured in the November 1, 1984, issue of Engineering News-Record was correctly analyzed and indicated high corner dead load uplift.

The important point shown in the example in Figures C2 and C3 is that seemingly small errors in modeling the structure can result in very substantial changes in the reactions, shears and moments. The designer must be aware of this potential when using two- or three-dimensional analysis techniques.

Sometimes modeling problems occur because user's manuals are not clear or because a "bug" exists, of which the author/vendor is unaware. Such a case is illustrated for a simply supported, partially curved and skewed bridge in Figure C4. Initially, this bridge was modeled with extra joints at locations other than diaphragms in an effort to improve live load determination. As a result, the number of points along each girder was not equal, but there was no indication of a potential problem in the descriptive literature. The resulting live load moment envelopes for the middle and two exterior girders, which are shown in Figure C4a, are obviously unusual in shape and possibly also in their order of maximum moment, i.e., No. 4, No. 5 and No. 3.

After these results were brought to the attention of the authors/vendors, it was decided that the live load processor was not responding properly to the unequal number of nodes per girder, that nodes should be essentially "radial," and that it was uncertain whether the nodes to which diaphragms were not connected were legitimate. The revised model, shown in Figure C4b, produced clearly better results, as is

SPECIFICATIONS

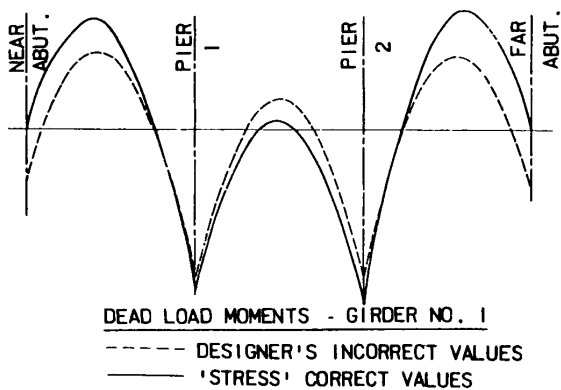
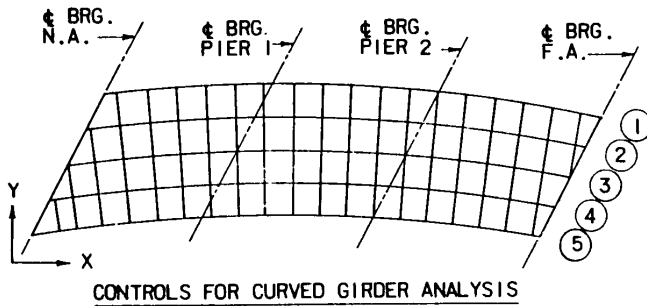
COMMENTARY

shown in the indicated live load moment envelopes. This example illustrates the need to review the output carefully and to communicate with the authors/vendors about the correct use of their programs.

In summary, two- and three-dimensional methods can provide better understanding of load distribution in girder bridges, but must be used with great care.

METRIC UNITS

GIRDER	RADIUS (m)	SPAN LENGTHS		
		1	2	3
1	297.00	29.31	29.64	29.84
2	294.04	29.77	29.95	30.05
3	291.05	30.28	30.28	30.28
4	288.10	30.81	30.61	30.51
5	285.11	31.39	30.99	30.73

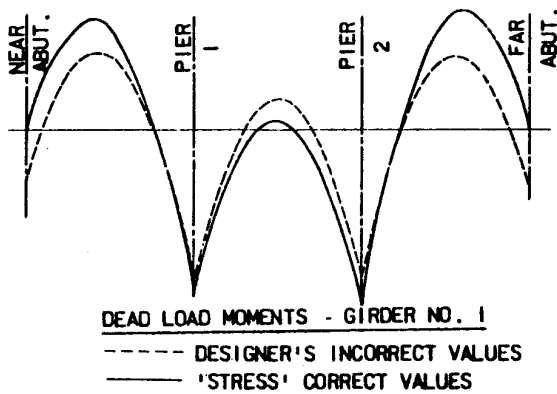
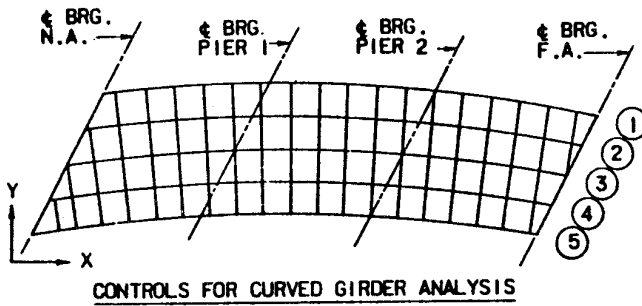


GIRD No.	SUPPORT REACTIONS				
	'STRESS' CORRECT SUPPORT CONDITION	DESIGNER'S INCORRECT REACTIONS	'STRESS' INCORRECT SUPPORT CONDITIONS		
	(VERT - kN)	(VERT - kN)	(VERT - kN)	(MOM - kN-m)	
NEAR ABUT.	1	288.81	-80.38	-79.09	-630.72
	2	300.11	401.74	401.30	-1,008.94
	3	289.56	394.76	394.63	-1,260.77
	4	288.59	261.72	261.36	-1,087.05
	5	335.07	750.96	748.73	-702.19
PIER 1	1	923.98	849.12	850.64	0.00
	2	860.38	822.84	819.37	0.00
	3	828.26	795.04	795.88	0.00
	4	927.05	882.31	882.79	0.00
	5	747.93	732.90	730.32	0.00
PIER 2	1	839.52	801.66	802.11	0.00
	2	899.56	851.48	847.61	0.00
	3	886.26	818.57	819.94	0.00
	4	895.74	823.59	823.99	0.00
	5	820.08	761.54	759.05	0.00
FAR ABUT.	1	296.59	994.66	993.02	1,099.80
	2	286.27	209.37	209.68	1,669.49
	3	288.81	383.82	380.26	1,667.19
	4	296.33	524.64	524.64	1,678.44
	5	308.96	-363.09	-362.56	1,102.78
TOTAL		11,607.99	11,617.24	11,608.08	

Figure C4.6.3.3-2 - Framing Plan, Comparative Dead Load Reactions and Moment Diagram Showing Effect of Proper and Improper Rotational Boundary Condition as Reflected in a Grid Analysis

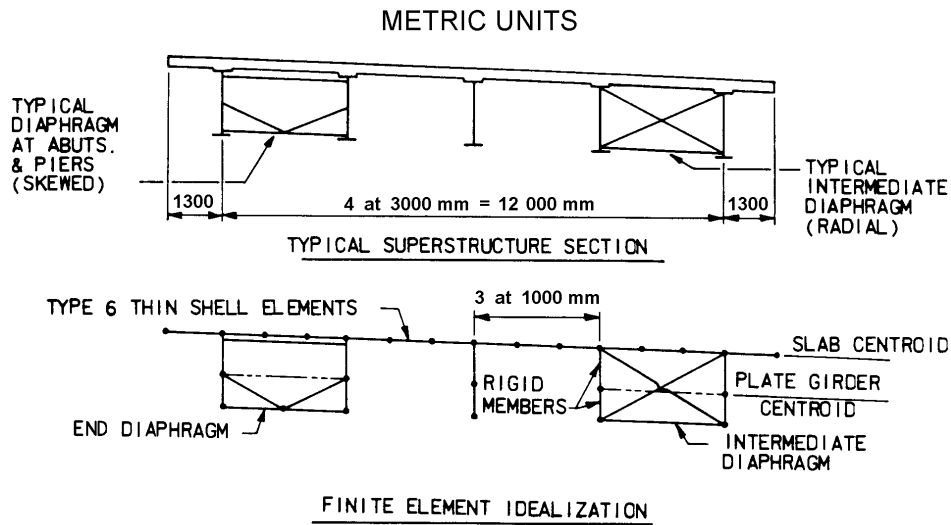
U. S. CUSTOMARY UNITS

GIRDER	RADIUS (FT.)	SPAN LENGTHS		
		1	2	3
1	974.4	96'-2"	97'-3"	97'-11"
2	964.7	97'-8"	98'-3"	98'-7"
3	954.9	99'-4"	99'-4"	99'-4"
4	945.2	101'-1"	100'-5"	100'-1"
5	935.4	103'-0"	101'-8"	100'-10"



GIRD. NO.	DEAD LOAD SUPPORT REACTIONS				
	'STRESS' CORRECT SUPPORT CONDITIONS	DESIGNER'S INCORRECT REACTIONS	'STRESS' INCORRECT SUPPORT CONDITIONS		
	(VERT - K)	(VERT - K)	(VERT - K)	(MOM X K-FT)	
NEAR ABUT.	1	64.93	-18.07	-17.78	-465.1
	2	67.47	90.32	90.22	-744.0
	3	65.10	88.75	88.72	-929.7
	4	64.88	58.84	58.76	-801.6
	5	75.33	168.83	168.33	-517.8
PIER 1	1	207.73	190.90	191.24	0
	2	193.43	184.99	184.21	0
	3	186.21	178.74	178.93	0
	4	208.42	198.36	198.47	0
	5	168.15	164.77	164.19	0
PIER 2	1	188.74	180.23	180.33	0
	2	202.24	191.43	190.56	0
	3	199.25	184.03	184.34	0
	4	201.38	185.16	185.25	0
	5	184.37	171.21	170.65	0
FAR ABUT.	1	66.68	223.62	223.25	811.0
	2	64.36	47.07	47.14	1231.1
	3	64.96	86.29	86.49	1229.4
	4	66.62	117.95	117.95	1237.7
	5	69.46	-81.63	-81.51	813.2
TOTAL	2609.71	2611.79	2609.73		

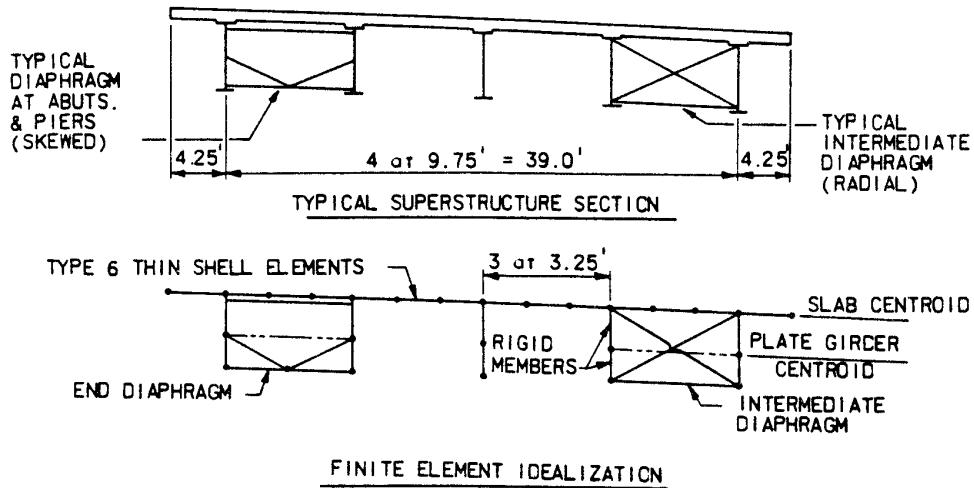
Figure C4.6.3.3-2 - Framing Plan, Comparative Dead Load Reactions and Moment Diagram Showing Effect of Proper and Improper Rotational Boundary Condition as Reflected in a Grid Analysis (Continued)



	BEAM NO	SAP NODE	FULL DEAD LOAD ON NON-COMPOSITE SECTION (kN)	STRESS FULL DEAD LOAD ON NON-COMPOSITE SECTION (kN)	SAP SLAB POURS 1 & 2 (kN)	SAP SLAB POUR 3 (kN)	SAP SLAB POUR 4 (kN)	SAP TOTAL OF COLUMNS 3,4,& 5 (kN)
NEAR ABUT.	5	8	238.8	251.3	256.6	-18.7	-1.7	236.1
	4	29	271.7	259.7	291.7	-6.6	-0.9	286.0
	3	64	249.0	246.8	265.9	-20.0	-2.2	243.7
	2	109	255.3	245.0	275.3	-10.2	-1.3	263.7
	1	167	290.0	290.9	326.4	-57.8	-12.9	256.6
PIER 1	5	282	579.1	602.2	419.8	100.0	268.6	788.6
	4	324	729.9	752.1	298.4	148.1	276.6	723.2
	3	363	763.7	725.4	332.2	146.7	298.0	777.0
	2	402	773.9	815.7	392.3	125.4	272.2	789.9
	1	444	666.7	673.4	285.1	130.7	270.8	686.7
PIER 2	5	576	761.9	742.3	330.4	162.8	295.3	788.6
	4	617	765.9	792.1	374.0	117.8	270.4	762.3
	3	656	785.9	773.9	373.6	135.2	288.6	797.5
	2	695	753.9	785.9	333.1	125.8	275.3	734.3
	1	736	737.0	734.3	326.4	114.3	282.8	723.6
FAR ABUT.	5	901	256.2	258.8	282.8	-50.3	-10.6	221.9
	4	935	245.9	243.3	261.1	-8.4	0.8	253.5
	3	959	248.2	246.4	265.5	-18.2	0.4	247.7
	2	979	259.7	255.7	285.5	-16.0	0.4	269.9
	1	991	261.9	268.2	287.7	-17.7	-2.6	267.3
			1011.9	1018.5				1011.9

Figure C4.6.3.3-3 - Finite Element Idealization and Reactions Obtained for Structure Shown in Figure C4.6.3.3-1

U. S. CUSTOMARY UNITS



		BEAM NO	SAP NCDE	SAP FULL DEAD LOAD ON NON-COMPOSITE SECTION	STRESS FULL DEAD LOAD ON NON-COMPOSITE SECTION	SAP SLAB POURS 1 & 2	SAP SLAB POUR 3	SAP SLAB POUR 4	SAP TOTAL OF COLUMNS 3, 4 & 5
NEAR ABUT.	5	8		53.7	56.5	57.7	-4.2	-0.4	53.1
	4	29		61.1	58.4	65.6	-1.5	0.2	64.3
	3	64		56.0	55.5	59.8	-4.5	-0.5	54.8
	2	109		57.4	55.1	61.9	-2.3	-0.3	59.3
	1	167		65.2	65.4	73.4	-13.0	-2.9	57.5
PIER 1	5	282		180.2	185.4	94.4	22.5	60.4	177.3
	4	324		164.1	169.1	67.1	33.3	62.2	162.6
	3	363		171.7	163.1	74.7	33.0	67.0	174.7
	2	402		174.0	183.4	88.2	28.2	61.2	177.6
	1	444		149.9	151.4	64.1	29.4	60.9	154.4
PIER 2	5	576		171.3	166.9	74.3	36.6	66.4	177.3
	4	617		172.2	178.1	84.1	26.5	60.8	171.4
	3	656		176.7	174.0	84.0	30.4	64.9	179.3
	2	695		169.5	176.7	74.9	28.3	61.9	165.1
	1	736		165.7	165.1	73.4	25.7	63.6	162.7
FAR ABUT.	5	901		57.6	58.2	63.6	-11.3	-2.4	49.9
	4	935		55.3	54.7	58.7	-1.9	0.2	57.0
	3	959		55.8	55.4	59.7	-4.1	0.1	55.7
	2	979		58.4	57.5	64.2	-3.6	0.1	60.7
	1	991		58.9	60.3	64.7	-4.0	-0.6	60.1
				2275	2290				2275

Figure C4.6.3.3-3 - Finite Element Idealization and Reactions Obtained for Structure Shown in Figure C4.6.3.3-1 (Continued)

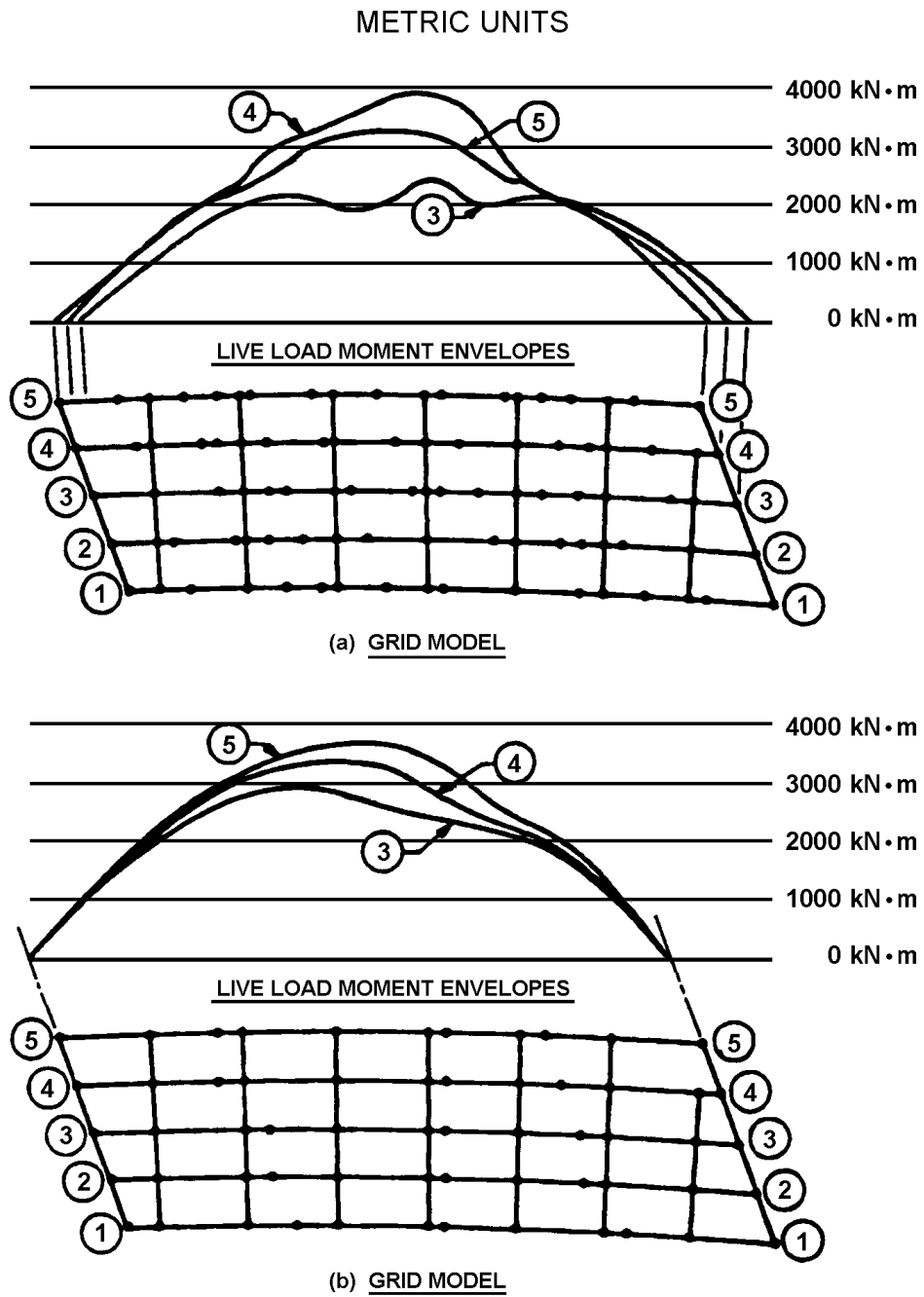


Figure C4.6.3.3-4 - Comparative Live Load Moment Envelopes for the Middle and Two Outside Girders of Curved Skewed Showing the Results of an Apparent "Bug" in Algorithm for Applying Live Load

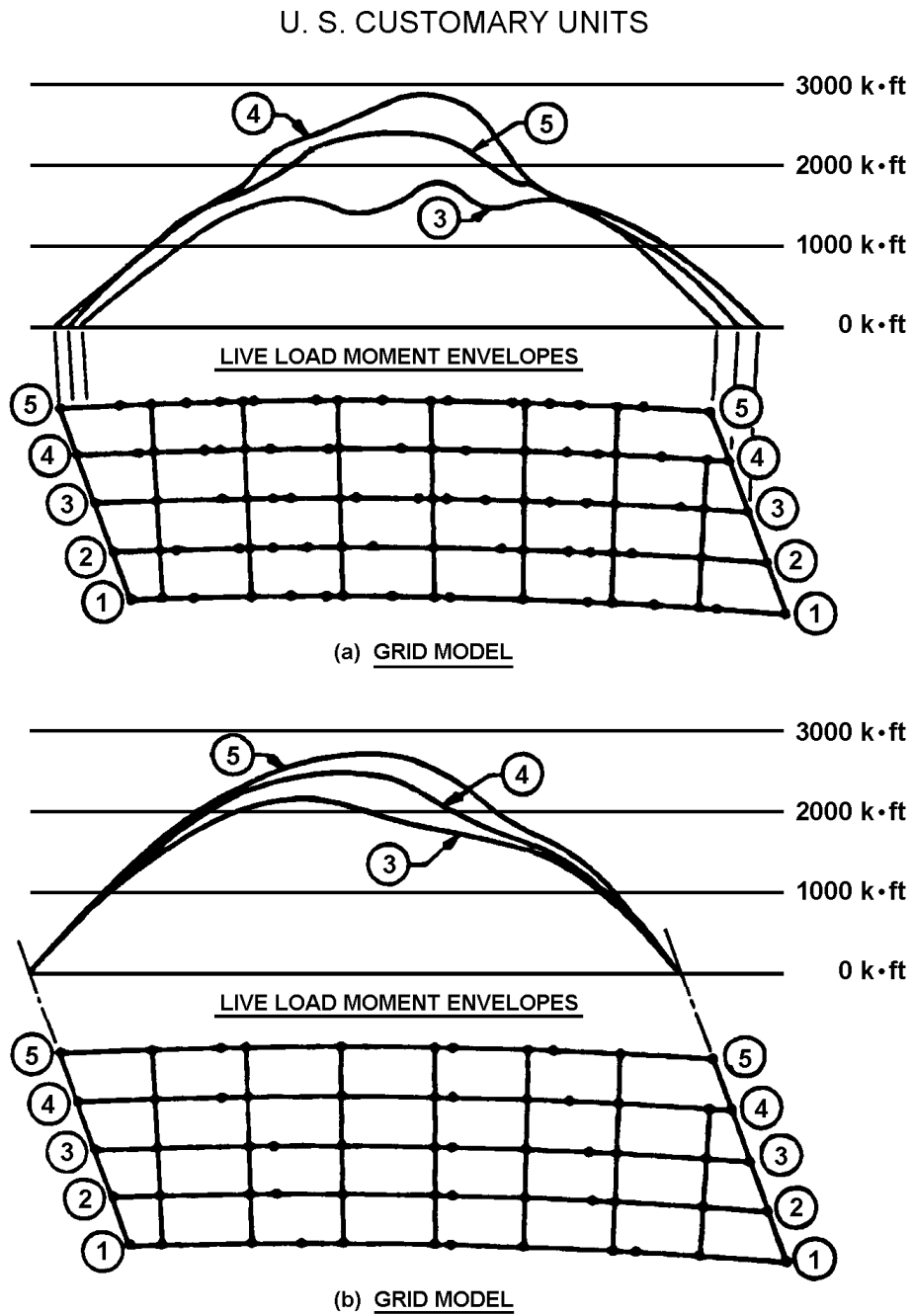


Figure C4.6.3.3-4 - Comparative Live Load Moment Envelopes for the Middle and Two Outside Girders of Curved Skewed Showing the Results of an Apparent "Bug" in Algorithm for Applying Live Load (Continued)

SPECIFICATIONS

COMMENTARY

4.6.4 Redistribution of Negative Moments in Continuous Beam Bridges

4.6.4.1 GENERAL

The following shall replace A4.6.4.1.

The redistribution of force effects in multi-span, multi-beam or girder superstructures is not permitted in the design of Pennsylvania bridges, except as described in D4.6.4.3.

4.6.4.2 REFINED METHOD

Delete A4.6.4.2

4.6.4.3 APPROXIMATE PROCEDURE

The following shall replace A4.6.4.3

A simplified redistribution procedure for compact steel beams given in A6.10.2.2 and D6.10.2.2 may be used.

4.7 DYNAMIC ANALYSIS**4.7.1 Basic Requirements of Structural Dynamics**

C4.7.1.4 DAMPING

The following shall supplement AC4.7.1.4.

Damping values obtained from field measurement or tests shall be approved by the Chief Bridge Engineer.

4.7.2 Elastic Dynamic Responses

4.7.2.2 WIND-INDUCED VIBRATION

4.7.2.2.1 Wind Velocities

The following shall supplement A4.7.2.2.1.

The Chief Bridge Engineer will decide if wind tunnel tests are warranted for a structure.

4.7.4 Analysis for Earthquake Loads

4.7.4.3 MULTI-SPAN BRIDGES

C4.7.4.3.1

4.7.4.3.1 Selection of Method

The following shall supplement A4.7.4.3.1.

A single-mode or a multi-mode analysis is acceptable for bridges whose skew angle is greater than 70° with a total span length less than 152 000 mm {500 ft.}. For major and unusual bridges, and bridges whose skew angle is less than 70°, use the multi-mode spectral analysis. Details of the single-mode spectral method of analysis procedure are given in A4.7.4.3.2.

Use the SEISAB computer program for seismic analysis. In addition, structural analysis programs (such as

The following shall replace AC4.7.4.3.1.

The selection of the method of analysis depends on seismic zone, regularity, and importance of the bridge.

Regularity is a function of the number of spans and the distribution of weight and stiffness. Regular bridges have less than seven spans, no abrupt or unusual changes in weight, stiffness, or geometry; and no large changes in these parameters from span-to-span or support-to-support, abutments excluded. A more rigorous analysis procedure may be used in lieu of the recommended minimum.

As a clarification of seismic analysis procedures, the Department will accept a multi-mode analysis in all cases.

SPECIFICATIONS

STAAD-III) may be used in lieu of SEISAB for unusual structures, for structures having substructure units with multi-column pier bents, and for structures with multiple simple spans.

Detailed seismic analysis is not required for single span bridges or for bridges in Seismic Zone 1. A seismic analysis may be performed for multi-span bridges in Seismic Zone 1 if designers feel such an analysis will more accurately reflect the connection forces and produce a more economical design.

The following shall replace Table A4.7.4.3.1-1.

Table 4.7.4.3.1-1 – Analysis Procedure

Seismic Zone	Bridges with Two or More Spans
1	None Required
2	A multi-mode analysis for all major and unusual bridges, and bridges whose skew angle is less than 70°. A single mode (or a multi-mode spectral) for bridges whose skew angle is greater than 70°, with total span length less than 152 000 mm {500 ft.}.

4.7.4.3.5P Determination of Elastic Forces and Displacements

For multiple span bridges in Seismic Zone 2, the elastic forces and displacements shall be determined independently along two perpendicular axes by use of a single-mode or multi-mode spectral method of analysis. The resulting forces shall then be combined as specified in A3.10.8. Typically the perpendicular axes are the longitudinal and transverse axes of the bridge, but the choice is open to the designer. The longitudinal axis of a curved bridge may be a chord connecting the two abutments. For single span bridges and bridges in Seismic Zone 1, the elastic forces and displacements shall also be combined as specified in A3.10.8.

4.7.4.4 MINIMUM DISPLACEMENT REQUIREMENTS

The following shall replace the definition of N in Equation A4.7.4.4-1.

N = minimum support length measured perpendicular to abutment or pier face from the end of the beam at the centerline of the bottom flange.

The following shall supplement A4.7.4.4.

The N calculated in Equation A1 shall not be taken less than 300 mm {12 in.}.

COMMENTARY

However, a multi-mode analysis is required when the bridge skew angle is less than 70° or the bridge is a major (total of span length greater than 152 000 mm {500 ft.}) or unusual structure. For other cases, a single-mode analysis will suffice.

SEISAB should be used for the seismic analysis. If SEISAB is not suitable for a structure, other structural analysis programs capable of seismic modeling (such as STAAD-III) may be used in lieu of SEISAB. The Designer must stipulate the reasons SEISAB is not suitable and obtain the Department's approval.

It has been found that, in most cases, seismic forces do not control the design. Therefore, when modeling foundations, it is acceptable for designers to perform a number of analyses (computer runs), based on assumptions which sufficiently bound the potential foundation stiffness and then use the worst resulting forces and displacements to design the structure. Use of this modeling procedure is generally acceptable when seismic forces do not control the design.

When seismic forces do control the design, an analysis which more closely models the superstructure and substructure stiffness is required.

C4.7.4.3.5P

When designing a component, it is important to recognize its geometric restraints and/or releases, the direction of the forces and displacements it must accommodate, as well as the skew effects.

C4.7.4.4

The following shall supplement AC4.7.4.4.

For bridges in Seismic Zone 2, the design displacements are specified as the maximum of those determined from the elastic analysis of A4.7.4.3 and D4.7.4.3 or the minimum specified support lengths given by Equation A4.7.4.4-1. This either/or specification was introduced to account for larger displacements that may occur from the analysis of more flexible bridges. It was the opinion of the PEP that displacement obtained from the elastic analysis of bridges should provide a reasonable

SPECIFICATIONS

NOTE: S in Equation A1 is based on AASHTO's definition of skew angle, see PP3.2.2 for PennDOT's and AASHTO's definition of skew angle.

The following shall replace Table A4.7.4.4-1.

Table 4.7.4.4-1 – Percentage N by Zone and Acceleration Coefficient

ZONE	ACCELERATION COEFFICIENT	SOIL TYPE	%N
1	<0.025	I or II	100
1	<0.025	III or IV	100
1	≥0.025	All	100
2	All Applicable	All	100
3	All Applicable	All	100
4	All Applicable	All	100

COMMENTARY

estimate of the displacements resulting from the inelastic response of the bridge. However, it must be recognized that displacements are very sensitive to the flexibility of the foundation; if the foundation is not included in the elastic analysis of A4.7.4.3 and D4.7.4.3, consideration should be given to increasing the specified displacements for bridges founded on very soft soils. This increase may be of the order of 50 percent or more, but, as with any generalization, considerable judgment is required. A better method is to determine upper and lower bounds from an elastic analysis which incorporates foundation flexibility. Special care in regard to foundation flexibility is required for bridges with high piers.

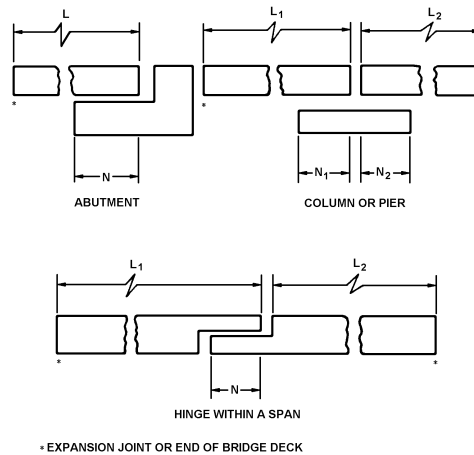


Figure C4.7.4.4-1 - Dimensions for Minimum Support Length Requirements

4.7.4.5P BASE ISOLATION DESIGN

4.7.4.5.1P General

This article includes the fundamental requirements for base isolation design, which greatly reduces the earthquake forces that a bridge must resist.

The same acceleration coefficient, A, is prescribed for base isolation design as for cases without base isolation. This coefficient is given on a county-by-county basis in Figure D3.10.2-1. However, a minimum value of 0.1 shall be used.

Seismic zone is not a delineator concerning method of analysis; however, minimum design requirements are governed by the seismic zone. Refer to Table A3.10.4-1 for the appropriate seismic zone designation.

The site coefficient for base isolation design, S_i, which accounts for the effects of the site condition on the elastic response coefficient, is given in Table 1. The soil profile types are the same as those described in A3.10.5.

The R-factors presented in Table A3.10.7.1-1 and A3.10.7.1-2 are used for base isolation design with the exception that the R-factor for all substructures shall not be

C4.7.4.5.1P

This article incorporates generic requirements for seismic isolation design. The isolation of structures from the damaging effects of earthquakes is not a new idea. The first patents for base isolation schemes were taken out at the turn of the century, but, until very recently, few structures were built which use these ideas. Early concerns were focused on the fear of uncontrolled displacements at the isolation interface, but these have been largely overcome by the successful development of mechanical energy dissipators. When used in combination with a flexible device, such as an elastomeric bearing or a sliding plate, an energy dissipator can control the response of an isolated structure by limiting both the displacements and the forces. Interest in base isolation, as an effective means of protecting bridges from earthquakes, has, therefore, revived in recent years. To date, there are several hundred bridges in New Zealand, Japan, Italy, and the United States which use base isolation principles and technology in their seismic design.

The intent of seismic isolation is to increase the fundamental period of vibration so that the structure is subjected to lower earthquake forces. However, the

SPECIFICATIONS

greater than 2.0.

Each statically stable segment of the structure shall be analyzed for the statically equivalent seismic force given in D4.7.4.5.2P. For Seismic Zone 2, the requirements of D4.7.4.5.6P shall apply.

Table 4.7.4.5.1P-1 – Site Coefficient for Base Isolation (S_i)

Site Coefficient	Soil Profile Type				
	I	II	III	IV	IV
S_i	1.0	1.5	2.0	3.0	3.0

COMMENTARY

reduction in force is accompanied by an increase in displacement demand which must be accommodated within the flexible mount. Furthermore, longer period bridges can be lively under service loads.

There are, therefore, three basic elements in those base isolation systems that have been used to date. These are:

- (a) A flexible mounting so that the period of vibration of the total system is lengthened sufficiently to reduce the force response.
- (b) A damper or energy dissipater so that the relative deflections across the flexible mounting can be limited to a practical design level.
- (c) A means of providing rigidity under low (service) load levels such as wind and braking forces.

Flexibility

An elastomeric bearing is not the only means of introducing flexibility into a structure, but it certainly appears to be the most practical and the one with the widest range of application. The idealized force response with increasing period (flexibility) is shown schematically in the force response curve in Figure C1. Reductions in base shear occur as the period of vibration of the structure is lengthened. The extent to which these forces are reduced is primarily dependent on the nature of the earthquake ground motion and the period of the fixed base structure. However, as noted above, the additional flexibility needed to lengthen the period of the structure will give rise to large relative displacements across the flexible mount. Figure C2 shows an idealized displacement response curve from which displacements are seen to increase with increasing period (flexibility).

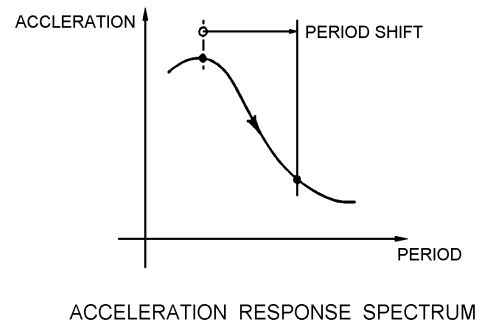
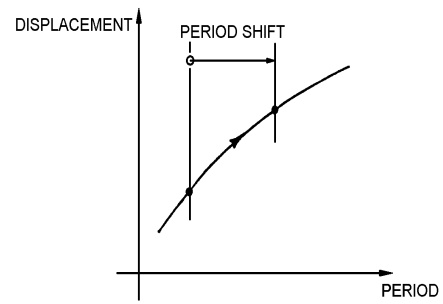


Figure C4.7.4.5.1P-1 - Idealized Force Response Curve

SPECIFICATIONS

COMMENTARY



DISPLACEMENT RESPONSE SPECTRUM

Figure C4.7.4.5.1P-2 - Idealized Displacement Response Curve

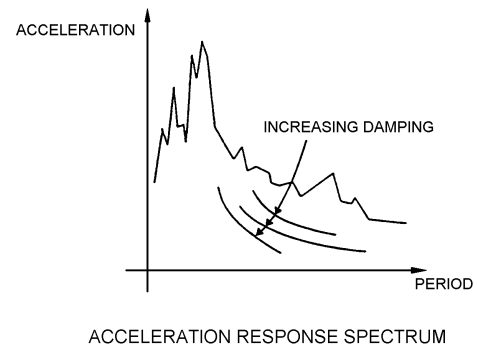
Energy Dissipation

Large relative displacements can be controlled if substantial additional damping is introduced into the structure at the isolation level. This is shown schematically in Figure C3. It can also be seen that higher damping removes much of the sensitivity to variations in ground motion characteristics, as is indicated by the smoother force response curves at higher damping.

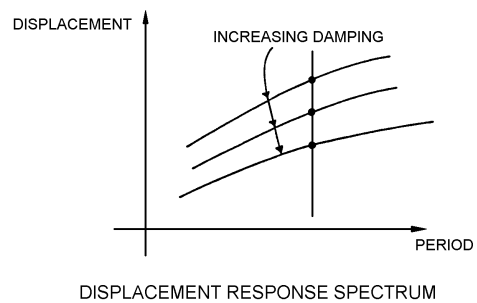
One of the most effective means of providing a substantial level of damping is through hysteretic energy dissipation. The term "hysteretic" refers to the offset between the loading and unloading curves under cyclic loading. Figure C4 shows an idealized force-displacement loop where the enclosed area is a measure of the energy dissipated during one cycle of motion. Mechanical devices which use the plastic deformation of either mild steel or lead to achieve this behavior have been developed.

SPECIFICATIONS

COMMENTARY

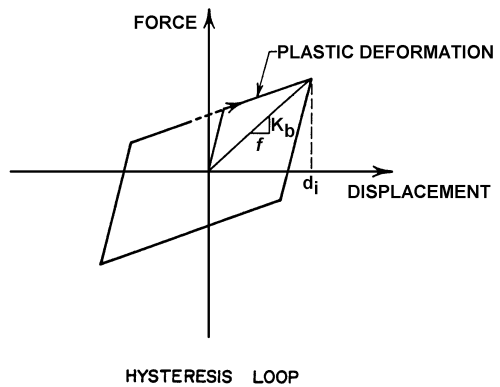


ACCELERATION RESPONSE SPECTRUM



DISPLACEMENT RESPONSE SPECTRUM

Figure C4.7.4.5.1P-3 - Response Curves for Increasing Damping



HYSTERESIS LOOP

Figure C4.7.4.5.1P-4 - Idealized Hysteresis Loop

Rigidity Under Low Lateral Loads

While lateral flexibility is highly desirable for high seismic loads, it is clearly undesirable to have a structural system that will vibrate perceptibly under frequently occurring loads such as wind loads or braking loads. Mechanical energy dissipators may be used to provide rigidity at these service loads by virtue of their high initial elastic stiffness. Alternately, some base isolation systems require a separate wind restraint device for this purpose - typically a rigid component which is designed to fail at a

given level of lateral load.

Design Application

The seismic design principles for base isolation are best illustrated by Figure C5 which was based on the AASHTO Standard Specification for Highway Bridges. The same basic concept concerning base isolation also applies to the LRFD Specification. The solid uppermost line is the realistic (elastic) ground response spectrum as recommended in the AASHTO Standard Specification for Highway Bridges for the highest seismic zone. This is the spectrum that is used to determine actual forces and displacements for conventional design. The lowest solid line is the design curve from the AASHTO Standard Specification for Highway Bridges. It is seen to be approximately one-fifth of the realistic forces given by the AASHTO Standard Specification for Highway Bridges. This reduction, to obtain the design forces, is consistent with an R-factor of 5 for a multi-column bent. Also shown is the probable overstrength of a bent so designed. Now if the bridge is isolated, the shear forces in this multi-column bent may be represented by an inelastic spectrum that incorporates the damping of the isolation system, as shown by the small dashed line in Figure C5.

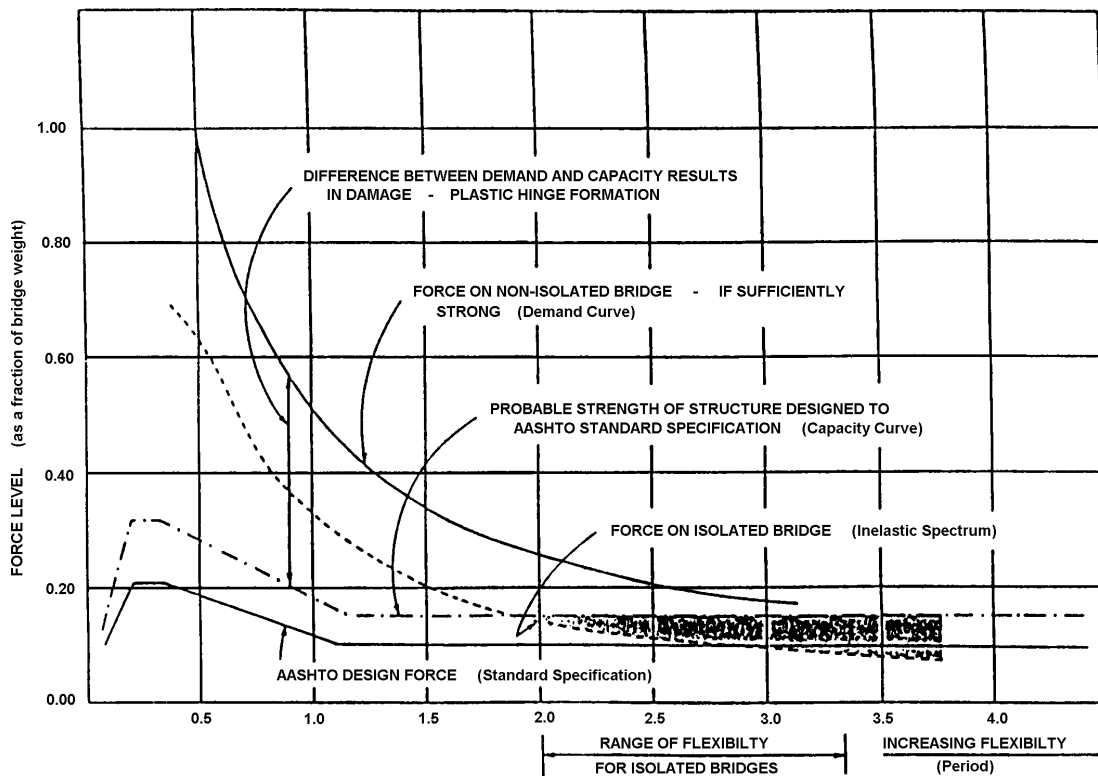


Figure C4.7.4.5.1P-5 – Earthquake Forces

SPECIFICATIONS

COMMENTARY

The period of the bridge will be in the 2.0- to 2.5-second range; in this range the overstrength (actual capacity) of the bent exceeds the realistic forces (demand) for the isolated bridge. This region has been shaded in Figure C5. There is, therefore, no inelastic deformation or ductility required of the bent, and elastic performance (without damage) is ensured. The benefits of seismic isolation for bridges may be summarized as follows:

- (a) Reduction in the realistic forces to which a bridge will be subjected by a factor of between 5 and 10.
- (b) Elimination of the ductility demand and, hence, damage to the piers.
- (c) Control of the distribution of the seismic forces to the substructure elements with appropriate sizing of the elastometric bearings.
- (d) Reduction in column design forces by a factor of approximately 2 in comparison with conventional design.
- (e) Reduction in foundation design forces by a factor of between 2 and 3 in comparison with conventional design.

The intent of seismic isolation design is to eliminate or significantly reduce damage (inelastic deformation) to the substructure. By limiting the R-factor to a maximum value of 2, the overstrength inherent in the substructures will ensure minimal ductility demand on the substructure for the design earthquake. For essential structures, consideration may be given to reducing the maximum value of R to as low as 1 to ensure complete elastic response of the substructure.

4.7.4.5.2P Statically Equivalent Seismic Force and Coefficient

The statically equivalent force is given by:

$$F = C_s W \quad (4.7.4.5.2P-1)$$

where:

C_s = elastic seismic response coefficient

W = weight of the superstructure segment supported by isolation bearings

The elastic seismic response coefficient, C_s , used to determine the equivalent force is given by the dimensionless relation:

C4.7.4.5.2P

For seismic isolation design, the elastic seismic coefficient is again related to the elastic ground response spectra. Here, the form is slightly different from that for non-isolation design (which involved $T^{2/3}$) and, for 5% damping, is given by

$$C_s = \frac{A S_i}{T} \quad (C4.7.4.5.2P-1)$$

In this case, A is once again the acceleration coefficient, S_i is the site coefficient for base isolation (Table D4.7.4.5.1P-1), and the $1/T$ factor accounts for the decrease in the response spectra ordinates as T increases. The specific S_i values reflect the fact that above a period of 1.0 second, there is a 1.0 to 1.5 to 2.0 to 3.0 relationship for the spectral accelerations for soil profile Types I, II, III and IV,

SPECIFICATIONS

$$C_s = \frac{K_b d_i}{W} \quad (4.7.4.5.2P-2)$$

where:

K_b = equivalent linear stiffness of all bearings supporting the superstructure segment

W = weight of the superstructure segment supported on the isolation bearings

d_i = displacement across the isolation bearings

The displacement d_i (mm) {in.} is given by

$$\text{Metric Units: } d_i = \frac{250AS_i T}{B} \quad (4.7.4.5.2P-3)$$

$$\text{U.S. Customary Units: } d_i = \frac{10AS_i T}{B}$$

where:

A = acceleration coefficient as defined in D4.7.4.5.1P

B = damping factor given in Table D4.7.4.5.2P-1

S_i = dimensionless site coefficient for isolation design for the given soil profile as designated in D4.7.4.5.1P

T = period of vibration (seconds) given by

$$T = 2\pi \sqrt{\frac{W}{K_b g}} \quad (4.7.4.5.2P-4)$$

where:

g = acceleration of gravity (mm/s²) {in/sec²}

COMMENTARY

respectively. Once again, C_s should not exceed a value of 2.5A.

If the effects of damping are included, the elastic seismic coefficient is given by

$$C_s = \frac{AS_i}{TB} \quad (C4.7.4.5.2P-2)$$

where B is the damping term given in Table D4.7.4.5.2P-1. Note that for 5% damping, $B = 1.0$.

The quantity C_s is a dimensionless design coefficient which, when multiplied by g , produces the spectral acceleration. This spectral acceleration, S_A , is related to the spectral displacement, S_D , by the relationship

$$S_A = \omega^2 S_D \quad (C4.7.4.5.2P-3)$$

Where ω is the circular natural frequency and is given by $2\pi/T$. Therefore, since $S_A \approx C_s g$, then

$$S_A = \left[\frac{AS_i}{TB} \right] g \quad (C4.7.4.5.2P-4)$$

and

Metric Units:

$$\begin{aligned} S_D &= \left[\frac{1}{\omega^2} \right] \left[\frac{AS_i}{TB} \right] g \\ &= \left[\frac{T^2}{2\pi} \right] \left[\frac{AS_i}{TB} \right] 9807 \text{ mm/s}^2 \\ &= \frac{248.4 AS_i T}{B} \text{ mm} \end{aligned} \quad (C4.7.4.5.2P-5)$$

U.S. Customary Units

$$\begin{aligned} S_D &= \left[\frac{1}{\omega^2} \right] \left[\frac{AS_i}{TB} \right] \\ &= \left[\frac{T^2}{2\pi} \right] \left[\frac{AS_i}{TB} \right] 386.4 \text{ in/sec}^2 \\ &= \frac{9.79 AS_i T}{B} \text{ in.} \end{aligned}$$

Denoting S_D as d_i , which is the displacement across the elastomeric bearings, the above is approximated to be

$$\text{Metric Units: } d_i = \frac{250 AS_i T}{B} \text{ mm} \quad (C4.7.4.5.2P-6)$$

SPECIFICATIONS

COMMENTARY

U.S. Customary Units: $d_i = \frac{10AS_iT}{B}$ in

An alternate form for C_s is possible. The quantity C_s is defined by the relationship

$$F = C_s W \tag{C4.7.4.5.2P-7}$$

where:

F = earthquake design force

W = weight of the structure

Therefore,

$$C_s = \frac{F}{W} = \frac{K_b d_i}{W}$$

where K_b is the equivalent linear spring of all bearings supporting the superstructure segment (see Figure DC4.7.4.5.1P-4). The equivalence of this form to the previous form is evident by recalling that $K_b = \omega^2 W/g$, from which

Metric Units:

$$C_s = \left[\frac{\omega^2 W}{g} \right] \left[\frac{d_i}{W} \right] = \left[\frac{2\pi^2}{T} \right] \left[\frac{1}{9807} \right] \left[\frac{248.4AS_iT}{B} \right] = \frac{AS_i}{BT} \tag{C4.7.4.5.2P-9}$$

U.S. Customary Units:

$$C_s = \left[\frac{\omega^2 W}{g} \right] \left[\frac{d_i}{W} \right] = \left[\frac{2\pi^2}{T} \right] \left[\frac{1}{386.4} \right] \left[\frac{9.79AS_iT}{B} \right] = \frac{AS_i}{BT}$$

Table 4.7.4.5.2P-1 – Damping Coefficient B

Damping (% of Critical)*	≤2	5	10	20	30	40	>50
B	0.8	1.0	1.2	1.5	1.7	1.9	2.0

*The percent of critical damping shall be verified by test of the isolation system’s characteristics. The damping coefficient shall be based on linear interpolation for damping levels other than those given.

4.7.4.5.3P Requirements for Elastic Force Determination

The statically equivalent force determined according to D4.7.4.5.2P, which is associated with the displacement across the isolation bearings, shall be applied independently along two perpendicular axes and combined as specified in

SPECIFICATIONS

COMMENTARY

A3.10.8.

Typically, the perpendicular axes are the longitudinal and transverse axes of the bridge, but the choice is open to the designer. The longitudinal axis of a curved bridge may be a chord connecting the two abutments.

4.7.4.5.4P Design Displacement for Other Loads

Adequate clearance must be provided to permit shear deflections in the bearings resulting from braking loads, wind loads and centrifugal forces. These deflections are a function of the force-deflection characteristics of the bearings.

4.7.4.5.5P Design Forces for Seismic Zone 1

The design force for the connection between superstructure and substructure at each bearing is given by

$$F_A = K_b d_i \quad (4.7.4.5.5P-1)$$

where:

K_b = equivalent linear stiffness of the isolation bearing

d_i = displacement of the isolated bridge deck as specified in D4.7.4.5.2P, using a minimum acceleration coefficient, A , of 0.10

4.7.4.5.6P Design Forces for Seismic Zone 2

The requirements of D4.7.4.5.2P shall apply, except that in the determination of seismic design forces an R-factor of 1 shall be used.

4.7.4.5.7P Substructure Design Requirements

4.7.4.5.7.1P Foundations and Abutments

The provisions of this document and the LRFD shall apply to the design of foundations and abutments.

4.7.4.5.7.2P Columns, Footings and Connections

4.7.4.5.7.2aP Structural Steel

The provisions of this document and the LRFD shall apply to the design of structural steel columns and connections.

4.7.4.5.7.2bP Reinforced Concrete

The provision of this document and the LRFD shall apply to the design of reinforced concrete columns, pier footings and connections.

C4.7.4.5.4P

To protect against fatigue under frequently occurring loads, deflections should be kept as small as practicable. As a guide, the deflection due to braking load should be less than 10% of the deformable rubber thickness, and that for extreme wind loads should be less than 25% of the deformable rubber thickness.

C4.7.4.5.5P

Seismic isolation design provides a significant reduction in the real elastic forces, and the exception of this section permits this force reduction to be utilized in the design of the bearings. However, it should be noted that the acceleration coefficient, which has a maximum value of 0.09 for bridges in Seismic Zone 1, is specified to have a minimum value of 0.10 if seismic isolation is used. This conservatism will ensure, for most areas in Seismic Zone 1, that the isolation bearings are capable of resisting twice the design earthquake. This level of conservatism is greater than that inherent in the requirement for bearings being designed for 0.2 times the dead load.

SPECIFICATIONS

COMMENTARY

4.8 ANALYSIS BY PHYSICAL MODELS

4.8.2 Bridge Testing

The following shall replace A4.8.2.

When approved by the Chief Bridge Engineer, existing bridges may be instrumented and results obtained under various conditions of traffic and/or environmental loads or load tested with special purpose vehicles to establish force effects and/or the load carrying capacity of the bridge.

PENNSYLVANIA DEPARTMENT OF TRANSPORTATION
DESIGN MANUAL

PART 4

VOLUME 1

PART B: DESIGN SPECIFICATIONS

SECTION 6 – STEEL STRUCTURES

SECTION 6 - TABLE OF CONTENTS

6.1 Scope	1
6.1.1P Restrictions of Steel Bridge Types	1
6.1.1.1P Steel Tied-Arch Bridges	1
6.2 Definitions	2
6.3 Notation	2
6.4 Materials.....	3
6.4.1 Structural Steels.....	3
6.4.3 Bolts, Nuts and Washers	4
6.4.3.1 Bolts.....	4
6.4.3.2 Nuts	5
6.4.3.3 Washers	5
6.4.3.4 Alternative Fasteners	5
6.4.3.5 Load Indicator Devices.....	5
6.4.7 Stainless Steel	6
6.5 Limit States.....	6
6.5.2 Service Limit State.....	6
6.5.3 Fatigue and Fracture Limit State.....	6
6.5.4 Strength Limit State	6
6.5.4.2 Resistance Factors	6
6.6 Fatigue and Fracture Considerations	7
6.6.1 Fatigue	7
6.6.1.2 Load-Induced Fatigue.....	7
6.6.1.2.1 Application	7
6.6.1.2.2 Design Criteria	7
6.6.1.2.4 Restricted Use Details	8
6.6.1.2.5 Fatigue Resistance	8
6.6.1.3 Distortion-Induced Fatigue.....	8
6.6.1.3.4P Distortion-Induced Fatigue: Unacceptable Details and Acceptable Alternative Details	9
6.6.2 Fracture.....	16
6.7 General Dimension and Detail Requirements	16
6.7.2 Dead Load Camber.....	16
6.7.2.1P Camber Due to Weight of Deck Slab	16
6.7.2.2P Camber Details for Design Drawings.....	16
6.7.2.3P Heat-Curve Camber Corrections	18
6.7.3 Minimum Thickness of Steel.....	19
6.7.4 Diaphragms and Cross-Frames.....	19
6.7.4.1 General	19
6.7.4.2 I-Section MEMBERS	20
6.7.4.3 Box Section MEMBERS	21
6.7.5 Lateral Bracing.....	23
6.7.5.2 I-Section MEMBERS	23
6.7.5.3 Tub Section MEMBERS	23
6.8 Tension Members.....	24
6.8.2 Tensile Resistance	24
6.8.2.2 Reduction Factor, U.....	24
6.8.2.3 Combined Tension and Flexure.....	24

6.8.3 Net Area.....	25
6.9 Compression Members.....	25
6.9.2 Compressive Resistance	25
6.9.2.2 Combined Axial Compression and Flexure	25
6.9.5 Composite Members.....	25
6.10 I-Sections In Flexure.....	25
6.10.0P Applicable Provisions.....	25
6.10.1 General	26
6.10.1.1.1 Stresses	27
6.10.1.1.1d Concrete Deck Stresses	28
6.10.1.1.1fP Lateral Support of Top Flanges Supporting Timber Decks	28
6.10.1.2 Noncomposite Sections	28
6.10.1.3 Hybrid Sections	29
6.10.1.4 Variable Web Depth Members	29
6.10.1.5 Stiffness	29
6.10.1.6 Flange Stresses And Member Bending Moment	29
6.10.1.7 Minimum Negative Flexure Concrete Deck Reinforcement	31
6.10.1.11p Lateral Support Of Top Flanges Supporting Timber Decks	32
6.10.3 Constructibility	32
6.10.3.2 Flexure.....	32
6.10.3.2.1 Discretely Braced Flanges in Compression.....	32
6.10.3.2.5.1P Slab Placement	32
6.10.3.2.5.2P Deck Slab Overhang Form Support	33
6.10.3.2.4.3P Deck Slab Overhang Rotation	37
6.10.3.5 Dead Load Deflection.....	37
6.10.4 Service Limit State.....	37
6.10.4.2 Permanent Deformation.....	37
6.10.4.2.1 General	37
C6.10.4.2.1	37
6.10.4.2.2 Flexure.....	37
6.10.5 Fatigue and Fracture Limit State.....	38
6.10.5.1 Fatigue	38
6.10.5.3 Special Fatigue Requirement for Webs	38
6.10.6 Strength Limit State	38
6.10.6.2 Flexure.....	38
6.10.6.2.2 Composite Sections in Positive Flexure	38
6.10.6.2.3 Composite Sections in Negative Flexure and Noncomposite Sections	38
6.10.8 Flexural Resistance - Composite Sections in Negative Flexure and Noncomposite Sections	39
6.10.8.2 Compression-Flange Flexural Resistance.....	39
6.10.8.2.3 Lateral Torsional Buckling Resistance	39
6.10.9 Shear Resistance	40
6.10.9.1 General	40
6.10.9.3.3 End Panels	40
6.10.10 Shear Connectors.....	40
6.10.10.1 General	40
6.10.10.1.1 Types	40
6.10.10.1.2 Pitch.....	40
6.10.10.1.3 Transverse Spacing.....	42
6.10.10.1.4 Cover and Penetration	42
6.10.10.1.5p Splice Locations	42
6.10.10.2 Fatigue Resistance	42
6.10.10.3 Special Requirements for Points of Permanent Load Contraflexure	43
6.10.10.4 Strength Limit State.....	43
6.10.10.4.2 Nominal Shear Force.....	43
6.10.11 Stiffeners.....	45
6.10.11.1 Transverse Intermediate Stiffeners	45
6.10.11.1.1 General	45
6.10.11.1.2 Projecting Width.....	45

6.10.11.3	Longitudinal Stiffeners	45
6.10.11.3.3	Moment of Inertia and Radius of Gyration.....	46
6.10.11.4P	Stiffeners in Rigid-Frame Knees	47
6.10.11.4.1P	Stiffener Spacing	47
6.10.11.4.2P	Stiffener Design	48
6.10.12	Cover Plates.....	49
6.10.12.3P	Cover Plate Length and Width	49
6.11	Box Sections in Flexure	49
6.11.1	General	49
6.11.1.1	Stress Determination.....	50
6.11.3	Constructibility	50
6.11.3.2	Flexure.....	50
6.11.5	Fatigue and Fracture Limit State	50
6.11.6	Strength Limit State	51
6.11.6.2	Flexure.....	51
6.11.6.2.2	Sections in Positive Flexure	51
6.11.9	Shear Resistance	51
6.11.10	Shear Connectors.....	51
6.11.11	Stiffeners.....	52
6.11.11.2	Longitudinal Compression-Flange Stiffeners	52
6.12	Miscellaneous Flexural Members	52
6.12.1	General	52
6.12.1.2	Strength Limit State.....	52
6.12.1.2.3	Shear.....	52
6.12.2	Nominal Flexural Resistance	52
6.12.2.2	Noncomposite Members	52
6.12.2.2.1	I- and H-Shaped Members.....	52
6.13	Connections and Splices	53
6.13.1	General	53
6.13.2	Bolted Connections	53
6.13.2.1	General	53
6.13.2.3	Bolts, Nuts and Washers.....	54
6.13.2.3.2	Washers	54
6.13.2.4	Holes.....	54
6.13.2.4.1	Types	54
6.13.2.4.1b	<i>Oversize Holes.....</i>	54
6.13.2.4.2	Size.....	54
6.13.2.5	Size of Bolts	55
6.13.2.6	Spacing of Bolts	56
6.13.2.6.6	Edge Distances	56
6.13.2.7	Shear Resistance.....	57
6.13.2.8	Slip Resistance.....	57
6.13.2.10	Tensile Resistance	58
6.13.2.10.3	Fatigue Resistance	58
6.13.2.11	Combined Tension and Shear.....	59
6.13.3	Welded Connections	59
6.13.3.1	General	59
6.13.3.8p	Intersecting Welds	59
6.13.3.9P	Intermittent Fillet Welds	60
6.13.3.10P	Minimum Edge Distance	60
6.13.4	Block Shear Rupture Resistance	60
6.13.6	Splices	60
6.13.6.1	Bolted Splices.....	60
6.13.6.1.1	General	60
6.13.6.1.4	Flexural Members.....	60
6.13.6.1.4a	<i>General.....</i>	61
6.13.6.1.4b	<i>Web Splices</i>	61
6.13.6.1.4c	<i>Flange Splices</i>	62

6.13.6.1.5 Fillers.....	63
6.13.6.2 Welded Splices	63
6.15 Piles	63
6.15.1 General	63
6.15.2 Structural Resistance.....	65
6.15.3P Compressive Resistance	66
6.15.3.1 Axial Compression	66
6.15.3.2 Combined Axial Compression and Flexure	67
6.15.3.3 Buckling	70
6.15.4 Maximum Permissible Driving Stresses	70
Appendix A – Flexural Resistance – Composite Sections in Negative Flexure and Noncomposite Sections with Compact or Noncompact Webs	71
Appendix B – Moment Redistribution from Interior-Pier Sections in Continuous-Span Bridges	71
Appendix C – Basic Steps for Steel Bridge Superstructures.....	71

SPECIFICATIONS

COMMENTARY

6.1 SCOPE

6.1.1P Restrictions of Steel Bridge Types

6.1.1.1P STEEL TIED-ARCH BRIDGES

Steel tied-arch bridges shall be used only after thorough consideration has been given to all factors in design, fabrication and erection, and if the design is approved by the Chief Bridge Engineer. In the preliminary stage, the tied-arch must show a marked economic advantage over alternate designs to warrant further consideration. Tied-arch structures are currently unacceptable to FHWA. Moreover, refer to the FHWA Technical Advisory T-5140.4, dated September 28, 1978, for the problems pertinent to tied-arch structures.

Transverse welds on the tie girders shall be avoided, where possible. Bolted connections shall be used instead of transverse welds.

On Langer-girder tied-arch bridges (those tied arches where the tie girder acts as the major flexural member in addition to providing horizontal reactions to the arch rib) with box girders functioning as tie girders, the internal diaphragms stiffening the box at the floorbeam connections shall be attached to both flanges, as well as the webs. A tie plate should be placed between the tie-girder flange and the floorbeam flange if they lie essentially in the same plane.

Hangers composed of multiple bridge strands shall have either spacers between the strands or dampers, or both.

The dynamic response of the bridge due to traffic shall be investigated by an appropriate three-dimensional, forced-vibration dynamic analysis, especially for tied-arch bridges that do not employ Langer-girders.

6.1.1.2P Steel Box Bridges

Steel box bridges shall be used only after thorough consideration has been given to all factors in design, fabrication, erection and future in-depth inspection, and if the design is approved by the Chief Bridge Engineer. In the preliminary stage, the steel box design must show a marked economic or aesthetic advantage over alternate designs to warrant further consideration.

C6.1.1.1P

Steel tied-arch bridges have experienced such problems as lamellar tearing in the hanger connections, detrimental vibration in the main structure and cables, and cracking in fracture-critical members. The design, detailing, and fabrication of the floorbeams are critical for long-term performance. Fatigue cracking has occurred in floorbeams due to out-of-plane distortion in combination with abrupt termination of the flange; proper coping and grinding of the cope were not performed.

The designer must use intuitive engineering judgment when selecting the type, location and number of spacers used between the strands of a hanger composed of multiple bridge strands. The need for spacers is not based upon a calculated analysis, but rather on the observation that some bridges without spacers experienced problems and were subsequently retrofitted with spacers.

C6.1.1.2P

Even though steel box girders may provide aesthetically pleasing and sometimes economical structures, the Department has major concerns about steel box girders which are:

- difficult inspection environment,
- inspection complexities,
- future cleaning, painting and/or repair difficulties.
- detailing complexities
- stability during erection

SPECIFICATIONS

COMMENTARY

6.2 Definitions

The following shall supplement A6.2.

Controlling Flange—top or bottom flange for the smaller section at a point of splice, whichever flange has the maximum elastic flexural stress at its mid-thickness due to the factored loads.

Non-controlling Flange—the flange at a point of splice opposite the controlling flange.

6.3 NOTATION

The following shall supplement A6.3

A_{bot}	=	area of the bottom flange (mm^2) { in.^2 } (D6.10.10.1.2)
A_d	=	minimum required cross-sectional area of a diagonal member of top lateral bracing for tub sections (mm^2) { in.^2 } (DC6.7.5.3)
F_{fat}	=	radial fatigue shear range per unit length, taken as the larger of either F_{fat1} or F_{fat2} (N/mm) {kip/in.} (D6.10.10.1.2)
F_{fat1}	=	radial fatigue shear range per unit length due to the effect of any curvature between brace points (N/mm) {kip/in.} (D6.10.10.1.2)
F_{fat2}	=	radial fatigue shear range per unit length due to torsion caused by effects other than curvature, such as skew (N/mm) {kip/in.} (D6.10.10.1.2)
F_p	=	total radial shear force in the concrete deck at the point of maximum positive live load plus impact moment for the design of the shear connectors at the strength limit state, taken equal to zero for straight spans or segments (N) {kip} (D6.10.10.4.2)
F_{rc}	=	net range of cross-frame force at the top flange (N) {kip} (D6.10.10.1.2)
F_T	=	total radial shear force in the concrete deck between the point of maximum positive live load plus impact moment and the centerline of an adjacent interior support for the design of shear connectors at the strength limit state, taken equal to zero for straight spans or segments (N) {kip} (D6.10.10.4.2)
f_{bu}	=	<u>largest value of the compressive stress throughout the unbraced length in the flange under consideration, calculated without consideration of flange lateral bending</u> (MPa) {ksi} (D6.10.1.6)
L_n	=	arc length between the point of maximum positive live load plus impact moment and the centerline of an adjacent interior support (mm) {ft.} (D6.10.10.4.2)
L_p	=	<u>arc length between an end of the girder and an adjacent point of maximum positive live load plus impact moment</u> (mm) {ft.} (D6.10.10.4.2)
M_u	=	<u>largest value of the major-axis bending moment throughout the unbraced length causing compression in the flange under consideration</u> (N-mm) {k-in.} (D6.10.1.6)
P_T	=	total longitudinal shear force in the concrete deck between the point of maximum positive live load plus impact moment and the centerline of an adjacent interior support for the design of the shear connectors at the strength limit state, taken as the sum of P_p and P_n (N){kip} (D6.10.10.4.2)
R	=	<u>minimum girder radius within a panel</u> (mm) {ft.} (D6.7.4.2)
r_σ	=	desired bending stress ratio in a horizontally curved I-girder, taken equal to $ f_t/f_{bu} $ (DC6.7.4.2)
V_{fat}	=	longitudinal fatigue shear range per unit length (N/mm) {kip/in.} (D6.10.10.1.2)
w	=	<u>effective length of deck assumed acting radial to the girder</u> (mm) {in.} (D6.10.10.1.2)
Z	=	<u>curvature parameter for determining required longitudinal web stiffener rigidity</u> (D6.10.11.3.3)
β	=	<u>curvature correction factor for longitudinal web stiffener rigidity</u> (D6.10.11.3.3)
σ_{flg}	=	range of longitudinal fatigue stress in the bottom flange without consideration of flange lateral bending (MPa) {ksi} (D6.10.10.1.2)

SPECIFICATIONS

COMMENTARY

6.4 MATERIALS

6.4.1 Structural Steels

The following shall supplement A6.4.1.

Poisson's ratio for structural steel shall be assumed to be 0.3 in the elastic range.

Unless directed otherwise, all structural steel shall conform to the specifications for structural steel, ASTM A 709/A 709M, Grade 250 {Grade 36}. Other types of steel, such as ASTM A 709/A 709M, Grades 345 and 345W {Grade 50 and 50W}, in combination with ASTM A 709/A 709M, Grade 250 {Grade 36}, or with each other may be considered for economy.

Steel grades 690 or 690W {Grades 100 or 100W} shall not be used unless written approval has been obtained from the Chief Bridge Engineer.

Unpainted ASTM A 709/A 709M, Grade 345W or HPS-485W {Grade 50W or HPS-70W}, steel shall not be specified without written approval of the Chief Bridge Engineer at the TS&L stage. This policy applies to state and local bridges and bridges where State or Federal funding is utilized. Use in contractor-designed alternates must also be approved at the TS&L stage. Use is not permitted in acidic or corrosive environments, in locations subject to salt water spray or fog, in depressed roadway sections (less than 6100 mm {20 ft.} clearance) where salt spray and other pollutants may be trapped, in low underclearance situations where the steel is either less than 1500 mm {5 ft.} from normal water elevation or continuously wet, or where the steel may be buried in soil. The use of Grade 345W or HPS-485W {Grade 50W or HPS-70W} steel is not permitted in bridge types where salt spray and dirt accumulation may be a concern (e.g., trusses or inclined-leg bridges) unless corrosion-susceptible regions are painted.

Do not use Grade 345W or HPS-485W {Grade 50W or HPS-70W} steel for expansion dams, or for stringers or other members under open steel decking.

Where the use of Grade 345W {Grade 50W} or Grade HPS-485W {Grade HPS-70W} unpainted weathering steel is permitted, the following criteria must be met:

- (a) The number of expansion joints shall be minimized.
- (b) Details to avoid retention of water and debris shall be incorporated in the design.
- (c) The steel shall be painted to a length of at least 1.5 times web depth and a minimum of 1500 mm {5 ft.} on each side of the expansion joint.
- (d) Drip plates shall be provided.

C6.4.1

The following shall supplement AC6.4.1.

For additional information on the economics of steel bridges, see PP4.3.

For additional information, refer to NCHRP Report No. 314, Guidelines for the Use of Weathering Steel in Bridges.

Drip bars attached as indicated on BC-753M.

SPECIFICATIONS

- (e) The substructure units shall be protected against staining. Use special drainage details for pier and abutment tops and/or protective coating for reinforced concrete surfaces in accordance with the Publication 408.
- (f) Mechanical fasteners made of ASTM A 325 and A 490, Type 3, weathering steels and stainless steels are suitable for weathering steel bridges. Do not use zinc and cadmium galvanized carbon-steel bolts for weathering steel bridges.
- (g) Load indicator washers are not recommended.

For existing bridges, where Grade 345W {Grade 50W} unpainted steel is used, clean and paint the beam ends up to 1500 mm {5 ft.} from leaking joints, or to where the weathering steel area is exposed to or subject to salt water spray.

6.4.3 Bolts, Nuts and Washers

6.4.3.1 BOLTS

The following shall replace A6.4.3.1.
Bolts shall conform to one of the following:

- the Standard Specification for Carbon Steel Bolts and Studs, 414 MPa {60 ksi} Tensile Strength, ASTM A 307,
- the Standard Specification for Structural Bolts, Steel, Heat-Treated, 827/724 MPa {120/105 ksi} Minimum Tensile Strength with a required minimum tensile strength of 827 MPa {120 ksi} for diameters 12.7 mm through 25.4 mm {1/2 in. through 1 in.} and 724 MPa {105 ksi} for diameters 28.6 mm through 38.1 mm {1 1/8 in. through 1 1/2 in.}, AASHTO M 164 (ASTM A 325), or
- the Standard Specification for Heat-Treated Steel Structural Bolts, 1034 MPa {150 ksi} Minimum Tensile Strength, AASHTO M 253 (ASTM A 490).

AASHTO M 253 (ASTM A 490) bolts are not allowed unless approved by the Chief Bridge Engineer. Type 1 bolts should be used with steels other than weathering steel. Type 3 bolts conforming with either ASTM A 325 or ASTM A 490 shall be used with weathering steels. AASHTO M 164 (ASTM A 325), Type 1, bolts may be mechanically galvanized in accordance with AASHTO M 298 (ASTM B 695), Class 50, when approved by the Engineer. Galvanized bolts shall be tension tested

COMMENTARY

Preferably for weathering steel bridges, use mechanical fasteners made of weathering steel. When stainless steel mechanical fasteners are used with weathering steel bridges, there is a possibility of galvanic corrosion of the weathering steel. Due to the small area of the bolt in relation to the material being bolted, the effect is usually negligible.

C6.4.3.1

The following shall supplement AC6.4.3.1.
Although there are metric high-strength bolt standards for ASTM A 325M and A 490M, as of this writing, no installation specification is available for metric high-strength bolts and no domestic high-strength bolt manufacturers are producing the metric bolts. The Department decided to use soft metric conversions of standard "English" high-strength bolts (ASTM A 325 and A 490) until these problems with the metric high-strength bolts are resolved (i.e., standard "English" high-strength bolts will be the same, except they will have a metric name).

A Lehigh University study shows that AASHTO M 253 (ASTM A 490) bolts are more sensitive to the number of threads in the grip than AASHTO M 164 (ASTM A 325) bolts. The decrease in tension in AASHTO M 253 (ASTM A 490) bolts after the maximum tension is reached is much more rapid than the unloading experienced in the AASHTO M 164 (ASTM A 325) bolt assembly. Also, the AASHTO M 253 (ASTM A 490) bolts have reduced ductility compared to the AASHTO M 164 (ASTM A 325) bolt

SPECIFICATIONS

after galvanizing, as required by AASHTO M 164 (ASTM A 325).

AASHTO M 253 (ASTM A 490) bolts shall not be galvanized.

Washers, nuts and bolts of any assembly shall be galvanized by the same process. The nuts should be overtapped to the minimum amount required for the fastener assembly, and shall be lubricated with a lubricant containing a visible dye.

6.4.3.2 NUTS

The following shall replace A6.4.3.2.

Except as noted below, nuts for AASHTO M 164 (ASTM A 325) bolts shall conform to either the Standard Specification for Carbon and Alloy Steel Nuts, AASHTO M 291 (ASTM A 563), Grades DH, DH3, C, C3, and D, or the Standard Specification for Carbon and Alloy Steel Nuts for Bolts for High-Pressure and High-Temperature Service, AASHTO M 292 (ASTM A 194), Grades 2 and 2H.

Nuts for AASHTO M 253 (ASTM A 490) bolts shall conform to the requirements of AASHTO M 291 (ASTM A 563), Grades DH and DH3 or AASHTO M 292 (ASTM A 194), Grade 2H.

Nuts to be galvanized shall be heat treated, Grade DH .

The provisions of D6.4.3.1 shall apply.

Plain nuts shall have a minimum hardness of 89 HRB.

Nuts to be used with AASHTO M 164 (ASTM A 325), Type 3 bolts shall be of Grade C3 or DH3. Nuts to be used with AASHTO M 253 (ASTM A 490), Type 3, bolts shall be of Grade DH3.

6.4.3.3 WASHERS

The following shall replace A6.4.3.3.

Washers shall conform to the Standard Specification for Hardened Steel Washers, AASHTO M 293 (ASTM F 436).

The provisions of D6.4.3.1 shall apply to galvanized washers.

6.4.3.4 ALTERNATIVE FASTENERS

The following shall replace the first portion of the first sentence of A6.4.3.4.

Other fasteners or fastener assemblies, not specified heretofore, may not be used unless approved by the Chief Bridge Engineer,

6.4.3.5 LOAD INDICATOR DEVICES

The following shall supplement A6.4.3.5.

For additional requirements concerning load indicator devices, see Publication 408.

COMMENTARY

having the same length of thread in the grip. Hot-dipped galvanized bolts are not permitted due to concerns associated with the quality of the threads.

C6.4.3.2

The following shall supplement AC6.4.3.2.

Following the same logic as given in DC6.4.3.1, a soft metric conversion of standard "English" nuts (ASTM A 563 and ASTM A 194) will be used.

SPECIFICATIONS

COMMENTARY

6.4.7 Stainless Steel

The following shall be added to the last sentence of the last paragraph of A6.4.7.
 "...and approved by the Chief Bridge Engineer."

6.5 LIMIT STATES

6.5.2 Service Limit State

The following shall replace the second paragraph of A6.5.2
 Flexural members shall be investigated at the service limit state as specified in A6.10, D6.10, A6.11, D6.11, DE6.10P and DE6.11P.

C6.5.2

The following shall replace AC6.5.2
 The intent of the service limit state provisions specified for flexural members in A6.10, D6.10, A6.11, D6.11, DE6.10P and DE6.11P is primarily to prevent objectionable permanent deformations due to localized yielding that would impair rideability under expected severe traffic loadings.

6.5.3 Fatigue and Fracture Limit State

The following shall replace the third paragraph of A6.5.3
 Flexural members shall be investigated at the fatigue and fracture limit state as specified in A6.10, D6.10, A6.11, D6.11, DE6.10P and DE6.11P.

6.5.4 Strength Limit State

6.5.4.2 RESISTANCE FACTORS

Replace all references to A 325M and A 490M with A 325 and A 490, respectively.

C6.5.4.2

The following shall replace the pile resistance factors in A6.5.4.2.

The following shall supplement AC6.5.4.2.
 The basis for the resistance factors for driven steel piles is described in DC6.15.2.

- for axial resistance of piles in compression and subject to damage due to severe driving conditions where use of a pile tip is necessary..... $\phi_c = 0.35$
- for axial resistance of piles in compression under good driving conditions where use of a pile tip is not necessary..... $\phi_c = 0.45$
- for axial resistance of piles bearing on soluble bedrock
 $\phi_c = 0.25$
- for axial resistance of steel portion of concrete filled pipe piles in compression..... $\phi_c = 0.35$
- for combined axial and flexural resistance of undamaged piles:
 - axial resistance $\phi_c = 0.60$

SPECIFICATIONS

COMMENTARY

- flexural resistance..... $\phi_f = 0.85$

6.6 FATIGUE AND FRACTURE CONSIDERATIONS

6.6.1 Fatigue

6.6.1.2 LOAD-INDUCED FATIGUE

6.6.1.2.1 Application

C6.6.1.2.1

Delete the second sentence of the first paragraph of A6.6.1.2.1

Delete the first paragraph of AC6.6.1.2.1.

6.6.1.2.2 Design Criteria

The following shall replace A6.6.1.2.2.
For load-induced fatigue considerations, each detail shall satisfy:

$$\gamma PTF \Delta f \leq \Delta F_n \quad (6.6.1.2.2-1)$$

where:

γ = load factor specified in Table A3.4.1-1 for the fatigue load combination

(Δf)= the force effect, live load stress range due to the passage of the fatigue load as specified in A3.6.1.4 (MPa) {ksi}

(ΔF)_n= the nominal fatigue resistance as specified in A6.6.1.2.5 and D3.6.1.4 (MPa) {ksi}

= $\frac{1}{2}(\Delta F)_{TH}$ as specified in A6.6.1.2.5 and D3.6.1.4 for Interstate and NHS bridges

PTF= Pennsylvania Traffic Factor as given in Table 1

SPECIFICATIONS

COMMENTARY

Table 6.6.1.2.2-1 - Pennsylvania Traffic Factor for Cases I, II and III

Case	Type of Road	ADTT	PTF
I	National Highway System	---	1.2
II	Freeways, Expressways, Major Highways and Streets	> 500	1.2
III	Other Highways and Streets not included in Case I or II	---	1.0

6.6.1.2.4 Restricted Use Details

C6.6.1.2.4P

The following shall supplement A6.6.1.2.4. Details defined as Category D or E in Table A6.6.1.2.3-1 are considered unacceptable for new designs. Such details shall be excluded from new designs, except when approved by the Chief Bridge Engineer.

Girder or floorbeam flanges inserted through a slot cut in the web of an intersecting member and then welded to one or both sides of the web to provide continuity are not acceptable. Moreover, such flanges butted flush against the web of the intersecting member and then welded to it are unacceptable.

Details involving the intersection of the flange of one girder with the web of another girder are unacceptable because a significant embedded crack-like interface may remain between members after the welding. Such a defect can quickly propagate, causing premature failure.

6.6.1.2.5 Fatigue Resistance

C6.6.1.2.5

Replace all references to A 325M and A 490M with A 325 and A 490, respectively.

The following shall replace Equation A6.6.1.2.5-2.

$$N = (365) (100) n (ADTT)_{SL} \quad (6.6.1.2.5-2P)$$

The following shall replace fourth paragraph of AC6.6.1.2.5.

PennDOT's design life is considered to be 100 years. In the overall development of the LRFD Specification, the design life has been considered to be 75 years. This is the reason that the 75 in Equation A6.6.1.2.5-2 is replaced with 100 in Equation D6.6.1.2.5-2P.

6.6.1.3 DISTORTION-INDUCED FATIGUE

C6.6.1.3

The following shall replace the second paragraph of A6.6.1.3.

To control web buckling and elastic flexing of the web, the provision of A6.10.5.3, D6.10.5.3 and DE6.10.6P shall be satisfied.

The following shall supplement AC6.6.1.3.

The interaction of primary and secondary components of steel bridge structures often results in cracking at unexpected locations in relatively short periods of time. Such cracking was first observed in the webs of girder-type bridges at short gaps between transverse web attachments

SPECIFICATIONS

6.6.1.3.4P Distortion-Induced Fatigue: Unacceptable Details and Acceptable Alternative Details

Members and fasteners shall be detailed to reduce the effect of repeated variations or reversals of stress due to out-of-plane deformations or secondary forces. Examples of details which have proven to be unacceptable, based upon this criteria, are shown in Figure 1. Acceptable alternatives to these unacceptable details are shown in Figure 2. These details do not include all possible variations of distortion-sensitive details, but they are considered typical and will provide guidance.

Lateral gusset plates near transverse stiffeners or coped around transverse stiffeners shall be rigidly attached to the transverse stiffener (either bolted or welded). If this rigid attachment is not provided, the potential for localized out-of-plane distortion cracking of the web is created near the juncture of the web and transverse stiffener.

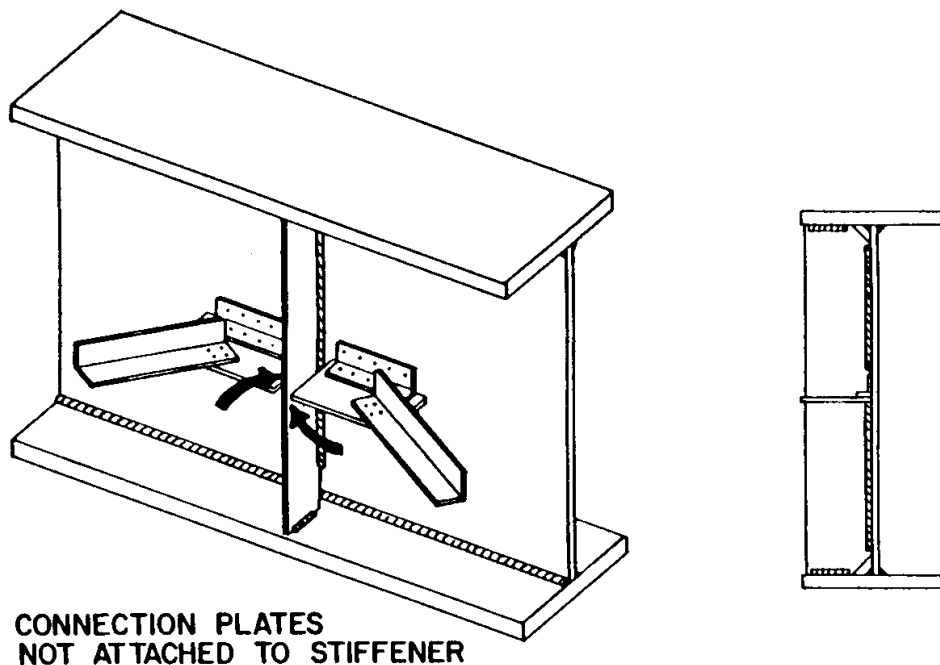
If lateral bracing is required, the preferred approach is to attach the gusset plate to the flange as shown in BD-620M and BC-754M. Welding of the gusset plate to the stiffener must be detailed to prevent intersecting walls.

COMMENTARY

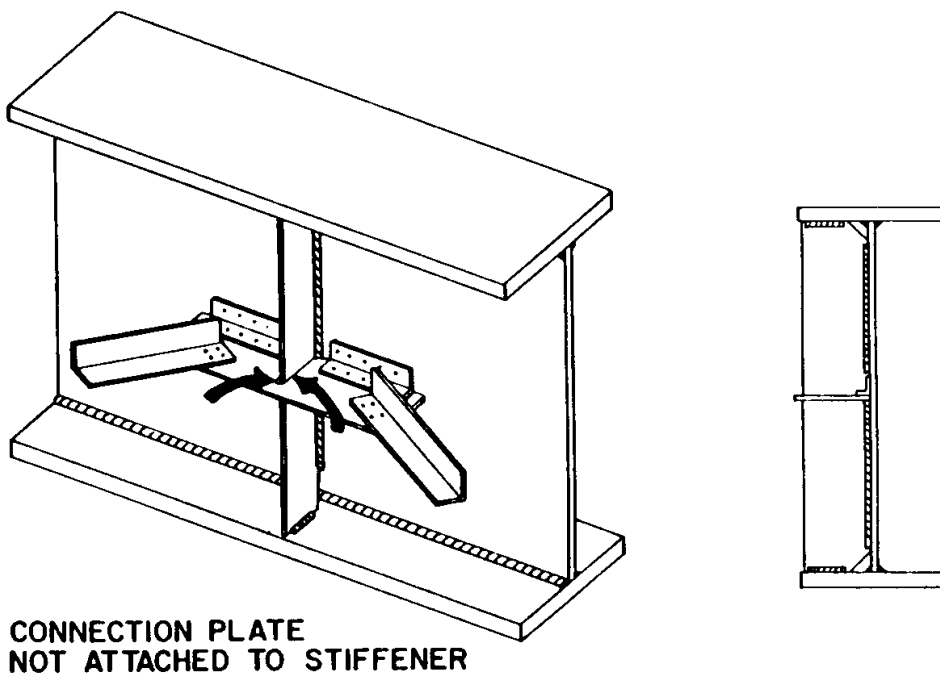
and the girder flanges. Investigations of this type of crack development suggest that the cracking is typical and is caused by out-of-plane displacements which result in large secondary web bending stresses. This is evident in the in-depth case studies presented by Mertz (1984). Fatigue crack growth resulting from displacement-induced secondary stresses is difficult to anticipate, since it involves the actual behavior of a structure, rather than the assumed behavior. The differences between the actual and the assumed behavior are most critical at very localized regions, such as at the ends of cut-short transverse connection plates. The present design idealization does not account for such localized behavior.

C6.6.1.3.4P

Rather than attempting to quantify the displacement-induced stresses and develop allowable values, it is the Department's philosophy that details susceptible to out-of-plane distortion are not acceptable. Through the design of better details, the inadequacy of the present design idealization in dealing with displacement-induced stresses is minimized. Connection plates for either diaphragms or floorbeams shall be rigidly attached to both girder flanges (either bolted or welded). Cutting the connection plate short or merely providing a tight fit to the flange is not acceptable, since the potential for localized out-of-plane distortion cracking of the web exists near the juncture of the web and flange.

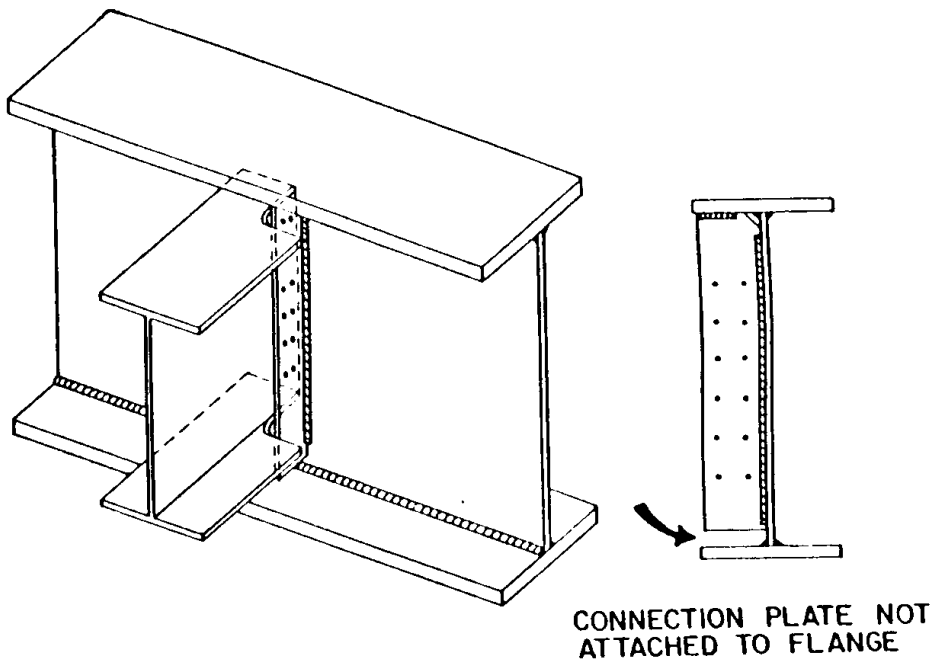


(a.) Lateral Connection Plate at Transverse Stiffener

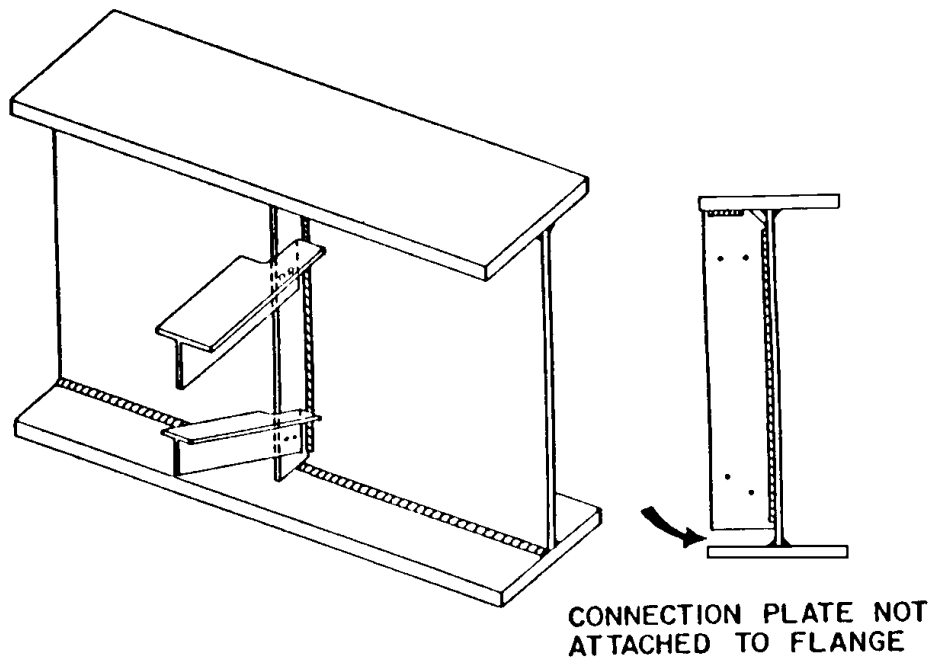


(b.) Lateral Connection Plate at Transverse Stiffener

Figure 6.6.1.3.4P-1 - Unacceptable Details

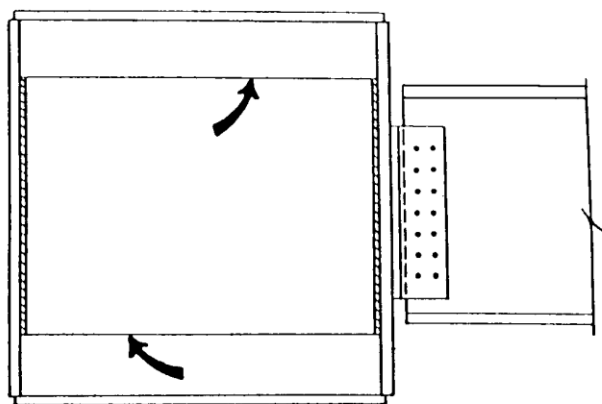


(c.) Girder-floorbeam Connection



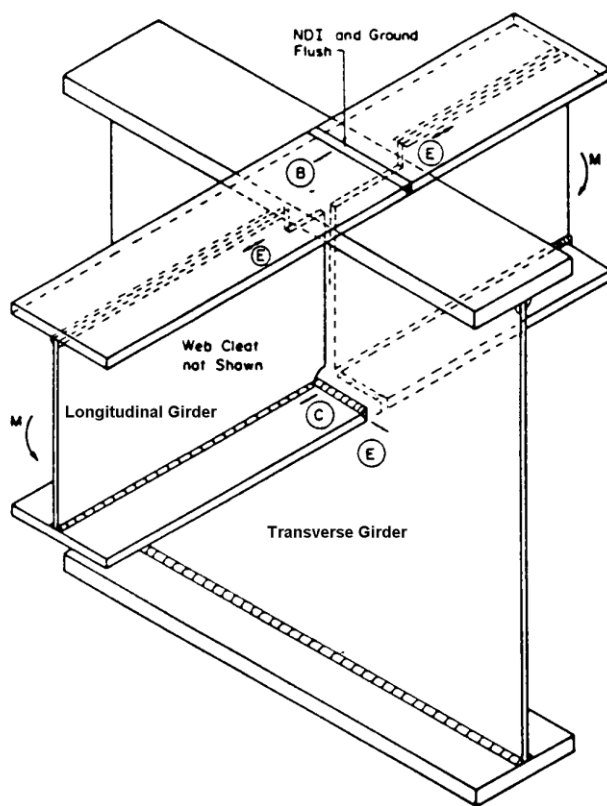
(d.) Girder-Cross - Frame Connection

Figure 6.6.1.3.4P-1 - Unacceptable Details (Continued)



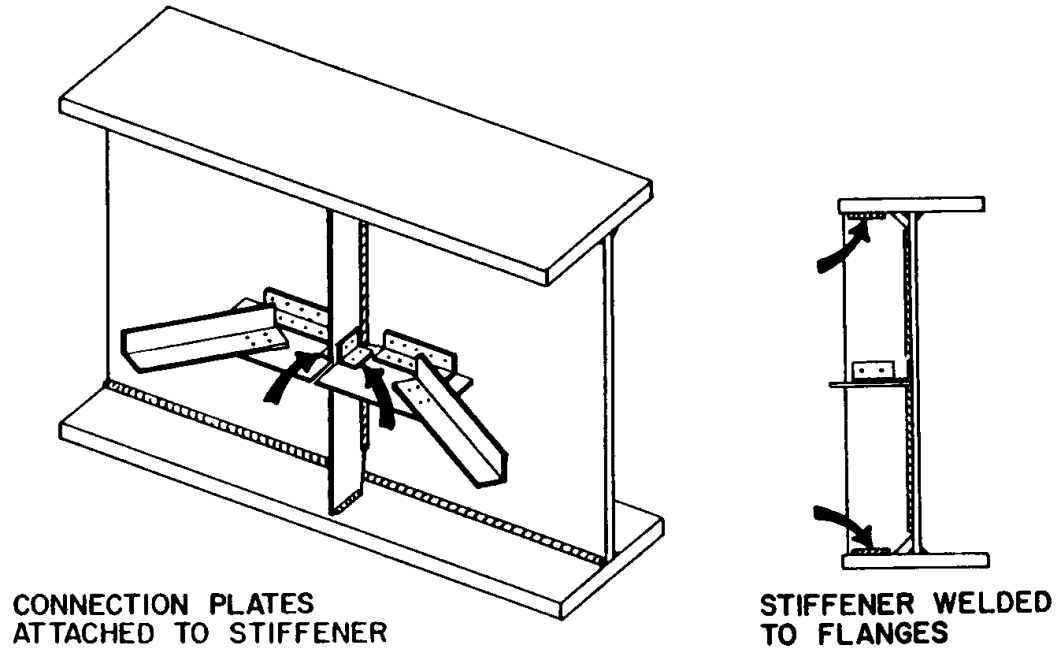
INTERNAL DIAPHRAGM NOT ATTACHED TO FLANGES

(e.) Internal Box Girder Diaphragm

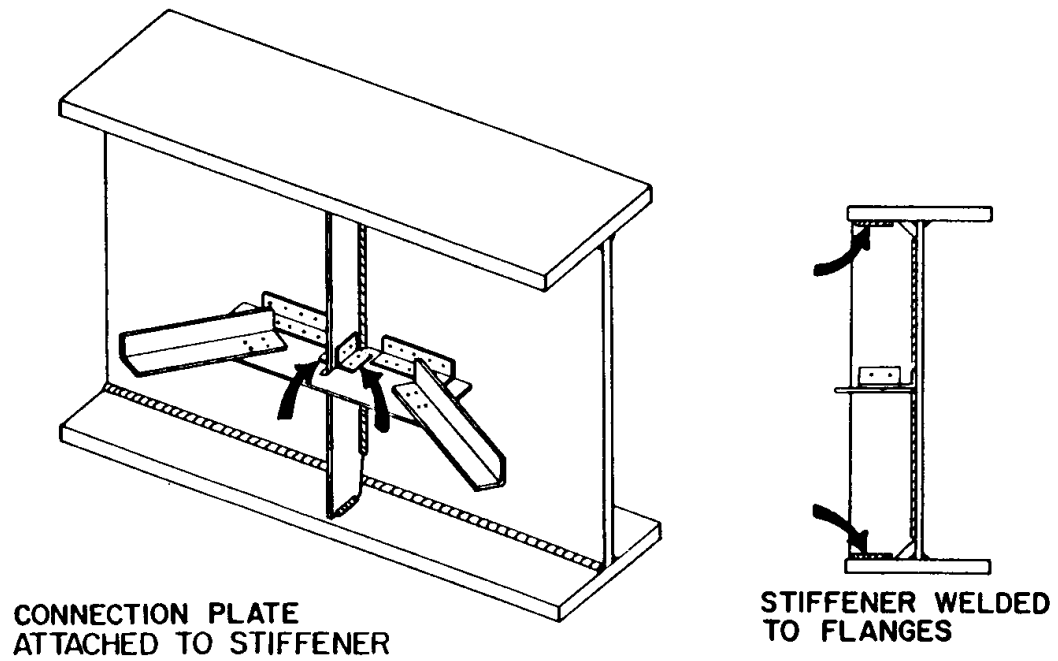


(f.) Longitudinal - to - Transverse Girder Connection

Figure 6.6.1.3.4P-1 - Unacceptable Details (Continued)

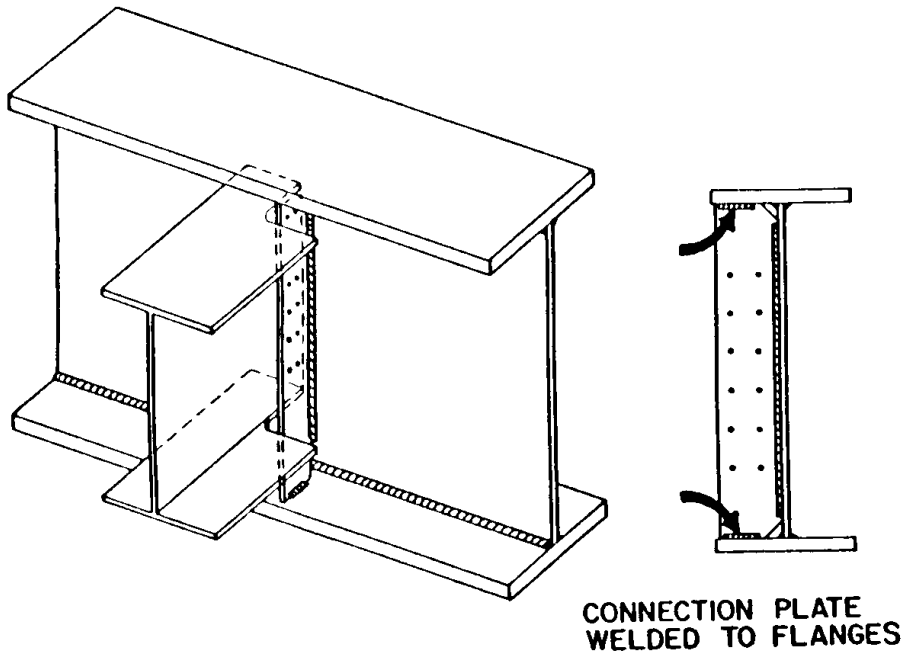


(a.) Lateral Connection Plate at Transverse Stiffener

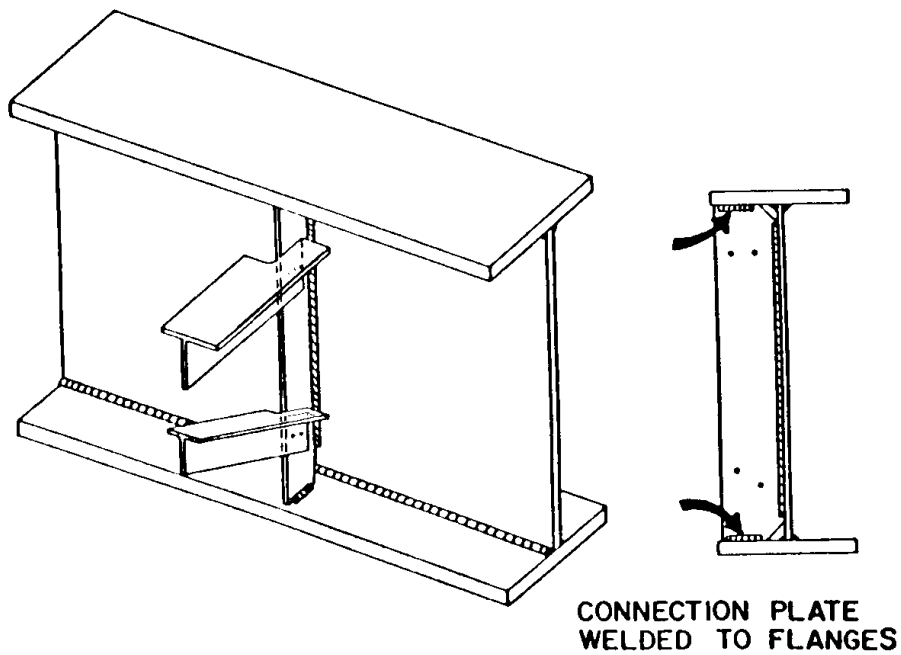


(b.) Lateral Connection Plate at Transverse Stiffener

Figure 6.6.1.3.4P-2 - Acceptable Alternatives Details

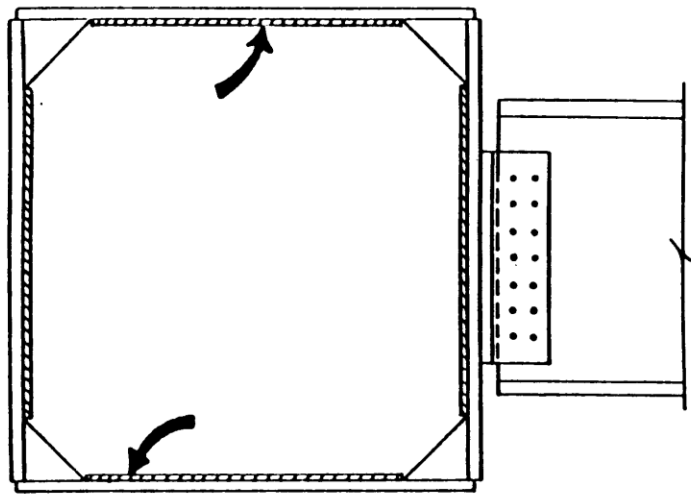


(c.) Girder Floorbeam Connection



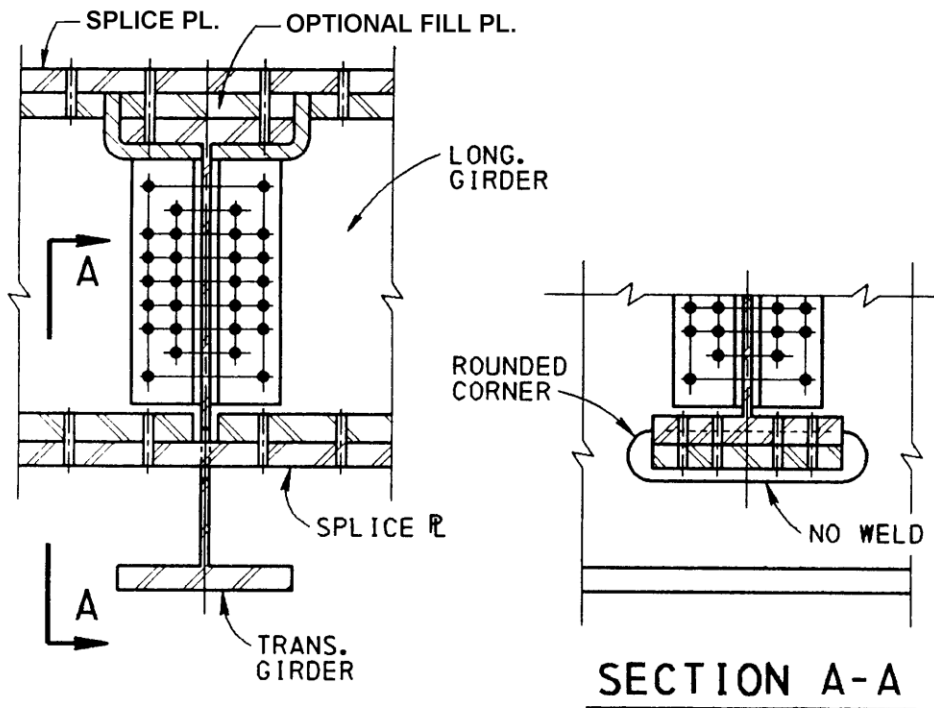
(d.) Girder - Cross-Frame Connection

Figure 6.6.1.3.4P-2 - Acceptable Alternatives Details (Continued)



**INTERNAL DIAPHRAGM
WELDED TO FLANGES**

(e.) Internal box Girder Diaphragm



(f.) Slotted Component Through Which Another Component Passes.

Figure 6.6.1.3.4P-2 - Acceptable Alternatives Details (Continued)

SPECIFICATIONS

COMMENTARY

6.6.2 Fracture

The following shall supplement A6.6.2.

Charpy V-Notch tests shall be performed as specified as per Publication 408, Section 1105.02(a)4. Diaphragms, cross-frames, bracing and connecting plates for curved girder bridges, straight girder bridges with skew less than 70°, or connections which are entirely welded and without any bolting are to be Charpy V-Notch tested. Typical shop welded, field bolted diaphragms on straight bridges do not require Charpy V-Notch testing (unless bridge skew is less than 70°). Under full dead load, beam ends and all bearing stiffeners, including bearing stiffeners at piers, are to be vertical.

6.7 GENERAL DIMENSION AND DETAIL REQUIREMENTS**6.7.2 Dead Load Camber**

C6.7.2P

The following shall supplement A6.7.2.

Camber is provided for the beams so that after all the dead loads (not including the future wearing surface) are applied, the beam is at the proper elevation. Camber is not used for the control of live load deflections.

For curved girders, the designer shall add the following note in the General Note section of the plans:

“Girder webs shall be plumb under the full dead load existing at the end of construction”

Full dead load includes the weight of pavement or overlays included in the initial construction. It does not include the future wearing surface.

6.7.2.1P CAMBER DUE TO WEIGHT OF DECK SLAB

The camber, due to the weight of deck slab, shall be determined from an analysis in which the weight of the deck slab is applied all at once.

6.7.2.2P CAMBER DETAILS FOR DESIGN DRAWINGS

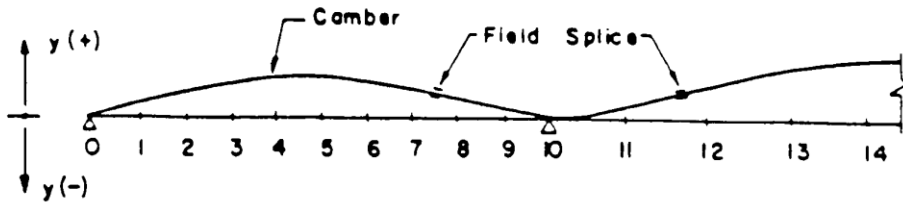
A diagram and a table of camber ordinates (see Figure 1) shall be shown on the contract plans. Ordinates shall be provided for all beams at one-tenth points and at field splice points (at dead load points of contraflexure if field splices are not provided) to account for the following:

- (a) Weight of steel
- (b) Weight of deck slab (see D6.7.2.1P)
- (c) Superimposed dead load (do not include future wearing surface)
- (d) Vertical curve
- (e) Superelevation

SPECIFICATIONS

COMMENTARY

- (f) 50% of heat curve camber (see D6.7.2.3P)
- (g) Total due to above



CAMBER ORDINATES y, MILLIMETERS (INCHES)

		POINT NO.							
Beam No.		1	2	3				Field Splice	
* Due to wt. of Steel	1								
	2								
	3								
* Due to wt. of Deck	1								
	2								
	3								
* Due to Super Load	1								
	2								
	3								
No Curve									
Total	1								
	2								
	3								

* Dead load deflection = - (Values tabulated)

Figure 6.7.2.2P-1 - Camber Details

SPECIFICATIONS

COMMENTARY

When total camber is less than the minimum that can be maintained in a beam (WF sections), no camber is required, but the following note shall be shown on the contract plans:

“Beams shall be placed with any mill camber up; the contractor shall consider and compensate for dead load deflection, due to the weight of the concrete, when forming and constructing the deck slab.”

Designers shall show theoretical dead load deflection data on plans even when no special camber is to be fabricated into the beams (i.e., when using mill camber), since this information is required by the contractor to construct the deck to the correct finished deck elevation.

The requirements for cross-section elevations at 3000 mm {10 ft.} intervals along the length of girder bridges are found in PP1.6.4.10.

6.7.2.3P HEAT-CURVE CAMBER CORRECTIONS

To compensate for possible loss of camber of heat-curved girders in service as residual stresses dissipate, the amount of camber in mm {in.}, Δ , at any section along the length of the girder shall be equal to:

$$\Delta = \frac{\Delta_{DL}}{\Delta_M} (\Delta_M + \Delta_R) \quad (6.7.2.3P-1)$$

where:

For $R < 305\,000$ mm {1,000 ft.}

Metric Units:

$$\Delta_R = \frac{0.02 L^2 F_y}{E Y_o} \left(\frac{305\,000 - R}{260\,000} \right) \quad (6.7.2.3P-2)$$

U.S. Customary Units:

$$\Delta_R = \frac{0.02 L^2 F_y}{E Y_o} \left(\frac{1,000 - R}{850} \right)$$

For $R > 305\,000$ mm {1,000 ft.}

$$\Delta_R = 0$$

R = radius of curvature of curved girder (mm) {ft.}

E = modulus of elasticity of the girder flange (MPa) {ksi}

C6.7.2.3P

Part of the heat-curve camber loss is attributable to construction loads and will occur during construction of the bridge; total heat-curve camber loss will be complete after several months of in-service loads. Therefore, a portion of the heat-curve camber increase (approximately 50%) should be included in the bridge profile. Camber losses of this nature (but generally smaller in magnitude) are also known to occur in straight beams and girders.

SPECIFICATIONS

- F_y = specified minimum yield strength of the girder flange (MPa) {ksi}
- Y_o = distance from the neutral axis to the extreme outer fiber (mm) {in.}
- L = span length for simple span; the distance between a simple end support and the dead load contraflexure point or the distance between points of dead load contraflexure points for continuous spans (mm) {in.}
- Δ_{DL} = camber at any point along L (mm) {in.}
- Δ_M = maximum value of Δ_{DL} within L (mm) {in.}

Heat-curve camber loss between dead load contraflexure points adjacent to piers is small and may be neglected.

6.7.3 Minimum Thickness of Steel

The following shall replace the first two paragraphs of A6.7.3.

Structural steel (including bracing, cross-frames, and all types of gusset plates), except for webs of certain rolled shapes, closed ribs in orthotropic decks, fillers and in railings shall not be less than 10 mm {3/8 in.} in thickness. For girders, the minimum flange plate thickness shall be 20 mm {3/4 in.} unless the fabricator can demonstrate the ability to satisfactorily fabricate and erect plate girders with thinner flange plates. For girders with longitudinal stiffeners, the minimum web thickness shall be 12 mm {1/2 in.}. The web thickness of rolled beams or channels shall not be less than 6 mm {0.23 in.}. The thickness of closed ribs in orthotropic decks shall not be less than 5 mm {3/16 in.}.

For girder flanges, bearing stiffeners and splice plates for bridges that are to be metallized, the width of the plates are to be oversized by 3 mm {1/8 in.} to account for edge grinding. The flange, bearing stiffener plates and splice plates to be shown on the plans shall be the oversized plates. For metallized bridges, the estimated quantity of fabricated structural steel shall be based on the oversized plates.

6.7.4 Diaphragms and Cross-Frames

6.7.4.1 GENERAL

The following shall supplement the first paragraph of A6.7.4.1.

The maximum spacing of cross-frames or diaphragms shall be 7600 mm {25 ft.}.

The following shall supplement A6.7.4.1.

Skew effects must be considered when designing diaphragms, especially when the skew angle is less than

COMMENTARY

C6.7.3P

This requirement of minimum web thickness for girders with longitudinal stiffeners was added to avoid web buckling and oil canning of deep girders. PennDOT has previously used 10 mm {3/8 in.} thickness resulting in web oil canning effect, specifically on I-476 over Conestoga Avenue. The New York Department of Transportation has successfully used the specified criteria.

For metallized bridges, the rolled edges of angles, channels and wide flange beams do not require edge grinding, therefore these components are not to be oversized.

C6.7.4.1

The following shall supplement AC6.7.4.1.

SPECIFICATIONS

70°. Proper consideration of unbraced length and diaphragm loads from non-uniform deflections is mandatory. Design calculations must consider the fact that cross-frames in skewed bridges connect different points of the span of adjacent girders and that these points will not deflect the same amount. Therefore, a check considering these differences must be made, and the resulting design forces must be used in the cross-frame design.

For sharply skewed bridges (typically, skews less than or equal to 60°), a cross-frame or diaphragm normal to the girder shall be located such as to minimize the effects of differential deflections, while satisfying the minimum cross-frame or diaphragm spacing requirement.

For additional analysis criteria for bridges with skew angles less than 70°, see D4.6.2.2.1.

Diaphragm and cross-frame members in horizontally curved bridges shall be considered primary members.

Diaphragm members in horizontally curved and skewed bridges may be used at support locations.

When support lines are skewed less than 70 degrees, intermediate diaphragms or cross-frames shall be placed normal to the girders in contiguous or discontinuous lines. When cross frames and diaphragms are normal to web near skewed supports, adequate girder restraint shall be provided.

6.7.4.2 I-SECTION MEMBERS

COMMENTARY

In locating intermediate cross-frames or diaphragms in sharply skewed bridges, the designer must consider distinct issues associated with each girder connected by the cross-frame or diaphragm. A cross-frame or diaphragm close to the bearing on one girder line may introduce forces into the system (cross-frame or diaphragm and girder flange) due to “nuisance stiffness,” where the deflection of one girder line cannot match the adjacent girder line. In these cases, elimination of a cross-frame or diaphragm is advisable. In addition, the initial cross-frame or diaphragm must be located such that the maximum permitted spacing is not exceeded in the adjacent connected girder. In some cases, the first interior line of cross-frames or diaphragms may not be full width across the superstructure, and the number of bays along a girder length may not be constant for each girder in the superstructure.

Bracing of horizontally curved members is more critical than for straight members. Diaphragm and cross-frame members resist forces that are critical to the proper functioning of curved-girder bridges. Since they transmit the forces necessary to provide equilibrium, they are considered primary members. Therefore, forces in the bracing members must be computed and considered in the design of these members. When the girders have been analyzed neglecting the effects of curvature according to the provisions of A4.6.1.2.4, the diaphragms or cross-frames may be analyzed by the V-load method (United States Steel 1984) or other rational means.

Solid plate diaphragms can be used at support locations in horizontally curved and skewed bridges. Replacing cross frames with solid plate diaphragms at abutment and pier locations has been shown to not adversely affect or appreciably benefit deformations during construction. For other intermediate locations along the bridge spans, diaphragms may cause higher stresses and deformations in the bridge structures during construction when compared to the use of cross frames.

Placement of cross frames parallel to the skew has been shown to induce significant localized lateral bending near support locations (AASHTO Subcommittee on Bridges & Structures, 2010).

C6.7.4.2P

SPECIFICATIONS

The article heading is changed from: Straight I-Sections.

The following shall supplement the first paragraph of A6.7.4.2

Cross frames and steel girders in curved and skewed bridges should both be detailed so that the webs are plumb under a specified loading condition.

Cross-frame members in horizontally curved bridges should contain diagonals and top and bottom chords.

The following shall replace the last two sentences of second paragraph of A6.7.4.2.

When the supports are skewed less than 70°, intermediate cross-frames shall be normal to the main members. If the supports are skewed, end cross-frames need not be co-linear with the line of bearings, see Standard Drawing BC-754M. For additional skewed cross-frame requirements, see D6.7.4.1.

The following shall supplement A6.7.4.2

The spacing, L_b , of intermediate diaphragms or cross-frames in horizontally curved I-girder bridges shall not exceed the following in the erected condition:

$$L_b \leq L_r \leq R/10 \quad (6.7.4.2-1)$$

where:

L_r = limiting unbraced length determined from Eq. A6.10.8.2.3-5 (mm) {ft.}

R = minimum girder radius within the panel (mm) {ft.}

In no case shall L_b exceed 7500 mm {25 ft}.

6.7.4.3 BOX SECTION MEMBERS

The article heading is changed from: Straight Box Sections.

The following shall replace the last two paragraphs of A6.7.4.3.

Intermediate internal diaphragms or cross-frames shall be provided. For all single box sections, horizontally curved sections, and multiple box sections in cross-sections of bridges not satisfying the requirements of A6.11.2.3 or with box flanges that are not fully effective according to the

COMMENTARY

End cross-frames must be parallel to centerline of bearings, but need not coincide with bearing line.

In curved and skewed bridges, cross-frame stresses can increase appreciably as a result of the locked-in stresses caused by inconsistent detailing. This increase may be more pronounced in bridges with larger cross frame spacings and also for cross frames near the bridge supports. For skewed bridges with skew angles between 90° and 70°, develop shop drawings which detail all webs plumb when girders are erected and diaphragms connected. For curved bridges and skewed bridges with skew angles less than 70°, develop shop drawings and erection procedures which detail all webs plumb after the full dead load (self weight of all structural and non-structural components, not including weight of the future wearing surface) is applied. See PennDOT Bridge Construction Standard BC-754, "Steel Diaphragms."

C6.7.4.3

The following shall replace the first sentence of the fourth paragraph of A6.7.4.3

For all horizontally curved box girder bridges, single box sections, and for box sections in bridges not satisfying the requirements of A6.11.2.3 or with box flanges that are not fully effective, cross-sectional distortion stresses are best controlled by the introduction of internal cross-frames or diaphragms.

SPECIFICATIONS**COMMENTARY**

provisions of A6.11.1.1 and D6.11.1.1 for curved bridges or DE6.11.1.1P for straight bridges, the internal bracing shall be spaced to control cross-section distortion, with the spacing not to exceed 7500 mm {25 ft}.

For all single box sections, horizontally curved sections, and multiple box sections in bridges not satisfying the requirements of A6.11.2.3 or with box flanges that are not fully effective according to the provisions of A6.11.1.1 and D6.11.1.1 for curved bridges or DE6.11.1.1P for straight bridges, the need for a bottom transverse member within the internal bracing shall be considered. Where provided, the transverse member shall be attached to the box flange unless longitudinal flange stiffeners are used, in which case the transverse member shall be attached to the longitudinal stiffeners by bolting. The cross-sectional area and stiffness of the top and bottom internal bracing members shall also not be less than the area and stiffness of the diagonal members.

SPECIFICATIONS

COMMENTARY

6.7.5 Lateral Bracing

6.7.5.2 I-SECTION MEMBERS

The article heading is changed from: Straight I-Sections.

6.7.5.3 TUB SECTION MEMBERS

The article title is changed from: Straight Tub Sections.

The following shall supplement the first paragraph of A6.7.5.3.

For horizontally curved girders, a full-length lateral bracing system shall be provided.

C6.7.5.2

The following shall supplement AC6.7.5.2.

Wherever possible, horizontal lateral bracing in or near the plane of the bottom flange should be eliminated from bridges, and the girders should be designed to carry the wind load between diaphragms according to A4.6.2.7.1.

Horizontal lateral bracing is relatively expensive because of the detail associated with it. Furthermore, there are often forces associated with horizontal lateral bracing which can result in distortion-induced fatigue; these forces are also a significant factor on steel bridges. Therefore, horizontal lateral bracing should not be considered for the improvement of redundancy.

When horizontal lateral bracing is required, it should be attached to the bottom flange wherever practical. (BD-620M permits attachment to the top flange.)

For horizontally curved bridges, when the curvature is sharp and temporary supports are not practical, it may be desirable to consider providing both top and bottom lateral bracing to ensure pseudo-box action while the bridge is under construction. Top and bottom lateral bracing provides stability to a pair of I-girders.

C6.7.5.3

The following shall replace the last sentence of the third paragraph of A6.7.5.3.

For both straight and horizontally curved tub sections, a full-length lateral bracing system forms a pseudo-box to help limit distortions brought about by temperature changes occurring prior to concrete deck placement, and to resist the torsion and twist caused by any eccentric loads acting on the

SPECIFICATIONS

COMMENTARY

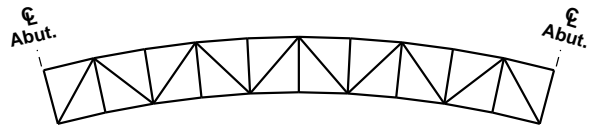


Figure C6.7.5.3-1 Warren-Type Single-Diagonal Top Lateral Bracing System for Tub Section Member: Plan View.

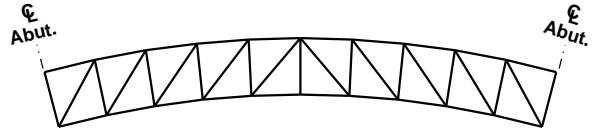


Figure C6.7.5.3-2 Pratt-Type Single-Diagonal Top Lateral Bracing System for Tub Section Member: Plan View.

Where the forces in the bracing members are not available from a refined analysis, the shear flow across the top of the pseudo-box section can be computed from Eq. C6.11.1.1-1 assuming the top lateral bracing acts as an equivalent plate. The resulting shear can then be computed by multiplying the resulting shear flow by the width w , and the shear can then be resolved into the diagonal bracing member(s). Should it become necessary for any reason to compute the St. Venant torsional stiffness of the pseudo-box section according to Eq. AC6.7.4.3-1, formulas are available (Kollbrunner and Basler 1966; Dabrowski 1968) to calculate the thickness of the equivalent plate for different possible configurations of top lateral bracing.

6.8 TENSION MEMBERS

6.8.2 Tensile Resistance

6.8.2.2 REDUCTION FACTOR, U

The following shall replace the first paragraph of A6.8.2.2. The reduction factors, specified in A6.8.2.2, shall be used to account for shear lag. Reduction factors developed from refined analysis or tests may be used if approved by the Chief Bridge Engineer.

6.8.2.3 COMBINED TENSION AND FLEXURE

The following shall replace the definition of M_{rx} in A6.8.2.3.

M_{rx} = factored flexural resistance about the x-axis taken as ϕ_f times the nominal flexural resistance about the x-axis determined as specified in DE6.10P, DE6.11P or A6.12, as applicable (N-mm) {kip-in.}

SPECIFICATIONS

6.8.3 Net Area

The following shall replace the first paragraph of A6.8.3. The net area, A_n , of an element is the product of the thickness of the element and its smallest net width. The net area, A_n , of a member is the sum of the net areas of each element. The width deducted for all holes; standard, oversized, and slotted; shall be taken as 1.6 mm {1/16 in.} greater than the hole size specified in D6.13.2.4.2. The net width shall be determined for each chain of holes extending across the member or element along any transverse, diagonal, or zigzag line.

6.9 COMPRESSION MEMBERS**6.9.2 Compressive Resistance****6.9.2.2 COMBINED AXIAL COMPRESSION AND FLEXURE**

The following shall replace the definition of M_{rx} in A6.8.2.3.

M_{rx} = factored flexural resistance about the x-axis taken equal to ϕ_f times the nominal flexural resistance about the x-axis determined as specified in DE6.10P, DE6.11P or A6.12, as applicable (N-mm) {kip-in.}

6.9.5 Composite Members**6.9.5.1 Nominal Compressive Resistance**

The following shall replace the definition of n in A6.9.5.1.

n = modular ratio of the concrete as specified in D5.4.2.1

6.10 I-SECTIONS IN FLEXURE**6.10.0P Applicable Provisions**

The provisions of D6.10 apply to steel I-girders curved in plan. The provisions of Appendix E apply to straight girder bridges.

Where Straight girders are referred to in A6.10 and D6.10, this reference should be ignored.

COMMENTARY

C6.8.3

Delete the first paragraph of AC6.8.3.

C6.10**C6.10.0P**

The provisions of D6.10 are based on the 2004 Third Edition of AASHTO-LRFD specifications as amended herein to account for the curved girder provisions that were incorporated in AASHTO LRFD by the 2005 interim specifications. The provisions of Appendix E are based on the 1998 Second Edition of the AASHTO-LRFD Design specifications with the 1999 through 2003 Interims. Using the earlier specifications for straight girder bridges will

SPECIFICATIONS

6.10.1 General

The following shall replace the first sentence in A6.10.1. The provisions of this article apply to flexure of rolled or fabricated kinked (chorded) continuous or horizontally curved steel I-section members symmetrical about the vertical axis in the plane of the web.

The following shall supplement A6.10.1.
Open-framed systems are those which have no horizontal lateral bracing in or near the plane of the bottom flange. Lateral bracing, when used, is provided to resist wind loads, but it is generally not needed since the girders can be

COMMENTARY

allow continuing using the existing STLRFD computer program, which is based on the Second Edition of AASHTO LRFD with modifications, with relatively few revisions. It is the intent of the Department to update the STLRFD computer program to correspond to the 2004 AASHTO-LRFD, including A6.10 and A6.11, at some point in the future. At which time, both straight and curved girders will be designed using the provisions of the 2004 Third Edition of the Specifications as amended by Design Manual Part 4. Any reference to straight girder bridges in D6.10 is meant to be used in the future when the Design Manual Part 4 and computer programs are fully updated to the third edition of the AASHTO-LRFD specifications.

C6.10.1

The following shall replace the first paragraph of AC6.10.1. This article addresses general topics that apply to all types of steel I-sections in horizontally curved bridges, or bridges containing both straight and curved segments. For the application of the provisions of A6.10 and D6.10, bridges containing both straight and curved segments are to be treated as horizontally curved bridges since the effects of curvature on the support reactions and girder deflections, as well as the effects of flange lateral bending, usually extend beyond the curved segments. Note that kinked (chorded) girders exhibit the same actions as curved girders, except that the effect of the noncollinearity of the flanges is concentrated at the kinks. Continuous kinked (chorded) girders should be treated as horizontally curved girders with respect to these Specifications.

The following shall supplement AC6.10.1.
For horizontally curved bridges, in addition to the potential sources of flange lateral bending discussed in the preceding paragraph, flange lateral bending effects due to curvature must always be considered at all limit states and also during construction.

Delete the reference to Appendix B from the first sentence of the second Paragraph of AC6.10.1.

The following shall replace the second sentence of the second paragraph of A6.10.1.

For the majority of straight non-skewed bridges, flange lateral bending effects tend to be most significant during construction and tend to be insignificant in the final constructed condition. Significant flange lateral bending may be caused by wind, by torsion from eccentric concrete deck overhang loads acting on cantilever forming brackets placed along exterior girders, and by the use of staggered cross-frames in conjunction with skew angles less than 70°.

The application of open-framed system distribution factors for closed-framed systems is generally conservative.

SPECIFICATIONS

designed to carry wind loads between the diaphragms. If horizontal lateral bracing is included, the open-framed system distribution factors shall be used. If a horizontal lateral bracing system is used, the connections must be detailed to ensure that the fatigue life of the bracing system is at least that of the girder.

Although the lateral wind bracing may not be required for the final constructed condition, the need for lateral wind bracing during construction shall be investigated.

6.10.1.1.1 Stresses

The following shall supplement A6.10.1.1.1
If concrete with expansive characteristics (except shrinkage-compensating concrete, which the Department is studying and may eventually exclude from this provision) is used, composite design shall be used with caution, and provision must be made in the design to accommodate the expansion. Composite section properties (see D6.10.3.1.1b) shall be assumed in the positive and negative moment regions for the calculation of design moments, shears and deflections.

6.10.1.1.1a Sequence of Loading

The following shall replace last paragraph of A6.10.1.1.1a
For unshored construction, permanent load applied before the concrete deck has attained 75% of its compressive strength shall be assumed carried by the steel section alone; permanent load and live load applied after this stage shall be assumed carried by the composite section. For shored construction, all permanent loads shall be assumed applied after the concrete deck has hardened or has been made composite and the contract documents shall so indicate. Use of shored systems requires the prior approval of the Chief Bridge Engineer.
For continuous spans, the final dead load moment at each design section shall be taken as the greater of either the dead load moment considering the weight of the concrete deck to be instantaneously applied or a moment based upon an incremental analysis of the specified slab placement sequence. Similarly, stresses should be computed based on the more critical of the incremental and instantaneously applied loads.

6.10.1.1.1b Stresses for Sections in Positive Flexure

Delete Equation A6.10.1.1.1b-1

COMMENTARY

If horizontal lateral bracing system is used, a rational analysis may consider a reduction in lateral live load distribution factor due to the quasi-box action of the closed-frame system.

Any reduction in live load distribution factor must be approved by the Chief Bridge Engineer.

The design procedure for evaluating the need for lateral bracing during construction shall be per BD-620M. As agreed upon by the APC Subcommittee for Steel Bridge Superstructures, the contractor is responsible for stability of the girders during erection, including providing wind bracing during erection as needed. This responsibility includes the analysis, design, material, fabrication and installation (and removal) of wind bracing during erection at no cost to the Department.

C6.10.1.1.1P

If the concrete is expansive, estimate expansion and properly design concrete to flange connection by adding additional shear studs.

C6.10.1.1.1a

Delete the first paragraph of AC6.10.1.1.1

C6.10.1.1.1b

The following shall replace AC6.10.1.1.1b

SPECIFICATIONS

The following shall supplement A6.10.1.1.1b:
For normal and low density concrete, the modular ratio is given in D5.4.2.1.

6.10.1.1.1c Stresses for Sections in Negative Flexure

The following shall replace A6.10.1.1.1c
For calculating flexural stresses in sections subjected to negative flexure, the composite section for both short-term and long-term moments shall consist of the steel section and the longitudinal reinforcement within the effective width of the concrete deck.

Cut-off points for the main reinforcement in cast-in-place decks over interior supports for continuity may be staggered as required by design.

Concrete on the tension side of the neutral axis shall not be considered in calculating resisting moments.

6.10.1.1.1d Concrete Deck Stresses

The following shall replace A6.10.1.1.1d
For calculating longitudinal flexural stresses in the concrete deck due to transient loads, the short-term modular ratio, n , shall be used. For calculating longitudinal flexural stresses in the concrete deck due to permanent loads, the long-term modular ratio, $3n$, shall be used.

6.10.1.1.1.fP Lateral Support of Top Flanges Supporting Timber Decks

The compression flanges of girders supporting timber floors shall not be considered to be laterally supported by the flooring, unless the floor and fastenings are specially designed to provide such support. Laminated timber decks shall be provided with steel clips designed to furnish adequate lateral support to the top flange.

6.10.1.2 NONCOMPOSITE SECTIONS

The following shall supplement A6.10.1.2
Whenever technically feasible, all structures shall be made composite.

COMMENTARY

It is preferable to proportion composite sections in simple spans and the positive moment regions of continuous spans so that the neutral axis lies below the top surface of the steel beam.

C6.10.1.1.1d

Delete AC6.10.1.1.1d

SPECIFICATIONS

COMMENTARY

6.10.1.3 HYBRID SECTIONS

The following shall supplement A6.10.1.3.
The use of girders with web yield strength higher than the flange yield strength requires the prior approval of the Chief Bridge Engineer.

6.10.1.4 VARIABLE WEB DEPTH MEMBERS

The following shall supplement A6.10.1.4.
The use of girders with variable web depth requires the prior approval of the Chief Bridge Engineer.

6.10.1.5 STIFFNESS

The following shall supplement A6.10.1.5
In the computation of flexural stiffness and flexural resistance of beams, the haunch shall be taken as zero. However, in the computation of dead load, the haunch shall be taken into account.

C6.10.1.5

The following shall supplement AC6.10.1.5
Field measured haunch depths may be used in the computation for flexural stiffness and resistance when rating existing bridges.
The following shall replace the second paragraph of AC6.10.1.5.
Field tests of composite continuous bridges have shown that there is considerable composite action in negative bending regions (Baldwin et al. 1978; Roeder and Eltvik 1985; Yen et al. 1995). Therefore, the stiffness of the full composite section is to be used over the entire bridge length for the analysis of composite flexural members, but not for stress calculations.
Other stiffness approximations which are based on sound engineering principles may be used if approved by the Chief Bridge Engineer.

6.10.1.6 FLANGE STRESSES AND MEMBER BENDING MOMENT

The following shall replace the fourth paragraph of A6.10.1.6 to the end of the article.
Lateral bending stresses in continuously braced flanges shall be taken equal to zero. Lateral bending stresses in discretely braced flanges shall be determined by structural analysis.
All discretely braced flanges shall satisfy:

$$\underline{f_{\ell} \leq 0.6F_{yf}} \quad (6.10.1.6-1)$$

The flange lateral bending stress, f_{ℓ} , may be determined directly from first-order elastic analysis in discretely braced compression flanges for which:

$$L_b \leq 1.2L_p \sqrt{\frac{C_b R_b}{f_{bu} / F_{yc}}} \quad (6.10.1.6-2)$$

C6.10.1.6

The following shall supplement the fourth paragraph of AC6.10.1.6
The determination of flange lateral bending moments due to curvature is addressed in A4.6.1.2.4b.
In all resistance equations, f_{bu} , M_u and f_{ℓ} are to be taken as positive in sign. However, for service and strength limit state checks at locations where the dead and live load contributions to f_{bu} , M_u or f_{ℓ} are of opposite sign, the signs of each contribution must be initially taken into account. In such cases, for both dead and live load, the appropriate net sum of the major-axis and lateral bending actions due to the factored loads must be computed, taking the signs into consideration, that will result in the most critical response for the limit state under consideration.

SPECIFICATIONS

COMMENTARY

or equivalently:

$$L_b \leq 1.2L_p \sqrt{\frac{C_b R_b}{M_u / M_{yc}}} \quad (6.10.1.6-3)$$

where:

C_b = moment gradient modifier specified in A6.10.8.2.3, D6.10.8.2.3 or Appendix A Article A6.3.3, as applicable.

f_{bu} = largest value of the compressive stress throughout the unbraced length in the flange under consideration, calculated without consideration of flange lateral bending (MPa) {ksi}

L_b = unbraced length (mm) {in.}

L_p = limiting unbraced length specified in A6.10.8.2.3 and D6.10.8.2.3 (mm) {in.}

M_u = largest value of the major-axis bending moment throughout the unbraced length causing compression in the flange under consideration (N-mm) {kip-in.}

M_{yc} = yield moment with respect to the compression flange determined as specified in AD6.2 (N-mm) {kip-in.}

R_b = web load-shedding factor determined as specified in A6.10.1.10.2

If Eq. 2, or Eq. 3 as applicable, is not satisfied, second-order elastic compression-flange lateral bending stresses shall be determined.

Second-order compression-flange lateral bending stresses may be determined by amplifying first-order values as follows:

$$f_\ell = \left(\frac{0.85}{1 - \frac{f_{bu}}{F_{cr}}} \right) f_{\ell 1} \geq f_{\ell 1} \quad (6.10.1.6-4)$$

or equivalently:

$$f_\ell = \left(\frac{0.85}{1 - \frac{M_u}{F_{cr} S_{xc}}} \right) f_{\ell 1} \geq f_{\ell 1} \quad (6.10.1.6-5)$$

SPECIFICATIONS

COMMENTARY

where:

f_{bu} = largest value of the compressive stress throughout the unbraced length in the flange under consideration, calculated without consideration of flange lateral bending (MPa) {ksi}

f_{l1} = first-order compression-flange lateral bending stress at the section under consideration, or the maximum first-order lateral bending stress in the compression flange under consideration throughout the unbraced length, as applicable (MPa) {ksi}

F_{cr} = elastic lateral torsional buckling stress for the flange under consideration determined from Eq. 6.10.8.2.3-8 or Eq. AA6.3.3-8. Eq. AA6.3.3-8 may only be applied for unbraced lengths in straight I-girder bridges in which the web is compact or noncompact.

M_{u} = largest value of the major-axis bending moment throughout the unbraced length causing compression in the flange under consideration (N-mm) {kip-in.}

S_{xc} = elastic section modulus about the major axis of the section to the compression flange taken as M_{yc}/F_{yc} (mm^3) {in.³}

6.10.1.7 MINIMUM NEGATIVE FLEXURE CONCRETE DECK REINFORCEMENT

C6.10.1.7

The following shall replace the first paragraph of A6.10.1.7 In negative flexure regions of any continuous span, the total cross-sectional area of the longitudinal reinforcement shall not be less than 1 percent of the total cross-sectional area of the slab. The reinforcement used to satisfy this requirement shall have a specified minimum yield strength not less than 420 MPa {60 ksi} and a size not exceeding No. 19 bars {No. 6}.

The required reinforcement shall be placed in two layers uniformly distributed across the slab width, and two-thirds shall be placed in the top layer. The individual bars shall be spaced at intervals not exceeding 300 mm {12 in} within each row.

Shear connectors shall be provided along the entire length of the girder to develop stresses on the plane joining the concrete and steel in accordance with A6.10.10 and D6.10.10.

Delete the second paragraph and last paragraph of A6.10.1.7 The following shall replace the last sentence in the paragraph before last in CA6.10.1.7. The above applies for members that are designed by the provisions of Article A6.10, Article D6.10 or Appendix A.

SPECIFICATIONS

COMMENTARY

6.10.1.11P LATERAL SUPPORT OF TOP FLANGES SUPPORTING TIMBER DECKS

The compression flanges of girders supporting timber floors shall not be considered to be laterally supported by the flooring, unless the floor and fastenings are specially designed to provide such support. Laminated timber decks shall be provided with steel clips designed to furnish adequate lateral support to the top flange.

6.10.3 Constructibility

6.10.3.2 FLEXURE

6.10.3.2.1 Discretely Braced Flanges in Compression

The following shall replace the definition of F_{nc} following Equation A6.10.3.2.1-3.

F_{nc} = nominal flexural resistance of the flange (MPa). F_{nc} shall be determined as specified in A6.10.8.2 and D6.10.8.2.. In computing F_{nc} for constructibility, the web load-shedding factor, R_b , shall be taken as 1.0.

6.10.3.2.5.1P Slab Placement

An analysis shall be performed to determine an acceptable slab placement sequence. The analysis shall address (but is not limited to) the following items:

- (a) Change in the stiffness in the girder as different segments of the slab are placed and as it affects both the temporary stresses and the potential for "locked-in" erection stresses
- (b) Bracing (or lack thereof) of the compression flange of girders and its effect on the stability and strength of the girder
- (c) Stability and strength of the girder through slab placement
- (d) Bracing of overhang deck forms
- (e) Uplift at bearings
- (f) *Temperature changes as prescribed in 3.12.2.1.1.*

The analysis of slab placement shall be done in an incremental fashion using a concrete modulus of elasticity

C6.10.3.2.1

The following shall supplement the fourth paragraph of AC6.10.3.2.1.

For horizontally curved bridges, flange lateral bending effects due to curvature must always be considered in discretely braced flanges during construction.

Delete the eighth paragraph of AC6.10.3.2.1.

C6.10.3.2.5.1P

During the mid-1980's, several of the Department's girder bridges experienced problems during placement of the slab. It is believed that bridges with highly unsymmetrical, deep steel girders combined with wide beam spacing and large overhang dimensions are more susceptible to problems during construction than are the typical earlier steel girder bridges which use more nearly symmetrical steel girders combined with closer beam spacing and smaller overhang dimensions. Since significant reduction in the construction cost of a bridge can be achieved by use of highly unsymmetrical, deep steel girders in conjunction with wide beam spacing and large overhang dimensions, an analysis must be performed to ensure that these types of girders provide adequate stability and strength through slab placement.

With skewed, curved, and/or continuous steel girder bridges, temporary uplift conditions at bearings can occur during the deck pour. Designers should evaluate the potential for uplift in bearings as part of the deck pour sequence evaluation. Designers should address temporary uplift conditions as follows:

- Where the temporary uplift is not detrimental to the

SPECIFICATIONS

equal to 70% of the concrete modulus elasticity at 28 days for concrete which is at least 24 hours old, assuming no retarder admixture is permitted. If retarder admixture is specified, it shall be indicated on the contract drawings, and the analysis shall be completed assuming 48 hours before gaining stiffness for lateral resistance. This means the stiffness of the model will change at the many different stages.

In no case shall the final design moment stresses or forces be less than those determined from an analysis in which the weight of the deck slab is applied all at once.

Slab concrete, which is less than 24 hours old (or 48 hours old when retarder is used), cannot be considered to provide lateral support for the embedded top flange of the girder. Conversely, slab concrete which is more than 24 hours old (or 48 hours old when retarder is used) can be considered to provide full lateral support for the embedded top flange of the girder. If the contractor can demonstrate that the concrete will provide lateral support for the embedded top flange in less than 24 hours (or 48 hours old when retarder is used), that limiting time may be used with the approval of the Chief Bridge Engineer.

From the results of the analysis of slab placement and lateral support conditions described above, the bending and shear strength of girder shall be checked.

6.10.3.2.5.2P Deck Slab Overhang Form Support

For the erection condition with the overhang form support system, the strength and stability of the fascia girder shall be ensured by applying the dead load of the overhang concrete and any construction equipment to the girder as follows:

- (a) The standard form support system, shown in Figure 1, may be used where:
 - (1) Girder web depth is less than 2400 mm {8'-0"}
 - (2) Deck slab overhang is less than 1400 mm {4'-9"}
 - (3) Slab thickness is equal to or less than 250 mm {10 in.}

COMMENTARY

long-term performance of the bearing, or does not result in adverse stability conditions, temporary uplift is permitted. In this case, the designer should identify in the construction plans the individual bearing locations where uplift is expected and during what stages of the deck pour the uplift will occur. A note stating that the uplift is temporary and permitted as part of construction should also be provided in the construction plans.

- Where uplift is determined to be unacceptable for individual bearing types or structure stability, the designer should identify in the construction plans the individual bearing locations where uplift is expected. Hold down forces and any other design requirements for restraining devices should be shown in the plans for the contractor's use in designing these components. Forces and design requirements for individual deck pour stages, as applicable, should be provided. The designer should verify the viability of at least one type of restraining device to meet the design requirements and provide schematic details of the device in the construction plans.

The effects from temperature change on the curved and skewed bridges are mostly functions of the girder support conditions. When minimum required restraint necessary for girder(s) global stability (i.e., prevention of global buckling of the girder or collection of girders) is provided, the applied temperature change may not have an appreciable impact on overall bridge deflections and stresses.

C6.10.3.2.5.2P

The requirements of this article can be met by reducing the length of some deck pours, or by increasing the size of the steel girder section, or by a combination of both. For original designs, the designer should obtain input from contractor and fabricators about the economics of those alternatives. Note, also, that only a relatively short length of the critical spans will be affected by the constructibility criterion.

The intent of the required checks is to control the buckling of the flanges and the webs of steel girders. It is felt that there is a potential for fatigue cracking if steel plates are allowed to buckle due to "oil-canning" effects.

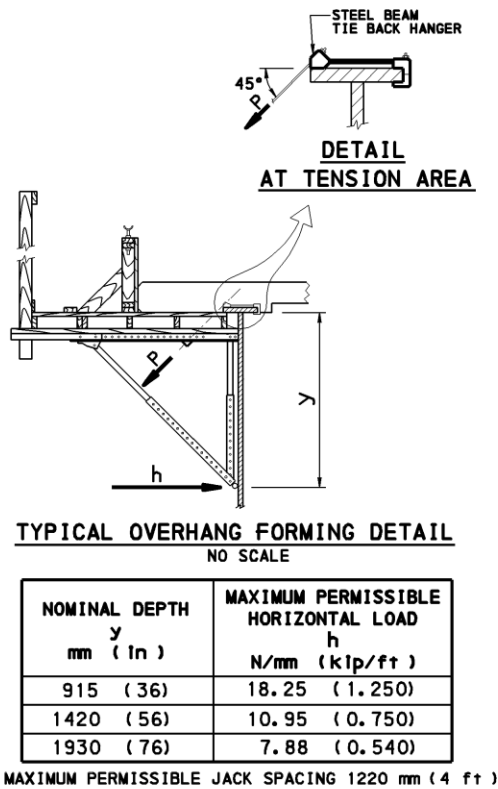
The preferred upper limit on the deck slab overhang is 1200mm {4'-0"} considering factors such as deck forming

SPECIFICATIONS

COMMENTARY

- (4) Transverse stiffener spacing does not exceed the depth of the girder
- (5) In regions where γ_w (see A6.10.3.2.1, D6.10.3.2.1 and A6.10.3.2.2) is less than 2.5, the factored dead load shear using a load factor of 4.0 is less than the buckling shear given in A6.10.9.3.

and deck finishing.



The fascia girders are designed for a temporary construction load applied to the web at a maximum 1220mm{4 ft.} interval. This load (see table) approximates the horizontal component of a deck overhang form support bracket and consists of an allowance for the weight of the concrete, forms and incidental loads, plus the deck finishing machine. Where a transverse stiffener spacing, less than that required for the final design shear, is indicated for constructibility, the spacing for the final design shear may be used if the overhang forms are supported from the bottom flange of the fascia girder, or if the girder web is adequately braced to prevent buckling due to loads from web-bearing form support brackets. The contractor has the option to modify the overhang bracket from that described herein provided working drawings including calculations, sealed by a professional engineer licensed in the Commonwealth of Pennsylvania, are submitted for review and acceptance and show the modifications do not cause unacceptable deformations or stresses in the bridge and it is understood the contractor is ultimately responsible for the satisfactory completion of the bridge.

Figure 6.10.3.2.5.2P-1 - Typical Overhang Forming Detail and Note

Where these requirements are satisfied, original designs of fascia girders shall provide transverse stiffeners throughout

For rolled beams spans, this is typically not a controlling design consideration with small deck overhangs less than

SPECIFICATIONS

the span at a maximum spacing of D, including the region where stiffeners are not required for the final design shear or where a spacing larger than D would be satisfactory for the final design shear. This requirement ensures reasonable constructibility. The stiffener spacings required for both constructibility and final design shear shall be shown on the contract drawings (preferably on the girder elevations), and the sketch and note from Figure 1 shall be included on the contract drawings.

- (b) For deck slab overhangs which do not meet the requirements of (a), the designer of the original structure shall review the condition with the Chief Bridge Engineer's office as part of the TS&L submission. If it is determined that web-supported overhang form brackets cannot be permitted, the following note shall be included in the general notes:

Support deck slab overhang forms from the bottom flange of the fascia girder, unless the girder web is adequately supported to prevent buckling due to loads from web-bearing form supports.

- (c) Contractor-designed alternates shall meet the requirements of this article. The stiffener spacing and a description of the deck overhang form support system, including the loads, shall be shown on the conceptual design drawings submitted for approval.
- (d) All DM-4 and appropriate LRFD provisions in regard to flange and web buckling must be checked.
- (e) For additional criteria on exterior girder rotation due to large cantilever deck slabs, see D9.7.1.5.1P.

COMMENTARY

600 mm {2 ft.} overhangs.

The revision to this note was developed by an APC Subcommittee for Stability of Steel Bridge Superstructures. The note was modified to provide more flexibility to the contractor to use deck overhang form brackets that have nominal depths greater than the typical 915 mm {3'-0"} bracket depth. The maximum permissible horizontal load value was developed based on field measurements of steel bridges constructed in 1999 in District 5-0 with deck overhangs in the range of 1422 mm {4'-8"} and a limited finite element analysis study of lateral web deflections of steel girders subjected to concentrated horizontal forces on the girder web.

Design modifications should consider web stress, overall web deformation, relative web deformation, the resulting deck overhang deflection, and the resulting effects on the finished deck profile. The contractor is responsible for selecting and providing calculations for the overhang forming system as required by Publication 408 Section 1050.3(c)2. Publication 408 Section 105.01 (c) specifies the responsibility of the work remains with the contractor regardless of reviews and/or acceptance of submitted working drawings by the Department.

Unacceptable deformations of the web or top flange results in deflection of the overhang bracket causing problematic deck finish and ride quality.

If an overhang is braced to within 6 inches of the bottom flange, it shall be considered braced to the bottom flange. Deck overhang forms for rolled beams spans, due to their shallow depth, are typically supported in this manner.

SPECIFICATIONS

6.10.3.2.4.3P Deck Slab Overhang Rotation

The designer shall consider the effects of out-of-plane girder rotations, common with skewed bridges, on deck elevations.

6.10.3.5 DEAD LOAD DEFLECTION

The following shall replace A6.10.3.5.
The provisions of A6.7.2 and D6.7.2 shall apply, as applicable.

6.10.4 Service Limit State

6.10.4.2 PERMANENT DEFORMATION

6.10.4.2.1 General

Delete the second paragraph of A6.10.4.2.1.

6.10.4.2.2 Flexure

Delete the first paragraph following the first where list in A6.10.4.2.2

COMMENTARY

C6.10.3.2.4.3P

Out-of-plane girder rotations will cause the overhang formwork to also rotate. In an increasing magnitude from the web of the fascia girder to the outside edge of the formwork, the formwork will move upward or downward, depending on the direction of rotation, during the deck pour. It may be desirable to pre-rotate the overhang formwork so that the as-designed deck overhang cross slope is obtained after the deck pour is complete. Additionally, it may be desirable to relocate the deck finishing machine support railing from its typical position on the overhang formwork to the fascia girders. This will minimize the upward and downward movements of the finishing machine during the deck pour due to out-of-plane girder rotations. Hand finishing work will be necessary for the deck area beyond the limits of the finishing machine.

The designer may consider approximating the anticipated girder rotation based on girder differential vertical displacements.

C6.10.4.2.1

Delete the second paragraph of A6.10.4.2.1.

C6.10.4.2.2

The following shall supplement AC6.10.4.2.2.

Lateral bending in the bottom flange is only a consideration at the service limit state for all horizontally curved I-girder bridges and for straight I-girder bridges with discontinuous cross-frame or diaphragm lines in conjunction with skews less than 70°. Wind load and deck overhang effects are not considered at the service limit state.

Delete the seventh paragraph of AC6.10.4.2.2.

SPECIFICATIONS

COMMENTARY

6.10.5 Fatigue and Fracture Limit State

6.10.5.1 FATIGUE

The following shall supplement A6.10.5.1
For horizontally curved I-girder bridges, the fatigue stress range due to major-axis bending plus lateral bending shall be investigated.

C6.10.5.1P

In horizontally curved I-girder bridges, the base metal adjacent to butt welds and welded attachments on discretely braced flanges subject to a net applied tensile stress must be checked for the fatigue stress range due to major-axis bending, plus flange lateral bending, at the critical transverse location on the flange. Examples of welded attachments for which this requirement applies include transverse stiffeners and gusset plates receiving lateral bracing members. The base metal adjacent to flange-to-web welds need only be checked for the stress range due to major-axis bending since the welds are located near the center of the flange. Flange lateral bending need not be considered for details attached to continuously braced flanges.

6.10.5.3 SPECIAL FATIGUE REQUIREMENT FOR WEBS

The following shall replace the first paragraph of A6.10.5.3
The live load flexural stress and shear stress resulting from the fatigue load, as specified in A3.6.1.4 and D3.6.1.4, shall be factored by two times the Pennsylvania Traffic Factor (PTF) and the fatigue load factor specified for the fatigue load combination in Table A3.4.1-1. The PTF is specified in D6.6.1.2.2.

For the purposes of this article, the factored fatigue load shall be taken as twice that calculated using the Fatigue load combination specified in Tables A3.4.1-1 and in D3.4.1.1P, with the fatigue live load taken as specified in A3.6.1.4 and D3.6.1.4, multiplied by the Pennsylvania Traffic Factor (PTF). The PTF is specified in D6.6.1.2.2.

6.10.6 Strength Limit State

6.10.6.2 FLEXURE

6.10.6.2.2 Composite Sections in Positive Flexure

The following shall replace A6.10.6.2.2.

Composite sections in kinked (chorded) continuous or horizontally curved steel girder bridges shall be considered as noncompact sections and shall satisfy the requirements of A6.10.7.2.

C6.10.6.2.2

The following shall replace AC6.10.6.2.2.
Composite sections in positive flexure in kinked (chorded) continuous or horizontally curved steel bridges are also to be designed at the strength limit state as noncompact sections as specified in A6.10.7.2. Research has not yet been conducted to support the design of these sections for a nominal flexural resistance exceeding the moment at first yield.

6.10.6.2.3 Composite Sections in Negative Flexure and

C6.10.6.2.3

SPECIFICATIONS

COMMENTARY

Noncomposite Sections

The following shall replace A6.10.6.2.3. Sections in kinked (chorded) continuous or horizontally curved steel girder bridges shall be proportioned according to provisions specified in A6.10.8 and D6.10.8.

The following shall replace AC6.10.6.2.3. For composite sections in negative flexure and noncomposite sections, the provisions of A6.10.8 and D6.10.8 limit the nominal flexural resistance to be less than or equal to the moment at first yield. As a result, the nominal flexural resistance for these sections is conveniently expressed in terms of the elastically computed flange stress.

For composite sections in negative flexure or noncomposite sections in horizontally curved bridges, the provisions of A6.10.8 and D6.10.8 must be used. Research has not yet been conducted to extend the provisions of Appendix A to sections in kinked (chorded) continuous or horizontally curved steel bridges.

6.10.8 Flexural Resistance - Composite Sections in Negative Flexure and Noncomposite Sections

6.10.8.2 COMPRESSION-FLANGE FLEXURAL RESISTANCE

6.10.8.2.3 Lateral Torsional Buckling Resistance

The following shall replace Equation A6.10.8.2.3-10.

f_1 = stress without consideration of lateral bending at the brace point opposite to the one corresponding to f_2 , calculated as the intercept of the most critical assumed linear stress variation passing through f_2 and either f_{mid} or f_0 , whichever produces the smaller value of C_b (MPa). f_1 may be determined as follows:

- When the variation in the moment along the entire length between the brace points is concave in shape:

$$f_1 = f_0 \quad (6.10.8.2.3-10)$$

- Otherwise:

$$f_1 = 2f_{mid} - f_2 \geq f_0 \quad (6.10.8.2.3-11)$$

SPECIFICATIONS

COMMENTARY

6.10.9 Shear Resistance

6.10.9.1 GENERAL

The following shall replace the first bulleted item of the third paragraph of A6.10.9.1.

- without a longitudinal stiffener and with a transverse stiffener spacing not exceeding 1.5D, or

The following shall replace the fourth paragraph of A6.10.9.1.

Provisions for end panels shall be as specified in A6.10.9.3.3 and D6.10.9.3.3.

The following shall supplement A6.10.9.1.
Transverse stiffener spacing shall also satisfy the requirements of D6.10.3.2.5.2P for deck slab overhang from support.

6.10.9.3.3 End Panels

The following shall replace the last paragraph of A6.10.9.3.3.

The transverse stiffener spacing for end panels without a longitudinal stiffener shall not exceed 0.5D. The transverse stiffener spacing of end panels with a longitudinal stiffener shall not exceed 0.5 times the maximum subpanel depth.

6.10.10 Shear Connectors

6.10.10.1 GENERAL

The following shall replace the third paragraph of A6.10.10.1.
Shear connectors are required along the entire length of the girder when a composite girder analysis has been performed.

6.10.10.1.1 Types

The following shall supplement A6.10.10.1.1.
The minimum diameter of studs shall be 19 mm {3/4 in.}.

6.10.10.1.2 Pitch

The following shall replace the part of the article starting immediately after Equation A6.10.10.1.2-1 to the end of A6.10.10.1.2.
in which:

$$V_{sr} = \text{horizontal fatigue shear range per unit length (N/mm) \{kip-in.\}}$$

C6.10.10.1P

Mechanical shear connectors provide for the horizontal shear at the interface between the concrete slab and the steel girder in the positive moment regions and the horizontal shear between the longitudinal reinforcement steel within the effective flange width and the steel girder in the negative moment regions.

C6.10.10.1.2

The following shall supplement A6.10.10.1.2.
At the fatigue limit state, shear connectors are designed for the range of live load shear between the deck and top flange of the girder. In straight girders, the shear range normally is due to only major-axis bending if torsion is ignored. Curvature, skew and other conditions may cause torsion, which introduces a radial component of the

SPECIFICATIONS

$$= \sqrt{V_{fat}^2 + F_{fat}^2} \quad (6.10.10.1.2-2)$$

$$V_{fat} = \text{longitudinal fatigue shear range per unit length (N/mm) \{kip/in.\}} \\ = \frac{V_f Q}{I} \quad (6.10.10.1.2-3)$$

F_{fat} = radial fatigue shear range per unit length (N/mm) {kip/in} taken as the larger of either:

$$F_{fat1} = \frac{A_{bot} \sigma_{flg} \ell}{wR} \quad (6.10.10.1.2-4)$$

or

$$F_{fat2} = \frac{F_{rc}}{w} \quad (6.10.10.1.2-5)$$

where:

σ_{flg} = range of longitudinal fatigue stress in the bottom flange without consideration of flange lateral bending (MPa) {ksi}

A_{bot} = area of the bottom flange (mm²) {in.²}

F_{rc} = net range of cross-frame or diaphragm force at the top flange (N) {kip}

I = moment of inertia of the short-term composite section (mm⁴) {in.⁴}

ℓ = distance between brace points (mm) {ft.}

n = number of shear connectors in a cross-section

p = pitch of shear connectors along the longitudinal axis (mm) {in.}

Q = first moment of the transformed short-term area of the concrete deck about the neutral axis of the short-term composite section (mm³) {in.³}

R = minimum girder radius within the panel (mm) {ft.}

V_f = vertical shear force range under the fatigue load combination specified in Table A3.4.1-1 and D3.4.1-1 with the fatigue live load taken as specified in A3.6.1.4 and D3.6.1.4 (N) {kip}

w = effective length of deck (mm) taken as 1220 mm {48 in.}, except at end supports where w may be

COMMENTARY

horizontal shear. These provisions provide for consideration of both of the components of the shear to be added vectorially according to Eq. 2.

The radial shear range, F_{fat} , typically is determined for the fatigue live load positioned to produce the largest positive and negative major-axis bending moments in the span. Therefore, vectorial addition of the longitudinal and radial components of the shear range is conservative because the longitudinal and radial shears are not produced by concurrent loads.

Eq. 4 may be used to determine the radial fatigue shear range resulting from the effect of any curvature between brace points. The shear range is taken as the radial component of the maximum longitudinal range of force in the bottom flange between brace points, which is used as a measure of the major-axis bending moment. The radial shear range is distributed over an effective length of girder flange, w . At end supports, w is halved. Eq. 4 gives the same units as V_{fat} .

Eq. 5 will typically govern the radial fatigue shear range where torsion is caused by effects other than curvature, such as skew. Eq. 5 is most likely to control only in regions adjacent to a skewed support for which the skew angle less than 70° in either a straight or horizontally curved bridge. Eqs. 4 and 5 yield approximately the same value if the span or segment is curved and there are no other sources of torsion in the region under consideration. Note that F_{rc} represents the net range of force transferred to the top flange from all cross-frames at the point under consideration due to the factored fatigue load plus impact. In lieu of a refined analysis, F_{rc} for an exterior girder, which is the critical case, may be taken as 111 200 N {25 kips}, and taken as zero for interior girders. Eq. 5 should only be checked using this value within the regions of a straight or horizontally curved girder in the region of a skewed support with a skew angle less than 70°. Regardless of whether F_{rc} is determined by refined analysis or taken as the above recommended value, it should be multiplied by the factor of 0.75 discussed in Article C6.6.1.2.1 and DC6.6.1.2.1 to account for the probability of two vehicles being in their critical relative position to cause the maximum range of cross-frame force at the top flange.

Eqs. 4 and 5 are provided to ensure that a load path is provided through the shear connectors to satisfy equilibrium at a transverse section through the girders, deck and cross-frame.

SPECIFICATIONS

COMMENTARY

taken as 610 mm {24 in.}

Z_r = shear fatigue resistance of an individual shear connector determined as specified in A6.10.10.2 and D6.10.10.2 (N) {kip}

For straight spans or segments, the radial fatigue shear range from Eq. 4 may be taken equal to zero. For straight or horizontally curved bridges with skews not less than 70°, the radial fatigue shear range from Eq. 5 may be taken equal to zero.

The center-to-center pitch of shear connectors shall not exceed 600 mm {24 in.} and shall not be less than six stud diameters.

The center-to-center pitch of channel shear connectors shall not exceed 600 mm {24 in.} and shall not be less than 150 mm {6 in.}.

6.10.10.1.3 Transverse Spacing

The following shall supplement A6.10.10.1.3.
The minimum number of studs in a group shall consist of two in a single transverse row.

6.10.10.1.4 Cover and Penetration

The following shall replace A6.10.10.1.4.
The clear depth of concrete cover over the tops of the shear connectors should not be less than 60 mm {2 1/2 in.}.
Shear connectors should penetrate at least 50 mm {2 in.} into the deck.

C6.10.10.1.4

Delete the second sentence of AC6.10.10.1.4.
For plan presentation, show cover and penetration limits; do not detail stud height (see BC-753M). Stud heights are determined in the field based on actual girder elevations.

6.10.10.1.5P SPLICE LOCATIONS

Shear connectors at splice locations shall be arranged to clear fasteners and shall be welded to the splice plate. Up to 20% fewer connectors, than required by design, are acceptable in the splice zone, provided that the deleted connectors are furnished as additional connectors adjacent to the splice.

6.10.10.2 FATIGUE RESISTANCE

C6.10.10.2

The following shall supplement A6.10.10.2.
The fatigue resistance of an individual channel shear connector, Z_r , shall be taken as:

The following shall supplement AC6.10.10.2.
Equations 3P and 4P were added because the LRFD specification does not address the fatigue resistance of channel shear connectors. Equations 3P and 4P were converted from Article 10.3.8.5.1.1 of AASHTO Standard Specification for Highway Bridges.

Metric Units:

$$Z_r = B w \leq 184 w \quad (6.10.10.2-3P)$$

U.S. Customary Units:

SPECIFICATIONS

COMMENTARY

$$Z_r = B w \leq 1.05 w$$

where:

Metric Units:

$$B = 1525 - 175 \text{ Log } N \quad (6.10.10.2-4P)$$

U.S. Customary Units:

$$B = 8.7 - \text{Log } N$$

w = length of channel shear connector measured in a transverse direction on the flange of a girder (mm)

N = number of cycles specified in A6.6.1.2.5 and D6.6.1.2.5

6.10.10.3 SPECIAL REQUIREMENTS FOR POINTS OF PERMANENT LOAD CONTRAFLEXURE

C6.10.10.3

Delete A6.10.10.3.

Delete AC6.10.10.3.

PennDOT requires composite girders to be composite full-length of the bridge with shear connectors full-length of the bridge.

6.10.10.4 STRENGTH LIMIT STATE

6.10.10.4.2 Nominal Shear Force

6.10.10.4.2

The following shall replace A6.10.10.4.2

For simple spans and for continuous spans that are noncomposite for negative flexure in the final condition, the total nominal shear force, P, between the point of maximum positive design live load plus impact moment and each adjacent point of zero moment shall be taken as:

The following shall supplement AC6.10.10.4.2.

The radial effect of curvature is included in Eqs. 4 and 9. For curved spans or segments, the radial force is required to bring into equilibrium the smallest of the longitudinal forces in either the deck or the girder. When computing the radial component, the longitudinal force is conservatively assumed to be constant over the entire length L_p or L_n , as applicable.

$$P = \sqrt{P_p^2 + F_p^2} \quad (6.10.10.4.2-1)$$

in which:

P_p = total longitudinal shear force in the concrete deck at the point of maximum positive live load plus impact moment (N) {kip} taken as the lesser of either:

$$P_{1p} = 0.85 f'_c b_s t_s \quad (6.10.10.4.2-2)$$

or

$$P_{2p} = F_{yw} D t_w + F_{yt} b_{ft} t_{ft} + F_{yc} b_{fc} t_{fc} \quad (6.10.10.4.2-3)$$

SPECIFICATIONS

COMMENTARY

F_p = total radial shear force in the concrete deck at the point of maximum positive live load plus impact moment (N) {kip} taken as:

$$F_p = P_p \frac{L_p}{R} \quad (6.10.10.4.2-4)$$

where:

b_s = effective width of the concrete deck (mm)

L_p = arc length between an end of the girder and an adjacent point of maximum positive live load plus impact moment (mm) {ft}

R = minimum girder radius over the length, L_p (mm) {ft.}

t_s = thickness of the concrete deck (mm) {in.}

For straight segments, F_p may be taken equal to zero. For continuous spans that are composite for negative flexure in the final condition, the total nominal shear force, P , between the point of maximum positive design live load plus impact moment and an adjacent end of the member shall be determined from Eq. 1. The total nominal shear force, P , between the point of maximum positive design live load plus impact moment and the centerline of an adjacent interior support shall be taken as:

$$P = \sqrt{P_T^2 + F_T^2} \quad (6.10.10.4.2-5)$$

in which:

P_T = total longitudinal shear force in the concrete deck between the point of maximum positive live load plus impact moment and the centerline of an adjacent interior support (N) {ft.} taken as:

$$P_T = P_p + P_n \quad (6.10.10.4.2-6)$$

P_n = total longitudinal shear force in the concrete deck over an interior support (N) {ft.} taken as the lesser of either:

$$P_{In} = F_{yw} D t_w + F_{yt} b_{ft} t_{ft} + F_{yc} b_{fc} t_{fc} \quad (6.10.10.4.2-7)$$

or

$$P_{2n} = 0.45 f'_c b_s t_s \quad (6.10.10.4.2-8)$$

SPECIFICATIONS

COMMENTARY

F_T = total radial shear force in the concrete deck between the point of maximum positive live load plus impact moment and the centerline of an adjacent interior support (N) {kip} taken as:

$$F_T = P_r \frac{L_n}{R} \quad (6.10.10.4.2-9)$$

where:

L_n = arc length between the point of maximum positive live load plus impact moment and the centerline of an adjacent interior support (mm) {ft.}

R = minimum girder radius over the length, L_n (mm) {ft.}

For straight segments, F_T may be taken equal to zero.

6.10.11 Stiffeners**6.10.11.1 TRANSVERSE INTERMEDIATE STIFFENERS****6.10.11.1.1 General**

The following shall supplement A6.10.11.1.1. Single-sided stiffeners on horizontally curved girders should be attached to both flanges. When pairs of transverse stiffeners are used on horizontally curved girders, they shall be fitted tightly to both flanges.

Transverse stiffeners shall also satisfy the requirements given in Standard Drawing BC-753M.

The following shall replace the third paragraph of A6.10.11.1.1.

The distance between the end of the web-to-stiffener weld and the near edge of the adjacent web-to-flange or longitudinal stiffener-to-web weld shall not be less than $4t_w$ but not to exceed the lesser of $6t_w$ and 100 mm {4 in.}.

6.10.11.1.2 Projecting Width

following shall supplement A6.10.11.1.2.

For tub sections in regions of negative flexure, b_f shall be taken as the full-width of the widest top flange within the field section under consideration.

6.10.11.3 LONGITUDINAL STIFFENERS**C6.10.11.1.1P**

When single-sided transverse stiffeners are used on horizontally curved girders, they should be attached to both flanges to help to restrain the flanges and to help retain the cross-sectional configuration of the girder when subjected to torsion. The fitting of pairs of transverse stiffeners against the flanges is required for the same reason.

The minimum distance between the end of the web-to-stiffener weld to the adjacent web-to-flange or longitudinal stiffener-to-web weld is set to relieve flexing of the unsupported segment of the web to avoid fatigue-induced cracking of the stiffener-to-web welds, and to avoid inadvertent intersecting welds. The $6t_w$ criterion for maximum distance is set to avoid vertical buckling of the unsupported web. The 100 mm {4 in.} criterion was arbitrarily selected to avoid a very large unsupported length where the web thickness has been selected for reasons other than stability, e.g., webs of bascule girders at trunnions.

SPECIFICATIONS

6.10.11.3.3 Moment of Inertia and Radius of Gyration

The following shall replace A6.10.11.3.3.
Longitudinal stiffeners shall satisfy:

$$I_{\ell} \geq Dt_w^3 \left[2.4 \left(\frac{d_o}{D} \right)^2 - 0.13 \right] \beta \quad (6.10.11.3.3-1)$$

and

$$r \geq \frac{0.16d_o \sqrt{\frac{F_{ys}}{E}}}{\sqrt{1 - 0.6 \frac{F_{yc}}{R_h F_{ys}}}} \quad (6.10.11.3.3-2)$$

in which:

β = curvature correction factor for longitudinal stiffener rigidity calculated as follows:

- For cases where the longitudinal stiffener is on the side of the web away from the center of curvature:

$$\beta = \frac{Z}{6} + 1 \quad (6.10.11.3.3-3)$$

- For cases where the longitudinal stiffener is on the side of the web toward the center of curvature:

$$\beta = \frac{Z}{12} + 1 \quad (6.10.11.3.3-4)$$

Z = curvature parameter:

$$= \frac{0.95d_o^2}{Rt_w} \leq 10 \quad (6.10.11.3.3-5)$$

where:

d_o = transverse stiffener spacing (mm) {in.}

I_{ℓ} = moment of inertia of the longitudinal stiffener including an effective width of the web equal to $18t_w$ taken about the neutral axis of the combined section (mm^4) {in.⁴}. If F_{yw} is smaller than F_{ys} , the strip of the web included in the effective section shall be reduced by the ratio F_{yw}/F_{ys} .

R = minimum girder radius in the panel (mm) {in.}

r = radius of gyration of the longitudinal stiffener including an effective width of the web equal to $18t_w$ taken about the neutral axis of the combined

COMMENTARY

C6.10.11.3.3

The following shall replace A6.10.11.3.3.

The rigidity required of longitudinal stiffeners on curved webs is greater than the rigidity required on straight webs because of the tendency of curved webs to bow. The factor β in Eq. 1 is a simplification of the requirement in the Hanshin (1988) provisions for longitudinal stiffeners used on curved girders. For longitudinal stiffeners on straight webs, Eq. 5 leads to $\beta = 1.0$.

SPECIFICATIONS

COMMENTARY

section (mm) {in.}. If F_{yw} is smaller than F_{ys} , the strip of the web included in the effective section shall be reduced by the ratio F_{yw}/F_{ys} .

6.10.11.4P STIFFENERS IN RIGID-FRAME KNEES

6.10.11.4.1P Stiffener Spacing

The spacing of stiffeners in rigid-frame knees shall satisfy both of the following equations:

$$f_a \leq F_{yc} - f_{cs} \quad (6.10.11.4.1P-1)$$

and

$$f_b \leq F_{yc} \quad (6.10.11.4.1P-2)$$

for which:

$$f_a = f_{cs} \left(\frac{3b^2}{Rt} \right) \left(\frac{\beta^2}{4 + 1.14\beta^4} \right) \quad (6.10.11.4.1P-3)$$

$$f_b = f_{cs} \left(\frac{3b^2}{Rt} \right) \left(\frac{\beta^3}{3.2 + \beta^3} \right) \quad (6.10.11.4.1P-4)$$

$$\beta = \frac{a}{b} \quad (6.10.11.4.1P-5)$$

where:

a = spacing of stiffeners (mm) {in.}

b = half of flange width (mm) {in.}

F_{yc} = specified minimum yield strength of a compression flange (MPa) {ksi}

f_{cs} = maximum compression Service I load flange stress (MPa) {ksi}

R = radius of flange curvature (mm) {in.}

t = thickness of flange (mm) {in.}

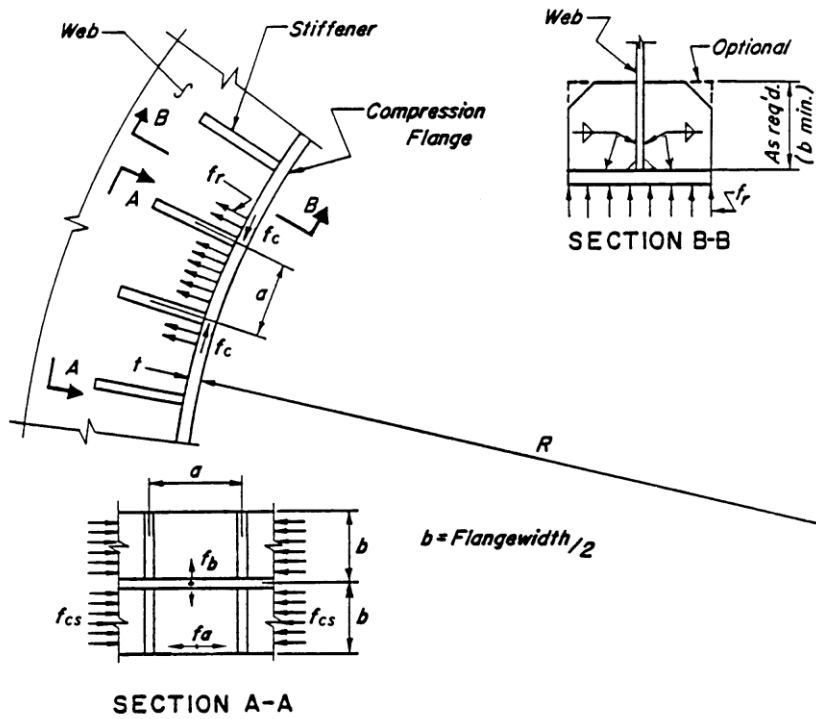


Figure 6.10.11.4.1P-1 - Stiffeners in Rigid-Frame Knees

6.10.11.4.2P Stiffener Design

The factored bearing resistance of stiffeners in rigid-frame knees, taken as specified in A6.10.11.2.3, shall be greater than P_b , taken as:

$$P_b = f_r ab \tag{6.10.11.4.2P-1}$$

for which:

$$f_r = \frac{f_c t}{R} \tag{6.10.11.4.2P-2}$$

where:

- a = spacing of stiffeners (mm) {in.}
- b = half of flange width (mm) {in.}
- f_c = maximum factored compression flange stress (MPa) {ksi}
- R = radius of flange curvature (mm) {in.}
- t = thickness of flange (mm) {in.}

SPECIFICATIONS

COMMENTARY

6.10.12 Cover Plates**6.10.12.3P COVER PLATE LENGTH AND WIDTH**

The length of any welded cover plate added to a rolled beam shall extend the full-length of the rolled beam, including the bearing area, or the full-length of the rolled beam field section in the case of a spliced beam unless otherwise approved by the Chief Bridge Engineer. The use of partial length cover plates is allowed for rehabilitation projects with detailed fatigue analysis. Partial length cover plates must be a bolted connection at the ends.

The width of the plate shall not exceed the width of the flange by 150 mm {6 in.}, or six times the thickness of the cover plate, whichever is less. Bottom flange cover plates preferably shall be wider than the bottom flange. Top flange cover plates shall be of constant width, preferably narrower than the top flange. When a cover plate narrower than the flange is used, the width of the plate shall be at least 50 mm {2 in.} less than the width of the flange. The width of a cover plate connected by fillet welds shall be no greater than 24 times the plate thickness.

6.11 BOX SECTIONS IN FLEXURE

The provisions of A6.11 and D6.11 apply to steel box I-girders curved in plan. The provisions of Appendix E, DE6.11P apply to straight box-girder bridges.

6.11.1 General**C6.10.12.3P**

The Department does not allow partial length cover plates for new designs.

C6.11P

The provisions of D6.11 are based on the 2004 Third Edition of AASHTO-LRFD Specifications as amended herein. The provisions of Appendix E are based on the 1998 Second Edition of the AASHTO-LRFD Design Specifications with the 1999 through 2003 Interims.

C6.11.1

The following shall replace the first sentence of the first paragraph of AC6.11.1.

A6.11.1 and D6.11.1 address general topics that apply to closed-box and tub sections used as flexural members in horizontally curved bridges, or bridges containing both straight and curved segments. For the application of the provisions of A6.11 and D6.11, bridges containing both straight and curved segments are to be treated as horizontally curved bridges since the effects of curvature on the support reactions and girder deflections, as well as the effects of flange lateral bending and torsional shear, usually extend beyond the curved segments.

The following shall supplement A6.11.1.

For horizontally curved boxes, flange lateral bending effects due to curvature and the effects of torsional shear must always be considered at all limit states and also during construction.

SPECIFICATIONS

COMMENTARY

6.11.1.1 STRESS DETERMINATION

C6.11.1.1

The following shall replace the third and fourth paragraphs of A6.11.1.1.

Delete the seventh paragraph of AC6.11.1.1

The section of an exterior member assumed to resist horizontal factored wind loading within these bridges may be taken as the bottom box flange acting as a web and 12 times the thickness of the web acting as flanges.

The provisions of A4.6.2.2.2b and D4.6.2.2.2b shall not apply to single or multiple box sections in horizontally curved bridges. For these sections, the effects of both flexural and St. Venant torsional shear shall be considered. The St. Venant torsional shear stress in box flanges due to the factored loads at the strength limit state shall not exceed the factored torsional shear resistance of the flange, F_{vr} , taken as:

$$F_{vr} = 0.75\phi_v \frac{F_{yf}}{\sqrt{3}} \quad (6.11.1.1-1)$$

6.11.3 Constructibility

6.11.3.2 FLEXURE

C6.11.3.2

The following shall replace the first four sentences of the third paragraph of AC6.11.3.2.

For horizontally curved girders, flange lateral bending effects due to curvature must always be considered during construction.

Delete the fourth paragraph of AC6.11.3.2.

6.11.5 Fatigue and Fracture Limit State

The following shall replace the first sentence of the fourth paragraph of A6.11.5.

Longitudinal warping stresses and transverse bending stresses due to cross-section distortion shall be considered for single and multiple box sections in horizontally curved bridges.

The following shall supplement the last paragraph of A6.11.5.

Unless adequate strength and stability of a damaged structure can be verified by refined analysis, in cross-sections comprised of two box sections, only the bottom flanges in the positive moment regions should be designated as fracture-critical. Where cross-sections contain more than two box girder sections, none of the components of the box sections should be considered fracture-critical.

SPECIFICATIONS

COMMENTARY

6.11.6 Strength Limit State

6.11.6.2 FLEXURE

6.11.6.2.2 Sections in Positive Flexure

The following shall replace A6.11.6.2.2
Sections in horizontally curved steel girder bridges shall be considered as noncompact sections and shall satisfy the requirements of A6.11.7.2 and A6.10.7.3.

6.11.9 Shear Resistance

The following shall replace the third paragraph of A6.11.9.
For all horizontally curved sections, V_u shall be taken as the sum of the flexural and St. Venant torsional shears.

6.11.10 Shear Connectors

The following shall replace the third paragraph of A6.11.10.
For horizontally curved sections, shear connectors shall be designed for the sum of the flexural and St. Venant torsional shears. The longitudinal fatigue shear range per unit length, V_{fat} , for one top flange of a tub girder shall be computed for the web subjected to additive flexural and torsional shears. The resulting shear connector pitch shall also be used for the other top flange. The radial fatigue shear range due to curvature, F_{fatL} , given by Eq. D6.10.10.1.2-4 may be ignored in the design of box sections in straight or horizontally curved spans or segments.

For checking the resulting number of shear connectors to satisfy the strength limit state, the cross-sectional area of

C6.11.6.2.2

The following shall replace AC6.11.6.2.2.
For sections in positive flexure in horizontally curved bridges the nominal flexural resistance is not permitted to exceed the moment at first yield. The nominal flexural resistance in these cases is therefore more appropriately expressed in terms of the elastically computed flange stress. If the section is part of a horizontally curved bridge, the section must be designed as a noncompact section. The ability of such sections to develop a nominal flexural resistance greater than the moment at first yield in the presence of potentially significant St. Venant torsional shear and cross-sectional distortion stresses has not been demonstrated.
Noncompact sections must also satisfy the ductility requirement specified in 6.10.7.3 to ensure a ductile failure. Satisfaction of this requirement ensures an adequate margin of safety against premature crushing of the concrete deck for sections utilizing 690-MPa {100 ksi} steels and/or for sections utilized in shored construction. This requirement is also a key limit in allowing web bend-buckling to be disregarded in the design of composite sections in positive flexure when the web also satisfies A6.11.2.1.2, as discussed in AC6.10.1.9.1.

6.11.10

Delete the second sentence of the first paragraph of A6.11.10.
The following shall supplement the second paragraph of A6.11.10.

Because of the inherent conservatism of these requirements, the radial fatigue shear range due to curvature need not be included when computing the horizontal fatigue shear range for box sections in either straight or horizontally curved spans or segments.

SPECIFICATIONS

COMMENTARY

the steel box section under consideration and the effective area of the concrete deck associated with that box shall be used in determining P by Eqs. D6.10.10.4.2-2, D6.10.10.4.2-3, D6.10.10.4.2-7, and D6.10.10.4.2-8.

The following shall replace the first sentence of last paragraph of A6.11.10.

For composite box flanges at the fatigue limit state, V_{sr} in Eq. A6.10.10.1.2-1 shall be determined as the vector sum of the longitudinal fatigue shear range given by Eq. D6.10.10.1.2-3 and the torsional fatigue shear range in the concrete deck

6.11.11 Stiffeners**6.11.11.2 LONGITUDINAL COMPRESSION-FLANGE STIFFENERS**

C6.11.11.2

The following shall supplement the first paragraph of A6.11.11.2.

For structural tees, b_{ℓ} should be taken as one-half the width of the flange.

6.12 MISCELLANEOUS FLEXURAL MEMBERS**6.12.1 General****6.12.1.2 STRENGTH LIMIT STATE****6.12.1.2.3 Shear**

The following shall replace the definition of n in A6.12.1.2.3.

V_n = nominal shear resistance specified in A6.10.9.2 and DE6.10.7.2P, as appropriate, for webs of noncomposite members and 6.12.3 for webs of composite members (N) {kip}

6.12.2 Nominal Flexural Resistance**6.12.2.2 NONCOMPOSITE MEMBERS****6.12.2.2.1 I- and H-Shaped Members**

The following shall replace the second paragraph of A6.12.2.2.1.

The provisions of A6.10, D6.10, DE6.10P and DE6.11p shall apply to flexure about an axis perpendicular to the web.

SPECIFICATIONS

6.13 CONNECTIONS AND SPLICES**6.13.1 General**

The following shall replace the first paragraph of A6.13.1. Except as specified otherwise, connections and splices for main members (both flanges and webs) shall be designed at the strength limit state for not less than the larger of:

- The average of the flexural moment-induced stress, shear, or axial force due to the factored loadings at the point of splice or connection and the factored flexural, shear, or axial resistance of the member or element at the same point, or
- 75 percent of the factored flexural, shear, or axial resistance of the member or element.

The following shall supplement A6.13.1.

If it is necessary to cope a flange in order to provide clearance at the end connection of a floorbeam or stringer, the bending resistance of the member at the cope location shall not be decreased by more than 50%. No sharp notches shall be introduced as a result of coping. The maximum practical radius shall be maintained at all copes with an absolute minimum radius of 50 mm {2 in.}.

Where diaphragms, cross-frames, lateral bracing, stringers, or floorbeams for straight or horizontally curved flexural members are included in the structural model used to determine force effects, or alternatively, are designed for explicitly calculated force effects from the results of a separate investigation, end connections for these bracing members shall be designed for the calculated factored member force effects. Otherwise, the end connections for these members shall be designed according to the 75 percent resistance provision contained herein.

6.13.2 Bolted Connections**6.13.2.1 GENERAL**

The following shall replace the second paragraph of A6.13.2.1. High-strength bolted joints shall be designated as slip-critical connections. Bearing-type connections may be used on rehabilitation projects if approved by the Chief Bridge Engineer.

COMMENTARY

C6.13.1

The following shall supplement AC6.13.1.

Often stresses on the top flange of a composite girder are low under design loads. This criteria would require a top splice plate to be about 75% of the area of the top flange, and have the appropriate number of bolts.

The exception for bracing members for straight or horizontally curved flexural members, that are included in the structural model used to determine force effects, results from experience with details developed invoking the 75 percent and average load provisions herein. These details tended to become so large as to be unwieldy resulting in large eccentricities and force concentrations. It has been decided that the negatives associated with these connections justifies the exception permitted herein.

C6.13.2.1P

When detailing bolted connections, tightening clearance between flange and web bolts need to be taken into account. Manual of Steel Construction, American Institute of Steel Construction, provides information on assembling clearances for threaded fasteners which can be used to avoid bolt interference problems.

SPECIFICATIONS

COMMENTARY

6.13.2.3 BOLTS, NUTS AND WASHERS

6.13.2.3.2 Washers

The following shall replace the third and fifth bulleted items of A6.13.2.3.2.

- AASHTO M 253 (ASTM A 490) bolts are to be installed in material having a specified minimum yield strength less than 345 MPa {50 ksi}, irrespective of the tightening method;
- AASHTO M 253 (ASTM A 490) bolts over 25.4 mm {1 in.} in diameter are to be installed in an oversize or short-slotted hole in an outer-ply, in which case a minimum thickness of 7.9 mm {5/16 in.} shall be used under both the head and the nut. Multiple hardened washers shall not be used.

6.13.2.4 HOLES

6.13.2.4.1 Types

6.13.2.4.1b Oversize Holes

The following shall replace A6.13.2.4.1b.
Approval of Chief Bridge Engineer must be obtained before oversize holes can be used in any or all plies of slip-critical connections. Oversize holes are not permitted in diaphragms or cross frames of curved girder bridges. Oversize holes shall not be used in bearing-type connections.

C6.13.2.4.1c Short-Slotted Holes

On skew bridges, short slotted holes for cross-frame connections should be utilized for adjustment for temporary and permanent conditions.

6.13.2.4.2 Size

The following shall replace Table A6.13.2.4.2-1.

SPECIFICATIONS

COMMENTARY

Table 6.13.2.4.2-1 - Maximum Hole Sizes

Metric Units				
Bolt Diameter d (mm)	Standard Hole Diameter (mm)	Oversize Hole Diameter (mm)	Short Slot Width x Length (mm x mm)	Long Slot Width x Length (mm x mm)
15.9	17.5	20.7	17.5 x 22	17.5 x 40
19.1	20.7	23.8	20.7 x 25	20.7 x 48
22.2	23.8	27.0	23.8 x 29	23.8 x 56
25.4	27.0	31.8	27.0 x 33	27.0 x 64
≥28.6	d+1.6	d+7.9	d+1.6 x d+9.5	d+1.6 x 2.5d

U.S. Customary Units				
Bolt Diameter d (in.)	Standard Hole Diameter (in.)	Oversize Hole Diameter (in.)	Short Slot Width x Length (in. x in.)	Long Slot Width x Length (in. x in.)
5/8	11/16	13/16	11/16 x 7/8	11/16 x 1-9/16
3/4	13/16	15/16	13/16 x 1	13/16 x 1-7/8
7/8	15/16	1-1/16	15/16 x 1-1/8	15/16 x 2-3/16
1	1-1/16	1-1/4	1-1/16 x 1-5/16	1-1/16 x 2-1/2
≥1-1/8	d+1/16	d+5/16	d+1/16 x d+3/8	d+1/16 x 2.5d

6.13.2.5 SIZE OF BOLTS

The following shall replace A6.13.2.5. Bolts shall not be less than 15.9 mm {5/8 in.} in diameter. Bolts 15.9 mm {5/8 in.} in diameter shall not be used in primary members, except in 64 mm {2.5 in.} legs of angles and in flanges of sections whose dimensions require 15.9 mm {5/8 in.} fasteners to satisfy other detailing provisions herein. Use of structural shapes which do not allow the use of 15.9 mm {5/8 in.} fasteners shall be limited to handrails.

Angles whose size is not determined by a calculated demand may use:

- 15.9 mm {5/8 in.} diameter bolts in 51 mm {2 in.} legs,
- 19.1 mm {3/4 in.} diameter bolts in 64 mm {2 1/2 in.} legs,
- 22.2 mm {7/8 in.} diameter bolts in 76 mm {3 in.} legs, and
- 25.4 mm {1 in.} diameter bolts in 89 mm {3 1/2 in.} legs.

C6.13.2.5P

Typically, high-strength bolts will be 22.2 mm {7/8 in.} diameter mechanically galvanized AASHTO M 164 (ASTM A 325) bolts. This is the typical high-strength bolt used in the past.

SPECIFICATIONS

COMMENTARY

The diameter of bolts in angles of primary members shall not exceed one-fourth the width of the leg in which they are placed.

Fasteners shall be of the size shown on the contract plans, but generally shall be 22.2 mm {7/8 in.} in diameter.

6.13.2.6 SPACING OF BOLTS

C6.13.2.6.1 Minimum Spacing and Clear Distance

The following shall supplement AC6.13.2.6.1. The preferred distance between centers of bolts in standard holes shall not be less than the values in Table 1:

Table C6.13.2.6.1-1 - Preferred Bolt Spacing

Metric Units		U.S. Customary Units	
Diameter Bolt (mm)	Preferred Distance between Centers of Bolts (mm)	Diameter Bolt (in.)	Preferred Distance between Centers of Bolts (in.)
15.9	60	5/8	2 1/4
19.1	65	3/4	2 1/2
22.2	75	7/8	3
25.4	90	1	3 1/2

6.13.2.6.6 Edge Distances

The following shall replace Table A6.13.2.6.6-1.

SPECIFICATIONS

COMMENTARY

Table 6.13.2.6.6-1 - Minimum Edge Distances

Metric Units			U.S. Customary Units		
Bolt Diameter (mm)	Sheared or Gas Cut Edges (mm)	Rolled Edges of Plates or Shapes (mm)	Bolt Diameter (in.)	Sheared or Gas Cut Edges (in.)	Rolled Edges of Plates or Shapes (in.)
15.9	29	22	5/8	1 1/8	7/8
19.1	32	25	3/4	1 1/4	1
22.2	38	29	7/8	1 1/2	1 1/8
25.4	44	32	1	1 3/4	1 1/4
28.6	51	38	1 1/8	2	1 1/2
31.8	57	41	1 1/4	2 1/4	1 5/8
34.9	60	44	1 3/8	2 3/8	1 3/4

6.13.2.7 SHEAR RESISTANCE

C6.13.2.7

The following shall supplement the first paragraph of AC6.13.2.7.

For steel plate girder flange splices greater than 1270 mm {50 in.} in length, the 20% reduction shall be applied to the nominal shear resistance of a bolt, calculated using Equation 1 and 2, because the axial force is parallel to the line of bolts. In such flange splices, the 1270 mm {50 in.} length is to be measured between the extreme bolts on only one side of the connection. The 20 percent reduction should not be applied for web bolts subjected to shear and moment.

6.13.2.8 SLIP RESISTANCE

C6.13.2.8

The following shall replace Table A6.13.2.8-1.

SPECIFICATIONS

COMMENTARY

Table 6.13.2.8-1 - Minimum Required Bolt Tension

Metric Units			U.S. Customary Units		
Bolt Diameter _t (mm)	Required Tension- P _t (kN)		Bolt Diameter (in.)	Required Tension- P _t (kip)	
	M 164 (A 325)	M 253 (A490)		M 164 (A 325)	M 253 (A 490)
15.9	84.5	120	5/8	19	24
19.1	125	178	3/4	28	35
22.2	173	245	7/8	39	49
25.4	227	325	1	51	64
28.6	249	409	1 1/8	56	80
31.8	320	516	1 1/4	71	102
34.9	378	618	1 3/8	85	121
38.1	463	752	1 1/2	103	148

The following shall replace the first bulleted item in the second paragraph (the definition of Class A surface).

- Class A surface: blast cleaned surfaces with Class A coatings

The following shall supplement A6.13.2.8.

For values of K_s , use Class A surface conditions for design, unless a paint is tested and proven to conform to Class B conditions. If Class B is used, field testing and controls must be specified in the contract drawings or construction specifications.

Delete the fourth paragraph in A6.13.2.8 which starts "The contract document shall specify that joints having..." and replace it with the following.

The following note shall be placed on the contact drawings:

"Blast clean the faying surfaces of splices and connections of all structural elements in accordance with Publication 408 Section 1060.3(b)3. Reblast unpainted elements that remain unassembled for a period of 12 months or more following the initial cleaning."

The following shall supplement AC6.13.2.8.

The revision to the definition of Class A and the requirement to blast clean all faying surfaces is based on results of research conducted jointly by the University of Texas at Austin and the FHWA in the early 1980's on weathering steel connections. An extensive testing program conducted in conjunction with the research showed that weathering steel connections with a mill scale surface had an average slip coefficient, K_s , less than the 0.33 value for Class A. Blast cleaned weathering steel achieved an average slip coefficient above the 0.50 value specified for a Class B contact surface. The testing program incorporated a wide range of variables, including exposure of test specimens to an open environment for periods up to 12 months.

The UT/FHWA research suggests that present LRFD design policy, which allows a mill scale surface for Class A, could result in weathering steel connections that do not meet the slip coefficient value for a Class A contact surface. The revision to the definition of Class A and the requirements to blast clean all faying surfaces will add desired safety into Department projects.

Inherent factors of safety in the design of connections should ensure the serviceability of in-place weathering steel structures where the slip critical condition controlled the design.

Designers are directed to review Publication 35 Bulletin 15 for current paint systems and corresponding slip coefficients.

6.13.2.10 Tensile Resistance

6.13.2.10.3 Fatigue Resistance

C6.13.2.10.3

SPECIFICATIONS

COMMENTARY

6.13.2.11 COMBINED TENSION AND SHEAR

Replace references to A 325M and A 490M with A 325 and A 490, respectively.

C6.13.2.11

6.13.3 Welded Connections

Replace references to A 325M with A 325.

6.13.3.1 GENERAL

C6.13.3.1

The following shall supplement A6.13.3.1. Field welding is generally prohibited. Provisions may be made for attachment of stay-in-place forms, bearing plates and sole plates of pot bearings (but not the pot bearing itself). All areas where field welding is permitted shall be specifically designated on the contract plans. The fatigue provisions of this specification shall apply to the design of all affected members.

The following shall supplement AC6.13.3.1. The AASHTO/AWS D1.5M/D1.5:2002 Bridge Welding Code describes the appropriate application of the types of NDT.

The regions of welded structures requiring non-destructive testing (NDT), along with the allowable types of NDT, shall be shown on the contract plans.

Use the AASHTO/AWS D1.1M/D1.1:2002 Structural Welding Code for the welding of new tubular structures, pipes, piles and existing steel which are not covered by AASHTO/AWS D1.5M/D1.5:2002.

6.13.3.8P INTERSECTING WELDS

Intersecting welds which provide a potential crack path into the web or flange of a girder from an attachment will not be permitted. The termination of the fillet weld to prevent the intersection shall provide a minimum clearance of 40 mm { 1 1/2 in. }, unless another clearance is required by other design documents. Transverse groove welds shall not be terminated to prevent the intersection.

SPECIFICATIONS

COMMENTARY

6.13.3.9P INTERMITTENT FILLET WELDS

Intermittent fillet welds are prohibited, unless they are incorporated in the final weld in accordance with AASHTO/AWS Bridge Welding Code.

6.13.3.10P MINIMUM EDGE DISTANCE

A minimum edge distance of 25 mm {1 in.} shall be maintained from a fillet weld termination to the edge of a base metal plate in the direction of the weld.

C6.13.3.10P

An example of minimum edge distance is graphically shown in Figure C1.

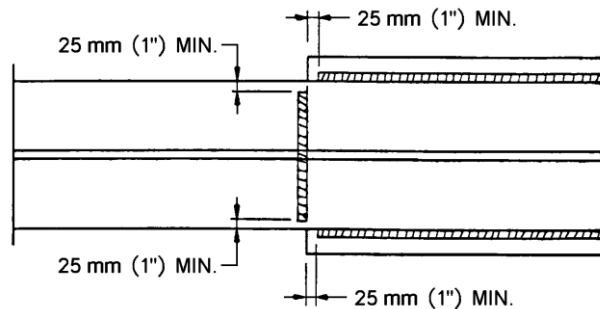


Figure C6.13.3.10P-1 - Minimum Edge Distance

6.13.4 Block Shear Rupture Resistance

The following shall replace the second sentence of the fourth paragraph of A6.13.4.

The net area shall be the gross area, minus the number of holes or fractional holes in the plane, multiplied by the nominal hole diameter specified in Table D6.13.2.4.2-1 plus 1.6 mm {1/16 in.} times the thickness of the component.

6.13.6 Splices

6.13.6.1 BOLTED SPLICES

6.13.6.1.1 General

The following shall replace A6.13.6.1.1.

Bolted splices shall be designed at the strength limit state to satisfy the requirements specified in A6.13.1 and D6.13.1. Where a section changes at a splice, the smaller of the two connected sections shall be used in the design. Develop bolted field splices for steel beams and girders in accordance with BD-616M. Splices shall be designed using the Department's SPLRFD program.

6.13.6.1.4 Flexural Members

C6.13.6.1.4P

A6.13.6.1.4a, A6.13.6.1.4b and A6.13.6.1.4c are revised

SPECIFICATIONS

COMMENTARY

below to give two sets of provisions. The straight girder provisions correspond to the AASHTO-LRFD Bridge Design Specifications, Second Edition, 1998. The horizontally curved girder provisions correspond to the AASHTO-LRFD Bridge Design Specifications, Third Edition, 2004. Both were revised for PennDOT use. Using the 1998 AASHTO-LRFD as basis for the design of straight girder splices allows the Department to continue using the existing steel splice design computer program (SPLRFD). It is the intent of the Department to update the SPLRFD computer program in the future to correspond to the provisions of the third edition of the AASHTO-LRFD Specifications.

6.13.6.1.4a General

A6.13.6.1.4a shall be revised as follows:

For straight bridges:

The following shall replace A6.13.6.1.4a.

Splice plates shall be investigated for fatigue of the base metal adjacent to slip-critical connections and specified in Table A6.6.1.2.3-1, using the gross section of the splice plates and member.

Splices subjected to tension shall satisfy the requirements specified in A6.13.5.2.

For horizontally curved bridges:

The following shall replace the fourth paragraph of A6.13.6.1.4a.

The factored flexural resistance of the flanges at the point of splice at the strength limit state shall satisfy the applicable provisions of A6.10.6.2, D6.10.6.2.

6.13.6.1.4b Web Splices

A6.13.6.1.4b shall be revised as follows:

For straight bridges:

The following shall replace A6.13.6.1.4b.

The elastic methods shall be used to determine the shear force in splice bolts. The ultimate strength method is not permitted.

Web splice plates and their connections shall be designed at the strength limit state for:

- The portion of the factored design moment, specified in A6.13.1 and D6.13.1, that is resisted by the web;
- The moment due to eccentricity of a notional shear determined as the shear due to the factored loading multiplied by the design moment specified in A6.13.1 and D6.13.1 and divided by the moment caused by the factored loads and the shear itself; and

C6.13.6.1.4b

A6.13.6.1.4b shall be revised as follows:

For straight bridges:

The following shall replace AC6.13.6.1.4b.

For bolt groups subjected to eccentric shear, a traditional conservative approach is often used in which the bolt group is treated as an elastic cross-section subjected to direct shear and torsion. A vector analysis is performed assuming that there is no friction and that the plates are rigid and the bolts are elastic.

SPECIFICATIONS

COMMENTARY

- The notional shear itself.

At the strength limit state, the flexural stress in the splice plates shall not exceed the specified minimum yield strength of the splice plates.

Web splice bolts shall be designed for the effects of moment due to the eccentric shear.

Web plates shall be spliced symmetrically by plates on each side. The splice plates for shear shall extend the full depth of the girder between flanges. There shall be not less than two rows of bolt on each side of the joint.

For bolted web splices with thickness differences of 2 mm {0.0625 in.} or less, no filler plates are required.

For horizontally curved bridges:

The following shall supplement A6.13.6.1.4b.

The elastic methods shall be used to determine the shear force in splice bolts. The ultimate strength method is not permitted.

The following shall replace the second sentence of the first paragraph of A6.13.6.1.4b.

For all single box sections, and for multiple box sections in bridges not satisfying the requirements of A6.11.2.3, including horizontally curved bridges, or with box flanges that are not fully effective according to the provisions of A6.11.1.1 and D6.11.1.1, the shear shall be taken as the sum of the flexural and St. Venant torsional shears in the web subjected to additive shears.

6.13.6.1.4c Flange Splices

A6.13.6.1.4c shall be revised as follows:

For straight bridges:

The following shall replace A6.13.6.1.4c.

At the strength limit state, the axial stress in the flange splice plate shall satisfy the requirements of A6.13.5.2 if in tension and A6.9.2 and D6.9.2 if compression.

For bolted flexural members, bolted splices in flange parts should not be used between field splices, unless approved by the Engineer. In any one flange, not more than one part should be spliced at the same cross-section. If practicable, splices should be located at points where there is an excess of section.

For horizontally curved bridges:

The following shall replace the first sentence of the paragraph before last of A6.13.6.1.4c.

For all single box sections, and for multiple box sections in bridges not satisfying the requirements of A6.11.2.3, including horizontally curved bridges, or with box flanges that are not fully effective according to the provisions of A6.11.1.1 and D6.11.1.1, longitudinal warping stresses due to cross-section distortion shall be considered when checking bolted flange splices for slip and for fatigue.

C6.13.6.1.4c

AC6.13.6.1.4c shall be revised as follows:

For straight bridges:

The following shall replace A6.13.6.1.4c.

For compression, use an unbraced length equal to zero, making $P_n = F_y A_s$

For horizontally curved bridges:

The following shall replace the first sentence of the tenth paragraph of AC6.10.6.1.4c.

For the box sections cited in this article, including sections in horizontally curved bridges, longitudinal warping stresses due to cross-section distortion can be significant under construction and service conditions and must therefore be considered when checking the connections of bolted flange splices for slip and for fatigue.

SPECIFICATIONS

COMMENTARY

6.13.6.1.5 Fillers

The following shall replace the third paragraph of A6.13.6.1.5.

Fillers 6.0 mm {1/4 in.} or more in thickness shall consist of not more than two plates, unless approved by the Chief Bridge Engineer.

The following shall replace the fifth paragraph of A6.13.6.1.5.

The specified minimum yield strength of fillers 6.0 mm {1/4 in.} or greater in thickness shall not be less than the larger of 70 percent of the specified minimum yield strength of the connected plate and 250 MPa {36 psi} unless approved by the Chief Bridge Engineer.

6.13.6.2 WELDED SPLICES

The following shall replace the third paragraph of A6.13.6.2.

Welded field splices shall not be used without written approval of the Chief Bridge Engineer.

6.15 PILES**6.15.1 General**

The following shall replace A 6.15.1.

Piles shall be designed as structural members capable of safely supporting all imposed loads.

For a pile group composed of only vertical piles which is subjected to lateral load, the pile structural analysis shall include explicit consideration of soil-structure interaction effects using a COM624P analysis (Wang and Reese, 1993) or LPILE 5.0 analysis.

Based on the parametric study conducted by the Department, which is described in the commentary, an abutment or retaining wall with a pile group composed of both vertical and battered piles which is subjected to lateral load shall be designed assuming that all lateral load is resisted by the horizontal component of the axial

The following shall replace the first sentence of the eleventh paragraph of AC6.10.6.1.4c.

In cases for straight girders where flange lateral bending is deemed significant, and for horizontally curved girders, the effects of the lateral bending must be considered in the design of the bolted splices for discretely braced top flanges of tub sections or discretely braced flanges of I-sections.

C6.13.6.2

The following shall supplement AC6.13.6.2.

Use the AASHTO/AWS D1.1M/D1.1:2002 Structural Welding Code for the welding of new tubular structures, pipes, piles, and existing which are not covered by AASHTO/AWS D1.5M/D1.5:2002.

C6.15.1

The following shall replace AC6.15.1.

To develop the recommended distribution of lateral load among piles supporting a typical bridge abutment, a parametric study (Kelly, et al, 1995) was performed using the program GROUP (Reese, et al, 1994). A second purpose of this parametric study was to determine if the Department's lateral deformation criteria of 12 mm {1/2 in.} for the service limit state and 25 mm {1 in.} for the strength limit state were satisfied. These criteria were met for all analyses representative of the Department's practice. The variables evaluated in the parametric study included:

- HP310X79 {HP12X53} and HP250X62 {HP10X42}

SPECIFICATIONS

capacity of the battered piles. The vertical load shall be distributed among piles in the group using a simple elastic procedure. The use of the above design procedure with any of the following conditions requires the approval of the Chief Bridge Engineer:

- Piles with a specified steel yield strength other than 250 MPa {36 ksi}
- Piles with bending stiffness properties less than HP250X62 {HP10X42}
- Very soft clays or very loose sands as defined in Standard Drawing BC-795M
- Piles with bending stiffness properties less than HP310X79 {HP12X53} in soft clays or loose sands as defined in Standard Drawing BC-795M
- Unfactored vertical load to horizontal load ratio less than 3.5 (excluding seismic forces)

COMMENTARY

piles with about four-pile diameters center-to-center spacing;

- End bearing piles on rock driven through a medium stiff-to-stiff clay deposit, and friction piles in deposits of medium dense and loose sand;
- Pile lengths of 3.0, 9.1 and 15.2 m {10, 30, and 50 ft.};
- Vertical and horizontal load levels consistent with common Department designs; and
- Pile-head fixity conditions of fixed, pinned and partially fixed.
- For typical pile groups containing battered piles designed using the simplified procedure, the pile study indicates that:
 - Combined stresses in upper portions of the battered and vertical piles due to axial load and bending are generally less than 82 to 95 MPa {11.9 to 13.8 ksi}, which is consistent with previous practice.
 - The fraction of the total lateral load resisted by bending of the vertical piles is generally less than about 20 percent.
 - The check of structural pile capacity for combined axial load and flexure in the upper portion of the pile using the LRFD Interaction Equations in A6.9.2.2 does not control the pile design.
 - Lateral deflections are well below acceptable magnitudes.
 - As pile stiffness increases, horizontal deformations and associated bending stresses decrease such that the simplified method remains applicable.

In cases for which pile and soil conditions differ significantly from those conditions examined in the parametric study, a suitable analysis should be performed which incorporates the necessary soil-structure interaction factors. This analysis may comprise finite element analysis, p-y analysis, or other applicable methods. Lateral deflections and maximum bending stresses for laterally-loaded pile groups generally occur within a depth below the pile cap equal to approximately 10 pile diameters. Therefore, the presence of poor material (very soft clays or very loose sands) within the upper 10 pile diameters invalidates use of the simplified method due to the potential for pile overstressing and excessive deformations under lateral loads. If these conditions exist, the designer may consider the following options:

SPECIFICATIONS

6.15.2 Structural Resistance

The following shall replace A 6.15.2.

Resistance factors, ϕ , for the strength limit state shall be taken as specified in D6.5.4.2. The resistance factors for axial resistance of piles in compression which are subject to damage due to driving shall be applied only to that section of the pile likely to experience damage.

Therefore, the specified ϕ factors of 0.35 and 0.45, specified in D6.5.4.2 for piles subject to damage, shall be applied only to the axial capacity of the pile. In addition, the ϕ factors of 0.60 and 0.85, specified in D6.5.4.2 for axial and flexural resistance, respectively, of undamaged piles, shall be applied to the combined axial and flexural resistance of the pile in the interaction equation for the compression and flexure terms respectively. This design approach is illustrated on Figure 1.

For piles bearing on soluble bedrock, the ϕ factor of 0.25 shall be applied to the axial capacity of the pile using a pile yield strength $F_y = 250 \text{ MPa}$ {36 ksi}.

COMMENTARY

- Improve in place or remove and replace the poor material. These may be viable options when the thickness of poor material is small and close to the ground surface.
- Perform a more rigorous, problem specific analysis to define pile stress levels and pile group deformations. This type of analysis may be performed using software such as GROUP, Reese, et al (1994).

A thin seam or lens of poor material below the upper 10 pile diameters will not typically affect the applicability of the simplified method.

C6.15.2

The following shall replace A 6.15.2.

Due to the nature of pile driving, additional factors must be considered in selection of resistance factors that are not normally accounted for in steel members. The factors considered in development of the specified resistance factors include:

- Unintended eccentricity of applied load about expected point of application,
- Variations in material properties of pile, and
- Pile damage due to driving.

These factors are discussed by Davisson (1983). While the resistance factors specified herein generally conform to the recommendations given by Davisson (1983), they have been modified to reflect the common practice of the Department. Specifically, the resistance factors presented in D6.5.4.2 have been selected in a manner such that, when combined with an average load factor of 1.45, the equivalent factor of safety calculated as the ratio of the appropriate load to resistance factor is comparable to the factor of safety previously used by the Department. The factored compressive resistance, P_r , includes reduction factors for unintended load eccentricity and material property variations, as well as a reduction for potential damage to piles due to driving, which is most likely to occur near the tip of the pile. The resistance factors for computation of the factored axial pile capacity near the tip of the pile are 0.35 and 0.45 for severe and good driving conditions, respectively. The ϕ factor of 0.25 for piles bearing on soluble bedrock is intended to safeguard against the potential of the loss of geotechnical capacity in soluble bedrock.

For steel piles, flexure occurs primarily toward the head of the pile. This upper zone of the pile is less likely to experience damage due to driving. Therefore, relative to combined axial compression and flexure, the resistance

SPECIFICATIONS

COMMENTARY

factor for axial resistance ($\phi_c = 0.60$) accounts for both unintended load eccentricity and pile material property variations, whereas the resistance factor for flexural resistance ($\phi_f = 0.85$) accounts only for variations in pile material properties.

Typically, due to the lack of a detailed soil-structure interaction analysis of pile groups containing both vertical and battered piles, evaluation of combined axial and flexural loading will only be applied to pile groups containing no battered piles.

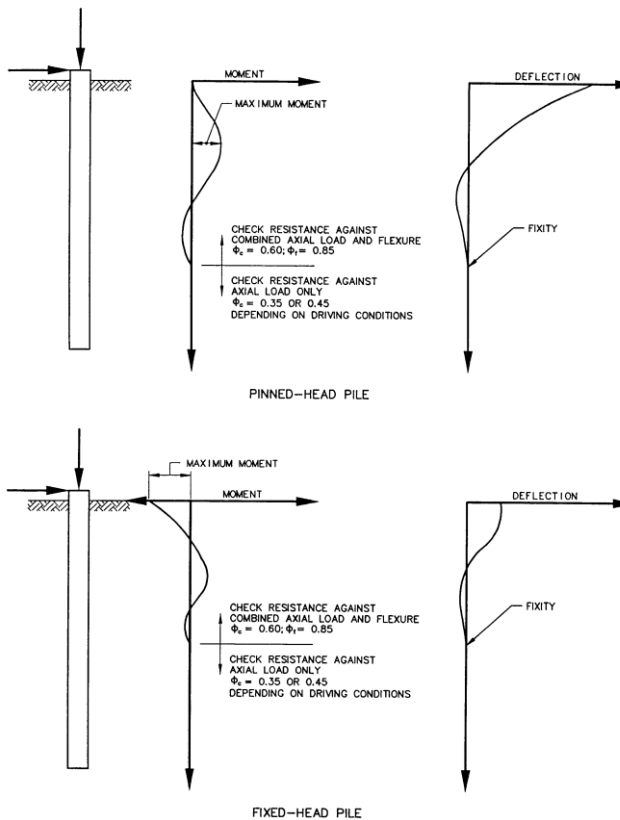


Figure 6.15.2-1 - Distribution of Moment and Deflection in Vertical Piles Subjected to Lateral Load

6.15.3P Compressive Resistance

The design of steel piles shall follow A6.9, except as specified herein.

6.15.3.1 AXIAL COMPRESSION

The following shall replace A 6.15.3.1.

For piles under axial load, the factored resistance of piles in compression, P_r , shall be taken as specified in A6.9.2.1 using the resistance factor, ϕ_c , specified in D6.5.4.2.

SPECIFICATIONS

COMMENTARY

6.15.3.2 COMBINED AXIAL COMPRESSION AND FLEXURE

C6.15.3.2

The following shall replace A 6.15.3.2.

Piles subjected to axial load and flexure shall be designed in accordance with A6.9.2.2 using the resistance factors, ϕ_c and ϕ_r , specified in D6.5.4.2.

Vertical H-pile foundations designed using COM624P or LPILE 5.0 per D10.7.3.12.2 may use the values given in Tables 1 and 2.

where:

- D = Depth of the pile.
- Area = Area of the pile.
- I_x, I_y = Moment of inertia about their respective axis.
- P_{uSERV} = COM624P or LPILE 5.0 pile load equivalent to pile resistance at Service Limit State.
- P_{uSTR} = COM624P or LPILE 5.0 pile load equivalent to pile resistance under severe driving conditions as defined in D6.15.2P.
- P_r = Factored axial resistance for combined axial and flexural resistance.
- M_{rx}, M_{ry} = Factored flexural resistance of the vertical pile in the x-axis and y-axis, respectively.

The factored flexural resistance, M_{rx} , is based on either the plastic or elastic moment of pile considering web and compression flange slenderness requirements. The factored flexural resistance, M_{ry} , is based on the plastic moment per AC6.12.2.2.1.

For these tables the piles are considered as braced. If very weak soils, scour or voids are expected, the buckling requirements of DM-4 6.15.3.3 must be considered and the values shown in Tables 1 and 2 are not applicable. P_{uSERV} and P_{uSTR} in Tables 1 and 2 are based on $0.25 \cdot f_y \cdot A_s$ and $0.35 \cdot f_y \cdot A_s$, respectively. For piles bearing on soluble rock (limestone, etc.) values for P_{uSERV} and P_{uSTR} equal to $0.16 \cdot f_y \cdot A_s$ and $0.25 \cdot f_y \cdot A_s$, respectively, are to be considered.

The section properties provided are for use in the COM624P or LPILE 5.0 analysis. The combined axial compression and flexural requirements of A6.9.2.2 shall be evaluated considering the results of the COM624P or LPILE 5.0 analysis and the resistances provided in the Tables 1 and 2.

The section properties may also be used in PENNDOT's Integral Abutment Spreadsheet. However; since the capacities in the tables do not consider unbraced length, the structural pile capacity of vertical piles used in an Integral Abutment must be checked in accordance with DM-4 Appendix G using the Integral Abutment Spreadsheet.

SPECIFICATIONS

COMMENTARY

Table 6.15.3.2P-1 – Pile Properties, Factored Axial and Flexural Resistances with Full Pile Section.
 $F_y = 250 \text{ MPa} \{36 \text{ ksi}\}$

Metric									
HP	Depth D (mm)	Area (mm ²)	I_x (10 ⁶ mm ⁴)	I_y (10 ⁶ mm ⁴)	P_{uSERV} (kN)	P_{uSTR} (kN)	P_r (kN)	M_{rx} (kN-m)	M_{ry} (kN-m)
360 x 174	361	22200	508	184	1378	1929	3306	679	310
360 x 152	356	19400	439	159	1204	1685	2889	589	270
360 x 132	351	16900	375	135	1049	1468	2517	455	231
360 x 108	346	13800	303	108	856	1199	2055	372	186
310 x 125	312	15900	270	88.2	987	1381	2368	417	180
310 x 110	308	14100	237	77.1	875	1225	2100	368	158
310 x 94	303	11900	196	63.9	738	1034	1772	274	132
310 x 79	299	10000	163	52.6	621	869	1489	232	110
250 x 85	254	10800	123	42.3	670	938	1608	232	104
250 x 62	246	7970	87.5	30.0	495	692	1187	151	75

US Customary Units									
HP	Depth D (in)	Area (in ²)	I_x (in ⁴)	I_y (in ⁴)	P_{uSERV} (kips)	P_{uSTR} (kips)	P_r (kips)	M_{rx} (kip-ft)	M_{ry} (kip-ft)
14 x 117	14.21	34.4	1220	443	310	434	743	495	228
14 x 102	14.01	30.0	1050	380	270	378	648	431	197
14 x 89	13.83	26.1	904	326	235	329	564	334	169
14 x 73	13.61	21.4	729	261	193	270	462	273	137
12 x 84	12.28	24.6	650	213	221	310	531	306	132
12 x 74	12.13	21.8	569	186	196	275	471	268	116
12 x 63	11.94	18.4	472	153	166	232	397	202	97
12 x 53	11.78	15.5	393	127	140	195	335	170	81
10 x 57	9.99	16.8	294	101	151	212	363	170	75
10 x 42	9.70	12.4	210	71.7	112	156	268	111	54

SPECIFICATIONS

COMMENTARY

Table 6.15.3.2P-2 – Factored Axial and Flexural Resistance with 1.5 mm (1/16") Section Loss. $F_y = 250$ MPa (36 ksi)

Metric									
HP	Depth D (mm)	Area (mm ²)	I_x (10 ⁶ mm ⁴)	I_y (10 ⁶ mm ⁴)	P_{uSERV} (kN)	P_{uSTR} (kN)	P_r (kN)	M_{rx} (kN-m)	M_{ry} (kN-m)
360 x 174	358	18530	424	152	1150	1610	2760	504	258
360 x 152	353	15730	355	127	976	1367	2343	428	217
360 x 132	348	13240	295	105	821	1150	1971	360	181
360 x 108	343	10210	224	79.7	634	887	1520	278	138
310 x 125	309	12780	217	70.1	793	1110	1903	299	145
310 x 110	305	10980	184	59.5	682	954	1636	257	124
310 x 94	300	8820	145	46.8	547	766	1313	206	98
310 x 79	296	6980	113	36.4	433	606	1039	163	77
250 x 85	251	8290	93.3	31.5	514	720	1,234	158	78
250 x 62	243	5470	59.9	20.2	339	475	814	105	51

US Customary Units									
HP	Depth D (in)	Area (in ²)	I_x (in ⁴)	I_y (in ⁴)	P_{uSERV} (kips)	P_{uSTR} (kips)	P_r (kips)	M_{rx} (kip-ft)	M_{ry} (kip-ft)
14 x 117	14.09	28.73	1019	365	259	362	620	369	189
14 x 102	13.89	24.39	853	305	219	307	527	313	159
14 x 89	13.71	20.51	708	253	185	258	443	263	133
14 x 73	13.49	15.83	537	192	142	199	342	203	101
12 x 84	12.16	19.81	521	168	178	250	428	219	106
12 x 74	12.01	17.02	443	143	153	215	368	188	90
12 x 63	11.82	13.66	349	112	123	172	295	151	72
12 x 53	11.66	10.81	272	87.5	97	136	234	119	56
10 x 57	9.87	12.84	224	75.6	116	162	277	116	57
10 x 42	9.58	8.48	143	48.5	76	107	183	77	37

SPECIFICATIONS

COMMENTARY

6.15.3.3 BUCKLING

The following shall replace the last sentence of A 6.15.3.3.
The depth to fixity shall be determined in accordance with D10.7.3.13.4 for battered piles or COM624P or LPILE 5.0 analyses for vertical piles. Figure D6.15.2-1 illustrates the depth to fixity as determined by COM624P or LPILE 5.0.

6.15.4 Maximum Permissible Driving Stresses

The following shall replace A 6.15.4.
Maximum permissible driving stresses for top driven steel piles shall be taken as specified in D10.7.8.

C6.15.3.3

The following shall replace AC 6.15.3.3.
The use of an approximate method in lieu of a P- Δ analysis is allowed if approved by the Chief Bridge Engineer.

SPECIFICATIONS

COMMENTARY

APPENDIX A – FLEXURAL RESISTANCE – COMPOSITE SECTIONS IN NEGATIVE FLEXURE AND NONCOMPOSITE SECTIONS WITH COMPACT OR NONCOMPACT WEBS

The following shall be added immediately after the heading of the appendix and before AA6.1.

The provisions of this Appendix are applicable to curved bridge components designed using the provisions of A6.10 and A6.11 as revised by D6.10 and D6.11. They are not applicable to straight bridge components designed using the provisions of Appendix DE.

APPENDIX B – MOMENT REDISTRIBUTION FROM INTERIOR-PIER SECTIONS IN CONTINUOUS-SPAN BRIDGES

Delete Appendix B in its entirety

The provisions of Appendix B correspond to the inelastic design procedures that are not allowed in Pennsylvania.

APPENDIX C – BASIC STEPS FOR STEEL BRIDGE SUPERSTRUCTURES

The following shall be added immediately after the heading of the appendix and before AC6.1.

The provisions of this Appendix are applicable to curved bridge components designed using the provisions of A6.10 and A6.11 as revised by D6.10 and D6.11. They are not applicable to straight bridge components designed using the provisions of Appendix DE.

REFERENCES

The following shall supplement the references of A5.

Albrecht, P., Coburn, S.K., Wattar, F.M., Tinklenberg, G.L. and W.P. Gallagher. Guidelines for the Use of Weathering Steel in Bridges. NCHRP Report 314. TRB, National Research Council, Washington, D.C., June 1989.

Mertz, D. R., "Displacement-Induced Fatigue Cracking in Welded Steel Bridges", Ph.D. dissertation, Lehigh University, 1984

**ADDITIONAL LATERAL STABILITY CRITERIA
FOR STRAIGHT STEEL GIRDER BRIDGES**

(APPLIES TO STRAIGHT AND CURVED BRIDGES)

1. THE DESIGN ENGINEER SHALL CHECK STRAIGHT BRIDGES FOR THE FOLLOWING LOADING CONDITIONS:

A) WIND LOADS ON THE STEEL SUPERSTRUCTURE PRIOR TO DECK PLACEMENT - THE PROCEDURES SHOULD FOLLOW THAT USED FOR THE STRAIGHT, UNDECKED BRIDGE. THE LANCED AREA SHALL BE THE VERTICAL PLANE AREA OF THE FANEA GIRDERS.

B) PARTIAL WIND LOADS UNDER STAGED CONSTRUCTION FOR FUTURE DECK REPLACEMENT AS DIRECTED BY THE DEPARTMENT.

C) VERTICAL AND LATERAL DEFLECTIONS SHALL BE EVALUATED FOR STEEL SELF-WEIGHT AND THE DEAD DEAD LOAD.

2. BEARINGS SHALL BE DESIGNED TO ACCOMMODATE GROUND ROTATION DURING THE DECK POUR BOTH IN AND OUT OF THE GIRDER PLANE. BEARINGS SHALL BE DESIGNED TO ACCOMMODATE GROUND ROTATION UNDER FULL DEAD LOAD. UP/LIFT SHALL BE CHECKED AT EACH BEARING FOR WORST LOADING CONDITION IN EACH CONSTRUCTION PHASE.

3. INCLUDE LATERAL WIND BRACING IN THE DESIGN OF GIRDERS THAT DO NOT MEET THE CRITERIA AS SHOWN ON SHEET L. DESIGN LATERAL BRACING TO CARRY WIND LOADS ONLY AND DETAIL THE BRACING SO THAT IT WILL NOT PARTICIPATE IN CARRYING PRIMARY STRUCTURE FORCES.

4. THE ENGINEER SHALL IDENTIFY THE NEED FOR AND LOCATION OF FALCROWK AND PROVIDE INFORMATION AS FOR DM4 DCLL2 17. HOWEVER, THE DESIGN AND FOUNDATION OF THE FALCROWK IS THE RESPONSIBILITY OF THE CONTRACTOR.

5. USE TOP OR BOTTOM FLANGE BRACING FOR STRAIGHT BRIDGES. FOR GIRDERS WITH NARROW TOP FLANGE WIDTH, IT IS RECOMMENDED TO USE ANTI-TURN FLANGE LATERAL BRACING.

6. RESPECTIVE OF THE GROSS FLANGE SPACING, GROSS FLANGE INCONSISTENT DETAILS SHALL BE AVOIDED AS SHOWN IN THE DETAILS FOR STRAIGHT STEEL BRIDGES. SO THAT THE WEBS ARE PLUMB UNDER FULL DEAD LOAD CONDITION FOR BEAR ANGLES BETWEEN 30° AND 70° AND FULL DEAD LOAD CONDITION FOR BEAR ANGLES LESS THAN 30°.

**ADDITIONAL LATERAL STABILITY CRITERIA
FOR CURVED STEEL BRIDGES**

1. THE DESIGN ENGINEER SHALL CHECK CURVED STEEL GIRDER BRIDGES FOR THE FOLLOWING LOADING CONDITIONS:

A) WIND LOADS ON THE STEEL SUPERSTRUCTURE PRIOR TO DECK PLACEMENT - THE PROCEDURES SHOULD FOLLOW THAT USED FOR STRAIGHT BRIDGES. THE LANCED AREA SHALL BE THE VERTICAL PLANE AREA OF THE LANCED GIRDERS. ALLOWABLE HORIZONTAL DEFLECTIONS SHALL BE BASED ON CRITERIA FOR STRAIGHT UNDECKED BRIDGES AND CHECKED PRIOR TO DECK PLACEMENT.

B) PARTIAL WIND LOADS UNDER STAGED CONSTRUCTION FOR FUTURE DECK REPLACEMENT AS DIRECTED BY THE DEPARTMENT.

C) VERTICAL AND LATERAL DEFLECTIONS SHALL ALSO BE EVALUATED FOR STEEL SELF-WEIGHT AND THE DEAD DEAD LOAD.

2. BEARINGS SHALL BE DESIGNED TO ACCOMMODATE GROUND ROTATION DURING THE DECK POUR BOTH IN AND OUT OF THE GIRDER PLANE. BEARINGS SHALL BE DESIGNED TO ACCOMMODATE GROUND ROTATION UNDER FULL DEAD LOAD. UP/LIFT SHALL BE EVALUATED AT EACH BEARING FOR WORST LOADING CONDITION IN EACH CONSTRUCTION PHASE.

3. INCLUDE LATERAL WIND BRACING IN THE DESIGN OF GIRDERS THAT DO NOT MEET THE CRITERIA AS SHOWN ON SHEET L. DESIGN LATERAL BRACING TO CARRY WIND LOADS ONLY AND DETAIL THE BRACING SO THAT IT WILL NOT PARTICIPATE IN CARRYING PRIMARY STRUCTURE FORCES.

4. THE ENGINEER SHALL IDENTIFY THE NEED FOR AND LOCATION OF FALCROWK AND PROVIDE INFORMATION AS FOR DM4 DCLL2 17. HOWEVER, THE DESIGN AND FOUNDATION OF THE FALCROWK IS THE RESPONSIBILITY OF THE CONTRACTOR.

5. DESIGN LATERAL BRACING FOR WIND LOADS. DESIGN AND DETAIL THE LATERAL BRACING SO THAT TORSIONAL FORCES FROM DEAD LOADS AND LIVE LOADS ON THE GIRDERS ARE NOT REDUCED BY THE LATERAL BRACING.

6. RESPECTIVE OF THE GROSS FLANGE SPACING, GROSS FLANGE INCONSISTENT DETAILS SHOULD BE AVOIDED AND GIRDERS AND CROSS FRAMES SHALL BE DETAIL SO THAT THE WEBS ARE PLUMB UNDER FULL DEAD LOAD CONDITION.

NOTE: EITHER ALL METRIC OR ALL ENGLISH VALUES MUST BE USED ON PLANS. METRIC AND ENGLISH VALUES SHOWN MAY NOT BE MIXED.

COMMONWEALTH OF PENNSYLVANIA
DEPARTMENT OF TRANSPORTATION
BUREAU OF DESIGN

STANDARD
STEEL GIRDER BRIDGES
LATERAL BRACING CRITERIA
AND DETAILS

REVISIONS	DATE	BY	APP. BY
RECOMMENDED APRIL 2004			
RECOMMENDED APRIL 2004			
RECOMMENDED APRIL 2004			